

FLUORINATION AND PHOTOCATALYSIS:

NEW HORIZONS

By

JON I. DAY

Bachelor of Arts/Science in Chemistry  
Oklahoma State University  
City, State  
2015

Submitted to the Faculty of the  
Graduate College of the  
Oklahoma State University  
in partial fulfillment of  
the requirements for  
the Degree of  
DOCTOR OF PHILOSOPHY  
May, 2020

FLUORINATION AND PHOTOCATALYSIS:  
NEW HORIZONS

Dissertation Approved:

Dr. Jimmie Dean Weaver III

---

Dissertation Adviser

Dr. Jeanne Bolliger

---

Dr. Elijah Schnitzler

---

Dr. Christopher Fennell

---

Dr. Marimuthu Andiappan

---

## ACKNOWLEDGEMENTS

### **Two-Headed Calf**

By Laura Gilpin

Tomorrow when the farm boys find this  
freak of nature, they will wrap his body  
in newspaper and carry him to the museum.  
But tonight he is alive and in the north  
field with his mother. It is a perfect  
summer evening: the moon rising over  
the orchard, the wind in the grass. And  
as he stares into the sky, there are  
twice as many stars as usual.

Name: JON I. DAY

Date of Degree: MAY, 2020

Title of Study: FLUORINATION AND PHOTOCATALYSIS: NEW HORIZONS

Major Field: CHEMISTRY

Abstract: Recently, the understanding of the importance of fluorination in organic compounds has exploded. It provides a handle for medicinal, agricultural and materials chemists to advantageously affect the properties of a molecule. Despite these enhancements, due to the absence of fluorine containing molecules in the natural world, the pool of molecules such as these from which chemists may draw to build larger and more elaborate molecules is very limited. Single fluorines can be installed into molecules, though this process is arduous, expensive, and inefficient. This problem is compounded when sequential fluorination processes are required. From a fundamentally different approach to fluorination in this way, installing fluorines everywhere, perfluorination, is straightforward and reliable. The fluorines may then be substituted one by one to give the desired molecule. It is toward this goal that the Weaver Lab has labored, developing methodology to perform new and interesting transformations on polyfluorinated molecules to not only reduce the fluorine content, but to do it selectively, and increase the complexity of the molecule as desired. Photocatalysis and  $S_NAr$  can serve in this capacity. Further, photocatalysis can be used in synthesis that does not involve fluorine, but rather take advantage of some of the other novel reactivities in which the photocatalytic cycle can be engaged. Expeditions into these realms are the subjects explored herein.



## TABLE OF CONTENTS

Chapter	Page
I. HISTORY LEADING TO WORKS HEREIN.....	1
1.1 Overview.....	1
1.2 Effects of Fluorination of Organic Molecules .....	1
1.3 Approaches to Synthesis of Fluorinated Molecules.....	4
1.4 Photocatalysis .....	6
1.41 Photochemical Isomerization in Nature.....	8
1.42 History of Photochemical Isomerization .....	8
1.43 History of E/Z Specific Synthesis.....	9
1.44 History of E to Z Isomerization in the Weaver Lab.....	10
1.45 Photocatalytic Hydrodefluorination.....	14
1.5 Other C–F Functionalizations .....	15
1.6 History of S <sub>N</sub> ArF.....	16
1.6 References.....	17
II. ADVANCES IN PHOTOCATALYSIS: A MICROREVIEW OF VISIBLE LIGHT MEDIATED RUTHENIUM AND IRIIDIUM CATALYZED ORGANIC TRANSFORMATIONS .....	33
2.1 Overview.....	33
2.2 Photocatalyst Physical Properties .....	35
2.3 Photocatalyst Details.....	36
2.3.1 <i>fac</i> -Ir(ppy) <sub>3</sub> .....	36
2.3.2 <i>fac</i> -Ir(2',4'-dF-ppy) <sub>3</sub> .....	37
2.3.3 <i>fac</i> -Ir(4'-F-ppy) <sub>3</sub> .....	38
2.3.4 <i>fac</i> -Ir(4'-CF <sub>3</sub> -ppy) <sub>3</sub> .....	38
2.3.5 [Ir(ppy) <sub>2</sub> (4,4'-dtb-bpy)]PF <sub>6</sub> .....	39
2.3.6 [Ir(2',4'-dF-5-CF <sub>3</sub> -ppy) <sub>2</sub> (bpy)]PF <sub>6</sub> .....	41
2.3.7 [Ir(2',4'-dF-5-me-ppy) <sub>2</sub> (4,4'-dtb-bpy)]PF <sub>6</sub> .....	42
2.3.8 [Ir(2',4'-dF-5-CF <sub>3</sub> -ppy) <sub>2</sub> (4,4'-dtb-bpy)]PF <sub>6</sub> .....	43
2.3.9 [Ir(3,4'-dm-ppy) <sub>2</sub> (4,4'-dtb-bpy)]PF <sub>6</sub> .....	45
2.3.10 [Ir(4,4'-dtb-ppy) <sub>2</sub> (3,4'-dtb-bpy)]PF <sub>6</sub> .....	46
2.3.11 [Ru(bpy) <sub>3</sub> ](PF <sub>6</sub> ) <sub>2</sub> .....	47
2.3.12 [Ru(bpz) <sub>3</sub> ](PF <sub>6</sub> ) <sub>2</sub> .....	48
2.3.13 [Ru(phen) <sub>3</sub> ](PF <sub>6</sub> ) <sub>2</sub> .....	49
2.3.14 [Ru(4,4'-dm-bpy) <sub>3</sub> ](PF <sub>6</sub> ) <sub>2</sub> .....	50
2.3.15 [Ru(4,4'-dtb-bpy) <sub>3</sub> ](PF <sub>6</sub> ) <sub>2</sub> .....	51

2.4 Conclusion .....	52
2.5 Acknowledgement .....	52
2.6 References.....	52
<b>III. SELECTIVE AND SCALABLE PERFLUOROARYLATION OF NITROALKANES.....</b>	<b>57</b>
3.1 Overview.....	57
3.2 Introduction.....	57
3.3 Results & Discussion .....	60
3.4 Conclusions.....	68
3.5 Experimental.....	68
3.6 Acknowledgements.....	73
3.1 References.....	73
<b>IV. VISIBLE LIGHT MEDIATED GENERATION OF TRANS- ARYLCYCLOHEXENES AND THEIR UTILIZATION IN THE SYNTHESIS OF CYCLIC BRIDGED ETHERS .....</b>	<b>132</b>
4.1 Overview.....	132
4.2 Introduction.....	133
4.3 Experimental.....	135
4.4 Mechanistic Investigation .....	138
4.5 Discussion.....	143
4.6 Conclusions.....	144
4.7 Acknowledgement .....	145
4.8 General Experimental .....	145
4.9 Synthesis of Substrates .....	145
4.10 Characterization .....	148
4.11 Spectra.....	152
4.12 Kinetic and Mechanistic Studies.....	184
4.12.1 Deuterium Incorporation.....	184
4.12.2 Evidence for Hydrogen Bonding .....	188
4.12.3 Competition between 1-Ph-Cyclohexene and 4.3.1f .....	191
4.12.4 Order of reactants.....	192
4.12.5 Proton Inventory .....	195
4.12.6 Calculations.....	196
4.12.7 References.....	210

V. SOLUBILITY OF IRIDIUM AND RUTHENIUM ORGANOMETALLIC PHOTOREDOX CATALYSTS .....	214
5.1 Overview.....	214
5.2 Introduction.....	214
5.3 Experimental.....	215
5.4 Discussion.....	217
5.5 Conclusion .....	230
5.6 References.....	230
VI. POLYFLUORO-POLYCYCLIC DEAROMATIVE ARYLATION: A PHOTOCATALYTIC BIRCH-LIKE REDUCTION PROVIDES ACCESS TO UNNATURAL CANNABINOIDS .....	232
6.1 Overview.....	232
6.2 Introduction.....	232
6.3 Optimization .....	235
6.4 Scope.....	237
6.5 Mechanism.....	239
6.6 Application.....	244
6.7 Conclusion .....	247
6.8 Acknowledgement .....	247
6.9 References.....	247
6.10 Experimental.....	266
6.10.1 Characterization.....	270
6.10.2 Spectra.....	284
6.10.3 Kinetic Isotope Effect Studies.....	389
6.10.4 Computational NMR spectra .....	394
6.10.5 Single crystal X-ray diffraction analysis.....	412
VII. Acknowledgments.....	416

## LIST OF TABLES

Table	Page
1 Some Select Fluorinated Molecules.....	2
2 Effect of Fluorination on pKa of Conjugate Acid and Relationship to Bioavailability .....	3
3 Select Photocatalyst Physical Attributes.....	7
4 Some Organic Triplet Sensitizers .....	9
5 Photophysical properties of selected commercially available photocatalysts .....	35
6 The importance of (poly)fluorinated arenes in medicinal and agricultural chemicals .....	57
7 Optimization of the SNAr reaction of pentafluoropyridine with nitromethanate...	60
8 Scope of the SNAr reaction of nitromethane with fluoroarenes.....	61
9 Investigation of the scope of the nucleophile .....	65
10 Reduction of nitromethyl arenes to amines .....	66
11 Optimization of reaction conditions.....	135
12 Scope of the Photochemical Isomerization.....	137
13 <i>fac</i> -Ir(ppy) <sub>3</sub> Solubility .....	218
14 <i>fac</i> -Ir(4'-Fppy) <sub>3</sub> Solubility .....	218
15 Ir(4'-CF <sub>3</sub> ppy) <sub>3</sub> Solubility.....	219
16 Ir(ppy) <sub>2</sub> (dtbbpy)PF <sub>6</sub> Solubility .....	219
17 Ru(dmb) <sub>3</sub> (PF <sub>6</sub> ) <sub>2</sub> Solubility.....	220
18 Ru(phen) <sub>3</sub> (PF <sub>6</sub> ) <sub>2</sub> Solubility.....	220
19 Ru(dtbbpy) <sub>3</sub> (PF <sub>6</sub> ) <sub>2</sub> Solubility .....	221
20 Ru(bpz) <sub>3</sub> (PF <sub>6</sub> ) <sub>2</sub> Solubility .....	221
21 Ru(bpy) <sub>3</sub> (PF <sub>6</sub> ) <sub>2</sub> Solubility.....	222
22 <i>fac</i> -Ir(Fppy) <sub>3</sub> Solubility .....	222
23 Ir(dtbbpy) <sub>2</sub> (dtbbpy)PF <sub>6</sub> Solubility .....	223
24 <i>fac</i> -Ir(tBuppy) <sub>3</sub> Solubility .....	223
25 Ir[dF(CF <sub>3</sub> )ppy] <sub>2</sub> (dtbbpy)PF <sub>6</sub> Solubility.....	224
26 Ir(dmppy) <sub>2</sub> (dtbbpy)PF <sub>6</sub> Solubility.....	224
27 Maximum solubility of various iridium and ruthenium complex photocatalysts in common organic solvents .....	226
28 Some Important Entries in the Fluoropharmacopeia .....	232
29 Optimization of the Reaction Conditions .....	235
30 Scope.....	238

## LIST OF FIGURES

Figure	Page
1 Photocatalyst Quenching Pathways .....	6
2 A hypothetical exploitation of the S <sub>N</sub> Ar mechanism for the formation of the monoarylated S <sub>N</sub> Ar product of pentafluoropyridine in contrast to Sandford and Cobb's 2012 work. ....	59
3a LUMO surfaces (upper) and MESP surfaces (lower) .....	64
3b Vertical cross section through electron density surface.....	64
4 Accessibility of the Biradical as a Function of Alkene Conjugation .....	138
5 Only the syn- and anti- diastereomers can lead to Oxabicyclic Etherification.....	139
6 Deuterium Incorporation under General Reaction Conditions with 4.3.1a and Computational identification of the Resultant Diastereomer.....	140
7 Proton Inventory .....	141
8 Geometry of the Presumptive Transition State.....	142
9 The solubility of photocatalysts in aqueous acetonitrile.....	217
10 Maximum Concentration of Uncharged Iridium Complex Photocatalysts in Various Organic Solvents.....	225
11 Maximum Concentration of Charged Iridium Complex Photocatalysts in Various Organic Solvents.....	225
12 Maximum Concentration of Charged Ruthenium Complex Photocatalysts in Various Organic Solvents.....	236
13 Darkening of Reaction as a Function of Equivalent Water Added .....	248

## LIST OF SCHEMES

Scheme	Page
1 “Hula–Twist” Photolysis and Photoisomerization in Humans at 290–315 nm .....	8
2 Schrock, Hoveyda Z Selective Alkene Metathesis Catalyst.....	10
3 Stereoconvergence discovered in Lu & Yoon, 2012. <i>Angewandte Chemie Int. Ed.</i> , 51, 10329.....	11
4 E to Z Photoisomerization in the Weaver Lab.....	11
5 Photocatalyst Size Matters for Isomerization .....	12
6a UV Mediated Solvolysis of E-Phenylcyclohexene .....	13
6b Strain Release in Synthesis .....	13
7 Mesolytic Fragmentation of a C–F Bond.....	14
8 Fluoroaryl Radical Abstraction of an H-atom leads to HDF .....	15
9 Fluoroaryl Radical Alkylation .....	15
10 Fluoroaryl Radical Arylation .....	16
11 Classic Stepwise S <sub>N</sub> ArF Mechanism .....	17
12 <i>fac</i> -Ir(ppy) <sub>3</sub> Reactions .....	36
13 <i>fac</i> -Ir(2',4'-dF-ppy) <sub>3</sub> Reactions.....	37
14 [Ir(ppy) <sub>2</sub> (4,4'-dtb-bpy)]PF <sub>6</sub> Reactions - Zheng .....	39
15 [Ir(ppy) <sub>2</sub> (4,4'-dtb-bpy)]PF <sub>6</sub> Reactions - Knowles .....	40
16 [Ir(ppy) <sub>2</sub> (4,4'-dtb-bpy)]PF <sub>6</sub> Reactions - Yu.....	40
17 [Ir(2',4'-dF-5-CF <sub>3</sub> -ppy) <sub>2</sub> (bpy)]PF <sub>6</sub> Reactions .....	41
18 [Ir(2',4'-dF-5-me-ppy) <sub>2</sub> (4,4'-dtb-bpy)]PF <sub>6</sub> Reactions .....	42
19 [Ir(2',4'-dF-5-CF <sub>3</sub> -ppy) <sub>2</sub> (4,4'-dtb-bpy)]PF <sub>6</sub> Reactions - Stephenson .....	43
20 [Ir(2',4'-dF-5-CF <sub>3</sub> -ppy) <sub>2</sub> (4,4'-dtb-bpy)]PF <sub>6</sub> Reactions - DiRocco .....	43
21 [Ir(2',4'-dF-5-CF <sub>3</sub> -ppy) <sub>2</sub> (4,4'-dtb-bpy)]PF <sub>6</sub> Reactions - MacMillan.....	44
22 [Ir(2',4'-dF-5-CF <sub>3</sub> -ppy) <sub>2</sub> (4,4'-dtb-bpy)]PF <sub>6</sub> Reactions - Yoon.....	44
23 [Ir(3,4'-dm-ppy) <sub>2</sub> (4,4'-dtb-bpy)]PF <sub>6</sub> Reactions .....	45
24 [Ru(bpy) <sub>3</sub> ](PF <sub>6</sub> ) <sub>2</sub> Reactions - Glorius.....	46
25 [Ru(bpy) <sub>3</sub> ](PF <sub>6</sub> ) <sub>2</sub> Reactions - Rueping .....	47
26 [Ru(bpz) <sub>3</sub> ](PF <sub>6</sub> ) <sub>2</sub> Reactions - Zheng.....	47
27 [Ru(bpz) <sub>3</sub> ](PF <sub>6</sub> ) <sub>2</sub> Reactions - Yoon .....	48
28 [Ru(phen) <sub>3</sub> ](PF <sub>6</sub> ) <sub>2</sub> Reactions - Jung & Han.....	49
29 [Ru(phen) <sub>3</sub> ](PF <sub>6</sub> ) <sub>2</sub> Reactions - Cho .....	49
30 [Ru(phen) <sub>3</sub> ](PF <sub>6</sub> ) <sub>2</sub> Reactions - Dolbier.....	49
31 [Ru(4,4'-dm-bpy) <sub>3</sub> ](PF <sub>6</sub> ) <sub>2</sub> Reactions - Gagné.....	50
32 [Ru(4,4'-dtb-bpy) <sub>3</sub> ](PF <sub>6</sub> ) <sub>2</sub> Reactions – Yoon .....	50
33 Strategies to achieve aryl fluorination .....	57

Scheme	Page
34 Effects of aryl hydrogen substituents on the regioselectivity of the S <sub>N</sub> Ar reaction .....	63
35 UV and visible light mediated double bond isomerization.....	132
36 Presumptive Mechanism, Kinetics and Deuterium Incorporation.....	143
37 Testing rates for the supersaturated literature reaction against variable concentrations of photocatalyst.....	215
38a Birch Reduction .....	234
38b This Work .....	234
39 Favoring Reduction.....	234
40 Cleavage of the Boc Protecting Group .....	238
41a Deuteration.....	241
41b KIE.....	241
42 Mechanistic Discussion .....	242
43a THC Fluoroanalog Target.....	243
43b Known Cannabinoid Fluoroanalogs .....	243
44 Deoxygenation.....	244
45 Reduction of the Michael System.....	245
46 Intramolecular Cyclization.....	245

## List of Abbreviations

ArF — fluoroarene

ArH — hydrocarbon arene

BDE — bond dissociation energy

DIPEA — diisopropylethylamine – Hünig's base

GCMS — Gas Chromatography Mass Spectrometry

HDF — hydrodefluorination

HF — Hartree-Fock theory level

HOMO — highest occupied molecular orbital

ISC — Intersystem Crossing

KIE — Kinetic Isotope Effect

LUMO — lowest unoccupied molecular orbital

MP2 — Second Order Møller-Plesset Perturbation Theory Level

NMR — Nuclear Magnetic Resonance

PC — photocatalyst

PCET — Proton Coupled Electron Transfer

PPM — Parts Per Million

PPT — Parts Per Thousand

SAR — Structure Activity Relationship

SET — single electron transfer

SNAr — Nucleophilic aromatic substitution

SNArF — Nucleophilic aromatic substitution of a C–F bond

SOMO — singly occupied molecular orbital

UV — ultraviolet



## CHAPTER I

### HISTORY LEADING TO WORKS HEREIN

#### 1.1 Overview

Over the course of the previous several years, I have endeavored to further several apparently disparate, yet tangentially related frontiers of synthetic chemistry. The areas of interest here are syntheses in visible light photocatalytic transformations for not only the interception of *trans*-cyclohexenes, but also functionalization of carbon fluorine (C–F) bonds, non-photocatalytic C–F functionalization through S<sub>N</sub>Ar.

#### 1.2 Effects of Fluorination in Organic Materials



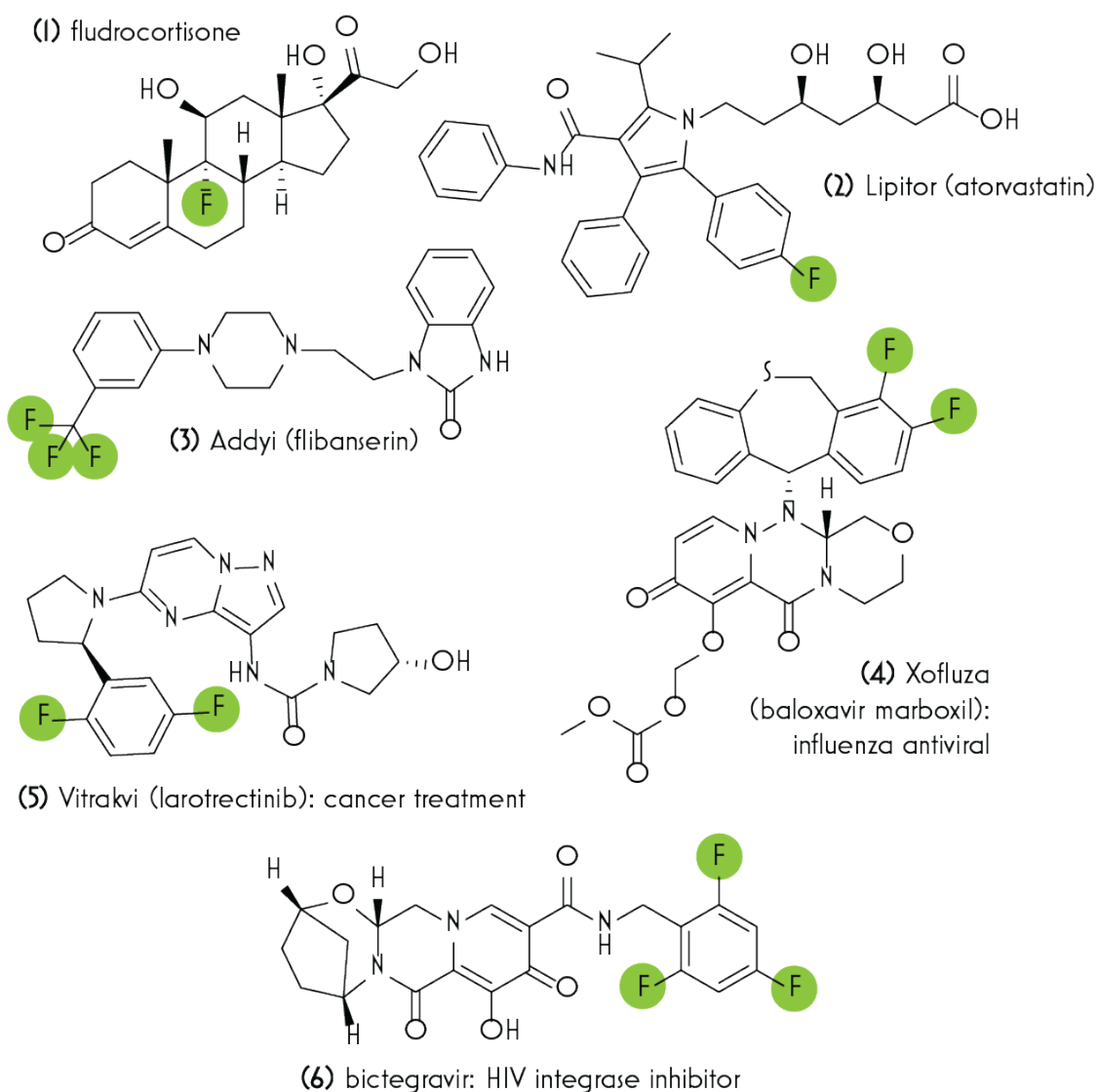
Fluorine is the hungriest element. It is hungry for electrons. This is because it is the most electronegative element.<sup>1</sup> When a fluorine is covalently bonded to a carbon, a C–F bond, something of an unusual situation is created. In comparison to some more common bonds, there are significant differences. Because fluorine is the most electronegative element, it pulls electron density toward itself, withdrawing it from the carbon to which it is attached. In comparison to a more common, electron donating hydrogen, or another carbon, the C–F dipole is inverted with respect to more common bonds. Fluorine is so electronegative, so hungry for electrons, that this hunger is manifested in several ways. For instance, it does not engage in dispersion or van der Waals interactions as readily as the vast majority of other common organic atoms that stem from the ability of bonds to be transiently polarized. Additionally, because of its impressive inductive effect, C–F bonds can substantially modulate the pK<sub>a</sub> for the deprotonation equilibrium of nearby acidic sites. Finally, because of its lone pairs of electrons, it can engage in hydrogen bonding, although only in the absence of other, stronger interactions.

Arguably, the properties that fluorine imparts to the molecules to which it is covalently bonded seem unusual because there are very few C–F bonds in the natural world. There are metabolites<sup>2</sup> derived from fluoroacetate,<sup>3</sup> fluorouracil isolated from a marine sponge *Phakellia fusca*,<sup>4</sup> and  $\omega$ -fluorooleic acid, the major toxin of *Dichapetalum toxicarium*.<sup>5</sup> It may

be at this point that the reader recognizes that these are all toxic, acting as antimetabolites that are recognized by enzymes as the native metabolite, interfering in these system.<sup>6</sup>

It could be speculated that because of this near absence of C–F bonds in the natural world, or perhaps due to the toxicity of the known compounds that contain them, reactions to synthesize natural products containing them were not investigated at the rate of more common bonds.<sup>7</sup> It became apparent, however, that the bioefficacy of molecules containing a C–F bond was intrinsically different than those nonfluorinated counterparts, as is evident in the development of the first drug containing a C–F bond, fludrocortisone (Table 1, structure 1), in the 1950s, which was discovered to be ten times more active as a glucocorticoid and 800 times more active as a mineralocorticoid than the nonfluorinated counterpart.<sup>8</sup>

Table 1: Some Select Fluorinated Molecules

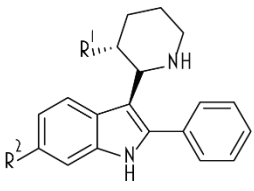


Many fluorinated bioactive molecules have since been discovered, including some of the bestselling and arguably most important pharmaceuticals,<sup>9-18</sup> biological probes,<sup>19-22</sup> and even PET radiotracers.<sup>23</sup> Some important mentions here, with a diverse range of application include atorvastatin (Lipitor) (Table 1, structure 2), a lipid reducing statin drug to prevent heart disease, (3) flibanserin (Addyi) – a sexual dysfunction treatment, (4) baloxavir marboxil (Xofluza) – an influenza antiviral, and (5) larotrectinib (Vitrakvi) – a cancer treatment.

Of the physical properties that fluorine modulates, one that has allowed its use more than many others is that the van der Waals radius of fluorine is small, at 1.47 Å, compared to hydrogen at 1.2 Å and oxygen at 1.52 Å.<sup>24</sup> The 1.340 Å bond length of a Csp<sup>2</sup>-F bond is comparable to the radii of both a C-H (1.09 Å) and a C-O bond (1.43 Å), often allowing a protein to recognize a fluorinated homologue of a hydrocarbon ligand, potentially substituting sterically for either bond in the active sites of proteins. Substituting for another electronegative element such as oxygen is clearly a closer substitution electronically, although as previously stated, such a substitution reduces the number of potential hydrogen bonding donors.<sup>15, 24-27</sup>

Fluorine's effects on pKa can also be substantial, and an interesting interdependence is evident between pKa and bioavailability.<sup>28</sup> As is apparent from an examination of the antipsychotic 2-phenyl-3-piperidinyl indole drugs, significant modulation can be effected through the inclusion of fluorine (Table 2a). For instance, the substitution of R<sup>1</sup> with fluorine instead of hydrogen increases the acidity of the conjugate acid of the piperidine, decreasing the likelihood of observing a molecule in the protonated ammonium form by ca. 2 orders of magnitude. This increases bioavailability substantially. Further fluorination of the indole ring at the R<sup>2</sup> position also increases the bioavailability, although this time the results are a little less straightforward. The argument has been made that aryl fluorination *always* makes a molecule more lipophilic.<sup>29</sup> One could instead make a more convincing

**Table 2a:** Effect of Fluorination on pKa of Conjugate Acid and Relationship to Bioavailability

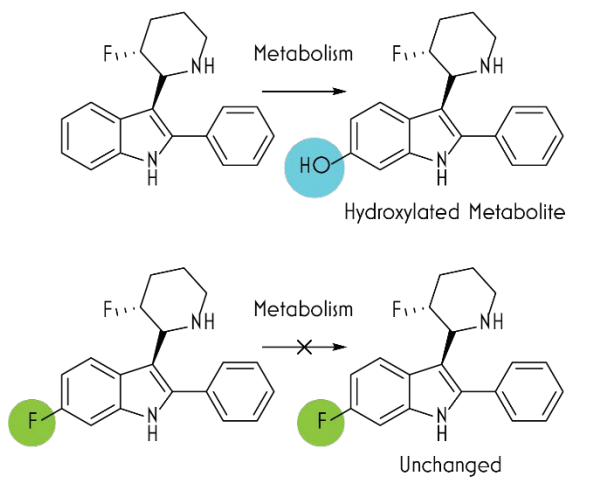


R 1	R 2	pK <sub>aH</sub>	5-HT <sub>2A</sub> <sup>a</sup>	F (%) <sup>b</sup>
H	H	10.4	0.99	poor
F	H	8.5	0.43	18
F	F	-	0.06	80

<sup>a</sup> Affinities at human cloned 5-HT<sub>2A</sub> receptor (nM).

<sup>b</sup> Bioavailability calculated from dosing at 0.5 - 2 mg/kg

**Table 2b:** Metabolic Effects of Fluorination



argument that the “lone pairs” of fluorine align nicely to the  $sp^2$   $\pi$  orbitals of the aryl carbons next door, and while electron density is withdrawn through the C–F  $\sigma$ -bond, it is donated through the  $\pi$  system,<sup>28</sup> analogous to back-bonding in transition metal systems. The net effect of this is that the bond, compared to its hydrocarbon counterpart is significantly less polarizable and therefore less hydrophilic. It is not therefore that the molecule becomes more lipophilic, but certainly it is less hydrophilic. Reduction in the number of hydrophilic regions in a molecule favors the ability to cross the blood-brain barrier,<sup>17, 30</sup> as it allows the easier transition to any lipid rich region, but there is a much better explanation as to why fluorination here improves the bioavailability.

Another important effect of fluorination again is derived from the fact that fluorine is the most electronegative element, and that the nearby electron density, as compared to the nonfluorinated analog, is pulled toward the fluorine. This effect is often used to overcome metabolic destruction. Sometimes, a drug candidate is efficacious in bioassays, but is destroyed metabolically, and still worse, sometimes converted to toxic metabolites that ultimately limit its potential utility. The mechanism of this destruction for lipophilic xenobiotics is often oxidation by the cytochrome p450 family of liver enzymes.<sup>31</sup> In order for this mechanism to be possible, electrons must be available for the molecule to be oxidized. As a strategy to alleviate destruction and subsequent excretion of a bioactive compound, a carbon that is susceptible to oxidation may be fluorinated (Table 2b). This fluorination removes the susceptibility of these electrons by not only relocating the electron density to less susceptible locations, but also blocking the position of oxidation with a nonhydrophilic functional group.

In summation, fluorination provides several ways to tune or modulate the properties of a molecule. Despite this usefulness for the synthetic chemist, fluorination strategies rely predominantly on linear installation of fluorine at the desired positions. For reasons described below, this is challenging and has limited the application of organofluorines.

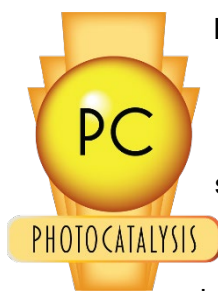
### 1.3 Approaches to Synthesis of Fluorinated Molecules

While methods for fluorination of aliphatic positions exist,<sup>32-34</sup> they are beyond the scope of this thesis. This thesis instead will focus on aromatic C–F bonds. Historically, installation of fluorine has been a laborious process with poor functional group tolerance, relying on diazotization followed by fluorination in a Balz-Schiemann reaction sequence, or perchlorination followed by a halogen exchange (HALEX) reaction to replace the chlorines with fluorines through  $S_NAr$ .<sup>35</sup> As can be expected, there has been significant recent work in fluorination strategies, typically relying on prefunctionalization,<sup>33, 36-41</sup> or directing group modulated C–H fluorination.<sup>42</sup> In recent years, it has been a central goal of the Weaver group to effect a fundamental inversion of fluorination strategy. Rather than installing fluorines one-by-one onto molecules, the Weaver lab has furthered the concept developed by others<sup>43-47</sup> of starting with materials that are fluorinated everywhere, which is relatively straightforward to accomplish on an industrial scale,<sup>48</sup> and then decrease the fluorine content through reduction to hydrogen or substitution to another functional group under mild, functional group tolerant conditions.

Some methods existed previously and have been developed since to approach reductions in the number of fluorines in a molecule, and especially pertinent to this discussion are fluoroaryl reactions. Of these methods, arguably some of the most promising for defluorination are transition metal catalyses involving oxidative metal insertions into the C–F bond,<sup>49-50</sup> Unfortunately these transformations typically suffer from difficulties of insertion of the transition metal into the remarkably strong C–F bond through oxidative addition (145 kcal/mol for homolytic cleavage of a C–F bond in C<sub>6</sub>F<sub>6</sub><sup>51</sup>), and poor (if any) turnover due to the formation of strong metal–fluorine bond, and catalysis therefore remains difficult. Some promise has been shown in reactions with hydridic metal complexes.<sup>52-56</sup> These methods are frequently sensitive to atmospheric water, and must be performed under Schlenk techniques or in a glovebox, limiting their ultimate utility.

Historic approaches to reduction in fluorine content have included metal reductions, which suffer from poor functional group tolerances, and frequently overreduction to complex mixtures of perturbations of polydefluorinated products, cyclohexadienes, and cyclohexenes.<sup>51, 57</sup> In these reactions, a solvated electron in ammonia solvent is transferred to the LUMO of a fluoroarene, generating a radical anion which subsequently fragments to give an aryl radical and an anion – fluoride. The aryl radical is typically further reduced to the aryl anion. Mechanistically, these reactions operate through a very important single electron transfer (SET), which was coming to prominence in the 1990s and 2000s in photocatalytic reactions popularized by the newly minted chemists such as Yoon,<sup>58</sup> and later with chemists such as MacMillan<sup>59</sup> and Stephenson.<sup>60</sup> It is the obvious next step to combine these two disparate ideas, providing a tractable approach to accomplish hydrodefluorination under milder conditions.

## 1.4 Photocatalysis



Photocatalysis is a subset of photochemistry, a method of synthesis in which a sub-stoichiometric photocatalyst (PC)

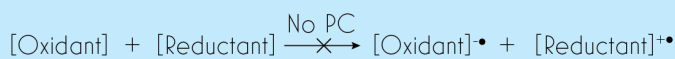
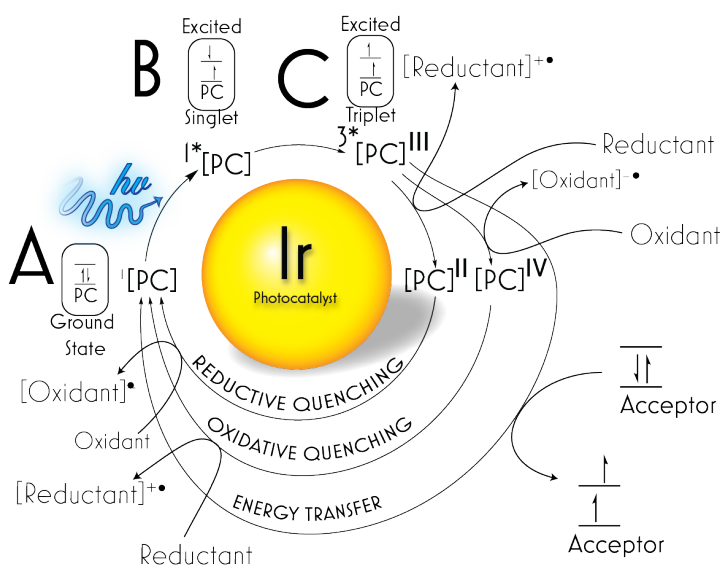
molecule, which absorbs light at a wavelength the substrate does not. Absorption of a photon facilitates the transformation through excitation of PC electrons to an excited electronic state.

Quenching of the excited PC is possible through a number of potential mechanisms that allow its return to the ground state, but usually involve the substrate. In other words, it is a way of engaging molecules in photochemistry by using a sensitizer to excite them indirectly. Photocatalysis and similar processes have been in practice

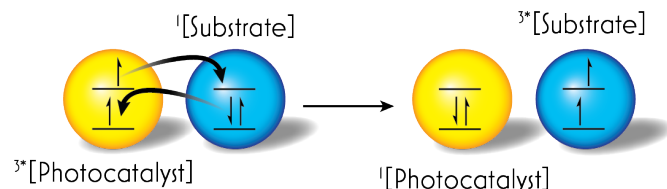
for a long time,<sup>61-64</sup> although it has only recently come into synthetic prominence because of the advantageous nature of advancements such as moving into the visible light range, where the difficulties inherent in using higher energy light are abated (see more on this below).<sup>65-66</sup> Many photocatalysts have been used, including organic dyes,<sup>67-68</sup> nanomaterials<sup>69</sup> and organometallic complexes.<sup>70-71</sup> For the sake of this brevity, only the organometallic complexes will be discussed, although there is a brief discussion of some organic sensitizers in the next section, 1.41.

Organometallic PCs are typically iridium or ruthenium centered, coordinatively saturated 18-electron complexes that absorb photons in the visible light region (Figure 1a). This allows electronic excitation of a HOMO electron to the LUMO orbital (Figure 1a, structure A to B). This singlet excited state then experiences an inter-system crossing event (B to C), in which the SOMO electron spin-flips, so that the molecule experiences a triplet excited state. As this triplet excited state is spin-forbidden to return to ground state, the triplet excited state is exceptionally long lived, yet high energy. The energy of this excited photocatalyst can be harnessed in three ways. It can undergo redox chemistry, either acting as an oxidant or as a reductant through SET or through an energy transfer process to complete the cycle. This energy transfer, because it originates from a triplet state, can be certainly described as a

**Figure 1a:** Photocatalyst Quenching Pathways

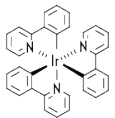
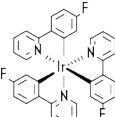
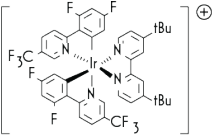
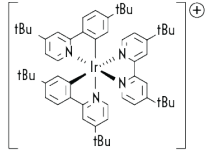


**Figure 1b:** Dexter Energy Transfer Mechanism



Dexter energy transfer mechanism.<sup>72</sup> A Dexter energy transfer mechanism is one in which electrons switch places from a donor (in this case, the PC), to an acceptor (in this case, the substrate), so that the triplet state is transferred from the PC to the substrate, and the PC is returned to ground state (Figure 1b). Each of these quenching mechanisms can come into play in different reactions, as will be shown. The energies related to these processes depend on various factors, including the identity of the metal and the ligands, and how much these structures stabilize the intermediate states along the catalytic cycle. For those PCs discussed herein, the energies and other select physical properties are displayed in Table 3.<sup>72-75</sup>

Table 3: Select Photocatalyst Physical Attributes

	radius <sup>a</sup> (Å)	E <sub>emis.</sub> (kcal/mol)	λ <sub>max</sub> excitation (nm)	λ <sub>max</sub> emission (nm)	E <sub>1/2</sub> Ox (V)	E <sub>1/2</sub> Red (V)	E <sub>1/2</sub> Ir <sup>II</sup> /Ir <sup>*</sup> (V)	E <sub>1/2</sub> Ir <sup>*</sup> /Ir <sup>IV</sup> (V)	τ (ns)
 fac-Ir(ppy) <sub>3</sub>	4.5	55.2	375	518	0.78	-2.20	-1.73	0.31	1900
 fac-Ir(4-F-ppy) <sub>3</sub>	4.57	58.6	380	488	0.955	-2.18	-1.905	0.685	2040
 Ir(dFCF <sub>3</sub> ppy) <sub>2</sub> dtbbpy PF <sub>6</sub>	5.02	60.1	380	470	1.69	-1.37	-0.89	1.21	2300
 Ir(dtbbpy) <sub>2</sub> dtbbpy PF <sub>6</sub>	N/A	49.4	N/A	583	1.13	N/A	-1.04	N/A	444

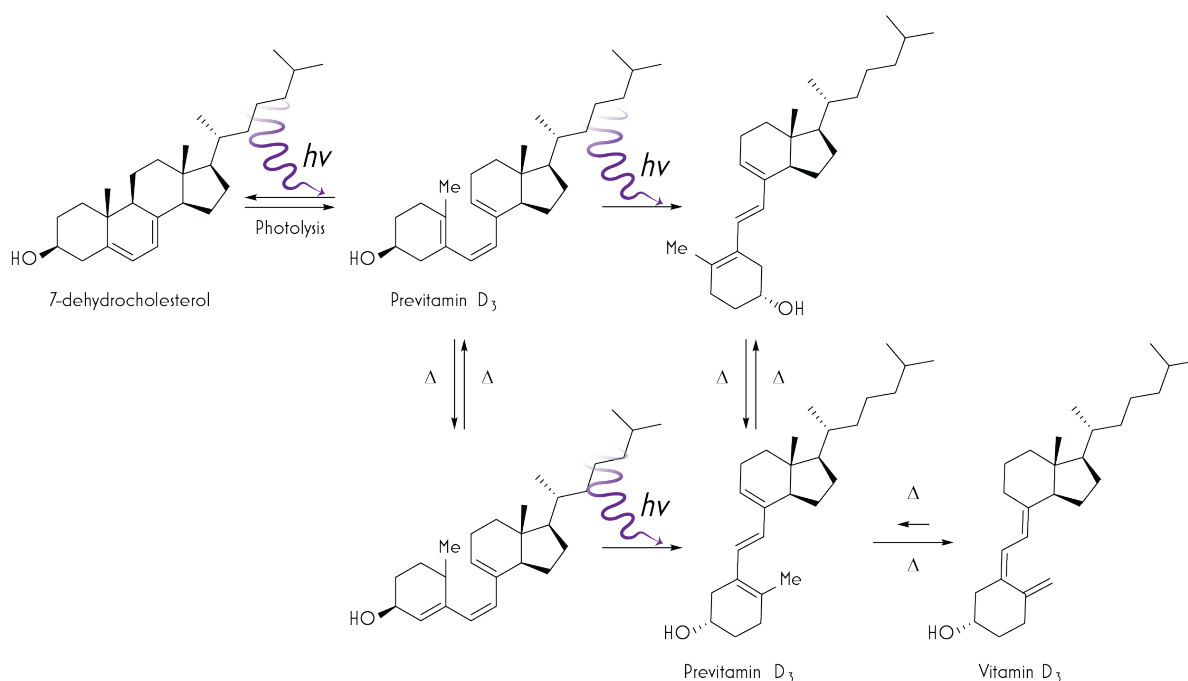
<sup>a</sup> Radius approximated as a sphere.

## 1.41 Photochemical Isomerization in Nature



Several photochemical isomerizations of alkenes are at work in the natural world. These photochemical isomerizations allow otherwise insurmountable thermal barriers to be overcome. For instance, one of these is the formation of vitamin D. Much work has been invested in the understanding the photon mediated formation of vitamin D.<sup>76-77</sup> Following penetration of a UV photon through human skin, provitamin D<sub>3</sub> (7-dehydrocholesterol) absorbs a photon and is photolyzed to previtamin D<sub>3</sub>. Previtamin D<sub>3</sub> can isomerize to vitamin D<sub>3</sub> (Scheme 1). This isomerization has been the subject of multiple investigations and has been characterized as taking place through a “hula-twist” mechanism, in which a molecule isomerizes around both an alkene and a conformationally restricted  $\sigma$  bond.<sup>78-79</sup> Additionally, a number of photosensing proteins, exist in the natural world, with chromophores such as the tetrapyrrole phytychromobilin, the polyenes retinal as in the rhodopsin protein, and coumaric acid all undergoing photochemical isomerization in the course of photosensing.<sup>80</sup> This isomerization typically initiates the transformation of the protein to a signaling state of which communicates photon absorption to a downstream signal transduction partner.

**Scheme 1:** “Hula-Twist” Photolysis and Photoisomerization in Humans at 290–315 nm



## 1.42 History of Photochemical Isomerization

Photochemical isomerization of alkenes has been known for a very long time.<sup>81-82</sup> In systems such as stilbenes, it has been recognized that excitation by absorption of a photon produces



a photoexcited state, in which excitation by a photon moves the molecule to a different energy landscape through electronic promotion. Although singlet excitations can occur and lead to isomerization,<sup>83</sup> as can electron transfer mediated isomerizations,<sup>84</sup> they are beyond the scope of this discussion. In the case of mechanisms that operate in a triplet excited state, either directly or *via* sensitization, the molecule can geometrically rearrange, overcoming thermal barriers that are otherwise insurmountably high. In the case of stilbenes, this excitation allows a molecule to change from a *Z*-conformation about the double bond to an *E*-conformation, or the other way around as well. Further investigations showed that preferential excitation of the *E* stilbene was possible, affecting an overall isomerization of the *E* stilbene to the higher energy ground state *Z*. It has been observed for decades that UV absorbing chromophores could act as triplet photosensitizers for indirect photoisomerization (Table 4),<sup>85-87</sup> exciting the substrate into a triplet energy landscape wherein formerly bonding alkene electrons repel each other and can then rotate about the C–C sigma bond either into an *E*- or *Z*-conformation.<sup>88-89</sup>

**Table 4:** Some Organic Triplet Sensitizers

Sensitizer	Triplet Energy [kcal/mol]
Acetone	79-82
Simple Olefins	78-82
p-Xylene	80.4
Acetophenone	74.1
Xanthone	74
Benzophenone	69.2
Triphenylene	66.5
Acetonaphthone	59.4
Conjugated Dienes	58-60
Eosin Y	43.6
Methylene Blue	33.3
$^1\Delta_gO_2$	22

### 1.43 History of E/Z Specific Synthesis

While it is an attractive approach to synthesize the *Z*-stereoisomers through formation of the more readily produced *E*-isomer and then isomerize it, UV light is typically too energetic to be useful for building starting materials and therefore leads to the degradation of many functional groups and motifs, selectivity for the higher energy *Z*-isomer of alkenes has been approached historically through diastereoselective olefin synthesis. Several common approaches will be laid out in the following paragraphs, including partial hydrogenation of an alkyne over a poisoned Lindlar's catalyst, alkynyl hydroboration, Wittig olefination, and alkene metathesis.

The most classic approach is the partial hydrogenation over a Lindlar catalyst–palladium on calcium carbonate, which has been poisoned with either sulfur, lead,<sup>90-92</sup> or ethylene diamine.<sup>93</sup> Since hydrogenation over palladium always takes place in a *syn* fashion, and the Lindlar catalyst is poisoned so that hydrogenation of alkynes takes place but the hydrogenation of alkenes does not, the single *syn*-addition of a molecular hydrogen molecule to the alkyne results in only the *Z*-isomer of the resultant alkene. While the reaction has seen substantial use, it is not particularly functional group tolerant, and multistep syntheses including it often involves protection/deprotection steps also.

Similarly, hydroboration of alkynes can give access exclusively to *Z*-isomers, as mechanistically the addition occurs *syn*.<sup>94</sup> This would go unnoticed in a standard hydroboration/oxidation reaction, however, because formation of the enol tautomerizes to the corresponding carbonyl, ablative of the stereochemical outcome since rotation about the

former double bonded carbons is permitted upon tautomerization. Therefore, in order to affect a Z-alkene, the intermediate borylated material must be intercepted or undergo proteodeboronation. Interception to make materials that may be further derivatized can be accomplished through halogenation of the intermediate borylated alkene followed by basic elimination to yield a Z-alkenyl bromide<sup>95</sup> or an E-alkenyl iodide, the difference in stereoisomers arising from a trans elimination of a dibrominated alkane intermediate in the case of the former, and a proposed formation of the hypoiodous acid followed by cis elimination of the boron in the case of the iodination.<sup>96</sup> Additional recent work has permitted the Z-borylated material to be produced in good yields from terminal alkynes, which can then be engaged in cross-couplings such as the Suzuki-Miyaura reaction to produce Z-alkenes.<sup>97</sup> Of course, in these multistep reactions, in order to use these reactions, more complex substrates must be insensitive to each reaction condition, or be protected/deprotected in an orthogonal manner, adding synthetic steps.

Additionally, olefination of aldehydes with phosphonium ylides, the classical Wittig reaction, can be harnessed to favor the formation of Z-stereoisomers.<sup>98-99</sup> For many circumstances, this approach can be advantageous. However, situations in which this reaction could be expected to be less than stellar are those in which other positions are sensitive either to base or to nucleophilic attack.

There are other, more modern methods to make Z-stereoisomers of acyclic alkenes, especially the use of Grubbs/Chauvin/Schrock<sup>100</sup> style olefin metathesis, with significant contributions provided by Hoveyda and many others.<sup>101-102</sup>

Typically, these reactions derive Z-selectivity through steric hindrance of catalyst ligands on the catalyst forcing the substrate constituents into the same direction (Scheme 2).

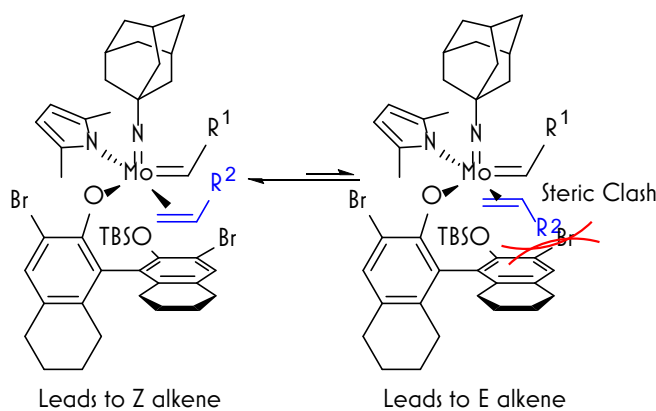
This method has been exceptional in facilitating syntheses, being

incorporated in a number of total syntheses of natural products, such as epothilone C, nakadomarin A, (+)-neopeltolide, (-)-disorazole C<sub>1</sub>, and mytilipin A.<sup>102</sup> While enabling, this methodology still requires an indirect, and somewhat circuitous route to building a Z-alkene.

#### 1.44 History of E to Z Isomerization in the Weaver Lab

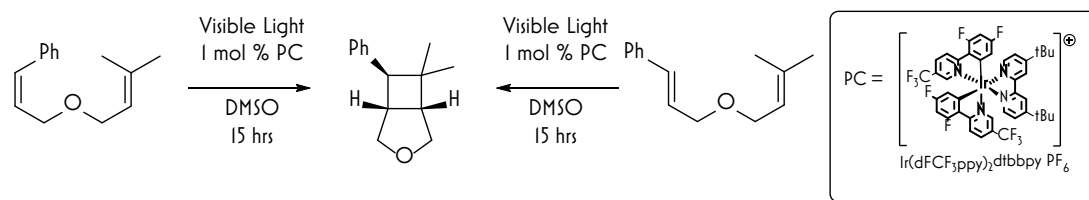
Setting the stage for the Weaver lab investigation of isomerizations of acyclic alkenyl systems beginning in 2014,<sup>103</sup> it is important to frame the reaction in light of a paper that had been released by Yoon in 2012.<sup>104</sup> In Yoon's paper, it was noted that during the exploration of scope, that a photoisomerization was occurring, such that the isomerization of styrenyl portion of the substrates occurred more rapidly than the [2+2] reaction that was being

**Scheme 2:** Schrock, Hoveyda Z Selective Alkene Metathesis Catalyst



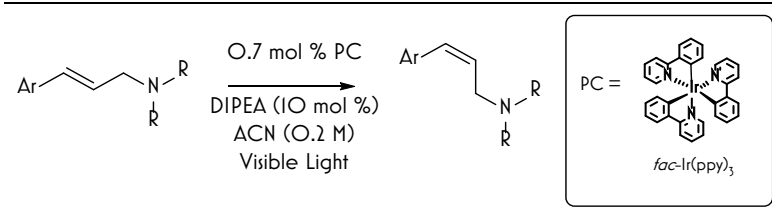
studied. Because the resultant product likely arose from a common triplet biradical intermediate beginning from either *E* or *Z* stereoisomers the process was stereoconvergent, (Scheme 3).

**Scheme 3:** Stereoconvergence discovered in Lu & Yoon, 2012. *Angewandte Chemie Int. Ed.*, 51, 10329.



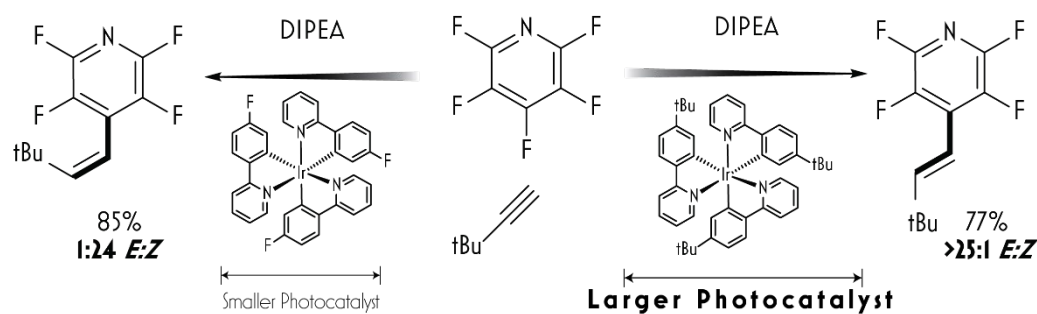
During investigation of olefins derived from cinnamyl systems, aryl prop-2-ene amines, it was discovered that in the presence of a photocatalyst and visible light, over time the reaction mixture coalesced toward almost exclusively the higher energy *Z*-isomer. This is significant, because of several reasons. For one, this method allows direct synthetic access to *Z*-acyclic alkenes *via* isomerization of the lower energy and more accessible *E*-stereoisomer. Further, it allows the reaction to take place under very mild conditions, whereas previously such reactivity was only known to take place under UV irradiation. For another reason, this reaction took place in the absence of a terminal reductant, yet was observed not to proceed to complete conversion without a catalytic amount of tertiary amine, DIPEA (Scheme 4).

**Scheme 4:** E to Z Photoisomerization in the Weaver Lab



At the same time, it was recognized in the field that with many photocatalysts, both triplet sensitization and SET were taking place. In order to sort out SET reactions mechanisms and energy transfer mechanisms, an additional investigation was initiated in the Weaver lab. Since it had been demonstrated that the photocatalytically generated fluoroaryl radical could intercept alkynes to generate alkenes, but yet the ability of the photocatalyst to act as a triplet sensitizer resulted in preferential formation of the *Z* stereoisomer of the product, as although the *E* was formed as both kinetic and thermodynamic stereoisomer, the propensity for isomerization was high enough that it was converted to the *Z*. It was shown that because the radius of the photocatalyst could be modified via ligand modification, selectivity could be achieved for only a SET mechanism or both a SET mechanism and a Dexter energy transfer mechanism (Scheme 5).

### Scheme 5: Photocatalysts Size Matters for Isomerization



Historically speaking, investigations of photoisomerizations were eventually conducted with cyclic, rather than acyclic alkenes. These systems also isomerize, but at first it was evident only in larger, less strained *trans*-cycloalkenes. Cycloalkenes can be isomerized from the *Z(cis)*- (lower energy system) to the *E(trans)*- (strained system) by UV photolysis, and for rings of 7 carbons or larger, they either are isolable,<sup>105-107</sup> or at least readily observable<sup>108-109</sup> through cuprous trapping. Evidence for *E(trans)*-cyclohexene was less forthcoming, however, presumably due to its calculated high strain (*ca.* 52 kcal/mol), this high energy would correspond to a short lifetime.

Much research was devoted to providing evidence of its existence.<sup>110</sup> During high speed pulsed photolysis experiments,<sup>111-112</sup> it was reported that researchers had observed a short lived species with a 9  $\mu$ s lifetime. It was determined that the intermediate had a *ca.* 7.5 kcal/mol barrier to isomerization back to the lower energy *Z*-isomer.

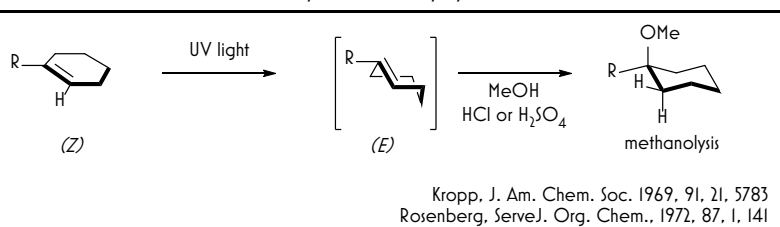
While irradiation with UV light led to multiple products, it has also been shown that if excited in acidic methanol, the *E*-phenylcyclohexene underwent methanolysis of the olefin<sup>109, 113-114</sup> (Scheme 6a). Additionally, Schuster<sup>115</sup> proposed a similar intermediate for the rearrangement of cyclohexenones. Further studies from the McClelland group with UV flash photolysis have demonstrated the presence of a transient cationic intermediate, which in some cases could be intercepted with a solvent.<sup>116</sup> Importantly, these precedents demonstrate the differential reactivity between the *Z(cis)*- and *E(trans)*-cyclohexenes, and the potential for productive syntheses because it loads strain energy into a bond, which then very much wants to release, and in doing so has the potential to drive chemical processes that we would otherwise not anticipate to be feasible.

The *release* of strain energy to facilitate chemical synthesis includes standouts (Scheme 6b) such as Danishefsky's work with cyclobutenone and cyclopentadiene [4+2] cycloadducts,<sup>117-119</sup> that of Garg with cycloarynes,<sup>120-122</sup> or that of Fox in which *trans* cyclooctenes react with tetrazines,<sup>123</sup> though there are many others.<sup>124-128</sup> The common feature in all of these systems is a distortion from typical bond geometries, which serves as not only a driving force, but also by the same reasoning often accelerates the subsequent reactions.

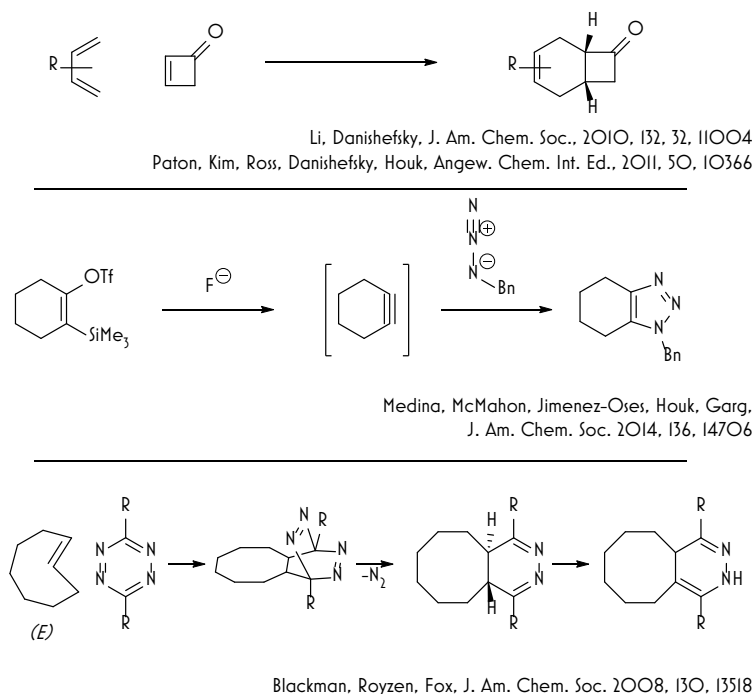
Despite these compelling early results, while larger *E*-cycloalkenes have been deployed in synthesis,<sup>129-130</sup> prior to the work presented herein, the application of *E*-cyclohexene in synthesis was almost non-existent, with the exception of the recent report from the Larionov group<sup>131</sup> of an exploitation of UV light mediated carboborative ring contraction. This sparsity is likely due, in part, to the use of UV light and historically strongly acidic conditions, such as with H<sub>2</sub>SO<sub>4</sub>,<sup>114</sup> which limit the functional group tolerance. A more challenging aspect in performing synthesis, however, is contending with the small energetic barrier to isomerization (*ca.* 7.5 kcal/mol). This barrier means that the

corresponding high energy *E*-cyclohexene does not have a long lifetime, and therefore interception of the species for productive synthesis must be more rapid. Further, while this was recognized as a novel, highly unusual transformation, its synthetic utility was limited by the requirement for the use of UV light either to directly excite the species, or through the use of an organic photosensitizer. Investigations into the use of organometallic triplet sensitizers which absorbed in the lower energy visible light range were sparse and centered on excited-state chemistry.<sup>132-133</sup> Chapter III examines the use of visible light generated cyclohexenes for synthesis.

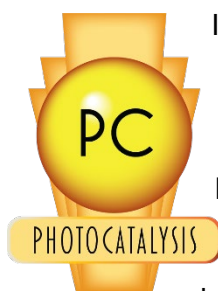
**Scheme 6a:** UV Mediated Solvolysis of *E*-Phenylcyclohexene



**Scheme 6b:** Strain Release in Synthesis

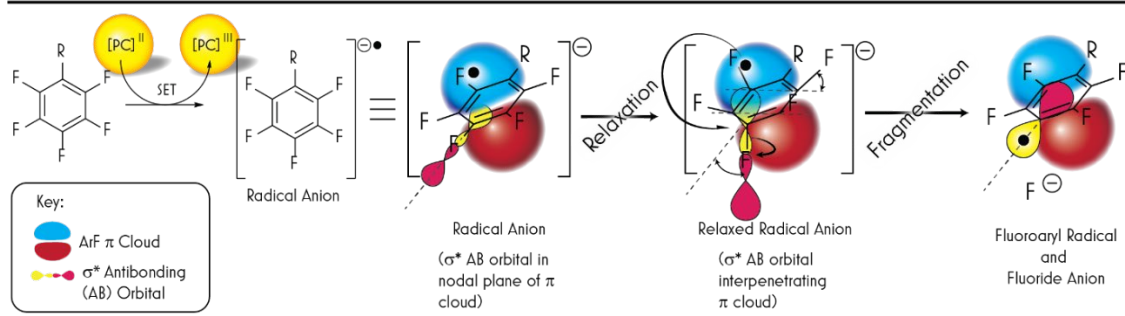


## 1.45 Photocatalytic Hydrodefluorination



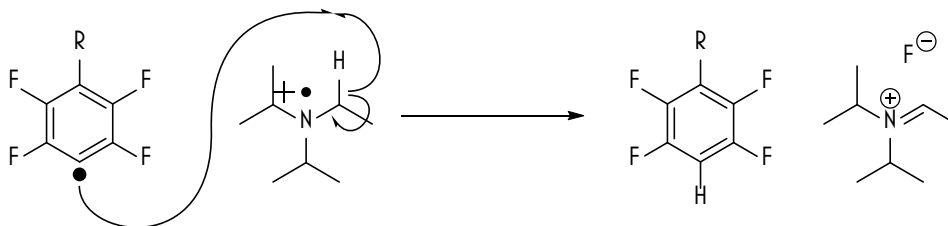
In the case of polyfluorinated arenes, the low-lying LUMO resulting from inductive stabilization of the  $\pi$  system by fluorines provides a place for which an electron can be placed *via* the reductive quenching pathway for some of the most common iridium based photocatalysts such as *fac*-tris[2-phenylpyridinato- $C^2,N$ ]iridium(III), Ir(ppy)<sub>3</sub>. This process allows for the fragmentation of a remarkably strong C–F bond (145 kcal/mol for C<sub>6</sub>F<sub>6</sub>)<sup>51</sup> Following excitation by visible light, the excited triplet PC accepts an electron from a sacrificial reductant, often in the Weaver lab being diisopropylethylamine (DIPEA,  $E_{ox}$  ca. 0.5 V vs. SCE<sup>134</sup>), and subsequently passes that electron on to a fluoroarene (ArF) (Table 1). This results in a fluoroaryl radical anion, which being a 7-electron system, is no longer aromatic. The nonaromatic fluoroaryl radical anion can then achieve a lower energy state by decreasing its rigidity, enjoying a steric decompression by moving fluorines out of the plane of the ring.<sup>135</sup> This decompressive relaxation allows the antibonding orbital of the C–F bond to jut abruptly into the  $\pi^*$ -like antibonding orbital, allowing what was previously a symmetry forbidden transformation to become allowed. As the radical populates the antibonding (AB) orbital, the C–F bond is weakened, and it fragments such that a fluoride leaves, and a radical occupies a p orbital in the position formerly occupied by the C–F bond, a mesolytic fragmentation (Scheme 7).<sup>51</sup>

**Scheme 7:** Mesolytic Fragmentation of a C–F Bond



This fluoroaryl radical is a high energy species, as is indirectly evidenced by the homolytic bond dissociation energy (BDE) of the corresponding C–H bond (114 kcal/mol for pentafluorobenzene).<sup>136</sup> Following a photocatalytic cycle such as this with DIPEA as the sacrificial reductant, the amine is oxidized to a radical cation. This amine radical cation has a significantly weakened  $\alpha$ -C–H bond at the position alpha to the nitrogen, at BDE ca. 42 kcal/mol as the radical cation,<sup>137-138</sup> (compared to ca. 90 kcal/mol as the neutral amine) presumably due to the formation of an iminium cation upon abstraction by the fluoroaryl radical which can form a salt with the fluoride anion previously produced, overall forming a hydrodefluorinated arene (Scheme 8).<sup>139</sup> It is important to note too that HAT is possible also from the neutral amine.

**Scheme 8:** Fluoroaryl Radical Abstraction of an H-atom leads to HDF

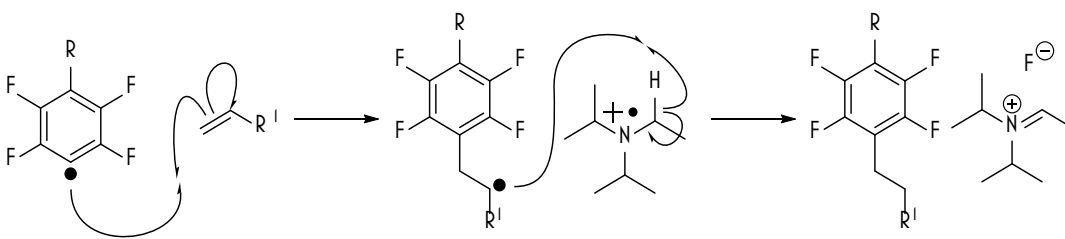


The generation of a fluoroaryl radical provided the possibility for it to be intercepted with another molecule, forming another bond instead of simply reducing the C–F bond to a C–H bond.

### 1.5 Other Photocatalytic C–F Functionalizations

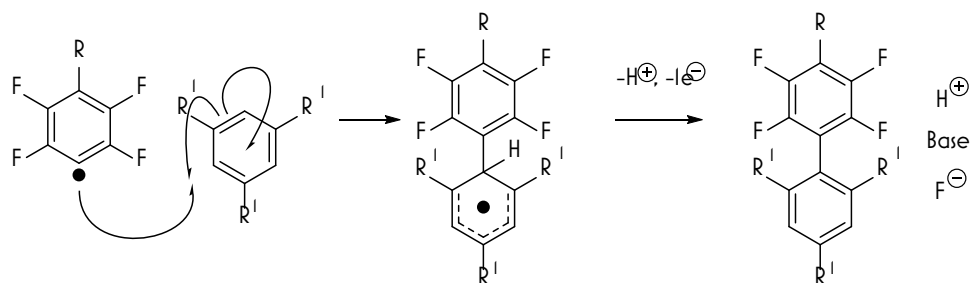
As is commonly taught in undergraduate organic chemistry courses, radical reactions take place with olefins. Radicals and olefins are friends. They get along famously.<sup>140</sup> It too is reasonable to expect that a fluoroaryl radical should do the same, and as has been shown repeatedly, it does.<sup>141-144</sup> Following generation of a fluoroaryl radical, as above in the hydrodefluorination, alkylations operate in much the same way, up to the point of mesolytic fragmentation. The likely mechanism diverges at that point. In this situation, the fluoroaryl radical couples with the olefin, (Scheme 9) resulting in a secondary radical which is subsequently quenched *via* HAT analogously to formation of the HDF product in Scheme 2. In this reaction, the caveat is that the rate of addition of the fluoroaryl radical must exceed the rate of abstraction of the H atom from the amine or amine radical cation, or the reaction will produce the HDF product instead of the alkylated product. This unintended side product is a consistently appearing contaminant in many photocatalytic reactions.

**Scheme 9:** Fluoroaryl Radical Alkylation



Similarly to reactions with  $sp^2$  hybridized olefin alkylations, reactions with aryl  $sp^2$  centers also work analogously. Rather than terminating with an HAT from an amine or an amine radical cation, following an addition to a hydrocarbon arene (ArH) (Scheme 10), the reaction terminates either with an HAT event to an unknown H-atom acceptor, or with a deprotonation. Given that the reaction operates better in the presence of  $K_2CO_3$ , it seems reasonable that deprotonation is the operative mechanism. Chapter V examines alternative reaction pathways for the presumed intermediate in this reaction.

### Scheme 10: Fluoroaryl Radical Arylation



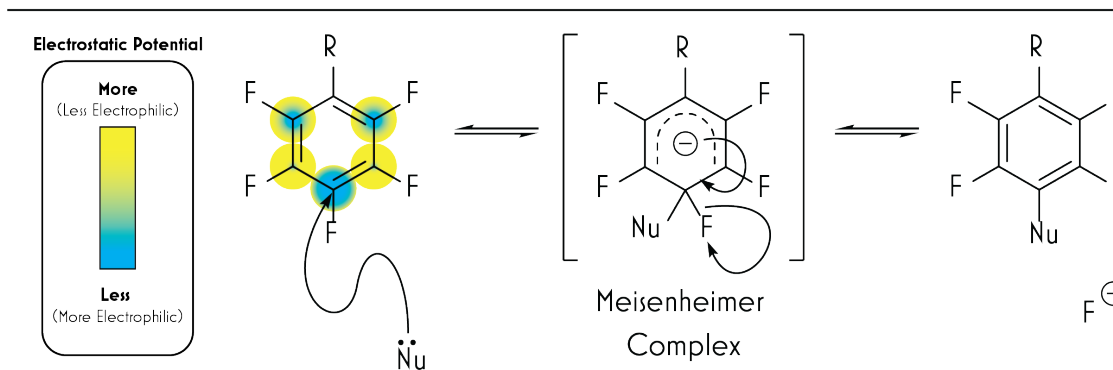
### 1.6 History of $S_NArF$



Nucleophilic aromatic substitution of a C–F bond ( $S_NArF$ ) can be viewed as a C–F functionalization as well, although obviously not a photocatalytic mechanism. It can, however serve as a complementary technique to some of the other technologies presented here. Mechanistically, a  $S_NAr$  reaction proceeds as a nucleophile attacks an electrophilic position on an aryl group (Scheme 11). Following the attack of the nucleophile, a tetrahedral intermediate, known variously as the Jackson-Meisenheimer intermediate, Meisenheimer intermediate,  $\sigma$ -intermediate, or all perturbations of this phraseology, but with “complex” instead of “intermediate.” For a long time, the belief that the mechanism for  $S_NAr$  reactions had been well established, with the intermediate Jackson-Meisenheimer complex having even been isolated and as salts in 1900 with further evidence reaching the literature in 1902.<sup>145</sup> By 1982, over 300  $^1H$  spectra had been published of these complexes. Although it was expected that the vast majority of these reactions operate through the stepwise mechanism depicted in Scheme 11, reports<sup>146</sup> have reached the literature of some, or as some authors propose, most<sup>147</sup>  $S_NAr$  reactions proceeding through a concerted reaction mechanism, forgoing the formation of such a complex entirely.<sup>148</sup> As the reactions presented herein have slower leaving groups (fluoride) and electron withdrawing groups (additional fluorines and electron withdrawing functional groups), it is reasonable to expect that the reactions proceed through a well-defined Meisenheimer complex because the electron withdrawing nature of the substituents certainly stabilizes the buildup of a negative charge, and therefore such an anionic intermediate could be expected to be significantly lower in energy than the transition states on either side of it.<sup>147</sup>



## Scheme II: Classic Stepwise S<sub>N</sub>ArF Mechanism



A number of leaving groups have been employed in S<sub>N</sub>Ar reactions, and their effect on otherwise identical reaction conditions can be ranked order of relative reaction rate of  $\text{F} > \text{Cl} \approx \text{Br} > \text{I}$ .<sup>149</sup> This is often held as evidence for a mechanism in which the addition of the nucleophile to the carbon at which the substitution is occurring is the rate determining step, the rate of which is increased by not only by the reduction in steric hindrance of the carbon by a smaller halogen, but also in an increased electrophilicity, a consequence of the electronegativity.<sup>150-151</sup>

Insofar as the selectivity of the reaction, multiple additions can occur if there are multiple sites that can be substituted, and in fact, this is one of the primary ways of forming the perfluorinated starting materials that often appear in this thesis, through the forced S<sub>N</sub>ArCl with a fluorine source through the HALEX process.<sup>35, 48</sup> The first addition typically occurs at the most electropositive position (Scheme 11) first (all other parameters being equal), and then subsequent reactions occur at the next most electropositive position. With perhalogenated, and especially perfluorinated materials, as is the focus of this work, many investigations have been undertaken in order to understand where substitution will occur and why. In the case of pentafluoropyridine, the substitution occurs primarily at the 4 position, and secondary additions can occur,<sup>152-153</sup> which can be influenced by a number of parameters. Selectivity for the desired number of additions can be achieved by lowering the temperature at which the reaction takes place, controlling the amount of nucleophile, and including additives which modify the energetics of the fragmenting halide.<sup>152, 154</sup>

### 1.7 References

1. Pauling, L., *J. Am. Chem. Soc.* **1932**, *54*, 3570.
2. Murphy, C. D.; Schaffrath, C.; O'Hagan, D., Fluorinated natural products: the biosynthesis of fluoroacetate and 4-fluorothreonine in *Streptomyces cattleya*. *Chemosphere* **2003**, *52* (2), 455-461.
3. Harper, D. B.; O'Hagan, D., *Nat. Prod. Rep* **1994**, *11*, 123.
4. Xu, X.-H.; Yao, G.-M.; Li, Y.-M.; Lu, J.-H.; Lin, C.-J.; Wang, X.; Kong, C.-H., 5-Fluorouracil derivatives from the sponge *Phakellia fusca*. *J. Nat. Prod.* **2003**, *66*, 285.
5. Tosaki, A.; Hearse, D. J., Fluoro-fatty acids and the impairment of cardiac function in the rat in vivo and in vitro. *Basic Res. Cardiol.* **1988**, (83), 158.
6. Welch, J. T., *Tetrahedron* **1987**, (43), 3123.
7. Gribble, G. W. In *Naturally occurring organofluorines*, Springer: 2002; pp 121-136.

8. Wang, J.; Sanchez-Rosello, M.; Acena, J. L.; del Pozo, C.; Sorochinsky, A. E.; Fustero, S.; Soloshonok, V. A.; Liu, H., Fluorine in pharmaceutical industry: fluorine-containing drugs introduced to the market in the last decade (2001-2011). *Chem Rev* **2014**, *114* (4), 2432-506.
9. Ismail, F. M. D., Important fluorinated drugs in experimental and clinical use. *J. Fluorine Chem.* **2002**, *118* (1), 27-33.
10. Böhm, H.-J.; Banner, D.; Bendels, S.; Kansy, M.; Kuhn, B.; Müller, K.; Obst-Sander, U.; Stahl, M., Fluorine in Medicinal Chemistry. **2004**, *5* (5), 637-643.
11. Isanbor, C.; O'Hagan, D., Fluorine in medicinal chemistry: A review of anti-cancer agents. *J. Fluorine Chem.* **2006**, *127* (3), 303-319.
12. Kirk, K. L., Fluorine in medicinal chemistry: Recent therapeutic applications of fluorinated small molecules. *J. Fluorine Chem.* **2006**, *127* (8), 1013-1029.
13. Morgenthaler, M.; Schweizer, E.; Hoffmann-Röder, A.; Benini, F.; Martin, R. E.; Jaeschke, G.; Wagner, B.; Fischer, H.; Bendels, S.; Zimmerli, D.; Schneider, J.; Diederich, F.; Kansy, M.; Müller, K., Predicting and Tuning Physicochemical Properties in Lead Optimization: Amine Basicities. **2007**, *2* (8), 1100-1115.
14. Müller, K.; Faeh, C.; Diederich, F., *Science* **2007**, *317*, 1881.
15. Kirk, K. L., Fluorination in Medicinal Chemistry: Methods, Strategies, and Recent Developments. *Organic Process Research & Development* **2008**, *12* (2), 305-321.
16. Hagmann, W. K., *J. Med. Chem.* **2008**, *51*, 4359.
17. Purser, S.; Moore, P. R.; Swallow, S.; Gouverneur, V., Fluorine in medicinal chemistry. *Chem. Soc. Rev.* **2008**, *37* (2), 320-330.
18. O'Hagan, D., Fluorine in health care: Organofluorine containing blockbuster drugs. *J. Fluorine Chem.* **2010**, *131* (11), 1071-1081.
19. Goekjian, P. G.; Wu, G.-Z.; Chen, S.; Zhou, L.; Jirousek, M. R.; Gillig, J. R.; Ballas, L. M.; Dixon, J. T., Synthesis of Fluorinated Macrocyclic Bis(indolyl)maleimides as Potential <sup>19</sup>F NMR Probes for Protein Kinase C. *J. Org. Chem.* **1999**, *64* (12), 4238-4246.
20. Moumné, R.; Pasco, M.; Prost, E.; Lecourt, T.; Micouin, L.; Tisné, C., Fluorinated Diaminocyclopentanes as Chiral Sensitive NMR Probes of RNA Structure. *J. Am. Chem. Soc.* **2010**, *132* (38), 13111-13113.
21. Cobb, S. L.; Murphy, C. D., <sup>19</sup>F NMR applications in chemical biology. *J. Fluorine Chem.* **2009**, *130* (2), 132-143.
22. Chen, H.; Viel, S.; Ziarelli, F.; Peng, L., <sup>19</sup>F NMR: a valuable tool for studying biological events. *Chem. Soc. Rev.* **2013**, *42* (20), 7971-7982.
23. Ametamey, S. M.; Honer, M.; Schubiger, P. A., Molecular Imaging with PET. *Chem. Rev.* **2008**, *108* (5), 1501-1516.
24. O'Hagan, D., Understanding organofluorine chemistry. An introduction to the C–F bond. *Chem. Soc. Rev.* **2008**, *37* (2), 308-319.
25. Böhm, H. J.; Banner, D.; Bendels, S.; Kansy, M.; Kuhn, B.; Müller, K.; Obst-Sander, U.; Stahl, M., Fluorine in Medicinal Chemistry. *ChemBioChem* **2004**, *5* (5), 637-643.
26. Hagmann, W. K., The Many Roles for Fluorine in Medicinal Chemistry. *J. Med. Chem.* **2008**, *51*, 4359.
27. Gillis, E. P.; Eastman, K. J.; Hill, M. D.; Donnelly, D. J.; Meanwell, N. A., Applications of Fluorine in Medicinal Chemistry. *J. Med. Chem.* **2015**, *58* (21), 8315-8359.
28. Purser, S.; Moore, P. R.; Swallow, S.; Gouverneur, V., Fluorine in medicinal chemistry. *Chemical Society Reviews* **2008**, *37* (2), 320-330.
29. Smart, B. E., Fluorine substituent effects (on bioactivity). *Journal of Fluorine Chemistry* **2001**, *109* (1), 3-11.

30. Shah, P.; Westwell, A. D., The role of fluorine in medicinal chemistry. *Journal of Enzyme Inhibition and Medicinal Chemistry* **2007**, *22* (5), 527-540.
31. Guengerich, F. P., Common and Uncommon Cytochrome P450 Reactions Related to Metabolism and Chemical Toxicity. *Chemical Research in Toxicology* **2001**, *14* (6), 611-650.
32. Bume, D. D.; Harry, S. A.; Lectka, T.; Pitts, C. R., Catalyzed and Promoted Aliphatic Fluorination. *The Journal of Organic Chemistry* **2018**, *83* (16), 8803-8814.
33. Szpera, R.; Moseley, D. F. J.; Smith, L. B.; Sterling, A. J.; Gouverneur, V., The Fluorination of C–H Bonds: Developments and Perspectives. *Angewandte Chemie International Edition* **2019**, *58* (42), 14824-14848.
34. Cheng, Q.; Ritter, T., New Directions in C–H Fluorination. *Trends in Chemistry* **2019**, *1* (5), 461-470.
35. Froese, R. D. J.; Whiteker, G. T.; Peterson, T. H.; Arriola, D. J.; Renga, J. M.; Shearer, J. W., Computational and Experimental Studies of Regioselective S<sub>N</sub>Ar Halide Exchange (Halex) Reactions of Pentachloropyridine. *The Journal of Organic Chemistry* **2016**, *81* (22), 10672-10682.
36. Ye, Y.; Schimler, S. D.; Hanley, P. S.; Sanford, M. S., Cu(OTf)<sub>2</sub>-Mediated Fluorination of Aryltrifluoroborates with Potassium Fluoride. *J. Am. Chem. Soc.* **2013**, *135* (44), 16292-16295.
37. Ichiishi, N.; Canty, A. J.; Yates, B. F.; Sanford, M. S., Cu-Catalyzed Fluorination of Diaryliodonium Salts with KF. *Org. Lett.* **2013**, *15* (19), 5134-5137.
38. Lee, H. G.; Milner, P. J.; Buchwald, S. L., An Improved Catalyst System for the Pd-Catalyzed Fluorination of (Hetero)Aryl Triflates. *Org. Lett.* **2013**, *15* (21), 5602-5605.
39. Fier, P. S.; Luo, J.; Hartwig, J. F., Copper-Mediated Fluorination of Arylboronate Esters. Identification of a Copper(III) Fluoride Complex. *J. Am. Chem. Soc.* **2013**, *135* (7), 2552-2559.
40. Fier, P. S.; Hartwig, J. F., Copper-Mediated Fluorination of Aryl Iodides. *J. Am. Chem. Soc.* **2012**, *134* (26), 10795-10798.
41. Tang, P.; Furuya, T.; Ritter, T., Silver-Catalyzed Late-Stage Fluorination. *J. Am. Chem. Soc.* **2010**, *132* (34), 12150-12154.
42. Truong, T.; Klimovica, K.; Daugulis, O., Copper-Catalyzed, Directing Group-Assisted Fluorination of Arene and Heteroarene C–H Bonds. *J. Am. Chem. Soc.* **2013**, *135* (25), 9342-9345.
43. Lentz, D.; Braun, T.; Kuehnel, M. F., Synthesis of Fluorinated Building Blocks by Transition-Metal-Mediated Hydrodefluorination Reactions. *Angew. Chem. Int. Ed. Engl.* **2013**, *52* (12), 3328-3348.
44. Ahrens, T.; Kohlmann, J.; Ahrens, M.; Braun, T., Functionalization of Fluorinated Molecules by Transition-Metal-Mediated C–F Bond Activation To Access Fluorinated Building Blocks. *Chem. Rev.* **2015**, *115* (2), 931-972.
45. Weaver, J.; Senaweera, S., C–F activation and functionalization of perfluoro- and polyfluoroarenes. *Tetrahedron* **2014**, *70* (41), 7413-7428.
46. Kiplinger, J. L.; Richmond, T. G.; Osterberg, C. E., Activation of Carbon-Fluorine Bonds by Metal Complexes. *Chem. Rev.* **1994**, *94* (2), 373-431.
47. Amii, H.; Uneyama, K., C–F Bond Activation in Organic Synthesis. *Chem. Rev.* **2009**, *109* (5), 2119-2183.
48. Sandford, G., Pentafluoropyridine. In *Encyclopedia of Reagents for Organic Synthesis*, 2005.
49. Sun, A. D.; Love, J. A., Nickel-Catalyzed Selective Defluorination to Generate Partially Fluorinated Biaryls. *Organic Letters* **2011**, *13* (10), 2750-2753.
50. Wang, T.; Keyes, L.; Patrick, B. O.; Love, J. A., Exploration of the Mechanism of Platinum(II)-Catalyzed C–F Activation: Characterization and Reactivity of Platinum(IV) Fluoroaryl Complexes Relevant to Catalysis. *Organometallics* **2012**, *31* (4), 1397-1407.

51. Konovalov, V. V.; Laev, S. S.; Beregovaya, I. V.; Shchegoleva, L. N.; Shteingarts, V. D.; Tsvetkov, Y. D.; Bilkis, I., Fragmentation of Radical Anions of Polyfluorinated Benzoates. *The Journal of Physical Chemistry A* **2000**, *104* (2), 352-361.
52. Arndt, P.; Spannenberg, A.; Baumann, W.; Burlakov, V. V.; Rosenthal, U.; Becke, S.; Weiss, T., Reactions of Zirconocene 2-Vinylpyridine Complexes with Diisobutylaluminum Hydride and Fluoride. *Organometallics* **2004**, *23* (20), 4792-4795.
53. Schneider, H.; Hock, A.; Jaeger, A. D.; Lentz, D.; Radius, U., NHC-Alane Adducts as Hydride Sources in the Hydrodefluorination of Fluoroaromatics and Fluoroolefins. *European Journal of Inorganic Chemistry* **2018**, *2018* (36), 4031-4043.
54. Edelbach, B. L.; Fazlur Rahman, A. K.; Lachicotte, R. J.; Jones, W. D., Carbon-Fluorine Bond Cleavage by Zirconium Metal Hydride Complexes. *Organometallics* **1999**, *18* (16), 3170-3177.
55. Aizenberg, M.; Milstein, D., Homogeneous rhodium complex-catalyzed hydrogenolysis of C-F bonds. *Journal of the American Chemical Society* **1995**, *117* (33), 8674-8675.
56. Aizenberg, M.; Milstein, D., Catalytic Activation of Carbon-Fluorine Bonds by a Soluble Transition Metal Complex. *Science* **1994**, *265* (5170), 359-361.
57. Laev, S. S.; Shteingarts, V. D.; Bilkis, I. I., On the difference in the results of reductive defluorination of pentafluorobenzoic acid by sodium and zinc in liquid ammonia medium. *Tetrahedron Letters* **1995**, *36* (26), 4655-4658.
58. Ischay, M. A.; Anzovino, M. E.; Du, J.; Yoon, T. P., Efficient Visible Light Photocatalysis of [2+2] Enone Cycloadditions. *Journal of the American Chemical Society* **2008**, *130* (39), 12886-12887.
59. Nicewicz, D. A.; MacMillan, D. W. C., Merging Photoredox Catalysis with Organocatalysis: The Direct Asymmetric Alkylation of Aldehydes. *Science* **2008**, *322* (5898), 77-80.
60. Narayanam, J. M. R.; Tucker, J. W.; Stephenson, C. R. J., Electron-Transfer Photoredox Catalysis: Development of a Tin-Free Reductive Dehalogenation Reaction. *Journal of the American Chemical Society* **2009**, *131* (25), 8756-8757.
61. Ciamician, G., THE PHOTOCHEMISTRY OF THE FUTURE. *Science* **1912**, *36* (926), 385-394.
62. Srinivasan, R., Use of a  $\pi$ -Complex of an Olefin as a Photochemical Catalyst. *Journal of the American Chemical Society* **1963**, *85* (19), 3048-3049.
63. Baldwin, J. E.; Greeley, R. H., Cycloadditions. IV. Mechanism of the Photoisomerization of cis,cis-1,5-Cyclooctadiene to Tricyclo[3.3.0.0<sup>2,6</sup>]octane. *Journal of the American Chemical Society* **1965**, *87* (20), 4514-4516.
64. Salomon, R. G.; Kochi, J. K., Copper(I) catalysis in photocycloadditions. I. Norbornene. *Journal of the American Chemical Society* **1974**, *96* (4), 1137-1144.
65. Twilton, J.; Le, C.; Zhang, P.; Shaw, M. H.; Evans, R. W.; MacMillan, D. W. C., The merger of transition metal and photocatalysis. *Nature Reviews Chemistry* **2017**, *1* (7), 0052.
66. Shaw, M. H.; Twilton, J.; MacMillan, D. W. C., Photoredox Catalysis in Organic Chemistry. *The Journal of Organic Chemistry* **2016**, *81* (16), 6898-6926.
67. Romero, N. A.; Nicewicz, D. A., Organic Photoredox Catalysis. *Chemical Reviews* **2016**, *116* (17), 10075-10166.
68. Fagnoni, M.; Dondi, D.; Ravelli, D.; Albini, A., Photocatalysis for the Formation of the C-C Bond. *Chemical Reviews* **2007**, *107* (6), 2725-2756.
69. Xu, C.; Ravi Anusuyadevi, P.; Aymonier, C.; Luque, R.; Marre, S., Nanostructured materials for photocatalysis. *Chemical Society Reviews* **2019**, *48* (14), 3868-3902.
70. Flamigni, L.; Barbieri, A.; Sabatini, C.; Ventura, B.; Barigelletti, F., Photochemistry and Photophysics of Coordination Compounds: Iridium. In *Photochemistry and Photophysics of Coordination Compounds II*, Balzani, V.; Campagna, S., Eds. Springer Berlin Heidelberg: Berlin, Heidelberg, 2007; pp 143-203.

71. You, Y.; Nam, W., Photofunctional triplet excited states of cyclometalated Ir(III) complexes: beyond electroluminescence. *Chemical Society Reviews* **2012**, *41* (21), 7061-7084.
72. Daub, M. E.; Jung, H.; Lee, B. J.; Won, J.; Baik, M.-H.; Yoon, T. P., Enantioselective [2+2] Cycloadditions of Cinnamate Esters: Generalizing Lewis Acid Catalysis of Triplet Energy Transfer. *Journal of the American Chemical Society* **2019**, *141* (24), 9543-9547.
73. Amador, A. G.; Sherbrook, E. M.; Yoon, T. P., A Redox Auxiliary Strategy for Pyrrolidine Synthesis via Photocatalytic [3+2] Cycloaddition. *Asian Journal of Organic Chemistry* **2019**, *8* (7), 978-985.
74. Lowry, M. S.; Hudson, W. R.; Pascal, R. A.; Bernhard, S., Accelerated Luminophore Discovery through Combinatorial Synthesis. *J. Am. Chem. Soc.* **2004**, *126* (43), 14129-14135.
75. Teegardin, K.; Day, J. I.; Chan, J.; Weaver, J., Advances in Photocatalysis: A Microreview of Visible Light Mediated Ruthenium and Iridium Catalyzed Organic Transformations. *Organic Process Research & Development* **2016**, *20* (7), 1156-1163.
76. Holick, M. F.; Smith, E.; Pincus, S., Skin as the Site of Vitamin D Synthesis and Target Tissue for 1,25-Dihydroxyvitamin D<sub>3</sub>: Use of Calcitriol (1,25-Dihydroxyvitamin D<sub>3</sub>) for Treatment of Psoriasis. *Archives of Dermatology* **1987**, *123* (12), 1677-1683a.
77. Fuß, W., Previtamin D: Z-E photoisomerization via a Hula-twist conical intersection. *Physical Chemistry Chemical Physics* **2019**, *21* (13), 6776-6789.
78. Liu, R. S. H., Photoisomerization by Hula-Twist: A Fundamental Supramolecular Photochemical Reaction. *Accounts of Chemical Research* **2001**, *34* (7), 555-562.
79. Müller, A. M.; Lochbrunner, S.; Schmid, W. E.; Fuß, W., Low-Temperature Photochemistry of Previtamin D: A Hula-Twist Isomerization of a Triene. *Angewandte Chemie International Edition* **1998**, *37* (4), 505-507.
80. van der Horst, M. A.; Hellingwerf, K. J., Photoreceptor Proteins, "Star Actors of Modern Times": A Review of the Functional Dynamics in the Structure of Representative Members of Six Different Photoreceptor Families. *Accounts of Chemical Research* **2004**, *37* (1), 13-20.
81. Lewis, G. N.; Magel, T. T.; Lipkin, D., The Absorption and Re-emission of Light by cis- and trans-Stilbenes and the Efficiency of their Photochemical Isomerization. *Journal of the American Chemical Society* **1940**, *62* (11), 2973-2980.
82. Hammond, G. S.; Saltiel, J.; Lamola, A. A.; Turro, N. J.; Bradshaw, J. S.; Cowan, D. O.; Counsell, R. C.; Vogt, V.; Dalton, C., Mechanisms of Photochemical Reactions in Solution. XXII.1 Photochemical cis-trans Isomerization. *Journal of the American Chemical Society* **1964**, *86* (16), 3197-3217.
83. Lewis, F. D.; Bassani, D. M.; Caldwell, R. A.; Unett, D. J., Singlet State Cis,Trans Photoisomerization and Intersystem Crossing of 1-Arylpropenes. *Journal of the American Chemical Society* **1994**, *116* (23), 10477-10485.
84. Foote, C. S., Mechanisms of Photosensitized Oxidation. *Science* **1968**, *162* (3857), 963-970.
85. Albin, A., Photosensitization in Organic Synthesis. *Synthesis* **1981**, *1981* (04), 249-264.
86. Ohno, T.; Lichtin, N. N., Electron transfer in the quenching of triplet methylene blue by complexes of iron(II). *Journal of the American Chemical Society* **1980**, *102* (14), 4636-4643.
87. Srivastava, V.; Singh, P. P., Eosin Y catalysed photoredox synthesis: a review. *RSC Advances* **2017**, *7* (50), 31377-31392.
88. Dilling, W. L., Photochemical cycloaddition reactions of nonaromatic conjugated hydrocarbon dienes and polyenes. *Chemical Reviews* **1969**, *69* (6), 845-877.
89. Turro, N. J., Triplet-triplet excitation transfer in fluid solution: Applications to organic photochemistry. *Journal of Chemical Education* **1966**, *43* (1), 13.
90. Lindlar, H., Ein neuer Katalysator für selektive Hydrierungen. *Helvetica Chimica Acta* **1952**, *35* (2), 446-450.

91. Lindlar, H.; Dubuis, R.; Jones, F. N.; McKusick, B. C., Palladium Catalyst for Partial Reduction of Acetylenes. *Organic Syntheses* **1966**, 46.
92. Overman, L. E.; Brown, M. J.; McCann, S. F.; Newbold, R. C.; Kende, A. S., (Z)-4-(Trimethylsilyl)-3-Buten-1-ol. *Organic Syntheses* **1990**, 68.
93. Campos, K. R.; Cai, D.; Journet, M.; Kowal, J. J.; Larsen, R. D.; Reider, P. J., Controlled Semihydrogenation of Aminoalkynes Using Ethylenediamine as a Poison of Lindlar's Catalyst. *The Journal of Organic Chemistry* **2001**, 66 (10), 3634-3635.
94. Tucker, C. E.; Davidson, J.; Knochel, P., Mild and stereoselective hydroborations of functionalized alkynes and alkenes using pinacolborane. *The Journal of Organic Chemistry* **1992**, 57 (12), 3482-3485.
95. Brown, H. C.; Hamaoka, T.; Ravindran, N., Stereospecific conversion of alkenylboronic acids into alkenyl bromides with inversion of configuration. Striking differences in the stereochemistry of the replacement of the boronic acid substituent by bromine and iodine and its significance in terms of the reaction mechanism. *Journal of the American Chemical Society* **1973**, 95 (19), 6456-6457.
96. Brown, H. C.; Hamaoka, T.; Ravindran, N., Reaction of alkenylboronic acids with iodine under the influence of base. Simple procedure for the stereospecific conversion of terminal alkynes into trans-1-alkenyl iodides via hydroboration. *Journal of the American Chemical Society* **1973**, 95 (17), 5786-5788.
97. McGough, J. S.; Butler, S. M.; Cade, I. A.; Ingleson, M. J., Highly selective catalytic trans-hydroboration of alkynes mediated by borenium cations and B(C<sub>6</sub>F<sub>5</sub>)<sub>3</sub>. *Chemical Science* **2016**, 7 (5), 3384-3389.
98. Bergelson, L. D.; Barsukov, L. I.; Shemyakin, M. M., The stereochemistry of the Wittig reaction with non-stabilized and semistabilized ylids. *Tetrahedron* **1967**, 23 (6), 2709-2720.
99. Stork, G.; Zhao, K., A stereoselective synthesis of (Z)-1-iodo-1-alkenes. *Tetrahedron Letters* **1989**, 30 (17), 2173-2174.
100. The Nobel Prize in Chemistry 2005.  
<https://www.nobelprize.org/prizes/chemistry/2005/press-release/> (accessed 3/15/2020).
101. Gottumukkala, A. L.; Madduri, A. V. R.; Minnaard, A. J., Z-Selectivity: A Novel Facet of Metathesis. *ChemCatChem* **2012**, 4 (4), 462-467.
102. Werrel, S.; Walker, J. C. L.; Donohoe, T. J., Application of catalytic Z-selective olefin metathesis in natural product synthesis. *Tetrahedron Letters* **2015**, 56 (38), 5261-5268.
103. Singh, K.; Staig, S. J.; Weaver, J. D., Facile synthesis of Z-alkenes via uphill catalysis. *J. Am. Chem. Soc.* **2014**, 136 (14), 5275-8.
104. Lu, Z.; Yoon, T. P., Visible Light Photocatalysis of [2+2] Styrene Cycloadditions by Energy Transfer. *Angewandte Chemie International Edition* **2012**, 51 (41), 10329-10332.
105. Stoll, M.; Hulstkamp, J.; Rouvé, A., Synthèses de produits macrocycliques à odeur musquée. 8e communication Synthèse de la civettone naturelle. *Helv. Chim. Acta* **1948**, 31 (2), 543-553.
106. Marshall, J., Trans-cycloalkenes and [a.b]betweenanenes, molecular jump ropes and double bond sandwiches. *Accounts Chem Res* **1980**, 13 (7), 213-218.
107. Cope, A. C.; Pike, R. A.; Spencer, C. F., Cyclic Polyolefins. XXVII. cis- and trans-Cycloöctene from N,N-Dimethylcycloöctylamine. *J. Am. Chem. Soc.* **1953**, 75 (13), 3212-3215.
108. Wallraff, G. M.; Michl, J., Low-temperature reactions of copper(I) triflate complexes of cis- and trans-cyclooctene cis- and trans-cycloheptene with trimethyl phosphite. Spectroscopic evidence for free trans-cycloheptene. *J Org Chem* **1986**, 51 (10), 1794-1800.
109. Inoue, Y.; Ueoka, T.; Kuroda, T.; Hakushi, T., Singlet photosensitization of simple alkenes. Part 4. cis-trans Photoisomerization of cycloheptene sensitized by aromatic esters. Some aspects of the chemistry of trans-cycloheptene. *J. Chem. Soc., Perkin Trans. 2* **1983**, 0 (7), 983-988.

110. Verbeek, J.; Van Lenthe, J. H.; Timmermans, P. J. J. A.; Mackor, A.; Budzelaar, P. H. M., On the existence of trans-cyclohexene. *The Journal of Organic Chemistry* **1987**, *52* (13), 2955-2957.
111. Bonneau, R.; Jousot-Dubien, J.; Salem, L.; Yarwood, A. J., A trans cyclohexene. *J. Am. Chem. Soc.* **1976**, *98* (14), 4329-4330.
112. Dauben, W. G.; Van Riel, H. C. H. A.; Hauw, C.; Leroy, F.; Jousot-Dubien, J.; Bonneau, R., Photochemical formation of trans-1-phenylcyclohexene. Chemical proof of structure. *J. Am. Chem. Soc.* **1979**, *101* (7), 1901-1903.
113. Kropp, P. J., Photochemistry of cycloalkenes. V. Effects of ring size and substitution. *J. Am. Chem. Soc.* **1969**, *91* (21), 5783-5791.
114. Rosenberg, H. M.; Serve, M. P., Photolysis of 1-phenylcyclohexene in methanol. *J Org Chem* **1972**, *37* (1), 141-142.
115. Schuster, D. I.; Brown, R. H.; Resnick, B. M., Photochemistry of ketones in solution. 53. Stereospecific triplet-state photorearrangements of chiral 2-cyclohexenones: type A lumiketone rearrangement and phenyl migrations. *J. Am. Chem. Soc.* **1978**, *100* (14), 4504-4512.
116. Cozens, F. L.; McClelland, R. A.; Steenken, S., Observation of cationic intermediates in the photolysis of 1-phenylcyclohexene. *J. Am. Chem. Soc.* **1993**, *115* (12), 5050-5055.
117. Li, X.; Danishefsky, S. J., Cyclobutenone as a highly reactive dienophile: expanding upon Diels-Alder paradigms. *J. Am. Chem. Soc.* **2010**, *132* (32), 11004-11005.
118. Paton, R. S.; Kim, S.; Ross, A. G.; Danishefsky, S. J.; Houk, K. N., Experimental Diels-Alder Reactivities of Cycloalkenones and Cyclic Dienes Explained through Transition-State Distortion Energies. *Angew. Chem. Int. Ed.* **2011**, *123* (44), 10550-10552.
119. Ross, A. G.; Li, X.; Danishefsky, S. J., Intramolecular Diels-Alder reactions of cycloalkenones: translation of high endo selectivity to trans junctions. *J. Am. Chem. Soc.* **2012**, *134* (38), 16080-16084.
120. Medina, J. M.; McMahon, T. C.; Jimenez-Oses, G.; Houk, K. N.; Garg, N. K., Cycloadditions of cyclohexynes and cyclopentyne. *J. Am. Chem. Soc.* **2014**, *136* (42), 14706-9.
121. Shah, T. K.; Medina, J. M.; Garg, N. K., Expanding the Strained Alkyne Toolbox: Generation and Utility of Oxygen-Containing Strained Alkynes. *J. Am. Chem. Soc.* **2016**, *138* (14), 4948-4954.
122. Medina, J. M.; Ko, J. H.; Maynard, H. D.; Garg, N. K., Expanding the ROMP Toolbox: Synthesis of Air-Stable Benzonorbornadiene Polymers by Aryne Chemistry. *Macromolecules* **2017**, *50* (2), 580-586.
123. Blackman, M. L.; Royzen, M.; Fox, J. M., Tetrazine ligation: fast bioconjugation based on inverse-electron-demand Diels-Alder reactivity. *J. Am. Chem. Soc.* **2008**, *130* (41), 13518-13519.
124. Tasdelen, M. A.; Yagci, Y., Light-induced click reactions. *Angew. Chem. Int. Ed.* **2013**, *52* (23), 5930-8.
125. Arumugam, S.; Popik, V. V., Light-induced hetero-Diels-Alder cycloaddition: a facile and selective photoclick reaction. *J. Am. Chem. Soc.* **2011**, *133* (14), 5573-9.
126. Wang, Y.; Song, W.; Hu, W. J.; Lin, Q., Fast alkene functionalization in vivo by Photoclick chemistry: HOMO lifting of nitrile imine dipoles. *Angew. Chem. Int. Ed.* **2009**, *48* (29), 5330-5333.
127. Hoyle, C. E.; Lowe, A. B.; Bowman, C. N., Thiol-click chemistry: a multifaceted toolbox for small molecule and polymer synthesis. *Chem. Soc. Rev.* **2010**, *39* (4), 1355-1387.
128. Poloukhine, A. A.; Mbua, N. E.; Wolfert, M. A.; Boons, G. J.; Popik, V. V., Selective labeling of living cells by a photo-triggered click reaction. *J. Am. Chem. Soc.* **2009**, *131* (43), 15769-76.
129. Nikolai, J.; Loe, Ø.; Dominiak, P. M.; Gerlitz, O. O.; Autschbach, J.; Davies, H. M. L., Mechanistic Studies of UV Assisted [4 + 2] Cycloadditions in Synthetic Efforts toward Vibsanin E. *J. Am. Chem. Soc.* **2007**, *129* (35), 10763-10772.
130. Dorr, H.; Rawal, V. H., The Intramolecular Diels-Alder Reactions of Photochemically Generated trans-Cycloalkenones. *J. Am. Chem. Soc.* **1999**, *121* (43), 10229-10230.

131. Jin, S.; Nguyen, V. T.; Dang, H. T.; Nguyen, D. P.; Arman, H. D.; Larionov, O. V., Photoinduced Carboborative Ring Contraction Enables Regio- and Stereoselective Synthesis of Multiply Substituted Five-Membered Carbocycles and Heterocycles. *J. Am. Chem. Soc.* **2017**, *139* (33), 11365-11368.
132. Ikezawa, H.; Kotal, C.; Yasufuku, K.; Yamazaki, H., Direct and sensitized valence photoisomerization of a substituted norbornadiene. Examination of the disparity between singlet- and triplet-state reactivities. *Journal of the American Chemical Society* **1986**, *108* (7), 1589-1594.
133. Islangulov, R. R.; Castellano, F. N., Photochemical Upconversion: Anthracene Dimerization Sensitized to Visible Light by a Rull Chromophore. *Angewandte Chemie International Edition* **2006**, *45* (36), 5957-5959.
134. McTiernan, C. D.; Morin, M.; McCallum, T.; Scaiano, J. C.; Barriault, L., Polynuclear gold(i) complexes in photoredox catalysis: understanding their reactivity through characterization and kinetic analysis. *Catalysis Science & Technology* **2016**, *6* (1), 201-207.
135. Shchegoleva, L. N.; Beregovaya, I. V.; Schastnev, P. V., Potential energy surface of C6F6-radical anion. *Chemical Physics Letters* **1999**, *312* (2), 325-332.
136. Clot, E.; Mégret, C.; Eisenstein, O.; Perutz, R. N., Exceptional Sensitivity of Metal-Aryl Bond Energies to ortho-Fluorine Substituents: Influence of the Metal, the Coordination Sphere, and the Spectator Ligands on M-C/H-C Bond Energy Correlations. *Journal of the American Chemical Society* **2009**, *131* (22), 7817-7827.
137. Beatty, J. W.; Stephenson, C. R. J., Amine Functionalization via Oxidative Photoredox Catalysis: Methodology Development and Complex Molecule Synthesis. *Accounts of Chemical Research* **2015**, *48* (5), 1474-1484.
138. Wayner, D. D. M.; Dannenberg, J. J.; Griller, D., Oxidation potentials of  $\alpha$ -aminoalkyl radicals: bond dissociation energies for related radical cations. *Chemical Physics Letters* **1986**, *131* (3), 189-191.
139. Senaweera, S. M.; Singh, A.; Weaver, J. D., Photocatalytic Hydrodefluorination: Facile Access to Partially Fluorinated Aromatics. *Journal of the American Chemical Society* **2014**, *136* (8), 3002-3005.
140. Kharasch, M. S.; Mayo, F. R., The Peroxide Effect in the Addition of Reagents to Unsaturated Compounds. I. The Addition of Hydrogen Bromide to Allyl Bromide. *Journal of the American Chemical Society* **1933**, *55* (6), 2468-2496.
141. Singh, A.; Kubik, J. J.; Weaver, J. D., Photocatalytic C-F alkylation; facile access to multifluorinated arenes. *Chemical Science* **2015**, *6* (12), 7206-7212.
142. Singh, A.; Fennell, C. J.; Weaver, J. D., Photocatalyst size controls electron and energy transfer: selectable E/Z isomer synthesis via C-F alkenylation. *Chem. Sci.* **2016**, *7* (11), 6796-6802.
143. Senaweera, S.; Weaver, J. D., Dual C-F, C-H Functionalization via Photocatalysis: Access to Multifluorinated Biaryls. *Journal of the American Chemical Society* **2016**, *138* (8), 2520-2523.
144. Priya, S.; Weaver, J. D., Prenyl Praxis: A Method for Direct Photocatalytic Defluoroprenylation. *Journal of the American Chemical Society* **2018**, *140* (47), 16020-16025.
145. Terrier, F., Rate and equilibrium studies in Jackson-Meisenheimer complexes. *Chemical Reviews* **1982**, *82* (2), 77-152.
146. Handel, H.; Pasquini, M. A.; Pierre, J. L., Effets de cryptands et activation de bases—VII11Partie précédente Réf. 1.: Réduction des halogénures de phényle par l'hydrure de potassium. *Tetrahedron* **1980**, *36* (22), 3205-3208.
147. Kwan, E. E.; Zeng, Y.; Besser, H. A.; Jacobsen, E. N., Concerted nucleophilic aromatic substitutions. *Nature Chemistry* **2018**, *10* (9), 917-923.
148. Neumann, C. N.; Hooker, J. M.; Ritter, T., Concerted nucleophilic aromatic substitution with (19)F(-) and (18)F(-). *Nature* **2016**, *534* (7607), 369-373.



149. Senger, N. A.; Bo, B.; Cheng, Q.; Keeffe, J. R.; Gronert, S.; Wu, W., The Element Effect Revisited: Factors Determining Leaving Group Ability in Activated Nucleophilic Aromatic Substitution Reactions. *The Journal of Organic Chemistry* **2012**, *77* (21), 9535-9540.
150. Bowler, J. T.; Wong, F. M.; Gronert, S.; Keeffe, J. R.; Wu, W., Reactivity in the nucleophilic aromatic substitution reactions of pyridinium ions. *Organic & Biomolecular Chemistry* **2014**, *12* (32), 6175-6180.
151. Bunnett, J. F.; Garbisch, E. W.; Pruitt, K. M., The "Element Effect" as a Criterion of Mechanism in Activated Aromatic Nucleophilic Substitution Reactions<sup>1,2</sup>. *Journal of the American Chemical Society* **1957**, *79* (2), 385-391.
152. Aksenov, V. V.; Vlasov, V. M.; Yakobson, G. G., Interaction of pentafluoropyridine with 4-nitrophenol and pentafluorophenol in the presence of potassium fluoride and 18-crown-6-ether. *Journal of Fluorine Chemistry* **1982**, *20* (4), 439-458.
153. Vlasov, V. M.; Aksenov, V. V.; Rodionov, P. P.; Beregovaya, I. V.; Shchegoleva, L. N., Unusual Lability of Pentafluorophenoxy Group in Reactions of Potassium Aroxides with Pentafluoropyridine. *Russian Journal of Organic Chemistry* **2002**, *38* (1), 115-125.
154. Rohrbach, S.; Smith, A. J.; Pang, J. H.; Poole, D. L.; Tuttle, T.; Chiba, S.; Murphy, J. A., Concerted Nucleophilic Aromatic Substitution Reactions. *Angewandte Chemie International Edition* **2019**, *58* (46), 16368-16388.
155. Singh, A.; Kubik, J. J.; Weaver, J. D., Photocatalytic C-F alkylation; facile access to multifluorinated arenes. *Chemical Science* **2015**.
156. Campagna, S.; Puntoriero, F.; Nastasi, F.; Bergamini, G.; Balzani, V., Photochemistry and Photophysics of Coordination Compounds: Ruthenium Photochemistry and Photophysics of Coordination Compounds I. *Top. Curr. Chem.* **2007**, *280*, 117-214.
157. Flamigni, L.; Barbieri, A.; Sabatini, C.; Ventura, B.; Barigelletti, F., Photochemistry and Photophysics of Coordination Compounds: Iridium Photochemistry and Photophysics of Coordination Compounds II. *Top. Curr. Chem.* **2007**, *281*, 143-203.
158. Prier, C. K.; Rankic, D. A.; MacMillan, D. W. C., Visible Light Photoredox Catalysis with Transition Metal Complexes: Applications in Organic Synthesis. *Chem. Rev.* **2013**, *113* (7), 5322-5363.
159. Kalyanasundaram, K.; Grätzel, M., Applications of functionalized transition metal complexes in photonic and optoelectronic devices. *Coord. Chem. Rev.* **1998**, *177* (1), 347-414.
160. Lowry, M. S.; Bernhard, S., Synthetically Tailored Excited States: Phosphorescent, Cyclometalated Iridium(III) Complexes and Their Applications. *Chem. Eur. J.* **2006**, *12* (31), 7970-7977.
161. Lalevee, J.; Peter, M.; Dumur, F.; Gimes, D.; Blanchard, N.; Tehfe, M.-A.; Morlet-Savary, F.; Fouassier, J. P., Subtle Ligand Effects in Oxidative Photocatalysis with Iridium Complexes: Application to Photopolymerization. *Chem. Eur. J.* **2011**, *17* (52), 15027-15031.
162. Ischay, M. A.; Anzovino, M. E.; Du, J.; Yoon, T. P., Efficient Visible Light Photocatalysis of [2+2] Enone Cycloadditions. *J. Am. Chem. Soc.* **2008**, *130* (39), 12886-12887.
163. Pac, C.; Ihama, M.; Yasuda, M.; Miyauchi, Y.; Sakurai, H., Tris(2,2'-bipyridine)ruthenium(2+)-mediated photoreduction of olefins with 1-benzyl-1,4-dihydronicotinamide: a mechanistic probe for electron-transfer reactions of NAD(P)H-model compounds. *J. Am. Chem. Soc.* **1981**, *103* (21), 6495-6497.
164. Fukuzumi, S.; Mochizuki, S.; Tanaka, T., Photocatalytic reduction of phenacyl halides by 9,10-dihydro-10-methylacridine: control between the reductive and oxidative quenching pathways of tris(bipyridine)ruthenium complex utilizing an acid catalysis. *J. Phys. Chem.* **1990**, *94* (2), 722-726.
165. Narayanam, J. M. R.; Stephenson, C. R. J., Visible light photoredox catalysis: applications in organic synthesis. *Chem. Soc. Rev.* **2011**, *40* (1), 102-113.

166. Terrett, J. A.; Clift, M. D.; MacMillan, D. W. C., Direct  $\beta$ -Alkylation of Aldehydes via Photoredox Organocatalysis. *J. Am. Chem. Soc.* **2014**, *136* (19), 6858-6861.
167. Slinker, J. D.; Gorodetsky, A. A.; Lowry, M. S.; Wang, J.; Parker, S.; Rohl, R.; Bernhard, S.; Malliaras, G. G., Efficient yellow electroluminescence from a single layer of a cyclometalated iridium complex. *J. Am. Chem. Soc.* **2004**, *126* (9), 2763-7.
168. Juris, A.; Balzani, V.; Belser, P.; von Zelewsky, A., Characterization of the Excited State Properties of Some New Photosensitizers of the Ruthenium (Polypyridine) Family. *Helv. Chim. Acta* **1981**, *64* (7), 2175-2182.
169. Rillema, D. P.; Allen, G.; Meyer, T. J.; Conrad, D., Redox properties of ruthenium(II) tris chelate complexes containing the ligands 2,2'-bipyrazine, 2,2'-bipyridine, and 2,2'-bipyrimidine. *Inorg. Chem* **1983**, *22* (11), 1617-1622.
170. Haga, M.; Dodsworth, E. S.; Eryavec, G.; Seymour, P.; Lever, A. B. P., Luminescence quenching of the tris(2,2'-bipyrazine)ruthenium(II) cation and its monoprotonated complex. *Inorg. Chem* **1985**, *24* (12), 1901-1906.
171. Young, R. C.; Meyer, T. J.; Whitten, D. G., Electron transfer quenching of excited states of metal complexes. *J. Am. Chem. Soc.* **1976**, *98* (1), 286-287.
172. Prier, C. K.; Rankic, D. A.; MacMillan, D. W., Visible light photoredox catalysis with transition metal complexes: applications in organic synthesis. *Chem. Rev.* **2013**, *113* (7), 5322-63.
173. Farney, E. P.; Yoon, T. P., Visible-Light Sensitization of Vinyl Azides by Transition Metal Photocatalysis. *Angew. Chem., Int. Ed.* **2014**, *53* (3), 793-797.
174. Dedeian, K.; Djurovich, P. I.; Garces, F. O.; Carlson, G.; Watts, R. J., A new synthetic route to the preparation of a series of strong photoreducing agents: fac-tris-ortho-metallated complexes of iridium(III) with substituted 2-phenylpyridines. *Inorg. Chem* **1991**, *30* (8), 1685-1687.
175. Grushin, V. V.; Herron, N.; LeCloux, D. D.; Marshall, W. J.; Petrov, V. A.; Wang, Y., New, efficient electroluminescent materials based on organometallic Ir complexes. *Chem. Commun.* **2001**, (16), 1494-1495.
176. Singh, A.; Teegardin, K.; Kelly, M.; Prasad, K. S.; Krishnan, S.; Weaver, J. D., Facile synthesis and complete characterization of homoleptic and heteroleptic cyclometalated Iridium(III) complexes for photocatalysis. *J. Organomet. Chem.* **2015**, *776*, 51-59.
177. Ladouceur, S.; Fortin, D.; Zysman-Colman, E., Enhanced Luminescent Iridium(III) Complexes Bearing Aryltriazole Cyclometallated Ligands. *Inorg. Chem* **2011**, *50* (22), 11514-11526.
178. Swanick, K. N.; Ladouceur, S.; Zysman-Colman, E.; Ding, Z., Correlating electronic structures to electrochemiluminescence of cationic Ir complexes. *RSC Adv.* **2013**, *3* (43), 19961-19964.
179. Anderson, B. L.; Maher, A. G.; Nava, M.; Lopez, N.; Cummins, C. C.; Nocera, D. G., Ultrafast Photoinduced Electron Transfer from Peroxide Dianion. *J. Phys. Chem.* **2015**, *119* (24), 7422-7429.
180. Zou, Y.-Q.; Lu, L.-Q.; Fu, L.; Chang, N.-J.; Rong, J.; Chen, J.-R.; Xiao, W.-J., Visible-Light-Induced Oxidation/3+2 Cycloaddition/Oxidative Aromatization Sequence: A Photocatalytic Strategy To Construct Pyrrolo 2,1-a isoquinolines. *Angew. Chem., Int. Ed.* **2011**, *50* (31), 7171-7175.
181. Damrauer, N. H.; Boussie, T. R.; Devenney, M.; McCusker, J. K., Effects of Intraligand Electron Delocalization, Steric Tuning, and Excited-State Vibronic Coupling on the Photophysics of Aryl-Substituted Bipyridyl Complexes of Ru(II). *J. Am. Chem. Soc.* **1997**, *119* (35), 8253-8268.
182. Bernhard, S.; Barron, J. A.; Houston, P. L.; Abruña, H. D.; Ruglovksy, J. L.; Gao, X.; Malliaras, G. G., Electroluminescence in Ruthenium(II) Complexes. *J. Am. Chem. Soc.* **2002**, *124* (45), 13624-13628.
183. Lv, H.; Cai, Y.-B.; Zhang, J.-L., Copper-Catalyzed Hydrodefluorination of Fluoroarenes by Copper Hydride Intermediates. *Angew. Chem., Int. Ed.* **2013**, *52* (11), 3203-3207.
184. Kalyanasundaram, K., Photophysics, photochemistry and solar energy conversion with tris(bipyridyl)ruthenium(II) and its analogues. *Coord. Chem. Rev.* **1982**, *46*, 159-244.

185. Bryant, G. M.; Fergusson, J. E.; Powell, H. K. J., Charge-transfer and intraligand electronic spectra of bipyridyl complexes of iron, ruthenium, and osmium. I. Bivalent complexes. *Aust. J. Chem.* **1971**, *24* (2), 257-273.
186. Bueldt, L. A.; Prescimone, A.; Neuburger, M.; Wenger, O. S., Photoredox Properties of Homoleptic d6 Metal Complexes with the Electron-Rich 4,4',5,5'-Tetramethoxy-2,2'-bipyridine Ligand. *Eur. J. Inorg. Chem.* **2015**, *2015* (28), 4666-4677.
187. McNally, A.; Prier, C. K.; MacMillan, D. W. C., Discovery of an  $\alpha$ -Amino C–H Arylation Reaction Using the Strategy of Accelerated Serendipity. *Science* **2011**, *334* (6059), 1114-1117.
188. Singh, A.; Arora, A.; Weaver, J. D., Photoredox-Mediated C-H Functionalization and Coupling of Tertiary Aliphatic Amines with 2-Chloroazoles. *Organic letters* **2013**, *15*, 5390-5393.
189. Qin, Q.; Yu, S., Visible-Light-Promoted Redox Neutral C-H Amidation of Heteroarenes with Hydroxylamine Derivatives. *Organic letters* **2014**, *16* (13), 3504-3507.
190. Kim, H.; Kim, T.; Lee, D. G.; Roh, S. W.; Lee, C., Nitrogen-centered radical-mediated C-H imidation of arenes and heteroarenes via visible light induced photocatalysis. *Chem. Commun.* **2014**, *50* (66), 9273-9276.
191. Arora, A.; Teegardin, K. A.; Weaver, J. D., Reductive Alkylation of 2-Bromoazoles via Photoinduced Electron Transfer: A Versatile Strategy to Csp<sup>2</sup>–Csp<sup>3</sup> Coupled Products. *Organic letters* **2015**, *17* (15), 3722-3725.
192. Uraguchi, D.; Kinoshita, N.; Kizu, T.; Ooi, T., Synergistic Catalysis of Ionic Bronsted Acid and Photosensitizer for a Redox Neutral Asymmetric  $\alpha$ -Coupling of N-Arylaminomethanes with Aldimines. *J. Am. Chem. Soc.* **2015**, *137* (43), 13768-13771.
193. Senaweera, S.; Weaver, J. D., Dual C-F, C-H Functionalization via Photocatalysis: Access to Multifluorinated Biaryls. *J. Am. Chem. Soc.* **2016**, *138* (8), 2520-3.
194. Nguyen, J. D.; Matsuura, B. S.; Stephenson, C. R. J., A Photochemical Strategy for Lignin Degradation at Room Temperature. *J. Am. Chem. Soc.* **2014**, *136* (4), 1218-1221.
195. Wang, J.; Zheng, N., The cleavage of a C-C Bond in cyclobutylanilines by visible-light photoredox catalysis: Development of a [4+2] annulation method. *Angew. Chem., Int. Ed.* **2015**, *54* (39), 11424-11427.
196. Rono, L. J.; Yayla, H. G.; Wang, D. Y.; Armstrong, M. F.; Knowles, R. R., Enantioselective Photoredox Catalysis Enabled by Proton-Coupled Electron Transfer: Development of an Asymmetric Aza-Pinacol Cyclization. *J. Am. Chem. Soc.* **2013**.
197. Qin, Q.; Yu, S., Visible-Light-Promoted Remote C(sp<sup>3</sup>)-H Amidation and Chlorination. *Organic letters* **2015**, *17* (8), 1894-1897.
198. Tellis, J. C.; Primer, D. N.; Molander, G. A., Single-electron transmetalation in organoboron cross-coupling by photoredox/nickel dual catalysis. *Science* **2014**, *345* (6195), 433-436.
199. Labadie, J. W.; Stille, J. K., Mechanisms of the palladium-catalyzed couplings of acid chlorides with organotin reagents. *J. Am. Chem. Soc.* **1983**, *105* (19), 6129-6137.
200. Finch, A.; Gardner, P. J.; Pearn, E. J.; Watts, G. B., Thermochemistry of triphenylboron, tricyclohexylboron and some phenylboron halides. *T. Faraday Soc.* **1967**, *63*, 1880.
201. Noble, A.; MacMillan, D. W. C., Photoredox  $\alpha$ -Vinylolation of  $\alpha$ -Amino Acids and N-Aryl Amines. *J. Am. Chem. Soc.* **2014**, *136* (33), 11602-11605.
202. Beatty, J. W.; Stephenson, C. R. J., Synthesis of (-)-Pseudotabersonine, (-)-Pseudovincadifformine, and (+)-Coronaridine Enabled by Photoredox Catalysis in Flow. *J. Am. Chem. Soc.* **2014**, *136* (29), 10270-10273.
203. Di Rocco, D. A.; Dykstra, K.; Krska, S.; Vachal, P.; Conway, D. V.; Tudge, M., Late-stage functionalization of biologically active heterocycles through photoredox catalysis. *Angew. Chem., Int. Ed.* **2014**, *53* (19), 4802-4806.

204. Minisci, F.; Bernardi, R.; Bertini, F.; Galli, R.; Perchinummo, M., Nucleophilic character of alkyl radicals—VI. *Tetrahedron* **1971**, *27* (15), 3575-3579.
205. Molander, G. A.; Colombel, V.; Braz, V. A., Direct Alkylation of Heteroaryls Using Potassium Alkyl- and Alkoxyethyltrifluoroborates. *Organic letters* **2011**, *13* (7), 1852-1855.
206. Noble, A.; McCarver, S. J.; MacMillan, D. W. C., Merging Photoredox and Nickel Catalysis: Decarboxylative Cross-Coupling of Carboxylic Acids with Vinyl Halides. *J. Am. Chem. Soc.* **2015**, *137* (2), 624-627.
207. Chu, L.; Lipshultz, J. M.; MacMillan, D. W., Merging Photoredox and Nickel Catalysis: The Direct Synthesis of Ketones by the Decarboxylative Arylation of  $\alpha$ -Oxo Acids. *Angew. Chem., Int. Ed.* **2015**, *54* (27), 7929-33.
208. Lu, Z.; Yoon, T. P., Visible Light Photocatalysis of [2+2] Styrene Cycloadditions by Energy Transfer. *Angew. Chem., Int. Ed.* **2012**, *51* (41), 10329-10332, S10329/1-S10329/128.
209. Sahoo, B.; Hopkinson, M. N.; Glorius, F., Combining Gold and Photoredox Catalysis: Visible Light-Mediated Oxy- and Aminoarylation of Alkenes. *J. Am. Chem. Soc.* **2013**, *135* (15), 5505-5508.
210. Singh, K.; Staig, S. J.; Weaver, J. D., Facile Synthesis of Z-Alkenes via Uphill Catalysis. *J. Am. Chem. Soc.* **2014**, *136* (14), 5275-5278.
211. Osawa, M.; Hoshino, M.; Wakatsuki, Y., A Light-Harvesting tert-Phosphane Ligand Bearing a Ruthenium(II) Polypyridyl Complex as Substituent. *Angew. Chem., Int. Ed.* **2001**, *40* (18), 3472-3474.
212. Fabry, D. C.; Ronge, M. A.; Rueping, M., Immobilization and Continuous Recycling of Photoredox Catalysts in Ionic Liquids for Applications in Batch Reactions and Flow Systems: Catalytic Alkene Isomerization by Using Visible Light. *Chem-Eur J* **2015**, *21* (14), 5350-5354.
213. Maity, S.; Zhu, M.; Shinabery, R. S.; Zheng, N., Intermolecular [3+2] Cycloaddition of Cyclopropylamines with Olefins by Visible-Light Photocatalysis. *Angew. Chem., Int. Ed.* **2012**, *51* (1), 222-226.
214. Blum, T. R.; Zhu, Y.; Nordeen, S. A.; Yoon, T. P., Photocatalytic Synthesis of Dihydrobenzofurans by Oxidative [3+2] Cycloaddition of Phenols. *Angew. Chem., Int. Ed.* **2014**, *53* (41), 11056-11059.
215. Tyson, E. L.; Niemeyer, Z. L.; Yoon, T. P., Redox Mediators in Visible Light Photocatalysis: Photocatalytic Radical Thiol-Ene Additions. *J. Org. Chem.* **2014**, *79* (3), 1427-1436.
216. Oh, S. H.; Malpani, Y. R.; Ha, N.; Jung, Y.-S.; Han, S. B., Vicinal Difunctionalization of Alkenes: Chlorotrifluoromethylation with CF<sub>3</sub>SO<sub>2</sub>Cl by Photoredox Catalysis. *Organic letters* **2014**, *16* (5), 1310-1313.
217. Iqbal, N.; Jung, J.; Park, S.; Cho, E. J., Controlled Trifluoromethylation Reactions of Alkynes through Visible-Light Photoredox Catalysis. *Angew. Chem., Int. Ed.* **2014**, *53* (2), 539-542.
218. Tang, X.-J.; Thomason, C. S.; Dolbier, W. R., Jr., Photoredox-Catalyzed Tandem Radical Cyclization of N-Arylacrylamides: General Methods To Construct Fluorinated 3,3-Disubstituted 2-Oxindoles Using Fluoroalkylsulfonyl Chlorides. *Organic letters* **2014**, *16* (17), 4594-4597.
219. Andrews, R. S.; Becker, J. J.; Gagné, M. R., Investigating the Rate of Photoreductive Glucosyl Radical Generation. *Organic letters* **2011**, *13* (9), 2406-2409.
220. Penning, T. D.; Talley, J. J.; Bertenshaw, S. R.; Carter, J. S.; Collins, P. W.; Docter, S.; Graneto, M. J.; Lee, L. F.; Malecha, J. W.; Miyashiro, J. M.; Rogers, R. S.; Rogier, D. J.; Yu, S. S.; Anderson, G. D.; Burton, E. G.; Cogburn, J. N.; Gregory, S. A.; Koboldt, C. M.; Perkins, W. E.; Seibert, K.; Veenhuizen, A. W.; Zhang, Y. Y.; Isakson, P. C., Synthesis and Biological Evaluation of the 1,5-Diarylpyrazole Class of Cyclooxygenase-2 Inhibitors: Identification of 4-[5-(4-Methylphenyl)-3-(trifluoromethyl)-1H-pyrazol-1-yl]benzenesulfonamide (SC-58635, Celecoxib). *J. Med. Chem.* **1997**, *40* (9), 1347-1365.
221. Wang, J.; Sanchez-Rosello, M.; Acena, J. L.; del Pozo, C.; Sorochinsky, A. E.; Fustero, S.; Soloshonok, V. A.; Liu, H., Fluorine in pharmaceutical industry: fluorine-containing drugs introduced to the market in the last decade (2001-2011). *Chem. Rev.* **2014**, *114* (4), 2432-506.

222. Schimler, S. D.; Ryan, S. J.; Bland, D. C.; Anderson, J. E.; Sanford, M. S., Anhydrous Tetramethylammonium Fluoride for Room-Temperature S<sub>N</sub>Ar Fluorination. *J. Org. Chem.* **2015**, *80* (24), 12137-12145.
223. Furuya, T.; Ritter, T., Fluorination of Boronic Acids Mediated by Silver(I) Triflate. *Org. Lett.* **2009**, *11* (13), 2860-2863.
224. Brooke, G. M., The preparation and properties of polyfluoro aromatic and heteroaromatic compounds. *J. Fluorine Chem.* **1997**, *86* (1), 1-76.
225. Campbell, M. G.; Ritter, T., Modern Carbon–Fluorine Bond Forming Reactions for Aryl Fluoride Synthesis. *Chem. Rev.* **2015**, *115* (2), 612-633.
226. Chambers, R. D.; Hutchinson, J.; Musgrave, W. K. R., Polyfluoro-heterocyclic compounds. Part I. The preparation of fluoro-, chlorofluoro-, and chlorofluorohydro-pyridines. *J. Chem. Soc.* **1964**, 3573.
227. Senaweera, S. M.; Weaver, J. D., Selective Perfluoro- and Polyfluoroarylation of Meldrum's Acid. *J. Org. Chem.* **2014**, *79* (21), 10466-10476.
228. Senaweera, S. M.; Weaver, J. D., Dual C–F, C–H Functionalization via Photocatalysis; Access to Multi-Fluorinated Biaryls. *J. Am. Chem. Soc.* **2016**, *138*, 2520-2523.
229. Singh, A.; Kubik, J. J.; Weaver, J. D., Photocatalytic C-F alkylation; facile access to multifluorinated arenes. *Chem. Sci.* **2015**, *6* (12), 7206-7212.
230. Senaweera, S. M.; Singh, A.; Weaver, J. D., Photocatalytic Hydrodefluorination: Facile Access to Partially Fluorinated Aromatics. *J. Am. Chem. Soc.* **2014**, *136* (8), 3002–3005.
231. Singh, A.; Kubik, J. J.; Weaver, J. D., Photocatalytic C-F alkylation; facile access to multifluorinated arenes. *Chemical Science* **2015**, *6* (12), 7206-7212.
232. Senaweera, S.; Weaver, J. D., Photocatalytic C-F Reduction and Functionalization. *Aldrichimica Acta* **2016**, *49*, 45.
233. Senaweera, S. M.; Singh, A.; Weaver, J. D., Photocatalytic Hydrodefluorination: Facile Access to Partially Fluorinated Aromatics. *J. Am. Chem. Soc.* **2014**, *136* (8), 3002-3005.
234. Arora, A.; Weaver, J. D., Visible Light Photocatalysis for the Generation and Use of Reactive Azolyl and Polyfluoroaryl Intermediates. *Acc. Chem. Res.* **2016**, *49* (10), 2273-2283.
235. Weaver, J. D., Hydrodefluorination of Perfluoroarenes Meets Visible Light Photocatalysis. *Synlett* **2014**, *25* (14), 1946-1952.
236. LaBerge, N. A.; Love, J. A., Activation and Formation of Aromatic C–F Bonds. In *Organometallic Fluorine Chemistry*, Braun, T.; Hughes, R. P., Eds. Springer International Publishing: Cham, 2015; pp 55-111.
237. Hu, J.-Y.; Zhang, J.-L., Hydrodefluorination Reactions Catalyzed by Transition-Metal Complexes. In *Organometallic Fluorine Chemistry*, Braun, T.; Hughes, R. P., Eds. Springer International Publishing: Cham, 2015; pp 143-196.
238. Chambers, R. D.; Martin, P. A.; Sandford, G.; Williams, D. L. H., Mechanisms of reactions of halogenated compounds: Part 7. Effects of fluorine and other groups as substituents on nucleophilic aromatic substitution. *J. Fluorine Chem.* **2008**, *129* (10), 998-1002.
239. Sun, Y.; Sun, H.; Jia, J.; Du, A.; Li, X., Transition-Metal-Free Synthesis of Fluorinated Arenes from Perfluorinated Arenes Coupled with Grignard Reagents. *Organometallics* **2014**, *33* (4), 1079-1081.
240. Chambers, R. D.; Hassan, M. A.; Hoskin, P. R.; Kenwright, A.; Richmond, P.; Sandford, G., Polyhalogenated heterocyclic compounds: Part 45. Reactions of perfluoro-(4-isopropylpyridine) with oxygen, nitrogen and carbon nucleophiles [1]. *J. Fluorine Chem.* **2001**, *111* (2), 135-146.
241. Beyki, K.; Haydari, R.; Maghsoodlou, M. T., Synthesis of 2,3,5,6-tetrafluoro-pyridine derivatives from reaction of pentafluoropyridine with malononitrile, piperazine and tetrazole-5-thiol. *SpringerPlus* **2015**, *4* (1), 757.

242. Ono, N., *The Nitro Group in Organic Synthesis*. Wiley-VCH: 2001.
243. Colgin, N.; Tatum, N. J.; Pohl, E.; Cobb, S. L.; Sandford, G., Synthesis and molecular structure of a perfluorinated pyridyl carbanion. *J. Fluorine Chem.* **2012**, *133*, 33-37.
244. Vaidyanathaswamy, R.; Radha, K.; Dharani, M.; Raguraman, T. S.; Anand, R., Reaction of nitroalkanes with polyfluoroaromatic compounds. *J. Fluorine Chem.* **2012**, *144*, 33-37.
245. Prat, D.; Pardigon, O.; Flemming, H.-W.; Letestu, S.; Ducandas, V.; Isnard, P.; Guntrum, E.; Senac, T.; Ruisseau, S.; Cruciani, P.; Hosek, P., Sanofi's Solvent Selection Guide: A Step Toward More Sustainable Processes. *Organic Process Research & Development* **2013**, *17* (12), 1517-1525.
246. Bug, T.; Lemek, T.; Mayr, H., Nucleophilicities of Nitroalkyl Anions. *J. Org. Chem.* **2004**, *69* (22), 7565-7576.
247. day, Prices of TMG and DBU.
248. Calculated using Advanced Chemistry Development (ACD/Labs) Software V11.02 (© 1994-2020 ACD/Labs).
249. Lee, L.; Kreutter, K. D.; Pan, W.; Crysler, C.; Spurlino, J.; Player, M. R.; Tomczuk, B.; Lu, T., 2-(2-Chloro-6-fluorophenyl)acetamides as potent thrombin inhibitors. *Bioorg. Med. Chem. Lett.* **2007**, *17* (22), 6266-6269.
250. Parikh, V. D.; Fray, A. H.; Kleinman, E. F., Synthesis of 8,9-difluoro-2-methyl-6-oxo-1,2-dihydropyrrolo[3,2,1-ij]quinoline-5-carboxylic acid. *J. Heterocyclic Chem.* **1988**, *25* (5), 1567-1569.
251. Pesti, J. A.; LaPorte, T.; Thornton, J. E.; Spangler, L.; Buono, F.; Crispino, G.; Gibson, F.; Lobben, P.; Papaioannou, C. G., Commercial Synthesis of a Pyrrolo-triazine-Fluoroindole Intermediate to Brivanib Alaninate: Process Development Directed toward Impurity Control. *Org. Process Res. Dev.* **2014**, *18* (1), 89-102.
252. Brooke, G. M.; Burdon, J.; Tatlow, J. C., 172. Aromatic polyfluoro-compounds. Part VII. The reaction of pentafluoronitrobenzene with ammonia. *J. Chem. Soc.* **1961**, (0), 802-807.
253. Teegardin, K. A.; Weaver, J. D., Polyfluoroarylation of oxazolones: access to non-natural fluorinated amino acids. *Chemical Communications* **2017**.
254. Senaweera, S.; Weaver, J. D., *Currently unpublished work under review* **2017**.
255. Shipilov, A. I.; Zolotkova, E. E.; Igumnov, S. M., Chloro- and Bromo-defluorination of Hexafluorobenzene and Octafluorotoluene. *Russian Journal of Organic Chemistry* **2004**, *40* (8), 1117-1120.
256. Politzer, P.; Murray, J. S.; Clark, T.,  $\sigma$ -Hole Bonding: A Physical Interpretation. In *Halogen Bonding I*, Springer International Publishing Switzerland 2014: 2014; Vol. Volume 358 of the series Topics in Current Chemistry, pp 19-42.
257. Politzer, P.; Laurence, P. R.; Jayasuriya, K., Molecular electrostatic potentials: an effective tool for the elucidation of biochemical phenomena. *Environmental Health Perspectives* **1985**, *61*, 191-202.
258. Bürgi, H. B.; Dunitz, J. D.; Lehn, J. M.; Wipff, G., Stereochemistry of reaction paths at carbonyl centres. *Tetrahedron* **1974**, *30* (12), 1563-1572.
259. Billica, H. R. A., Homer, Catalyst, Raney Nickel, W-6. *Org. Synth.* **1949**, *29*, 24.
260. Subramanian, H.; Jasperse, C. P.; Sibi, M. P., Characterization of Bronsted acid-base complexes by 19F DOSY. *Org. Lett.* **2015**, *17* (6), 1429-32.
261. Gaussian 09, R. C.; Frisch, M. J.; Trucks, G. W.; Schlegel, H. B.; Scuseria, G. E.; Robb, M. A.; Cheeseman, J. R.; Scalmani, G.; Barone, V.; Mennucci, B.; Petersson, G. A.; Nakatsuji, H.; Caricato, M.; Li, X.; Hratchian, H. P.; Izmaylov, A. F.; Bloino, J.; Zheng, G.; Sonnenberg, J. L.; Hada, M.; Ehara, M.; Toyota, K.; Fukuda, R.; Hasegawa, J.; Ishida, M.; Nakajima, T.; Honda, Y.; Kitao, O.; Nakai, H.; Vreven, T.; J. A. Montgomery, J.; Peralta, J. E.; Ogliaro, F.; Bearpark, M.; Heyd, J. J.; Brothers, E.; Kudin, K. N.; Staroverov, V. N.; Keith, T.; Kobayashi, R.; Normand, J.; Raghavachari, K.; Rendell, A.; Burant, J. C.; Iyengar, S. S.; Tomasi, J.; Cossi, M.; Rega, N.; Millam, J. M.; Klene, M.; Knox, J. E.; Cross,

- J. B.; Bakken, V.; Adamo, C.; Jaramillo, J.; Gomperts, R.; Stratmann, R. E.; Yazyev, O.; Austin, A. J.; Cammi, R.; Pomelli, C.; Ochterski, J. W.; Martin, R. L.; Morokuma, K.; Zakrzewski, V. G.; Voth, G. A.; Salvador, P.; Dannenberg, J. J.; Dapprich, S.; Daniels, A. D.; Farkas, O.; Foresman, J. B.; Ortiz, J. V.; Cioslowski, J.; Fox, D. J., *Gaussian, Inc., Wallingford CT* **2010**.
262. Corey, E. J.; Tada, M.; LaMahieu, R.; Libit, L., trans-2-Cycloheptenone. *J. Am. Chem. Soc.* **1965**, *87* (9), 2051-2052.
263. Singh, K.; Fennell, C. J.; Coutsias, E. A.; Latifi, R.; Hartson, S.; Weaver, J. D., Light Harvesting for Rapid and Selective Reactions: Click Chemistry with Strain-Loadable Alkenes. *Chem-Us* **2018**, *4* (1), 124-137.
264. Wei, X.-J.; Boon, W.; Hessel, V.; Noël, T., Visible-Light Photocatalytic Decarboxylation of  $\alpha,\beta$ -Unsaturated Carboxylic Acids: Facile Access to Stereoselective Difluoromethylated Styrenes in Batch and Flow. *ACS Catalysis* **2017**, *7* (10), 7136-7140.
265. Straathof, N. J. W.; Cramer, S. E.; Hessel, V.; Noël, T., Practical Photocatalytic Trifluoromethylation and Hydrotrifluoromethylation of Styrenes in Batch and Flow. *Angew. Chem. Int. Ed.* **2016**, *55* (50), 15549-15553.
266. Lin, Q.-Y.; Xu, X.-H.; Qing, F.-L., Chemo-, Regio-, and Stereoselective Trifluoromethylation of Styrenes via Visible Light-Driven Single-Electron Transfer (SET) and Triplet-Triplet Energy Transfer (TTET) Processes. *J. Org. Chem.* **2014**, *79* (21), 10434-10446.
267. Metternich, J. B.; Gilmour, R., A Bio-Inspired, Catalytic E  $\rightarrow$  Z Isomerization of Activated Olefins. *J. Am. Chem. Soc.* **2015**, *137* (35), 11254-11257.
268. Metternich, J. B.; Gilmour, R., One Photocatalyst, n Activation Modes Strategy for Cascade Catalysis: Emulating Coumarin Biosynthesis with (-)-Riboflavin. *J. Am. Chem. Soc.* **2016**, *138* (3), 1040-1045.
269. Metternich, J. B.; Gilmour, R., Photocatalytic E  $\rightarrow$  Z Isomerization of Alkenes. *Synlett* **2016**, *27* (18), 2541-2552.
270. Rackl, D.; Kreitmeier, P.; Reiser, O., Synthesis of a polyisobutylene-tagged fac-Ir(ppy)<sub>3</sub> complex and its application as recyclable visible-light photocatalyst in a continuous flow process. *Green Chem.* **2016**, *18* (1), 214-219.
271. Rono, L. J.; Yayla, H. G.; Wang, D. Y.; Armstrong, M. F.; Knowles, R. R., Enantioselective Photoredox Catalysis Enabled by Proton-Coupled Electron Transfer: Development of an Asymmetric Aza-Pinacol Cyclization. *J. Am. Chem. Soc.* **2013**, *135* (47), 17735-17738.
272. Lian, J.-J.; Chen, P.-C.; Lin, Y.-P.; Ting, H.-C.; Liu, R.-S., Gold-Catalyzed Intramolecular [3 + 2]-Cycloaddition of Arenyne-Yne Functionalities. *J. Am. Chem. Soc.* **2006**, *128* (35), 11372-11373.
273. Monkman, A. P.; Burrows, H. D.; Hamblett, I.; Navarathnam, S.; Svensson, M.; Andersson, M. R., The effect of conjugation length on triplet energies, electron delocalization and electron-electron correlation in soluble polythiophenes. *J. Chem. Phys.* **2001**, *115* (19), 9046-9049.
274. Dexter, D. L., A Theory of Sensitized Luminescence in Solids. *J. Chem. Phys.* **1953**, *21* (5), 836-850.
275. Head-Gordon, M.; Pople, J. A.; Frisch, M. J., MP2 energy evaluation by direct methods. *Chem. Phys. Lett.* **1988**, *153* (6), 503-506.
276. Cramer, C., *Essentials of Computational Chemistry: Theories and Models*. II ed.; John Wiley & Sons: 2004; p 216.
277. Dunning, T. H., Gaussian basis sets for use in correlated molecular calculations. I. The atoms boron through neon and hydrogen. *J. Chem. Phys.* **1989**, *90* (2), 1007-1023.
278. Banister, S. D.; Arnold, J. C.; Connor, M.; Glass, M.; McGregor, I. S., Dark Classics in Chemical Neuroscience:  $\Delta^9$ -Tetrahydrocannabinol. *ACS Chemical Neuroscience* **2019**, *10* (5), 2160-2175.

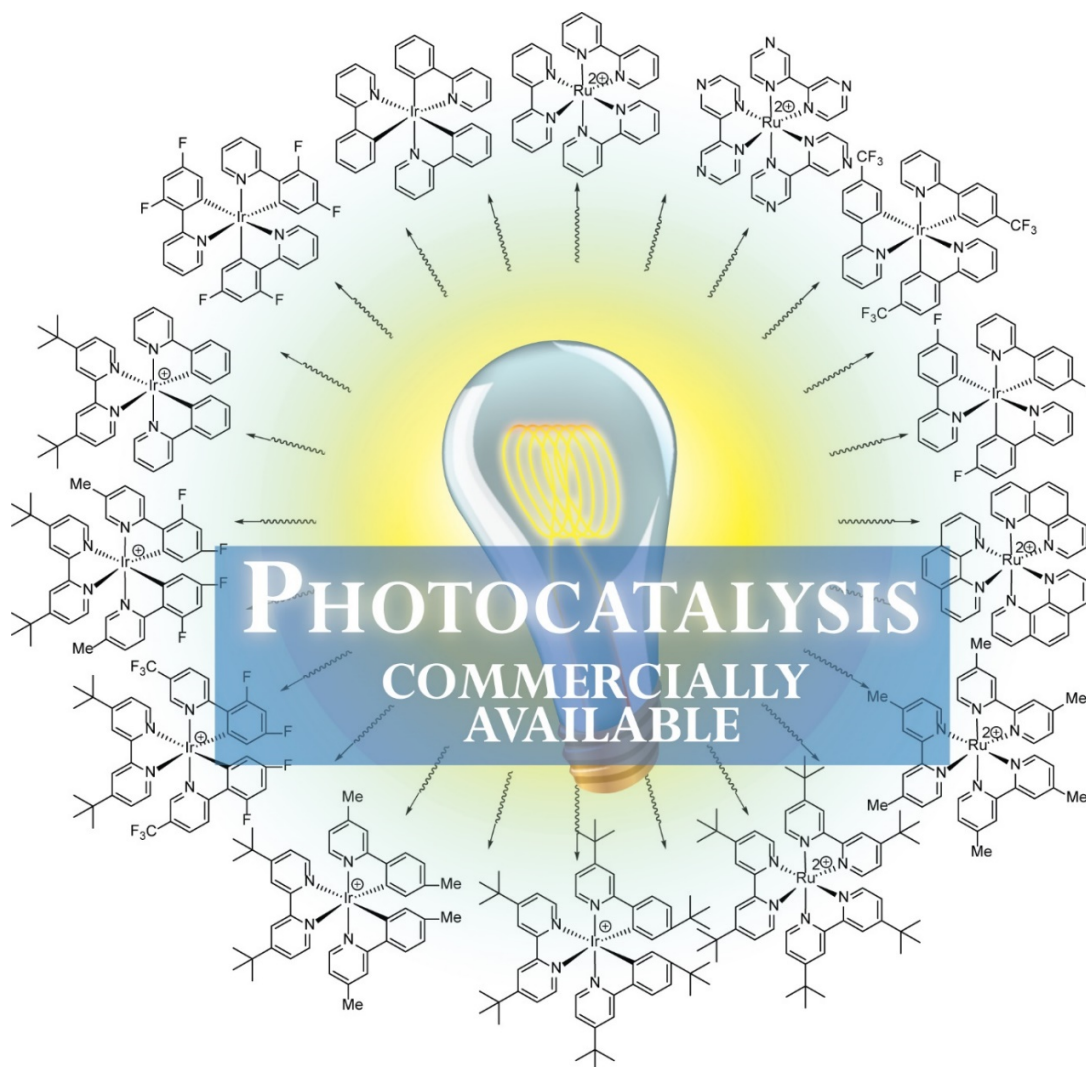
279. Teegardin, K.; Day, J. I.; Chan, J.; Weaver, J., Advances in Photocatalysis: A Microreview of Visible Light Mediated Ruthenium and Iridium Catalyzed Organic Transformations. *Org. Process Res. Dev.* **2016**, *20* (7), 1156-1163.
280. Johnson, R. P.; DiRico, K. J., Ab Initio Conformational Analysis of trans-Cyclohexene. *J Org Chem* **1995**, *60* (4), 1074-1076.
281. Bally, T.; Rablen, P. R., Quantum-Chemical Simulation of <sup>1</sup>H NMR Spectra. 2. Comparison of DFT-Based Procedures for Computing Proton-Proton Coupling Constants in Organic Molecules. *J Org Chem* **2011**, *76* (12), 4818-4830.
282. Anslyn, E.; Dougherty, D., Isotope Effects. In *Modern Physical Organic Chemistry*, University Science Books: 2006; pp 429-430.
283. Chandrasekhar, S.; Chandrashekar, G.; Reddy, M. S.; Srihari, P., A facile and chemoselective conjugate reduction using polymethylhydrosiloxane (PMHS) and catalytic B(C<sub>6</sub>F<sub>5</sub>)<sub>3</sub>. *Organic & Biomolecular Chemistry* **2006**, *4* (9), 1650-1652.
284. Günther, H., Chemical Shifts Through Hydrogen Bonding. In *NMR Spectroscopy*, John Wiley & Sons: 1995; pp 97-99.
285. Plata, R. E.; Singleton, D. A., A Case Study of the Mechanism of Alcohol-Mediated Morita Baylis-Hillman Reactions. The Importance of Experimental Observations. *J. Am. Chem. Soc.* **2015**, *137* (11), 3811-3826.
286. Winter, A., Making a bad calculation. *Nature Chem.* **2015**, *7*, 473.
287. Pettersen, E. F.; Goddard, T. D.; Huang, C. C.; Couch, G. S.; Greenblatt, D. M.; Meng, E. C.; Ferrin, T. E., UCSF Chimera--a visualization system for exploratory research and analysis. *J. Comput. Chem.* **2004**, *25* (13), 1605-12.
288. Singh, A.; Teegardin, K.; Kelly, M.; Prasad, K. S.; Krishnan, S.; Weaver, J. D., Facile synthesis and complete characterization of homoleptic and heteroleptic cyclometalated Iridium(III) complexes for photocatalysis. *Journal of Organometallic Chemistry* **2015**, *776*, 51-59.
289. Bally, T.; Rablen, P. R., Quantum-Chemical Simulation of <sup>1</sup>H NMR Spectra. 2. Comparison of DFT-Based Procedures for Computing Proton-Proton Coupling Constants in Organic Molecules. *The Journal of Organic Chemistry* **2011**, *76* (12), 4818-4830.



## CHAPTER II

### ADVANCES IN PHOTOCATALYSIS: A MICROREVIEW OF VISIBLE LIGHT MEDIATED RUTHENIUM AND IRIIDIUM CATALYZED ORGANIC TRANSFORMATIONS

#### 2.1 Overview

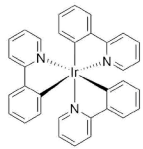
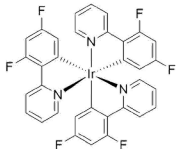
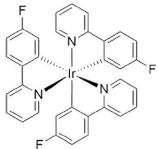
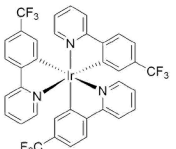
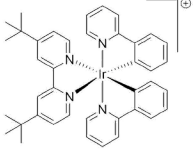
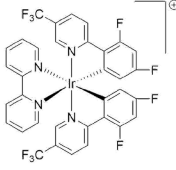
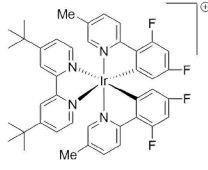
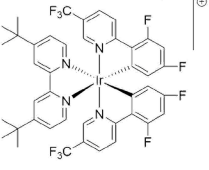
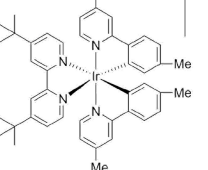
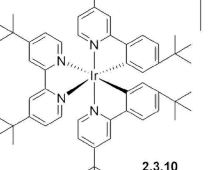
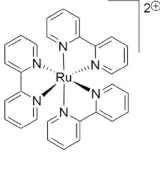
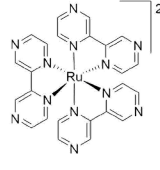
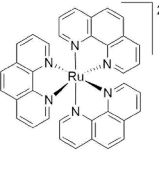
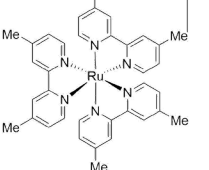
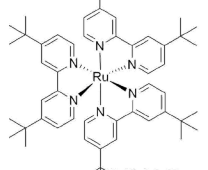


Herein is contained materials adapted from *Org. Process Res. Dev.* 2016, 20, 7, 1156-1163, which as of this thesis has been cited 104 times. This publication was an invited review of some noteworthy reactions, but more than anything was a convenient vehicle for the publication of a collection of physical data, Table 5, which I have been informed is tacked to many corkboards.

Over the course of the preceding 30 years, there have been substantial developments utilizing cyclometalated ruthenium and iridium complexes in photochemistry.<sup>155-158</sup> Historically these complexes have been primarily employed in solar cells,<sup>159</sup> light emitting diodes (LEDs),<sup>160</sup> and as initiators in free radical polymerizations.<sup>161</sup> Both of the prototypical complexes, Ru(bpy)<sub>3</sub><sup>2+</sup> and Ir(ppy)<sub>3</sub> are d<sup>6</sup>, coordinatively saturated, 18-electron complexes. When excited by visible light they undergo a metal-to-ligand-charge transfer (MLCT) from the highest occupied molecular orbital of the metal (HOMO) to the lowest unoccupied molecular orbital of the ligand (LUMO).<sup>156-157</sup> Ligands coordinated to the metal stabilize charged and singly occupied molecular orbitals (SOMOs). As a consequence, these complexes undergo both reductive and oxidative quenching pathways with relative ease,<sup>156-158</sup> which can be rationally applied in organic transformations.<sup>59, 162-165</sup> Comparison of the potential of the photocatalyst to a substrate that may undergo a redox event can suggest the likelihood of an electron transfer. However, caution should be exercised because the conditions under which the redox properties were determined are almost certainly different than the reaction conditions, and in addition may involve a nonreversible step. The former may affect the necessary potential and the latter can facilitate reactions that appear to have an underpotential.

While electron transfer serves as a means for these complexes to return to the ground state, this can also be accomplished by energy transfer to other molecules with orbitals of the appropriate energy level. Importantly, modification of the ligand scaffold provides many opportunities to tune the photophysical properties of these complexes as can be seen in surveys of the various ruthenium and iridium complexes found in current literature.<sup>156-158</sup> However, the number of complexes commercially available for use in catalysis is currently more limited. In this review, we will briefly discuss some of the electrochemical and photophysical properties of ruthenium and iridium photocatalysts which are commercially available<sup>65</sup> (Table 5) and highlight a select number of the diverse organic transformations enabled by each catalyst.

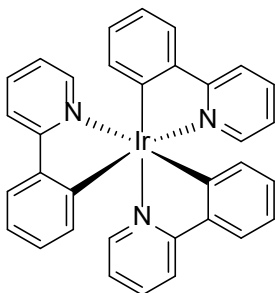
## 2.2 Photocatalyst Physical Properties

 <p><b>Section 2.3.1</b></p> <p><b>fac-Ir(ppy)<sub>3</sub></b> CAS 94928-86-6</p> <table border="1"> <thead> <tr> <th><math>\lambda_{\text{max}}</math> (excitation) nm</th> <th><math>\lambda_{\text{max}}</math> (emission) nm</th> </tr> </thead> <tbody> <tr> <td>375</td> <td>518</td> </tr> <tr> <th><math>\tau</math> ns</th> <th>Emission kcal/mol</th> </tr> <tr> <td>1900</td> <td>55.2</td> </tr> <tr> <th>E<sub>1/2</sub> Ox V</th> <th>E<sub>1/2</sub> Red V</th> </tr> <tr> <td>0.78</td> <td>-2.20</td> </tr> <tr> <th>E<sub>1/2</sub> (M<sup>+/M<sup>+</sup>) V</sup></th> <th>E<sub>1/2</sub> (M<sup>+/M<sup>+</sup>) V</sup></th> </tr> <tr> <td>-1.73</td> <td>0.31</td> </tr> <tr> <th>E<sub>gap</sub> eV</th> <th>Ref</th> </tr> <tr> <td>2.75</td> <td>23, 24, 27, 68a</td> </tr> </tbody> </table>	$\lambda_{\text{max}}$ (excitation) nm	$\lambda_{\text{max}}$ (emission) nm	375	518	$\tau$ ns	Emission kcal/mol	1900	55.2	E <sub>1/2</sub> Ox V	E <sub>1/2</sub> Red V	0.78	-2.20	E <sub>1/2</sub> (M <sup>+/M<sup>+</sup>) V</sup>	E <sub>1/2</sub> (M <sup>+/M<sup>+</sup>) V</sup>	-1.73	0.31	E <sub>gap</sub> eV	Ref	2.75	23, 24, 27, 68a	 <p><b>2.3.2</b></p> <p><b>fac-Ir(2',4'-dF-ppy)<sub>3</sub></b> CAS 387859-70-3</p> <table border="1"> <thead> <tr> <th><math>\lambda_{\text{max}}</math> (excitation) nm</th> <th><math>\lambda_{\text{max}}</math> (emission) nm</th> </tr> </thead> <tbody> <tr> <td>378</td> <td>476</td> </tr> <tr> <th><math>\tau</math> ns</th> <th>Emission kcal/mol</th> </tr> <tr> <td>1570</td> <td>60.1</td> </tr> <tr> <th>E<sub>1/2</sub> Ox V</th> <th>E<sub>1/2</sub> Red V</th> </tr> <tr> <td>0.935</td> <td>-1.87</td> </tr> <tr> <th>E<sub>1/2</sub> (M<sup>+/M<sup>+</sup>) V</sup></th> <th>E<sub>1/2</sub> (M<sup>+/M<sup>+</sup>) V</sup></th> </tr> <tr> <td>-1.28</td> <td>0.36</td> </tr> <tr> <th>E<sub>gap</sub> eV</th> <th>Ref</th> </tr> <tr> <td>2.21</td> <td>3, 24, 27, 34, 68b</td> </tr> </tbody> </table>	$\lambda_{\text{max}}$ (excitation) nm	$\lambda_{\text{max}}$ (emission) nm	378	476	$\tau$ ns	Emission kcal/mol	1570	60.1	E <sub>1/2</sub> Ox V	E <sub>1/2</sub> Red V	0.935	-1.87	E <sub>1/2</sub> (M <sup>+/M<sup>+</sup>) V</sup>	E <sub>1/2</sub> (M <sup>+/M<sup>+</sup>) V</sup>	-1.28	0.36	E <sub>gap</sub> eV	Ref	2.21	3, 24, 27, 34, 68b	 <p><b>2.3.3</b></p> <p><b>fac-Ir(4'-F-ppy)<sub>3</sub></b> CAS 370878-69-6</p> <table border="1"> <thead> <tr> <th><math>\lambda_{\text{max}}</math> (excitation) nm</th> <th><math>\lambda_{\text{max}}</math> (emission) nm</th> </tr> </thead> <tbody> <tr> <td>380</td> <td>488</td> </tr> <tr> <th><math>\tau</math> ns</th> <th>Emission kcal/mol</th> </tr> <tr> <td>2040</td> <td>58.6</td> </tr> <tr> <th>E<sub>1/2</sub> Ox V</th> <th>E<sub>1/2</sub> Red V</th> </tr> <tr> <td>0.955</td> <td>-2.18</td> </tr> <tr> <th>E<sub>1/2</sub> (M<sup>+/M<sup>+</sup>) V</sup></th> <th>E<sub>1/2</sub> (M<sup>+/M<sup>+</sup>) V</sup></th> </tr> <tr> <td>-1.905</td> <td>0.685</td> </tr> <tr> <th>E<sub>gap</sub> eV</th> <th>Ref</th> </tr> <tr> <td>2.86</td> <td>24, 27, 68c</td> </tr> </tbody> </table>	$\lambda_{\text{max}}$ (excitation) nm	$\lambda_{\text{max}}$ (emission) nm	380	488	$\tau$ ns	Emission kcal/mol	2040	58.6	E <sub>1/2</sub> Ox V	E <sub>1/2</sub> Red V	0.955	-2.18	E <sub>1/2</sub> (M <sup>+/M<sup>+</sup>) V</sup>	E <sub>1/2</sub> (M <sup>+/M<sup>+</sup>) V</sup>	-1.905	0.685	E <sub>gap</sub> eV	Ref	2.86	24, 27, 68c	 <p><b>2.3.4</b></p> <p><b>fac-Ir(4'-CF<sub>3</sub>-ppy)<sub>3</sub></b> CAS 500295-52-3</p> <table border="1"> <thead> <tr> <th><math>\lambda_{\text{max}}</math> (excitation) nm</th> <th><math>\lambda_{\text{max}}</math> (emission) nm</th> </tr> </thead> <tbody> <tr> <td>372</td> <td>507</td> </tr> <tr> <th><math>\tau</math> ns</th> <th>Emission kcal/mol</th> </tr> <tr> <td>2160</td> <td>56.4</td> </tr> <tr> <th>E<sub>1/2</sub> Ox V</th> <th>E<sub>1/2</sub> Red V</th> </tr> <tr> <td>1.065</td> <td>-2.175</td> </tr> <tr> <th>E<sub>1/2</sub> (M<sup>+/M<sup>+</sup>) V</sup></th> <th>E<sub>1/2</sub> (M<sup>+/M<sup>+</sup>) V</sup></th> </tr> <tr> <td>-1.695</td> <td>0.59</td> </tr> <tr> <th>E<sub>gap</sub> eV</th> <th>Ref</th> </tr> <tr> <td>2.76</td> <td>24, 27, 68d</td> </tr> </tbody> </table>	$\lambda_{\text{max}}$ (excitation) nm	$\lambda_{\text{max}}$ (emission) nm	372	507	$\tau$ ns	Emission kcal/mol	2160	56.4	E <sub>1/2</sub> Ox V	E <sub>1/2</sub> Red V	1.065	-2.175	E <sub>1/2</sub> (M <sup>+/M<sup>+</sup>) V</sup>	E <sub>1/2</sub> (M <sup>+/M<sup>+</sup>) V</sup>	-1.695	0.59	E <sub>gap</sub> eV	Ref	2.76	24, 27, 68d	 <p><b>2.3.5</b></p> <p><b>[Ir(ppy)<sub>2</sub>(4,4'-dtb-bpy)]PF<sub>6</sub></b> CAS 676525-77-2</p> <table border="1"> <thead> <tr> <th><math>\lambda_{\text{max}}</math> (excitation) nm</th> <th><math>\lambda_{\text{max}}</math> (emission) nm</th> </tr> </thead> <tbody> <tr> <td>410</td> <td>581</td> </tr> <tr> <th><math>\tau</math> ns</th> <th>Emission kcal/mol</th> </tr> <tr> <td>557</td> <td>49.21</td> </tr> <tr> <th>E<sub>1/2</sub> Ox V</th> <th>E<sub>1/2</sub> Red V</th> </tr> <tr> <td>1.21</td> <td>-1.51</td> </tr> <tr> <th>E<sub>1/2</sub> (M<sup>+/M<sup>+</sup>) V</sup></th> <th>E<sub>1/2</sub> (M<sup>+/M<sup>+</sup>) V</sup></th> </tr> <tr> <td>-0.96</td> <td>0.66</td> </tr> <tr> <th>E<sub>gap</sub> eV</th> <th>Ref</th> </tr> <tr> <td>n/a</td> <td>17, 18, 23, 68e</td> </tr> </tbody> </table>	$\lambda_{\text{max}}$ (excitation) nm	$\lambda_{\text{max}}$ (emission) nm	410	581	$\tau$ ns	Emission kcal/mol	557	49.21	E <sub>1/2</sub> Ox V	E <sub>1/2</sub> Red V	1.21	-1.51	E <sub>1/2</sub> (M <sup>+/M<sup>+</sup>) V</sup>	E <sub>1/2</sub> (M <sup>+/M<sup>+</sup>) V</sup>	-0.96	0.66	E <sub>gap</sub> eV	Ref	n/a	17, 18, 23, 68e
$\lambda_{\text{max}}$ (excitation) nm	$\lambda_{\text{max}}$ (emission) nm																																																																																																							
375	518																																																																																																							
$\tau$ ns	Emission kcal/mol																																																																																																							
1900	55.2																																																																																																							
E <sub>1/2</sub> Ox V	E <sub>1/2</sub> Red V																																																																																																							
0.78	-2.20																																																																																																							
E <sub>1/2</sub> (M <sup>+/M<sup>+</sup>) V</sup>	E <sub>1/2</sub> (M <sup>+/M<sup>+</sup>) V</sup>																																																																																																							
-1.73	0.31																																																																																																							
E <sub>gap</sub> eV	Ref																																																																																																							
2.75	23, 24, 27, 68a																																																																																																							
$\lambda_{\text{max}}$ (excitation) nm	$\lambda_{\text{max}}$ (emission) nm																																																																																																							
378	476																																																																																																							
$\tau$ ns	Emission kcal/mol																																																																																																							
1570	60.1																																																																																																							
E <sub>1/2</sub> Ox V	E <sub>1/2</sub> Red V																																																																																																							
0.935	-1.87																																																																																																							
E <sub>1/2</sub> (M <sup>+/M<sup>+</sup>) V</sup>	E <sub>1/2</sub> (M <sup>+/M<sup>+</sup>) V</sup>																																																																																																							
-1.28	0.36																																																																																																							
E <sub>gap</sub> eV	Ref																																																																																																							
2.21	3, 24, 27, 34, 68b																																																																																																							
$\lambda_{\text{max}}$ (excitation) nm	$\lambda_{\text{max}}$ (emission) nm																																																																																																							
380	488																																																																																																							
$\tau$ ns	Emission kcal/mol																																																																																																							
2040	58.6																																																																																																							
E <sub>1/2</sub> Ox V	E <sub>1/2</sub> Red V																																																																																																							
0.955	-2.18																																																																																																							
E <sub>1/2</sub> (M <sup>+/M<sup>+</sup>) V</sup>	E <sub>1/2</sub> (M <sup>+/M<sup>+</sup>) V</sup>																																																																																																							
-1.905	0.685																																																																																																							
E <sub>gap</sub> eV	Ref																																																																																																							
2.86	24, 27, 68c																																																																																																							
$\lambda_{\text{max}}$ (excitation) nm	$\lambda_{\text{max}}$ (emission) nm																																																																																																							
372	507																																																																																																							
$\tau$ ns	Emission kcal/mol																																																																																																							
2160	56.4																																																																																																							
E <sub>1/2</sub> Ox V	E <sub>1/2</sub> Red V																																																																																																							
1.065	-2.175																																																																																																							
E <sub>1/2</sub> (M <sup>+/M<sup>+</sup>) V</sup>	E <sub>1/2</sub> (M <sup>+/M<sup>+</sup>) V</sup>																																																																																																							
-1.695	0.59																																																																																																							
E <sub>gap</sub> eV	Ref																																																																																																							
2.76	24, 27, 68d																																																																																																							
$\lambda_{\text{max}}$ (excitation) nm	$\lambda_{\text{max}}$ (emission) nm																																																																																																							
410	581																																																																																																							
$\tau$ ns	Emission kcal/mol																																																																																																							
557	49.21																																																																																																							
E <sub>1/2</sub> Ox V	E <sub>1/2</sub> Red V																																																																																																							
1.21	-1.51																																																																																																							
E <sub>1/2</sub> (M <sup>+/M<sup>+</sup>) V</sup>	E <sub>1/2</sub> (M <sup>+/M<sup>+</sup>) V</sup>																																																																																																							
-0.96	0.66																																																																																																							
E <sub>gap</sub> eV	Ref																																																																																																							
n/a	17, 18, 23, 68e																																																																																																							
 <p><b>2.3.6</b></p> <p><b>[Ir(2',4'-dF-5-CF<sub>3</sub>-ppy)<sub>2</sub>(bpy)]PF<sub>6</sub></b> CAS n/a</p> <table border="1"> <thead> <tr> <th><math>\lambda_{\text{max}}</math> (excitation) nm</th> <th><math>\lambda_{\text{max}}</math> (emission) nm</th> </tr> </thead> <tbody> <tr> <td>405</td> <td>473</td> </tr> <tr> <th><math>\tau</math> ns</th> <th>TSE kcal/mol</th> </tr> <tr> <td>2280</td> <td>60.4</td> </tr> <tr> <th>E<sub>1/2</sub> Ox V</th> <th>E<sub>1/2</sub> Red V</th> </tr> <tr> <td>1.23</td> <td>-1.23</td> </tr> <tr> <th>E<sub>1/2</sub> (M<sup>+/M<sup>+</sup>) V</sup></th> <th>E<sub>1/2</sub> (M<sup>+/M<sup>+</sup>) V</sup></th> </tr> <tr> <td>-0.97</td> <td>0.97</td> </tr> <tr> <th>E<sub>gap</sub> eV</th> <th>Ref</th> </tr> <tr> <td>2.20</td> <td>3, 24, 37, 68f</td> </tr> </tbody> </table>	$\lambda_{\text{max}}$ (excitation) nm	$\lambda_{\text{max}}$ (emission) nm	405	473	$\tau$ ns	TSE kcal/mol	2280	60.4	E <sub>1/2</sub> Ox V	E <sub>1/2</sub> Red V	1.23	-1.23	E <sub>1/2</sub> (M <sup>+/M<sup>+</sup>) V</sup>	E <sub>1/2</sub> (M <sup>+/M<sup>+</sup>) V</sup>	-0.97	0.97	E <sub>gap</sub> eV	Ref	2.20	3, 24, 37, 68f	 <p><b>2.3.7</b></p> <p><b>[Ir(2',4'-dF-5-me-ppy)<sub>2</sub>(4,4'-dtb-bpy)]PF<sub>6</sub></b> CAS 1335047-34-1</p> <table border="1"> <thead> <tr> <th><math>\lambda_{\text{max}}</math> (excitation) nm</th> <th><math>\lambda_{\text{max}}</math> (emission) nm</th> </tr> </thead> <tbody> <tr> <td>360</td> <td>475</td> </tr> <tr> <th><math>\tau</math> ns</th> <th>Emission kcal/mol</th> </tr> <tr> <td>1221</td> <td>60.2</td> </tr> <tr> <th>E<sub>1/2</sub> Ox V</th> <th>E<sub>1/2</sub> Red V</th> </tr> <tr> <td>1.51</td> <td>-1.43</td> </tr> <tr> <th>E<sub>1/2</sub> (M<sup>+/M<sup>+</sup>) V</sup></th> <th>E<sub>1/2</sub> (M<sup>+/M<sup>+</sup>) V</sup></th> </tr> <tr> <td>-0.92</td> <td>0.97</td> </tr> <tr> <th>E<sub>gap</sub> eV</th> <th>Ref</th> </tr> <tr> <td>2.97</td> <td>28, 29, 68g</td> </tr> </tbody> </table>	$\lambda_{\text{max}}$ (excitation) nm	$\lambda_{\text{max}}$ (emission) nm	360	475	$\tau$ ns	Emission kcal/mol	1221	60.2	E <sub>1/2</sub> Ox V	E <sub>1/2</sub> Red V	1.51	-1.43	E <sub>1/2</sub> (M <sup>+/M<sup>+</sup>) V</sup>	E <sub>1/2</sub> (M <sup>+/M<sup>+</sup>) V</sup>	-0.92	0.97	E <sub>gap</sub> eV	Ref	2.97	28, 29, 68g	 <p><b>2.3.8</b></p> <p><b>[Ir(2',4'-dF-5-CF<sub>3</sub>-ppy)<sub>2</sub>(4,4'-dtb-bpy)]PF<sub>6</sub></b> CAS 870987-63-6</p> <table border="1"> <thead> <tr> <th><math>\lambda_{\text{max}}</math> (excitation) nm</th> <th><math>\lambda_{\text{max}}</math> (emission) nm</th> </tr> </thead> <tbody> <tr> <td>380</td> <td>470</td> </tr> <tr> <th><math>\tau</math> ns</th> <th>Emission kcal/mol</th> </tr> <tr> <td>2300</td> <td>60.1</td> </tr> <tr> <th>E<sub>1/2</sub> Ox V</th> <th>E<sub>1/2</sub> Red V</th> </tr> <tr> <td>1.69</td> <td>-1.37</td> </tr> <tr> <th>E<sub>1/2</sub> (M<sup>+/M<sup>+</sup>) V</sup></th> <th>E<sub>1/2</sub> (M<sup>+/M<sup>+</sup>) V</sup></th> </tr> <tr> <td>-0.89</td> <td>1.21</td> </tr> <tr> <th>E<sub>gap</sub> eV</th> <th>Ref</th> </tr> <tr> <td>2.20</td> <td>18, 23, 27, 68h</td> </tr> </tbody> </table>	$\lambda_{\text{max}}$ (excitation) nm	$\lambda_{\text{max}}$ (emission) nm	380	470	$\tau$ ns	Emission kcal/mol	2300	60.1	E <sub>1/2</sub> Ox V	E <sub>1/2</sub> Red V	1.69	-1.37	E <sub>1/2</sub> (M <sup>+/M<sup>+</sup>) V</sup>	E <sub>1/2</sub> (M <sup>+/M<sup>+</sup>) V</sup>	-0.89	1.21	E <sub>gap</sub> eV	Ref	2.20	18, 23, 27, 68h	 <p><b>2.3.9</b></p> <p><b>[Ir(3,4'-dm-ppy)<sub>2</sub>(4,4'-dtb-bpy)]PF<sub>6</sub></b> CAS 1607469-49-7</p> <table border="1"> <thead> <tr> <th><math>\lambda_{\text{max}}</math> (excitation) nm</th> <th><math>\lambda_{\text{max}}</math> (emission) nm</th> </tr> </thead> <tbody> <tr> <td>450</td> <td>597</td> </tr> <tr> <th><math>\tau</math> ns</th> <th>Emission kcal/mol</th> </tr> <tr> <td>n/a</td> <td>47.89</td> </tr> <tr> <th>E<sub>1/2</sub> Ox V</th> <th>E<sub>1/2</sub> Red V</th> </tr> <tr> <td>1.208</td> <td>-1.524</td> </tr> <tr> <th>E<sub>1/2</sub> (M<sup>+/M<sup>+</sup>) V</sup></th> <th>E<sub>1/2</sub> (M<sup>+/M<sup>+</sup>) V</sup></th> </tr> <tr> <td>-0.868</td> <td>0.552</td> </tr> <tr> <th>E<sub>gap</sub> eV</th> <th>Ref</th> </tr> <tr> <td>2.076</td> <td>16, 68i</td> </tr> </tbody> </table>	$\lambda_{\text{max}}$ (excitation) nm	$\lambda_{\text{max}}$ (emission) nm	450	597	$\tau$ ns	Emission kcal/mol	n/a	47.89	E <sub>1/2</sub> Ox V	E <sub>1/2</sub> Red V	1.208	-1.524	E <sub>1/2</sub> (M <sup>+/M<sup>+</sup>) V</sup>	E <sub>1/2</sub> (M <sup>+/M<sup>+</sup>) V</sup>	-0.868	0.552	E <sub>gap</sub> eV	Ref	2.076	16, 68i	 <p><b>2.3.10</b></p> <p><b>[Ir(4,4'-dtb-ppy)<sub>2</sub>(3,4'-dtb-bpy)]PF<sub>6</sub></b> CAS 808142-80-5</p> <table border="1"> <thead> <tr> <th><math>\lambda_{\text{max}}</math> (excitation) nm</th> <th><math>\lambda_{\text{max}}</math> (emission) nm</th> </tr> </thead> <tbody> <tr> <td>n/a</td> <td>583</td> </tr> <tr> <th><math>\tau</math> ns</th> <th>Emission kcal/mol</th> </tr> <tr> <td>444</td> <td>49.04</td> </tr> <tr> <th>E<sub>1/2</sub> Ox V</th> <th>E<sub>1/2</sub> Red V</th> </tr> <tr> <td>n/a</td> <td>n/a</td> </tr> <tr> <th>E<sub>1/2</sub> (M<sup>+/M<sup>+</sup>) V</sup></th> <th>E<sub>1/2</sub> (M<sup>+/M<sup>+</sup>) V</sup></th> </tr> <tr> <td>n/a</td> <td>n/a</td> </tr> <tr> <th>E<sub>gap</sub> eV</th> <th>Ref</th> </tr> <tr> <td>n/a</td> <td>18, 68j</td> </tr> </tbody> </table>	$\lambda_{\text{max}}$ (excitation) nm	$\lambda_{\text{max}}$ (emission) nm	n/a	583	$\tau$ ns	Emission kcal/mol	444	49.04	E <sub>1/2</sub> Ox V	E <sub>1/2</sub> Red V	n/a	n/a	E <sub>1/2</sub> (M <sup>+/M<sup>+</sup>) V</sup>	E <sub>1/2</sub> (M <sup>+/M<sup>+</sup>) V</sup>	n/a	n/a	E <sub>gap</sub> eV	Ref	n/a	18, 68j
$\lambda_{\text{max}}$ (excitation) nm	$\lambda_{\text{max}}$ (emission) nm																																																																																																							
405	473																																																																																																							
$\tau$ ns	TSE kcal/mol																																																																																																							
2280	60.4																																																																																																							
E <sub>1/2</sub> Ox V	E <sub>1/2</sub> Red V																																																																																																							
1.23	-1.23																																																																																																							
E <sub>1/2</sub> (M <sup>+/M<sup>+</sup>) V</sup>	E <sub>1/2</sub> (M <sup>+/M<sup>+</sup>) V</sup>																																																																																																							
-0.97	0.97																																																																																																							
E <sub>gap</sub> eV	Ref																																																																																																							
2.20	3, 24, 37, 68f																																																																																																							
$\lambda_{\text{max}}$ (excitation) nm	$\lambda_{\text{max}}$ (emission) nm																																																																																																							
360	475																																																																																																							
$\tau$ ns	Emission kcal/mol																																																																																																							
1221	60.2																																																																																																							
E <sub>1/2</sub> Ox V	E <sub>1/2</sub> Red V																																																																																																							
1.51	-1.43																																																																																																							
E <sub>1/2</sub> (M <sup>+/M<sup>+</sup>) V</sup>	E <sub>1/2</sub> (M <sup>+/M<sup>+</sup>) V</sup>																																																																																																							
-0.92	0.97																																																																																																							
E <sub>gap</sub> eV	Ref																																																																																																							
2.97	28, 29, 68g																																																																																																							
$\lambda_{\text{max}}$ (excitation) nm	$\lambda_{\text{max}}$ (emission) nm																																																																																																							
380	470																																																																																																							
$\tau$ ns	Emission kcal/mol																																																																																																							
2300	60.1																																																																																																							
E <sub>1/2</sub> Ox V	E <sub>1/2</sub> Red V																																																																																																							
1.69	-1.37																																																																																																							
E <sub>1/2</sub> (M <sup>+/M<sup>+</sup>) V</sup>	E <sub>1/2</sub> (M <sup>+/M<sup>+</sup>) V</sup>																																																																																																							
-0.89	1.21																																																																																																							
E <sub>gap</sub> eV	Ref																																																																																																							
2.20	18, 23, 27, 68h																																																																																																							
$\lambda_{\text{max}}$ (excitation) nm	$\lambda_{\text{max}}$ (emission) nm																																																																																																							
450	597																																																																																																							
$\tau$ ns	Emission kcal/mol																																																																																																							
n/a	47.89																																																																																																							
E <sub>1/2</sub> Ox V	E <sub>1/2</sub> Red V																																																																																																							
1.208	-1.524																																																																																																							
E <sub>1/2</sub> (M <sup>+/M<sup>+</sup>) V</sup>	E <sub>1/2</sub> (M <sup>+/M<sup>+</sup>) V</sup>																																																																																																							
-0.868	0.552																																																																																																							
E <sub>gap</sub> eV	Ref																																																																																																							
2.076	16, 68i																																																																																																							
$\lambda_{\text{max}}$ (excitation) nm	$\lambda_{\text{max}}$ (emission) nm																																																																																																							
n/a	583																																																																																																							
$\tau$ ns	Emission kcal/mol																																																																																																							
444	49.04																																																																																																							
E <sub>1/2</sub> Ox V	E <sub>1/2</sub> Red V																																																																																																							
n/a	n/a																																																																																																							
E <sub>1/2</sub> (M <sup>+/M<sup>+</sup>) V</sup>	E <sub>1/2</sub> (M <sup>+/M<sup>+</sup>) V</sup>																																																																																																							
n/a	n/a																																																																																																							
E <sub>gap</sub> eV	Ref																																																																																																							
n/a	18, 68j																																																																																																							
 <p><b>2.3.10</b></p> <p><b>[Ru(bpy)<sub>3</sub>](PF<sub>6</sub>)<sub>2</sub></b> CAS 60804-74-2</p> <table border="1"> <thead> <tr> <th><math>\lambda_{\text{max}}</math> (excitation) nm</th> <th><math>\lambda_{\text{max}}</math> (emission) nm</th> </tr> </thead> <tbody> <tr> <td>452</td> <td>615</td> </tr> <tr> <th><math>\tau</math> ns</th> <th>Emission kcal/mol</th> </tr> <tr> <td>1100</td> <td>46.49</td> </tr> <tr> <th>E<sub>1/2</sub> Ox V</th> <th>E<sub>1/2</sub> Red V</th> </tr> <tr> <td>1.29</td> <td>-1.33</td> </tr> <tr> <th>E<sub>1/2</sub> (M<sup>+/M<sup>+</sup>) V</sup></th> <th>E<sub>1/2</sub> (M<sup>+/M<sup>+</sup>) V</sup></th> </tr> <tr> <td>-0.81</td> <td>0.77</td> </tr> <tr> <th>E<sub>gap</sub> eV</th> <th>Ref</th> </tr> <tr> <td>n/a</td> <td>19, 23, 68k</td> </tr> </tbody> </table>	$\lambda_{\text{max}}$ (excitation) nm	$\lambda_{\text{max}}$ (emission) nm	452	615	$\tau$ ns	Emission kcal/mol	1100	46.49	E <sub>1/2</sub> Ox V	E <sub>1/2</sub> Red V	1.29	-1.33	E <sub>1/2</sub> (M <sup>+/M<sup>+</sup>) V</sup>	E <sub>1/2</sub> (M <sup>+/M<sup>+</sup>) V</sup>	-0.81	0.77	E <sub>gap</sub> eV	Ref	n/a	19, 23, 68k	 <p><b>2.3.12</b></p> <p><b>[Ru(bpz)<sub>3</sub>](PF<sub>6</sub>)<sub>2</sub></b> CAS 80907-56-8</p> <table border="1"> <thead> <tr> <th><math>\lambda_{\text{max}}</math> (excitation) nm</th> <th><math>\lambda_{\text{max}}</math> (emission) nm</th> </tr> </thead> <tbody> <tr> <td>443</td> <td>591</td> </tr> <tr> <th><math>\tau</math> ns</th> <th>Emission kcal/mol</th> </tr> <tr> <td>740</td> <td>48.38</td> </tr> <tr> <th>E<sub>1/2</sub> Ox V</th> <th>E<sub>1/2</sub> Red V</th> </tr> <tr> <td>1.86</td> <td>-0.80</td> </tr> <tr> <th>E<sub>1/2</sub> (M<sup>+/M<sup>+</sup>) V</sup></th> <th>E<sub>1/2</sub> (M<sup>+/M<sup>+</sup>) V</sup></th> </tr> <tr> <td>-0.26</td> <td>1.45</td> </tr> <tr> <th>E<sub>gap</sub> eV</th> <th>Ref</th> </tr> <tr> <td>n/a</td> <td>21, 23, 68l</td> </tr> </tbody> </table>	$\lambda_{\text{max}}$ (excitation) nm	$\lambda_{\text{max}}$ (emission) nm	443	591	$\tau$ ns	Emission kcal/mol	740	48.38	E <sub>1/2</sub> Ox V	E <sub>1/2</sub> Red V	1.86	-0.80	E <sub>1/2</sub> (M <sup>+/M<sup>+</sup>) V</sup>	E <sub>1/2</sub> (M <sup>+/M<sup>+</sup>) V</sup>	-0.26	1.45	E <sub>gap</sub> eV	Ref	n/a	21, 23, 68l	 <p><b>2.3.13</b></p> <p><b>[Ru(phen)<sub>3</sub>](PF<sub>6</sub>)<sub>2</sub></b> CAS 28277-60-3</p> <table border="1"> <thead> <tr> <th><math>\lambda_{\text{max}}</math> (excitation) nm</th> <th><math>\lambda_{\text{max}}</math> (emission) nm</th> </tr> </thead> <tbody> <tr> <td>447</td> <td>610</td> </tr> <tr> <th><math>\tau</math> ns</th> <th>Emission kcal/mol</th> </tr> <tr> <td>500</td> <td>46.87</td> </tr> <tr> <th>E<sub>1/2</sub> Ox V</th> <th>E<sub>1/2</sub> Red V</th> </tr> <tr> <td>1.26</td> <td>-1.36</td> </tr> <tr> <th>E<sub>1/2</sub> (M<sup>+/M<sup>+</sup>) V</sup></th> <th>E<sub>1/2</sub> (M<sup>+/M<sup>+</sup>) V</sup></th> </tr> <tr> <td>-0.87</td> <td>0.82</td> </tr> <tr> <th>E<sub>gap</sub> eV</th> <th>Ref</th> </tr> <tr> <td>2.18</td> <td>22, 23, 35, 68m</td> </tr> </tbody> </table>	$\lambda_{\text{max}}$ (excitation) nm	$\lambda_{\text{max}}$ (emission) nm	447	610	$\tau$ ns	Emission kcal/mol	500	46.87	E <sub>1/2</sub> Ox V	E <sub>1/2</sub> Red V	1.26	-1.36	E <sub>1/2</sub> (M <sup>+/M<sup>+</sup>) V</sup>	E <sub>1/2</sub> (M <sup>+/M<sup>+</sup>) V</sup>	-0.87	0.82	E <sub>gap</sub> eV	Ref	2.18	22, 23, 35, 68m	 <p><b>2.3.14</b></p> <p><b>[Ru(4,4'-dm-bpy)<sub>2</sub>](PF<sub>6</sub>)<sub>2</sub></b> CAS 83605-44-1</p> <table border="1"> <thead> <tr> <th><math>\lambda_{\text{max}}</math> (excitation) nm</th> <th><math>\lambda_{\text{max}}</math> (emission) nm</th> </tr> </thead> <tbody> <tr> <td>457</td> <td>632</td> </tr> <tr> <th><math>\tau</math> ns</th> <th>Emission kcal/mol</th> </tr> <tr> <td>875</td> <td>45.32</td> </tr> <tr> <th>E<sub>1/2</sub> Ox V</th> <th>E<sub>1/2</sub> Red V</th> </tr> <tr> <td>1.14</td> <td>-1.43</td> </tr> <tr> <th>E<sub>1/2</sub> (M<sup>+/M<sup>+</sup>) V</sup></th> <th>E<sub>1/2</sub> (M<sup>+/M<sup>+</sup>) V</sup></th> </tr> <tr> <td>n/a</td> <td>0.22</td> </tr> <tr> <th>E<sub>gap</sub> eV</th> <th>Ref</th> </tr> <tr> <td>2.57</td> <td>30, 31, 32, 36, 68n</td> </tr> </tbody> </table>	$\lambda_{\text{max}}$ (excitation) nm	$\lambda_{\text{max}}$ (emission) nm	457	632	$\tau$ ns	Emission kcal/mol	875	45.32	E <sub>1/2</sub> Ox V	E <sub>1/2</sub> Red V	1.14	-1.43	E <sub>1/2</sub> (M <sup>+/M<sup>+</sup>) V</sup>	E <sub>1/2</sub> (M <sup>+/M<sup>+</sup>) V</sup>	n/a	0.22	E <sub>gap</sub> eV	Ref	2.57	30, 31, 32, 36, 68n	 <p><b>2.3.15</b></p> <p><b>[Ru(4,4'-dtb-bpy)<sub>2</sub>](PF<sub>6</sub>)<sub>2</sub></b> CAS 75777-87-6</p> <table border="1"> <thead> <tr> <th><math>\lambda_{\text{max}}</math> (excitation) nm</th> <th><math>\lambda_{\text{max}}</math> (emission) nm</th> </tr> </thead> <tbody> <tr> <td>459</td> <td>614</td> </tr> <tr> <th><math>\tau</math> ns</th> <th>Emission kcal/mol</th> </tr> <tr> <td>990</td> <td>46.56</td> </tr> <tr> <th>E<sub>1/2</sub> Ox V</th> <th>E<sub>1/2</sub> Red V</th> </tr> <tr> <td>n/a</td> <td>n/a</td> </tr> <tr> <th>E<sub>1/2</sub> (M<sup>+/M<sup>+</sup>) V</sup></th> <th>E<sub>1/2</sub> (M<sup>+/M<sup>+</sup>) V</sup></th> </tr> <tr> <td>n/a</td> <td>n/a</td> </tr> <tr> <th>E<sub>gap</sub> eV</th> <th>Ref</th> </tr> <tr> <td>n/a</td> <td>18, 31, 32, 33, 68o</td> </tr> </tbody> </table>	$\lambda_{\text{max}}$ (excitation) nm	$\lambda_{\text{max}}$ (emission) nm	459	614	$\tau$ ns	Emission kcal/mol	990	46.56	E <sub>1/2</sub> Ox V	E <sub>1/2</sub> Red V	n/a	n/a	E <sub>1/2</sub> (M <sup>+/M<sup>+</sup>) V</sup>	E <sub>1/2</sub> (M <sup>+/M<sup>+</sup>) V</sup>	n/a	n/a	E <sub>gap</sub> eV	Ref	n/a	18, 31, 32, 33, 68o
$\lambda_{\text{max}}$ (excitation) nm	$\lambda_{\text{max}}$ (emission) nm																																																																																																							
452	615																																																																																																							
$\tau$ ns	Emission kcal/mol																																																																																																							
1100	46.49																																																																																																							
E <sub>1/2</sub> Ox V	E <sub>1/2</sub> Red V																																																																																																							
1.29	-1.33																																																																																																							
E <sub>1/2</sub> (M <sup>+/M<sup>+</sup>) V</sup>	E <sub>1/2</sub> (M <sup>+/M<sup>+</sup>) V</sup>																																																																																																							
-0.81	0.77																																																																																																							
E <sub>gap</sub> eV	Ref																																																																																																							
n/a	19, 23, 68k																																																																																																							
$\lambda_{\text{max}}$ (excitation) nm	$\lambda_{\text{max}}$ (emission) nm																																																																																																							
443	591																																																																																																							
$\tau$ ns	Emission kcal/mol																																																																																																							
740	48.38																																																																																																							
E <sub>1/2</sub> Ox V	E <sub>1/2</sub> Red V																																																																																																							
1.86	-0.80																																																																																																							
E <sub>1/2</sub> (M <sup>+/M<sup>+</sup>) V</sup>	E <sub>1/2</sub> (M <sup>+/M<sup>+</sup>) V</sup>																																																																																																							
-0.26	1.45																																																																																																							
E <sub>gap</sub> eV	Ref																																																																																																							
n/a	21, 23, 68l																																																																																																							
$\lambda_{\text{max}}$ (excitation) nm	$\lambda_{\text{max}}$ (emission) nm																																																																																																							
447	610																																																																																																							
$\tau$ ns	Emission kcal/mol																																																																																																							
500	46.87																																																																																																							
E <sub>1/2</sub> Ox V	E <sub>1/2</sub> Red V																																																																																																							
1.26	-1.36																																																																																																							
E <sub>1/2</sub> (M <sup>+/M<sup>+</sup>) V</sup>	E <sub>1/2</sub> (M <sup>+/M<sup>+</sup>) V</sup>																																																																																																							
-0.87	0.82																																																																																																							
E <sub>gap</sub> eV	Ref																																																																																																							
2.18	22, 23, 35, 68m																																																																																																							
$\lambda_{\text{max}}$ (excitation) nm	$\lambda_{\text{max}}$ (emission) nm																																																																																																							
457	632																																																																																																							
$\tau$ ns	Emission kcal/mol																																																																																																							
875	45.32																																																																																																							
E <sub>1/2</sub> Ox V	E <sub>1/2</sub> Red V																																																																																																							
1.14	-1.43																																																																																																							
E <sub>1/2</sub> (M <sup>+/M<sup>+</sup>) V</sup>	E <sub>1/2</sub> (M <sup>+/M<sup>+</sup>) V</sup>																																																																																																							
n/a	0.22																																																																																																							
E <sub>gap</sub> eV	Ref																																																																																																							
2.57	30, 31, 32, 36, 68n																																																																																																							
$\lambda_{\text{max}}$ (excitation) nm	$\lambda_{\text{max}}$ (emission) nm																																																																																																							
459	614																																																																																																							
$\tau$ ns	Emission kcal/mol																																																																																																							
990	46.56																																																																																																							
E <sub>1/2</sub> Ox V	E <sub>1/2</sub> Red V																																																																																																							
n/a	n/a																																																																																																							
E <sub>1/2</sub> (M <sup>+/M<sup>+</sup>) V</sup>	E <sub>1/2</sub> (M <sup>+/M<sup>+</sup>) V</sup>																																																																																																							
n/a	n/a																																																																																																							
E <sub>gap</sub> eV	Ref																																																																																																							
n/a	18, 31, 32, 33, 68o																																																																																																							

**TABLE 5.** Photophysical properties of selected commercially available photocatalysts.<sup>74, 156-157, 166-186,68</sup> Potentials vs. saturated calomel electrode (SCE). n/a: information not available.

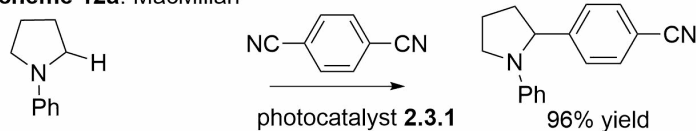
## 2.3 Photocatalyst Details

### 2.3.1 *fac*-Ir(ppy)<sub>3</sub>

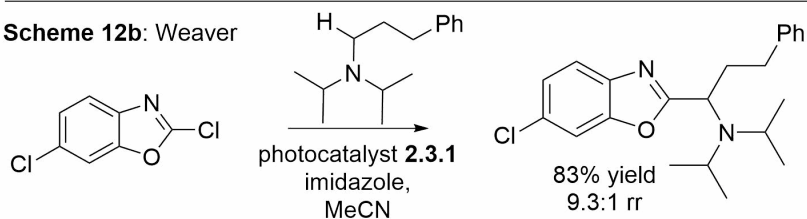


There has been significant progress in  $\alpha$ -C–H functionalization of amines in photocatalysis, including the arylation of tertiary amines by MacMillan and coworkers,<sup>187</sup> (Scheme 12a), the azoylation of aliphatic amines by our own lab<sup>188</sup> (Scheme 12b), and the C–H amidation of unfunctionalized indoles with hydroxyl amines by Yu and coworkers<sup>189</sup> (Scheme 12c), all of which use the prototypical catalyst **2.3.1**.

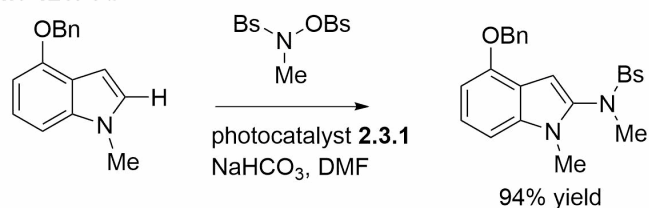
Scheme 12a: MacMillan



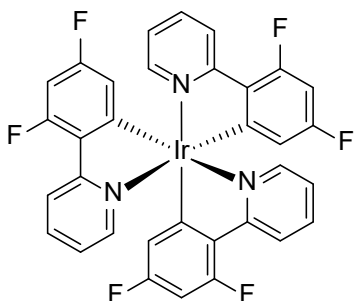
Scheme 12b: Weaver



Scheme 12c: Yu

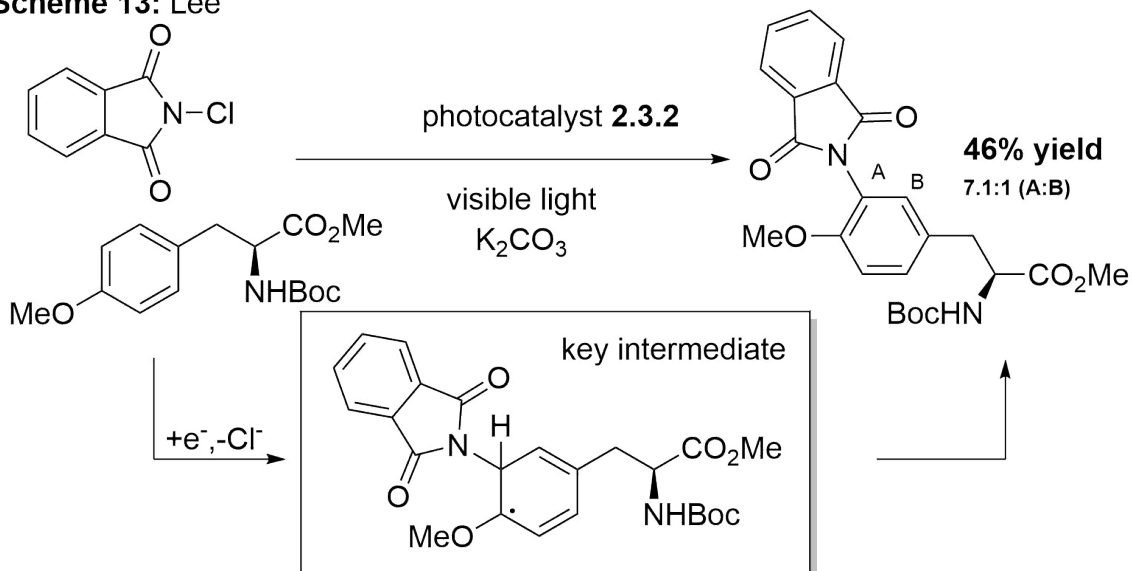


### 2.3.2 *fac*-Ir(2',4'-dF-ppy)<sub>3</sub>

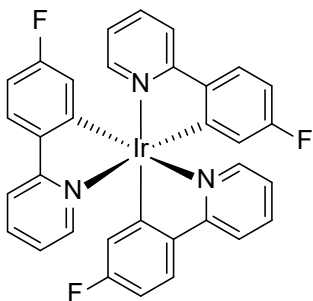


Lee and coworkers<sup>190</sup> utilized **2.3.2** to initiate a C–H imidation of heteroarenes with *N*-chlorophthalimide. After initially investigating **2.3.1**, photocatalyst **2.3.2** proved to be the superior catalyst. The reaction likely proceeds through a *N*-radical intermediate initiated by electron transfer from excited **2.3.2**, which undergoes radical addition to the arene partner. The hexadienyl radical serves to reduce the catalyst leading to rearomatization (Scheme 13). The scope consists of various substituted arenes with modest yields and regioselectivity.

**Scheme 13:** Lee

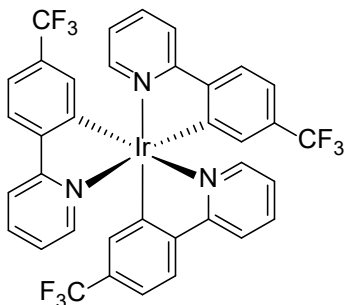


### 2.3.3 *fac*-Ir(4'-F-ppy)<sub>3</sub>



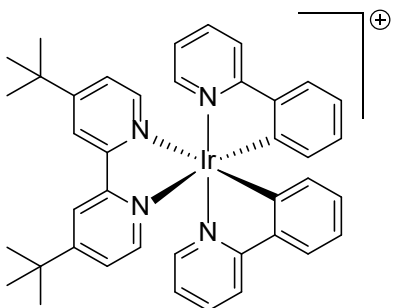
While current literature references are limited, and transformations that utilize photocatalyst **2.3.3** as an optimal catalyst are presently absent, it is noteworthy that the catalyst is being employed. Our group<sup>155, 191</sup> has routinely used **2.3.3** in our standard catalyst screen, and likewise Ooi and coworkers<sup>192</sup> synthesized this catalyst in their asymmetric  $\alpha$ -coupling of *N*-arylaminoethanes and used the photocatalyst in their optimization experiments. **2.3.3** is thus included in order to provide electrochemical and photophysical data.

### 2.3.4 *fac*-Ir(4'-CF<sub>3</sub>-ppy)<sub>3</sub>



Photocatalyst **2.3.4** is another photocatalyst that has now become commercially available but has yet to have been demonstrated to be an optimal catalyst in current organic transformations. Our group<sup>155, 193</sup> has and will continue to employ **2.3.4** in our standard catalyst screens.

### 2.3.5 [Ir(ppy)<sub>2</sub>(4,4'-dtb-bpy)]PF<sub>6</sub>

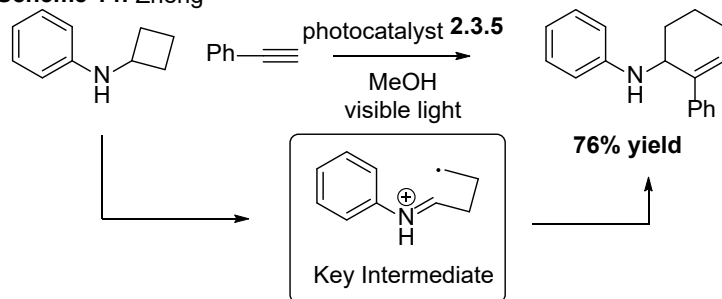


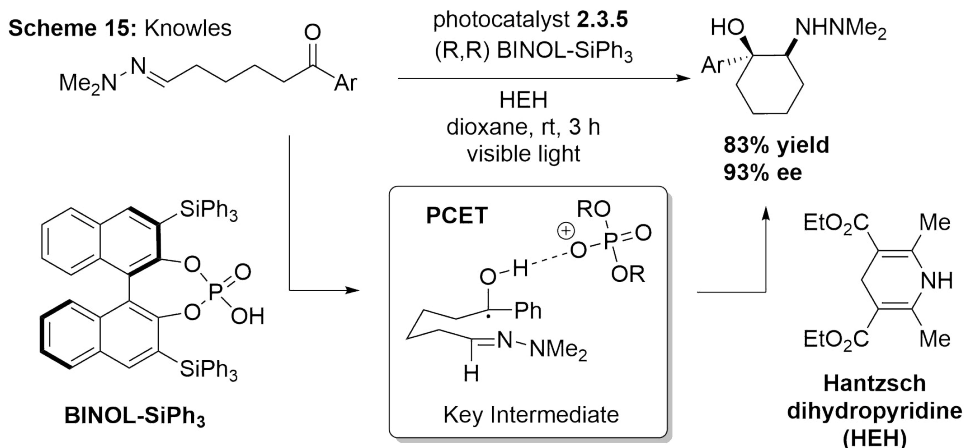
Advances have been made recently in photocatalytic biomass remediation. Stephenson and coworkers<sup>194</sup> utilized visible light and **2.3.5** in a photoflow reactor to degrade lignin biomass model substrates, in a two-step reaction sequence (not shown).

In 2015, Zheng<sup>195</sup> demonstrated that cyclobutylanilines could undergo a ring-opening [4+2] reaction with alkynes using **2.3.5**. They proposed that the reaction likely proceeds through a distonic radical cation. Excellent yields were achieved using various aliphatic cyclobutylanilines and bicyclic amines (Scheme 14).

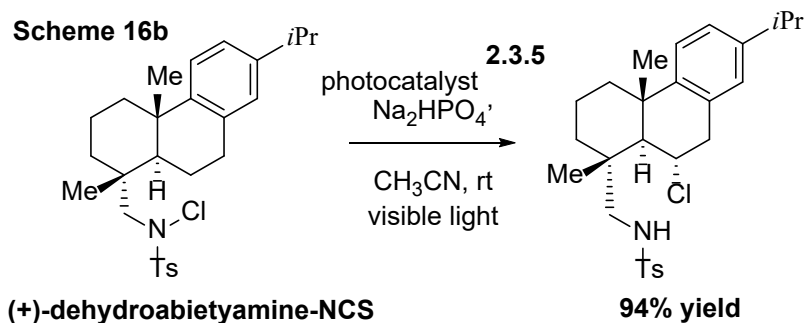
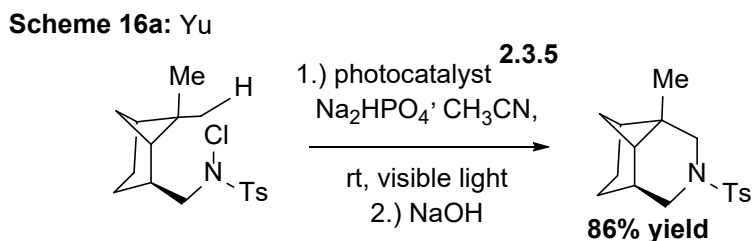
In 2013, Knowles and coworkers<sup>196</sup> used **2.3.5** in concert with binol-derived phosphoric acid to perform an asymmetric aza-pinacol cyclization with excellent yields and enantiomeric excess (ee) (Scheme 15). Electron transfer to the ketone only occurred when it was protonated by the chiral acid, allowing the C–C formation to take place enantioselectively.

Scheme 14: Zheng



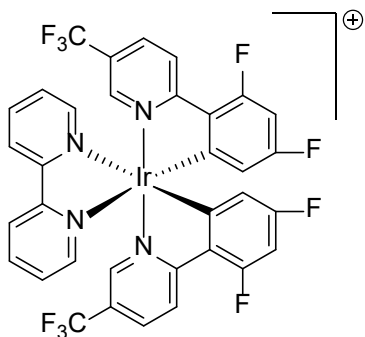


In 2015, Yu<sup>197</sup> reported a visible light mediated remote C–H chlorination of aliphatic and benzylic amines (Scheme 16a) using **2.3.5** which took advantage of the ease of *N*-chlorination to functionalize a distant and far less reactive C–H bond on the same molecule. The reaction likely takes place via a 1,5-atom transfer, which upon addition of NaOH provides the subsequent cyclization product. Yu went on to apply the methodology to the late stage functionalization of the antitumor drug (+)-dehydroabietyamine (Scheme 16b) to produce a chlorinated version of the pharmacophore.



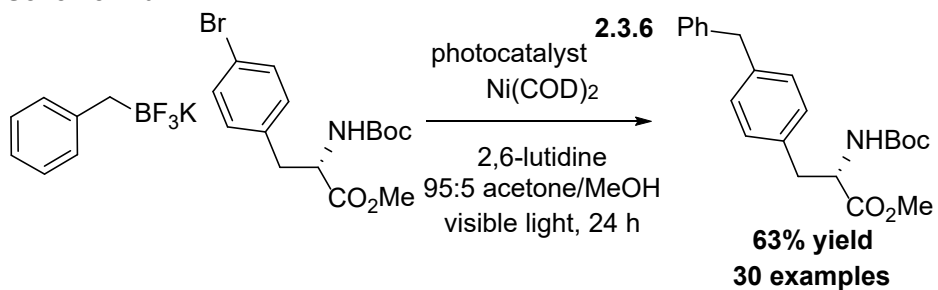


### 2.3.6 [Ir(2',4'-dF-5-CF3-ppy)<sub>2</sub>(bpy)]PF<sub>6</sub>

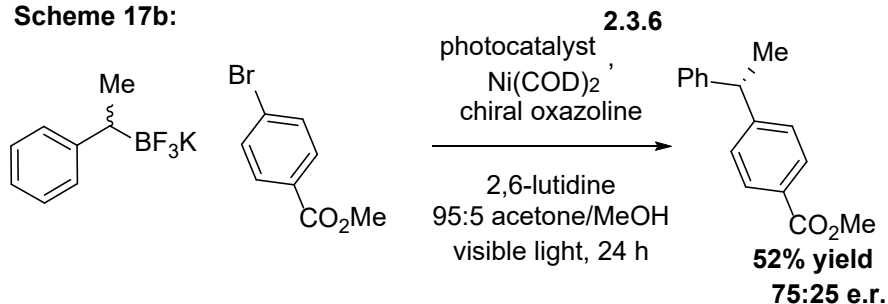


While photocatalysis has resulted in a number of enabling methods, there has also been a significant increase in the development and use of photocatalysis in concert with other transition-metal chemistry, which is just beginning to reveal new mechanistic possibilities. Molander<sup>198</sup> demonstrated a recent example of photocatalysis being used in concert with other transition-metal catalysis. The group demonstrated a single-electron transmetalation in organoboron cross-coupling using Ni(0). The traditional two-electron transmetalation cleaves the C–B bond heterolytically, giving lower or no reactivity in regards to sp<sup>3</sup> hybridized carbons.<sup>199</sup> Molander and coworkers demonstrated that a photocatalytic single-electron transfer (SET) using **2.3.6** enables cleavage of the C–B bond to occur homolytically, effectively reversing the order of reactivity (sp<sup>3</sup>>sp<sup>2</sup>>sp) and correlates to radical stability.<sup>200</sup> A wide variety of aryl halide partners were shown to be compatible (Scheme 17a). Furthermore, it was demonstrated that stereoselectivity is possible with help of photoredox cross-coupling and a chiral ligand (Scheme 17b).

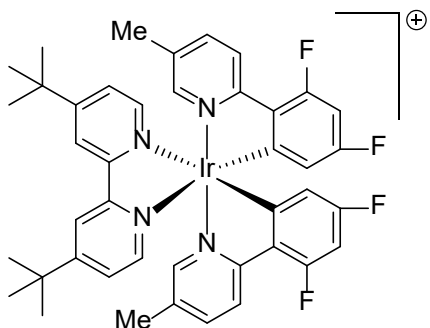
**Scheme 17a:**



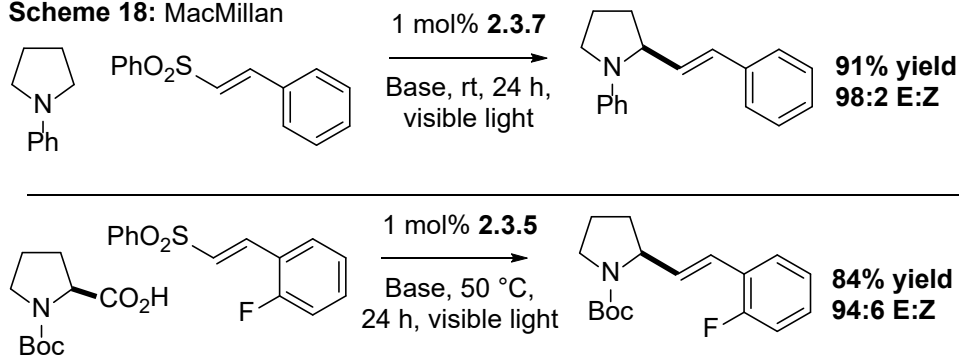
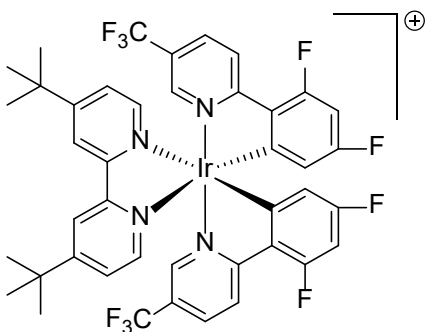
**Scheme 17b:**



**2.3.7**  $[\text{Ir}(\text{2}',\text{4}'\text{-dF-5-me-ppy})_2(\text{4},\text{4}'\text{-dtb-bpy})]\text{PF}_6$



MacMillan et al. showed that *N*-aryl amines could undergo selective C–H vinylation utilizing vinyl sulfones and photocatalyst **2.3.7** in good yields and E:Z selectivity. The methodology could be extended to *N*-Boc  $\alpha$ -amino acids as well (via decarboxylation), though a change to catalyst **2.3.5** was necessary (Scheme 18).<sup>201</sup>

**Scheme 18: MacMillan****2.3.8** [Ir(2',4'-dF-5-CF<sub>3</sub>-ppy)<sub>2</sub>(4,4'-dtb-bpy)]PF<sub>6</sub>

Photocatalysis has also been used in the derivatization of natural products into biologically interesting molecules in both early and late stages. In 2014, Stephenson utilized **2.3.8** to access a key intermediate via an oxidative ring fragmentation of (+)-catharanthine (**19a**) in a photoflow reactor early in the synthetic process (Scheme 19), presumably generating a transient cyclic iminium (**19b**) which underwent cyanation to produce the intermediate species (**19c**) in 96% yield, followed by acid mediated rearrangement to reach (-)-pseudotabersonine (**19d**) in 90% yield.<sup>202</sup>

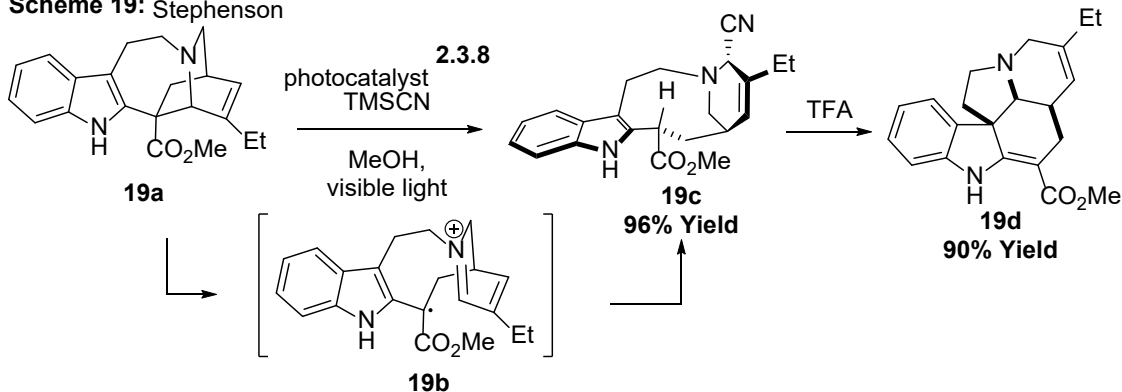
DiRocco and coworkers demonstrated the efficacy of the same photocatalyst to perform late stage functionalization (LSF) by methylation, ethylation, or cyclopropylation of various complex medicinal and agrochemical molecules by visible light photocatalysis (Scheme 20).<sup>203</sup> Established methods such as Minisci's persulfate mediated decarboxylation required high temperatures<sup>204</sup> and are often too harsh for large, complex molecules. While increases to the scope have been made,<sup>205</sup> DiRocco's method to overcome these issues represents a significant advancement in LSF, in part, because the catalyst can help regulate the concentration of the reactive species.

In 2015, MacMillan showed that photocatalysts **2.3.7**<sup>206</sup> or **2.3.8**<sup>207</sup> could be combined synergistically with a NiCl<sub>2</sub>•dtbbpy catalyst for the formation of olefins and aryl ketones (Scheme 21).

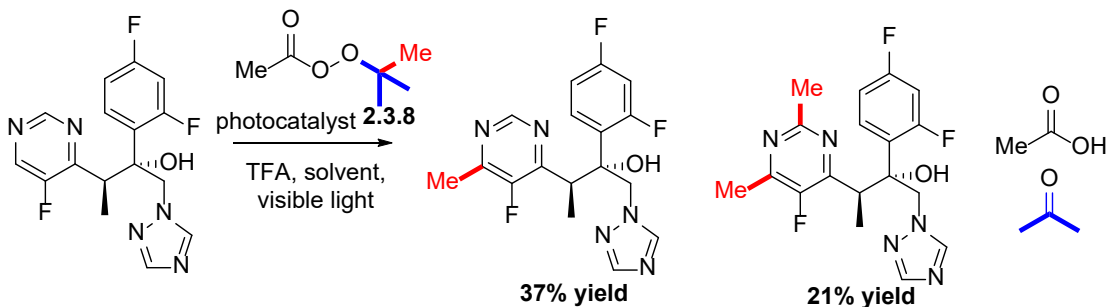
In 2008, Yoon demonstrated the [2+2] intramolecular cycloaddition took place via an electron transfer mechanism with catalytic amounts of **2.3.11**, *vide infra*, (Scheme 22a).<sup>162</sup> Then, in 2012, he also demonstrated that an energy transfer

pathway could be used for substrates that were unlikely to undergo electron transfer (Scheme 23b). **2.3.8** was selected not only because the excited state oxidation potential cannot initialize radical cation cycloadditions, but also because the energy of the catalyst's excited state is comparable to the triplet state energy of excited styrenes.<sup>208</sup>

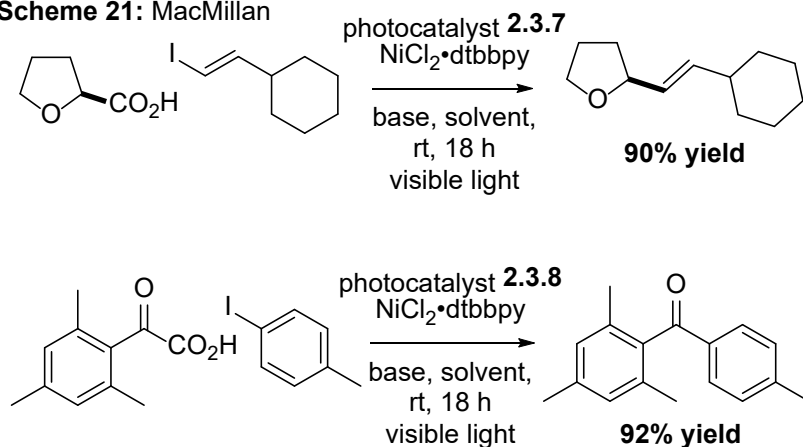
**Scheme 19:** Stephenson



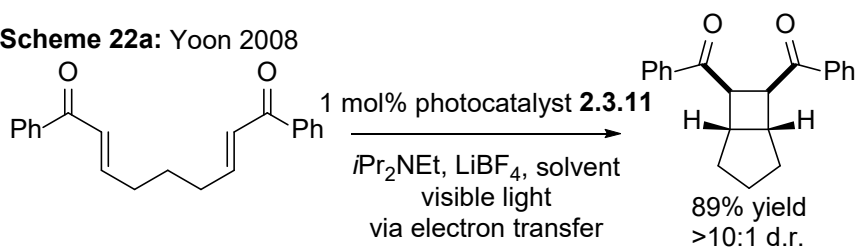
**Scheme 20:** DiRocco



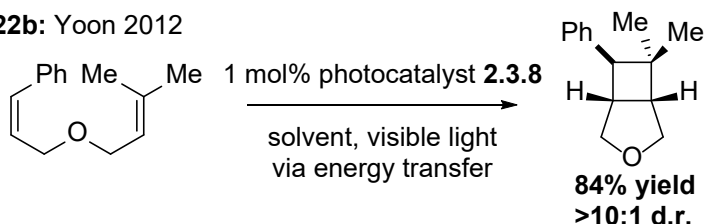
**Scheme 21:** MacMillan



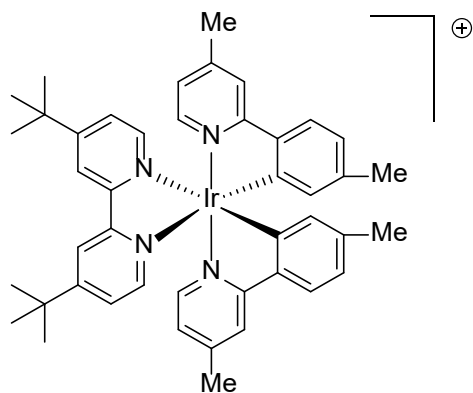
**Scheme 22a:** Yoon 2008



**Scheme 22b:** Yoon 2012

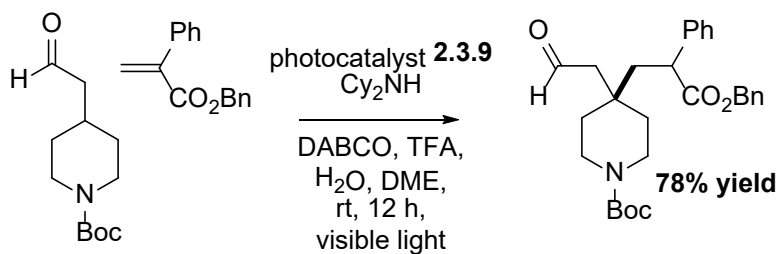


### 2.3.9 [Ir(3,4'-dm-ppy)<sub>2</sub>(4,4'-dtb-bpy)]PF<sub>6</sub>

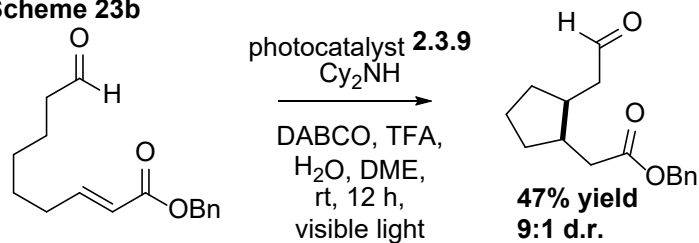


In 2014, MacMillan and coworkers reported a method that utilizes **2.3.9** to directly couple a Michael acceptor and an aldehyde at the  $\beta$ -position (Scheme 23a). The  $\beta$ -functionalization of the aldehydes (as opposed to  $\alpha$ -functionalization) via any method has little precedence and demonstrates the enabling nature of photocatalysis. It also allows for intramolecular 5- or 6-exo-trig radical cyclizations onto aldehydes that are unsaturated and possess a terminal electron withdrawing group (Scheme 23b).<sup>166</sup>

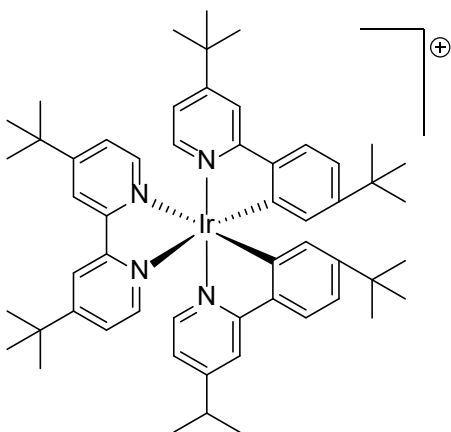
**Scheme 23a: MacMillan**



**Scheme 23b**

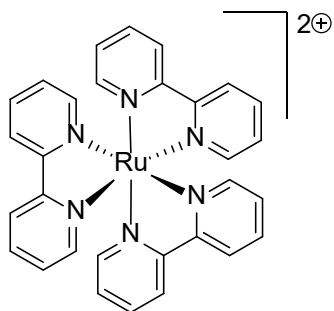


**2.3.10** [Ir(4,4'-dtb-ppy)<sub>2</sub>(3,4'-dtb-bpy)]PF<sub>6</sub>



Current literature references for catalyst **2.3.10** are limited and it is included in order to provide electrochemical and photophysical data.

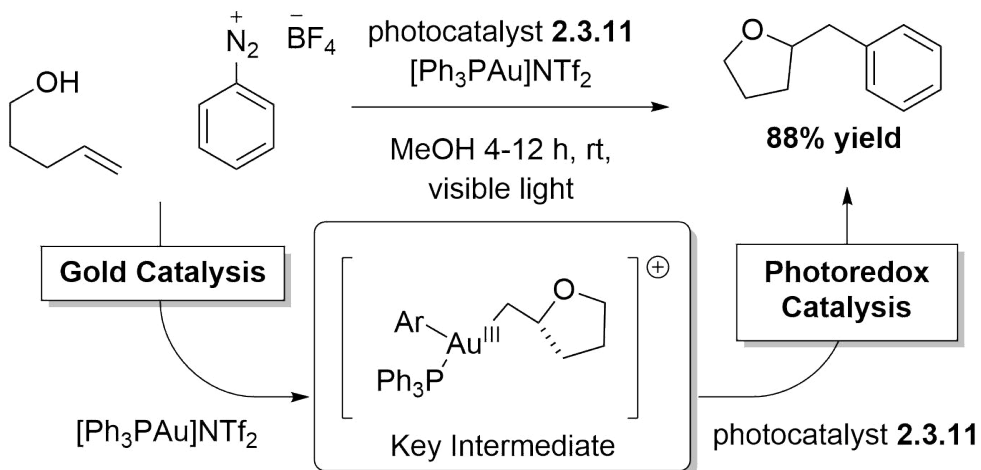
### 2.3.11 [Ru(bpy)<sub>3</sub>](PF<sub>6</sub>)<sub>2</sub>

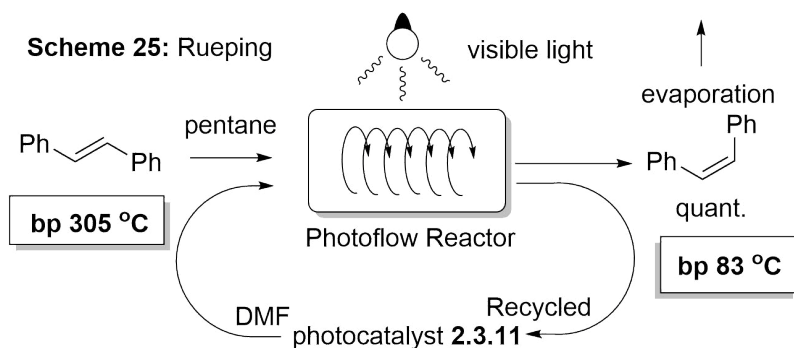


In another example of merging catalytic cycles of transition-metal catalysis and photocatalysis, Glorius and coworkers<sup>209</sup> merged gold catalysis and photocatalysis (Scheme 24), with oxidation of the gold complex by **2.3.11** during the reaction. Moderate to good yields of oxy- and amino arylated alkenes were realized using [Ph<sub>3</sub>PAu]NTf<sub>2</sub> and vinyl alcohols.

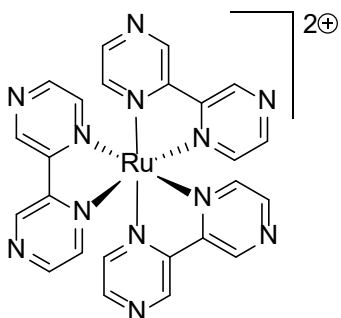
Our group<sup>210</sup> has shown that visible light and **2.3.11** can facilitate (E)- to (Z)-isomerizations of substituted styrenes. Osawa's group<sup>211</sup> has also shown isomerizations of stilbene derivatives with photocatalyst **2.3.11**. Rueping<sup>212</sup> and coworkers produced an economical and practical two-phase photoflow setup using **2.3.11**, achieving quantitative yields of *cis*-stilbene on a 1.8 g scale (Scheme 25). The catalyst/DMF mixture and (E)-stilbene/pentane was circulated through an illuminated glass microreactor. As the more volatile (Z)-stilbene was evaporated, the catalyst and the unreacted high boiling (E)-stilbene were pumped back into system for further isomerization.

**Scheme 24:** Glorius



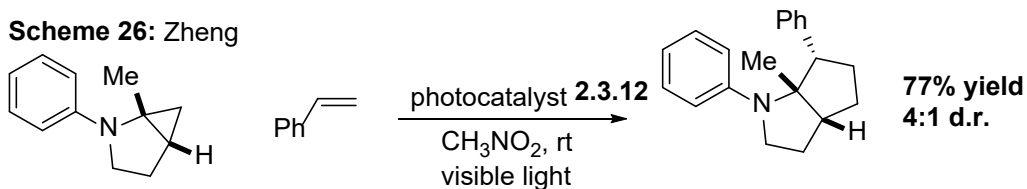


### 2.3.12 [Ru(bpz)<sub>3</sub>](PF<sub>6</sub>)<sub>2</sub>



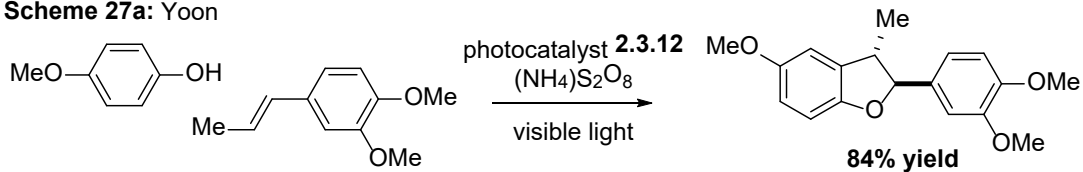
In 2012, Zheng and coworkers<sup>213</sup> utilized **2.3.12** for an intermolecular [3+2] cycloaddition of olefins with cyclopropylanilines, monocyclic, and bicyclic amines, giving good yields and diastereomeric ratios (Scheme 26).

In 2014, utilizing **2.3.12** with an external oxidant Yoon and coworkers<sup>214</sup> detailed an oxidative [3+2] cycloaddition of phenols with alkenes (Scheme 27a) which demonstrated a modular synthesis of dihydrobenzofurans. In the same year they developed a thio-ene “click” reaction of thiols with alkenes (Scheme 27b).<sup>215</sup>

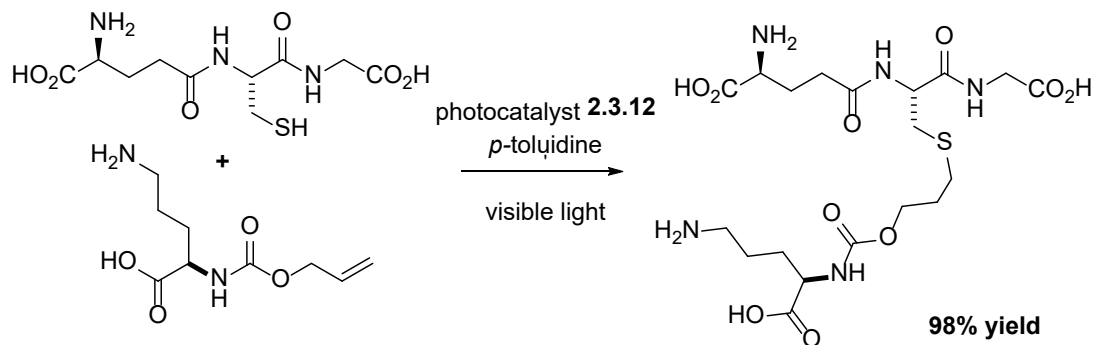




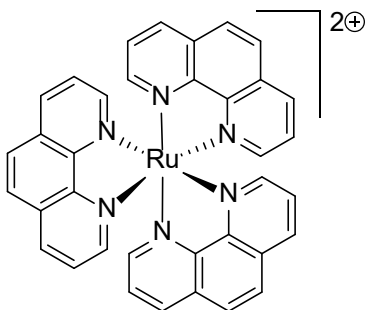
**Scheme 27a: Yoon**



**Scheme 27b**



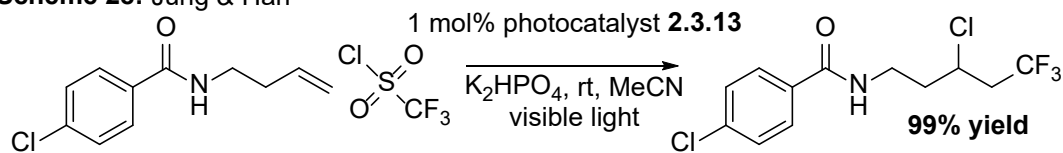
### **2.3.13** $[\text{Ru}(\text{phen})_3](\text{PF}_6)_2$



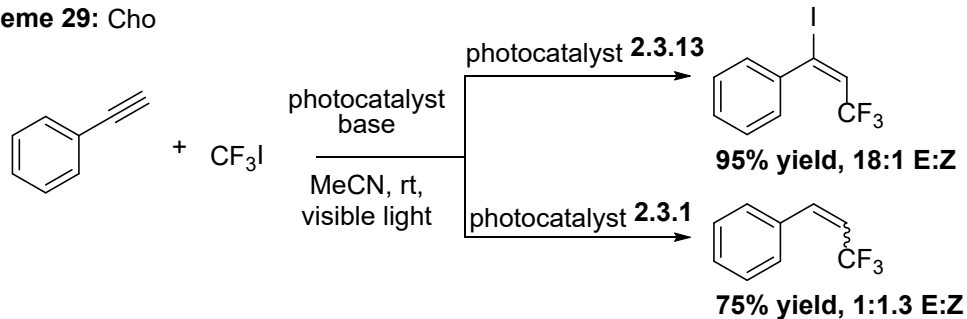
In 2014, using **2.3.13**, Jung and Han reported a convenient method to trifluoromethylate and vicinally chlorinate both internal and terminal alkenes (Scheme 28). **2.3.1** gave similar conversion in initial screening.<sup>216</sup> In the same year, Cho and coworkers synthesized difunctionalized alkenes from alkynes using  $\text{CF}_3$ .<sup>217</sup> In Cho's work, however, it was shown that a switch in catalyst from **2.3.13** to **2.3.1**, resulted in the hydrotrifluoromethylated product, albeit with poor E:Z selectivity (Scheme 29).

Dolbier and coworkers showed that with **2.3.13** and a trifluoromethylsulfonyl chloride, *N*-arylacrylamides could be cyclized through the trifluoromethyl radical to produce 3,3-disubstituted 2-oxoindoles (Scheme 30). The scope was expanded to include the use of the  $\text{CF}_2\text{H}$  radical, though it required a change of photocatalyst to **2.3.1**.<sup>218</sup>

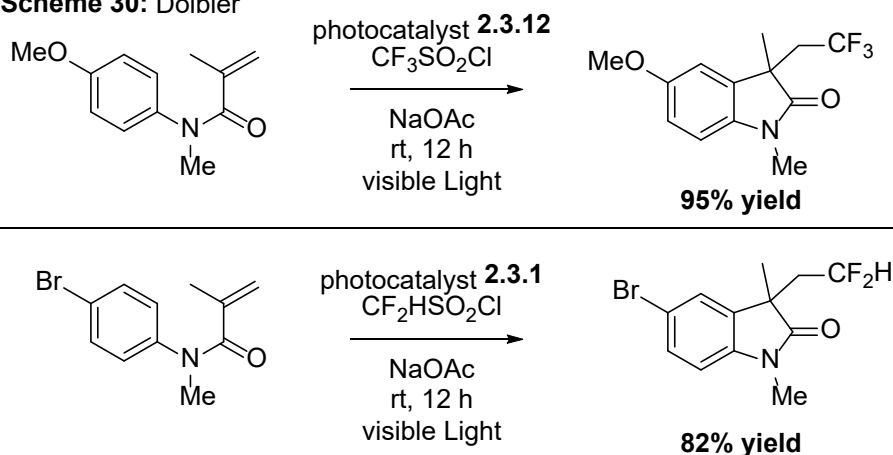
**Scheme 28:** Jung & Han



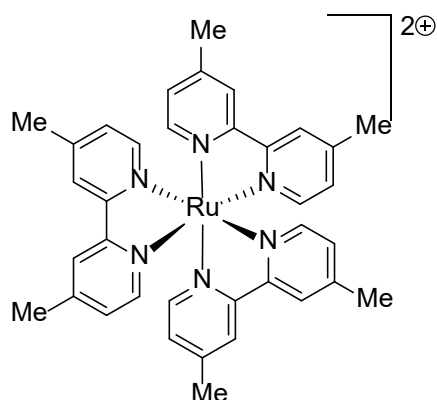
**Scheme 29:** Cho



**Scheme 30:** Dolbier

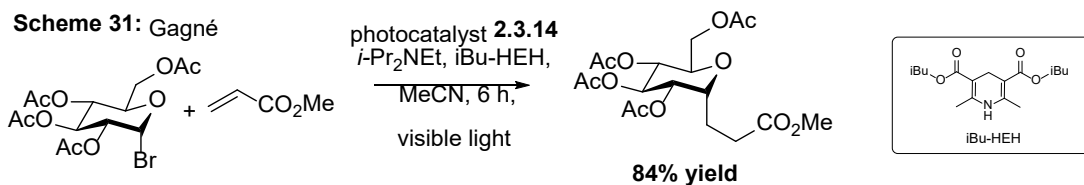


### **2.3.14** $[\text{Ru}(4,4'\text{-dm-bpy})_3](\text{PF}_6)_2$

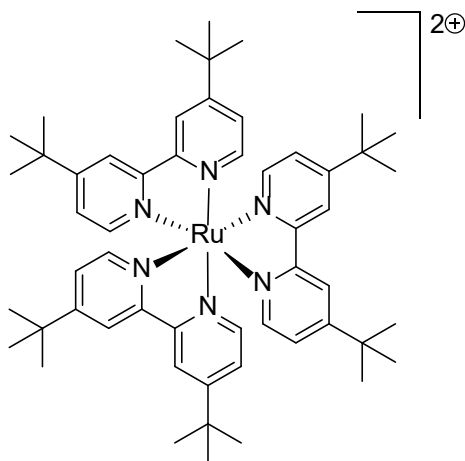


Investigating the radical mediated C–C bond formation between an  $\alpha$ -glucosylbromide and methyl acrylate in 2011, Gagné et al. reported that while the common photocatalyst **2.3.11** accomplished the desired transformation, the rate was exceptionally slow. By changing the solvent and the catalyst to **2.3.14**

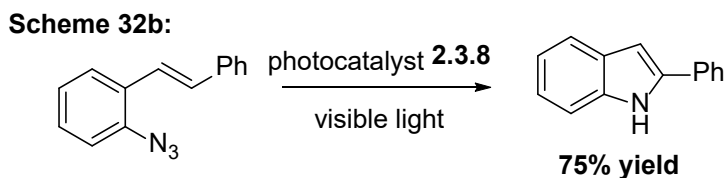
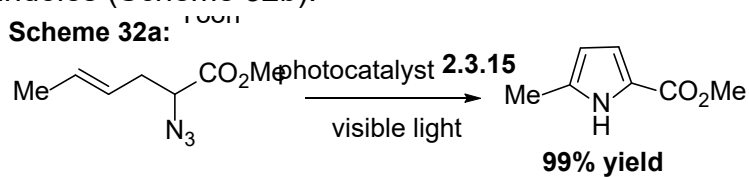
(Scheme 31), the rates of conversion were enhanced.<sup>219</sup> In 2012, utilizing similar conditions, Gagné investigated the permeation of light into the reaction mixture using a photoflow reactor and also expanded the scope to include acroleins.



### 2.3.15 [Ru(4,4'-dtb-bpy)<sub>3</sub>](PF<sub>6</sub>)<sub>2</sub>



In 2014, Yoon and coworkers utilized the energy transfer mechanism of **2.3.15**. Following energy transfer, the substrate expelled the N<sub>2</sub> to produce a nitrene intermediate, which underwent subsequent intramolecular insertion to produce pyrroles in good yields (Scheme 32a). Similarly, photocatalyst **2.3.8** transformed ortho alkenylated aryl azides to provide access to substituted indoles (Scheme 32b).<sup>173</sup>



## 2.4 Conclusions

We have shown a handful of examples of the rapidly growing and diverse repertoire of reactions and collected electro- and photophysical data for a set of commercially available photocatalysts. We have shown some of the distinct mechanisms in which these catalysts can participate and based on this versatility, we expect to see new directions continue to emerge from this powerful new set of catalysts.

## 2.5 Acknowledgement

Jon Day and Kip Teegardin shared first authorship on this publication

## 2.6 References

1. Singh, A.; Kubik, J. J.; Weaver, J. D., Photocatalytic C-F alkylation; facile access to multifluorinated arenes. *Chemical Science* **2015**.
2. Campagna, S.; Puntoriero, F.; Nastasi, F.; Bergamini, G.; Balzani, V., Photochemistry and Photophysics of Coordination Compounds: Ruthenium Photochemistry and Photophysics of Coordination Compounds I. *Top. Curr. Chem.* **2007**, *280*, 117-214.
3. Flamigni, L.; Barbieri, A.; Sabatini, C.; Ventura, B.; Barigelletti, F., Photochemistry and Photophysics of Coordination Compounds: Iridium Photochemistry and Photophysics of Coordination Compounds II. *Top. Curr. Chem.* **2007**, *281*, 143-203.
4. Prier, C. K.; Rankic, D. A.; MacMillan, D. W. C., Visible Light Photoredox Catalysis with Transition Metal Complexes: Applications in Organic Synthesis. *Chem. Rev.* **2013**, *113* (7), 5322-5363.
5. Kalyanasundaram, K.; Grätzel, M., Applications of functionalized transition metal complexes in photonic and optoelectronic devices. *Coord. Chem. Rev.* **1998**, *177* (1), 347-414.
6. Lowry, M. S.; Bernhard, S., Synthetically Tailored Excited States: Phosphorescent, Cyclometalated Iridium(III) Complexes and Their Applications. *Chem. Eur. J.* **2006**, *12* (31), 7970-7977.
7. Lalevee, J.; Peter, M.; Dumur, F.; Gigmès, D.; Blanchard, N.; Tehfe, M.-A.; Morlet-Savary, F.; Fouassier, J. P., Subtle Ligand Effects in Oxidative Photocatalysis with Iridium Complexes: Application to Photopolymerization. *Chem. Eur. J.* **2011**, *17* (52), 15027-15031.
8. Ischay, M. A.; Anzovino, M. E.; Du, J.; Yoon, T. P., Efficient Visible Light Photocatalysis of [2+2] Enone Cycloadditions. *J. Am. Chem. Soc.* **2008**, *130* (39), 12886-12887.

9. Nicewicz, D. A.; MacMillan, D. W. C., Merging Photoredox Catalysis with Organocatalysis: The Direct Asymmetric Alkylation of Aldehydes. *Science* **2008**, *322* (5898), 77-80.
10. Pac, C.; Ihama, M.; Yasuda, M.; Miyauchi, Y.; Sakurai, H., Tris(2,2'-bipyridine)ruthenium(2+)-mediated photoreduction of olefins with 1-benzyl-1,4-dihydronicotinamide: a mechanistic probe for electron-transfer reactions of NAD(P)H-model compounds. *J. Am. Chem. Soc.* **1981**, *103* (21), 6495-6497.
11. Fukuzumi, S.; Mochizuki, S.; Tanaka, T., Photocatalytic reduction of phenacyl halides by 9,10-dihydro-10-methylacridine: control between the reductive and oxidative quenching pathways of tris(bipyridine)ruthenium complex utilizing an acid catalysis. *J. Phys. Chem.* **1990**, *94* (2), 722-726.
12. Narayanam, J. M. R.; Stephenson, C. R. J., Visible light photoredox catalysis: applications in organic synthesis. *Chem. Soc. Rev.* **2011**, *40* (1), 102-113.
13. Terrett, J. A.; Clift, M. D.; MacMillan, D. W. C., Direct  $\beta$ -Alkylation of Aldehydes via Photoredox Organocatalysis. *J. Am. Chem. Soc.* **2014**, *136* (19), 6858-6861.
14. Slinker, J. D.; Gorodetsky, A. A.; Lowry, M. S.; Wang, J.; Parker, S.; Rohl, R.; Bernhard, S.; Malliaras, G. G., Efficient yellow electroluminescence from a single layer of a cyclometalated iridium complex. *J. Am. Chem. Soc.* **2004**, *126* (9), 2763-7.
15. Lowry, M. S.; Hudson, W. R.; Pascal, R. A.; Bernhard, S., Accelerated Lumiphore Discovery through Combinatorial Synthesis. *J. Am. Chem. Soc.* **2004**, *126* (43), 14129-14135.
16. Juris, A.; Balzani, V.; Belser, P.; von Zelewsky, A., Characterization of the Excited State Properties of Some New Photosensitizers of the Ruthenium (Polypyridine) Family. *Helv. Chim. Acta* **1981**, *64* (7), 2175-2182.
17. Rillema, D. P.; Allen, G.; Meyer, T. J.; Conrad, D., Redox properties of ruthenium(II) tris chelate complexes containing the ligands 2,2'-bipyrazine, 2,2'-bipyridine, and 2,2'-bipyrimidine. *Inorg. Chem* **1983**, *22* (11), 1617-1622.
18. Haga, M.; Dodsworth, E. S.; Eryavec, G.; Seymour, P.; Lever, A. B. P., Luminescence quenching of the tris(2,2'-bipyrazine)ruthenium(II) cation and its monoprotonated complex. *Inorg. Chem* **1985**, *24* (12), 1901-1906.
19. Young, R. C.; Meyer, T. J.; Whitten, D. G., Electron transfer quenching of excited states of metal complexes. *J. Am. Chem. Soc.* **1976**, *98* (1), 286-287.
20. Prier, C. K.; Rankic, D. A.; MacMillan, D. W., Visible light photoredox catalysis with transition metal complexes: applications in organic synthesis. *Chem. Rev.* **2013**, *113* (7), 5322-63.
21. Farney, E. P.; Yoon, T. P., Visible-Light Sensitization of Vinyl Azides by Transition Metal Photocatalysis. *Angew. Chem., Int. Ed.* **2014**, *53* (3), 793-797.
22. Dedeian, K.; Djurovich, P. I.; Garces, F. O.; Carlson, G.; Watts, R. J., A new synthetic route to the preparation of a series of strong photoreducing agents: fac-tris-ortho-metallated complexes of iridium(III) with substituted 2-phenylpyridines. *Inorg. Chem* **1991**, *30* (8), 1685-1687.
23. Grushin, V. V.; Herron, N.; LeCloux, D. D.; Marshall, W. J.; Petrov, V. A.; Wang, Y., New, efficient electroluminescent materials based on organometallic Ir complexes. *Chem. Commun.* **2001**, (16), 1494-1495.

24. Singh, A.; Teegardin, K.; Kelly, M.; Prasad, K. S.; Krishnan, S.; Weaver, J. D., Facile synthesis and complete characterization of homoleptic and heteroleptic cyclometalated Iridium(III) complexes for photocatalysis. *J. Organomet. Chem.* **2015**, *776*, 51-59.
25. Ladouceur, S.; Fortin, D.; Zysman-Colman, E., Enhanced Luminescent Iridium(III) Complexes Bearing Aryltriazole Cyclometallated Ligands. *Inorg. Chem.* **2011**, *50* (22), 11514-11526.
26. Swanick, K. N.; Ladouceur, S.; Zysman-Colman, E.; Ding, Z., Correlating electronic structures to electrochemiluminescence of cationic Ir complexes. *RSC Adv.* **2013**, *3* (43), 19961-19964.
27. Anderson, B. L.; Maher, A. G.; Nava, M.; Lopez, N.; Cummins, C. C.; Nocera, D. G., Ultrafast Photoinduced Electron Transfer from Peroxide Dianion. *J. Phys. Chem.* **2015**, *119* (24), 7422-7429.
28. Zou, Y.-Q.; Lu, L.-Q.; Fu, L.; Chang, N.-J.; Rong, J.; Chen, J.-R.; Xiao, W.-J., Visible-Light-Induced Oxidation/ 3+2 Cycloaddition/Oxidative Aromatization Sequence: A Photocatalytic Strategy To Construct Pyrrolo 2,1-a isoquinolines. *Angew. Chem., Int. Ed.* **2011**, *50* (31), 7171-7175.
29. Damrauer, N. H.; Boussie, T. R.; Devenney, M.; McCusker, J. K., Effects of Intraligand Electron Delocalization, Steric Tuning, and Excited-State Vibronic Coupling on the Photophysics of Aryl-Substituted Bipyridyl Complexes of Ru(II). *J. Am. Chem. Soc.* **1997**, *119* (35), 8253-8268.
30. Bernhard, S.; Barron, J. A.; Houston, P. L.; Abruña, H. D.; Ruglovksy, J. L.; Gao, X.; Malliaras, G. G., Electroluminescence in Ruthenium(II) Complexes. *J. Am. Chem. Soc.* **2002**, *124* (45), 13624-13628.
31. Lv, H.; Cai, Y.-B.; Zhang, J.-L., Copper-Catalyzed Hydrodefluorination of Fluoroarenes by Copper Hydride Intermediates. *Angew. Chem., Int. Ed.* **2013**, *52* (11), 3203-3207.
32. Kalyanasundaram, K., Photophysics, photochemistry and solar energy conversion with tris(bipyridyl)ruthenium(II) and its analogues. *Coord. Chem. Rev.* **1982**, *46*, 159-244.
33. Bryant, G. M.; Fergusson, J. E.; Powell, H. K. J., Charge-transfer and intraligand electronic spectra of bipyridyl complexes of iron, ruthenium, and osmium. I. Bivalent complexes. *Aust. J. Chem.* **1971**, *24* (2), 257-273.
34. Bueldt, L. A.; Prescimone, A.; Neuburger, M.; Wenger, O. S., Photoredox Properties of Homoleptic d6 Metal Complexes with the Electron-Rich 4,4',5,5'-Tetramethoxy-2,2'-bipyridine Ligand. *Eur. J. Inorg. Chem.* **2015**, *2015* (28), 4666-4677.
35. McNally, A.; Prier, C. K.; MacMillan, D. W. C., Discovery of an  $\alpha$ -Amino C-H Arylation Reaction Using the Strategy of Accelerated Serendipity. *Science* **2011**, *334* (6059), 1114-1117.
36. Singh, A.; Arora, A.; Weaver, J. D., Photoredox-Mediated C-H Functionalization and Coupling of Tertiary Aliphatic Amines with 2-Chloroazoles. *Organic letters* **2013**, *15*, 5390-5393.
37. Qin, Q.; Yu, S., Visible-Light-Promoted Redox Neutral C-H Amidation of Heteroarenes with Hydroxylamine Derivatives. *Organic letters* **2014**, *16* (13), 3504-3507.

38. Kim, H.; Kim, T.; Lee, D. G.; Roh, S. W.; Lee, C., Nitrogen-centered radical-mediated C-H amidation of arenes and heteroarenes via visible light induced photocatalysis. *Chem. Commun.* **2014**, 50 (66), 9273-9276.
39. Arora, A.; Teegardin, K. A.; Weaver, J. D., Reductive Alkylation of 2-Bromoazoles via Photoinduced Electron Transfer: A Versatile Strategy to Csp<sup>2</sup>-Csp<sup>3</sup> Coupled Products. *Organic letters* **2015**, 17 (15), 3722-3725.
40. Uraguchi, D.; Kinoshita, N.; Kizu, T.; Ooi, T., Synergistic Catalysis of Ionic Bronsted Acid and Photosensitizer for a Redox Neutral Asymmetric  $\alpha$ -Coupling of N-Arylaminoethanes with Aldimines. *J. Am. Chem. Soc.* **2015**, 137 (43), 13768-13771.
41. Senaweera, S.; Weaver, J. D., Dual C-F, C-H Functionalization via Photocatalysis: Access to Multifluorinated Biaryls. *J. Am. Chem. Soc.* **2016**, 138 (8), 2520-3.
42. Nguyen, J. D.; Matsuura, B. S.; Stephenson, C. R. J., A Photochemical Strategy for Lignin Degradation at Room Temperature. *J. Am. Chem. Soc.* **2014**, 136 (4), 1218-1221.
43. Wang, J.; Zheng, N., The cleavage of a C-C Bond in cyclobutylanilines by visible-light photoredox catalysis: Development of a [4+2] annulation method. *Angew. Chem., Int. Ed.* **2015**, 54 (39), 11424-11427.
44. Rono, L. J.; Yayla, H. G.; Wang, D. Y.; Armstrong, M. F.; Knowles, R. R., Enantioselective Photoredox Catalysis Enabled by Proton-Coupled Electron Transfer: Development of an Asymmetric Aza-Pinacol Cyclization. *J. Am. Chem. Soc.* **2013**.
45. Qin, Q.; Yu, S., Visible-Light-Promoted Remote C(sp<sup>3</sup>)-H Amidation and Chlorination. *Organic letters* **2015**, 17 (8), 1894-1897.
46. Tellis, J. C.; Primer, D. N.; Molander, G. A., Single-electron transmetalation in organoboron cross-coupling by photoredox/nickel dual catalysis. *Science* **2014**, 345 (6195), 433-436.
47. Labadie, J. W.; Stille, J. K., Mechanisms of the palladium-catalyzed couplings of acid chlorides with organotin reagents. *J. Am. Chem. Soc.* **1983**, 105 (19), 6129-6137.
48. Finch, A.; Gardner, P. J.; Pearn, E. J.; Watts, G. B., Thermochemistry of triphenylboron, tricyclohexylboron and some phenylboron halides. *T. Faraday Soc.* **1967**, 63, 1880.
49. Noble, A.; MacMillan, D. W. C., Photoredox  $\alpha$ -Vinylolation of  $\alpha$ -Amino Acids and N-Aryl Amines. *J. Am. Chem. Soc.* **2014**, 136 (33), 11602-11605.
50. Beatty, J. W.; Stephenson, C. R. J., Synthesis of (-)-Pseudotabersonine, (-)-Pseudovincadifformine, and (+)-Coronaridine Enabled by Photoredox Catalysis in Flow. *J. Am. Chem. Soc.* **2014**, 136 (29), 10270-10273.
51. Di Rocco, D. A.; Dykstra, K.; Krska, S.; Vachal, P.; Conway, D. V.; Tudge, M., Late-stage functionalization of biologically active heterocycles through photoredox catalysis. *Angew. Chem., Int. Ed.* **2014**, 53 (19), 4802-4806.
52. Minisci, F.; Bernardi, R.; Bertini, F.; Galli, R.; Perchinummo, M., Nucleophilic character of alkyl radicals—VI. *Tetrahedron* **1971**, 27 (15), 3575-3579.

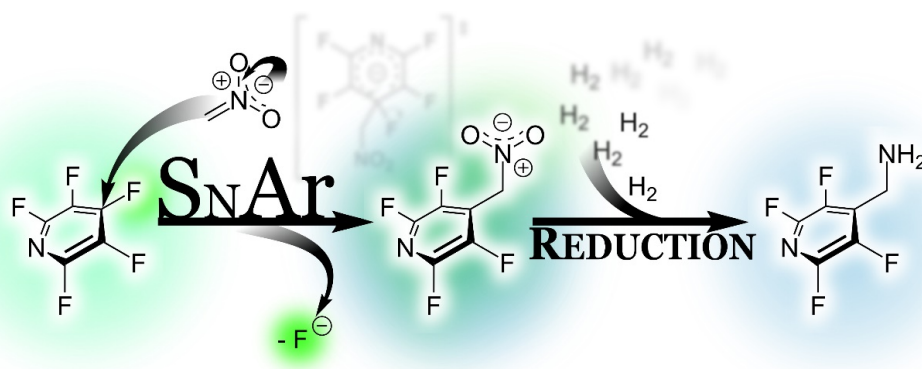
53. Molander, G. A.; Colombel, V.; Braz, V. A., Direct Alkylation of Heteroaryls Using Potassium Alkyl- and Alkoxyethyltrifluoroborates. *Organic letters* **2011**, *13* (7), 1852-1855.
54. Noble, A.; McCarver, S. J.; MacMillan, D. W. C., Merging Photoredox and Nickel Catalysis: Decarboxylative Cross-Coupling of Carboxylic Acids with Vinyl Halides. *J. Am. Chem. Soc.* **2015**, *137* (2), 624-627.
55. Chu, L.; Lipshultz, J. M.; MacMillan, D. W., Merging Photoredox and Nickel Catalysis: The Direct Synthesis of Ketones by the Decarboxylative Arylation of alpha-Oxo Acids. *Angew. Chem., Int. Ed.* **2015**, *54* (27), 7929-33.
56. Lu, Z.; Yoon, T. P., Visible Light Photocatalysis of [2+2] Styrene Cycloadditions by Energy Transfer. *Angew. Chem., Int. Ed.* **2012**, *51* (41), 10329-10332, S10329/1-S10329/128.
57. Sahoo, B.; Hopkinson, M. N.; Glorius, F., Combining Gold and Photoredox Catalysis: Visible Light-Mediated Oxy- and Aminoarylation of Alkenes. *J. Am. Chem. Soc.* **2013**, *135* (15), 5505-5508.
58. Singh, K.; Staig, S. J.; Weaver, J. D., Facile Synthesis of Z-Alkenes via Uphill Catalysis. *J. Am. Chem. Soc.* **2014**, *136* (14), 5275-5278.
59. Osawa, M.; Hoshino, M.; Wakatsuki, Y., A Light-Harvesting tert-Phosphane Ligand Bearing a Ruthenium(II) Polypyridyl Complex as Substituent. *Angew. Chem., Int. Ed.* **2001**, *40* (18), 3472-3474.
60. Fabry, D. C.; Ronge, M. A.; Rueping, M., Immobilization and Continuous Recycling of Photoredox Catalysts in Ionic Liquids for Applications in Batch Reactions and Flow Systems: Catalytic Alkene Isomerization by Using Visible Light. *Chem. Eur. J.* **2015**, *21* (14), 5350-5354.
61. Maity, S.; Zhu, M.; Shinabery, R. S.; Zheng, N., Intermolecular [3+2] Cycloaddition of Cyclopropylamines with Olefins by Visible-Light Photocatalysis. *Angew. Chem., Int. Ed.* **2012**, *51* (1), 222-226.
62. Blum, T. R.; Zhu, Y.; Nordeen, S. A.; Yoon, T. P., Photocatalytic Synthesis of Dihydrobenzofurans by Oxidative [3+2] Cycloaddition of Phenols. *Angew. Chem., Int. Ed.* **2014**, *53* (41), 11056-11059.
63. Tyson, E. L.; Niemeyer, Z. L.; Yoon, T. P., Redox Mediators in Visible Light Photocatalysis: Photocatalytic Radical Thiol-Ene Additions. *J. Org. Chem.* **2014**, *79* (3), 1427-1436.
64. Oh, S. H.; Malpani, Y. R.; Ha, N.; Jung, Y.-S.; Han, S. B., Vicinal Difunctionalization of Alkenes: Chlorotrifluoromethylation with CF<sub>3</sub>SO<sub>2</sub>Cl by Photoredox Catalysis. *Organic letters* **2014**, *16* (5), 1310-1313.
65. Iqbal, N.; Jung, J.; Park, S.; Cho, E. J., Controlled Trifluoromethylation Reactions of Alkynes through Visible-Light Photoredox Catalysis. *Angew. Chem., Int. Ed.* **2014**, *53* (2), 539-542.
66. Tang, X.-J.; Thomason, C. S.; Dolbier, W. R., Jr., Photoredox-Catalyzed Tandem Radical Cyclization of N-Arylacrylamides: General Methods To Construct Fluorinated 3,3-Disubstituted 2-Oxindoles Using Fluoroalkylsulfonyl Chlorides. *Organic letters* **2014**, *16* (17), 4594-4597.
67. Andrews, R. S.; Becker, J. J.; Gagné, M. R., Investigating the Rate of Photoreductive Glucosyl Radical Generation. *Organic letters* **2011**, *13* (9), 2406-2409.



## CHAPTER III

### SELECTIVE AND SCALABLE PERFLUOROARYLATION OF NITROALKANES

#### 3.1 Overview



Herein is contained materials adapted from *J. Org. Chem.* 2017, 82, 13, 6801-6810. This publication outlines selectivity and scope of a competent nucleophile nitroalkane with perfluoroarenes, and outlines some mechanistic insight into the selectivity of the addition. The reaction conditions are demonstrated on a large scale, in order to show the synthetic utility of the reaction.

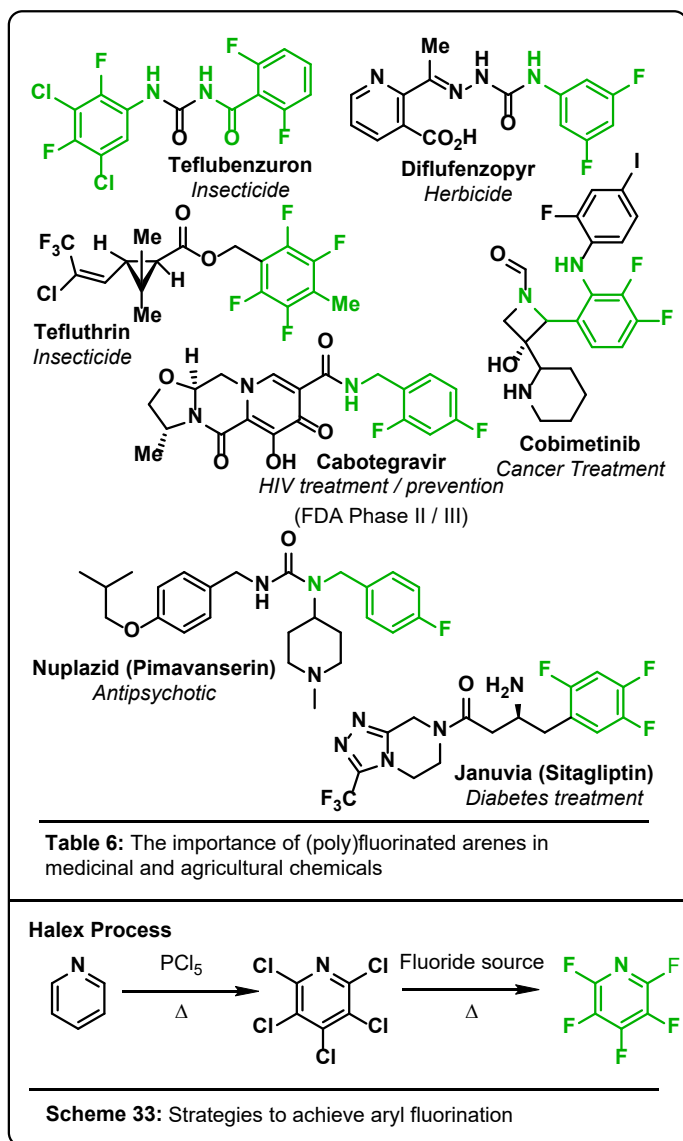
#### 3.2 Introduction

The bioefficacy of small molecules developed for use in medicinal and agricultural products has been shown repeatedly to be significantly augmented by the introduction of a fluorine substituent, or in many cases multiple fluorines (Figure 1).<sup>17, 27, 220-221</sup> While some elegant solutions<sup>41, 222-223</sup> to introduce a single fluorine have recently been published, if a *poly*fluorinated moiety is desired, these strategies of installing fluorines one-at-a-time can become prohibitively unwieldy because the prerequisite starting materials are a synthetic challenge in their own right. For this reason, the commercial availability of, or synthetic access to polyfluorinated precursors is relatively limited compared to that of monofluorinated analogs. This presents the need for a complementary set of synthetic methodologies that will allow for the simple, high yielding syntheses of diverse, functionalized polyfluorinated molecules that will enable rapid

incorporation into larger compounds. Accomplishing this goal will allow for more complete evaluations of the decisive role fluorine plays within functional molecules.

While individual replacement of hydrogens on an arene can be complex, complete replacement of the hydrogen content of an arene with fluorine is synthetically straightforward,<sup>224-226</sup> through methods such as perchlorination followed by nucleophilic halogen exchange (halex) sequences (Scheme 33). As a result, many important perfluorinated arene motifs are commercially available. Congruent with strategies championed by others,<sup>44, 46-47</sup> rather than selectively installing fluorine on each of the desired carbons, our goal is to develop syntheses that begin with inexpensive commercially available perfluorinated starting materials and realize polyfluorination patterns through selective functionalization<sup>227-231</sup> or reduction<sup>232-233</sup> of the undesired C–F bonds under mild conditions. As evidenced by the sophistication of and number of recent C–F functionalization reactions,<sup>142, 193, 227, 232, 234-237</sup> there is an increasing need to functionalize the inchoate highly fluorinated arene cores so that they may be easily incorporated into more elaborate molecules with interesting properties.

Uncatalyzed nucleophilic substitution reactions of fluoroarenes are well established.<sup>224, 238</sup> Though the literature predominantly features heteroatom nucleophiles, examples are present that utilize carbon nucleophiles such as Grignard reagents,<sup>239</sup> and carbanions<sup>240-241</sup> directly. The advantage of utilizing a nucleophile generated from deprotonation of a nitroalkane (i.e. a nitronate) in a reaction with polyfluorinated arene motif is that in one step a highly versatile benzylic nitro group is installed, which can allow further elaboration. This versatility is due in part to its acidifying effect as well as the variable oxidation state of the nitro group. As a synthetic handle, a benzylic nitro group can be readily employed in the Michael reaction, the nitro-



Henry reaction, the Nef reaction, or reduced to an amine (vide infra), among many other transformations.<sup>242</sup> We present herein conditions for the substitution of a C–F bond of polyfluoroarenes with nitroalkanes. The method efficiently yields the monoarylated nitroalkane, is regioselective, highly scalable, and can be performed largely without the use of column chromatography.

In 2012, Sandford and Cobb<sup>243</sup> noted the expected importance of the polyfluorinated heteroaromatic amines and approached this goal through a similar strategy as that presented here, speculating that it could be reached through perfluoroarylation of nitromethane followed by reduction, but rather produced the bipyridyl species (Figure 2, **3.1.2f**), which likely arises through a subsequent substitution of the initial product. While the desired monoarylated product was not obtained under these conditions, Sandford's work does provide strong evidence that the nitronate is sufficiently nucleophilic to undergo substitution and highlights the complicating chemistry with which we would need to contend.

In 2012, Vaidyanathaswamy showed that nitromethane could be used as a nucleophile in the addition to both pentafluorobenzonitrile and methyl pentafluorobenzoate, also indicating the feasibility of the reaction.<sup>244</sup> In their work, the addition was accomplished using 1,8-diazabicyclo[5.4.0]undec-7-ene (DBU) as the base, diethyl ether as the solvent, and required a different isolation technique for every product. Given our intention of scaling the reaction to provide substantial quantities, we were concerned about the generality of the reaction, the cost of DBU and its removal from the product, the ability to use diethyl ether on scale (which is banned in all Sanofi<sup>245</sup> processes), as well as the unique isolation techniques. We sought to develop a general method with greater scope, higher yield, lower overall cost, and which was more amenable to scaling.

A simple analysis of the generally accepted  $S_NAr$  mechanism (Figure 2) led us to suspect that it might be possible to favor the formation of the monoaryl product, **3.1.2e**. The addition of the nitromethane to an aryl group gives rise to a new pronucleophile, (**3.1.2c**), which was expected to be deprotonated under any conditions capable of deprotonating nitromethane, given the acidifying effect of the highly fluorinated aryl group. This was expected to give rise to the nitronate **3.1.2d**, which is also able to participate in a subsequent substitution, leading to **3.1.2f**. Likely this pathway leads to the diarylated species isolated by Sandford and Cobb. However, the nitronate **3.1.2d** was expected to be considerably less nucleophilic<sup>246</sup> than **3.1.2b**, due to not only the difference in  $pK_a$  of the respective conjugate acids, but also due to the increased steric demand of **3.1.2d**. Therefore, we suspected that we could take advantage of the decreased nucleophilicity to effect the desired selectivity for the monoarylated product, **3.1.2e**. Nonetheless, in the presence of additional fluoroarene, the subsequent arylation was expected take place (**2f**, **3.1.2g**).

We speculated that it might be possible to outcompete the relatively slow second arylation event of **3.1.2d** by ensuring that the starting fluoroarene **3.1.2a** was completely

consumed by reaction with nitromethanate **3.1.2b** before a subsequent arylation event could occur. This could be realized by lowering the amount of thermal energy present in the system, and through the addition of another equivalent of base, which would generate a superstoichiometric amount of the intended nucleophile, **3.1.2b**.

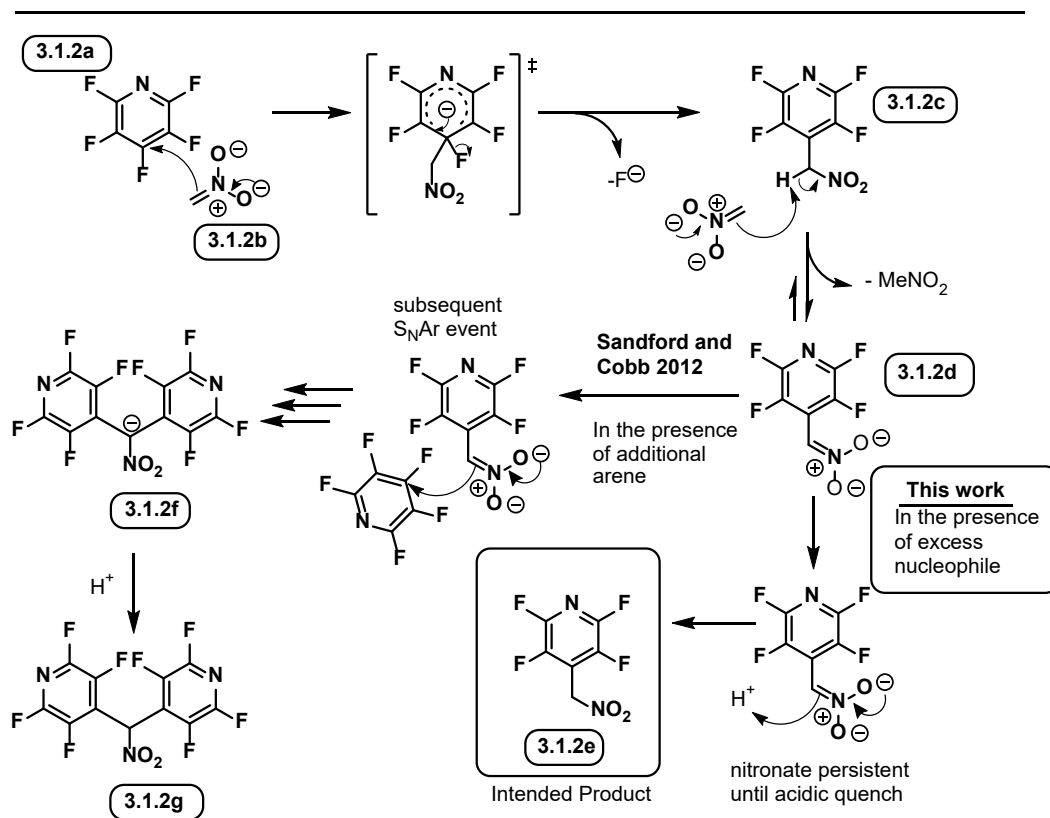
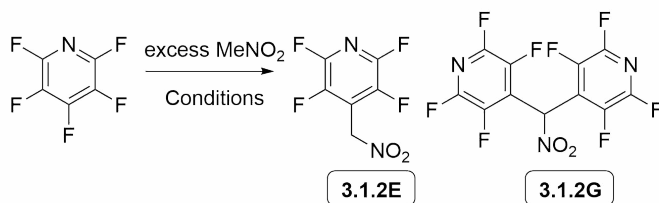


**Figure 2:** A hypothetical exploitation of the  $S_NAr$  mechanism for the formation of the monoarylated  $S_NAr$  product of pentafluoropyridine in contrast to Sandford and Cobb's 2012 work.

### 3.3 Results and Discussion

With a hypothesis developed, we began probing the reaction conditions, starting with the reaction of nitromethanate and pentafluoropyridine, (Table 7). Initial screenings of reaction conditions produced only the biaryl product when triethylamine was used as the base (entries 1). Some of the intended product resulted following the use of DBU to generate nitromethanate **3.1.2b** (entry 2). Next, 1,1,3,3-tetramethylguanidine (TMG) was tried and gave comparable or slightly better results than DBU (entry 3 vs. 2). Given the cost of TMG being ca. 1/4 the cost of DBU<sup>247</sup>, we opted to utilize TMG for further study (entries 3-13). It is further important to note that although experimental values are not available, the predicted log  $P^{222}$  is significantly different,  $1.1 \pm 0.6$  for DBU and  $-0.3 \pm 0.2$  for TMG, indicating TMG possess a 26 times greater preference to partition into an aqueous layer than DBU. Increasing the amount of TMG effected complete conversion of the starting arene, and a substantial increase in the amount of the intended product (entry 4). It was found that the use of TMG necessitated a drop in temperature in order

avoid the addition of TMG to the perfluoroarene (entries 3, 5, and 6). The first drop in temperature from room temperature to 0 °C increased the selectivity of the reaction toward monoarylation by reducing the available energy of the system to facilitate the apparently more sluggish second arylation event, as evidenced by the decrease in the



formation of the biaryl product (**3.1.2g**). Further decreasing the temperature of the reaction to -25 °C led to substantially fewer side products, but also a diminishment of the overall conversion (entry 6). Nonetheless, the majority of the mass balance was now either the desired product (**3.1.2e**) or starting material. The quantity of the nucleophile generated was then investigated, which showed a steady increase in conversion which varied directly with the equivalents of TMG used (entries 6-10). It was not until the equivalents of base, and therefore

Entry	Temp.	Base	Equiv. Base	Conversion to monoaryl product <b>3.1.2E</b>	Conversion to biaryl product <b>3.1.2G</b>	Conversion
1	rt	TEA	1.1	0%	36%	66%
2	rt	DBU	1.0	3%	63%	95%
3	rt	TMG	1.0	6%	28%	82%
4	rt	TMG	1.5	21%	53%	100%
5	0 °C	TMG	1.0	18%	1%	72%
6	-25 °C	TMG	1.0	57%	<1%	66%
7	-25 °C	TMG	1.25	63%	<1%	71%
8	-25 °C	TMG	1.5	79%	<1%	83%
9	-25 °C	TMG	1.75	79%	<1%	93%
10	-25 °C	TMG	2.0	84%	<1%	96%
11	-25 °C	TMG	2.1	98%	0%	99%
12	-25 °C	TMG	2.5	92%	0%	97%
13	-35 °C	TMG	2.1	>99%	0%	>99%

**Table 7:** Optimization of the S<sub>N</sub>Ar reaction of pentafluoropyridine with nitromethane

All reactions run in excess nitromethane; TEA = triethylamine, DBU = 1,8-diazabicyclo[5.4.0]undec-7-ene, TMG = 1,1,3,3-tetramethylguanidine; NMR scale; Conversion determined by relative integration of NMR peaks. Products other than 2E and 2G were not characterized fully.

nitromethane **3.1.2b**, exceeded 2.0 equivalents that the amount of other side products declined sharply in entry 11. Further increasing the amount of TMG to 2.5 equivalents (entry 12) had a deleterious effect on the reaction, however. Further decreasing the temperature was found to have completely suppressed the arylation of the TMG, and gave complete conversion to the intended product **3.1.2e** (entry 13).

Results of an exploration of the scope of fluoroarenes that were investigated are shown in Scheme 3. In reactions in which the perfluoroarene contained a strong electron withdrawing group (**3.3.3a-3.3.3d**), it was found that the reactions were complete in a very short time, i.e. less than 5 minutes after completion of the addition of the fluoroarene. With less activated fluoroarenes (**3.3.3e-3.3.3i**), nitromethane underwent noticeably slower substitution. Consequently, TMG addition was competitive and only became more problematic as the reaction temperature was increased. Thus, a change

to the more expensive but less nucleophilic DBU was required to generate the nucleophile.

Initially, workup of the reaction mixtures consisted of quenching the reaction with aqueous acid in order to protonate the anion of the product (Figure 2, **3.1.2e**) and any remaining base.  $^{19}\text{F}$  NMR analysis of the aqueous layer revealed that the products were,

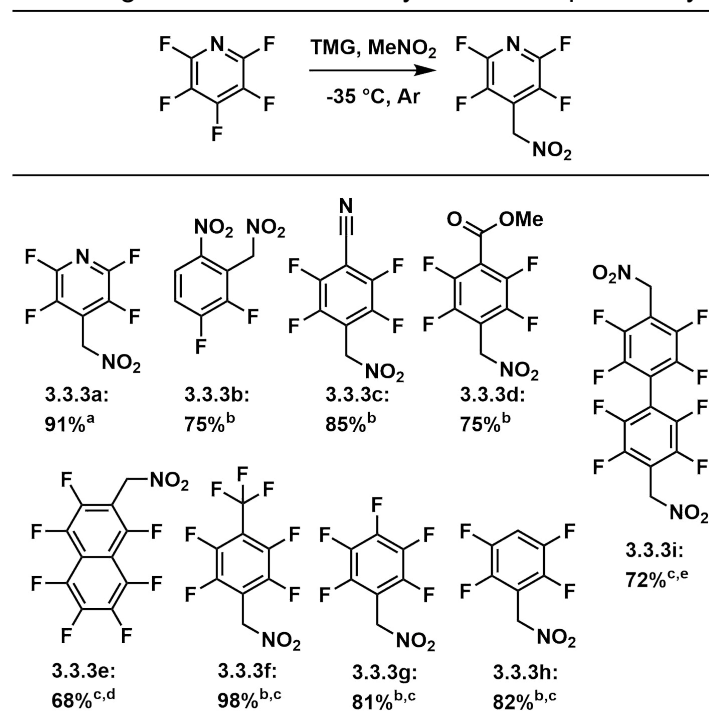


**Table 8:** Scope of the  $\text{S}_{\text{N}}\text{Ar}$  reaction of nitromethane with fluoroarenes

Isolated yields, <sup>a</sup> 20 g scale, <sup>b</sup> 1 g scale. <sup>c</sup> DBU instead of TMG, rt. <sup>d</sup> 250 mg scale. <sup>e</sup> 50 mg scale.

to varying degrees, soluble in water. It was also found that although it was possible to triturate the materials in order to purify them, substantial loss of material resulted.

In order to mitigate this loss, the crude reaction mixtures were acidified following the reaction with a sodium chloride saturated acidic solution. Immediately, better mass recovery was observed. Presumably, the increase in the ionic strength of the aqueous layer discouraged dissolution of the product therein, resulting in improved partitioning of the product into the ethyl acetate organic layer and increasing the overall recovery. The resultant mixture

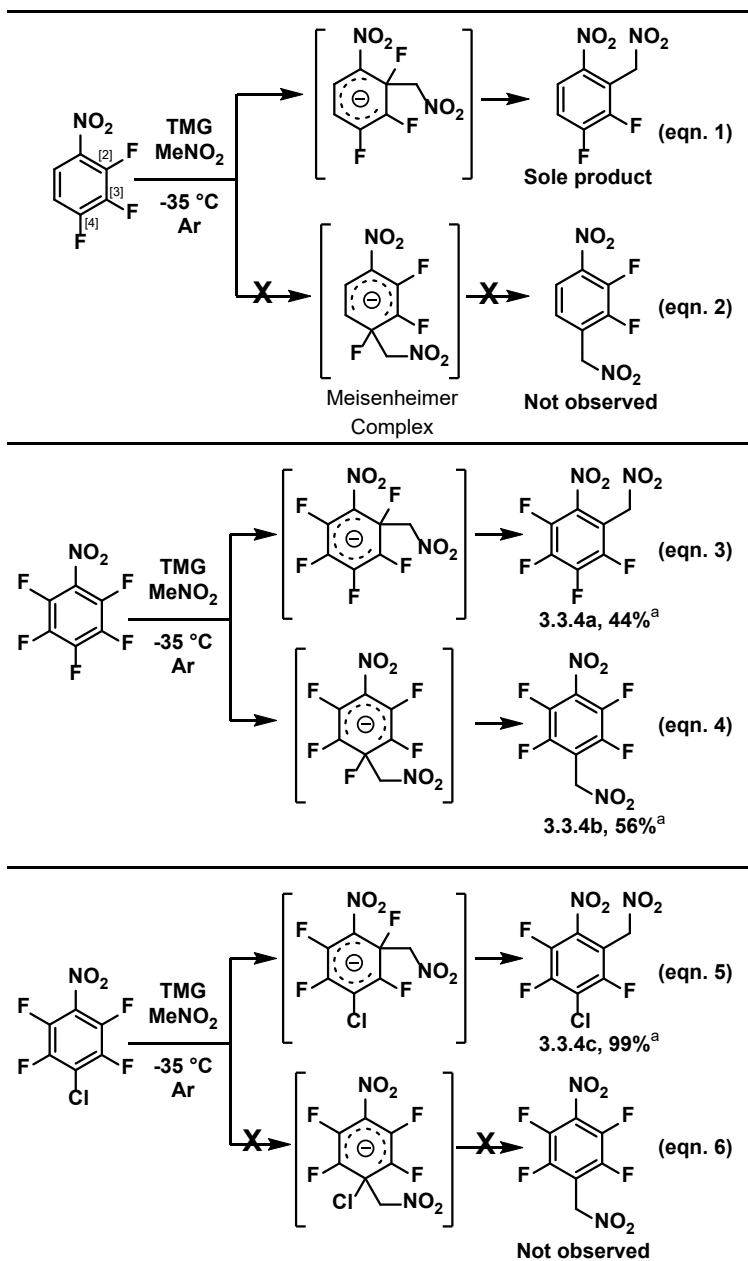
was then separated and the organic layer washed with a small amount of dilute aqueous acid which was not saturated with sodium chloride (General Procedure 3.5.A). In the case of the less activated arenes **3.3.3f-3.3.3h**, which utilized DBU it was found that the standard workup conditions did not free the product completely from the base, and it was necessary to extract the resultant reaction mixtures with a nonpolar solvent following the above workup conditions in order to obtain pure product (General Procedure 3.5.B). These workup conditions resulted in a simple, chromatography-free, easily scalable workup that afforded analytically pure product from the reaction mixture.

With reaction and workup conditions in hand, we attempted to scale up the reaction. This was accomplished on a 20 g scale of the reaction of pentafluoropyridine, which proceeded cleanly to a single product (**3.3.3a**) in a 91% yield. However, upon scaling we found that a cosolvent which could help dissipate the heat was necessary. Initially, diethyl ether was used which is not an ideal solvent for industrial processes, so it was additionally run on a 1 g scale using heptane as the solvent, but otherwise the same. Though the reaction was biphasic, and the nucleophile salt solidified while cooling,

at -35 °C it proceeded to a single product in 96% yield, though the reaction time had to be increased to 4 hours. It is important to note that care was taken to slowly add the fluoroarene to the pregenerated nitromethanate, as the reaction generates significant heat, and increases in temperature were found to lead to the formation of unintended side products, namely that of the substitution of TMG.

The selectivity of the  $S_NAr$  reaction with 1,2,3-trifluoro-4-nitrobenzene ( $F_3NB$ ) to produce **3.3.3b**<sup>248-250</sup> is interesting when compared to pentafluoronitrobenzene<sup>251</sup> (PFNB) because it demonstrates the impact the fluorination pattern has on the regioselectivity of substitution with a highly reactive, yet sterically small nucleophile such as nitromethanate (Scheme 34, **3.3.4b**, and **3.3.4c**). It has been posited<sup>238</sup> that in reference to the site of substitution, ortho- and meta-fluorines facilitate the addition of nucleophiles inductively, whereas, ortho- and para-fluorines hinder the addition by destabilization of the Meisenheimer intermediate via resonance. Thus, the major product of addition to  $F_3NB$  occurs with excellent selectivity ortho to the nitro group (Scheme 34, eqns. 1, 2). Attack by the nitromethanate at the C2 position could potentially maximize both the inductive and resonance effects because both the electron withdrawing nitro group and the fluorine ortho and meta to the site of substitution promote it. The directing effect of fluorine is dramatically observed when this result is compared with the addition to PFNB, which results in a poorly selective addition (eqns. 3,4). In fact, the major product (albeit only slightly) switches to the para-substituted product. This switch in selectivity can be rationalized by the aforementioned reasons. First, para substitution to the nitro group is favored by two additional ortho and meta fluorines. Secondly, addition ortho to the nitro group is retarded by the presence of a fluorine located in the position para to the site of substitution. The net effect is that both products are produced. It should be noted that that this selectivity is notably lower than other carbonucleophiles, Meldrum's acid or oxazolone, which give the para addition in *ca.* 86:14 ratio.<sup>227, 252</sup>

Hoping to probe the nuances of this mechanism, the reaction was repeated with 1-chloro-2,3,5,6-tetrafluoro-4-nitrobenzene (1-Cl- $F_4NB$ ) which recently became accessible.<sup>253</sup> Nucleophilic aromatic substitution reactions are generally thought to have two transition states. The first is the attack of the nucleophile, which leads to formation of the Meisenheimer complex, and the second is the breakdown of that complex. Commonly, formation is the slow step, but the latter has been observed to be the rate-determining.<sup>254</sup> Thus, we posited that replacing the 4-fluoro substituent would allow us to probe the reversibility of the first step. If the breakdown of the Meisenheimer complex was the rate-limiting step following a reversible addition of the nucleophile, one could expect that the incorporation of the para chlorine would lead to exclusive substitution at the chlorinated position because the fragmentation of the chloride should be more exothermic. This is not observed, however. With nitromethanate, the substitution of 1-Cl- $F_4NB$  occurs exclusively at the ortho position (Scheme 34, eqns. 5, 6, **3.3.4c**), suggesting that attack of the nucleophile on the arene is not reversible and other forces are responsible for the observed selectivity.



**Scheme 34:** Effects of aryl hydrogen substituents on the regioselectivity of the S<sub>N</sub>Ar reaction

<sup>a</sup> Percent conversion of arene to products. Relative concentration of products 4a : 4b determined by <sup>19</sup>F NMR integrations, with complete conversion of starting arene.

In order to elucidate the factors responsible for the shift in selectivity (**3.3.4c** vs **3.3.4b**), DFT calculated molecular electrostatic potential energy surfaces<sup>255-256</sup> (MESPs) were generated for the three substrates (Figure 3A). While the relative size of the LUMO does not change appreciably across the substrates, the MESP is more supportive of the experimentally observed selectivity. For F<sub>3</sub>NB, the MESP shows significant partial positive electrostatic anisotropy at the position ortho to the nitro group, suggesting that the initial Coulombic attraction of the nucleophile contributes to the selective formation of the product **3.3.3b**.

In the reaction of PFNB with nitromethanate which leads to products **3.3.4a** (ortho substitution) and **3.3.4b** (para substitution) in 44% and 56% conversion respectively, this hypothesis of electrostatic attraction of the nucleophile is further supported by the DFT calculations. The MESP surface illustrates that the potential energy is more

positive at the para position than that at the ortho position. The observed selectivity can potentially be rationalized, however, by the fact that because there are two ortho positions at which substitutions may occur, there is a greater statistical probability of substitution at these positions compared to the para position, leading to an essentially unselective substitution in which the para position is favored, albeit only slightly.



In the substitution of 1-Cl-F<sub>4</sub>NB, the reaction is completely selective for the position ortho to the nitro group. The MESP surface for this substrate indicates that the most electropositive carbon has shifted in relation to that of the PFNB, from the position para to the nitro group to the ortho position.

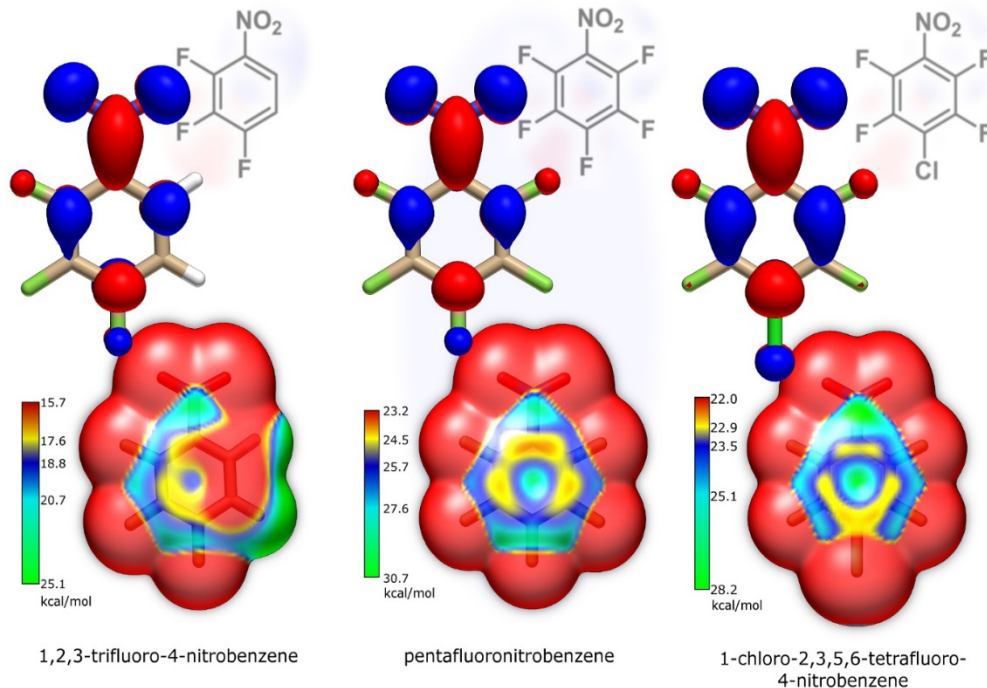


Figure 3a: LUMO surfaces (upper), and MESP surfaces (lower).

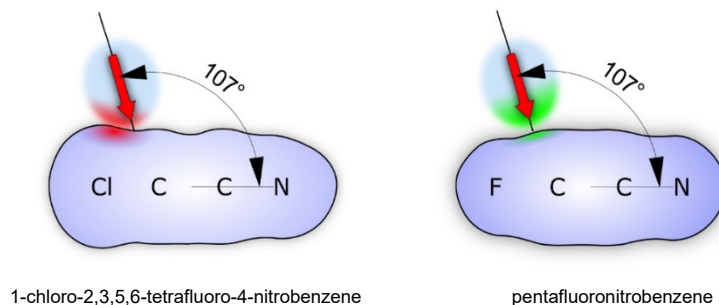
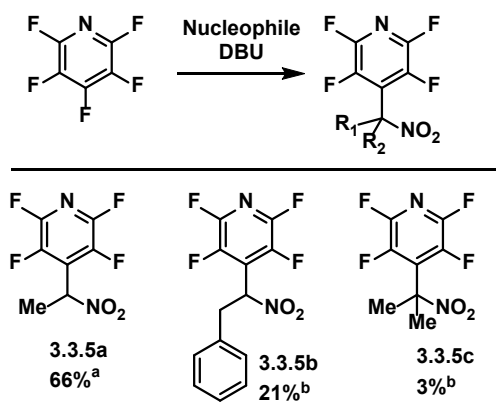


Figure 3b: Vertical cross section through electron density surface. Incoming nucleophile added for illustrative purposes.

An additional factor that may contribute to the change in the selectivity may be due to the fact that the chlorine is significantly larger than a fluorine substituent. A side-view of a cross section of the electron density surface (through C1 and C4 perpendicular to the molecular plane) indicates that attack of the nucleophile at C1 may be somewhat occluded by the attached chlorine approaching at the Bürgi–Dunitz angle,<sup>257</sup> (Figure 3B). Curiously, this is in contrast to our previous observation,<sup>252</sup> in which the addition of an oxazolone enolate to 4-chlorotetrafluoropyridine gave substitution at the 4 position as the

major product, which is the same as the fluorinated analog. Of all the factors discussed, they all seem to support the observed selectivity of the reaction, however, the relative contribution of each is still unclear.



**Table 9:** Investigation of the scope of the nucleophile

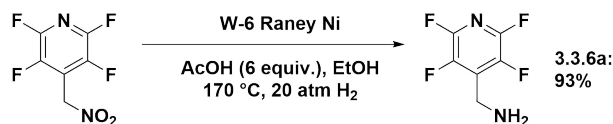
Isolated yields; a reacted at -25 °C; b reacted at 0 °C.

found to take place (**3.3.5b** and **3.3.5c**), albeit with modest to poor yields. The majority of the mass balance was presumed to be addition of the base, though the other products were not fully characterized. It should be noted that no further optimization was performed which may have increased yields. Nonetheless, these reactions do indicate that the reaction can work with other enolizable nitroalkanes and can rapidly give rise to highly elaborated polyfluorinated arenes.

Polyfluorinated benzylic amines are a useful and biologically important moiety, as can be seen in Table 6. The structures of cabotegravir and pimavanserin are particularly interesting because, after reduction of the nitro group, the products of Figure 3 could conceivably serve as uninvestigated, fluorinated analogs with improved properties. In order for this to happen, we first had to find conditions that would facilitate the reduction of the aliphatic nitro group to an amine, (Table 10). One complicating factor is that the resultant amine itself could act as a nucleophile and undergo subsequent addition to the substrate, especially at the elevated temperatures frequently used in nitro-reductions.

In order to reduce the aliphatic nitro group, a variety of catalytic reductions of **3.3.3a** was carried out under acidic conditions (Table 10). We hoped the presence of an acid would protonate the product amine immediately upon formation, thus preventing further nucleophilic substitution. Refluxing of **3.3.3a** with iron dust and concentrated HCl yielded some of the intended product, albeit very slowly (entry 1). We then focused on a catalytic palladium reduction with a hydrogen atmosphere. The reaction did not reduce the nitro group under an atmosphere of hydrogen (balloon pressure, entry 2), but upon increasing the H<sub>2</sub> pressure in a pressure reactor in the presence of formic acid (entries 3, 4), slowly gave the desired product. The same reaction conditions but with acetic, instead of formic, acid did not result in a detectable amount of the intended product (entry 5). We next focused on Raney nickel reductions. Reaction with off-the-shelf activated Raney Ni

in water resulted in none of the intended amine (entry 6). Questioning the activity of the pre-activated Raney Ni, W-6 Raney Ni was prepared according to literature.<sup>258</sup> Screening the activity of the W-6 Raney Ni with 3 equivalents of acetic acid for only 1



Isolated yield, ca. 500 mg scale; isolated as the hydrochloride salt

Entry	Reductant	Catalyst	Time (hrs)	Solvent	Acid (equiv.)	Temp.	Pressure	SM remaining	Conversion to Intended Product <sup>a</sup>
1	HCl	Fe	144	EtOH	HCl	100 °C	–	0%	28%
2	H <sub>2</sub>	Pd/C	42	MeOH	AcOH (4.4)	80 °C	–	0%	0%
3	H <sub>2</sub>	Pd/C	72	MeOH	CHOOH (2)	60 °C	5.5 atm	0%	5%
4	H <sub>2</sub>	Pd/C	72	MeOH	CHOOH (2)	100 °C	6.8 atm	0%	5%
5	H <sub>2</sub>	Pd/C	72	MeOH	AcOH (10)	100 °C	6.8 atm	0%	trace
6	H <sub>2</sub>	Raney Ni	72	MeOH	–	40 °C	6.8 atm	0%	0%
7	H <sub>2</sub>	Raney Ni (W6)	1	EtOH	AcOH (3)	rt	6.8 atm	0%	0%
8	H <sub>2</sub>	Raney Ni (W6)	1	EtOH	AcOH (3)	50 °C	6.8 atm	0%	7%
9	H <sub>2</sub>	Raney Ni (W6)	1	EtOH	AcOH (3)	100 °C	6.8 atm	0%	8%
10	H <sub>2</sub>	Raney Ni (W6)	1	EtOH	AcOH (3)	100 °C	21 atm	0%	13%
11	H <sub>2</sub>	Raney Ni (W6)	1	EtOH	AcOH (3)	150 °C	21 atm	0%	56%
12	H <sub>2</sub>	Raney Ni (W6)	1	EtOH	AcOH (6)	150 °C	21 atm	0%	78%
13	H <sub>2</sub>	Raney Ni (W6)	1	EtOH	AcOH (9)	150 °C	21 atm	0%	72%
14	H <sub>2</sub>	Raney Ni (W6)	3	EtOH	AcOH (6)	150 °C	21 atm	0%	98%

<sup>a</sup> Conversion to intended product determined by relative integration of <sup>19</sup>F peaks

**Table 10:** Reduction of nitromethyl arenes to amines

hour at room temperature, 50 °C, and 100 °C resulted in 0%, 7%, and 8% of the intended amine, (entries 7, 8, and 9, respectively). Increasing the pressure of hydrogen gas resulted in better yields, with 13% (entry 10). At this point, increasing the temperature to 150 °C led to a substantial increase in the yield to (56%, entry 11). Increasing the acetic acid to 6 equivalents, further improved the yield to 78% (entry 12). However, further increases (9 equiv) proved slightly detrimental to the yield (entry 13). Returning to the conditions in entry 19 but extending the reaction time to 3 hours resulted in 98% conversion (entry 14) and an isolated yield of 93%.

We wanted to avoid the use of a column to isolate the product and to be able to isolate it in such a way that it would be stable. The following workup allowed us to both isolate it and safely store it as the HCl salt. After filtration and evaporation of the solvent, the heterogeneous mixture showed a greenish discoloration and the NMR signals were degraded, potentially due to the presence of nickel salts. Both the discoloration and

NMR signal degradation resolved upon extraction with acidic water and washing with ether. Increasing the pH of the aqueous layer and extraction of the aqueous layer into ether led to the isolation of the amine, which was precipitated as the hydrochloride salt from anhydrous ethereal hydrochloric acid.

### 3.4 Conclusion

We have demonstrated a highly scalable method to quickly and easily functionalize and replace a C–F bond in a variety of perfluorinated and polyfluorinated arenes utilizing inexpensive reagents and mild reaction conditions. This will successively help facilitate C–F functionalization as a viable strategy for the synthesis of multifluorinated arenes. Furthermore, we were able to demonstrate for the first time the elusive monoarylation of nitromethane with pentafluoropyridine and provided conditions for its reduction to the benzylic amine. Thus, by using this method, we have shown that more complex molecules can be produced in short order from commercially available poly- and perfluorinated arenes, adding to the collective knowledge for the synthesis of versatile building blocks which will enable the synthesis of many useful highly fluorinated arenes.

### 3.5 Experimental

NMR spectra were obtained on a Bruker A400 instrument. High resolution mass spectra were obtained on a ThermoFisher LTQ-OrbitrapXL using electrospray ionization. Chemicals were obtained from commercial sources and used as received, except as noted. <sup>19</sup>F DOSY performed according to Sibi and Jasperse's technique.<sup>259</sup> 1 gram scale means that the general procedures were scaled *ad valorem* 1 gram of the intended product with 100% theoretical yield.

#### General procedures for the S<sub>N</sub>Ar–F Arylation of nitromethane:

**General Procedure 3.5.A:** To a clean, dry round bottom flask, 12 equivalents of nitromethane were added. The round bottom flask was fitted with a magnetic stir bar, rubber septum, internal thermometer, and a ventilation needle. The solution was degassed with bubbling argon for 10 minutes. While under continuous argon flow, 2.1 equivalents of TMG were added and the solution was stirred for an additional 20 minutes. The solution and the arene to be added were then cooled to -35 °C. Then, the chilled fluoroarene was added dropwise. The addition of the fluoroarene was done such that the reaction temperature did not rise more than 5 °C. The reaction was complete in less than 5 minutes following the completion of the addition, and was then quenched with a solution of 1 M HCl (2.3 equivalents) that had been saturated with NaCl. The resultant crude mixture was extracted with ethyl acetate (3 x 5 reaction volumes), the combined organic layer was washed with successive small amounts (~0.5 reaction volumes) of HCl (0.1 M), separated, and the organic layer was stripped of solvent, *in vacuo*. Generally purity was sufficient so as to negate the need for further purification. Variations are noted per substrate.

**General Procedure 3.5.B:** To a clean, dry round bottom flask, 12 equivalents of nitromethane were added. The round bottom flask was fitted with a magnetic stir bar. Then, 2.1 equivalents of DBU were added and the solution was stirred for an additional 10 minutes. Next, the fluoroarene was added dropwise, and allowed to stir for 1 hour.

The reaction was then quenched with a solution of 1 M HCl (2.3 equivalents) that had been saturated with NaCl. The resultant crude mixture was extracted twice with ethyl acetate (2 x 5 reaction volumes), the combined organic layer was washed with a small amount (~0.5 reaction volume) of HCl (0.1 M), separated, and the combined organic layer was stripped of solvent *in vacuo*. The product was extracted from the resultant oily material (5 x ~20 mL hexanes) and carefully decanted, leaving the denser, colored layer behind each time. The combined hexanes layer was stripped of solvent *in vacuo*. Generally purity was sufficient so as to negate the need for further purification. Variations are noted per substrate.

**3.3.3a: 2,3,5,6-tetrafluoro-4-(nitromethyl)pyridine:** General Procedure 3.5.A was followed in a 500 mL RB, pentafluoropyridine (95.2 mmol, 10.45 mL), TMG (200.0 mmol, 25.10 mL), MeNO<sub>2</sub> (1142.4 mmol, 61.10 mL), NaCl saturated-1M HCl (210 mL), diethyl ether (100 mL). Deviation from standard reaction conditions: After the reaction, the crude material was ground by mortar and pestle and washed with approximately 800 mL 0.1 M HCl over vacuum filtration until no further lightening of coloration was observed. Resulted in a pale yellow-orange crystalline solid, mass 18.197 g, 91% yield. MP 69-71 °C. <sup>19</sup>F NMR (376 MHz, Chloroform-*d*) δ -87.79 (dq, *J* = 28.2, 13.1 Hz, 2F), -141.45 – -141.72 (m, 2F). <sup>1</sup>H NMR (400 MHz, Chloroform-*d*) δ 5.70 (s, 2H). <sup>13</sup>C{<sup>1</sup>H} NMR (101 MHz, Chloroform-*d*) δ 143.4 (app. dddd, *J*=251.3, 15.5, 12.2, 3.3 Hz, 2C), 140.7 (app. dd, *J*=264.6, 35.5 Hz, 2C), 121.3 (tt, *J* = 15.6, 3.0 Hz, 1C), 65.4 (s, 1C). <sup>19</sup>F DOSY mass: calcd. 210; found 216. HRMS (*m/z*): [M - H]<sup>-</sup> calcd for [C<sub>6</sub>HF<sub>4</sub>N<sub>2</sub>O<sub>2</sub>]<sup>-</sup> 208.9979; found 208.9966

**3.3.3a: 2,3,5,6-tetrafluoro-4-(nitromethyl)pyridine: (in heptane)** as in the above procedure, except on a 1 g scale with 10 mL heptane instead of diethyl ether, and reaction time was increased to 4 hours. The initial temperature was -35 °C and was allowed to slowly increase to 0 °C over the course of the reaction. Workup was the same as the standard conditions, but the solidified material was ground in a mortar and pestle and washed with ~ 50 mL aq. HCl (0.1 M) over vacuum filtration. 0.9551 g, 96% yield. <sup>19</sup>F & <sup>1</sup>H NMR spectra agreed with characterization above.

**3.3.3b: 1,2-difluoro-4-nitro-3-(nitromethyl)benzene:** General Procedure 3.5.A was followed on a 1 g scale, using 4-Nitro-1,2,3-trifluorobenzene (4.58 mmol, 0.53 mL) with TMG (9.63 mmol, 1.21 mL) and nitromethane (55.02 mmol, 2.98 mL), except the resultant material had to be successively washed with 0.1 M aq. HCl to remove the base. 0.753 g pale yellowish crystalline solid, 75% yield. MP 86-91 °C. <sup>19</sup>F NMR (376 MHz, Chloroform-*d*) δ -123.28 (m, 2F), -133.39 (m, 2F). <sup>1</sup>H NMR (400 MHz, Chloroform-*d*) δ 8.16 (ddd, *J* = 9.3, 4.4, 2.1 Hz, 1H), 7.52 (dt, *J* = 9.3, 8.1 Hz, 1H), 5.94 (d, *J* = 1.8 Hz, 2H). <sup>13</sup>C{<sup>1</sup>H} NMR (101 MHz, Chloroform-*d*) δ 154.0 (dd, *J* = 262.4, 13.8 Hz), 149.8 (dd, *J* = 256.8, 14.3 Hz), 143.9, 122.6 (dd, *J* = 7.9, 3.9 Hz), 119.2 (dd, *J* = 18.7, 1.8 Hz), 115.9 (dd, *J* = 14.0, 1.4 Hz), 67.6 (dd, *J* = 5.9, 1.7 Hz). HRMS (*m/z*): [M - H]<sup>-</sup> calcd for [C<sub>7</sub>H<sub>3</sub>F<sub>2</sub>N<sub>2</sub>O<sub>4</sub>]<sup>-</sup> 217.0066; found 217.0053.

**3.3.3c: 2,3,5,6-tetrafluoro-4-(nitromethyl)benzotrile:** General Procedure 3.5.A was followed on a 1 g scale, with pentafluorobenzotrile (4.27 mmol, 0.54 mL), TMG (8.97 mmol, 1.13 mL), and nitromethane (51.26 mmol, 2.78 mL) in a 100 mL RBF, except with 10 mL diethyl ether. The organic layer was washed with 3 mL 0.1 M HCl total, resulting in an peach colored crystalline solid. 0.852 g, 85% yield. MP 67-71 °C (lit. 65–65.5 °C)<sup>244</sup> <sup>19</sup>F NMR (376 MHz, Chloroform-*d*) δ -87.80 (dq, *J* = 27.9, 13.1 Hz, 2F), -141.47 – -141.70 (m, 2F). <sup>1</sup>H NMR (400 MHz, Chloroform-*d*) δ 5.70 (s, 2H). <sup>13</sup>C{<sup>1</sup>H} NMR (101

MHz, Chloroform-*d*)  $\delta$  143.6 (dddd,  $J = 248.1, 17.0, 12.4, 3.3$  Hz, 2C), 140.9 (d,  $J = 264.7$  Hz, 2C), 121.5 (tt,  $J = 15.3, 2.9$  Hz, 1C), 65.6 (s, 1C). HRMS ( $m/z$ ):  $[M - H]^-$  calcd for  $[C_8HF_4N_2O_2]^-$  232.9979; found 232.9965.

**3.3.3d: methyl 2,3,5,6-tetrafluoro-4-(nitromethyl)benzoate:** General Procedure 3.5.A was followed on a 1 gram scale, with methyl pentafluorobenzoate (3.74 mmol, 0.55 mL), TMG (7.86 mmol, 0.99 mL) and nitromethane (44.92 mmol, 2.43 mL) except the instead of washing the organic layers with 0.1 M HCl, crude material was dissolved in methanol and triturated by dripping the solution into DI water, resulting in an amber colored crystalline solid. 0.746 g, 75% yield. MP 35-36 °C (lit. m.p. 30–31 °C)<sup>244</sup>  $^{19}F$  NMR (376 MHz, Chloroform-*d*)  $\delta$  -137.85 – -138.07 (m, 2F), -139.64 – -139.84 (m, 2F).  $^1H$  NMR (400 MHz, Chloroform-*d*)  $\delta$  5.58 (s, 2H), 3.95 (s, 3H).  $^{13}C\{^1H\}$  NMR (101 MHz, Chloroform-*d*)  $\delta$  159.4 (s, 1C), 145.4 (ddt,  $J = 254.0, 14.8, 4.7$  Hz, 2C), 144.4 (ddt,  $J = 258.3, 14.9, 4.7$  Hz, 2C), 115.2 (td,  $J = 16.3, 4.1$  Hz, 1C), 111.2 (t,  $J = 17.6$  Hz, 1C), 65.6 (s, 1C), 53.7 (d,  $J = 2.3$  Hz, 1C). HRMS ( $m/z$ ):  $[M - H]^-$  calcd for  $[C_9H_4F_4NO_4]^-$  266.0082; found 266.0071.

**3.3.3e: 1,2,3,4,5,6,8-heptafluoro-7-(nitromethyl)naphthalene:** General Procedure 3.5.B was followed on a 250 mg scale, with octafluoronaphthalene (0.80 mmol, 217.24 mg), DBU (1.68 mmol, 0.25 mL), and nitromethane (9.58 mmol, 0.52 mL), except the reaction time was increased to 3 hours. The product was separated by normal phase liquid chromatography with the product eluting at 5% EtOAc in hexanes. 0.1688 g off white crystalline solid, 68% yield. MP 96-98 °C.  $^{19}F$  NMR (376 MHz, Chloroform-*d*)  $\delta$  -118.32 (ddt,  $J = 67.7, 19.4, 3.9$  Hz, 1F), -138.15 (ddq,  $J = 16.7, 8.1, 4.1$  Hz, 1F), -142.39 (dtt,  $J = 67.8, 16.8, 4.6$  Hz, 1F), -144.72 (dddt,  $J = 58.1, 19.1, 14.9, 2.4$  Hz, 1F), -147.07 (dtt,  $J = 58.1, 18.1, 4.7$  Hz, 1F), -149.98 (dddt,  $J = 20.2, 17.6, 8.4, 4.2$  Hz, 1F), -153.57 (ddtd,  $J = 19.5, 17.1, 7.4, 4.0$  Hz, 1F).  $^1H$  NMR (400 MHz, Chloroform-*d*)  $\delta$  5.75 (s, 1H).  $^{13}C\{^1H\}$  NMR (101 MHz, Chloroform-*d*)  $\delta$  151.9 (d,  $J = 263.7$  Hz), 145.6 (dd,  $J = 254.5, 14.3$  Hz), 141.8 (d,  $J = 261.1$  Hz), 141.4 (d,  $J = 255.3$  Hz), 140.8 (dt,  $J = 258.9, 15.1$  Hz), 140.6 (d,  $J = 259.7$  Hz), 139.1 (dt,  $J = 256.3, 14.9$  Hz), 112.8, 107.7 (t,  $J = 13.5$  Hz), 107.2 (t,  $J = 19.2$  Hz), 65.9 (p,  $J = 2.1$  Hz). Structure Assigned by  $^{13}C : ^1H$  HMBC. HRMS ( $m/z$ ):  $[M - H]^-$  calcd for  $[C_{11}HF_7NO_2]^-$  311.9901; found 311.9893.

**3.3.3f: 1,2,4,5-tetrafluoro-3-(nitromethyl)-6-(trifluoromethyl)benzene:** General Procedure 3.5.B was followed on a 1 gram scale, with octafluorotoluene (3.61 mmol, 0.51 mL), DBU (7.58 mmol, 1.13 mL), and nitromethane (43.31 mmol, 2.35 mL) resulting in a colorless crystalline solid. 0.9362 g, 98% yield. MP 46-51 °C.  $^{19}F$  NMR (376 MHz, Chloroform-*d*)  $\delta$  -56.16 – -56.95 (m), -138.25 – -139.03 (m).  $^1H$  NMR (400 MHz, Chloroform-*d*)  $\delta$  5.67 (s, 2H).  $^{13}C\{^1H\}$  NMR (101 MHz, Chloroform-*d*)  $\delta$  145.7 (d,  $J = 257.2$  Hz, 2C), 144.1 (d,  $J = 264.6$  Hz, 2C), 120.4 (q,  $J = 275.3$  Hz, 1C), 113.0 – 112.3 (m, 2C), 65.4 (t,  $J = 2.5$  Hz, 1C). HRMS ( $m/z$ ):  $[M - H]^-$  calcd for  $[C_8HF_7NO_2]^-$  275.9901; found 275.9881.

**3.3.3g: 1,2,3,4,5-pentafluoro-6-(nitromethyl)benzene:** General Procedure 3.5.B was followed on a 1 gram scale, with hexafluorobenzene (4.40 mmol, 0.508 mL), DBU (9.25 mmol, 1.38 mL), and nitromethane (52.84 mmol, 2.86 mL), except with reaction time extended to 4 hours. Resulted in a light tan liquid. 0.833 g, 83% yield.  $^{19}F$  NMR (376 MHz, Chloroform-*d*)  $\delta$  -140.82 – -140.95 (m, 2F), -149.28 (tt,  $J = 20.8, 3.3$  Hz, 1F), -160.56 – -160.89 (m, 2F).  $^1H$  NMR: (400 MHz, Chloroform-*d*)  $\delta$  5.51 (t,  $J = 1.50, 2H$ ).  $^{13}C\{^1H\}$  NMR (101 MHz, Chloroform-*d*)  $\delta$  146.1 (dddt,  $J = 252.7, 11.4, 7.6, 4.1$  Hz), 143.2

(dt,  $J = 258.8, 13.3, 5.3$  Hz, 1C), 137.9 (d,  $J = 253.2$ , Hz, 2C), 104.1 (td,  $J = 17.3, 4.2$  Hz, 2C), 65.5 (s, 1C). HRMS (m/z): [M - H]<sup>-</sup> calcd for [C<sub>7</sub>HF<sub>5</sub>NO<sub>2</sub>]<sup>-</sup> 225.9933; found 225.9916.

**3.3.3h: 1,2,4,5-tetrafluoro-3-(nitromethyl)benzene:** General Procedure 3.5.B was followed on a 2 gram scale, with pentafluorobenzene (9.56 mmol, 1.06 mL), DBU (20.09 mmol, 3.00 mL), and nitromethane (114.78 mmol, 6.22 mL), but the reaction time was lengthened to 18 hours, resulting in a light tan liquid., 1.852 g, 93% yield. <sup>19</sup>F NMR: (400 MHz, Chloroform-*d*) δ -140.87 (m, 2F), -149.28 (tt,  $J=20.85$  Hz, 3.33 Hz 1F), -160.73 (m, 2F). <sup>1</sup>H NMR: (400 MHz, Chloroform-*d*) δ 5.51 (t,  $J=1.50$ , 2H). <sup>13</sup>C{<sup>1</sup>H} Proton decoupled NMR (101 MHz, CDCl<sub>3</sub>) δ 146.1 (dddt,  $J=252.73$  Hz, 11.35 Hz, 7.62 Hz, 4.10 Hz, 2C), δ 143.7 (m, 1C), δ 137.9 (m, 2C), δ 104.1 (td,  $J=17.26$  Hz, 4.18 Hz, 1C), δ 65.5 (s, 1C). HRMS (m/z): [M - H]<sup>-</sup> calcd for [C<sub>7</sub>H<sub>2</sub>F<sub>4</sub>NO<sub>2</sub>]<sup>-</sup> 208.0027; found 208.0022.

**3.3.3i: 2,2',3,3',5,5',6,6'-octafluoro-4,4'-bis(nitromethyl)-1,1'-biphenyl:** General Procedure 3.5.B was followed on a 50 mg scale, with decafluorobiphenyl (0.12 mmol, 40.1 mg), DBU (0.25 mmol, 40 μL), and nitromethane (1.44 mmol, 80 μL), except the reaction was conducted at 60 °C. Following concentration, the material was purified by normal phase flash chromatography, with the product eluting at 25% ethyl acetate in hexanes. 36 mg yield, 72%. MP 171-173 °C. <sup>19</sup>F NMR (376 MHz, Chloroform-*d*) δ -135.81 – -136.38 (m, 4F), -139.33 – -139.58 (m, 4F). <sup>1</sup>H NMR (400 MHz, Chloroform-*d*) δ 5.65 (t,  $J = 1.4$  Hz, 4H). <sup>13</sup>C{<sup>1</sup>H} NMR (101 MHz, Chloroform-*d*) δ 145.5 (dd,  $J = 254.8, 11.7$  Hz, 4C), 144.0 (dd,  $J = 254.9, 15.3$  Hz, 4C), 110.9 (t,  $J = 16.7$  Hz, 2C), 109.3 (s, 2C), 65.8 (s, 2C). HRMS (m/z): [M - H]<sup>-</sup> calcd for [C<sub>14</sub>H<sub>3</sub>F<sub>8</sub>N<sub>2</sub>O<sub>4</sub>]<sup>-</sup> 414.9970; found 414.9944

**3.3.4a: 1,2,3,4-tetrafluoro-5-nitro-6-(nitromethyl)benzene and 3.3.3b: 1,2,4,5-tetrafluoro-3-nitro-6-(nitromethyl)benzene.** General Procedure 3.5.A was followed, resulting in both. Relative integrations were 44% : 56% respectively by <sup>19</sup>F NMR, with complete consumption of starting material. Separated by normal phase liquid chromatography on silica gel, ethyl acetate/Hexanes with 3a eluting at 5% ethyl acetate, retention time 15 m. The concentration of ethyl acetate was then increased, and 3b eluted at 10% ethyl acetate after 25 minutes. Both 4a and 4b were somewhat viscous liquids.

**3.3.4a: 1,2,3,4-tetrafluoro-5-nitro-6-(nitromethyl)benzene:** <sup>19</sup>F NMR (376 MHz, Chloroform-*d*) δ -135.53 (dddt,  $J = 21.4, 10.0, 6.2, 1.8$  Hz, 1F), -141.91 (ddd,  $J = 21.8, 10.2, 8.3$  Hz, 1F), -144.97 (ddd,  $J = 21.5, 20.1, 8.3$  Hz, 1F), -145.77 (ddd,  $J = 21.6, 20.0, 6.2$  Hz, 1F). <sup>1</sup>H NMR (400 MHz, Chloroform-*d*) δ 5.67 (t,  $J = 2.2$  Hz, 2H). <sup>13</sup>C{<sup>1</sup>H} NMR (101 MHz, Chloroform-*d*) δ 146.6 (dddd,  $J = 256.4, 11.5, 4.3, 2.5$  Hz, 1C), 143.2 (dddd,  $J = 264.9, 17.1, 11.9, 3.2$  Hz, 1C), 142.6 (d,  $J = 263.5$  Hz, 1C), 135.0 (s, 1C), 129.3 – 126.8 (m, 1C), 109.3 (ddd,  $J = 16.3, 4.6, 2.0$  Hz, 1C), 66.8 (s, 1C). HRMS (m/z): [M - H]<sup>-</sup> calcd for [C<sub>7</sub>HF<sub>4</sub>N<sub>2</sub>O<sub>4</sub>]<sup>-</sup> 252.9878; found 252.9869.

**3.3.4b: 1,2,4,5-tetrafluoro-3-nitro-6-(nitromethyl)benzene** <sup>19</sup>F NMR (376 MHz, Chloroform-*d*) δ -136.27 – -136.45 (m, 2F), -144.49 – -144.88 (m, 2F). <sup>1</sup>H NMR (400 MHz, Chloroform-*d*) δ 5.69 (t,  $J = 1.5$  Hz, 2H). <sup>13</sup>C{<sup>1</sup>H} NMR (101 MHz, Chloroform-*d*) δ 145.7 (dd,  $J = 257.4, 23.0$  Hz), 140.2 (dd,  $J = 265.0, 22.1$  Hz), 132.0, 112.5 (t,  $J = 16.9$  Hz), 65.4 (p,  $J = 2.1$  Hz). HRMS (m/z): [M - H]<sup>-</sup> calcd for [C<sub>7</sub>HF<sub>4</sub>N<sub>2</sub>O<sub>4</sub>]<sup>-</sup> 252.9878; found 252.9869.

**3.3.4c: 1-chloro-2,3,6-trifluoro-4-nitro-5-(nitromethyl)benzene** Beginning with starting materials prepared as in literature,<sup>253</sup> General Procedure 3.5.A was followed on a 0.218 mmol scale, with 1-chloro-2,3,5,6-tetrafluoro-4-nitrobenzene, (0.218 mmol, 50 mg), TMG (0.46 mmol, 60  $\mu$ L), and nitromethane (2.62 mmol, 140  $\mu$ L) with reaction time extended to 3 hours, resulting in a light brown oil, 31 mg, 53% yield. <sup>19</sup>F NMR (376 MHz, Chloroform-*d*)  $\delta$  -114.00 – -114.19 (m, 1F), -123.57 – -124.11 (m, 1F), -142.87 – -143.54 (m, 1F). <sup>1</sup>H NMR (400 MHz, Chloroform-*d*)  $\delta$  5.68 (s, 2H). <sup>13</sup>C{<sup>1</sup>H} NMR (101 MHz, Chloroform-*d*)  $\delta$  152.5 (d, *J* = 255.5 Hz, 1C), 148.6 (ddd, *J* = 262.2, 14.5, 4.3 Hz, 1C), 140.9 (ddd, *J* = 266.4, 15.7, 4.6 Hz, 1C), 136.7 (m, 1C), 116.4 (dd, *J* = 23.5, 17.8 Hz, 1C), 107.6 (d, *J* = 19.5 Hz, 1C), 66.1 (s, 1C). HRMS (*m/z*): [M - H]<sup>-</sup> calcd for [C<sub>7</sub>HCIF<sub>3</sub>N<sub>2</sub>O<sub>4</sub>]<sup>-</sup> 268.9582; found 268.9564.

**3.3.5a: 2,3,5,6-tetrafluoro-4-(1-nitroethyl)pyridine:** General Procedure 3.5.A was followed on a 1 g scale, with pentafluoropyridine (4.76 mmol, 0.52 mL), TMG (10.00 mmol, 1.25 mL), and nitroethane (57.12 mmol, 4.08 mL), with crude reaction mixture separated by normal phase liquid chromatography over silica gel, eluting at 5% DCM in Hexanes, yielding 0.6652 g pale golden liquid, 66% yield. <sup>19</sup>F NMR (376 MHz, Chloroform-*d*)  $\delta$  -88.23 – -88.66 (m, 2F), -142.21 – -142.44 (m, 2F). <sup>1</sup>H NMR (400 MHz, Chloroform-*d*)  $\delta$  5.88 (q, *J* = 7.2 Hz, 1H), 2.04 (d, *J* = 7.2 Hz, 3H). <sup>13</sup>C{<sup>1</sup>H} NMR (101 MHz, Chloroform-*d*)  $\delta$  143.7 (dddd, *J* = 247.5, 16.5, 12.6, 3.1 Hz, 2C), 140.1 (d, *J* = 263.0 Hz, 2C), 128.1 (tt, *J* = 13.9, 2.7 Hz, 1C), 74.8, 17.5 (t, *J* = 2.4 Hz, 1C). HRMS (*m/z*): [M - H]<sup>-</sup> calcd for [C<sub>7</sub>H<sub>3</sub>F<sub>4</sub>N<sub>2</sub>O<sub>2</sub>]<sup>-</sup> 223.0136; found 223.0142.

**3.3.5b: 2,3,5,6-tetrafluoro-4-(1-nitro-2-phenylethyl)pyridine:** General Procedure 3.5.B was followed on a 0.95 g scale, but 2.2 equiv. (2-nitroethyl)benzene (6.93 mmol, 1.047 g), prepared according to literature, was added to DBU (7.62 mmol, 1.14 mL) in 20 mL diethyl ether, vigorously stirring, followed by 250 mg silica gel. The reaction mixture was cooled to 0 °C, and pentafluoropyridine (3.15 mmol, 0.346 mL) in 5 mL diethyl ether (chilled) was added dropwise. Workup was the same as the general procedure. The resultant mixture was separated from the nitroalkene by reverse phase liquid chromatography, C-18 column, eluting at 45-55% acetonitrile in water after 40 minutes. Fractions were stripped of organic solvent, extracted with DCM, dry loaded onto silica gel, and further purified by normal phase liquid chromatography on a silica gel column, with the product eluting at 5% DCM in hexanes. 0.2001 g viscous yellowish liquid, 21% yield. <sup>19</sup>F NMR (376 MHz, Methylene Chloride-*d*<sub>2</sub>)  $\delta$  -89.31 – -89.57 (m, 2F), -141.47 – -141.71 (m, 2F). <sup>1</sup>H NMR (400 MHz, Methylene Chloride-*d*<sub>2</sub>)  $\delta$  7.36 – 7.11 (m, 5H), 6.11 (dd, *J* = 10.0, 6.4 Hz, 1H), 4.11 (dd, *J* = 13.9, 6.4 Hz, 1H), 3.56 (dd, *J* = 13.9, 10.0 Hz, 1H). <sup>13</sup>C{<sup>1</sup>H} NMR (101 MHz, Methylene Chloride-*d*<sub>2</sub>)  $\delta$  144.1 (dddd, *J* = 246.4, 16.7, 12.8, 3.0 Hz, 2C), 140.9 (d, *J* = 262.7 Hz, 2C), 133.9 (s, 1C), 129.7 (s, 2C), 129.4 (s, 2C), 128.6 (s, 1C), 127.0 (tt, *J* = 13.9, 2.8 Hz, 1C), 80.8 (t, *J* = 2.0 Hz, 1C), 37.7 (t, *J* = 2.2 Hz, 1C). HRMS (*m/z*): [M - H]<sup>-</sup> calcd for [C<sub>13</sub>H<sub>7</sub>F<sub>4</sub>N<sub>2</sub>O<sub>2</sub>]<sup>-</sup> 299.0449; found 299.0429.

**3.3.5c: 2,3,5,6-tetrafluoro-4-(2-nitropropan-2-yl)pyridine** General Procedure 3.5.B was followed on a 4.60 mmol scale, but 2.2 equiv. 2-nitropropane (10.12 mmol, 0.92 mL) was used instead of nitromethane, with pentafluoropyridine (4.60 mmol, 0.51 mL), and DBU (9.66 mmol, 1.44 mL). The reaction mixture was cooled to 0 °C. Workup was the same as the general procedure. Crude material purified by normal phase liquid chromatography over silica gel, with the intended product eluting at 10% EtOAc in Hexanes, 17-20 minutes retention. Evaporation yielded 31.4 mg (3% yield) brownish



crystalline solid, MP 124-129 °C.  $^{19}\text{F}$  NMR (376 MHz, Chloroform-*d*)  $\delta$  -90.16 – -90.46 (m, 2F), -162.99 – -163.40 (m, 2F).  $^1\text{H}$  NMR (400 MHz, Chloroform-*d*)  $\delta$  1.80 – 1.69 (m, 6H).  $^{13}\text{C}\{^1\text{H}\}$  NMR (101 MHz, Chloroform-*d*)  $\delta$  145.4 – 145.1 (m, 1C), 143.7 (d,  $J$  = 241.5 Hz, 2C), 132.7 (d,  $J$  = 254.1 Hz, 2C), 91.6 (s, 1C), 23.1 (s, 2C). HRMS ( $m/z$ ):  $[\text{M} - \text{H}]^-$  calcd for  $[\text{C}_8\text{H}_5\text{F}_4\text{N}_2\text{O}_2]^-$  237.02926; found 237.0278.

Procedure for the reduction of **3.3.3a** to **3.3.6a**: (**perfluoropyridin-4-yl**)methanamine W-6 Raney Ni was prepared according to literature.<sup>258</sup> To a 450 mL glass jacketed stirring pressure reactor was added 100 mL anhydrous ethanol, 1 equivalent **1a**, 6 equivalents acetic acid, and 40% m/m Raney Ni. The reactor was then sealed, stirring commenced, and the atmosphere filled and vented with 21 ATM hydrogen gas 5X. The reactor was again filled to 21 ATM and heated to 150 °C. The reaction was stirred at 150 °C for 3 hours. The reactor was then cooled in an ice bath to room temperature, vented, and the opened. The resultant solution was vacuum filtered through celite and stripped of solvent in vacuo. The solids that formed were dissolved in a 1 M aqueous HCl and washed with diethyl ether, the organic phase then being discarded. The aqueous layer was made basic with 2 M aqueous NaOH, at which time, visible white precipitate formed. The aqueous layer was then extracted with diethyl ether. The organic layer was dried with  $\text{MgSO}_4$ , and made acidic with anhydrous ethereal HCl. White solids precipitated and were separated by vacuum filtration, washed with additional anhydrous diethyl ether, and dried over vacuum.

**3.3.6a: (perfluoropyridin-4-yl)methanamine hydrochloride** slightly off-white solid. 2.23 mmol scale, 452 mg, 93% yield. MP 264 °C (vaporized/decomposed).  $^{19}\text{F}$  NMR (376 MHz, Deuterium Oxide)  $\delta$  -90.92 – -91.20 (m, 2F), -142.13 – -143.11 (m, 2F).  $^1\text{H}$  NMR (400 MHz, Deuterium Oxide)  $\delta$  4.49 (s, 2H).  $^{13}\text{C}\{^1\text{H}\}$  NMR (101 MHz, DMSO- $d_6$ )  $\delta$  142.3 (dt,  $J$  = 242.9, 15.4 Hz, 2C), 140.6 (d,  $J$  = 259.5 Hz, 2C), 127.6 (t,  $J$  = 16.4 Hz, 1C), 30.5 (s, 1C). HRMS ( $m/z$ ):  $[\text{M} + \text{H}]^+$  calcd for  $[\text{C}_6\text{H}_5\text{F}_4\text{N}_2]^+$  181.0383; found 181.0377.

### Computational Methods

Structures were built and optimized at MM2 levels using PerkinElmer Chem3D 15.0.0.106. They were then optimized at the B3LYP theory level with basis set 6-311+G(2d,p), with cube files for LUMO, electron density, and electrostatic potential generated in Gaussian 09.<sup>260</sup> The electron density surface was rendered at 0.001 au, and mapped with the electrostatic density cube in UCSF Chimera 1.11.2.

### 3.6 Acknowledgements

The authors would like to thank Dr. Anuradha Singh for an initial experimental result, and Dr. Chris Fennell for his computational assistance.

### 3.7 References

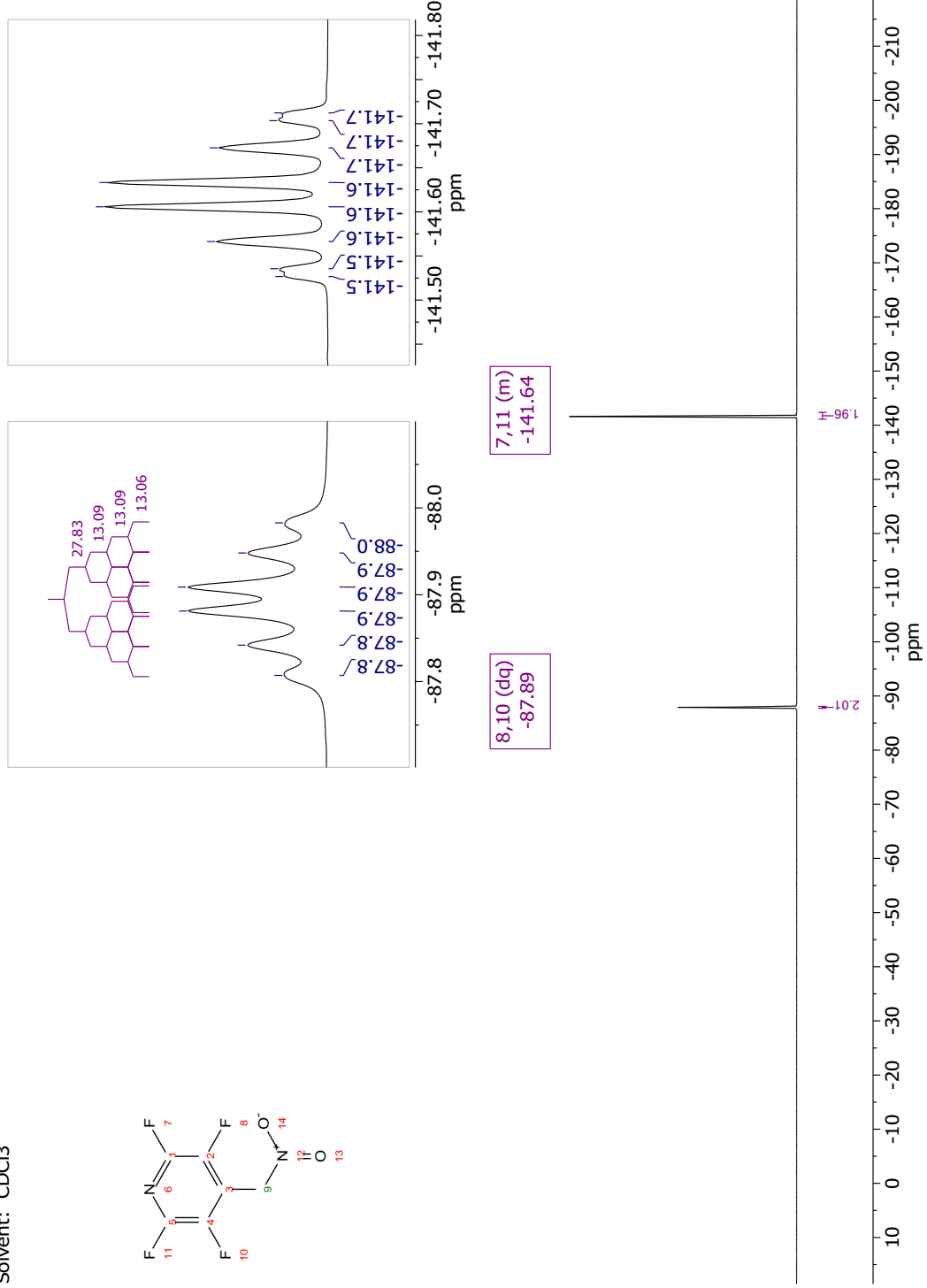
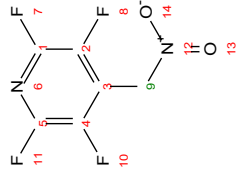
1. Penning, T. D.; Talley, J. J.; Bertenshaw, S. R.; Carter, J. S.; Collins, P. W.; Docter, S.; Graneto, M. J.; Lee, L. F.; Malecha, J. W.; Miyashiro, J. M.; Rogers, R. S.; Rogier, D. J.; Yu, S. S.; Anderson, G. D.; Burton, E. G.; Cogburn, J. N.; Gregory, S. A.; Koboldt, C. M.; Perkins, W. E.; Seibert, K.; Veenhuizen, A. W.; Zhang, Y. Y.; Isakson, P. C., Synthesis and Biological Evaluation of the 1,5-Diarylpyrazole Class of Cyclooxygenase-2 Inhibitors: Identification of 4-[5-(4-Methylphenyl)-3-(trifluoromethyl)-1H-pyrazol-1-yl]benzenesulfonamide (SC-58635, Celecoxib). *J. Med. Chem.* **1997**, *40* (9), 1347-1365.

2. Purser, S.; Moore, P. R.; Swallow, S.; Gouverneur, V., Fluorine in medicinal chemistry. *Chem. Soc. Rev.* **2008**, *37* (2), 320-330.
3. Gillis, E. P.; Eastman, K. J.; Hill, M. D.; Donnelly, D. J.; Meanwell, N. A., Applications of Fluorine in Medicinal Chemistry. *J. Med. Chem.* **2015**, *58* (21), 8315-8359.
4. Wang, J.; Sanchez-Rosello, M.; Acena, J. L.; del Pozo, C.; Sorochinsky, A. E.; Fustero, S.; Soloshonok, V. A.; Liu, H., Fluorine in pharmaceutical industry: fluorine-containing drugs introduced to the market in the last decade (2001-2011). *Chem. Rev.* **2014**, *114* (4), 2432-506.
5. Schimler, S. D.; Ryan, S. J.; Bland, D. C.; Anderson, J. E.; Sanford, M. S., Anhydrous Tetramethylammonium Fluoride for Room-Temperature SNAr Fluorination. *J. Org. Chem.* **2015**, *80* (24), 12137-12145.
6. Tang, P.; Furuya, T.; Ritter, T., Silver-Catalyzed Late-Stage Fluorination. *J. Am. Chem. Soc.* **2010**, *132* (34), 12150-12154.
7. Furuya, T.; Ritter, T., Fluorination of Boronic Acids Mediated by Silver(I) Triflate. *Org. Lett.* **2009**, *11* (13), 2860-2863.
8. Brooke, G. M., The preparation and properties of polyfluoro aromatic and heteroaromatic compounds. *J. Fluorine Chem.* **1997**, *86* (1), 1-76.
9. Campbell, M. G.; Ritter, T., Modern Carbon-Fluorine Bond Forming Reactions for Aryl Fluoride Synthesis. *Chem. Rev.* **2015**, *115* (2), 612-633.
10. Chambers, R. D.; Hutchinson, J.; Musgrave, W. K. R., Polyfluoro-heterocyclic compounds. Part I. The preparation of fluoro-, chlorofluoro-, and chlorofluorohydro-pyridines. *J. Chem. Soc.* **1964**, 3573.
11. Kiplinger, J. L.; Richmond, T. G.; Osterberg, C. E., Activation of Carbon-Fluorine Bonds by Metal Complexes. *Chem. Rev.* **1994**, *94* (2), 373-431.
12. Ahrens, T.; Kohlmann, J.; Ahrens, M.; Braun, T., Functionalization of Fluorinated Molecules by Transition-Metal-Mediated C-F Bond Activation To Access Fluorinated Building Blocks. *Chem. Rev.* **2015**, *115* (2), 931-972.
13. Amii, H.; Uneyama, K., C-F Bond Activation in Organic Synthesis. *Chem. Rev.* **2009**, *109* (5), 2119-2183.
14. Senaweera, S. M.; Weaver, J. D., Selective Perfluoro- and Polyfluoroarylation of Meldrum's Acid. *J. Org. Chem.* **2014**, *79* (21), 10466-10476.
15. Senaweera, S. M.; Weaver, J. D., Dual C-F, C-H Functionalization via Photocatalysis; Access to Multi-Fluorinated Biaryls. *J. Am. Chem. Soc.* **2016**, *138*, 2520-2523.
16. Singh, A.; Kubik, J. J.; Weaver, J. D., Photocatalytic C-F alkylation; facile access to multifluorinated arenes. *Chem. Sci.* **2015**, *6* (12), 7206-7212.
17. Senaweera, S. M.; Singh, A.; Weaver, J. D., Photocatalytic Hydrodefluorination: Facile Access to Partially Fluorinated Aromatics. *J. Am. Chem. Soc.* **2014**, *136* (8), 3002-3005.
18. Singh, A.; Kubik, J. J.; Weaver, J. D., Photocatalytic C-F alkylation; facile access to multifluorinated arenes. *Chemical Science* **2015**, *6* (12), 7206-7212.
19. Senaweera, S.; Weaver, J. D., Photocatalytic C-F Reduction and Functionalization. *Aldrichimica Acta* **2016**, *49*, 45.
20. Senaweera, S. M.; Singh, A.; Weaver, J. D., Photocatalytic Hydrodefluorination: Facile Access to Partially Fluorinated Aromatics. *J. Am. Chem. Soc.* **2014**, *136* (8), 3002-3005.
21. Arora, A.; Weaver, J. D., Visible Light Photocatalysis for the Generation and Use of Reactive Azolyl and Polyfluoroaryl Intermediates. *Acc. Chem. Res.* **2016**, *49* (10), 2273-2283.
22. Senaweera, S.; Weaver, J. D., Dual C-F, C-H Functionalization via Photocatalysis: Access to Multifluorinated Biaryls. *J. Am. Chem. Soc.* **2016**, *138* (8), 2520-3.

23. Singh, A.; Fennell, C. J.; Weaver, J. D., Photocatalyst size controls electron and energy transfer: selectable E/Z isomer synthesis via C-F alkenylation. *Chem. Sci.* **2016**, *7* (11), 6796-6802.
24. Weaver, J. D., Hydrodefluorination of Perfluoroarenes Meets Visible Light Photocatalysis. *Synlett* **2014**, *25* (14), 1946-1952.
25. LaBerge, N. A.; Love, J. A., Activation and Formation of Aromatic C–F Bonds. In *Organometallic Fluorine Chemistry*, Braun, T.; Hughes, R. P., Eds. Springer International Publishing: Cham, 2015; pp 55-111.
26. Hu, J.-Y.; Zhang, J.-L., Hydrodefluorination Reactions Catalyzed by Transition-Metal Complexes. In *Organometallic Fluorine Chemistry*, Braun, T.; Hughes, R. P., Eds. Springer International Publishing: Cham, 2015; pp 143-196.
27. Chambers, R. D.; Martin, P. A.; Sandford, G.; Williams, D. L. H., Mechanisms of reactions of halogenated compounds: Part 7. Effects of fluorine and other groups as substituents on nucleophilic aromatic substitution. *J. Fluorine Chem.* **2008**, *129* (10), 998-1002.
28. Sun, Y.; Sun, H.; Jia, J.; Du, A.; Li, X., Transition-Metal-Free Synthesis of Fluorinated Arenes from Perfluorinated Arenes Coupled with Grignard Reagents. *Organometallics* **2014**, *33* (4), 1079-1081.
29. Chambers, R. D.; Hassan, M. A.; Hoskin, P. R.; Kenwright, A.; Richmond, P.; Sandford, G., Polyhalogenated heterocyclic compounds: Part 45. Reactions of perfluoro-(4-isopropylpyridine) with oxygen, nitrogen and carbon nucleophiles [1]. *J. Fluorine Chem.* **2001**, *111* (2), 135-146.
30. Beyki, K.; Haydari, R.; Maghsoodlou, M. T., Synthesis of 2,3,5,6-tetrafluoro-pyridine derivatives from reaction of pentafluoropyridine with malononitrile, piperazine and tetrazole-5-thiol. *SpringerPlus* **2015**, *4* (1), 757.
31. Ono, N., *The Nitro Group in Organic Synthesis*. Wiley-VCH: 2001.
32. Colgin, N.; Tatum, N. J.; Pohl, E.; Cobb, S. L.; Sandford, G., Synthesis and molecular structure of a perfluorinated pyridyl carbanion. *J. Fluorine Chem.* **2012**, *133*, 33-37.
33. Vaidyanathaswamy, R.; Radha, K.; Dharani, M.; Raguraman, T. S.; Anand, R., Reaction of nitroalkanes with polyfluoroaromatic compounds. *J. Fluorine Chem.* **2012**, *144*, 33-37.
34. Prat, D.; Pardigon, O.; Flemming, H.-W.; Letestu, S.; Ducandas, V.; Isnard, P.; Guntrum, E.; Senac, T.; Ruisseau, S.; Cruciani, P.; Hosek, P., Sanofi's Solvent Selection Guide: A Step Toward More Sustainable Processes. *Organic Process Research & Development* **2013**, *17* (12), 1517-1525.
35. Bug, T.; Lemek, T.; Mayr, H., Nucleophilicities of Nitroalkyl Anions. *J. Org. Chem.* **2004**, *69* (22), 7565-7576.
36. day, Prices of TMG and DBU.
37. Calculated using Advanced Chemistry Development (ACD/Labs) Software V11.02 (© 1994-2020 ACD/Labs).
38. Lee, L.; Kreutter, K. D.; Pan, W.; Crysler, C.; Spurlino, J.; Player, M. R.; Tomczuk, B.; Lu, T., 2-(2-Chloro-6-fluorophenyl)acetamides as potent thrombin inhibitors. *Bioorg. Med. Chem. Lett.* **2007**, *17* (22), 6266-6269.
39. Parikh, V. D.; Fray, A. H.; Kleinman, E. F., Synthesis of 8,9-difluoro-2-methyl-6-oxo-1,2-dihydropyrrolo[3,2,1-ij]quinoline-5-carboxylic acid. *J. Heterocyclic Chem.* **1988**, *25* (5), 1567-1569.
40. Pesti, J. A.; LaPorte, T.; Thornton, J. E.; Spangler, L.; Buono, F.; Crispino, G.; Gibson, F.; Lobben, P.; Papaioannou, C. G., Commercial Synthesis of a Pyrrolotriazine–Fluoroindole Intermediate to Brivanib Alaninate: Process Development Directed toward Impurity Control. *Org. Process Res. Dev.* **2014**, *18* (1), 89-102.

41. Brooke, G. M.; Burdon, J.; Tatlow, J. C., 172. Aromatic polyfluoro-compounds. Part VII. The reaction of pentafluoronitrobenzene with ammonia. *J. Chem. Soc.* **1961**, (0), 802-807.
42. Teegardin, K. A.; Weaver, J. D., Polyfluoroarylation of oxazolones: access to non-natural fluorinated amino acids. *Chemical Communications* **2017**.
43. Senaweera, S.; Weaver, J. D., *Currently unpublished work under review* **2017**.
44. Shipilov, A. I.; Zolotkova, E. E.; Igumnov, S. M., Chloro- and Bromo-defluorination of Hexafluorobenzene and Octafluorotoluene. *Russian Journal of Organic Chemistry* **2004**, *40* (8), 1117-1120.
45. Politzer, P.; Murray, J. S.; Clark, T.,  $\sigma$ -Hole Bonding: A Physical Interpretation. In *Halogen Bonding I*, Springer International Publishing Switzerland 2014: 2014; Vol. Volume 358 of the series Topics in Current Chemistry, pp 19-42.
46. Politzer, P.; Laurence, P. R.; Jayasuriya, K., Molecular electrostatic potentials: an effective tool for the elucidation of biochemical phenomena. *Environmental Health Perspectives* **1985**, *61*, 191-202.
47. Bürgi, H. B.; Dunitz, J. D.; Lehn, J. M.; Wipff, G., Stereochemistry of reaction paths at carbonyl centres. *Tetrahedron* **1974**, *30* (12), 1563-1572.
48. Billica, H. R. A., Homer, Catalyst, Raney Nickel, W-6. *Org. Synth.* **1949**, *29*, 24.
49. Subramanian, H.; Jasperse, C. P.; Sibi, M. P., Characterization of Bronsted acid-base complexes by <sup>19</sup>F DOSY. *Org. Lett.* **2015**, *17* (6), 1429-32.
50. Gaussian 09, R. C.; Frisch, M. J.; Trucks, G. W.; Schlegel, H. B.; Scuseria, G. E.; Robb, M. A.; Cheeseman, J. R.; Scalmani, G.; Barone, V.; Mennucci, B.; Petersson, G. A.; Nakatsuji, H.; Caricato, M.; Li, X.; Hratchian, H. P.; Izmaylov, A. F.; Bloino, J.; Zheng, G.; Sonnenberg, J. L.; Hada, M.; Ehara, M.; Toyota, K.; Fukuda, R.; Hasegawa, J.; Ishida, M.; Nakajima, T.; Honda, Y.; Kitao, O.; Nakai, H.; Vreven, T.; J. A. Montgomery, J.; Peralta, J. E.; Ogliaro, F.; Bearpark, M.; Heyd, J. J.; Brothers, E.; Kudin, K. N.; Staroverov, V. N.; Keith, T.; Kobayashi, R.; Normand, J.; Raghavachari, K.; Rendell, A.; Burant, J. C.; Iyengar, S. S.; Tomasi, J.; Cossi, M.; Rega, N.; Millam, J. M.; Klene, M.; Knox, J. E.; Cross, J. B.; Bakken, V.; Adamo, C.; Jaramillo, J.; Gomperts, R.; Stratmann, R. E.; Yazyev, O.; Austin, A. J.; Cammi, R.; Pomelli, C.; Ochterski, J. W.; Martin, R. L.; Morokuma, K.; Zakrzewski, V. G.; Voth, G. A.; Salvador, P.; Dannenberg, J. J.; Dapprich, S.; Daniels, A. D.; Farkas, O.; Foresman, J. B.; Ortiz, J. V.; Cioslowski, J.; Fox, D. J., *Gaussian, Inc., Wallingford CT* **2010**.

1a: 2,3,5,6-tetrafluoro-4-(nitromethyl)pyridine  
Nucleus:  $^{19}\text{F}$   
Solvent:  $\text{CDCl}_3$

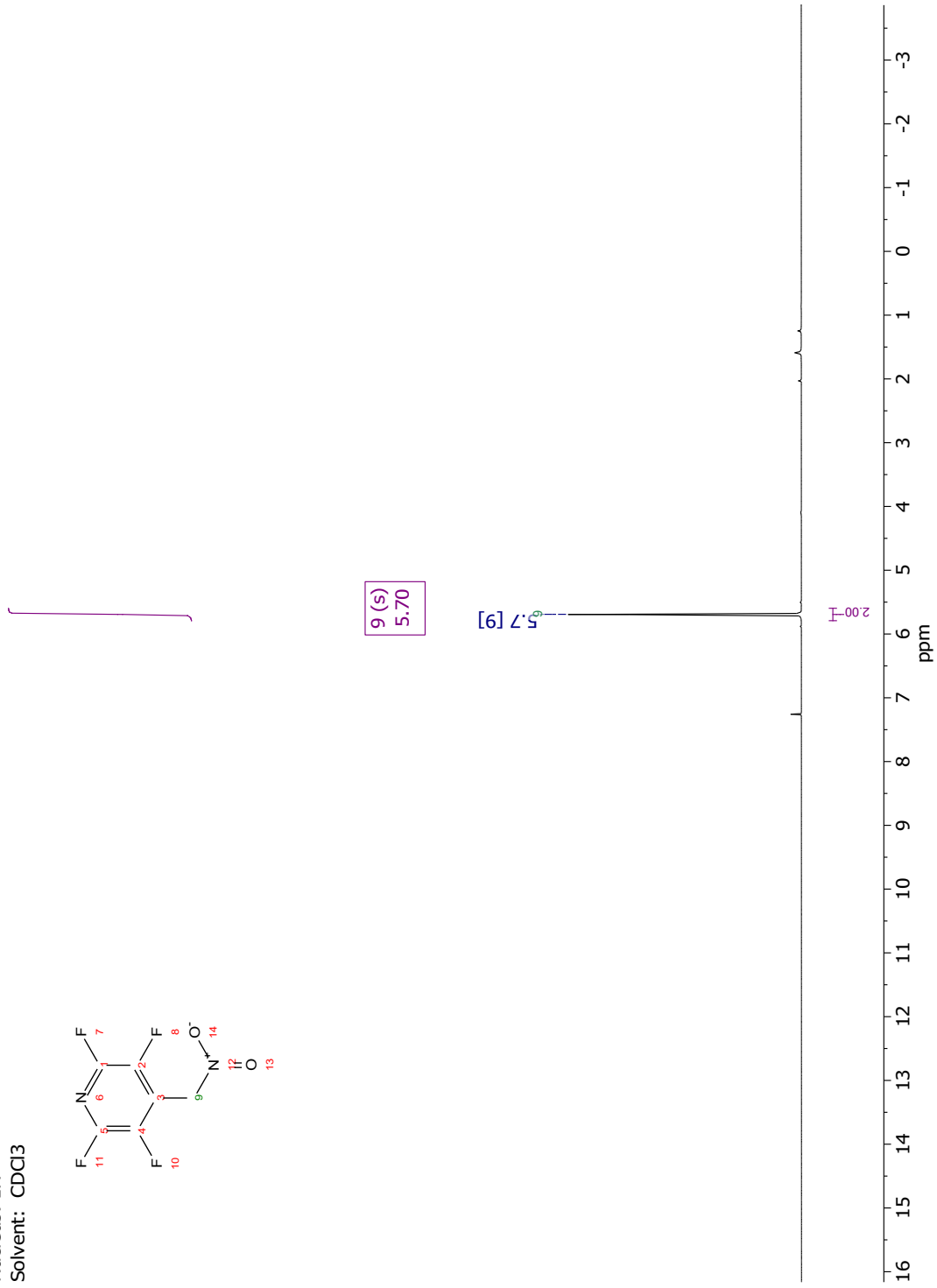
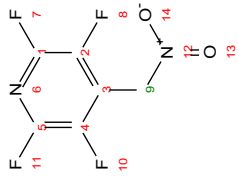


3.3.2e

1a: 2,3,5,6-tetrafluoro-4-(nitromethyl)pyridine

Nucleus: <sup>1</sup>H

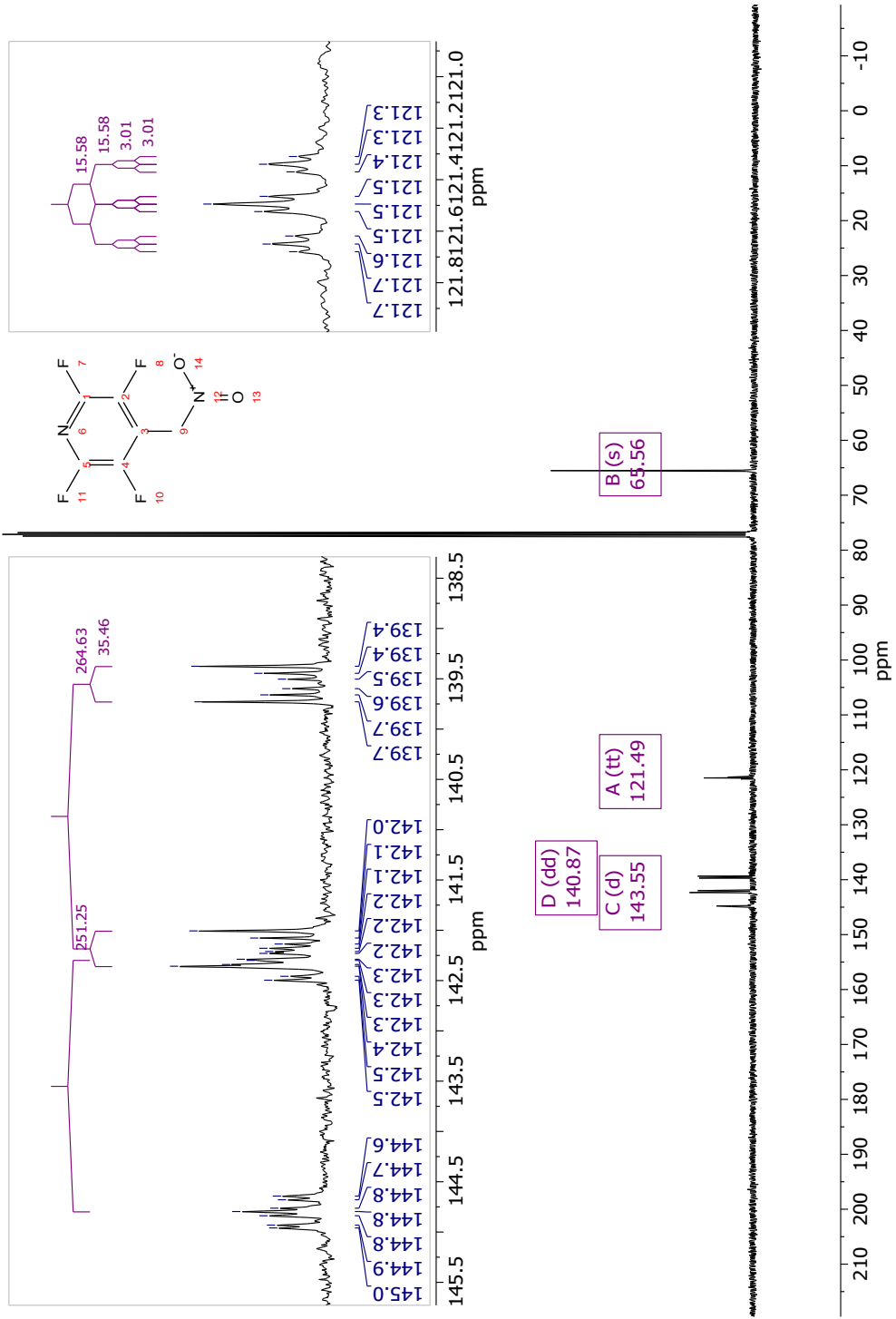
Solvent: CDCl<sub>3</sub>

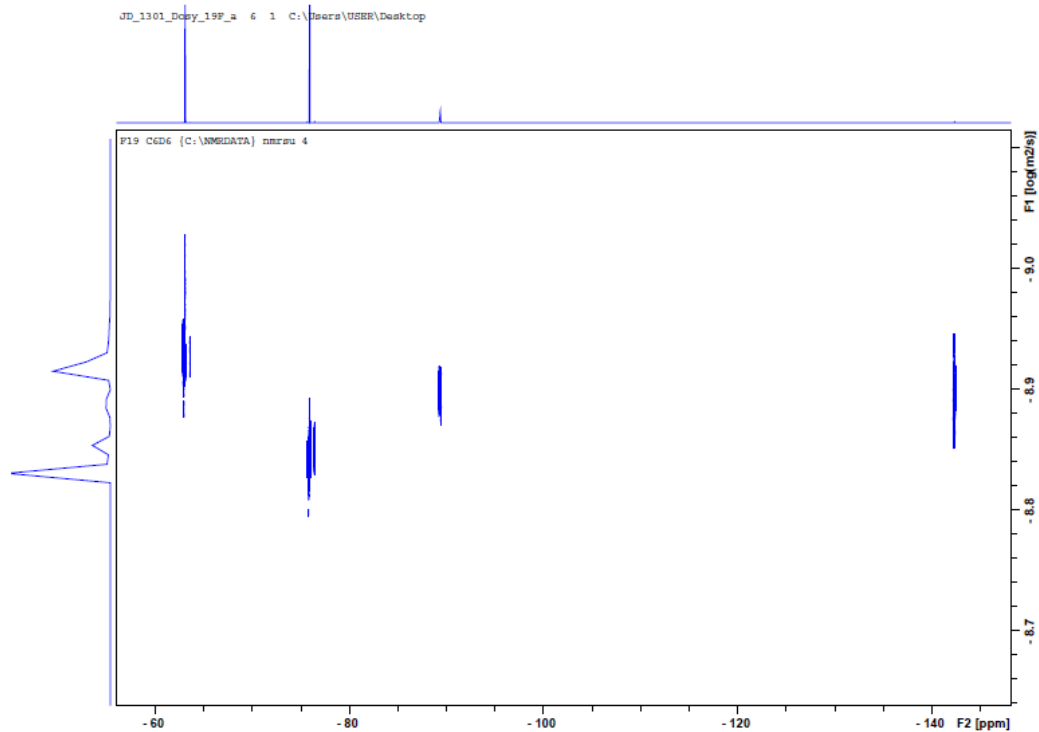


3.3.2e 2,3,5,6-tetrafluoro-4-(nitromethyl)pyridine

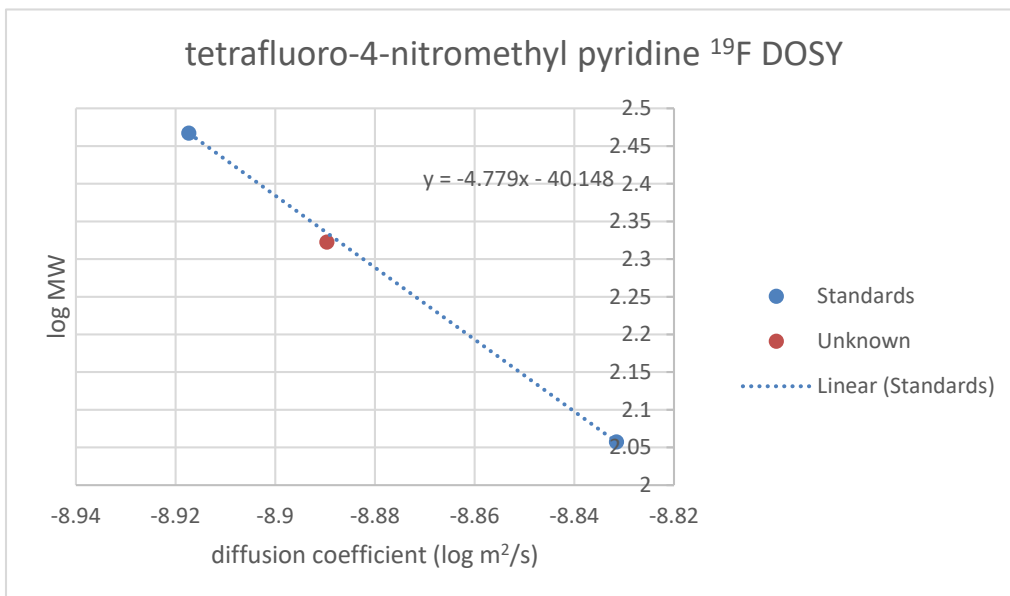
nucleus: <sup>13</sup>C

Solvent: CDCl<sub>3</sub>





	log d	mw	log mw	calc mass	%difference
bis-3,5-(CF3)-bromobenzene	-8.9173	293.1	2.467016		
TFA	-8.8315	114.02	2.056981		
tetrafluoro-4-nitromethylpyridine	-8.8896	210.09	2.322405	216.4703	3.04%





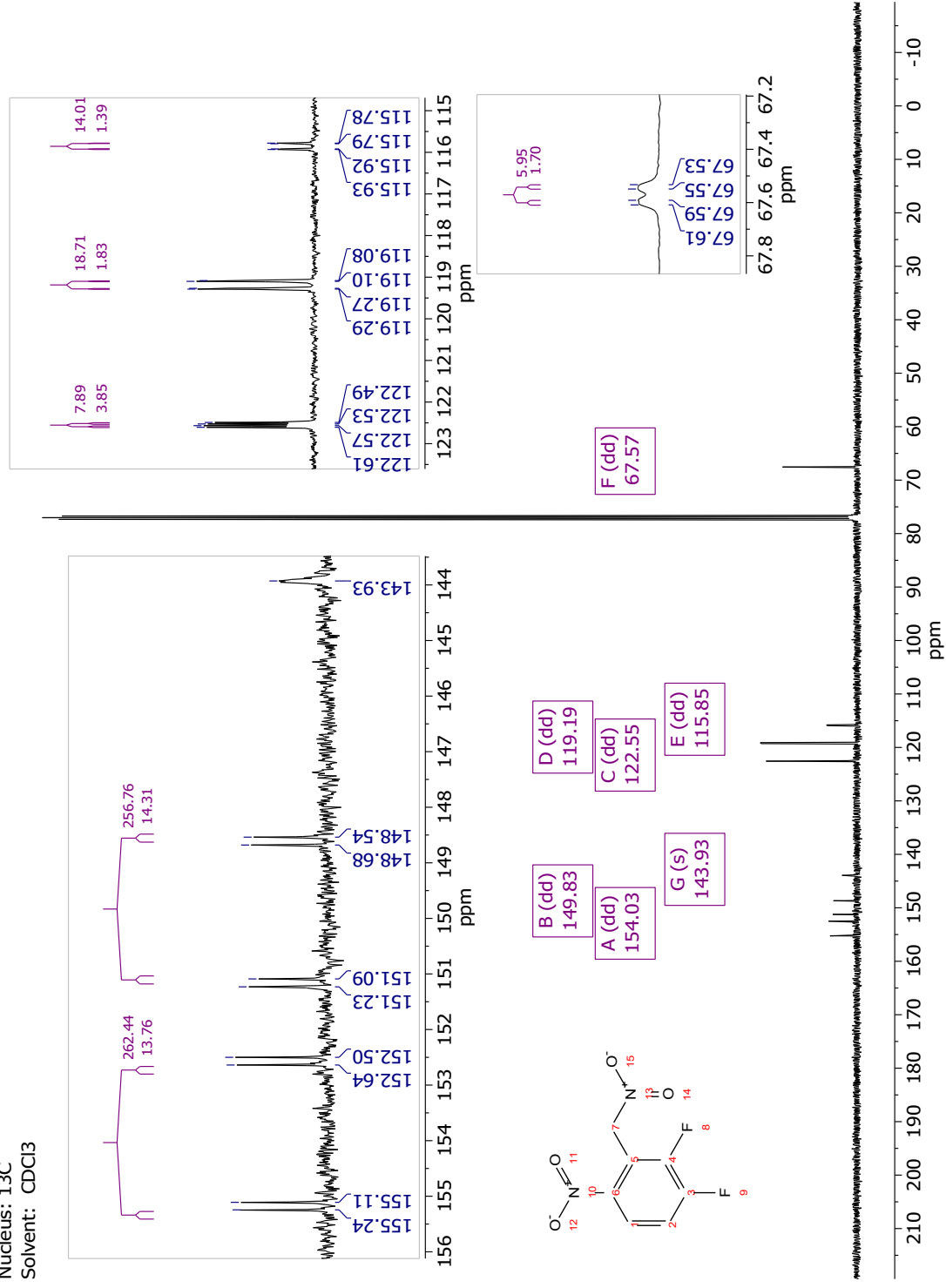


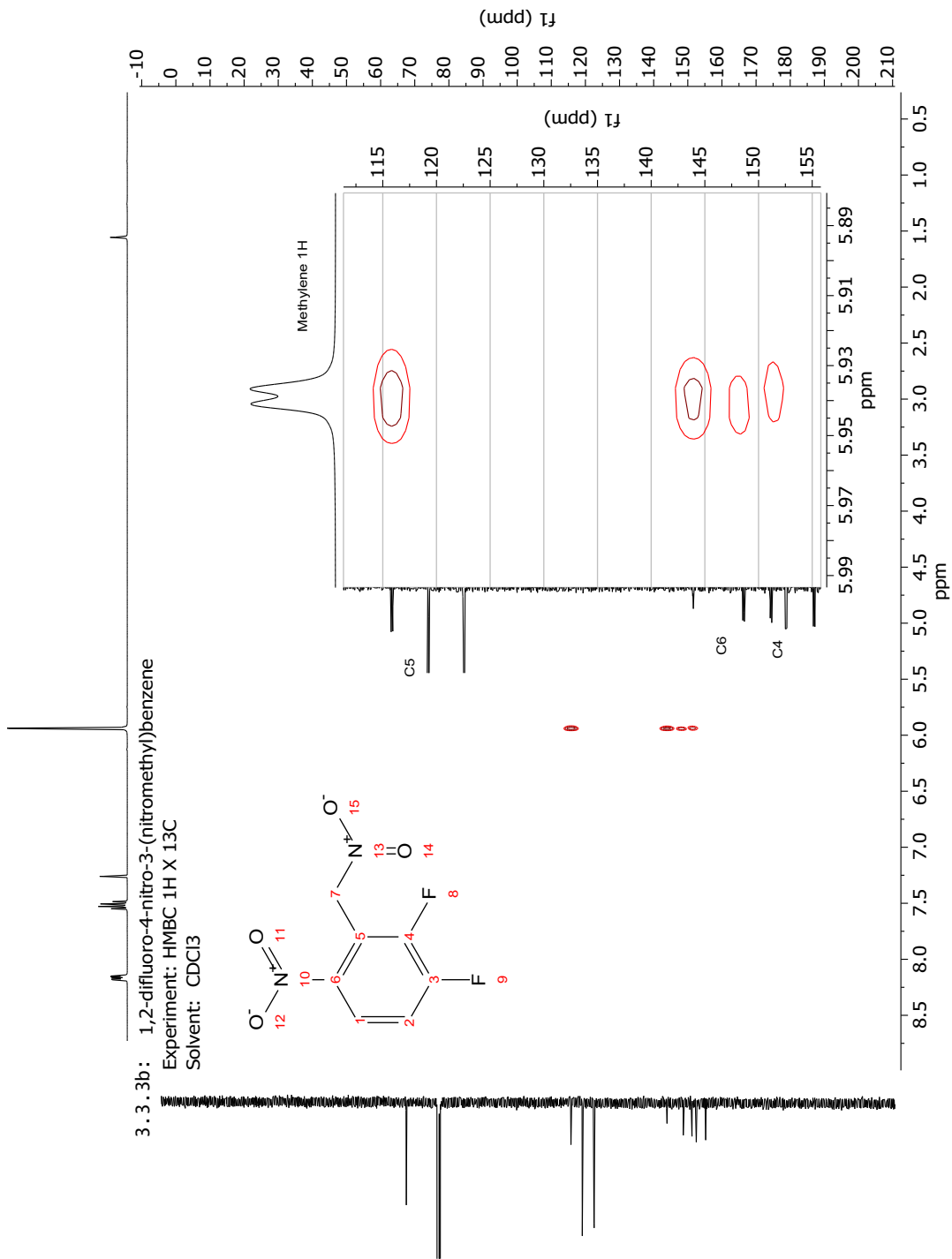


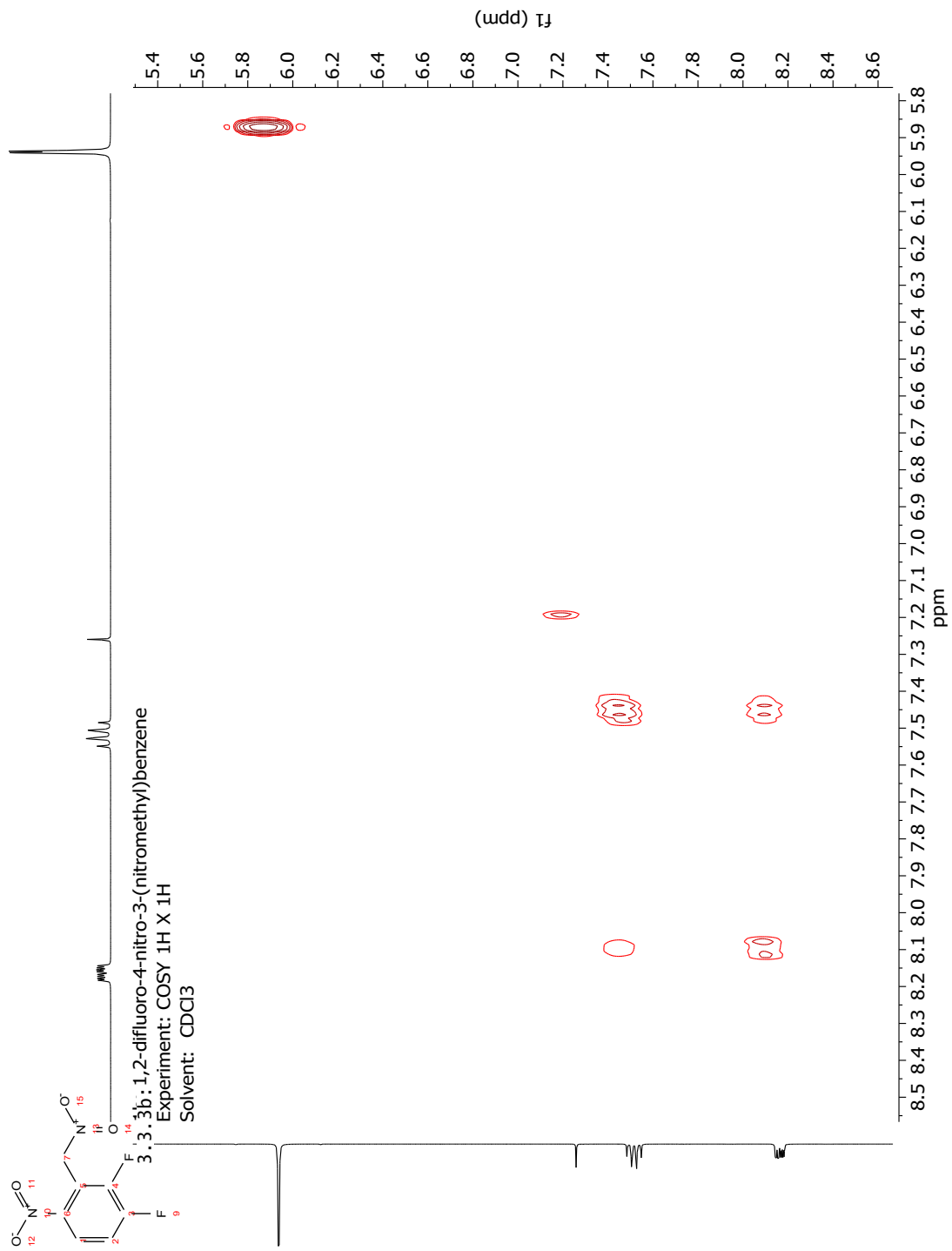
3. 3. 3b: 1,2-difluoro-4-nitro-3-(nitromethyl)benzene

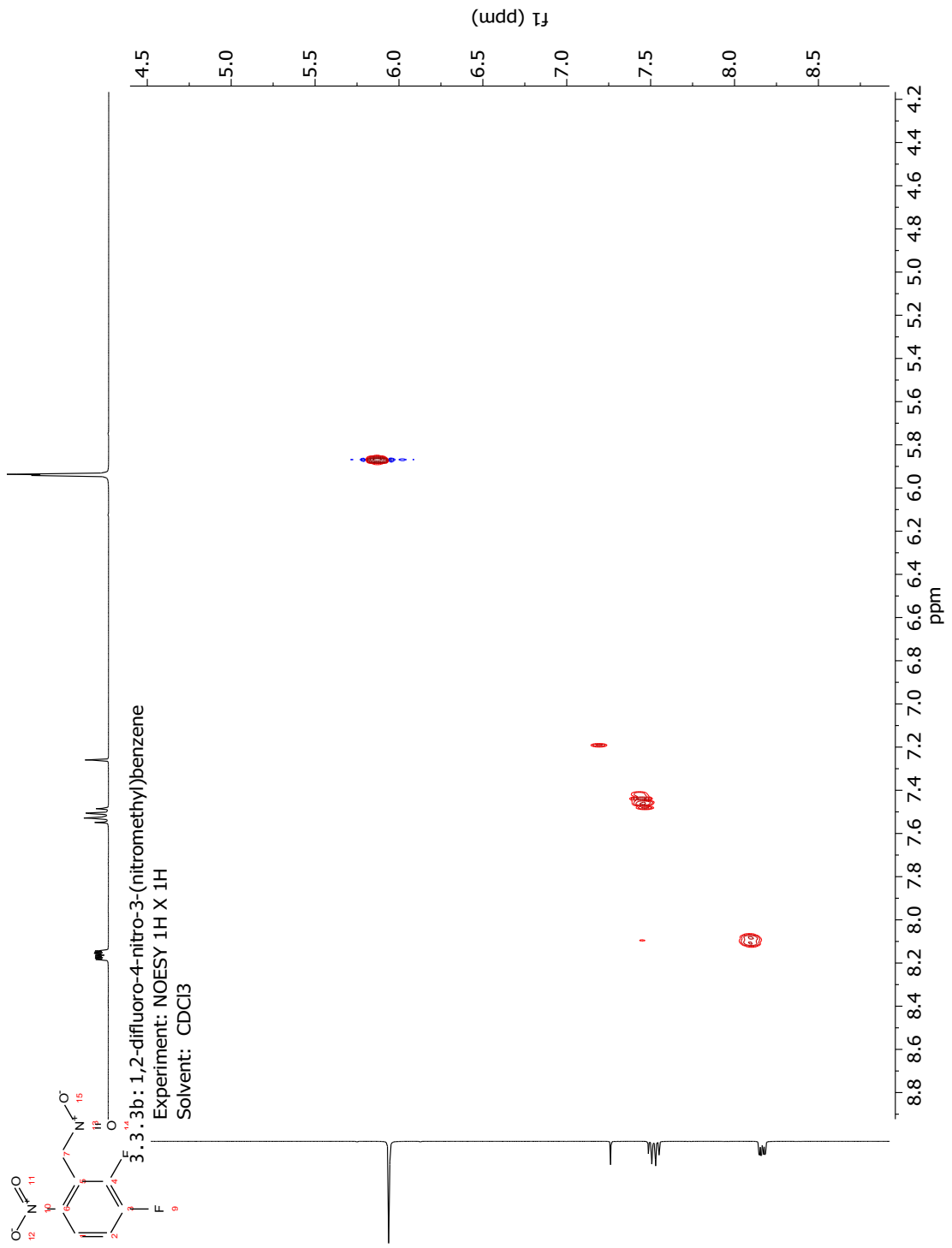
Nucleus: <sup>13</sup>C

Solvent: CDCl<sub>3</sub>



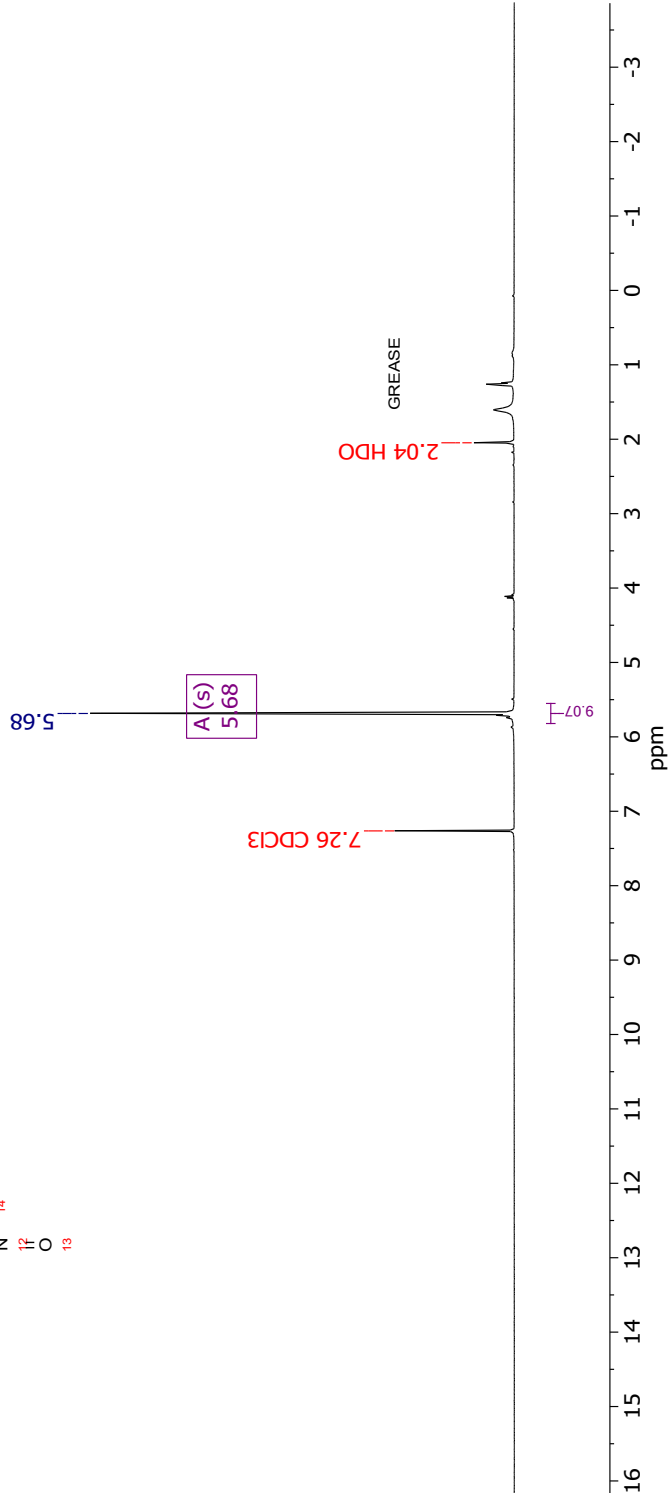
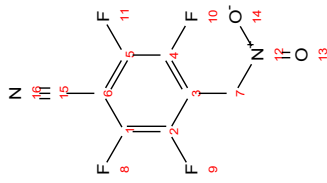






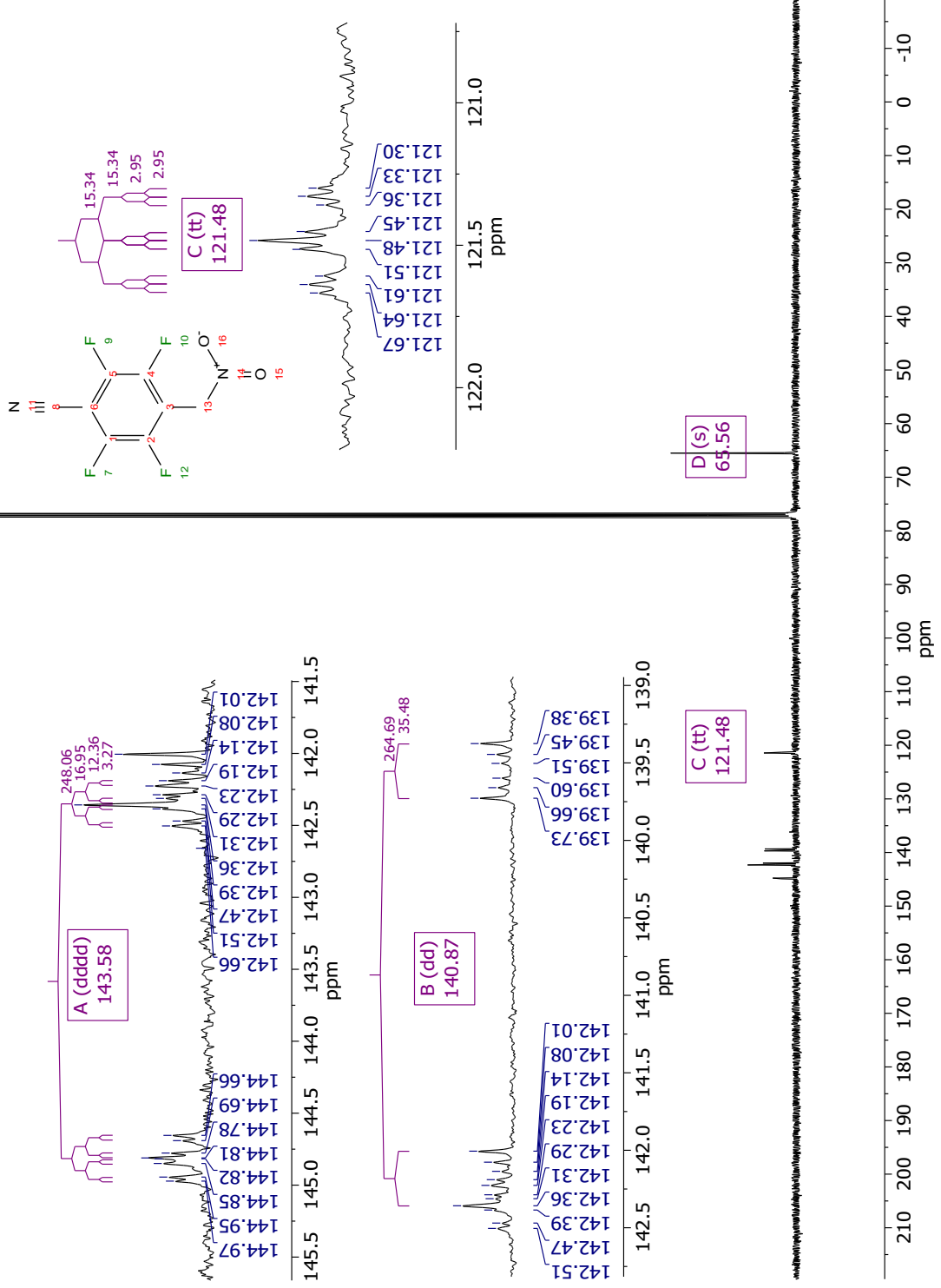


3.3.3c: 2,3,5,6-tetrafluoro-4-(nitromethyl)benzotrile  
Nucleus: <sup>1</sup>H  
Solvent: CDCl<sub>3</sub>





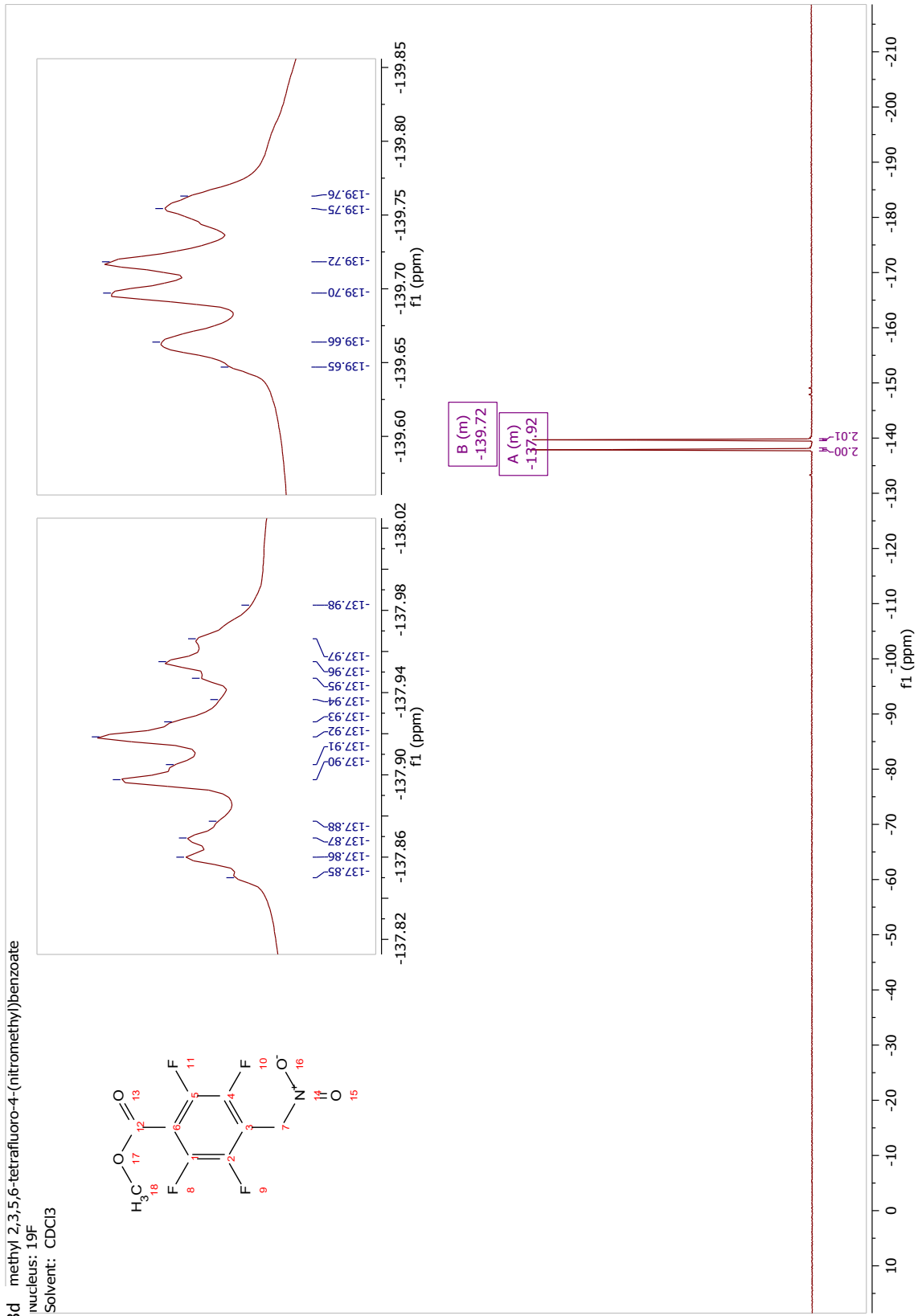
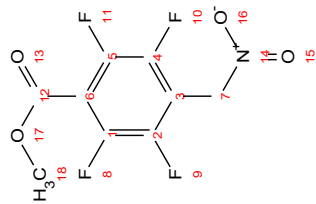
3.3.3c: 2,3,5,6-tetrafluoro-4-(nitromethyl)benzonitrile  
<sup>13</sup>C CDCl<sub>3</sub>



3.3.3d methyl 2,3,5,6-tetrafluoro-4-(nitromethyl)benzoate

nucleus:  $^{19}\text{F}$

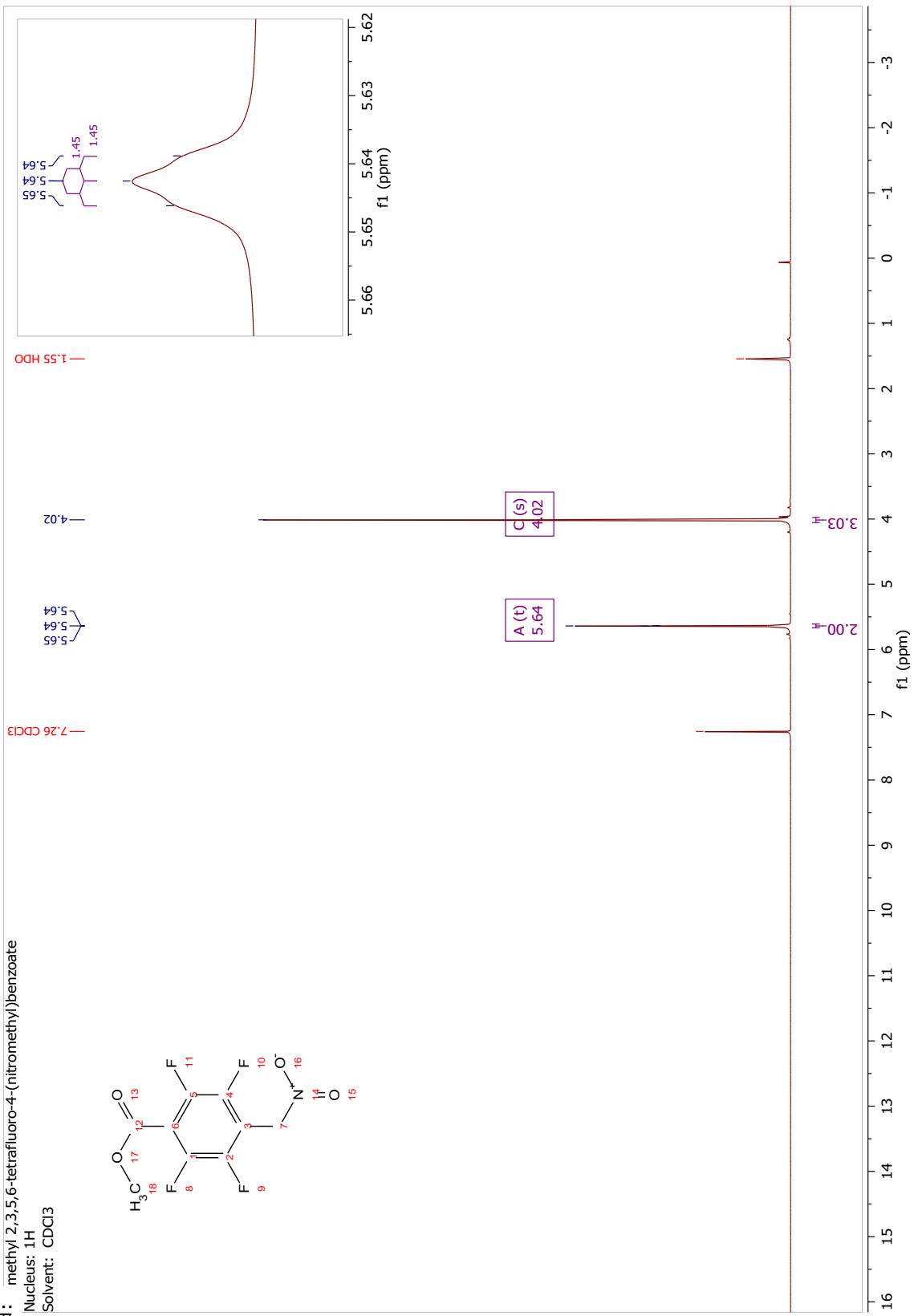
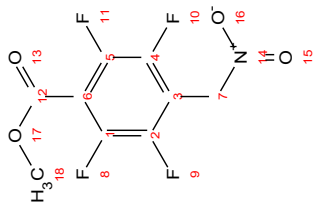
Solvent: CDCl<sub>3</sub>



3.3.3d: methyl 2,3,5,6-tetrafluoro-4-(nitromethyl)benzoate

Nucleus:  $^1\text{H}$

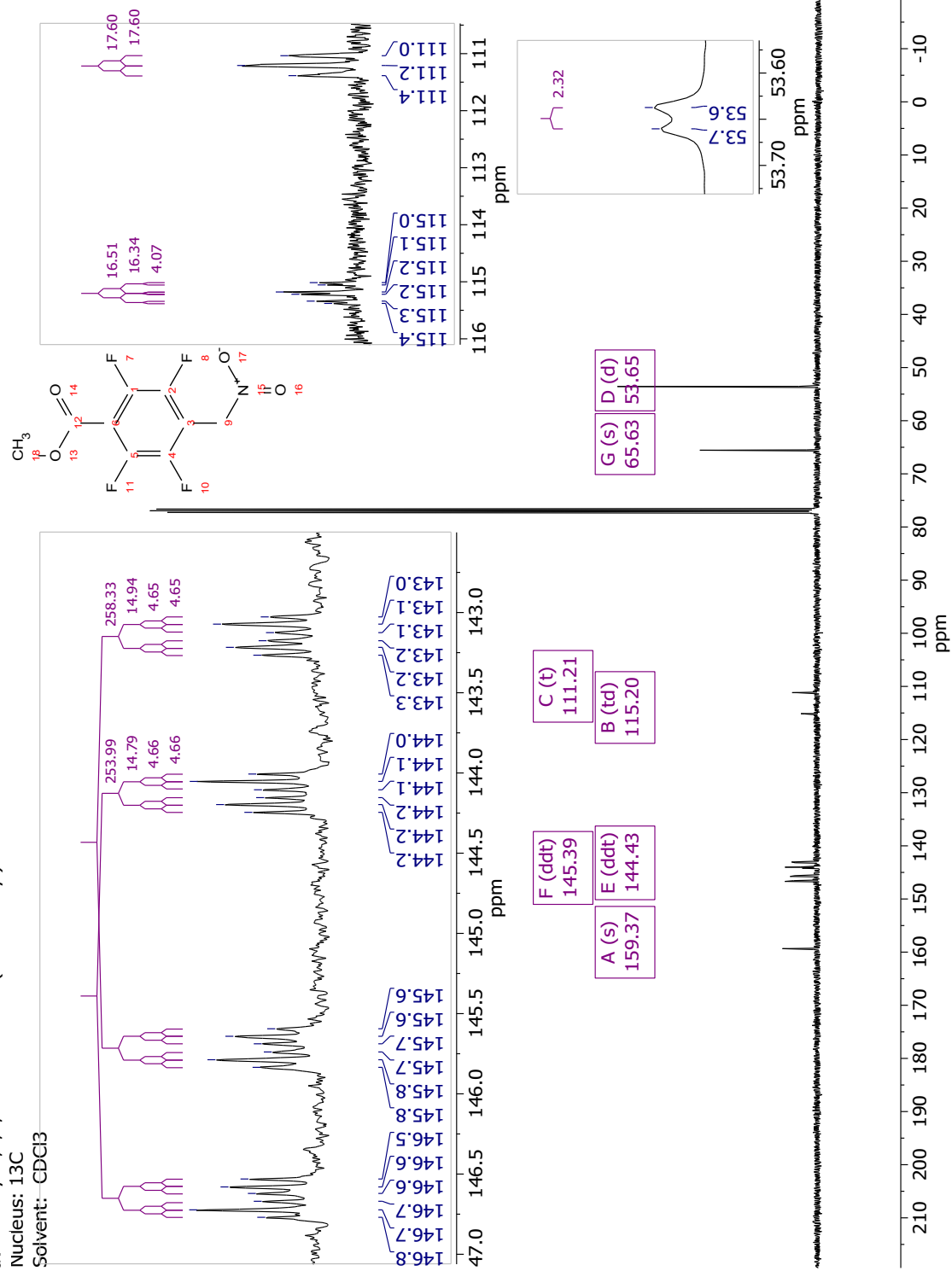
Solvent:  $\text{CDCl}_3$



3.3.3d: methyl 2,3,5,6-tetrafluoro-4-(nitromethyl)benzoate

Nucleus:  $^{13}\text{C}$

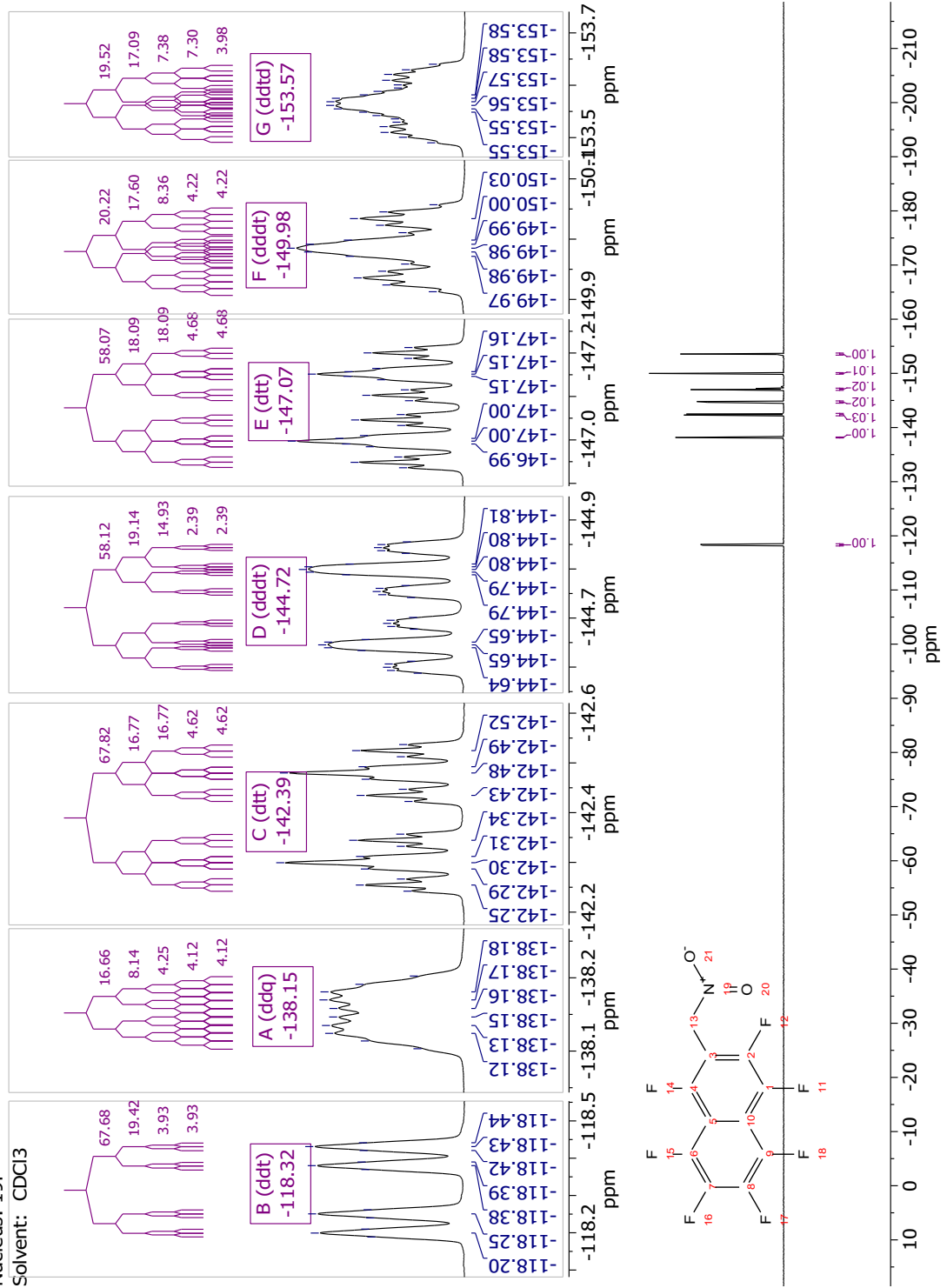
Solvent: CDCl<sub>3</sub>



3.3.3e 1,2,3,4,5,6,8-heptafluoro-7-(nitromethyl)naphthalene

Nucleus:  $^{19}\text{F}$

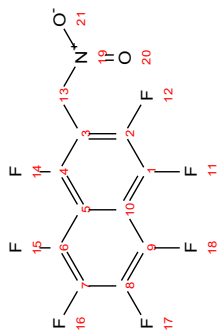
Solvent:  $\text{CDCl}_3$



3.3.3e: 1,2,3,4,5,6,8-heptafluoro-7-(nitromethyl)naphthalene

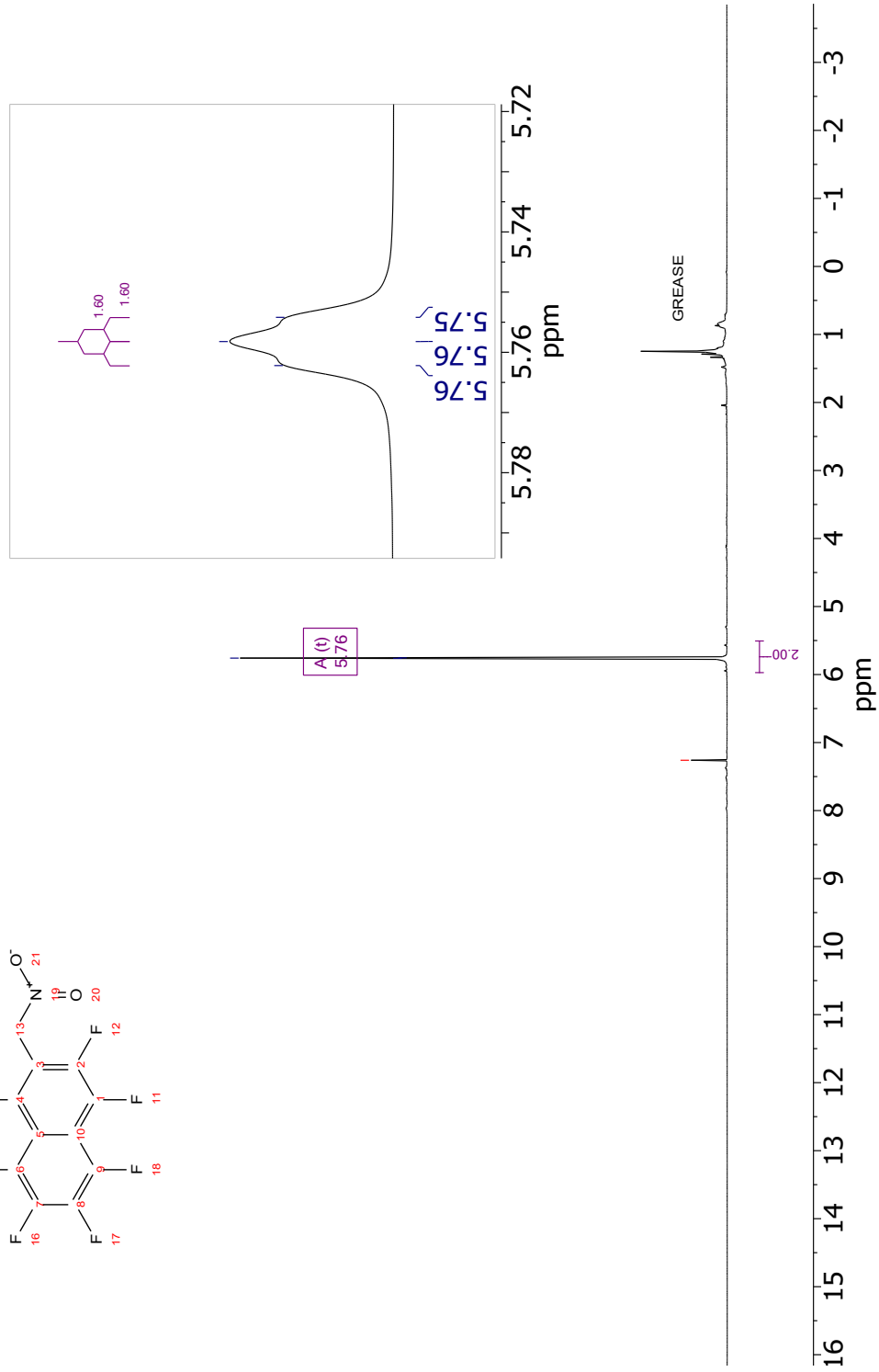
Nucleus: <sup>1</sup>H

Solvent: CDCl<sub>3</sub>

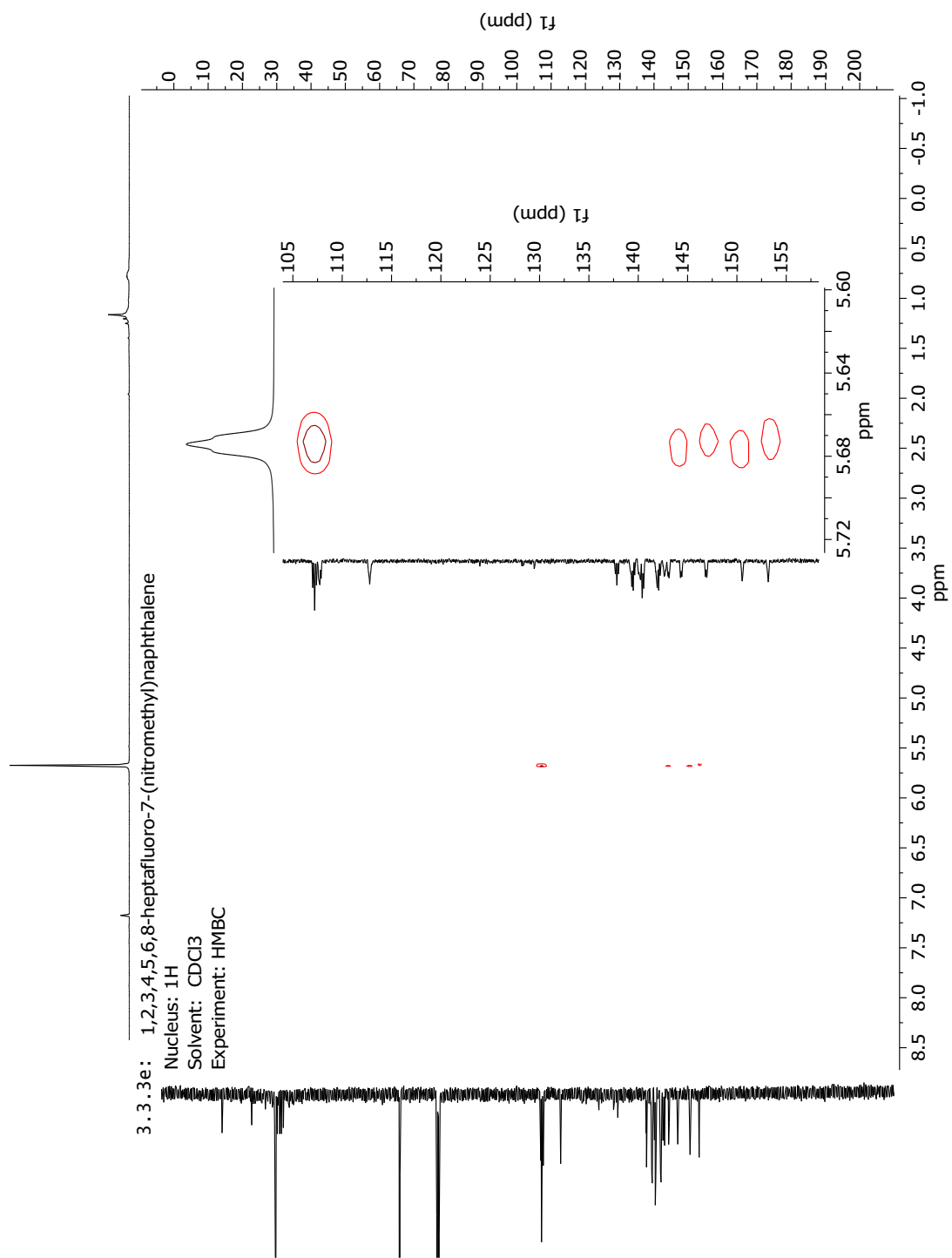


7.3 CDCl<sub>3</sub>

5.8  
5.8  
5.8  
5.8





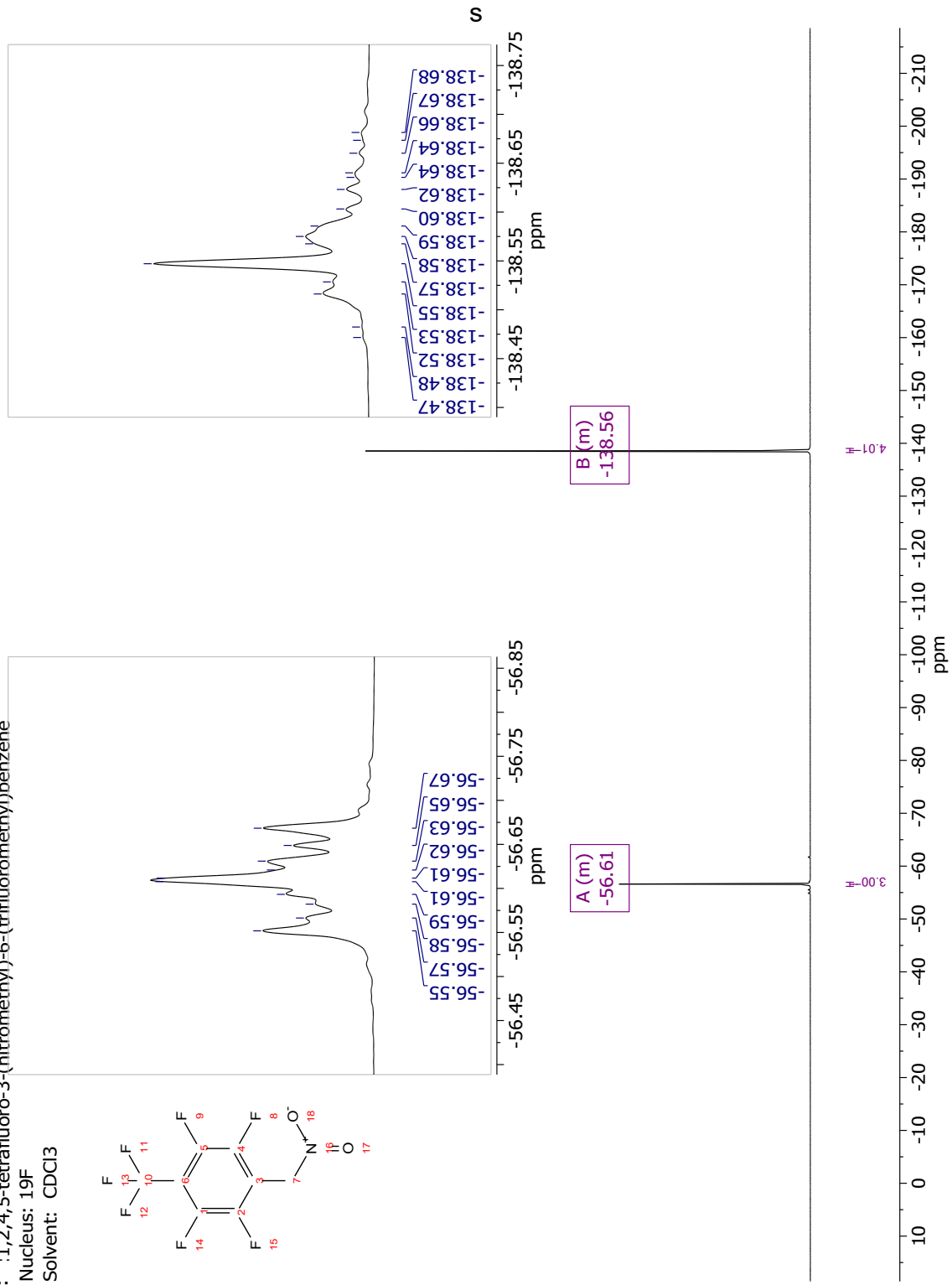
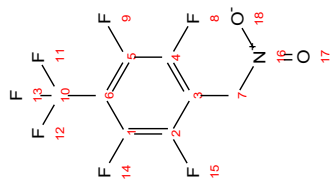




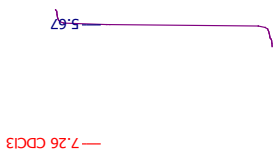
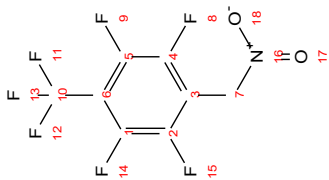
3.3.3f: :1,2,4,5-tetrafluoro-3-(nitromethyl)-6-(trifluoromethyl)benzene

Nucleus: <sup>19</sup>F

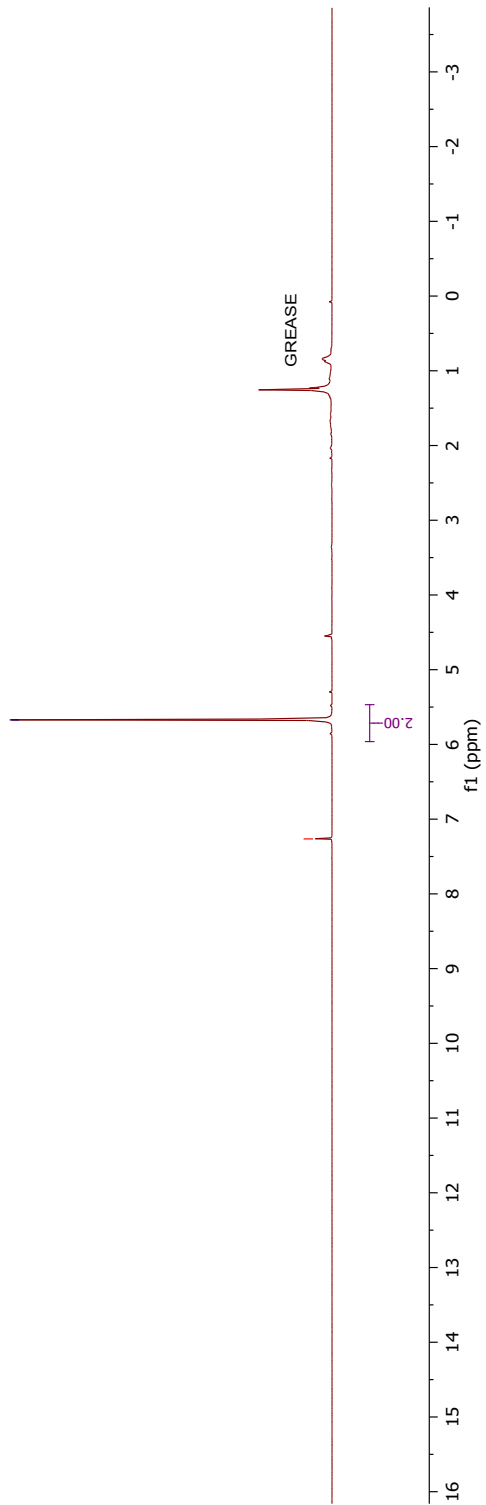
Solvent: CDCl<sub>3</sub>



3 . 3 . 3f 1,2,4,5-tetrafluoro-3-(nitromethyl)-6-(trifluoromethyl)benzene  
Nucleus: <sup>1</sup>H  
Solvent: CDCl<sub>3</sub>



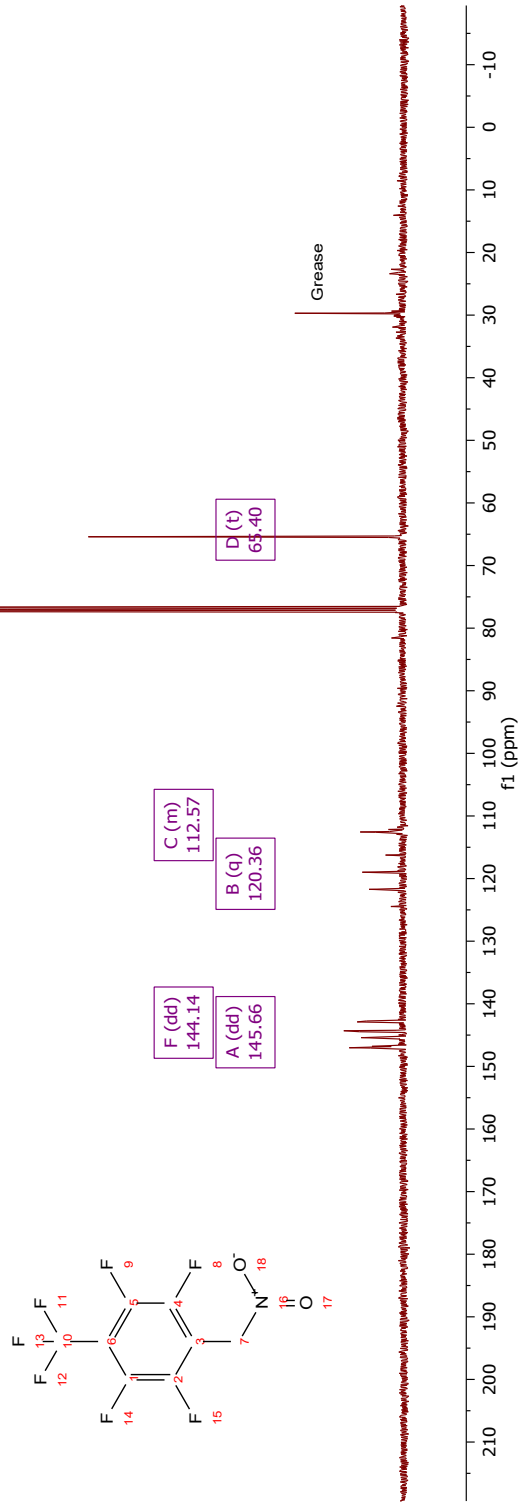
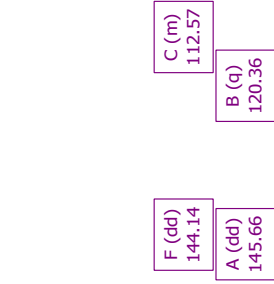
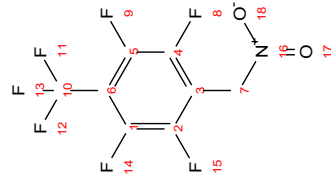
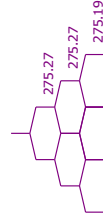
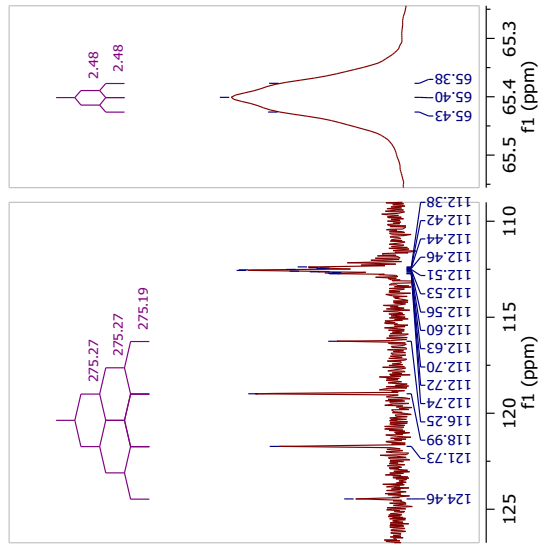
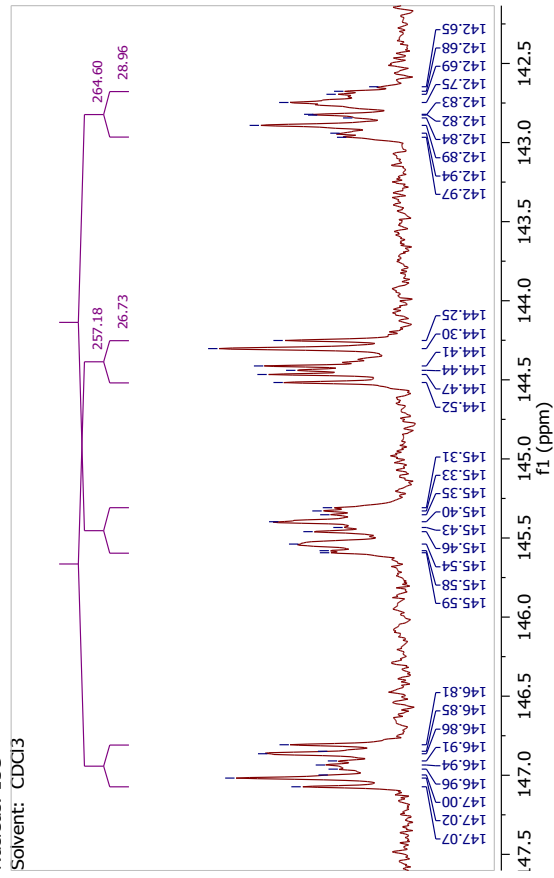
A (s)  
5.67



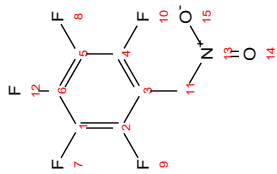
3.3.3f 1,2,4,5-tetrafluoro-3-(nitromethyl)-6-(trifluoromethyl)benzene

Nucleus:  $^{13}\text{C}$

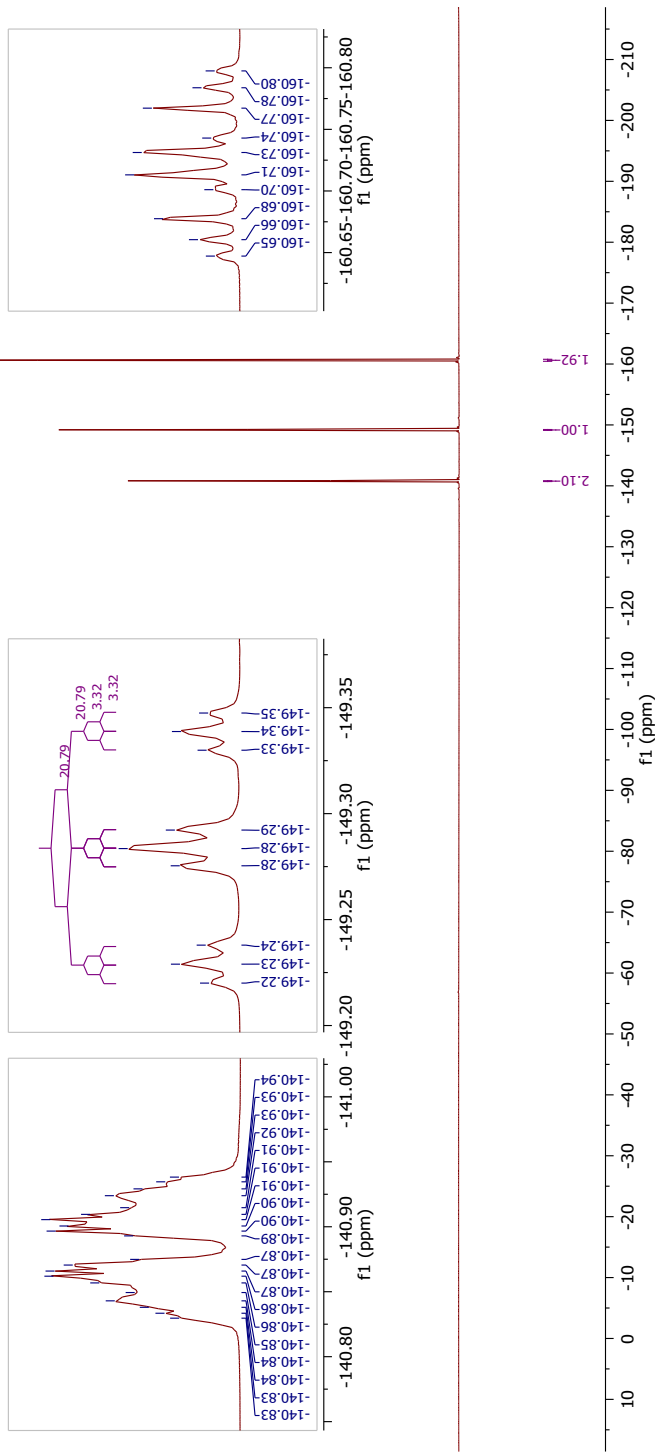
Solvent:  $\text{CDCl}_3$



3.3.3g: 1,2,3,4,5-pentafluoro-6-(nitromethyl)benzene  
 Nucleus:  $^{19}\text{F}$   
 Solvent:  $\text{CDCl}_3$



B (tt) -149.28  
 A (m) -140.88  
 C (m) -160.73



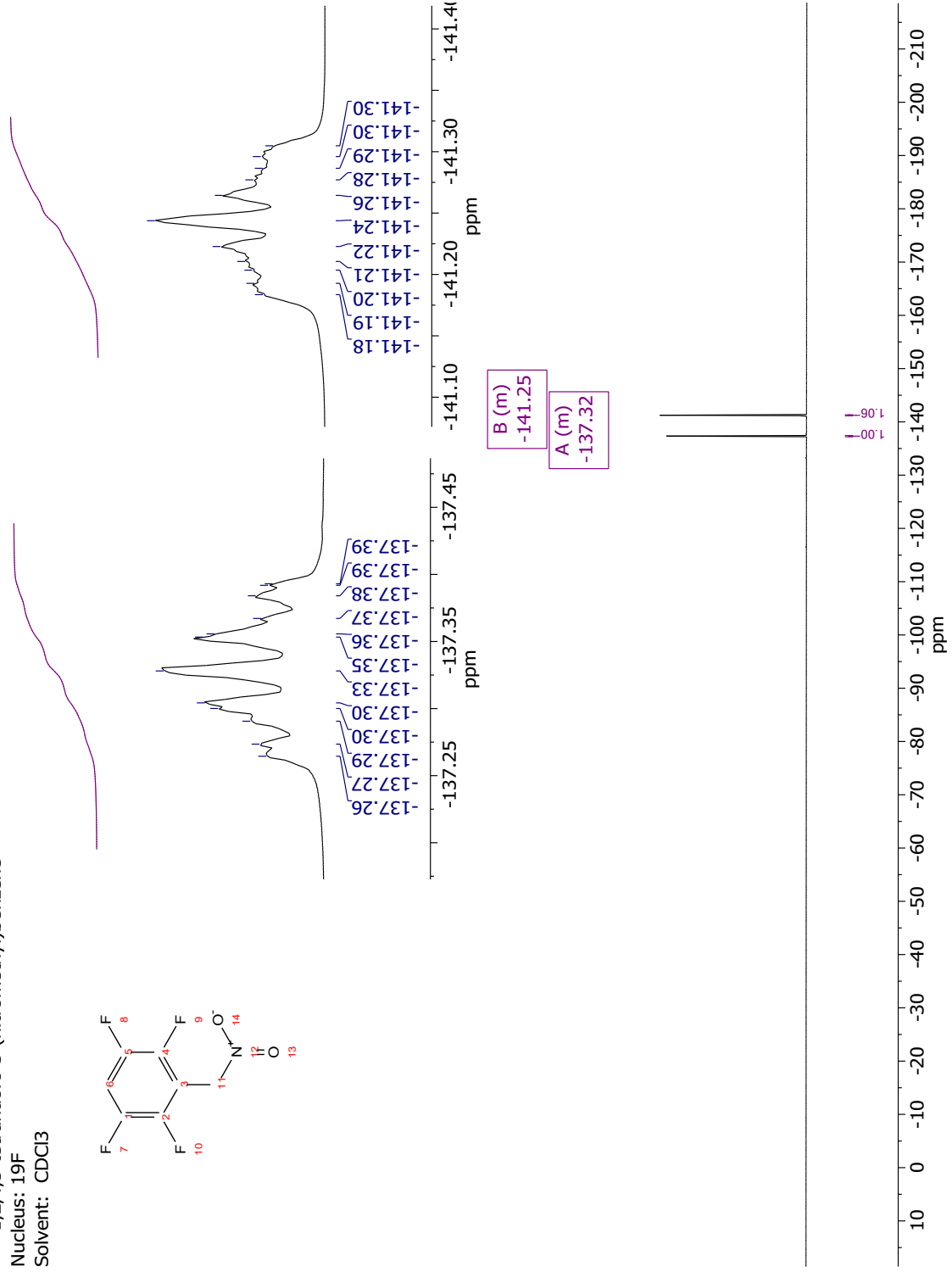
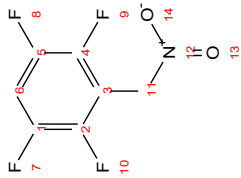




3.3.3h 1,2,4,5-tetrafluoro-3-(nitromethyl)benzene

Nucleus:  $^{19}\text{F}$

Solvent:  $\text{CDCl}_3$

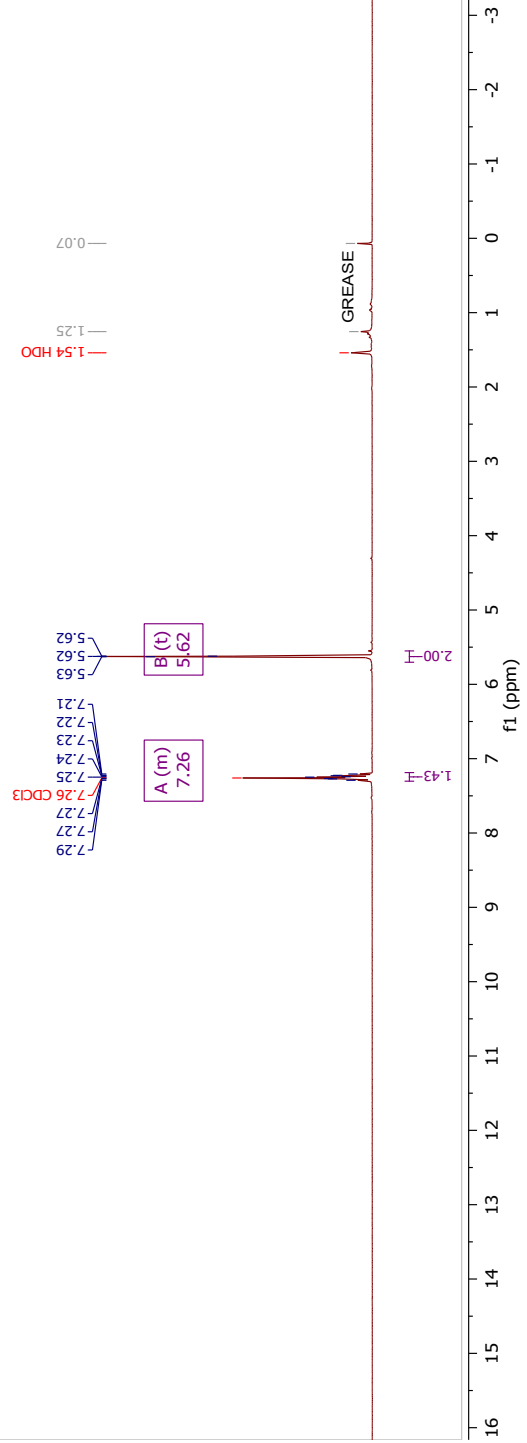
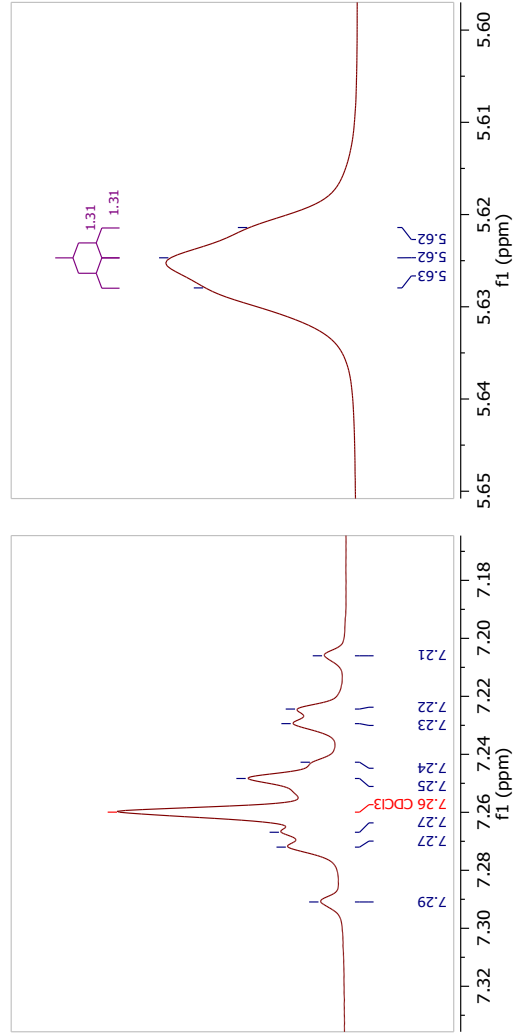
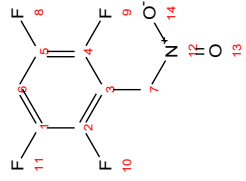


3.3.3h:

1,2,4,5-tetrafluoro-3-(nitromethyl)benzene

Nucleus: <sup>1</sup>H

Solvent: CDCl<sub>3</sub>

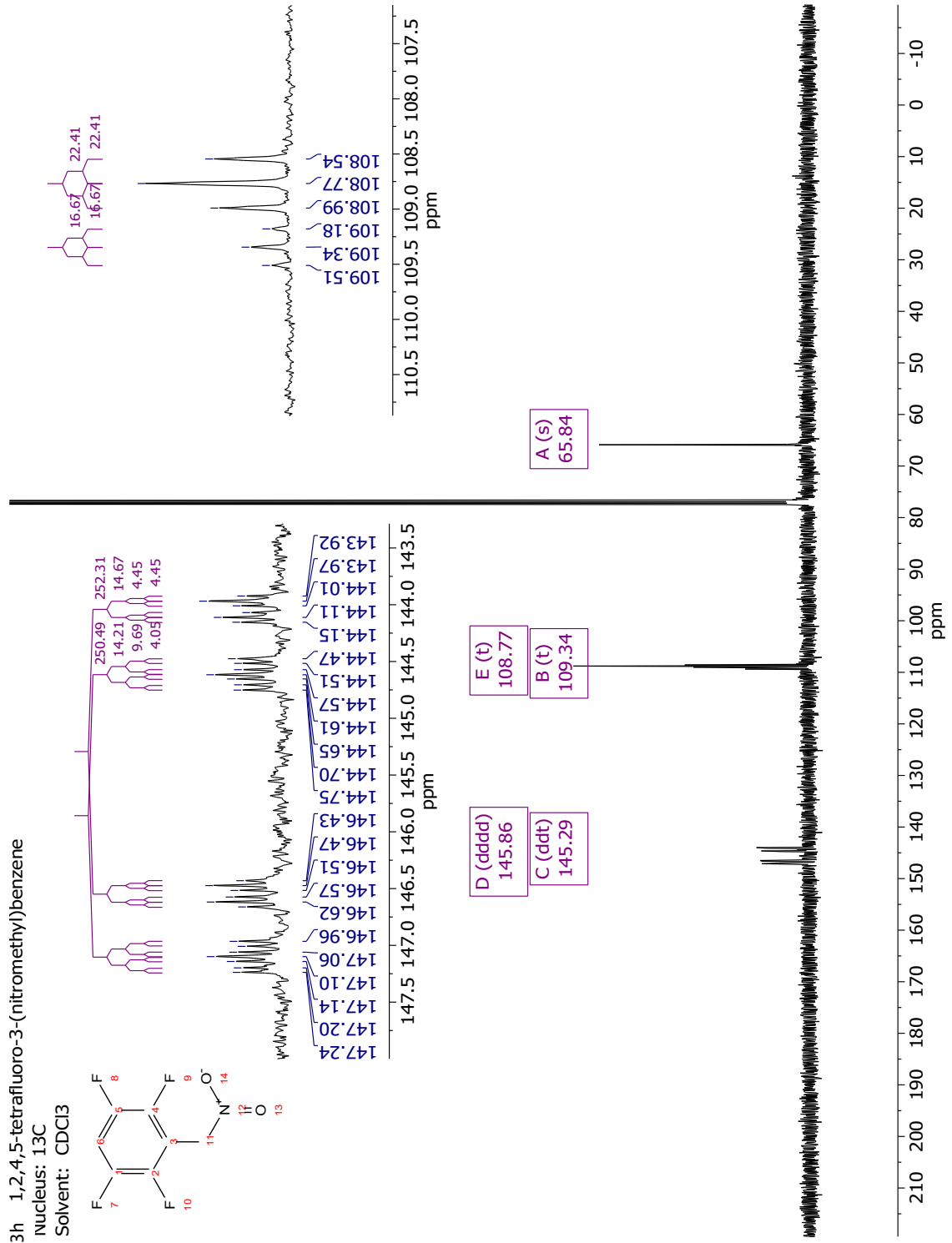
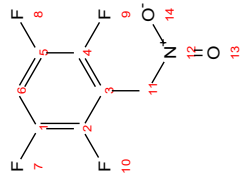




3.3.3h 1,2,4,5-tetrafluoro-3-(nitromethyl)benzene

Nucleus:  $^{13}\text{C}$

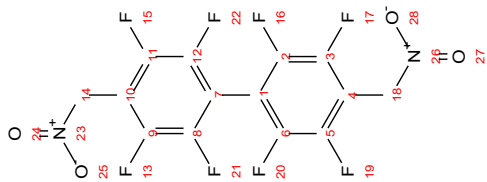
Solvent:  $\text{CDCl}_3$



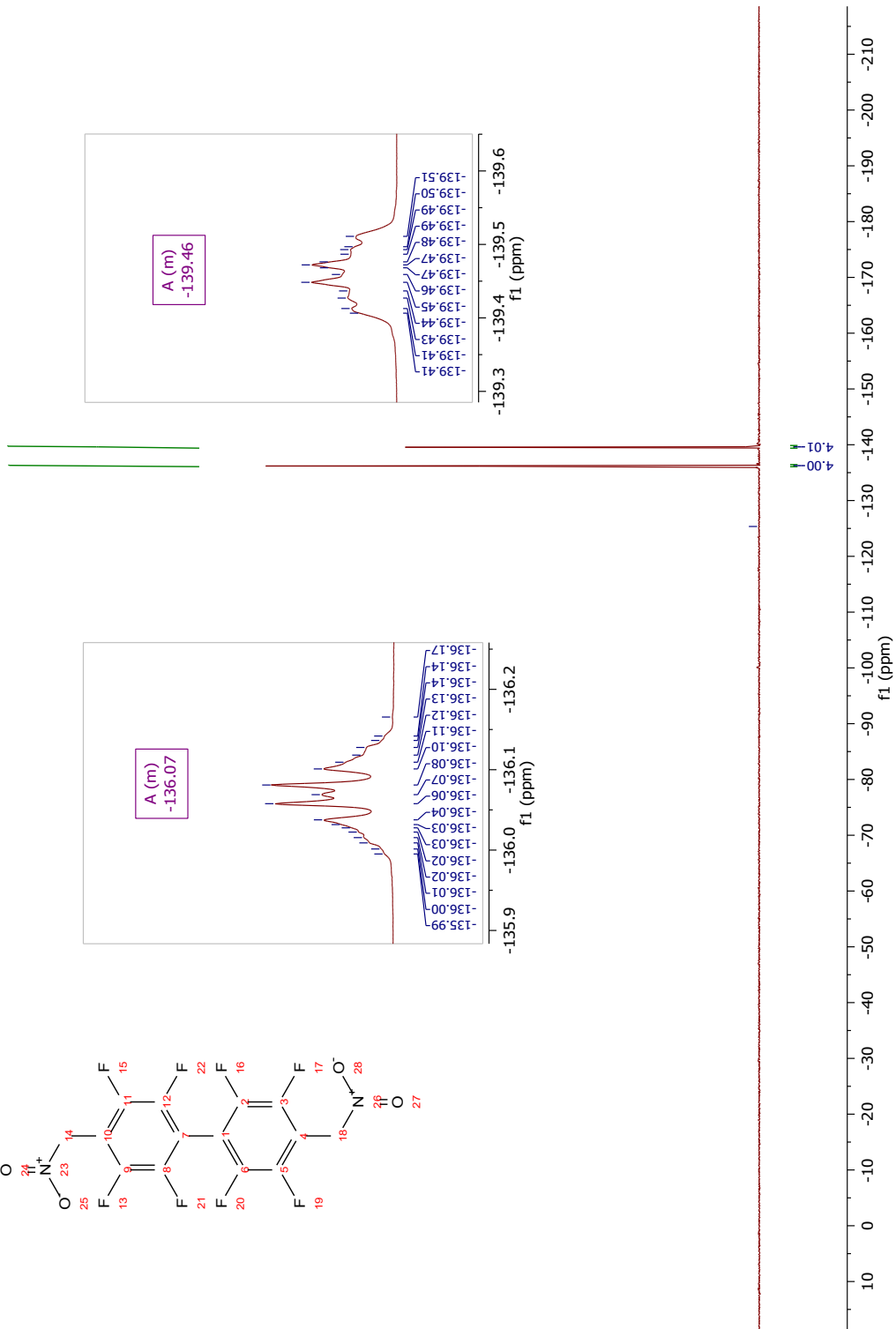
3.3.31 2,2',3,3',5,5',6,6'-octafluoro-4,4'-bis(nitromethyl)-1,1'-biphenyl:

Nucleus: <sup>19</sup>F

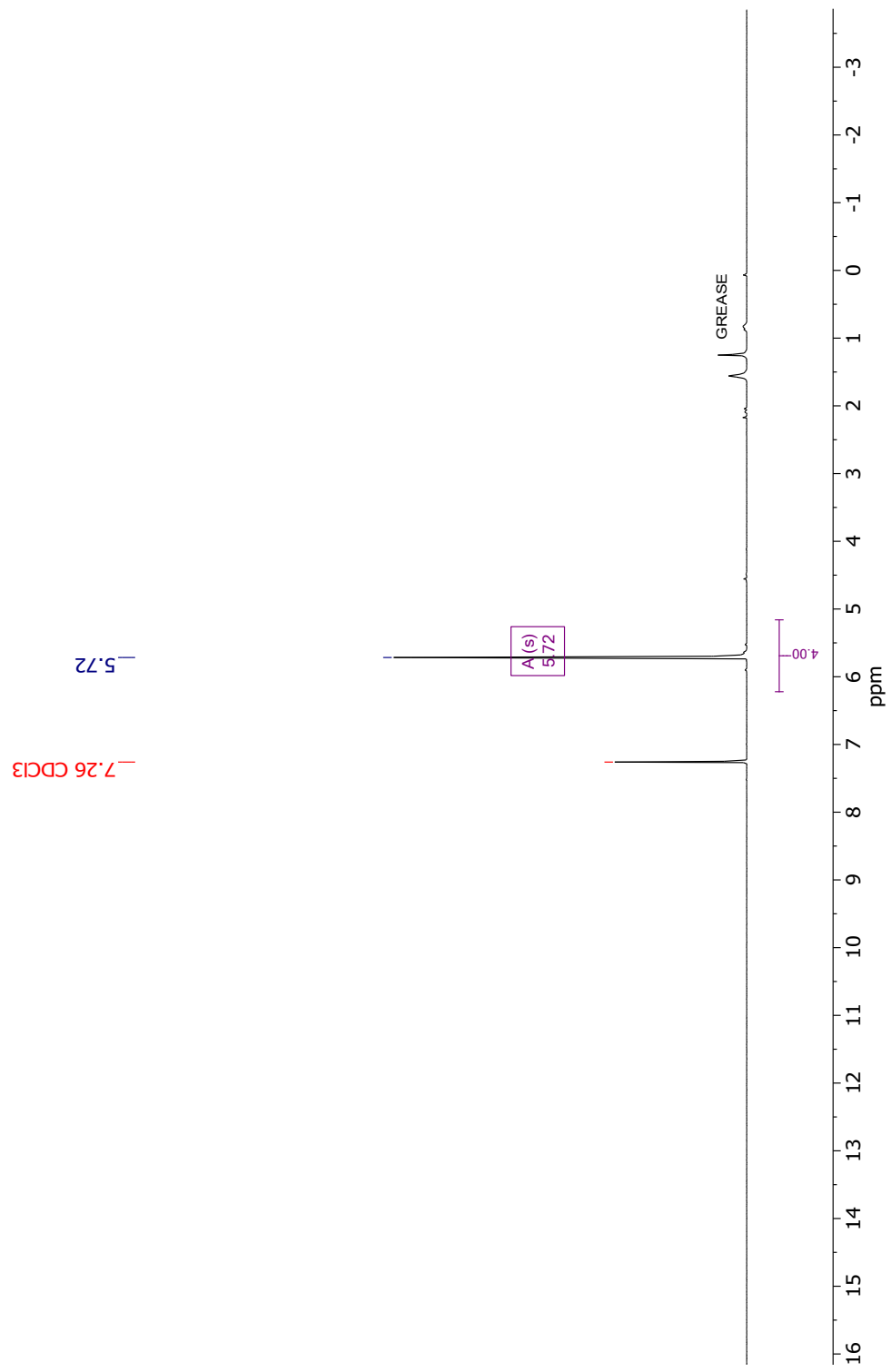
Solvent: CDCl<sub>3</sub>



— -125.19



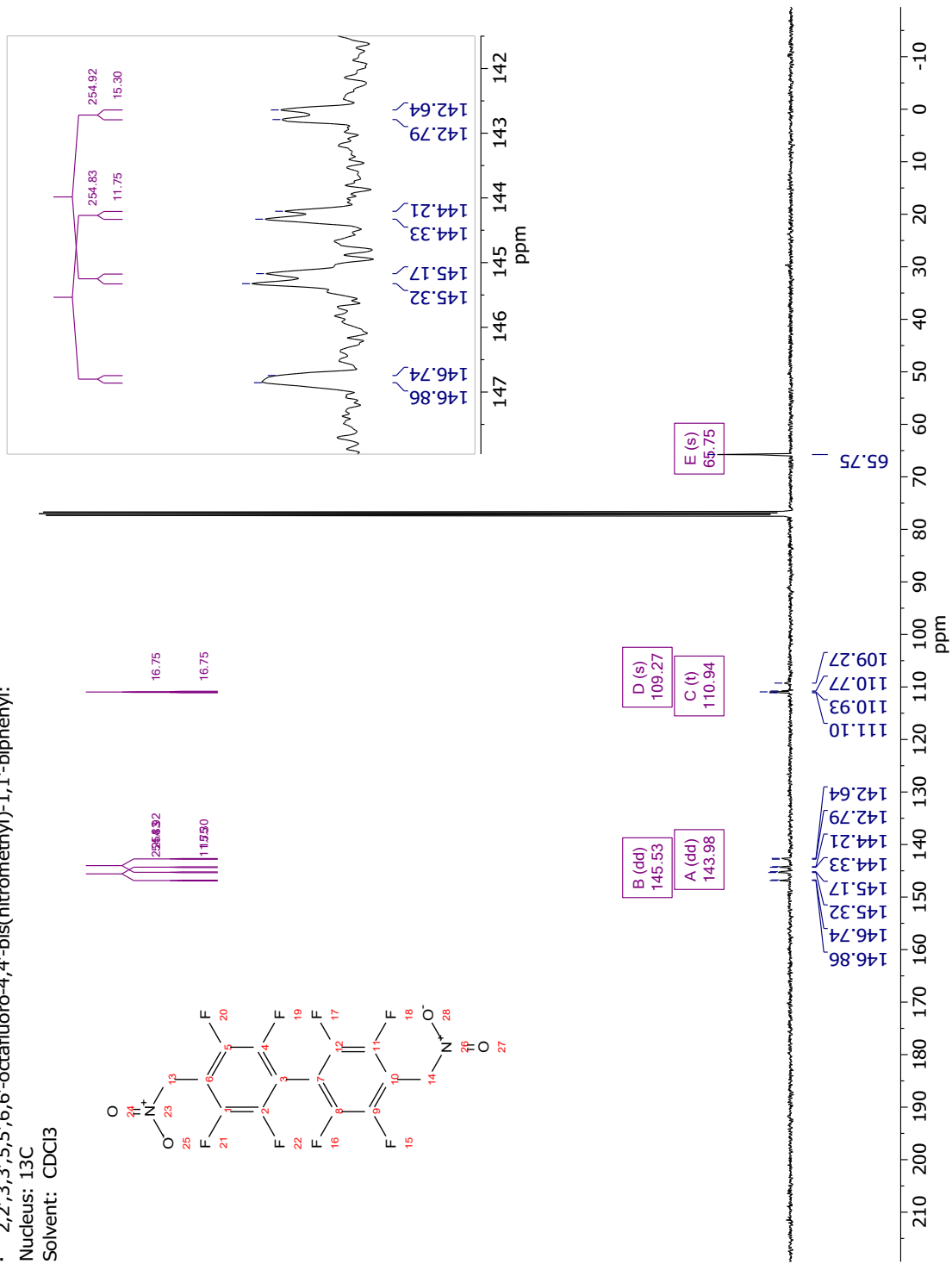
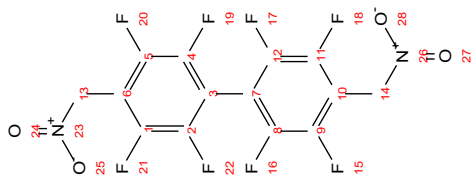
3.3.3i 2,2',3,3',5,5',6,6'-octafluoro-4,4'-bis(nitromethyl)-1,1',1'-diphenyl:  
nucleus: 1H  
Solvent: CDCl3



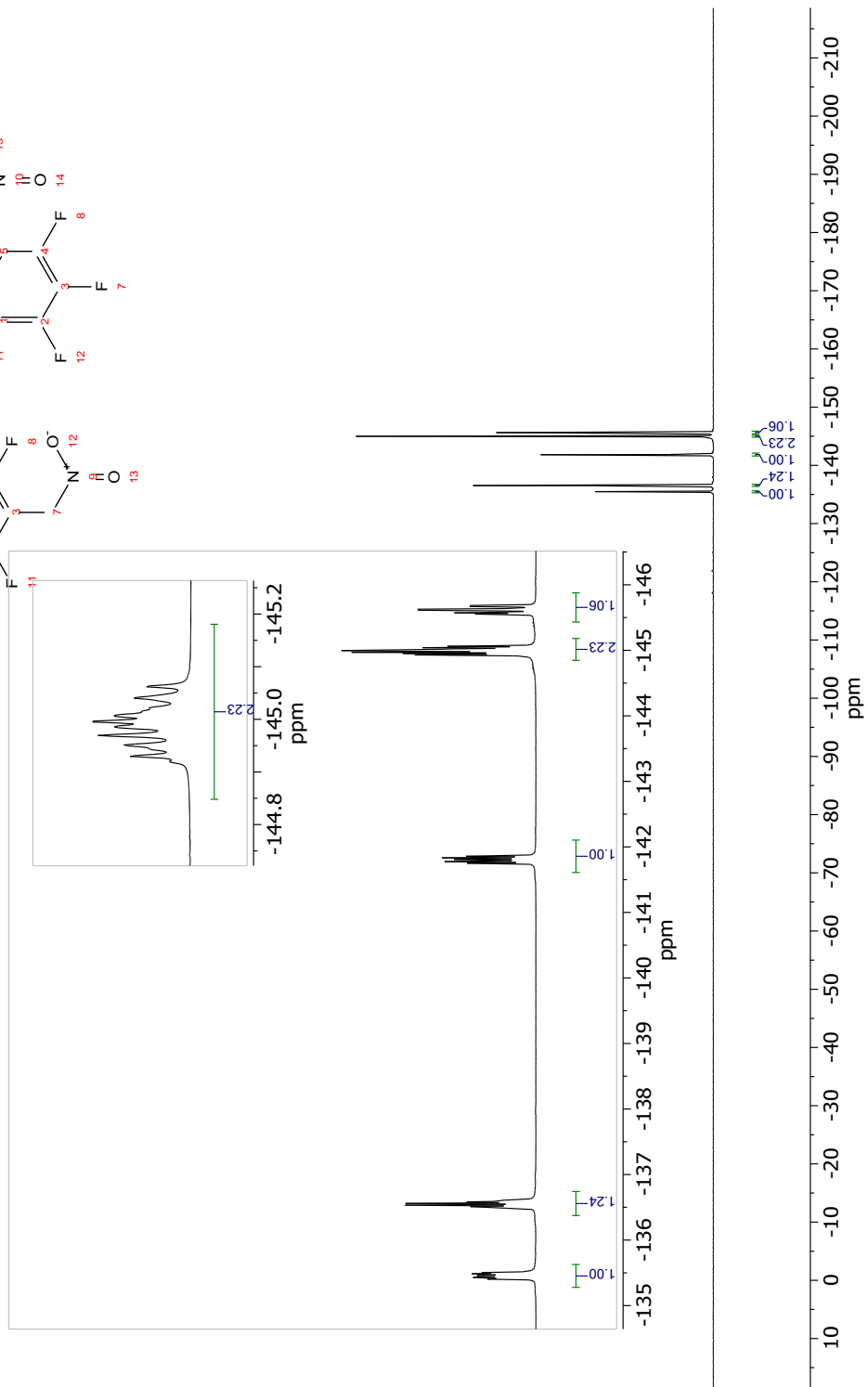
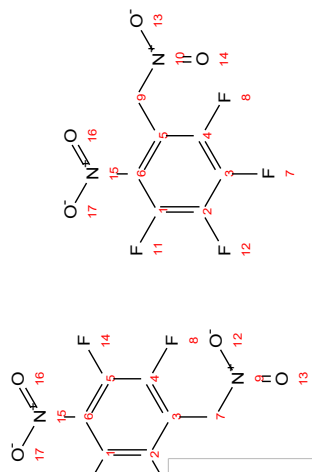
3.3.3i: 2,2',3,3',5,5',6,6'-octafluoro-4,4'-bis(nitromethyl)-1,1'-biphenyl:

Nucleus:  $^{13}\text{C}$

Solvent:  $\text{CDCl}_3$



3.3.4a: 1,2,3,4-tetrafluoro-5-nitro-6-(nitromethyl)benzene  
 mixed regioisomers following workup  
 Nucleus: <sup>19</sup>F  
 Solvent: CDCl<sub>3</sub>

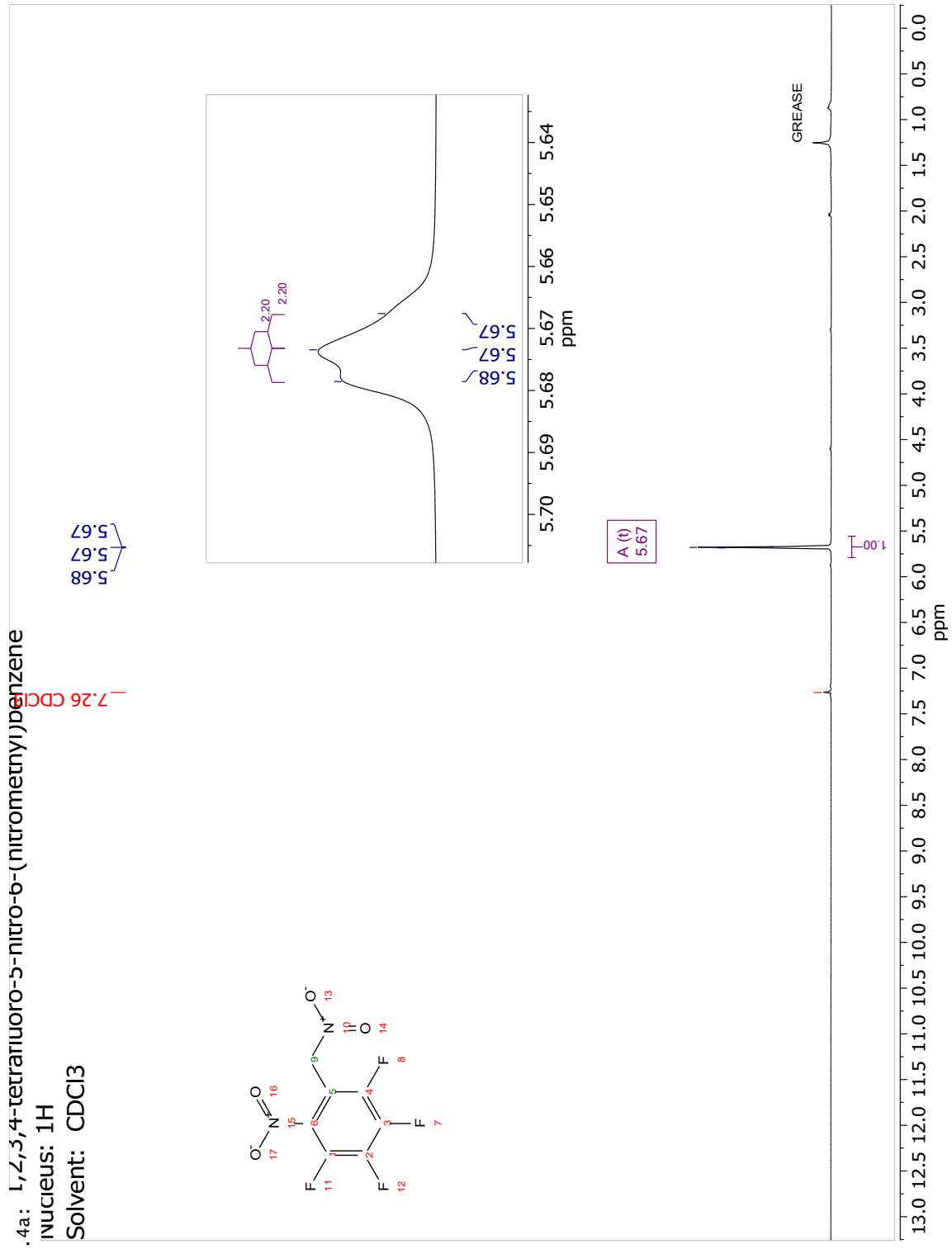




3.3.4a: 1,2,3,4-tetrafluoro-5-nitro-6-(nitromethyl)benzene

Nucleus:  $^1\text{H}$

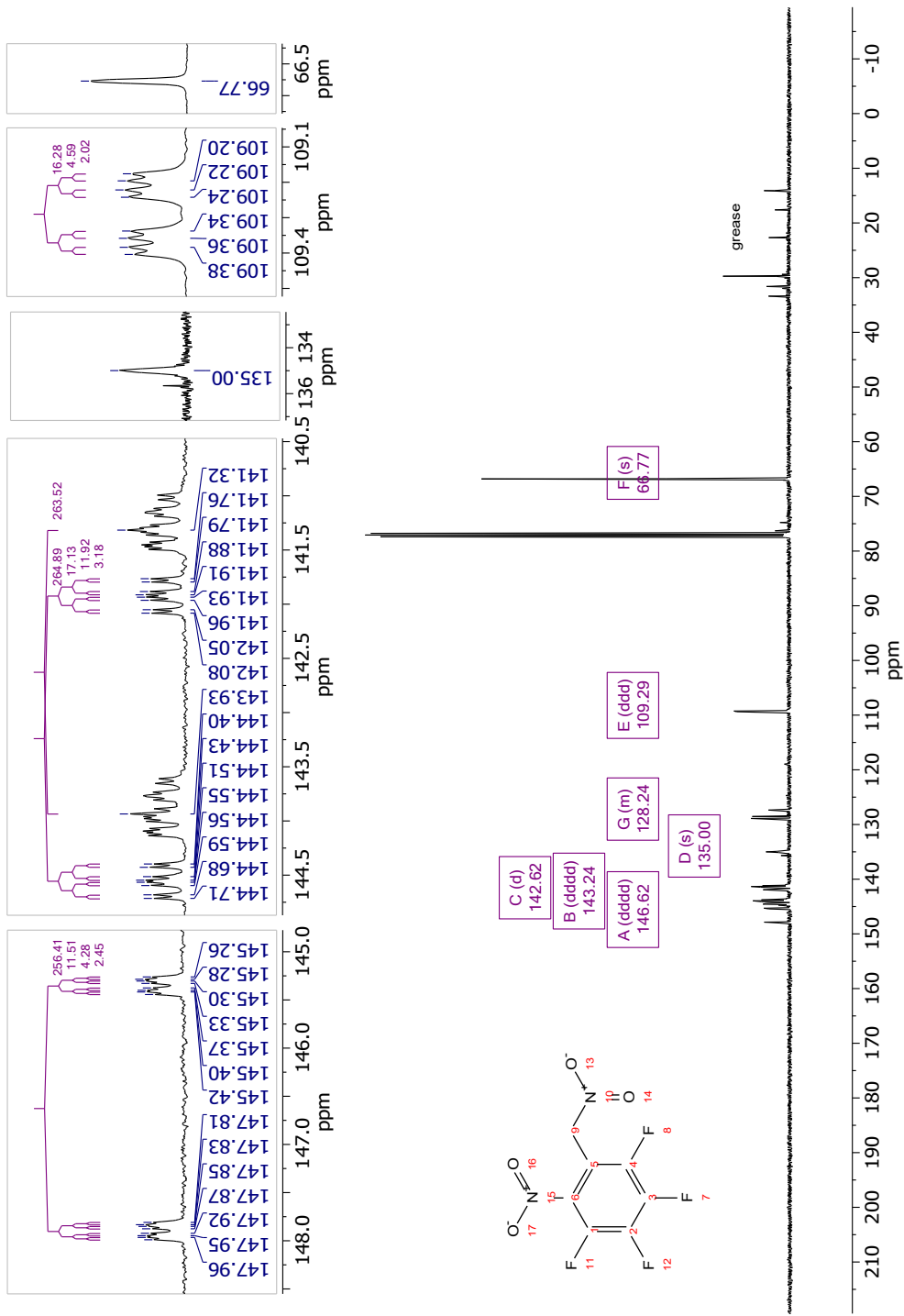
Solvent:  $\text{CDCl}_3$



3.3.4a: 1,2,3,4-tetrafluoro-5-nitro-b-(nitrometny) benzene

Nucleus: <sup>13</sup>C

Solvent: CDCl<sub>3</sub>

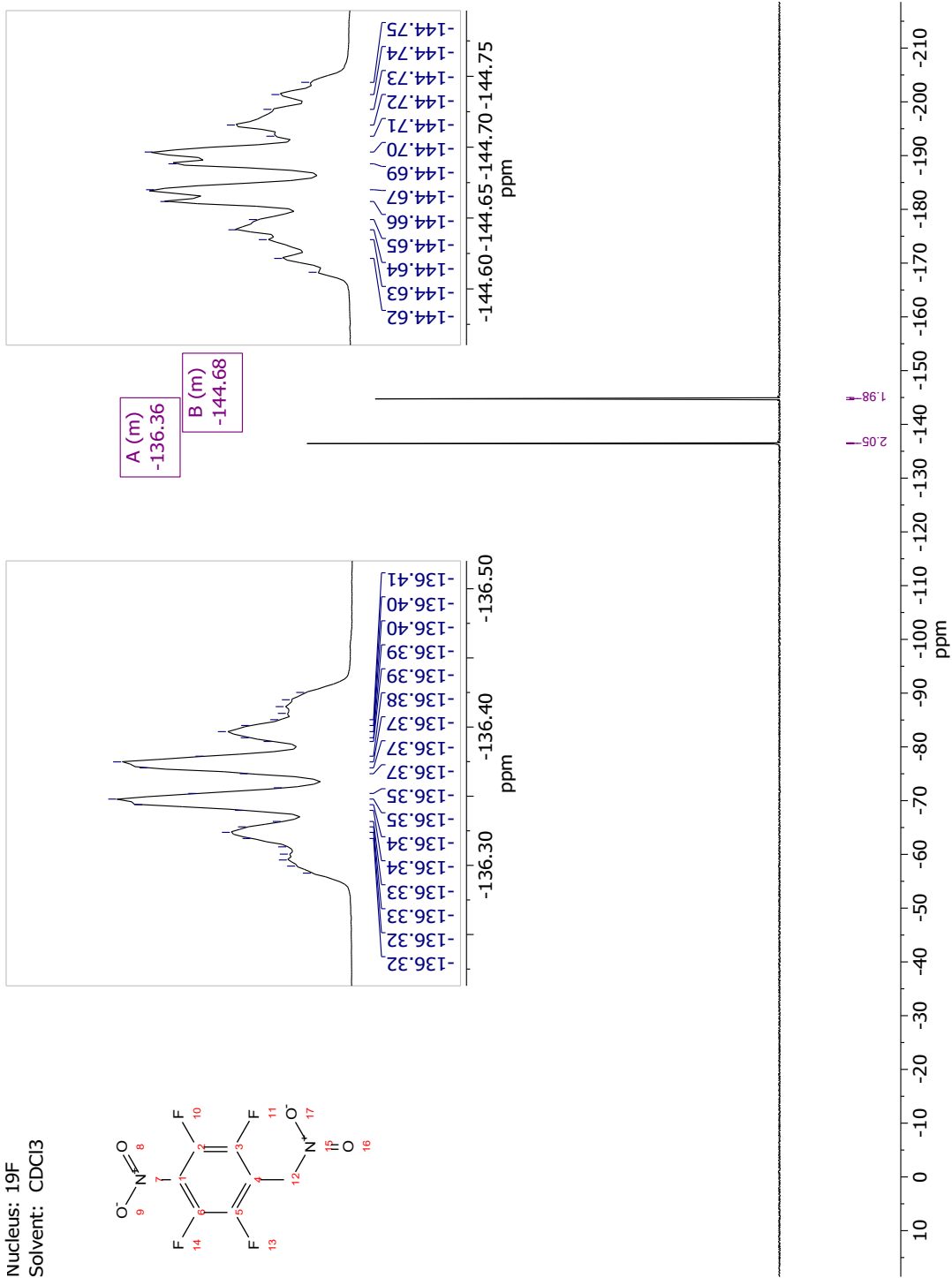
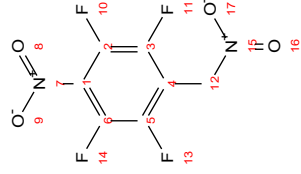




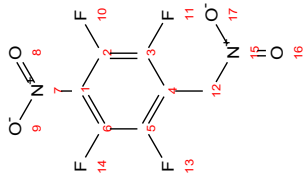
3.3.4b: 1,2,4,5-tetrafluoro-3-nitro-6-(nitromethyl)benzene

Nucleus: <sup>19</sup>F

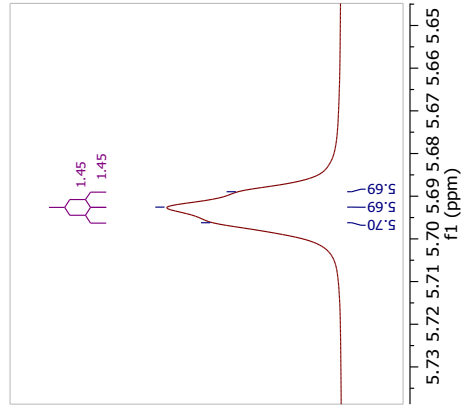
Solvent: CDCl<sub>3</sub>



3.3.4b: 1,2,4,5-tetrafluoro-3-nitro-6-(nitromethyl)benzene  
Nucleus:  $^1\text{H}$   
Solvent:  $\text{CDCl}_3$

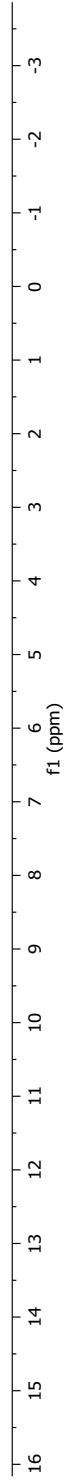


7.26  $\text{CDCl}_3$

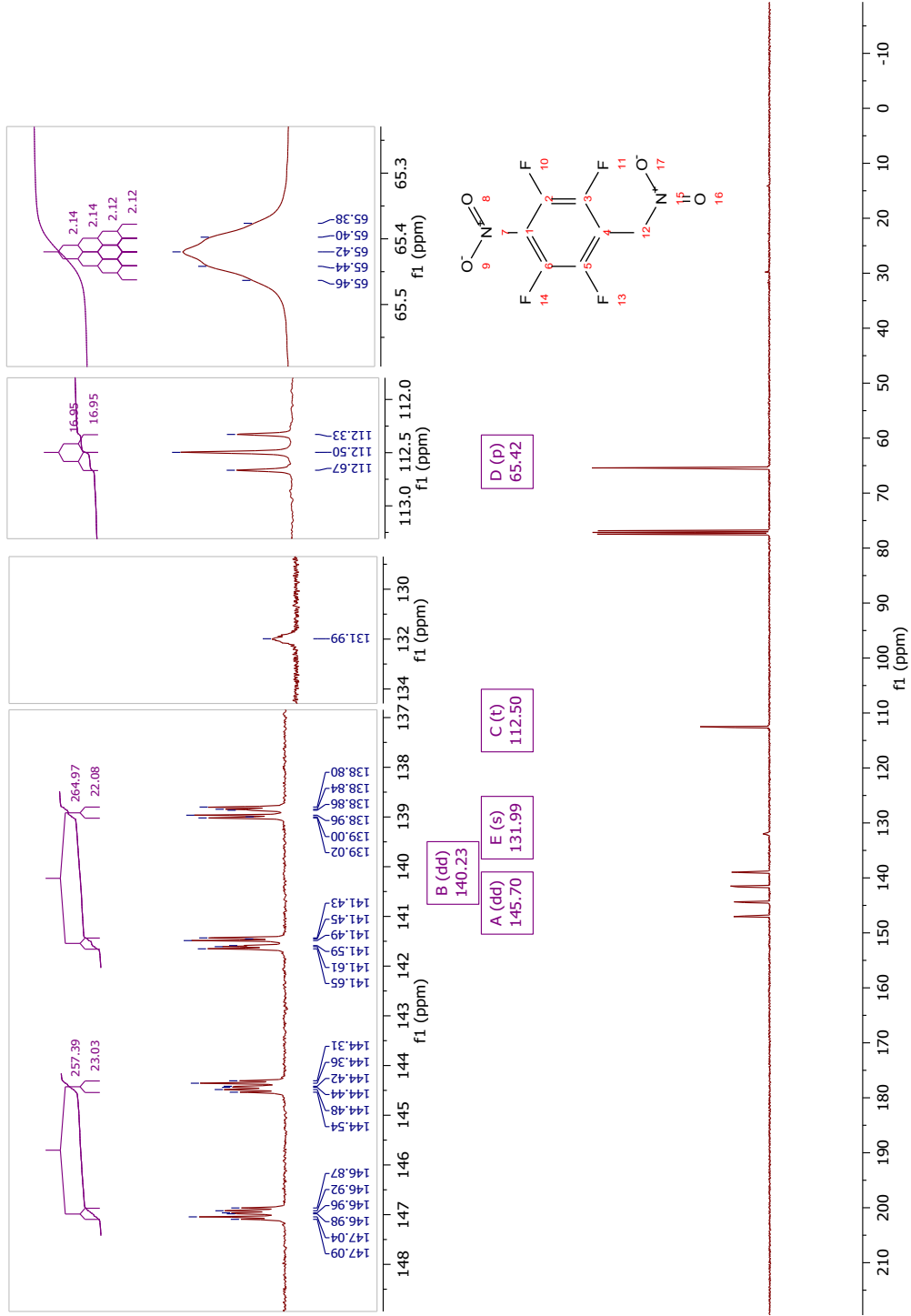


B (t)  
5.69

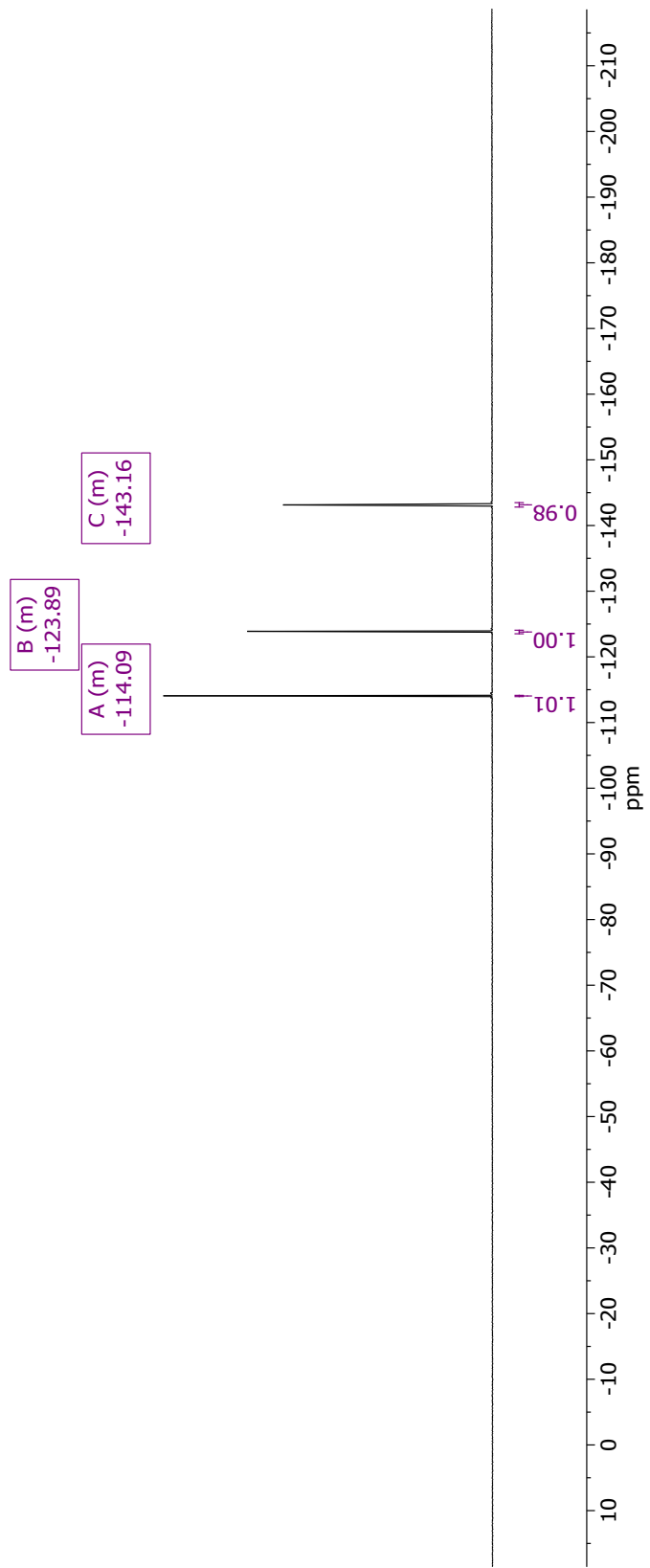
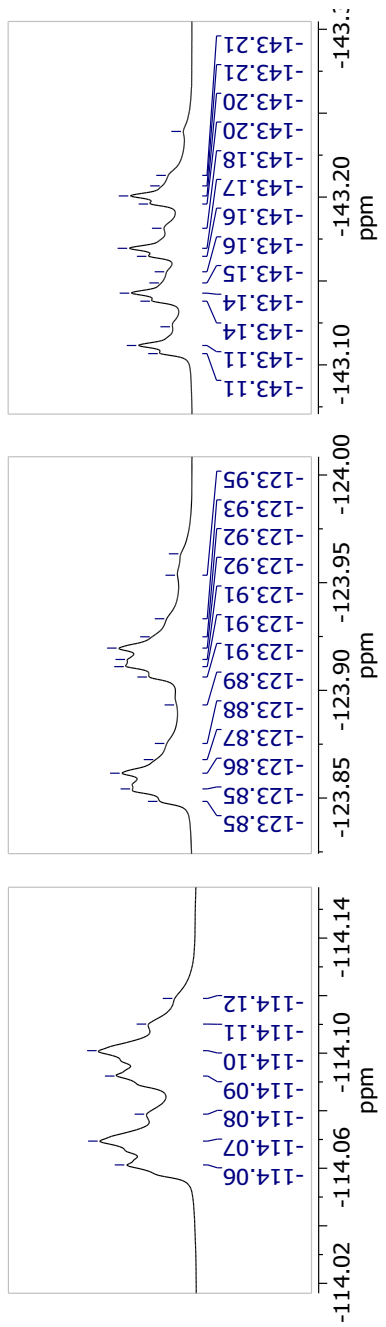
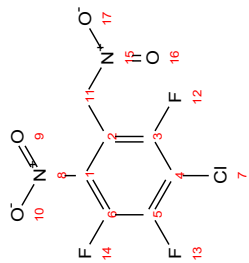
2.00 I



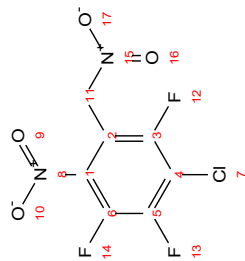
3.3.4b : 1,2,4,5-tetrafluoro-3-nitro-6-(nitromethyl)benzene  
 Nucleus:  $^{13}\text{C}$   
 Solvent:  $\text{CDCl}_3$



3.3.4c: 1-chloro-2,3,6-trifluoro-4-nitro-5-(nitromethyl)benzene  
 solvent: CDCl<sub>3</sub>  
 Nucleus: 19F



3.3.4c: 1-chloro-2,3,6-trifluoro-4-nitro-5-(nitromethyl)benzene  
solvent: CDCl<sub>3</sub>  
Nucleus: <sup>1</sup>H



A (s)  
5.68

5.7

7.3 CDCl<sub>3</sub>

1.6 H<sub>2</sub>O

Grease

2.00

ppm

-3

-2

-1

0

1

2

3

4

5

6

7

8

9

10

11

12

13

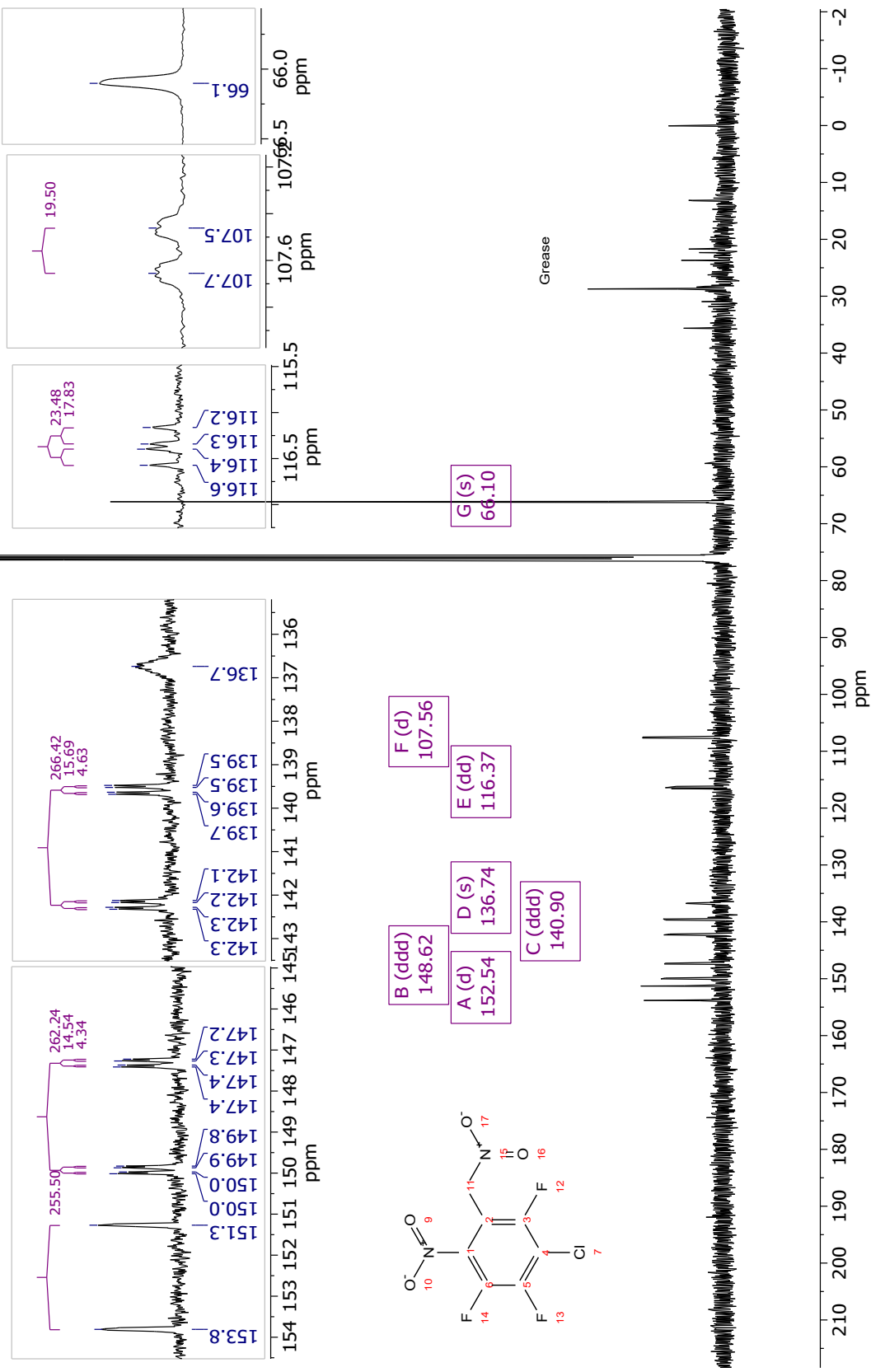
14

15

3. 3. 4c: 1-chloro-2,3,6-trifluoro-4-nitro-5-(nitromethyl)benzene

Solvent: CDCl<sub>3</sub>

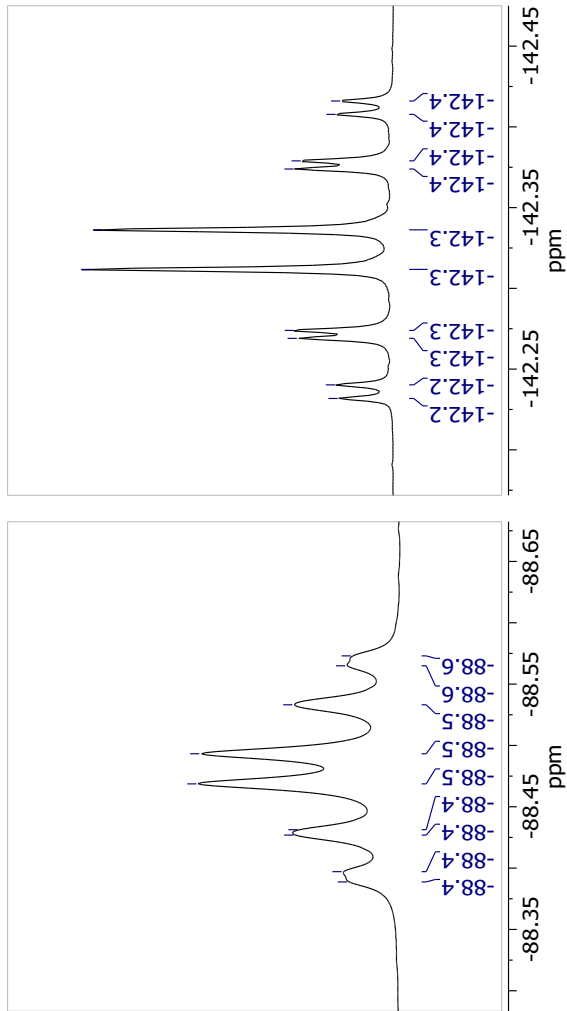
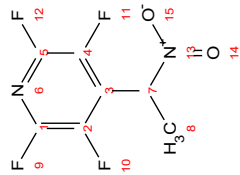
Nucleus: <sup>13</sup>C



3.3.5a: 2,3,5,6-tetrafluoro-4-(1-nitroethyl)pyridine

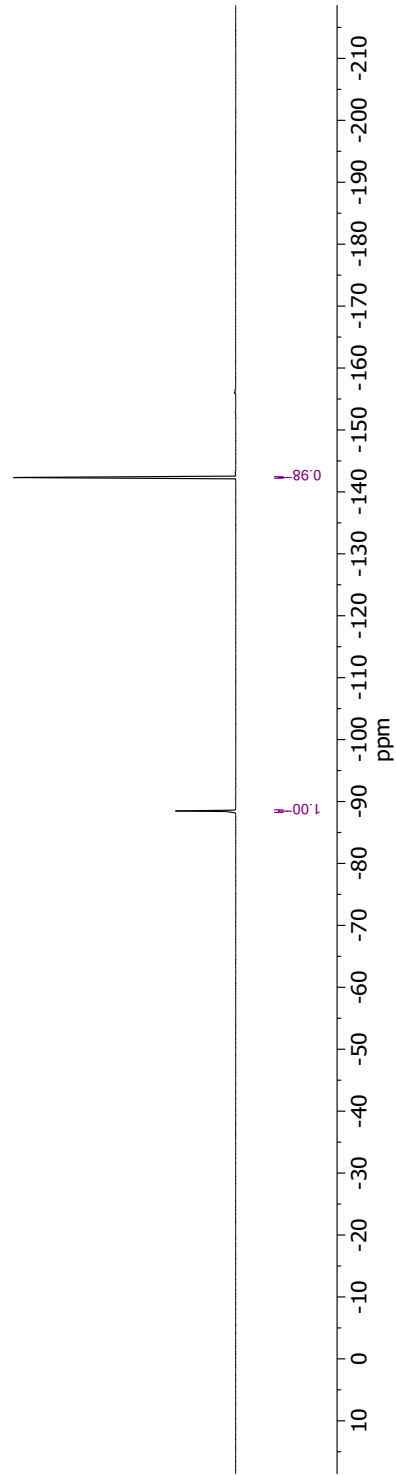
Nucleus:  $^{19}\text{F}$

Solvent:  $\text{CDCl}_3$



A (m)  
-88.49

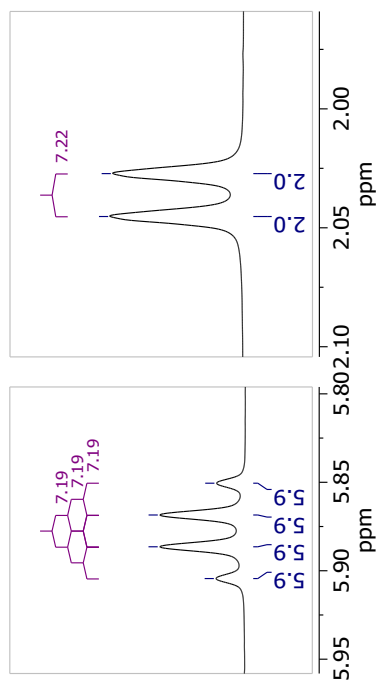
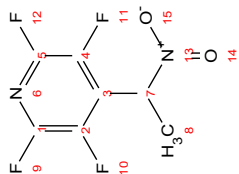
B (m)  
-142.32



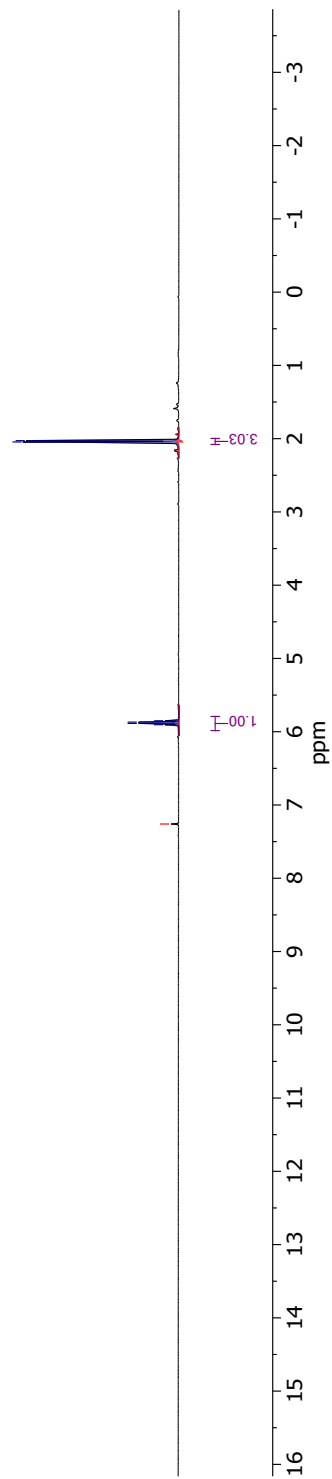
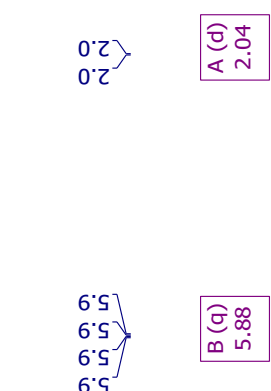
3.3.5a 2,3,5,6-tetrafluoro-4-(1-nitroethyl)pyridine

Nucleus:  $^1\text{H}$

Solvent:  $\text{CDCl}_3$



-7.3  $\text{CDCl}_3$

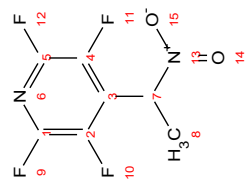
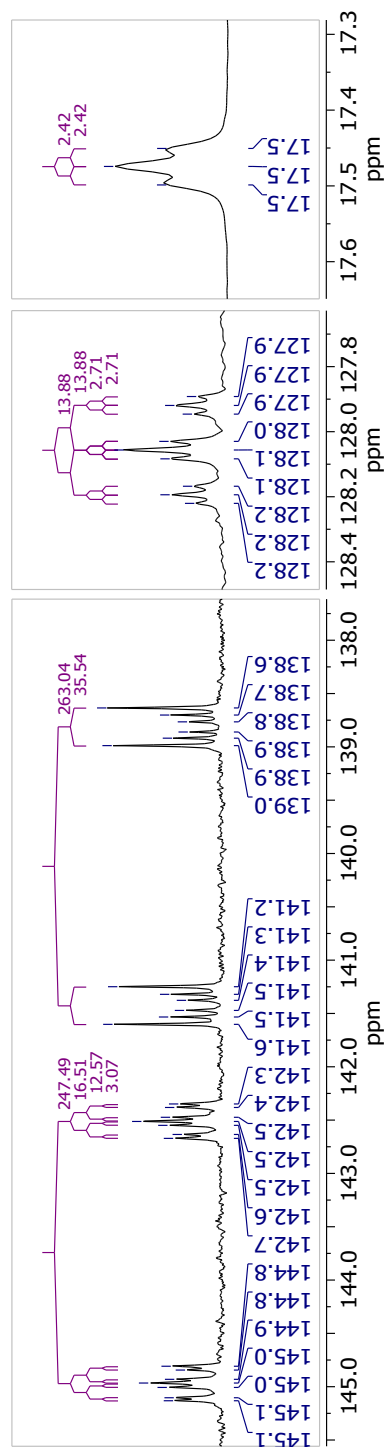




3.3.5a: 2,3,5,6-tetrafluoro-4-(1-nitroethyl)pyridine

Nucleus:  $^{13}\text{C}$

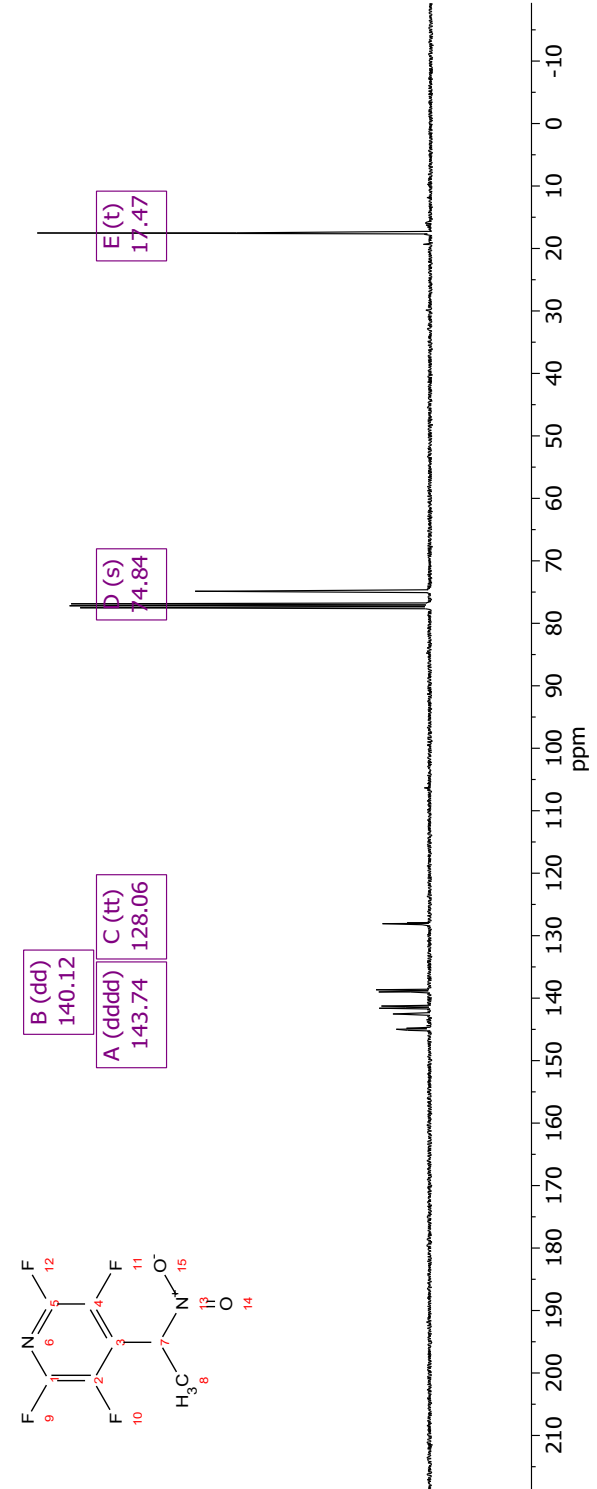
Solvent:  $\text{CDCl}_3$



B (dd) 140.12  
 A (dddd) 143.74  
 C (tt) 128.06

D (s) 74.84

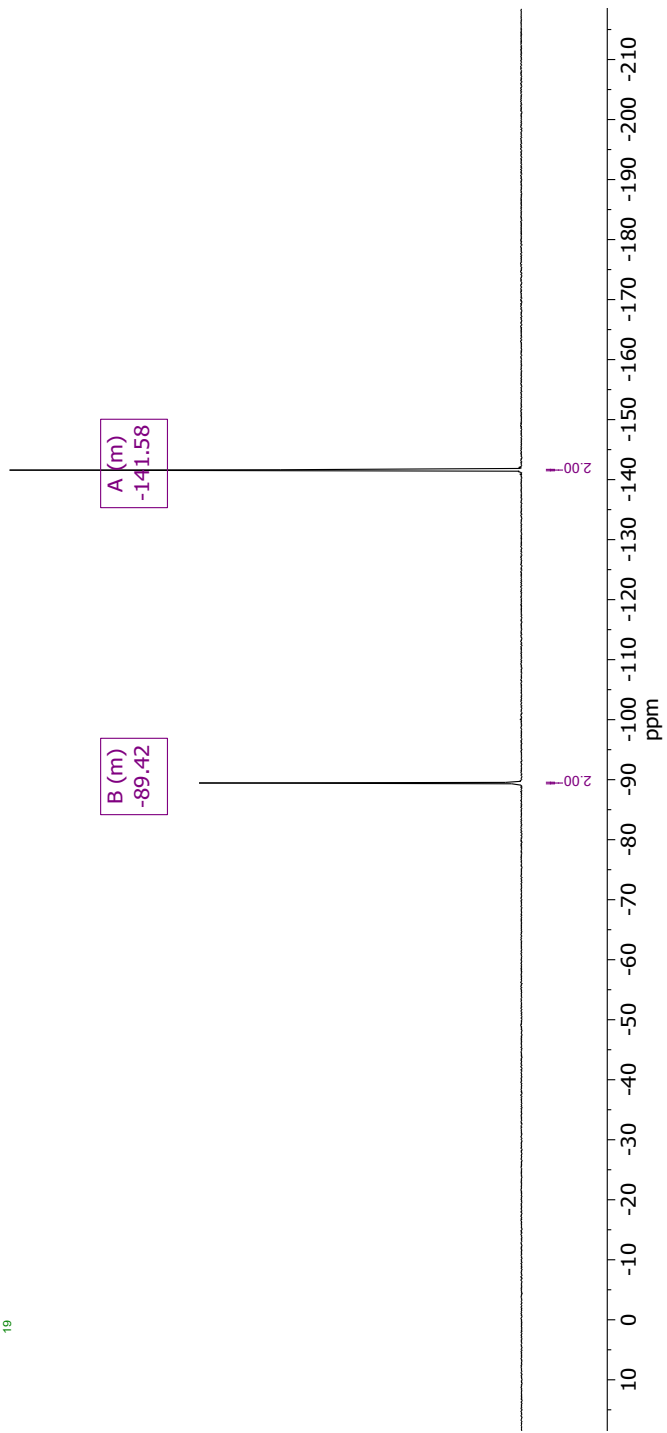
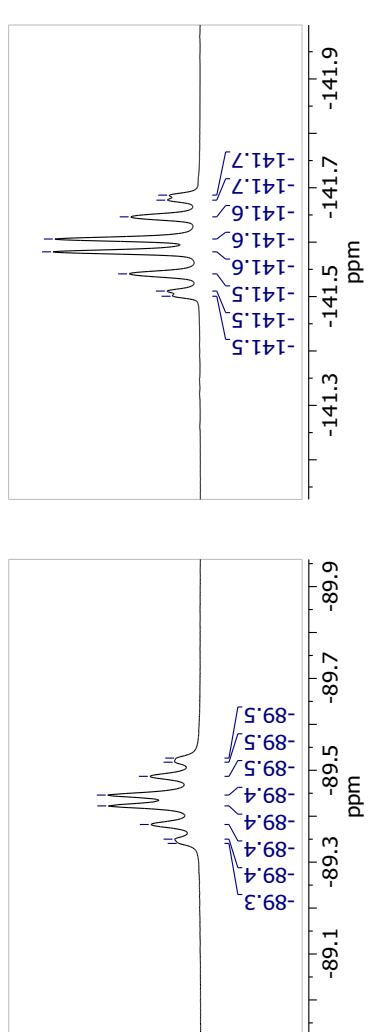
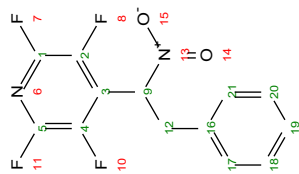
E (t) 17.47



3.3.5b: 2,3,5,6-tetrafluoro-4-(1-nitro-2-phenylethyl)pyridine

Nucleus: <sup>19</sup>F

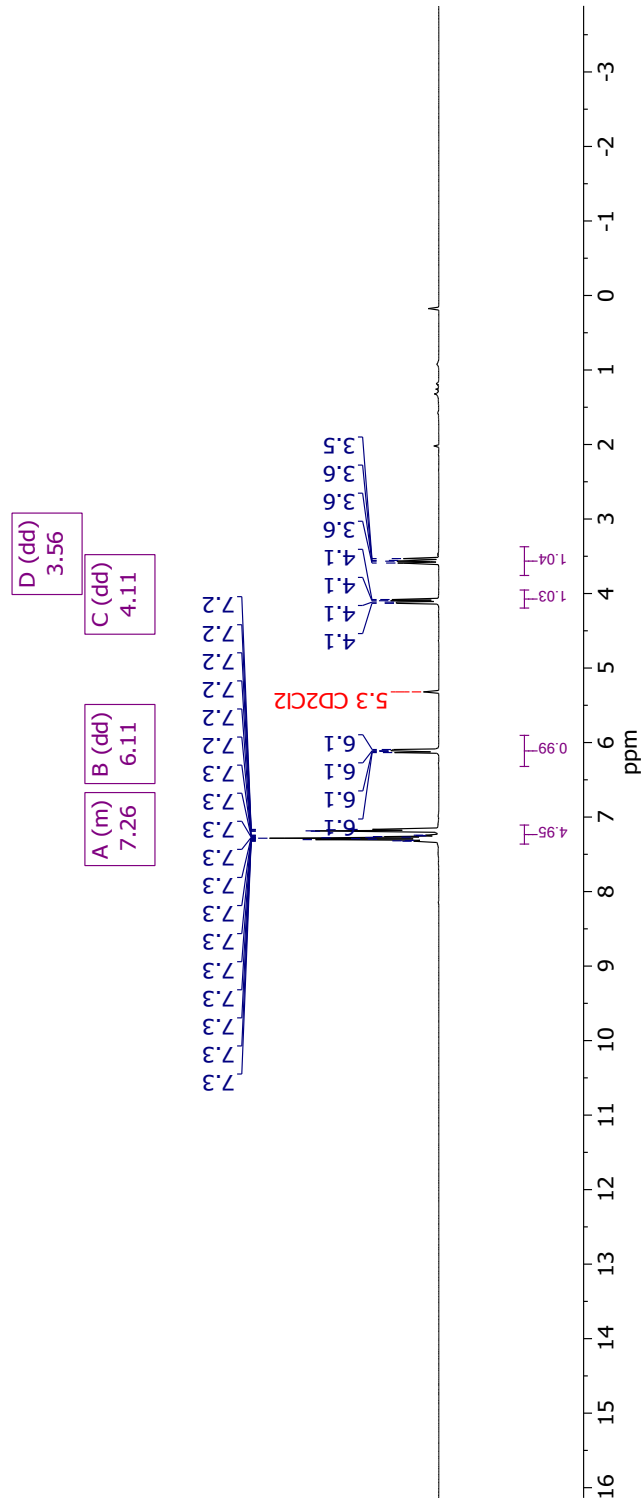
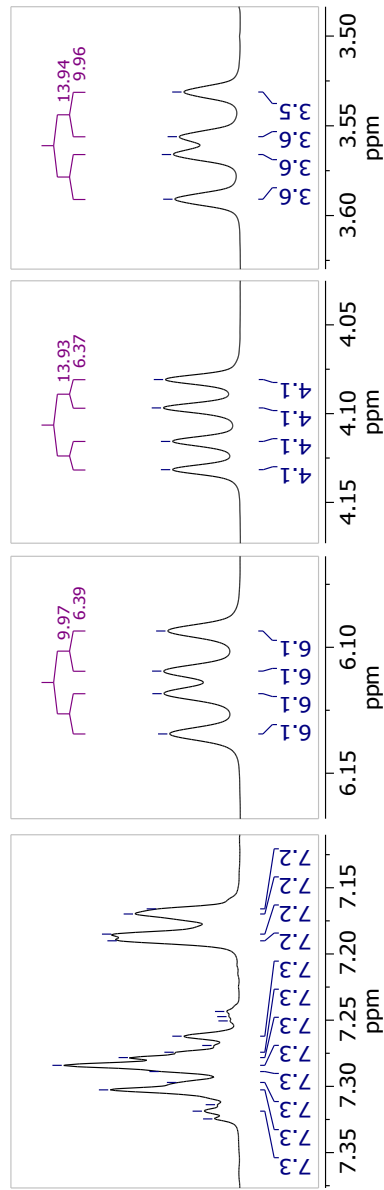
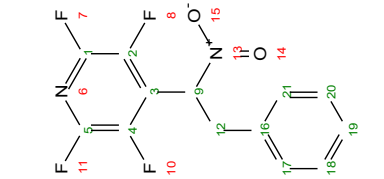
Solvent: CD<sub>2</sub>Cl<sub>2</sub>



3.3.5b: 2,3,5,6-tetrafluoro-4-(1-nitro-2-phenylethyl)pyridine

nucleus: <sup>1</sup>H

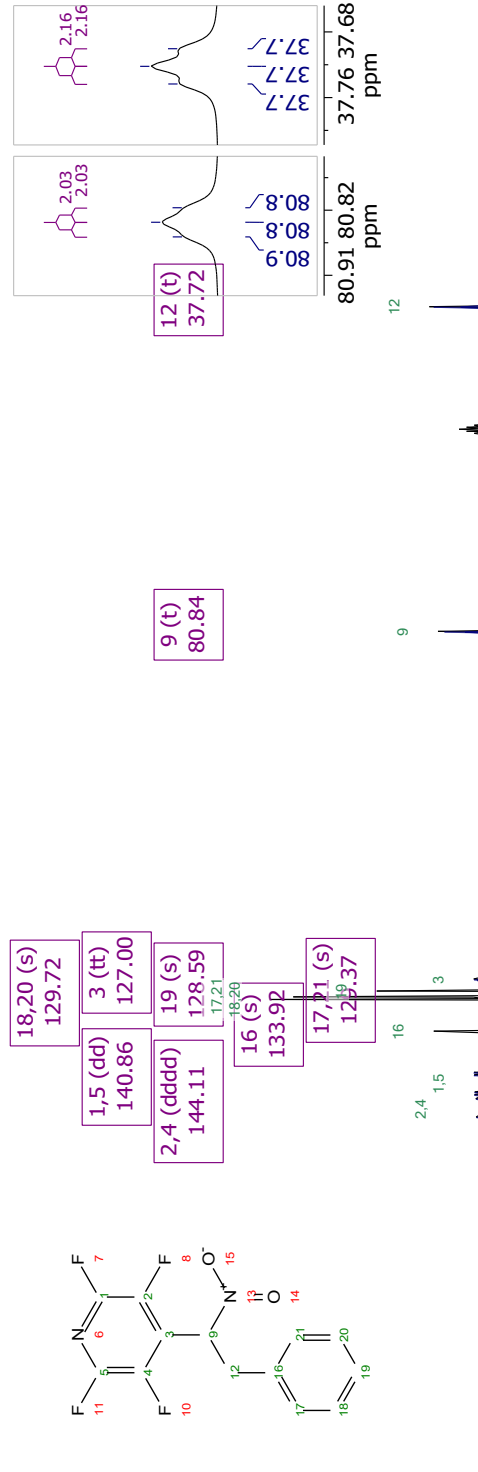
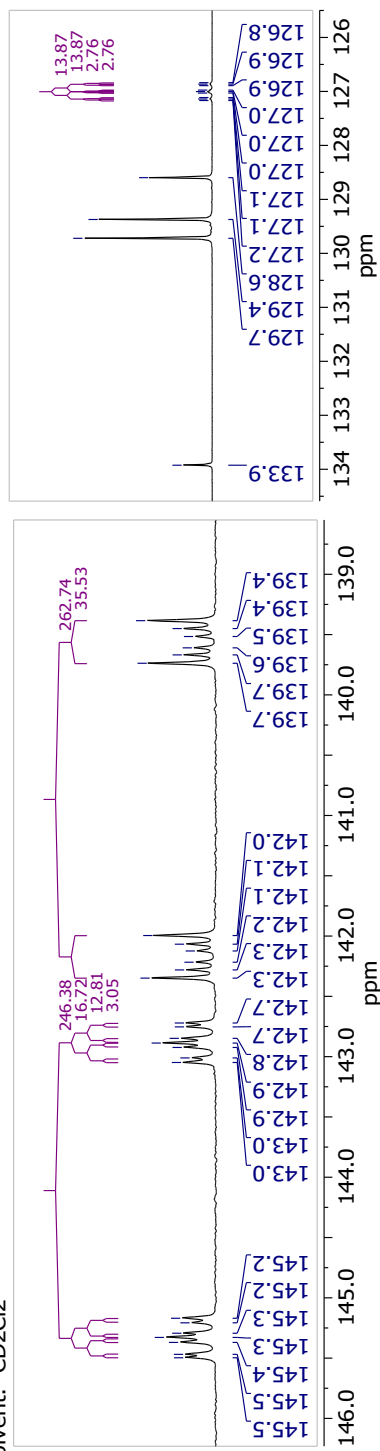
Solvent: CD<sub>2</sub>Cl<sub>2</sub>



3.3.5b: 2,3,5,6-tetrafluoro-4-(1-nitro-2-phenylethyl)pyridine

Nucleus: <sup>13</sup>C

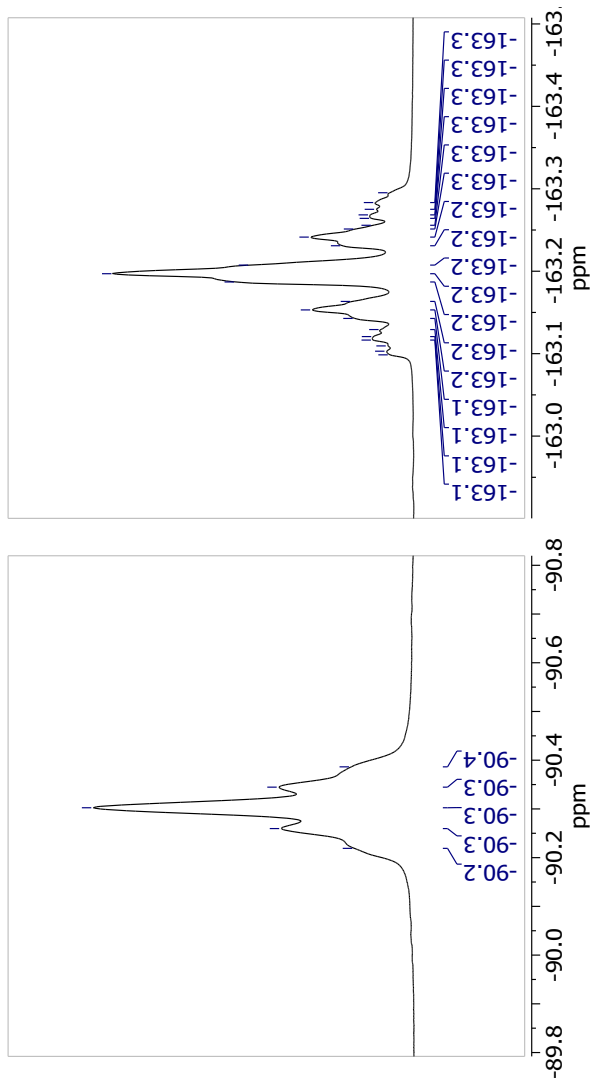
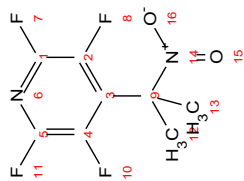
Solvent: CD<sub>2</sub>Cl<sub>2</sub>



3.3.5c: 2,3,5,6-tetrafluoro-4-(2-nitropropan-2-yl)pyridine

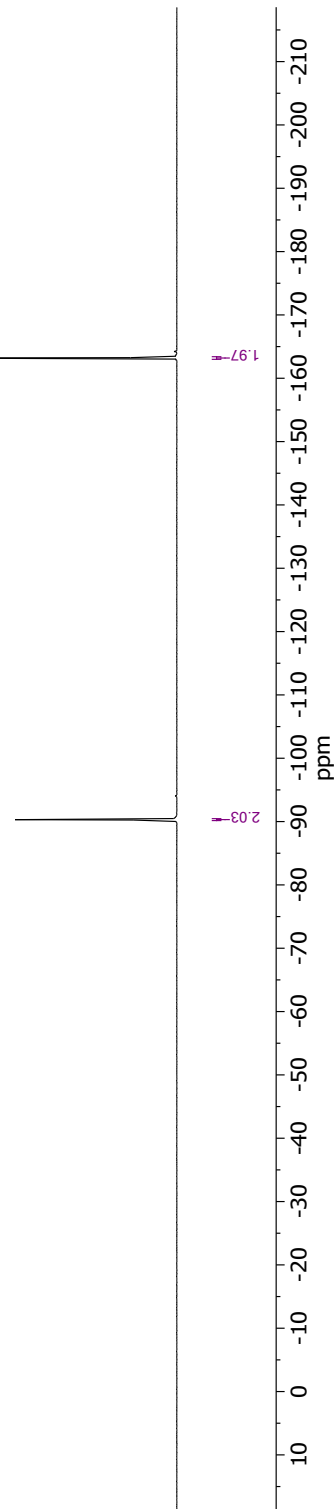
Nucleus: <sup>19</sup>F

Solvent: CDCl<sub>3</sub>



A (m)  
-90.32

B (m)  
-163.19

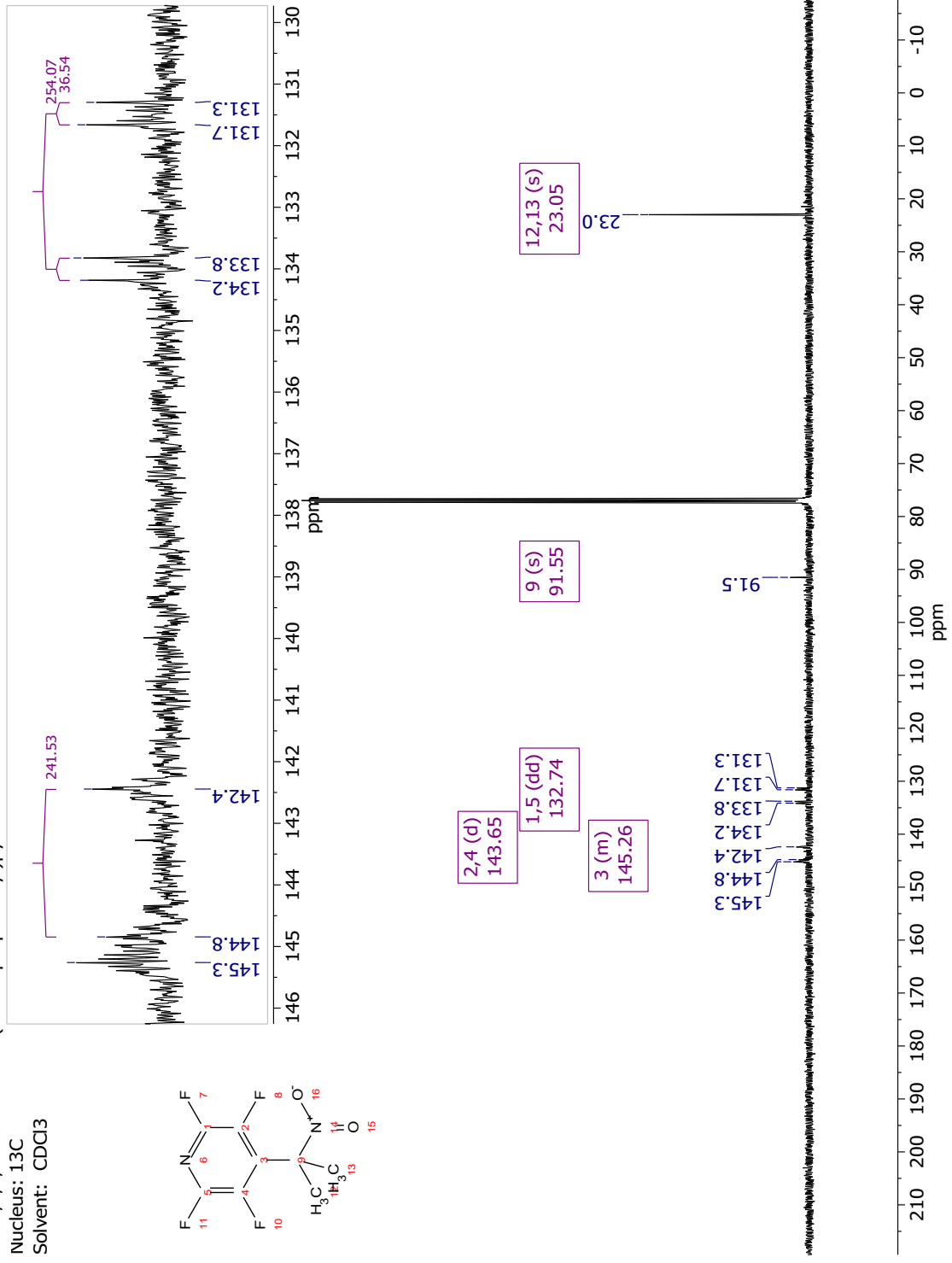
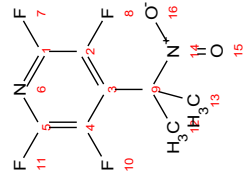


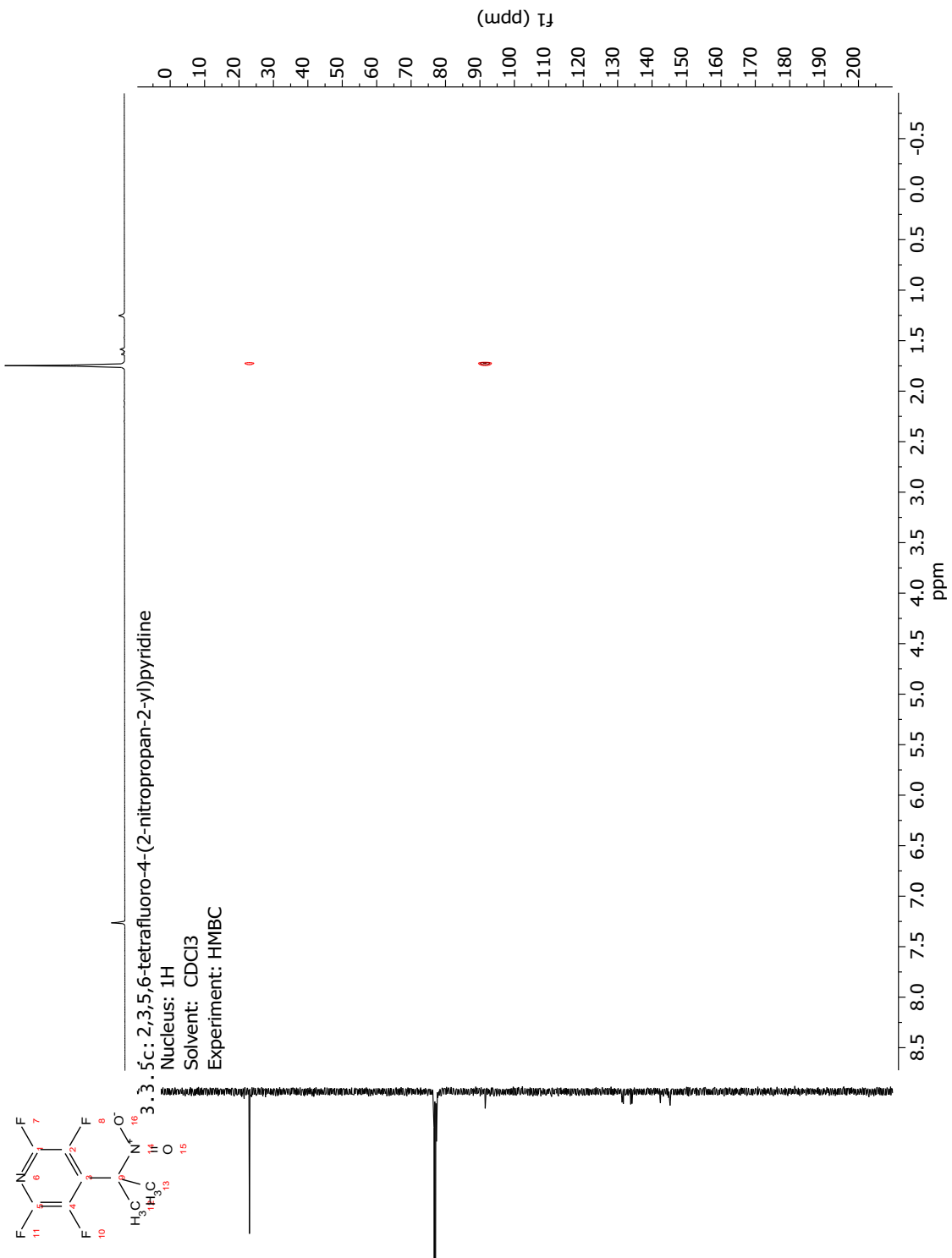


3.3.5c: 2,3,5,6-tetrafluoro-4-(2-nitropropan-2-yl)pyridine

Nucleus:  $^{13}\text{C}$

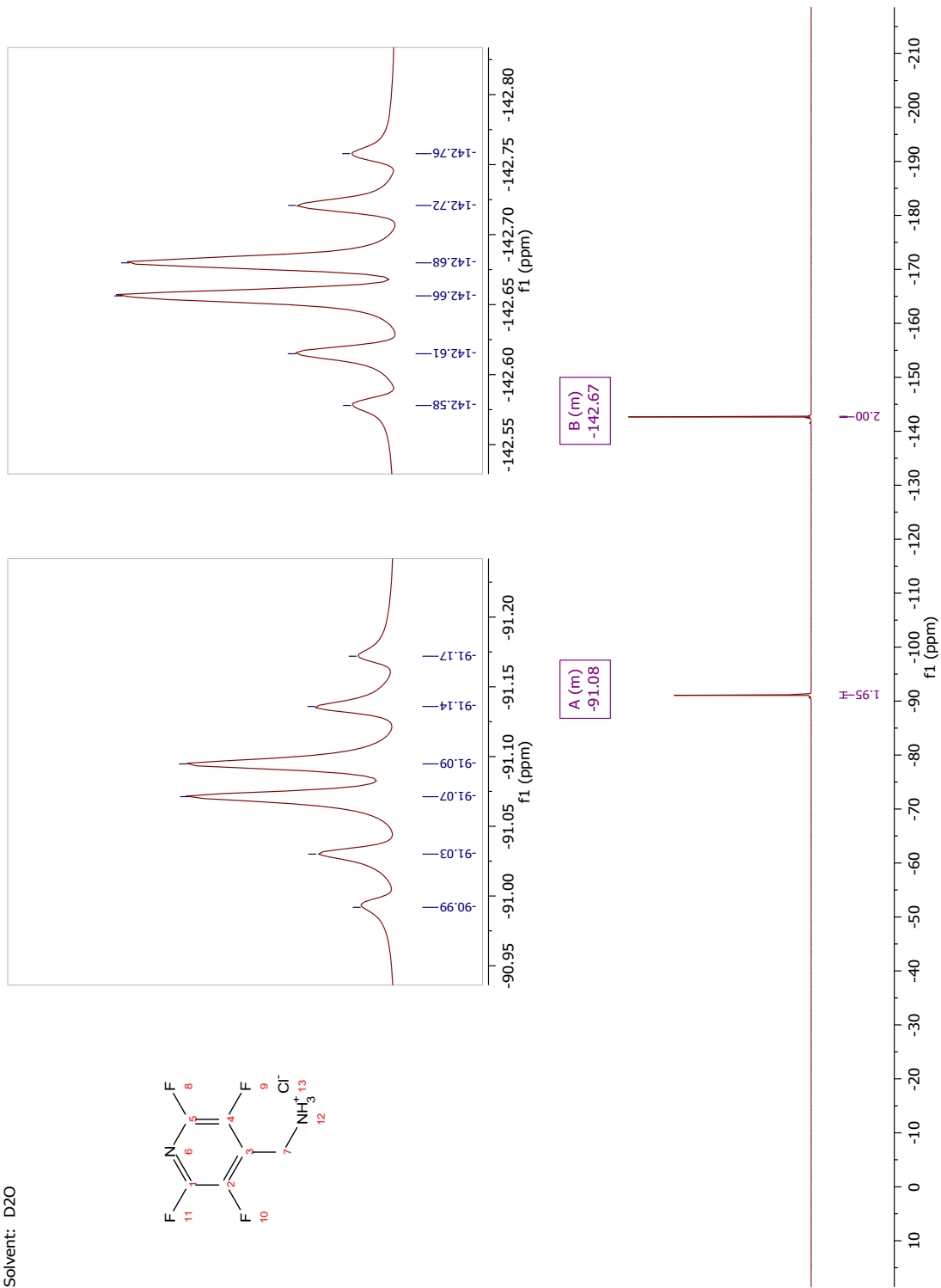
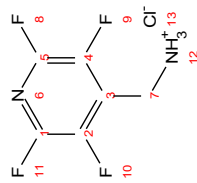
Solvent: CDCl<sub>3</sub>



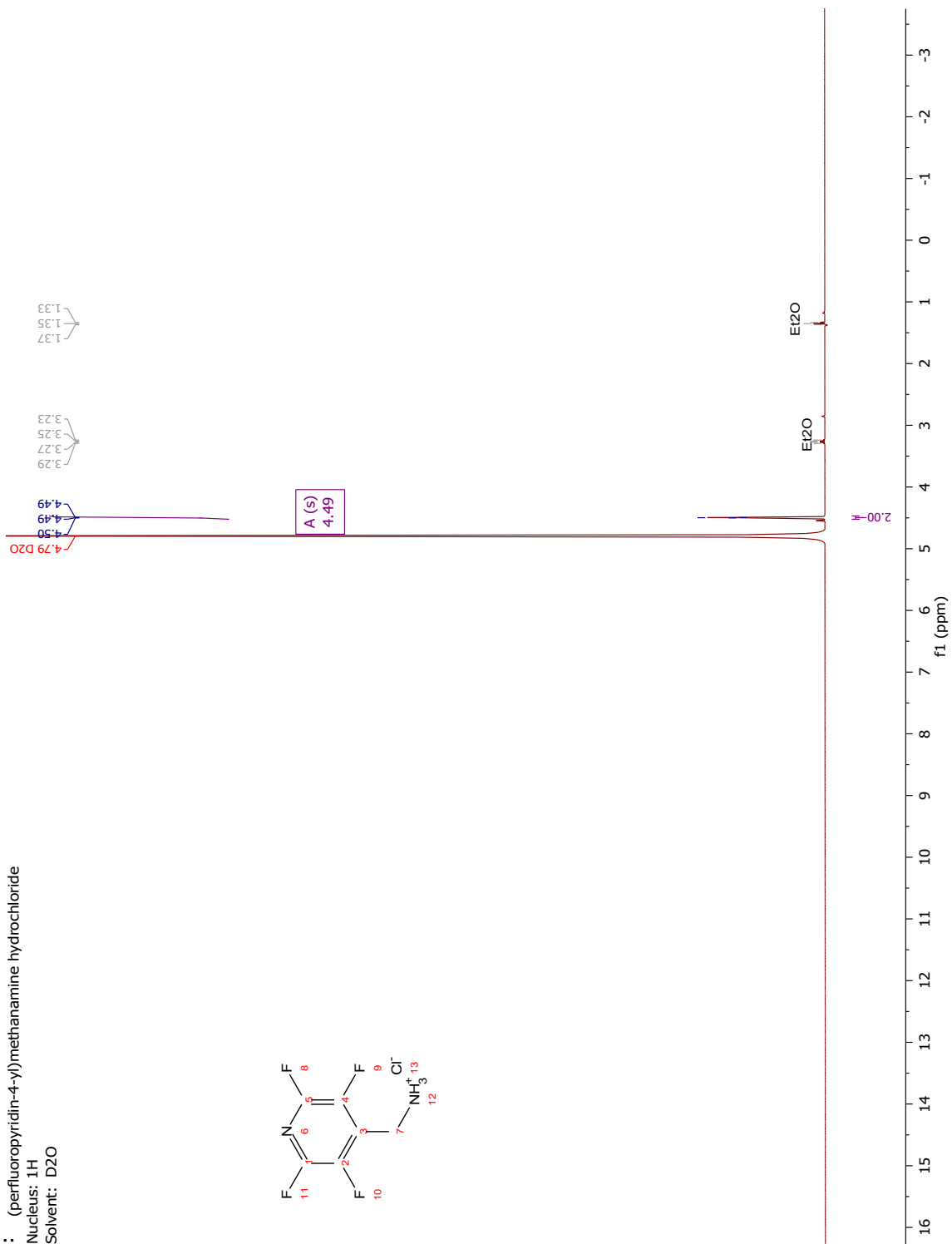
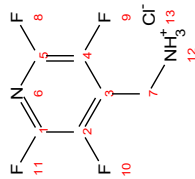




3.3.6a: (perfluoropyridin-4-yl)methanamine hydrochloride  
Nucleus:  $^{19}\text{F}$   
Solvent: D<sub>2</sub>O



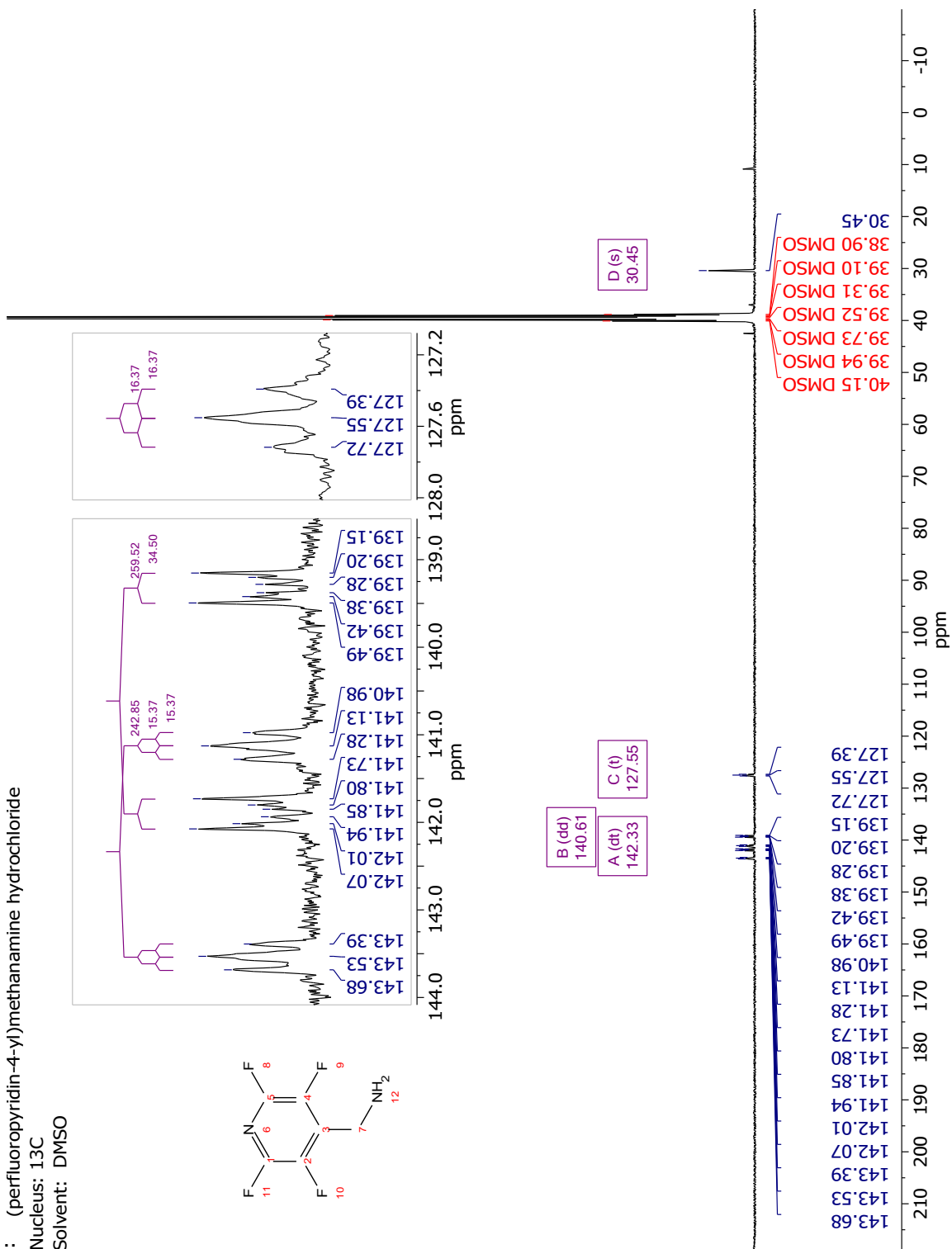
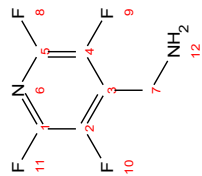
3.3.6a: (perfluoropyridin-4-yl)methanamine hydrochloride  
Nucleus: <sup>1</sup>H  
Solvent: D2O



3.3.6a: (perfluoropyridin-4-yl)methanamine hydrochloride

Nucleus:  $^{13}\text{C}$

Solvent: DMSO



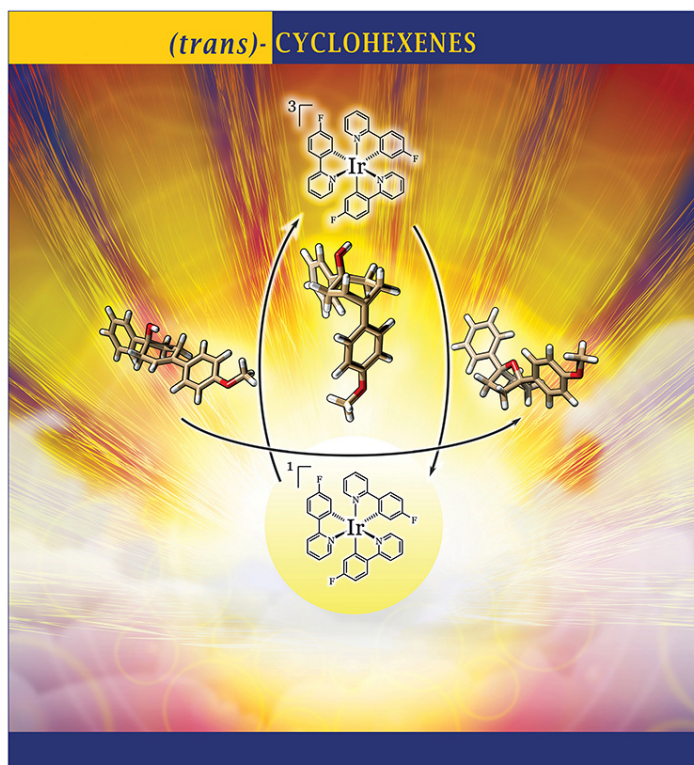
## CHAPTER IV

### VISIBLE LIGHT MEDIATED GENERATION OF TRANS-ARYLCYCLOHEXENES AND THEIR UTILIZATION IN THE SYNTHESIS OF CYCLIC BRIDGED ETHERS

#### 4.1 Overview

August 8, 2018  
Volume 140  
Number 31  
pubs.acs.org/JACS

**J | A | C | S**  
JOURNAL OF THE AMERICAN CHEMICAL SOCIETY



Herein is contained materials adapted from *J. Am. Chem. Soc.* 2018, 140, 31, 9934. With this publication we were invited to submit supplementary cover artwork, which is pictured at the left

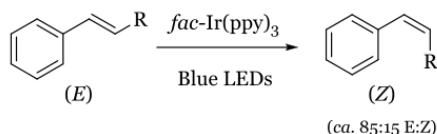
## 4.2 INTRODUCTION

The *release* of strain energy to facilitate chemical synthesis includes standouts such as Danishefsky's work with cyclobutenone and cyclopentadiene [4+2] cycloadducts,<sup>117-119</sup> that of Garg with cycloarynes,<sup>120-122</sup> or that of Fox in which *trans* cyclooctenes react with tetrazines,<sup>123</sup> though there are many others.<sup>124-128</sup> The release of this built in or chemically triggered strain can make otherwise challenging transformations possible. In contrast to a one-time event, an attractive alternative approach to building in triggers or integral molecular strain is to capture energy from visible light, as this could alleviate the difficulty associated with performing chemistry on prestrained molecules, or the difficulty associated with the installation of functional groups that serve as the trigger. With this in mind, we were drawn to E.J. Corey's communication from 1965 reporting the formation of *trans*-2-cycloheptenone,<sup>261</sup> in which the *cis*-cycloheptenone was photoexcited with UV light *in situ* with cyclopentadiene, which yielded only a [4+2] type product that appeared to be generated through a pericyclic reaction with the *trans*-isomer, elegantly demonstrating the potential of even transient strain to promote synthesis.

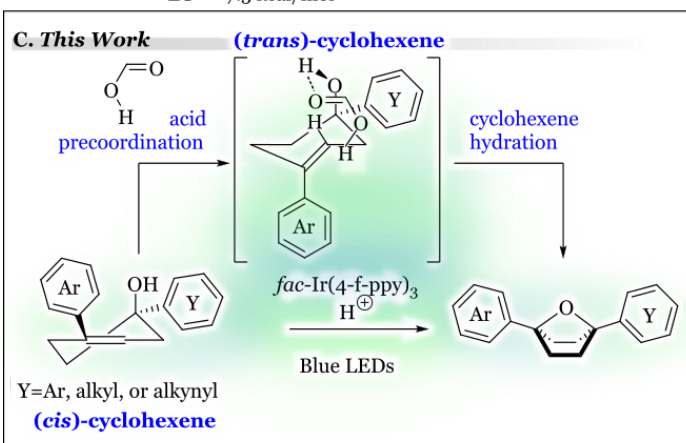
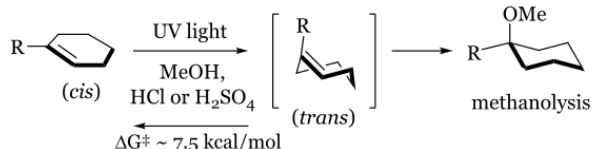
In our previous work,<sup>103, 142, 262</sup> we used visible light and Ir-based photocatalysts to

**Scheme 35** : UV and visible light mediated double bond isomerizations

### A. Visible Light Mediated Styrenyl Isomerization



### B. UV-light Mediated Isomerization & Methanol Trapping



dynamically isomerize styrenoids, and generate a photostationary state of alkenes highly enriched in the *Z*-configuration (Scheme 35A). While works have demonstrated the diverse utility of these and transformations, such as the Noël group's trifluoromethylation, hydrotrifluoromethylation, and difluoromethylation,<sup>263-264</sup> the Qing group's stereoselective trifluoromethylation of styrenes,<sup>265</sup> the Gilmour group's work with riboflavin mediated isomerizations<sup>266</sup> and corresponding synthetic routes to coumarins,<sup>267-268</sup> the Rueping<sup>212</sup> and Reiser<sup>269</sup> groups' works toward applications in process, we sought to further build on this foundation, suspecting that it would be possible to use visible light photocatalysis to generate a

strained and therefore reactive *trans*-cycloalkene in a controlled manner. For this, we were drawn to *trans*-cyclohexenes.

Larger, less strained *trans*-cycloalkenes can be generated by UV photolysis, and are isolable,<sup>105-107</sup> or at least readily observable.<sup>108-109</sup> Evidence for *trans*-cyclohexene was less forthcoming, however, presumably due to its high strain (*ca.* 52 kcal/mol), and correspondingly short lifetime. During pulsed photolysis experiments, Jousset-Dubien<sup>111</sup> and Dauben<sup>111-112</sup> reported having observed a transient species with a 9  $\mu$ s lifetime at room temperature and a *ca.* 7.5 kcal/mol barrier to isomerization back to the starting material. While irradiation with UV light led to multiple products, it has also been shown that if excited in acidic methanol, the *trans*-phenylcyclohexene underwent methanolysis of the olefin<sup>109, 113-114</sup> (Scheme 35B). Additionally, Schuster<sup>115</sup> proposed a similar intermediate for the rearrangement of cyclohexenones. Further studies from the McClelland group with UV flash photolysis have demonstrated the presence of a transient cationic intermediate, which in some cases could be intercepted with a solvent.<sup>116</sup> Importantly, these precedents demonstrated the differential reactivity between the *cis*- and *trans*-cyclohexenes, and the potential for productive syntheses.

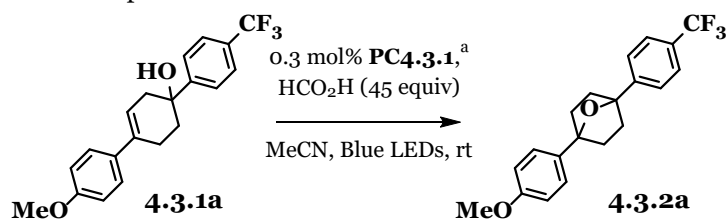
Despite these compelling early results, while larger *trans*-cycloalkenes have been deployed in synthesis,<sup>129-130</sup> the application of *trans*-cyclohexene in synthesis is still almost non-existent, with the exception of the recent report from the Larionov group<sup>131</sup> of an elegant exploitation of UV light mediated carboborative ring contraction. This sparsity is likely due, in part, to the use of UV light and historically strongly acidic conditions (i.e. H<sub>2</sub>SO<sub>4</sub>),<sup>114</sup> which limit the functional group tolerance. A more challenging aspect in performing synthesis, however, is contending with the small energetic barrier to isomerization (*ca.* 7.5 kcal/mol). In order to accomplish this, we reasoned that precoordination of the reactive partner would be the key to overcoming the difficulties of the short lifetime of the *trans*-alkene, because it would allow the entropic penalty to be paid before the transition state, thus bringing down the energy barrier.

We postulated that an alcohol group could hydrogen bond with an acid prior to isomerization (Scheme 35C), preparing ahead of time for the short lived, high-energy *trans*-cyclohexene, ultimately facilitating the protonation of the alkene by pre-positioning the acid near the alkene. The generated carbenium ion and the internal alcohol could then undergo ring closure to form the ether product. In addition, use of a tertiary benzylic alcohol, prone to acid catalyzed elimination, would demonstrate the increased reactivity of the *trans*-cyclohexene. The expected reactivity of *trans*-cyclohexene in relation to its *cis*-isomer would be orthogonal because it would circumvent the expected elimination of the tertiary alcohol and allow reaction to take place only when stimulated by light. Further, we reasoned that the use of a photocatalyst would allow us to generate the requisite *trans*-cyclohexene indirectly with visible light, preventing side reactions that typically accompany UV photolysis.

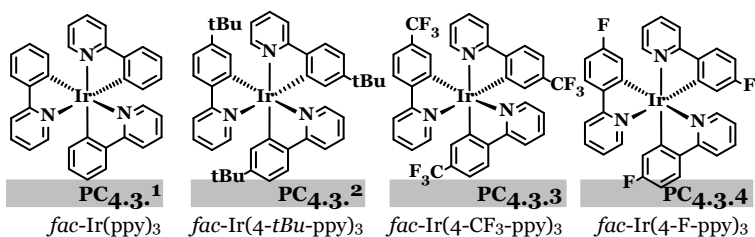
### 4.3 EXPERIMENTAL

To begin our investigation, we subjected cyclohexenol **4.3.1a** to catalytic amounts of **PC4.3.1** ( $\text{Ir}(\text{ppy})_3$ ), formic acid which we anticipated would not induce elimination, due to its weak acidity, and blue LEDs (Table 11, entry 1). We were pleased to observe the formation of the desired bicyclic ether in good conversion (78%). Control reactions established the necessity of all three components (entry 2). Attempts to use a stronger Brønsted acid, such as HCl, simply led to elimination of water (entry 3).

Next, we evaluated the effect of the photocatalyst on the reaction (entries 4-6). We found, as previously demonstrated,<sup>142</sup> that both the steric volume and the emissive energy of the catalyst affect the rate of the reaction. Sterically larger photocatalysts such as **PC4.3.2** with its much larger molecular radius effectively suppressed reactivity (entry 4 vs. 5), despite very similar emissive energy to **PC4.3.1** (54.5 vs. 55.2 kcal/mol), indicating the likelihood of an energy transfer pathway. The most effective catalysts were relatively smaller (entries 5 and 6). The optimal catalyst was found to be **P4.3.4**, whose emissive energy is 58.6 kcal/mol, but is only slightly larger than standard **PC4.3.1**. **PC4.3.4** was used for further optimization. Evaluation of several carboxylic acids (entries 7-10), revealed that a 90% solution of formic acid was optimal, where both weaker and stronger acids were detrimental to the reaction.

**Table 11.** Optimization of Reaction Conditions.

Entry	Modification of conditions	Conversion to <b>2a</b> <sup>b</sup>	Time
1	None	19 / 78%	3.3 h / 24 h
2	No acid, no photocatalyst, or no light	0%	24 h
3	HCl instead of <b>PC4.3.1</b> and formic acid <sup>c</sup>	0%	24 h
4	<b>PC4.3.2</b> instead of <b>PC4.3.1</b>	3%	3.3 h
5	<b>PC4.3.3</b> instead of <b>PC4.3.1</b>	56%	3.3 h
6	<b>PC4.3.4</b> instead of <b>PC 1</b>	91%	3.3 h
7	<b>PC4.3.4</b> and 20 equiv of formic acid	98%	8 h
8	<b>PC4.3.4</b> and 20 equiv of acetic acid	60%	8 h
9	<b>PC4.3.4</b> and 20 equiv of trichloroacetic acid	7%	8 h
10	<b>PC4.3.4</b> and 20 equiv of trifluoroacetic acid	0%	8 h
11	<b>PC4.3.4</b> at -20 °C	41%	2 h
12	<b>PC4.3.4</b> at -10 °C	48%	2 h
13	<b>PC4.3.4</b> at 0 °C	17%	2 h
14	<b>PC4.3.4</b> at 30 °C	29%	2 h
15	<b>PC4.3.4</b> at 45 °C	61%	2 h
16	<b>PC4.3.4</b> at 60 °C	59%	2 h



<b>radius:</b> <sup>[16]</sup>	4.5	5.0	4.8	4.57 (Å)
<b>E<sub>emis.</sub></b> <sup>:[16,40]</sup>	55.2	54.5	56.4	58.6 (kcal/mol)

<sup>a</sup> A stock solution of **b** catalyst was used. The concentration of **4.3.1a** was 0.05 M. Determined by <sup>19</sup>F NMR. <sup>c</sup>The dehydrated product was detected by GCMS.

We initiated our exploration of the scope of the reaction by varying the substituent attached at the carbinol carbon. The reaction was remarkably tolerant to various substitution at this position, giving the cyclized product in very good yields for electron poor arenes (**4.3.2a-4.3.2d**), electron neutral arenes (**4.3.2e** and **4.3.2f**), alkynyl (**4.3.2g**), and alkyl substituents (**4.3.2h**). The propensity of some of the carbinols to ionize under acidic conditions (i.e. tertiary benzylic<sup>270</sup> or propargylic alcohols<sup>271</sup>), highlights the

Analysis of the optimal temperature revealed maximal reaction rate at 45 °C (entry 15). Curiously, examination at early timepoints revealed a bifurcation of the rate constant, which increased with temperatures both higher and lower than 0 °C (entries 11-16). This unusual result is consistent with a highly reactive intermediate, in which lower temperatures extend the lifetime of the reactive species by reducing the free energy available for thermal reversion to the *cis*-cyclohexene species. Conversely, we expected that increased temperatures increase the rate either by increasing the probability of the *cis*-cyclohexene encountering an excited photocatalyst to generate the reactive *trans*-cyclohexene, or alternatively, could populate higher energy conformations, which would be more capable of energy transfer. We explore these possibilities below.

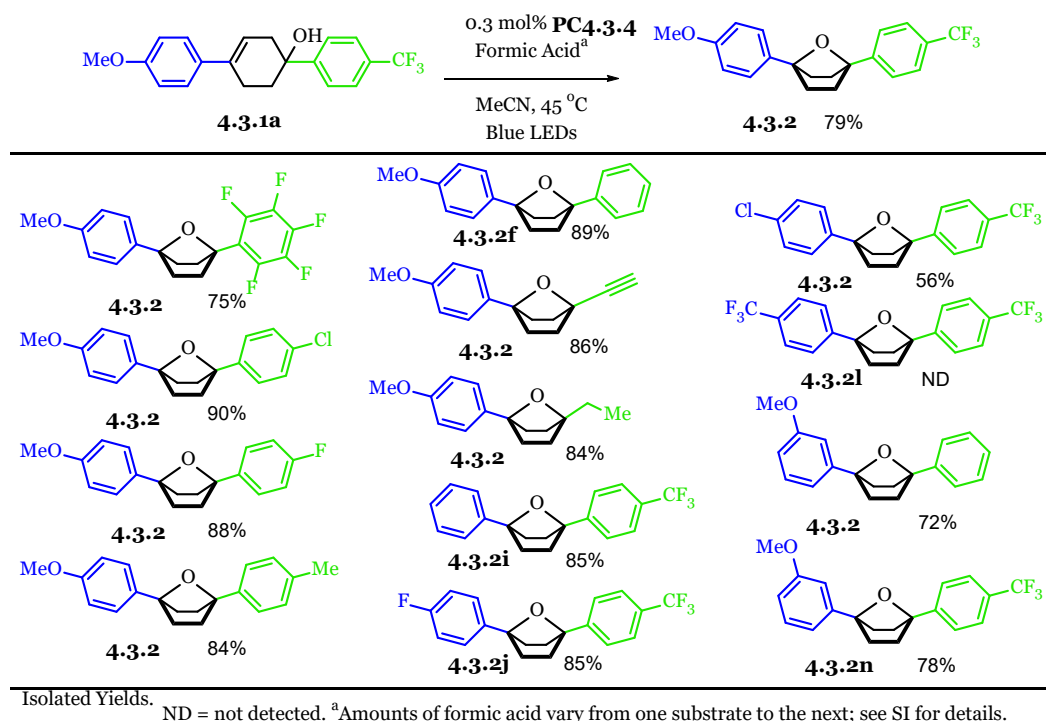


importance of using a weak acid, and demonstrates the enhanced basicity of *trans*-cyclohexene. We next explored the vinyl arene substituent (**4.3.2a** vs. **4.3.2i-4.3.2n**). The arene is an essential component of the substrate as it makes the triplet state of the alkene energetically accessible through visible light photocatalysis.<sup>32</sup>

Because the conjugation is an important facet to triplet stabilization,<sup>272</sup> it is unlikely that the reaction would proceed with ortho substituents which dramatically disrupt the conjugation both in the ground state and the vertically excited triplet. Within this limitation, the arene was quite amenable to substitution with electron rich (**4.3.2a**), neutral (**4.3.2i**), and moderately electron poor (**4.3.2j** and **4.3.2k**) arenes. However, strongly electron deficient arenes (**4.3.2l**) failed to give any cyclized product. This failure may result from very sluggish protonation of the *trans*-alkene, which instead undergoes thermal reversion to the relaxed *cis*- starting material, although electronic modulation of the HOMO–LUMO gap is possible as well, and may prevent excitation by the photocatalyst.

At this point in the investigation, several key assumptions about the reaction had been made. It was assumed that, as established previously in related transformations,<sup>103, 142, 212, 262, 269</sup> photochemical energy from a photon in the visible light region is absorbed by a photosensitizer, which after photoexcitation to a singlet, ultimately leads to a long-lived triplet excited state.<sup>70</sup> Because the catalyst is in a triplet state, and photocatalyst radii dependency is observed (Table 11, entry 4), then the energy transfer most likely occurs via a Dexter<sup>273</sup> mechanism, exciting the substrate to a triplet biradical. This triplet biradical is capable of bond rotation about the former double bond. The triplet biradical rotates to an orthogonal position because not only do the formerly  $\pi$  electrons now repel each other, but rotation also serves to relieve 1,2-eclipsing interactions. Upon returning to the ground state from the triplet landscape via a non-radiative crossing event (ISC; conical intersection) at, or very near the transition state for rotation about the double bond, the former alkene can then further rotate and relax to form either the *trans*-cyclohexene which can engage in subsequent reactivity, or unproductively reform the *cis*-alkene, evolving its energy as heat.

There were, however, several mechanistic quandaries, such as what purpose does the acid serve? Does the acid serve only as a proton source, or does it actually precoordinate as we have supposed? These questions ultimately culminate in the penultimate question: what does the transition state look like? We therefore sought to probe these questions, beginning by investigating the geometry of the transient reactive species.

**Table 12** Scope of the Photocatalytic Cyclization.

#### 4.4 MECHANISTIC INVESTIGATION

To gain further insight to the reaction, and determine if the geometries we were envisioning were feasible, we set out to perform conformational analyses computationally. Since triplet state energies would be of interest here, we settled on using Møller-Plesset (MP2)<sup>274</sup> theory, ultimately with large, correlation consistent basis sets.<sup>275-276</sup> First, we minimized the starting alcohol and performed two dihedral drivers at the freely rotatable C–C bonds connecting the three rings (Figure 4A). The carbinol phenyl (C<sup>1</sup>) preferred to rotate 90° from the adjacent ring, presumably to avoid allylic strain. Looking at the styrenyl phenyl revealed a more complex landscape, in which the lowest energy conformer has the two rings 28° out of planarity. We subjected the 90° cross section to an increased number of scan points for rotational angles (Figure 4B). Next, we subjected select structures to a higher level of computational theory, in order to provide insight into the relationship between the thermal and the excited state landscapes.

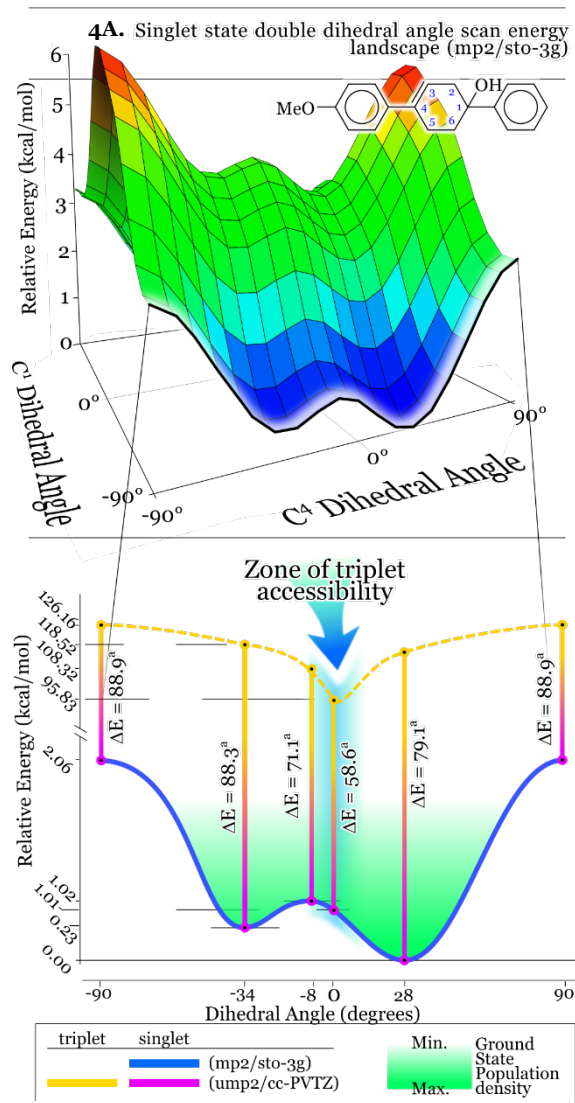
Beginning from the minimized geometry with the methoxyphenyl ring canted 28° from planarity with the *cis*-cyclohexene ring, a vertical excitation from the singlet to the triplet state was calculated using the cc-PVTZ basis set.<sup>276</sup> The energy difference for this excitation was found to be in excess of the emissive energy of the photocatalyst. This is because the minimized geometry favors deconjugation of the methoxyphenyl dihedral angle at C<sup>4</sup> of the *cis*-cyclohexene, and therefore puts the singlet to triplet excitation

energy out of reach of the photocatalyst. At ca. 1 kcal/mol higher energy, rotation of the methoxyphenyl ring into planarity with the *cis*-cyclohexene double bond is easily thermally accessible at a reaction temperature of 45 °C. Based on a Boltzmann distribution population analysis,<sup>40</sup> increasing reaction temperature from 0 °C to 45 °C increases the frequency of observing a molecule in the fully conjugated conformer by ca. 30%, based on the relative energies of these conformers. This provides some insight to support our prior supposition as to the bifurcation of reaction rate in relation to reaction temperature (Table 11, entries 13-16).

Vertical excitations from the singlet to the triplet state were calculated at minima and maxima of this landscape, as well as 0°. In lieu of performing an exhaustive and correspondingly computationally expensive ring conformer search on the cyclohexene ring, dihedral angles for rotation about the C<sup>4</sup>-methoxyphenyl ring were frozen, and a simple geometry optimization was performed on the ground state singlet, in the gas phase. While absolute energy differences for singlet to triplet excitation are greater than expected, the trend of the gap demonstrates the importance of conjugation. Conjugation of the alkene with the methoxyphenyl  $\pi$  cloud brings the calculated excitation energy to a minimum, which is known experimentally to be within the range of the emission energy of the photocatalyst (58.6 kcal/mol).<sup>277</sup>

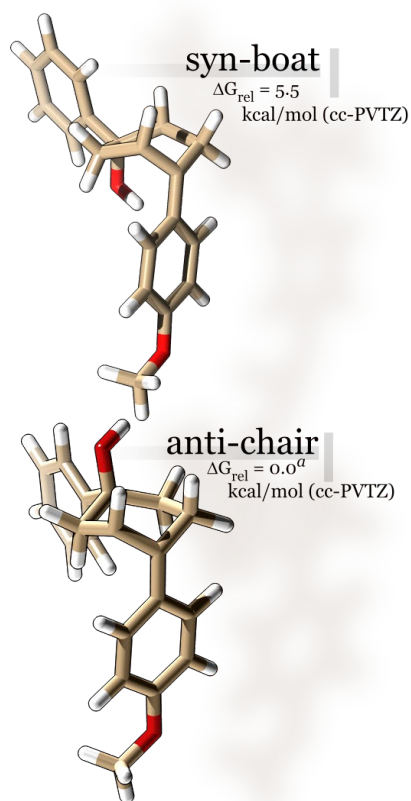
Next, we considered the strained *trans*-cyclohexene species. Importantly, upon ISC, the formation of the *trans*-cyclohexene generates four potential diastereomers, of which only two could lead to ring closure (axial-OH). We have termed these the *syn*-boat and the *anti*-chair (Figure 5). Calculations of the ground state energies of these species indicated

**Figure 4:** Accessibility of the Biradical as a Function of Alkene Conjugation



**4B.** Singlet state energies as a function of c4 dihedral angle and vertical excitations to triplet state energies. <sup>a</sup>Excitation values scaled to the experimentally determined maximum value for excitation at 0° - 58.6 kcal/mol, the emission energy of the photocatalyst; other triplet state energies relative to this. Energies along ordinate axis are relative to the lowest energy point in the singlet landscape. Singlet curve developed at MP2/STO3G; energies scaled to values determined at MP2/cc-PVTZ.<sup>[29]</sup>

**Figure 5:** Only the *syn*- and *anti*- diastereomers of the *trans*-cyclohexane can lead to oxabicyclic etherification



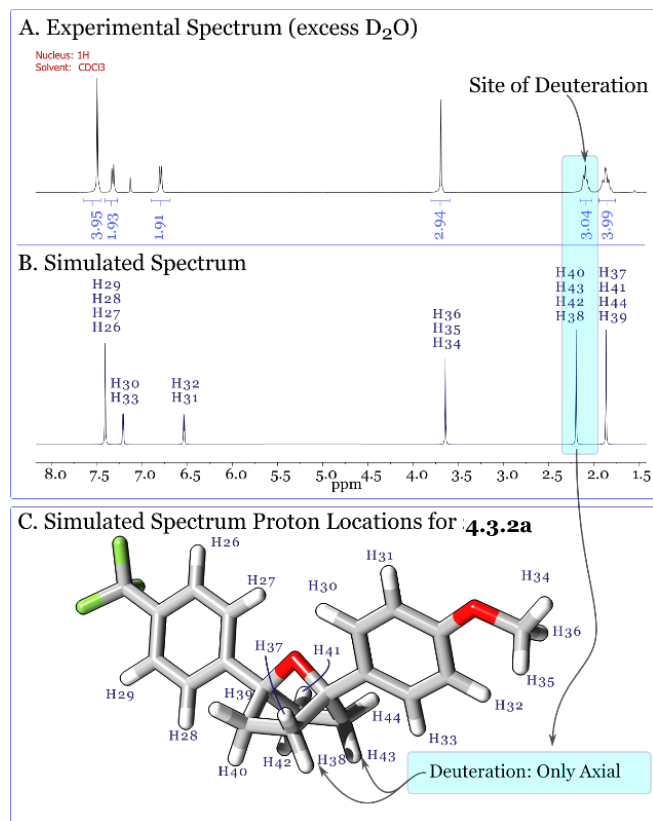
<sup>a</sup> $\Delta G_{\text{rel}} = 51.7$  kcal/mol relative to product - Scheme 36D

that the *anti*-chair would be lower in energy by *ca.* 5.5 kcal/mol, which is consistent with the work of Johnson.<sup>278</sup> This energy difference cannot be used to anticipate the reactive conformer, however, since both are lower than the triplet state energy and thus accessible therefrom. In order to discern the reaction pathway, we would need stereochemical evidence. Since the upper limit for the energy to excite the *cis*-cyclohexane is the emission energy of the photocatalyst, then the maximum height conical intersection on the singlet state landscape must also be bounded by this restriction. It is of note that the difference between the ground state energy of the *anti*-chair *trans*-cyclohexene and the  $\lambda_{\text{max}}$  emissive energy of the photocatalyst is approximately the same as not only the value that Dauben found for reversion of *trans*-phenylcyclohexene to the *cis*-starting material, but also the computationally determined value determined by Johnson for simple cyclohexene.

It was envisioned that a deuterium label could provide stereochemical evidence of the geometry of the bond which undergoes hydroalkoxylation, as the face of incorporation and the number of sites deuterated would provide mechanistic insight with regard to the reversibility of the protonation step. Submitting **4.3.1a** to reaction conditions in which a large excess of D<sub>2</sub>O was added resulted in deuterium incorporation only on the face of the cyclohexene ring opposite that of the forming ether, so that the deuterated product shows signal attenuation equivalent to the incorporation of 1 hydrogen only in the axial position of the product (Figure 6A). This was affirmed by correlation with computational NMR simulation (Figure 6B).<sup>40, 279</sup>

The presence of isotopic scrambling only on the formerly vinyl carbon indicated that the protonation/deuteration was essentially irreversible, and could have occurred in two ways. *Exo* protonation of the *syn*-boat can be ruled out, since it would lead to incorporation of the deuterium on the same side of the ring as the forming ether, not the experimentally observed product. Similarly, *endo* protonation of the *anti*-chair conformer should be ruled out because it too leads to the incorrect deuterated regioisomer. It is possible that the protonation/deuteration could have occurred from the *endo* face of the

**Figure 6:** Deuterium Incorporation under General Reaction Conditions with **4.3.1a** and Computational Identification of the Resultant Diastereomer



*syn-boat trans-cyclohexene* ring. However, because the *endo* face is the more sterically congested, it seemed unlikely to be the face of protonation. Conceivably, the C<sup>1</sup> hydroxyl could have been serving to protonate the *endo* face of the *syn-boat* conformer. Assessment of this scenario reveals that the proton or deuterium would subsequently have to travel through the van der Waals cloud of the cyclohexane ring, likely requiring a tunneling event to arrive at the proper orbital to generate the experimentally observed product. If this did occur, one could expect a very large kinetic isotope effect (KIE), ( $k_H/k_D > 40$ ),<sup>280</sup> but it was not observed (*vide infra*). The simplest explanation is that the deuteration event happens from the *exo* face of the *anti-chair*. Although the *exo* protonation of the *anti-chair* conformer seemed the most likely, the question still to be answered

was how that *exo* protonation occurred.

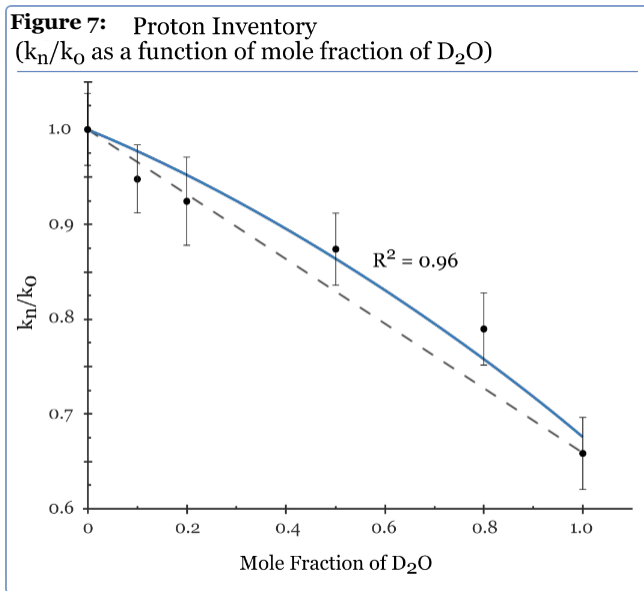
In order to probe this, we next began investigating the kinetics of the reaction. Initial rates experiments indicate that the reaction is first order with respect to catalyst. With the substrate, the reaction appeared to have zero order kinetics.<sup>40</sup> With formic acid, at low loadings there was a linear response to concentration, while at higher loadings it fell out of the rate expression.<sup>40</sup> This led us to suspect that the acid may be undergoing a pre-rate determining step equilibrium, i.e. a precoordination event. Further support for the latter idea was observed in <sup>1</sup>H NMR via titration of the tertiary alcohol starting material (**4.3.1f**) with formic acid under anhydrous conditions, which resulted in a slight deshielding of the hydroxyl signal in the reaction solvent, acetonitrile.<sup>48</sup> This is consistent with hydrogen bonding of the proton with an H-bond acceptor, such as an oxygen in formic acid. It is remarkable that this interaction can be observed at all, given that acetonitrile can compete with other hydrogen bond acceptors, and overshadow many nonbonding or partially bonding interactions.<sup>281</sup>

This precoordination of the substrate and acid serve to reduce the entropy of the transition state. Importantly, we anticipate such precoordination provides a proximal

proton to the *trans*-alkene upon its genesis, and that this is essential to harnessing the strain energy. Similarly, while not discussed in Larionov's<sup>131</sup> recent carboborative ring contraction, we suspect that the absence of dimerization products or products of other reaction pathways is due to the precoordination of a Lewis acidic trialkyl borane with the alkene, which serves a similar role to immediate protonation. We conducted tandem rate experiments with phenyl-cyclohexene, which is devoid of a hydroxyl group, and **4.3.1f**<sup>40</sup> under the standard reaction conditions in order to investigate the relative effect of the precoordination (section 4.12.3). These experiments revealed much faster reactivity with the substrate capable of precoordination (**4.3.1f**) than the phenyl-cyclohexene could achieve without a hydrogen bond to the formic acid, supportive of the assumption that the precoordination aids the reactivity.

When the aqueous environment of the reaction was replaced with D<sub>2</sub>O,<sup>282</sup> we observed a solvent KIE  $k_H/k_D$  of 1.5. This is unusual because it is outside the ranges for what would be expected for either a primary (greater than 2) or a secondary normal KIE (1 to 1.4).<sup>280</sup> Furthermore, in the case of a rehybridization from an sp<sup>2</sup> to sp<sup>3</sup> carbon in the rate determining step, one would expect to observe an inverse KIE (0.8 to 1). Further obfuscating the interpretation of the observed KIE is that there are multiple sites for deuterium exchange, not only at the site observed in the final product, but also in the hydroxyl, and in formic acid itself. Additionally, if the proton/deuteron being transferred is from a formic acid coordinated to the hydroxyl group, then a nonlinear transition state is expected, and thus a diminished KIE would be expected as well. What could be said at this point was that it further suggests that the protonation of the alkene is not occurring from the endo face of the *syn*-boat conformer. If it was, it would have to travel through the van der Waals cloud of the cyclohexene ring and would therefore likely have tunneling characteristics.<sup>280</sup>

In order to sort out the possibilities, we conducted a proton inventory experiment (Figure 7). Although the data is noisy, the plotted result showed an upward curvature. Curvature is consistent with the transfer of multiple protons in the rate-determining step. The upward curvature could be consistent with a transition state that possesses a significant degree of inverse character.<sup>283-284</sup> This result is consistent with the rehybridization of an sp<sup>2</sup> carbon to sp<sup>3</sup> in the rate determining step in which not only is a proton transferred to the substrate,

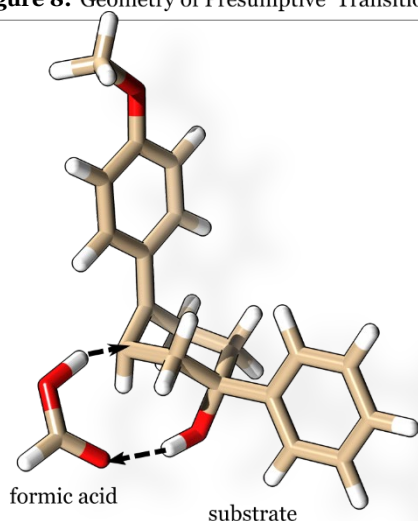


Dashed line added for emphasis of curvature.



but also the forming formate anion is simultaneously abstracting a proton from the hydroxyl group.

**Figure 8:** Geometry of Presumptive Transition State



Geometry identified at HF/3-21G. Proton transfer pathways indicated with dashed lines

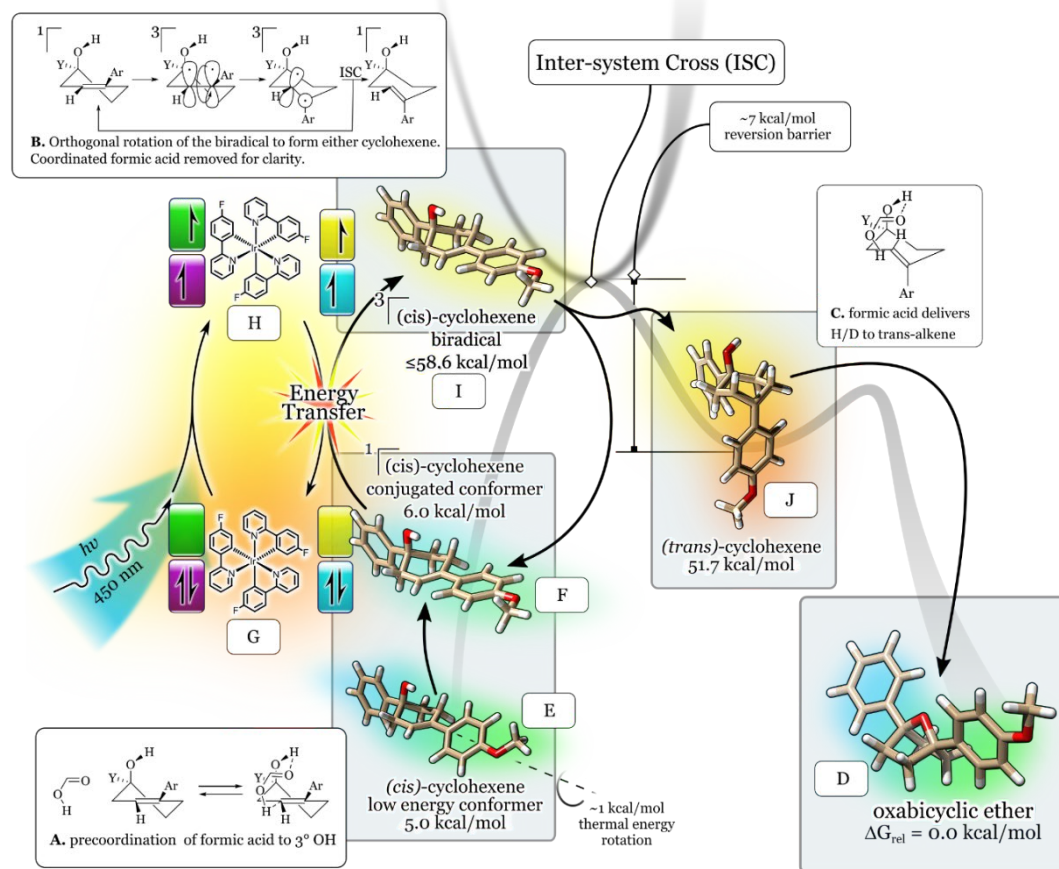
We then sought to combine the evidence of hydrogen bonding between the hydroxyl proton and formic acid with our conformational analysis of the *trans*-cyclohexene. Since *exo* protonation of the *anti*-chair *trans*-cyclohexene is most likely, we sought to model a hydrogen bonded formic acid molecule with the *anti*-chair geometry to see if a potential transition state would be geometrically feasible. Optimization of the aforementioned geometries with a transition state minimization at low basis set and theory level (HF/3-21G) resulted in the geometry in Figure 8. This model clearly demonstrates the possibility of such a transition state in which a formic acid bridges the gap and allows the *exo*-protonation. While we are hesitant to assign the identity of the transition state due to the inherent difficulties therein,<sup>285-286</sup> this geometry explains a nonlinear transition state and a corresponding smaller KIE.

#### 4.5 DISCUSSION

Combining all of these ideas into a cohesive, tentative mechanistic proposal (Scheme 2), we believe key features include the precoordination of a formic acid with the hydroxyl proton (Scheme 2A). Upon excitation from the ground state photocatalyst (G) an excited triplet state photocatalyst (H) intercepts a *cis*-cyclohexene substrate, which is in the proper conjugated conformer with an accessible triplet state energy (F). The triplet state photocatalyst and the singlet ground state substrate undergo Dexter energy transfer to produce the excited triplet state *cis*-cyclohexene biradical (I) and regenerate the ground state singlet photocatalyst (G). The excited triplet state substrate biradical (I) is then no longer bonding and undergoes rotation about the remaining C–C  $\sigma$  bond so that the singly occupied orbitals rotate orthogonal to each other (structures in Scheme 2B). The substrate biradical is then close in both geometry and energy to the thermal transition state for rotation, and undergoes an intersystem crossing event. Upon crossing from the triplet back into the singlet energy landscape, it can either relax to the *cis*-cyclohexene starting material (F) or continue to rotate to the *trans*-cyclohexene *anti*-chair conformer (J), which is still coordinated with the formic acid through a hydrogen bond (C). The protonation of the alkene through an apparent *exo*-protonation of the *anti*-chair

diastereomer of the *trans*-cyclohexene likely transfers more than one hydrogen in the rate-determining step via a nonlinear transition state (Figure 4). Protonation of the alkene generates a carbenium ion, which is rapidly attacked by the alcohol oxygen to produce the oxabicyclic ether (D).

**Scheme 36:** Presumptive Mechanism, Kinetics and Deuterium incorporation



#### 4.6 CONCLUSIONS

In conclusion, we have exploited the ability to dynamically capture energy from visible light, and we have developed a strategy to exploit this energy to synthesize new organic molecules. We have highlighted some of the intricacies that should be considered when thinking about energy transfer photocatalysis, such as appropriate choice of photocatalyst not only energetically, but also geometrically, and in addition have highlighted the importance of the accessibility of the triplet state as a function of conformer conjugation. A key hydrogen bonded precoordination event makes possible the singular reactivity, and results in a product that is not otherwise accessible. Its short lifetime is a general and persistent issue that for many years has resulted in *trans*-cyclohexene's recalcitrance with regard to synthesis. We have demonstrated how precoordination with the reactive partner (an acid) can be used to overcome this



obstinacy without resorting to the use of UV light, and provided a methodology that will hopefully make synthesis involving *trans*-cyclohexene more tractable.

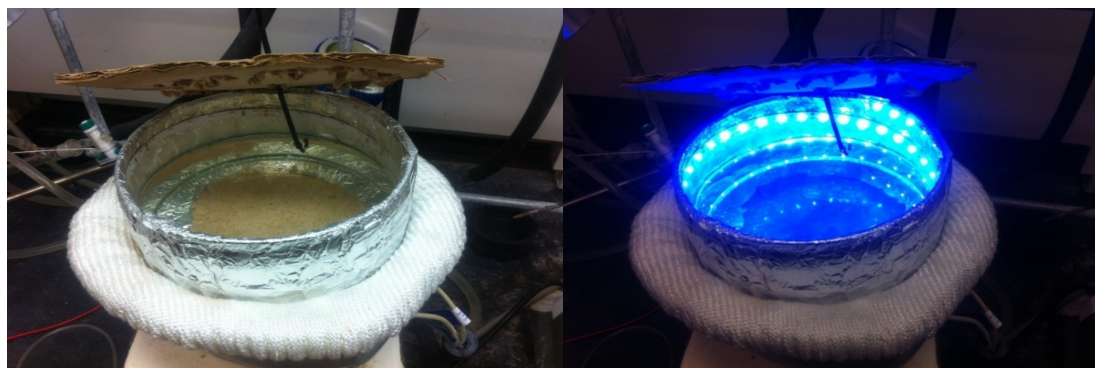
#### 4.7 ACKNOWLEDGMENT

Special thanks to Sonal Priya for help in editing this manuscript.

#### 4.8 General Experimental:

All reagents were obtained from commercial suppliers (Aldrich, Oakwood chemicals, VWR) and used without further purification unless otherwise noted. Acetonitrile (CH<sub>3</sub>CN) was dried using molecular sieves. PC1 was synthesized by using our previous method<sup>288</sup>. Reactions were monitored by thin layer chromatography (TLC), obtained from sorbent technology Silica XHL TLC Plates, w/UV254, glass backed, 250 μm, 20 x 20 cm, and were visualized with ultraviolet light, potassium permanganate stain and GC-MS (QP 2010S, Shimadzu equipped with auto sampler).

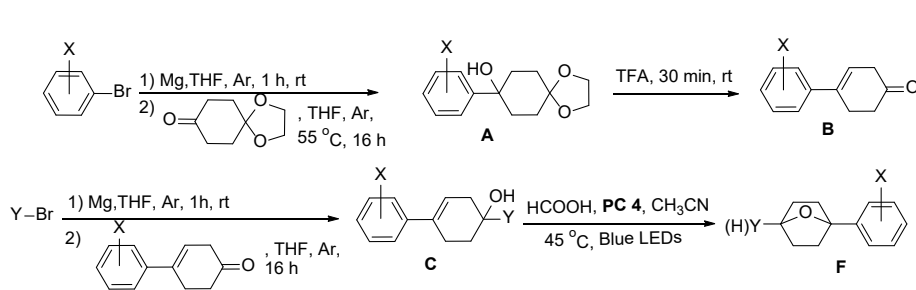
Photocatalytic reactions were set up in a light bath which is depicted below. Strips of blue LEDs, (18 LEDs/ft) were purchased from Solid Apollo and were wrapped around on



the walls of glass crystallization dish and secured with masking tape and then wrapped with aluminum foil. A lid which rest on the top was fashioned from cardboard and holes were made such that reaction tubes (12 X 75 mm cultural borosilicate tube) were held firmly in the cardboard lid which was placed on the top of bath. Water was added to the bath such that the tubes were submerged in the water which was maintained at 45 °C with the aid of a sand bath connected to a thermostat.

NMR spectra were obtained on 400 MHz Bruker Advance III spectrometer. <sup>1</sup>H and <sup>13</sup>C NMR chemical shifts are reported in ppm relative to the residual protio solvent peak (<sup>1</sup>H, <sup>13</sup>C). IR spectra were recorded on Perkin Elmer 2000 FT-IR. Melting points were determined on Stuart SMP10 melting point apparatus and reported uncorrected.

#### 4.9 Synthesis of substrates



**General Procedure A1 for the synthesis of A.<sup>2</sup>**  
 To an oven dried round bottom flash equipped with magnetic stir

bar was added magnesium metal (56.1 mmol, 2.5 equiv), a pinch of I<sub>2</sub>, THF (0.5 M) then 1-bromo-4-methoxybenzene (44.9 mmol, 2.0 equiv) was added portion-wise. The mixture was stirred at room temperature for 1 hour. After the complete consumption of 1-bromo-4-methoxybenzene, the reaction mixture was cooled to 0 °C, and 1,4 cyclohexanedione monoethylene acetal (22.5 mmol, 1 equiv) in THF was added drop-wise to the reaction mixture. The reaction mixture was heated at 55 °C until completion in between 16-24 h. After completion, the reaction mixture was quenched by saturated NH<sub>4</sub>Cl (50 mL) and extracted with EtOAc (3 x 50 mL). The combined organic layers were washed with 0.1M NaOH (40 mL). The organic layer was separated, dried over MgSO<sub>4</sub>, and concentrated to obtain the crude product that was purified by normal phase chromatography. Normal phase chromatography was performed with Teledyne ISCO automated chromatography system using Hexane: Ethyl acetate (80:20) over 0-70 column volumes using flow rate from 35-80 mL/min on Rediseq column with product detection at 254 and 288 nm.

Table 1: Summary of various substrates A with their yields.

S.No.	X	% yield (over two steps)
1a-h	4-Methoxy	46
1i	Hydrogen	41
1j	4-Fluorine	33
1k	4-Chlorine	40
1l	4-Trifluoromethyl	30
1m,n	3-Methoxy	84

**General Procedure B1 for the synthesis of B.<sup>2</sup>**

To an oven dried round bottom flash equipped with magnetic stir bar was added A (1 equiv) and TFA (1 M). The mixture was stirred at room temperature for 30 min. After the completion, the mixture was neutralized by the addition of saturated NaHCO<sub>3</sub>, and extracted with CH<sub>2</sub>Cl<sub>2</sub> (2 x 30 mL). The combined organic layers were washed with distilled water (10 mL). The organic layer was separated, dried over MgSO<sub>4</sub>, and concentrated to obtain the crude product that was purified by normal phase chromatography. Normal phase chromatography was performed with Teledyne ISCO automated chromatography system using Hexane: Ethyl acetate (80:20) over 0-70 volume columns using flow rated from 35-80 mL/min on Rediseq column of 40-80 g with product detection at 254 and 288 nm.

Table 2: Summary of various substrates B with their yields.

S.No	X	% yield
1a-h	Methoxy	62

1i	Hydrogen	92
1j	Fluorine	45
1k	Chlorine	96
1l	Trifluoromethyl	35
1m,n	3-Methoxy	90

General procedure A was followed to synthesize C.

Table 3: Summary of various substrates C with their yields.

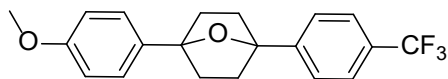
S.No	X	Y	% yield (over two steps)
1a	4-Methoxy	4-Trifluoromethylbenzene	12
1c	4-Methoxy	4-Chlorobenzene	13
1d	4-Methoxy	4-Fluorobenzene	35
1b	4-Methoxy	Pentafluorobenzene	5
1e	4-Methoxy	4-Methylbenzene	35
1f	4-Methoxy	Phenyl	42
1g	4-Methoxy	Ethyne	45
1h	4-Methoxy	Ethyl	25
1i	Hydrogen	4-Trifluoromethylbenzene	42
1k	4-Chlorine	4-Trifluoromethylbenzene	18
1j	4-Fluorine	4-Trifluoromethylbenzene	14
1l	4-Trifluoromethylbenzene	4-Trifluoromethylbenzene	4
1m	3-Methoxy	Phenyl	35
1n	3-Methoxy	4-Trifluoromethylbenzene	48

General procedure F (Photocatalytic reactions and characterization)

A 20 mL disposable scintillation vial was charged with compound cyclohexene substrate (1.0 equiv), catalyst PC4 (0.3 mol%) in MeCN. The mixture was divided in equal amount into NMR tubes. The sealed glass capillary containing C<sub>6</sub>D<sub>6</sub> was put into each NMR tube to aid in the locking process. The NMR tubes were capped with rubber septum and the reaction mixture was degassed with argon bubbling for 10 minutes, then placed in the light bath such that the lower portion of the tube was submerged under water. The reaction was monitored periodically by <sup>1</sup>H NMR. After the complete consumption of starting material, the reaction mixture was neutralized with saturated sodium bicarbonate solution and the layers were separated. The organic layer was washed with brine, dried over MgSO<sub>4</sub> and concentrated to obtain the crude product that was purified by normal phase chromatography using silica gel as stationary phase and ethyl acetate/hexanes as mobile phase unless otherwise noted.

## 4.10 Characterization

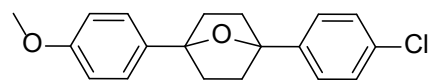
### 4.3.2a (1-(4-methoxyphenyl)-4-(4-(trifluoromethyl)phenyl)-7-oxabicyclo[2.2.1]heptane)



general procedure A was followed using 4''-methoxy-4-(trifluoromethyl)-3',6'-dihydro-[1,1':4',1''-terphenyl]-1'(2'H)-ol (100.0 mg, 0.28 mmol), catalyst PC4 (0.6 mg, 0.3 mol%), and

formic acid (580 mg, 12.6 mmol) was used to afford 1a in 79% yield (79 mg, 0.22 mmol) as a white solid. The crude material was purified by flash chromatography using hexanes: ethyl acetate with product eluting at 5%. <sup>1</sup>H NMR (400 MHz, CDCl<sub>3</sub>) δ 7.62 (s, 4H), 7.45 (d, *J* = 8.7 Hz, 2H), 6.92 (d, *J* = 8.7 Hz, 2H), 3.83 (s, 3H), 2.30 – 2.17 (m, 4H), 2.09 – 1.92 (m, 4H). <sup>13</sup>C NMR (101 MHz, CDCl<sub>3</sub>) δ 158.8, 147.1, 134.6, 129.1 (q, *J* = 32.3 Hz), 126.5, 125.5, 125.1 (q, *J* = 3.6 Hz), 124.3 (q, *J* = 271.9 Hz), 113.6, 87.4, 86.9, 55.3, 38.7, 38.6. <sup>19</sup>F NMR (376 MHz, CDCl<sub>3</sub>) δ -62.4 (s, 3F). FT-IR cm<sup>-1</sup> 2955, 1514, 1333, 1106. GC/MS (*m/z*, relative intensity) 348 (M<sup>+</sup>, 15), 160 (30), 135 (100), 77 (38). Melting point 99-101 °C.

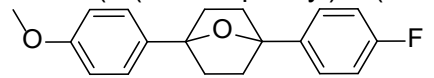
### 4.3.2c (1-(4-chlorophenyl)-4-(4-methoxyphenyl)-7-oxabicyclo[2.2.1]heptane)



The general procedure F was followed using 4-chloro-4''-methoxy-3',6'-dihydro-[1,1':4',1''-terphenyl]-1'(2'H)-ol (100.0 mg, 0.32 mmol), 5.4 mL of stock

solution of PC4 (2.0 mg, 0.0028 mmol, 20 mL CH<sub>3</sub>CN), and formic acid (98.6 mg, 2.14 mmol) was used to afford 2a in 90% yield (90 mg, 0.29 mmol) as a white solid. The crude material was purified by flash chromatography using hexanes: ethyl acetate with product eluting at 10%. <sup>1</sup>H NMR (400 MHz, CDCl<sub>3</sub>) δ 7.51 – 7.44 (m, 4H), 7.36 (d, *J* = 8.4 Hz, 2H), 6.94 (d, *J* = 8.6 Hz, 2H), 3.85 (s, 3H), 2.22 (d, *J* = 7.4 Hz, 4H), 2.11 – 1.93 (m, 4H). <sup>13</sup>C NMR (101 MHz, CDCl<sub>3</sub>) δ 158.7 141.5, 134.8, 132.7, 128.3, 126.7, 126.5, 113.6, 87.3, 86.8, 55.3, 38.7, 38.6. FT-IR cm<sup>-1</sup> 2953, 1515, 1254, 1088. GC/MS (*m/z*, relative intensity) 314 (M<sup>+</sup>, 20), 279 (10), 135 (100), 77 (45). Melting point 98-99 °C.

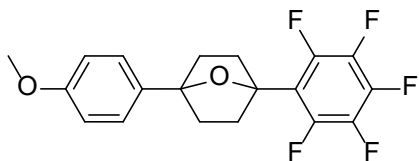
### 4.3.2d (1-(4-fluorophenyl)-4-(4-methoxyphenyl)-7-oxabicyclo[2.2.1]heptanes)



The general procedure F was followed using 4-fluoro-4''-methoxy-3',6'-dihydro-[1,1':4',1''-terphenyl]-1'(2'H)-ol (100.0 mg, 0.34 mmol, 1.0 equiv), catalyst PC4 (0.7

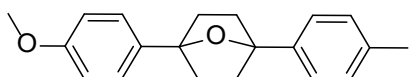
mg, 0.3 mol%), and formic acid (148.2 mg, 2.14 mmol) was used to afford 2a in 88% yield (90 mg, 0.30 mmol) as a white solid. The crude material was purified by flash chromatography using hexanes: ethyl acetate with product eluting at 5%. <sup>1</sup>H NMR (400 MHz, CDCl<sub>3</sub>) δ 7.64 – 7.42 (m, 4H), 7.16 – 7.02 (m, 2H), 7.02 – 6.87 (m, 2H), 3.84 (s, 3H), 2.41 – 2.15 (m, 4H), 2.15 – 1.86 (m, 4H). <sup>13</sup>C NMR (101 MHz CDCl<sub>3</sub>) δ 162.3 (d, *J* = 244.7 Hz), 159.1, 139.2, 135.3, 127.4 (d, *J* = 7.9 Hz), 126.9, 115.4 (d, *J* = 21.3 Hz), 114.1, 87.6, 87.3, 55.7, 39.2, 39.1. <sup>19</sup>F NMR (376 MHz, CDCl<sub>3</sub>) δ -115.87 (m, 1F)(FT-IR cm<sup>-1</sup> 2952, 1511, 1247, 1172. GC/MS (*m/z*, relative intensity) 298 (M<sup>+</sup>, 100), 270 (30), 135 (100), 77 (50). Melting point 99-100 °C.

### 4.3.2b (1-(4-methoxyphenyl)-4-(perfluorophenyl)-7-oxabicyclo[2.2.1]heptanes)



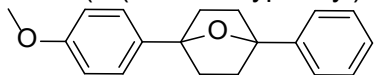
The general procedure F was followed using 2,3,4,5,6-pentafluoro-4''-methoxy-3',6'-dihydro-[1,1':4',1''-terphenyl]-1'(2'H)-ol (60.0 mg, 0.16 mmol, 1.0 equiv), catalyst PC4 (0.3 mg, 0.3 mol%), and formic acid (171.4 mg, 3.73 mmol) was used to afford 4a in 75% yield (45 mg, 0.12 mmol) as a white solid. The crude material was purified by flash chromatography using hexanes: ethyl acetate with product eluting at 5%. <sup>1</sup>H NMR (400 MHz, CDCl<sub>3</sub>) δ 7.42 (d, *J* = 8.8 Hz, 2H), 6.91 (d, *J* = 8.7 Hz, 2H), 3.86 – 3.78 (m, 3H), 2.37 (dq, *J* = 11.2, 5.0, 3.3, 2.4 Hz, 2H), 2.24 – 2.07 (m, 4H), 2.04 – 1.92 (m, 2H). <sup>13</sup>C NMR (101 MHz, CDCl<sub>3</sub>) δ 158.8, 144.7 (d, *J* = 255.9 Hz), 140.2 (d, *J* = 233.5 Hz), 137.7 (d, *J* = 231.8 Hz), 134.1, 126.4, 116.1 – 115.5 (m), 113.7, 87.1, 83.8, 55.3, 38.0 (t, *J* = 2.8 Hz), 37.6. <sup>19</sup>F NMR (376 MHz, CDCl<sub>3</sub>) δ -138.30 (dd, *J* = 22.5, 7.2 Hz, 2F), -156.24 (tt, *J* = 21.3, 4.2 Hz, 1F), -162.31 – -162.63 (m, 2F). FT-IR cm<sup>-1</sup> 2920, 1488, 1248, 1179. GC/MS (*m/z*, relative intensity) 370 (M<sup>+</sup>, 20), 342 (80), 135 (50), 77 (20). Melting point 133-134 °C.

#### 4.3.2e (1-(4-methoxyphenyl)-4-(p-tolyl)-7-oxabicyclo[2.2.1]heptane)



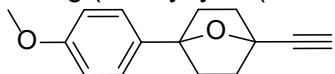
The general procedure F was followed using 4''-methoxy-4-methyl-3',6'-dihydro-[1,1':4',1''-terphenyl]-1'(2'H)-ol (100.0 mg, 0.34 mmol, 1.0 equiv), catalyst PC4 (0.7 mg, 0.3 mol%), CH<sub>3</sub>CN (7.1 mL), and formic acid (243.9 mg, 5.3 mmol) was used to afford 5a in 84% yield (84 mg, 0.29 mmol) as a white solid. The crude material was purified by flash chromatography using hexanes: ethyl acetate with product eluting at 5%. <sup>1</sup>H NMR (400 MHz, CDCl<sub>3</sub>) δ 7.50 – 7.43 (m, 2H), 7.43 – 7.38 (m, 2H), 7.18 (d, *J* = 7.9 Hz, 2H), 6.96 – 6.87 (m, 2H), 3.82 (s, 3H), 2.35 (s, 3H), 2.19 (d, *J* = 8.3 Hz, 4H), 2.00 (d, *J* = 6.7 Hz, 4H). <sup>13</sup>C NMR (101 MHz, CDCl<sub>3</sub>) δ 158.7, 140.0, 136.6, 135.2, 128.9, 126.58, 125.2, 113.6, 87.2, 87.1, 55.3, 38.8, 38.7, 21.2. FT-IR cm<sup>-1</sup> 2956, 1514, 1247, 1174. GC/MS (*m/z*, relative intensity) 294 (M<sup>+</sup>, 30), 150 (40), 135(100), 91 (45). Melting point 101-102 °C.

#### 4.3.2f (1-(4-methoxyphenyl)-4-phenyl-7-oxabicyclo[2.2.1]heptane)



The general procedure F was followed using 4''-methoxy-3',6'-dihydro-[1,1':4',1''-terphenyl]-1'(2'H)-ol (100.0 mg, 0.36 mmol, 1.0 equiv), catalyst PC4 (0.8 mg, 0.3 mol%), CH<sub>3</sub>CN (7.5 mL), and formic acid (135.5 mg, 2.944 mmol) was used to afford 6a in 89% yield (89 mg, 0.32 mmol) as a white solid. The crude material was purified by flash chromatography using hexanes: ethyl acetate with product eluting at 10%. <sup>1</sup>H NMR (400 MHz, CDCl<sub>3</sub>) δ 7.63 – 7.50 (m, 2H), 7.50 – 7.43 (m, 2H), 7.37 (d, *J* = 7.6 Hz, 2H), 7.33 – 7.27 (m, 1H), 7.03 – 6.85 (m, 2H), 3.82 (s, 3H), 2.32 – 2.12 (m, 4H), 2.12 – 1.92 (m, 4H). <sup>13</sup>C NMR (101 MHz, CDCl<sub>3</sub>) δ 158.7, 143.1, 135.1, 128.3, 127.0, 126.6, 125.3, 113.7, 87.3, 87.13, 55.3, 38.8, 38.7. FT-IR cm<sup>-1</sup> 2950, 1515, 1248, 1174. GC/MS (*m/z*, relative intensity) 280 (M<sup>+</sup>, 20), 150 (40), 135 (100), 77 (100). Melting point 58-60 °C.

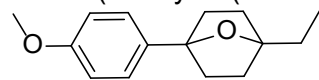
#### 4.3.2g (1-ethynyl-4-(4-methoxyphenyl)-7-oxabicyclo[2.2.1]heptane)



The general procedure F was followed using 4''-methoxy-3',6'-dihydro-[1,1':4',1''-terphenyl]-1'(2'H)-ol (100.0 mg, 0.44 mmol, 1.0 equiv), catalyst PC4 (0.9 mg, 0.3 mol%), and formic acid (907 mg, 19.7 mmol) was used to afford 7a in 86% yield (86 mg, 0.38 mmol)

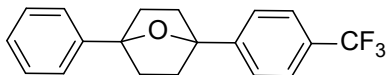
as a white solid. The crude material was purified by flash chromatography using hexanes: ethyl acetate with product eluting at 5%. <sup>1</sup>H NMR (400 MHz, CDCl<sub>3</sub>) δ 7.36 (d, *J* = 8.8 Hz, 2H), 6.87 (d, *J* = 8.8 Hz, 2H), 3.80 (s, 3H), 2.64 (s, 1H), 2.20 – 2.11 (m, 2H), 2.11 – 2.01 (m, 4H), 2.00 – 1.87 (m, 2H). <sup>13</sup>C NMR (101 MHz, CDCl<sub>3</sub>) δ 158.8, 133.8, 126.5, 113.6, 87.7, 82.7, 77.2, 74.4, 55.3, 38.5, 37.8. FT-IR cm<sup>-1</sup> 3238, 2922, 1513, 1255. GC/MS (m/z, relative intensity) 228 (M<sup>+</sup>, 15), 135 (100), 77 (70), 39 (65). Melting point 130-131 °C

#### 4.3.2h (1-ethyl-4-(4-methoxyphenyl)-7-oxabicyclo[2.2.1]heptane)



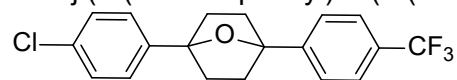
The general procedure F was followed using 4-ethyl-4'-methoxy-2,3,4,5-tetrahydro-[1,1'-biphenyl]-4-ol (90.0 mg, 0.39 mmol), catalyst 4.3.PC4 (0.8 mg, 0.3 mol%), and formic acid (561.4 mg, 12.2 mmol) was used to afford 8a in 84% yield (75.6 mg, 0.33 mmol) as a clear oil. The crude material was purified by flash chromatography using hexanes: ethyl acetate with product eluting at 5%. <sup>1</sup>H NMR (400 MHz, CDCl<sub>3</sub>) δ 7.37 (d, *J* = 8.7 Hz, 2H), 6.88 (d, *J* = 8.7 Hz, 2H), 3.80 (s, 3H), 2.10 – 2.01 (m, 2H), 1.96 – 1.82 (m, 4H), 1.82 – 1.64 (m, 4H), 1.04 (t, *J* = 7.6 Hz, 3H). <sup>13</sup>C NMR (101 MHz, CDCl<sub>3</sub>) δ 158.9, 135.8, 126.9, 113.9, 87.7, 86.9, 55.7, 38.8, 35.7, 28.9, 9.9. FT-IR cm<sup>-1</sup> 2964, 1515, 1245, 1175. GC/MS (m/z, relative intensity) 232 (M<sup>+</sup>, 20), 189 (20), 150 (30), 135 (100).

#### 4.3.2i (1-phenyl-4-(4-(trifluoromethyl)phenyl)-7-oxabicyclo[2.2.1]heptane)



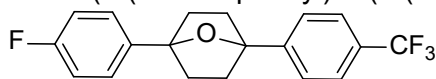
The general procedure F was followed using 4-(trifluoromethyl)-3',6'-dihydro-[1,1':4',1''-terphenyl]-1'(2'H)-ol (100.0 mg, 0.31 mmol), catalyst PC4 (0.7 mg, 0.3 mol%), and formic acid (639.7 mg, 13.9 mmol) was used to afford 9a in 85% yield (85 mg, 0.27 mmol) as a white solid. The crude material was purified by flash chromatography using hexanes: ethyl acetate with product eluting at 5%. <sup>1</sup>H NMR (400 MHz, CDCl<sub>3</sub>) δ 7.56 (s, 4H), 7.46 (d, 2H), 7.31 (t, *J* = 7.5 Hz, 2H), 7.23 (d, *J* = 7.3 Hz, 1H), 2.28 – 2.07 (m, 4H), 2.04 – 1.85 (m, 4H). <sup>13</sup>C NMR (101 MHz, CDCl<sub>3</sub>) δ 147.0, 142.5, 129.2 (q, *J* = 32.2 Hz), 128.3, 127.2, 125.5, 125.2, 125.2, 124.3 (q, *J* = 32.2 Hz), 87.6, 86.9, 38.7, 38.6. <sup>19</sup>F NMR (376 MHz, CDCl<sub>3</sub>) δ -62.39 (s, 3F). FT-IR cm<sup>-1</sup> 2953, 1323, 1154, 1109. GC/MS (m/z, relative intensity) 318 (M<sup>+</sup>, 20), 145 (50), 105 (100), 77 (80). Melting point 72- 74 °C.

#### 4.3.2j (1-(4-chlorophenyl)-4-(4-(trifluoromethyl)phenyl)-7-oxabicyclo[2.2.1]heptane)



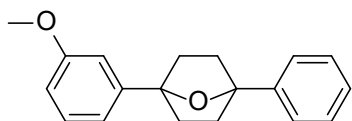
The general procedure F was followed using 4''-chloro-4-(trifluoromethyl)-3',6'-dihydro-[1,1':4',1''-terphenyl]-1'(2'H)-ol (100.0 mg, 0.28 mmol), catalyst PC4 (0.6 mg, 0.3 mol%), CH<sub>3</sub>CN (5.9 mL) and formic acid (588.1 mg, 12.78 mmol) was used to afford 10a in 57% yield (57 mg, 0.16 mmol) as a white solid. The crude material was purified by flash chromatography using hexanes: ethyl acetate with product eluting at 5%. <sup>1</sup>H NMR (400 MHz, CDCl<sub>3</sub>) δ 7.63 (s, 4H), 7.50 – 7.43 (m, 2H), 7.39 – 7.33 (m, 2H), 2.33 – 2.16 (m, 4H), 2.05 – 1.94 (m, 4H). <sup>13</sup>C NMR (101 MHz, CDCl<sub>3</sub>) δ 146.7 (d, *J* = 1.5 Hz), 141.1, 132.9, 129.3 (q, *J* = 32.4 Hz), 128.4, 126.6, 125.5, 125.2 (q, *J* = 3.8 Hz), 124.2 (q, *J* = 271.9 Hz), 87.1, 87.1, 38.6, 38.8. <sup>19</sup>F NMR (376 MHz, CDCl<sub>3</sub>) δ -62.40 (s, 3F). FT-IR cm<sup>-1</sup> 2922, 1321, 1124, 1067. GC/MS (m/z, relative intensity) 352 (M<sup>+</sup>, 20), 173 (30), 139 (100), 115 (60). Melting point 102-104 °C.

4.3.2k (1-(4-fluorophenyl)-4-(4-(trifluoromethyl)phenyl)-7-oxabicyclo[2.2.1]heptane)



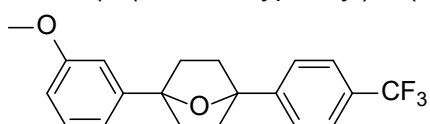
The general procedure F was followed using 4''-fluoro-4-(trifluoromethyl)-3',6'-dihydro-[1,1':4',1''-terphenyl]-1'(2'H)-ol (100.0 mg, 0.30 mmol), catalyst PC4 (0.6 mg, 0.3 mol%), and formic acid (616.2 mg, 13.39 mmol) was used to afford 11a in 85% yield (85 mg, 0.25 mmol) as a white solid. The crude material was purified by flash chromatography using hexanes: ethyl acetate with product eluting at 5%. <sup>1</sup>H NMR (400 MHz, CDCl<sub>3</sub>) δ 7.54 (s, 4H), 7.37 (d, *J* = 8.0 Hz, 2H), 7.26 (d, *J* = 8.2 Hz, 2H), 2.28 – 2.06 (m, 4H), 1.90 (d, *J* = 7.5 Hz, 4H). <sup>13</sup>C NMR (101 MHz, CDCl<sub>3</sub>) δ 161.8 (d, *J* = 245.2 Hz), 146.6, 138.1 (d, *J* = 3.1 Hz), 129.1 (q, *J* = 32.3 Hz), 126.7 (d, *J* = 8.0 Hz), 125.3, 125.0 (q, *J* = 3.7 Hz), 124.1 (q, *J* = 271.9 Hz), 114.9 (d, *J* = 21.3 Hz), 87.0, 86.9, 38.5, 38.5. <sup>19</sup>F NMR (376 MHz, CDCl<sub>3</sub>) δ -62.38 (s, 3F), -115.50 – -115.66 (m, 1F). FT-IR cm<sup>-1</sup> 2949, 1510, 1324, 1119 GC/MS (*m/z*, relative intensity) 336 (M<sup>+</sup>, 20) 173 (20), 123 (100), 95 (50). Melting point 65-68 °C.

4.3.2m (1-(3-methoxyphenyl)-4-phenyl-7-oxabicyclo[2.2.1]heptane)



The general procedure F was followed using 3''-methoxy-3',6'-dihydro-[1,1':4',1''-terphenyl]-1'(2'H)-ol (50.0 mg, 0.18 mmol), catalyst PC4 (0.4 mg, 0.3 mol%), and formic acid (152.3 mg, 3.31 mmol) was used to afford 12a in 72% yield (36.4 mg, 0.13 mmol) as a colorless oil. The crude material was purified by flash chromatography using hexanes: ethyl acetate with product eluting at 5%. <sup>1</sup>H NMR (400 MHz, CDCl<sub>3</sub>) δ 7.55 (d, *J* = 7.8 Hz, 2H), 7.40 (t, *J* = 7.5 Hz, 2H), 7.35 – 7.27 (m, 2H), 7.21 – 7.04 (m, 2H), 6.85 (dd, *J* = 8.2, 2.5 Hz, 1H), 3.86 (s, 3H), 2.24 (d, *J* = 6.7 Hz, 4H), 2.03 (d, *J* = 5.8 Hz, 4H). <sup>13</sup>C NMR (101 MHz, CDCl<sub>3</sub>) δ 159.6, 144.7, 143.0, 129.4, 128.3, 127.1, 125.3, 117.7, 112.5, 111.0, 87.45, 87.38, 55.4, 38.80, 38.75.

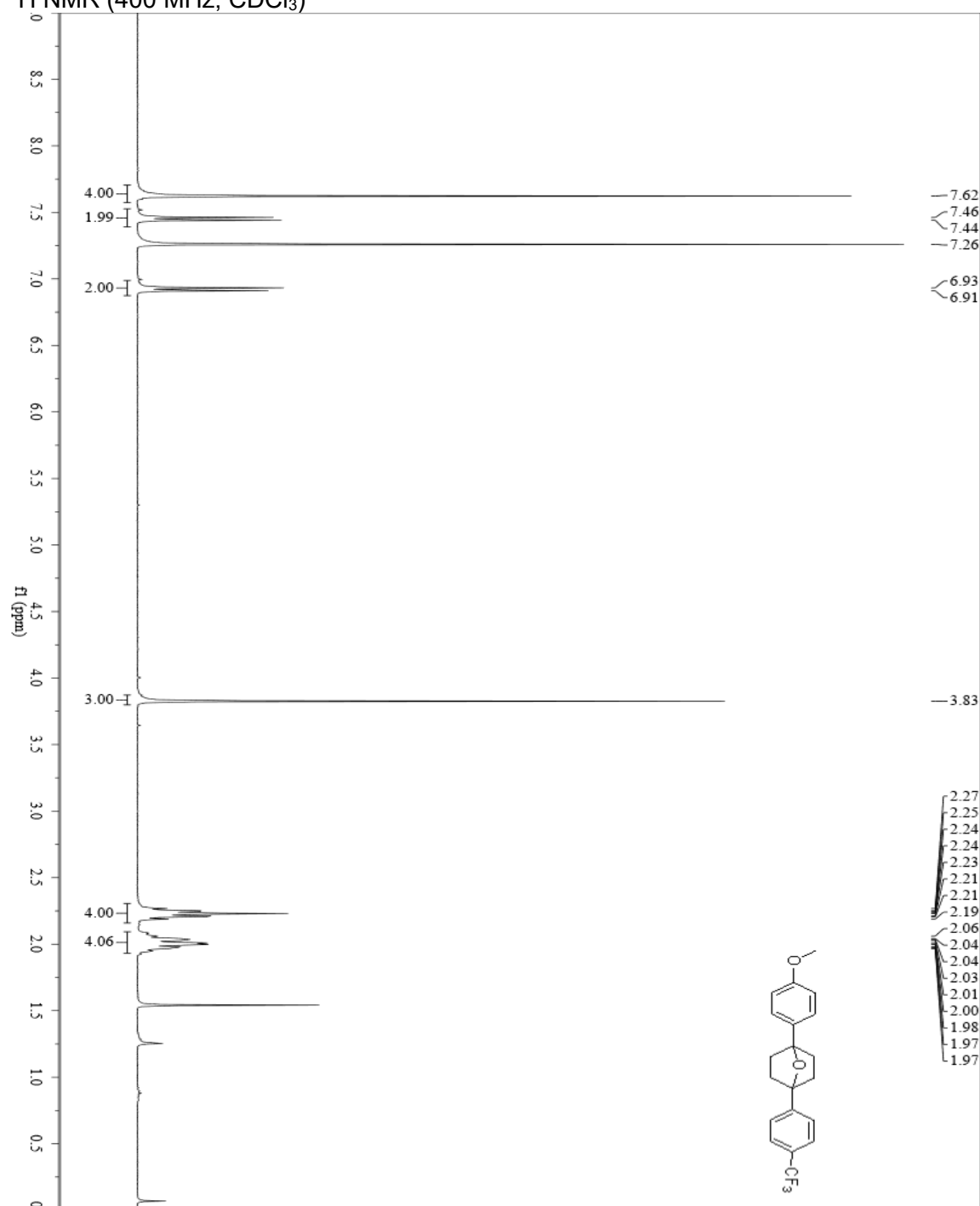
4.3.2n (1-(3-methoxyphenyl)-4-(4-(trifluoromethyl)phenyl)-7-oxabicyclo[2.2.1]heptane)



The general procedure F was followed using 3''-methoxy-4-(trifluoromethyl)-3',6'-dihydro-[1,1':4',1''-terphenyl]-1'(2'H)-ol (90.0 mg, 0.26 mmol), catalyst PC4 (0.4 mg, 0.3 mol%), and formic acid (239.3 mg, 5.20 mmol) was used to afford 13a in 78% yield (70.0 mg, 0.20 mmol) as a white solid. The crude material was purified by flash chromatography using hexanes: ethyl acetate with product eluting at 8%. <sup>1</sup>H NMR (400 MHz, CDCl<sub>3</sub>) δ 7.65 (s, 4H), 7.32 (t, *J* = 7.9 Hz, 1H), 7.19 – 7.07 (m, 2H), 6.93 – 6.81 (m, 1H), 3.86 (s, 3H), 2.33 – 2.19 (m, 4H), 2.12 – 1.92 (m, 4H). <sup>13</sup>C NMR (101 MHz, CDCl<sub>3</sub>) δ 159.7, 147.1, 144.3, 129.5 (2C), 129.4 (q, *J* = 120.0 Hz), 125.6 (2C), 125.3 (q, *J* = 3.8 Hz), 117.7, 112.5, 111.1, 87.7, 87.0, 55.4, 38.7 (4C). <sup>19</sup>F NMR (376 MHz, CDCl<sub>3</sub>) δ -62.37 (s, 3F).

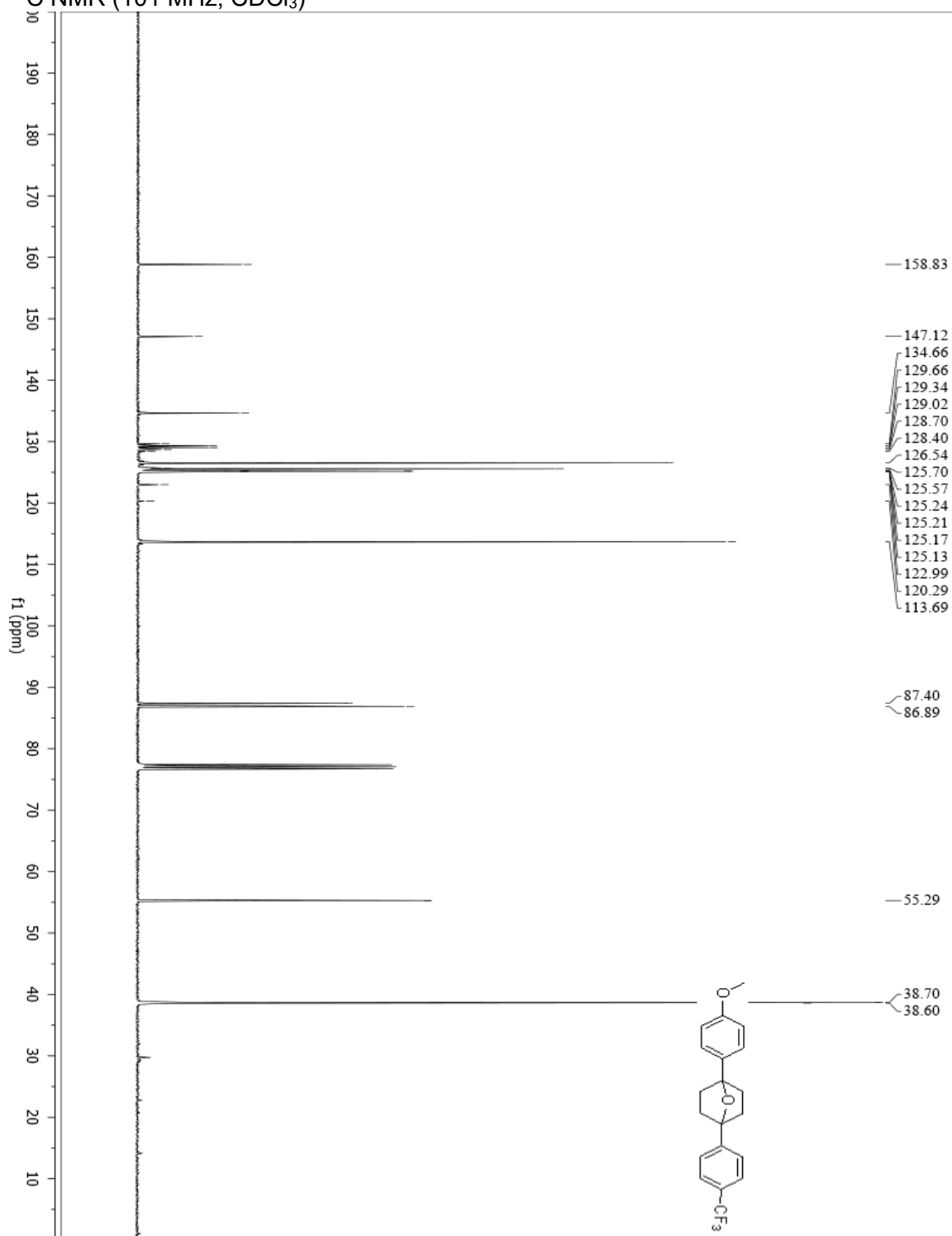
## 4.11 Spectra

### 4.3.1a (1-(4-methoxyphenyl)-4-(4-(trifluoromethyl)phenyl)-7-oxabicyclo[2.2.1]heptane) <sup>1</sup>H NMR (400 MHz, CDCl<sub>3</sub>)

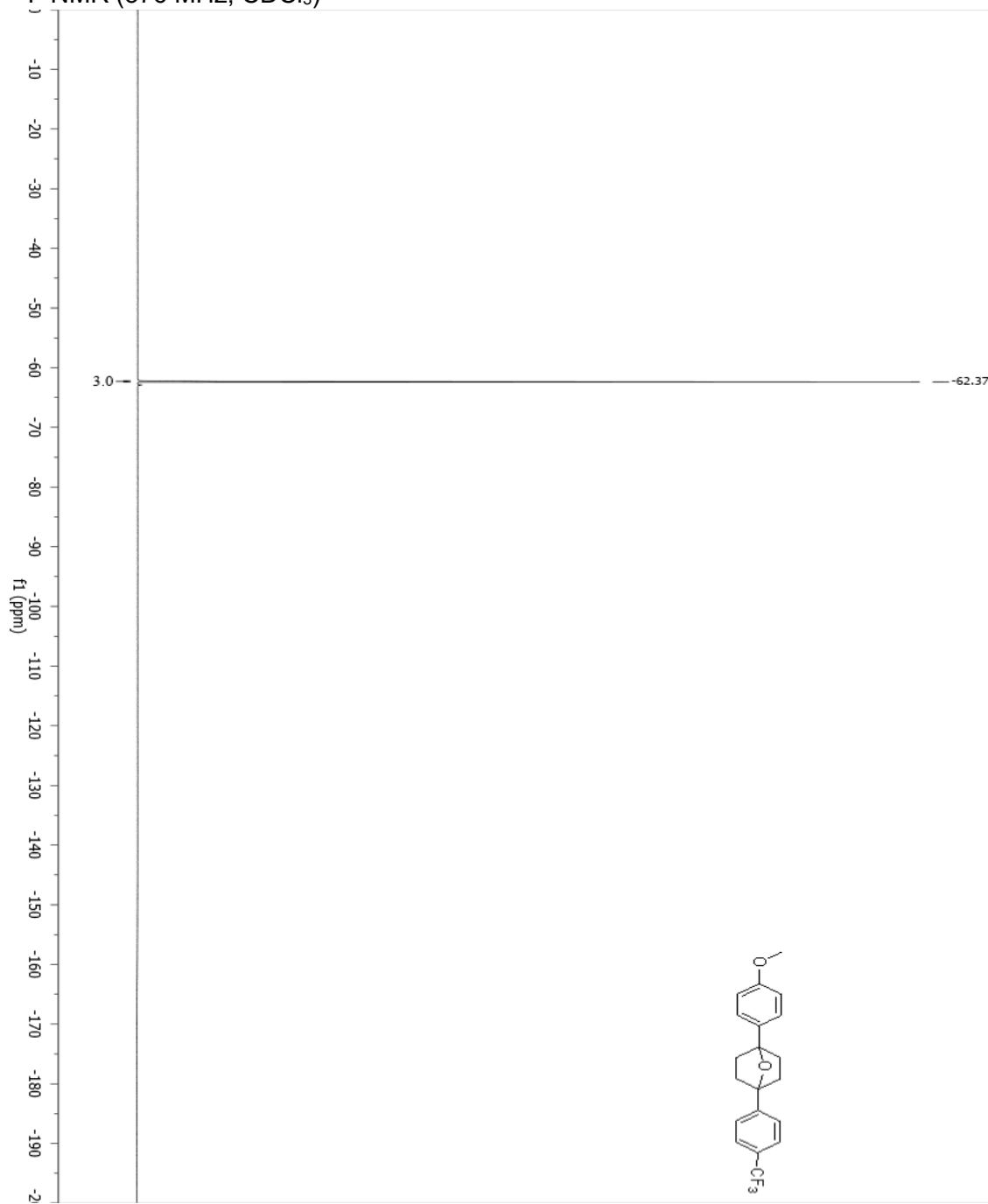




4.3.1a (1-(4-methoxyphenyl)-4-(4-(trifluoromethyl)phenyl)-7-oxabicyclo[2.2.1]heptane)  
<sup>13</sup>C NMR (101 MHz, CDCl<sub>3</sub>)

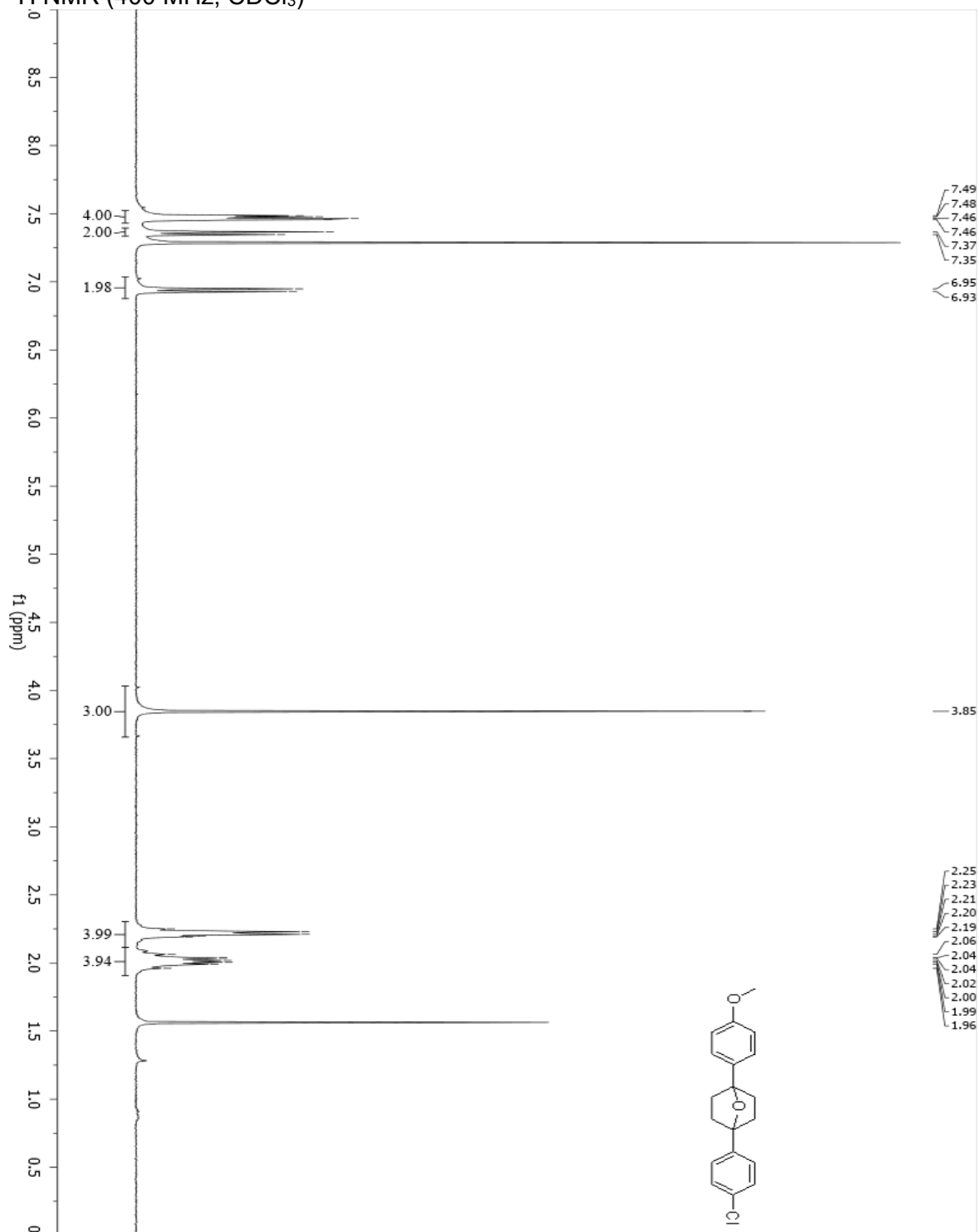


4.3.1a (1-(4-methoxyphenyl)-4-(4-(trifluoromethyl)phenyl)-7-oxabicyclo[2.2.1]heptane)  
<sup>19</sup>F NMR (376 MHz, CDCl<sub>3</sub>)

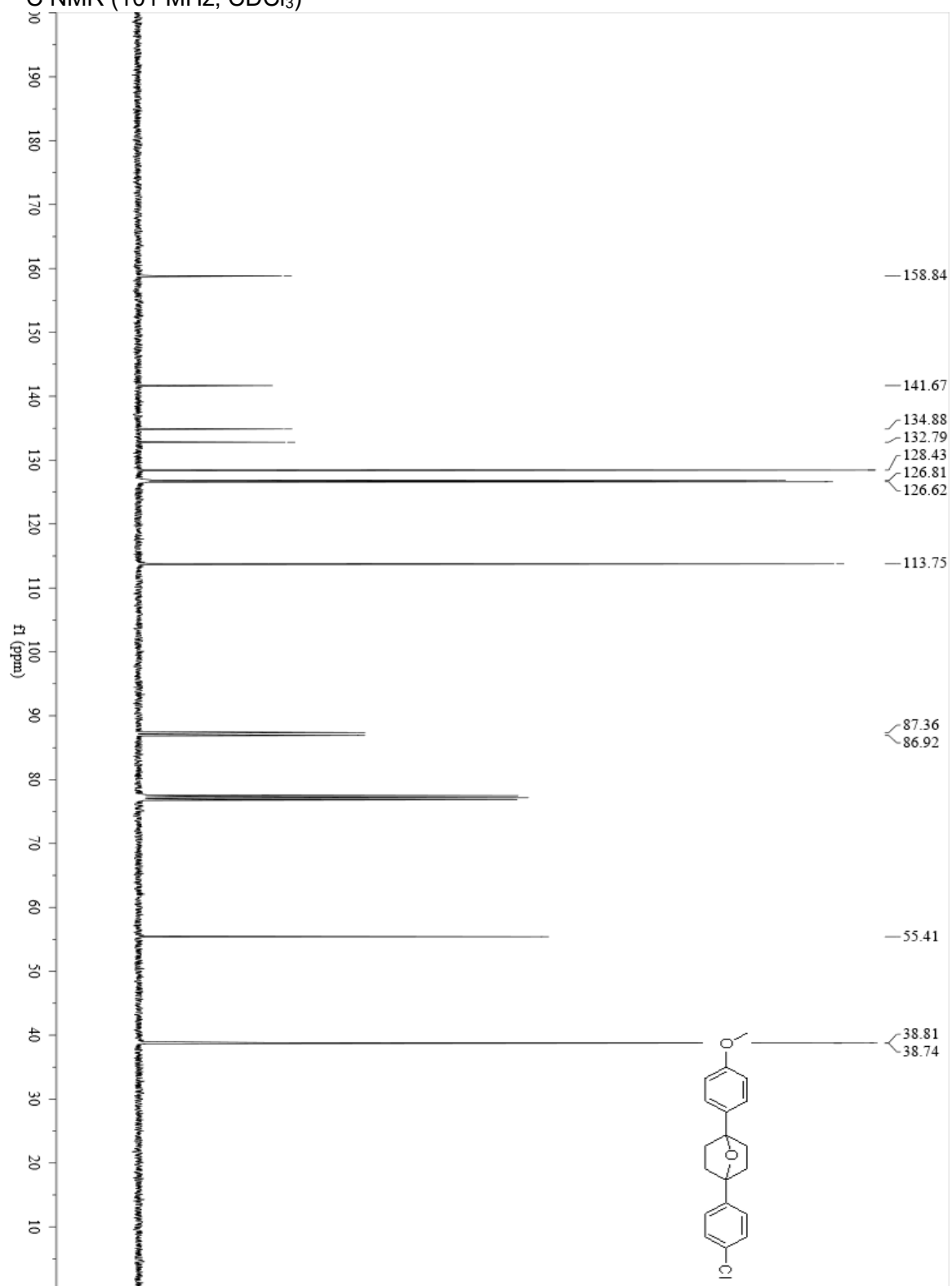


4.3.1a (1-(4-methoxyphenyl)-4-(4-(trifluoromethyl)phenyl)-7-oxabicyclo[2.2.1]heptane)  
Fluorine

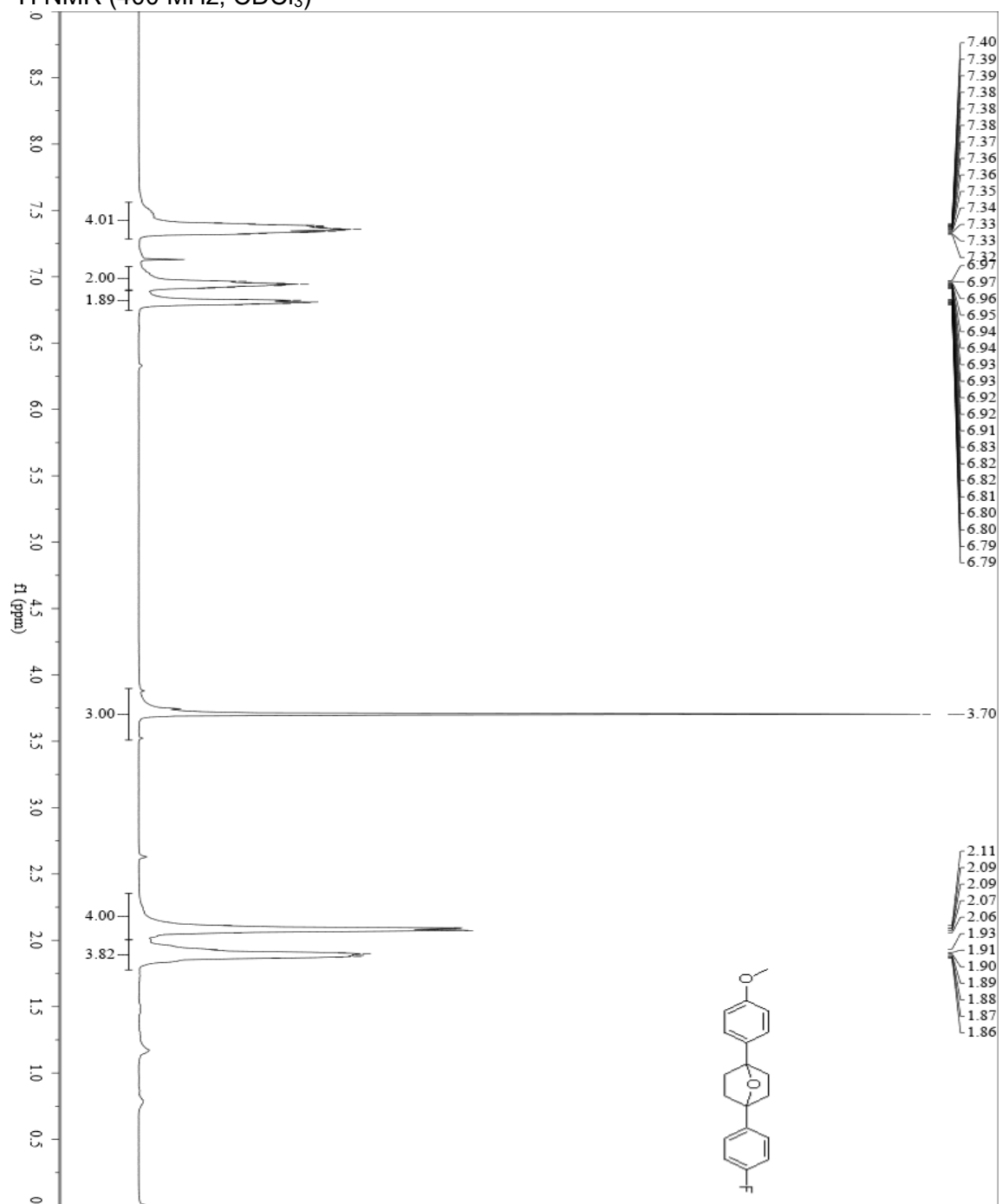
$^1\text{H}$  NMR (400 MHz,  $\text{CDCl}_3$ )



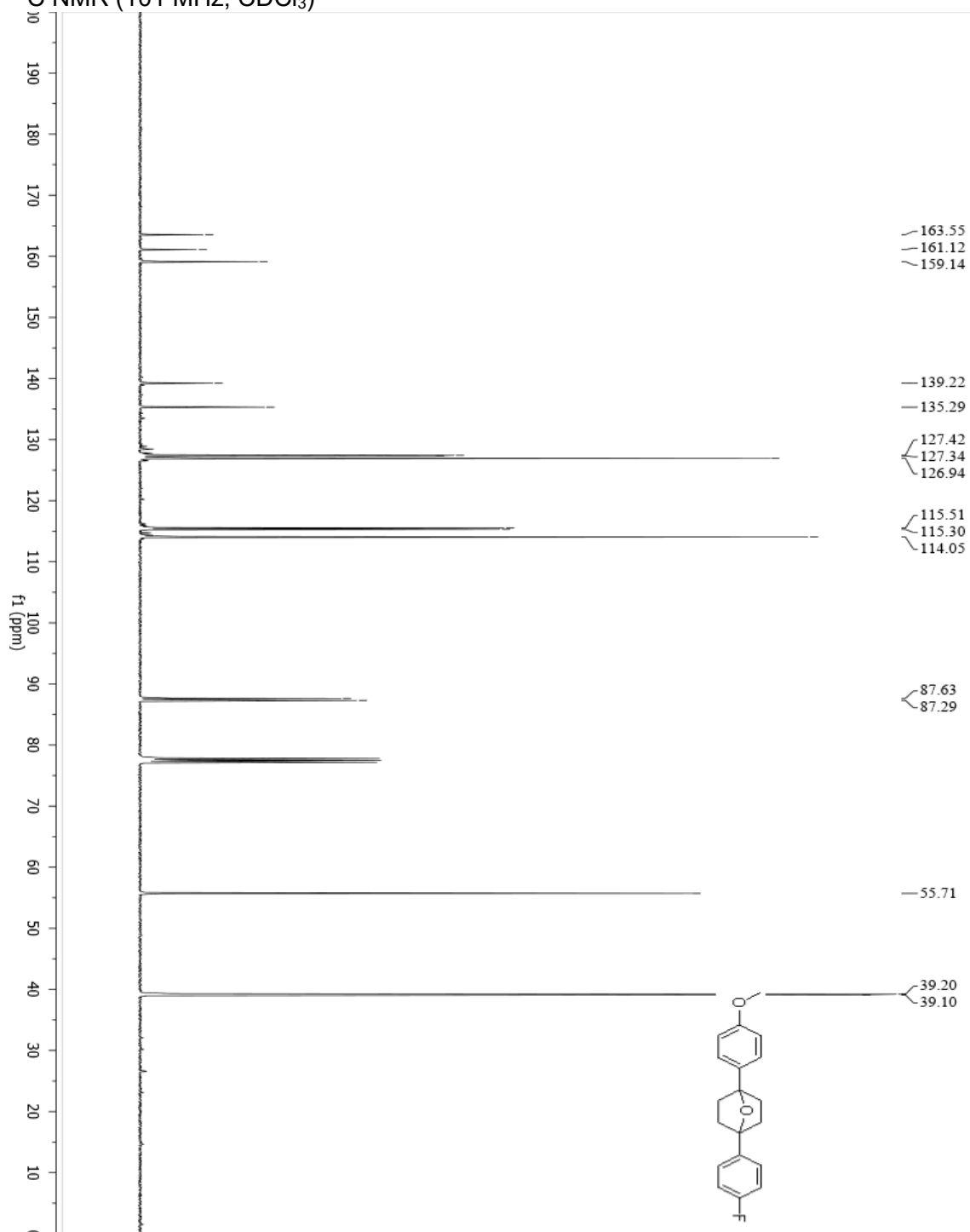
4.3.2c (1-(4-chlorophenyl)-4-(4-methoxyphenyl)-7-oxabicyclo[2.2.1]heptane)  
<sup>13</sup>C NMR (101 MHz, CDCl<sub>3</sub>)



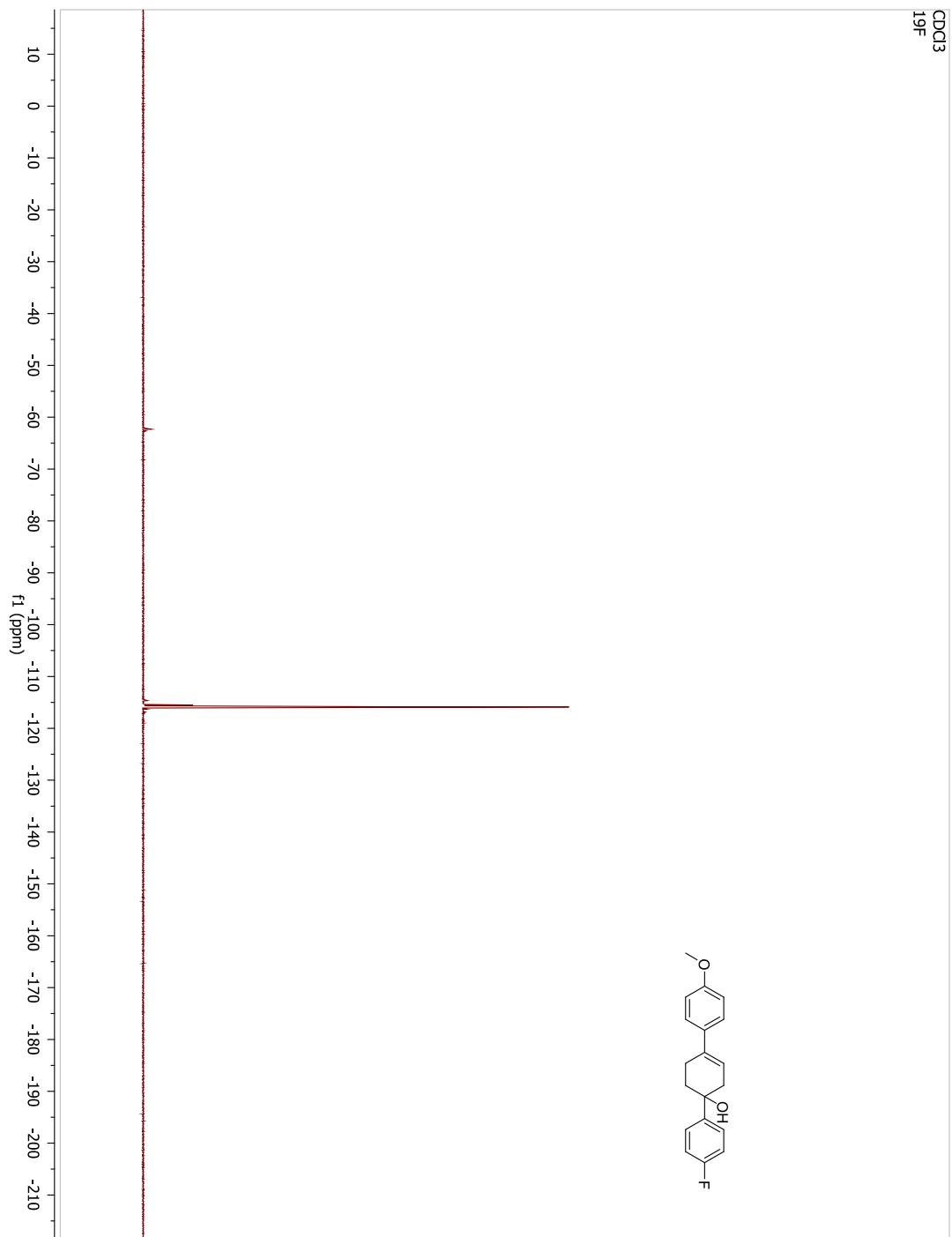
4.3.2c (1-(4-chlorophenyl)-4-(4-methoxyphenyl)-7-oxabicyclo[2.2.1]heptane)- Carbon  
<sup>1</sup>H NMR (400 MHz, CDCl<sub>3</sub>)



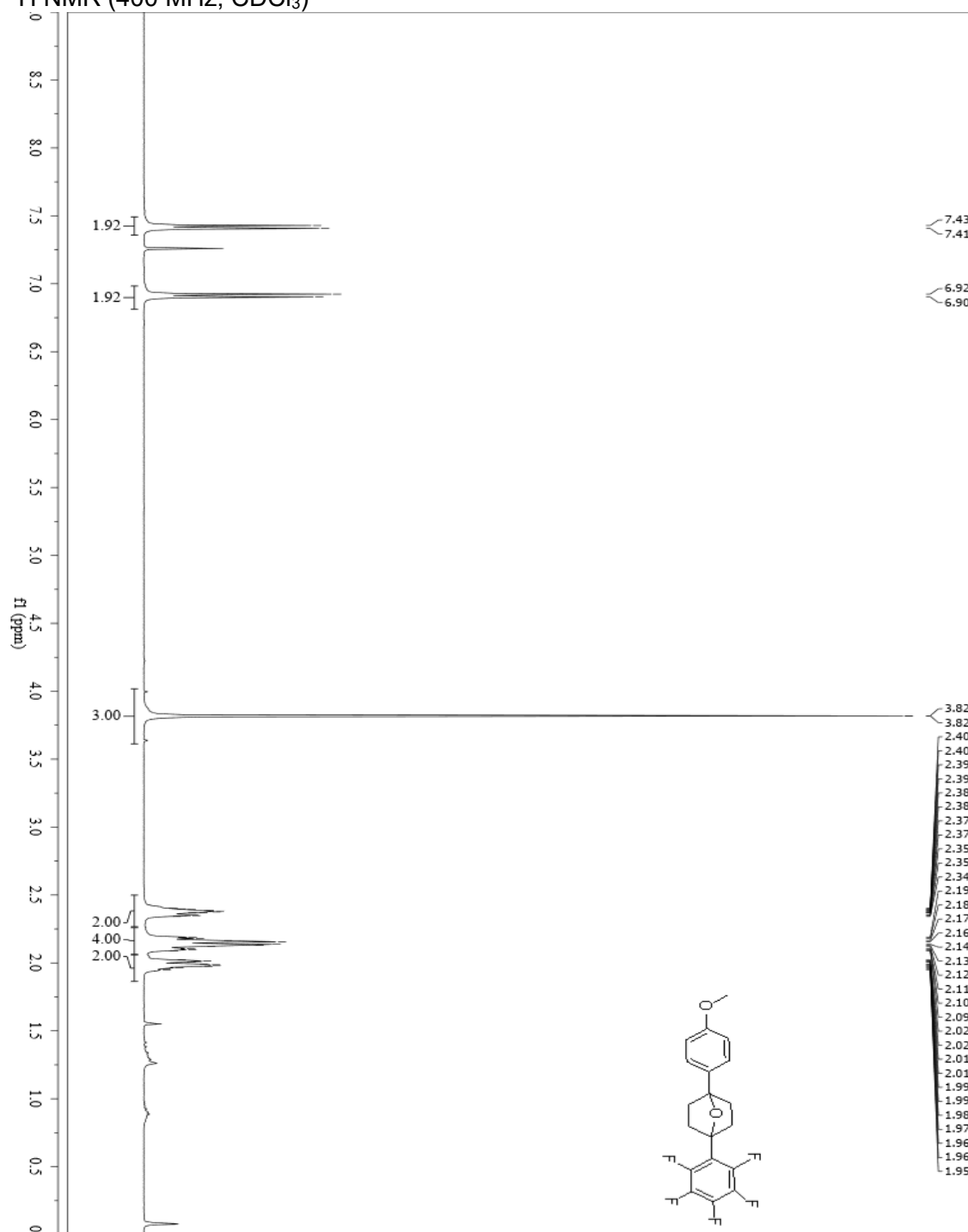
4.3.2c (1-(4-fluorophenyl)-4-(4-methoxyphenyl)-7-oxabicyclo[2.2.1]heptanes)  
<sup>13</sup>C NMR (101 MHz, CDCl<sub>3</sub>)



4.3.2c (1-(4-fluorophenyl)-4-(4-methoxyphenyl)-7-oxabicyclo[2.2.1]heptanes)  
<sup>19</sup>F NMR (376 MHz, CDCl<sub>3</sub>)

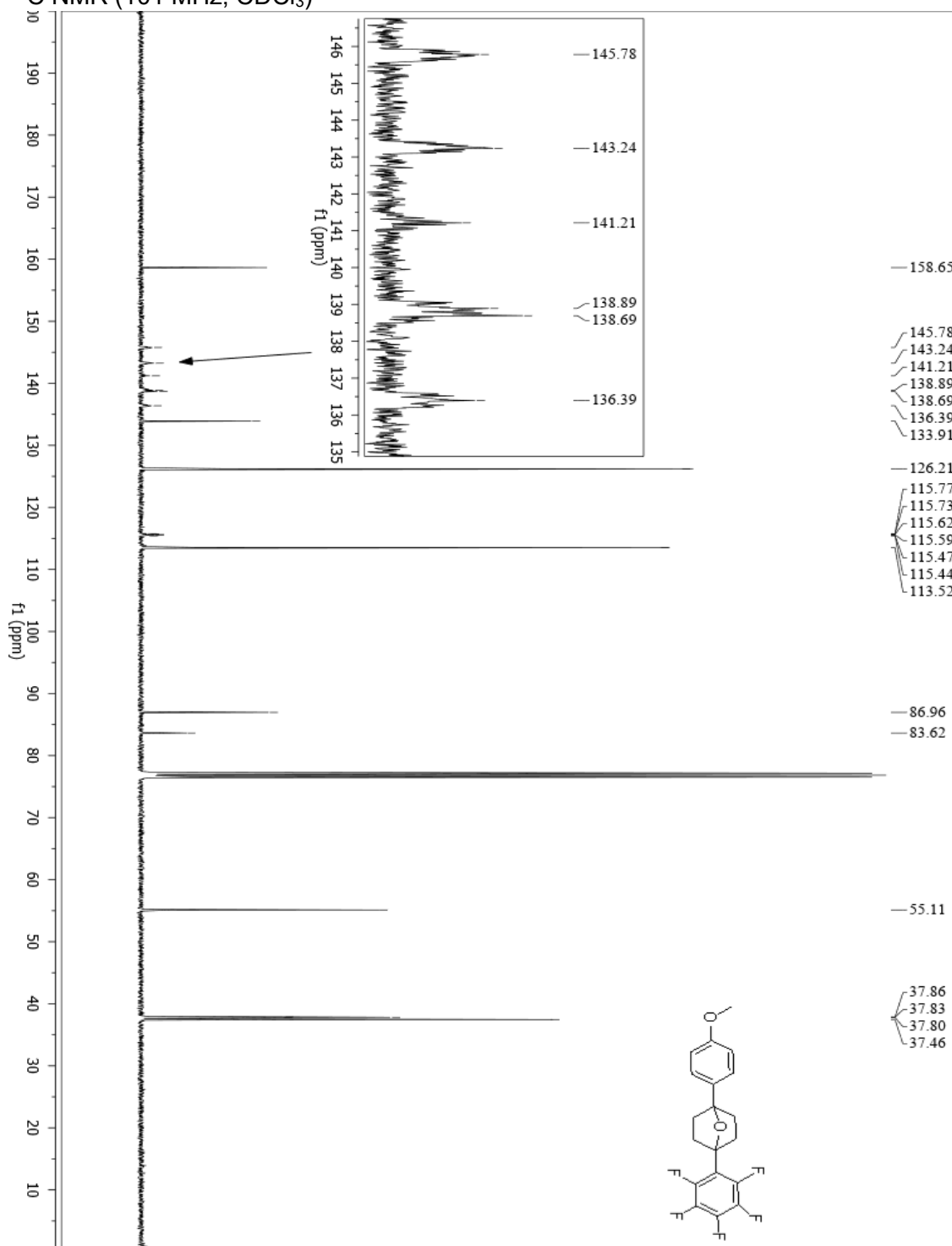


4.3.2c (1-(4-fluorophenyl)-4-(4-methoxyphenyl)-7-oxabicyclo[2.2.1]heptanes)  
<sup>1</sup>H NMR (400 MHz, CDCl<sub>3</sub>)

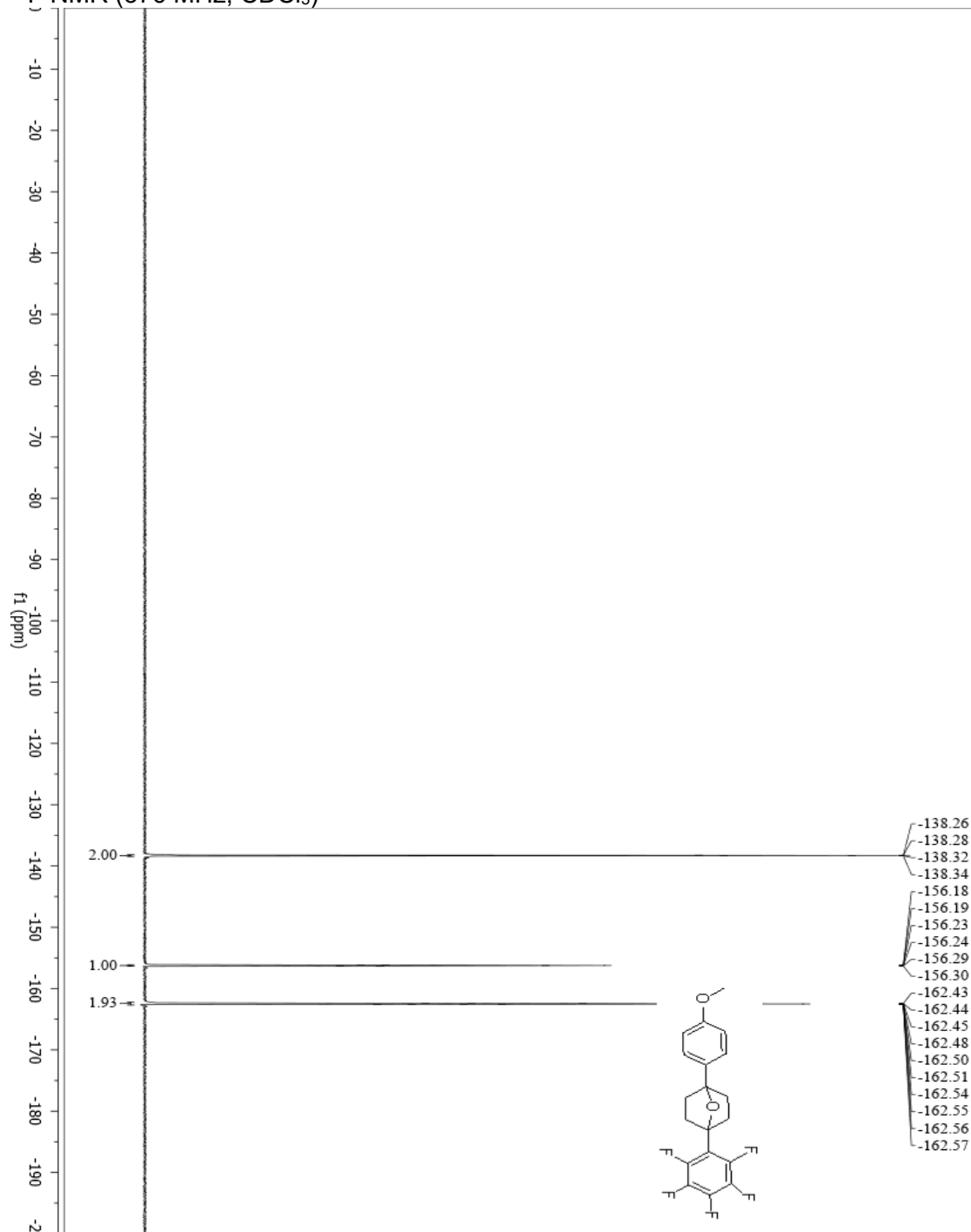




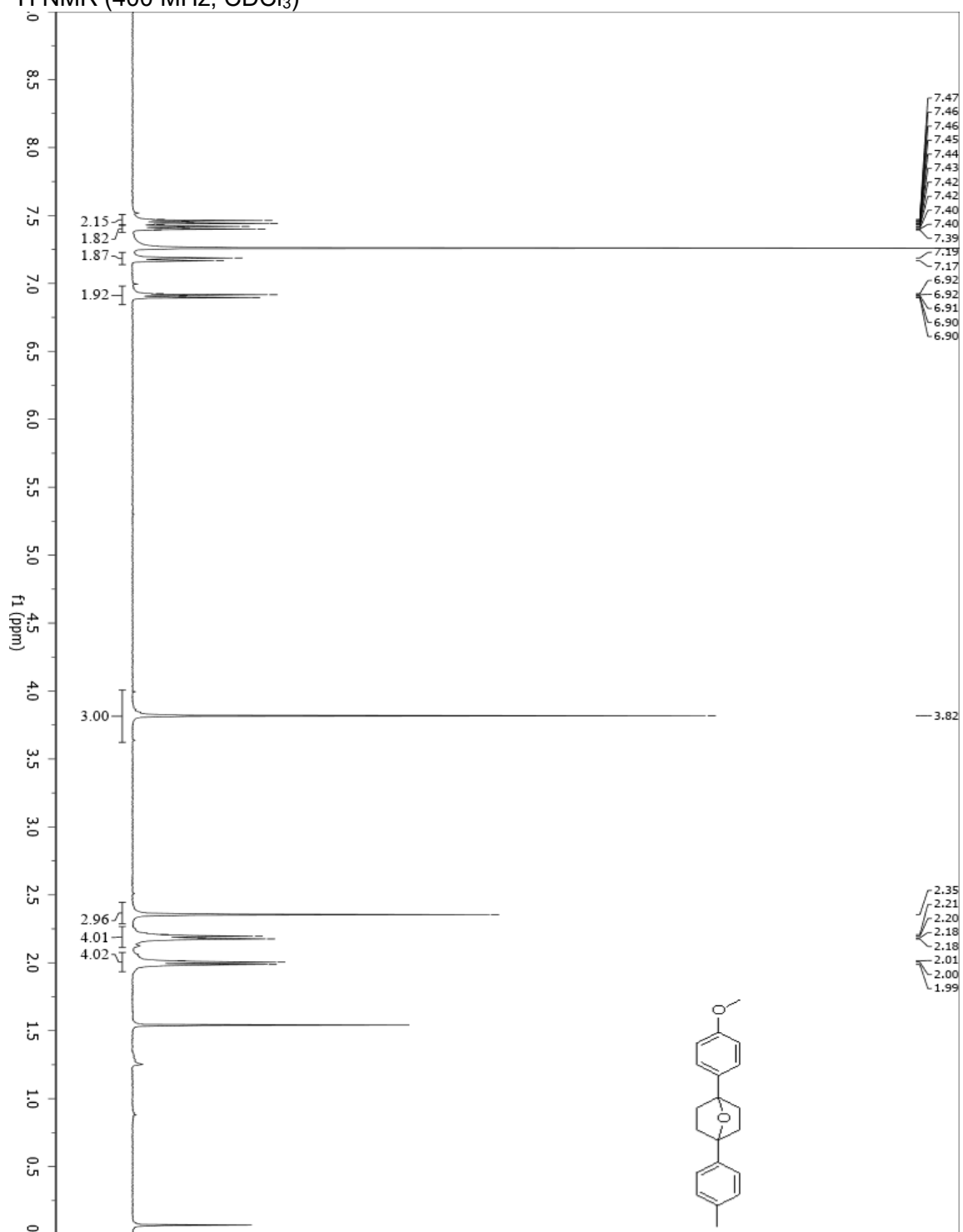
4.3.2b (1-(4-methoxyphenyl)-4-(perfluorophenyl)-7-oxabicyclo[2.2.1]heptanes)  
<sup>13</sup>C NMR (101 MHz, CDCl<sub>3</sub>)



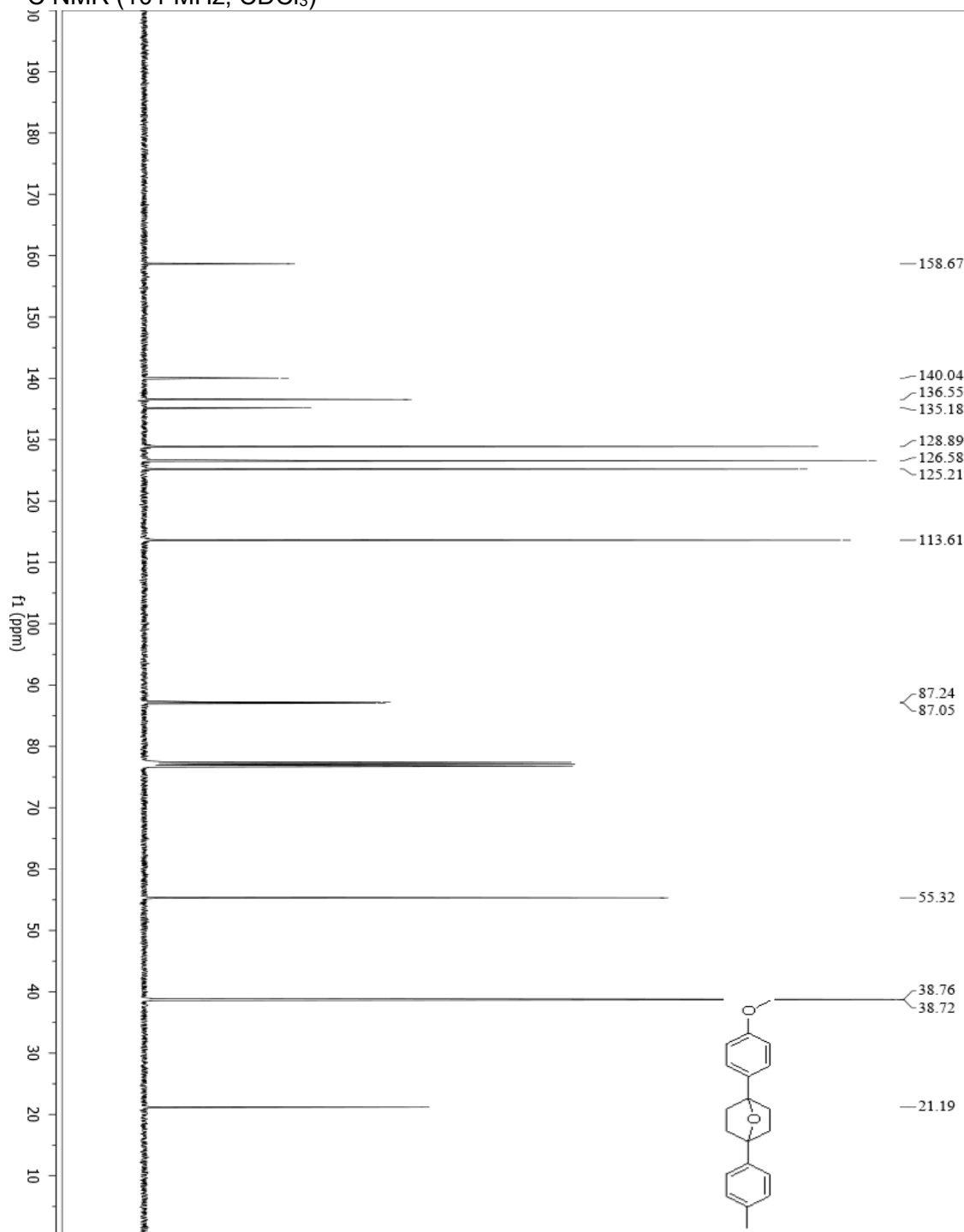
4.3.2b (1-(4-methoxyphenyl)-4-(perfluorophenyl)-7-oxabicyclo[2.2.1]heptanes)- Carbon  $^{19}\text{F}$  NMR (376 MHz,  $\text{CDCl}_3$ )



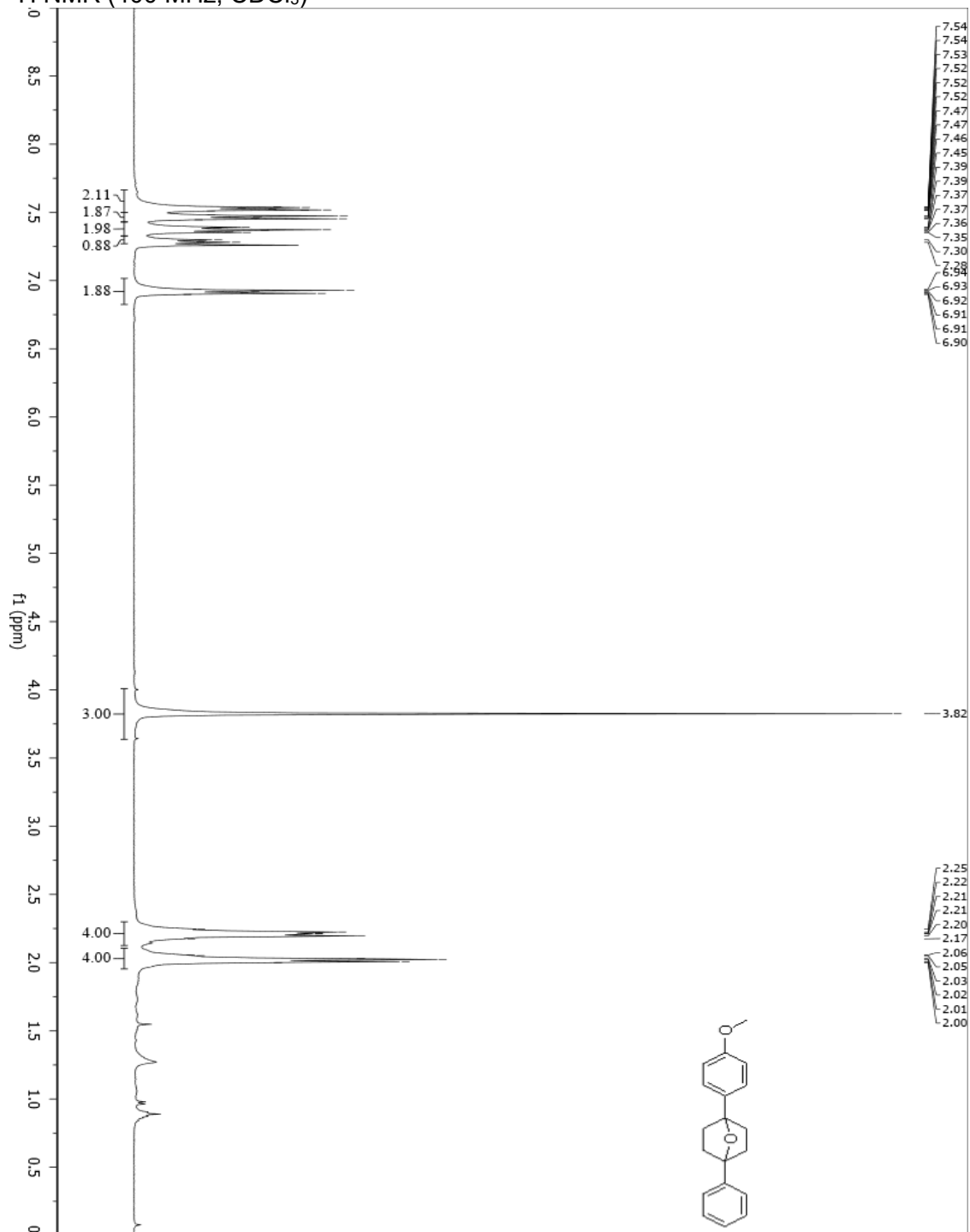
4.3.2b (1-(4-methoxyphenyl)-4-(perfluorophenyl)-7-oxabicyclo[2.2.1]heptanes)- Fluorine  
 $^1\text{H}$  NMR (400 MHz,  $\text{CDCl}_3$ )



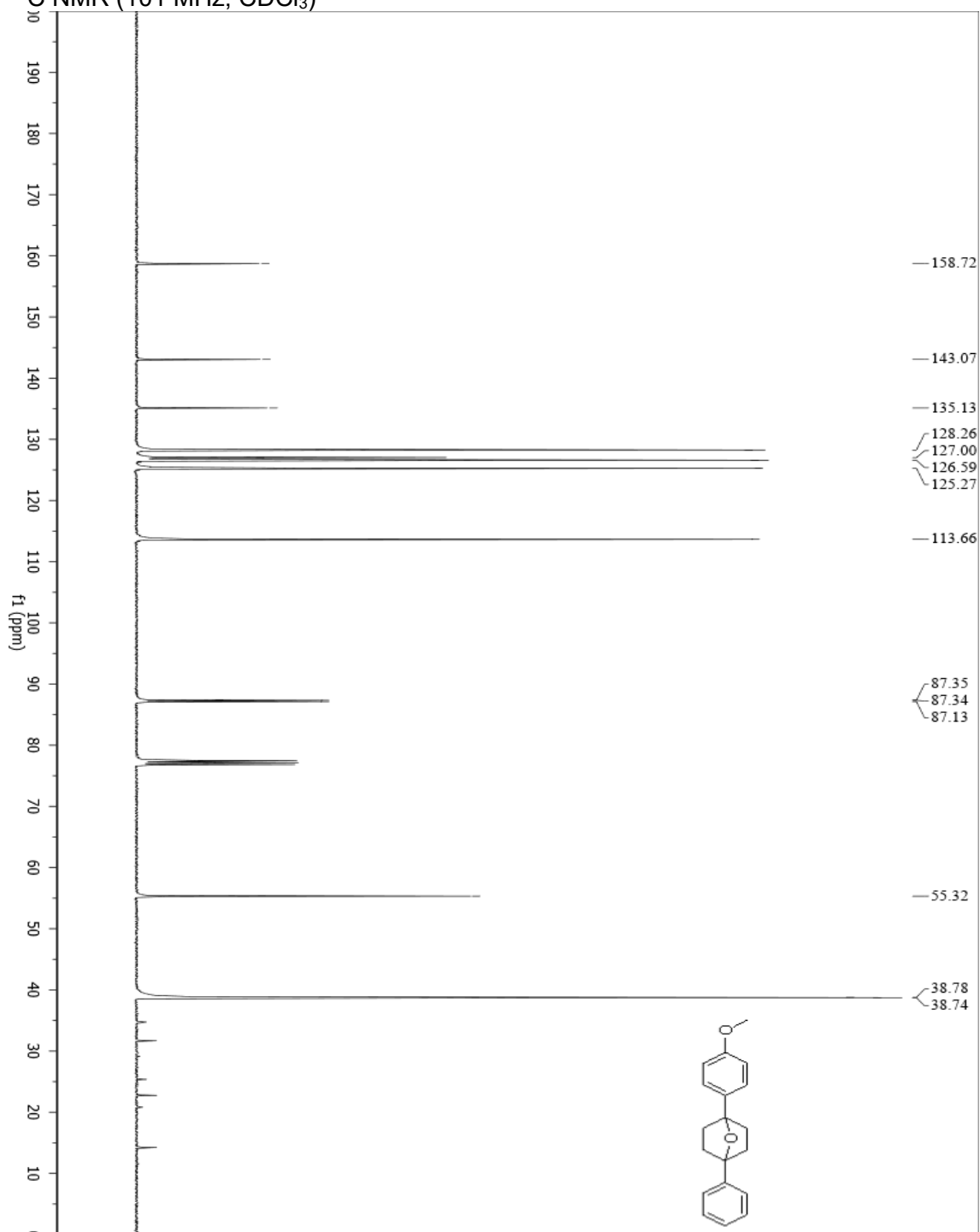
4.3.2e (1-(4-methoxyphenyl)-4-(p-tolyl)-7-oxabicyclo[2.2.1]heptane)  
<sup>13</sup>C NMR (101 MHz, CDCl<sub>3</sub>)



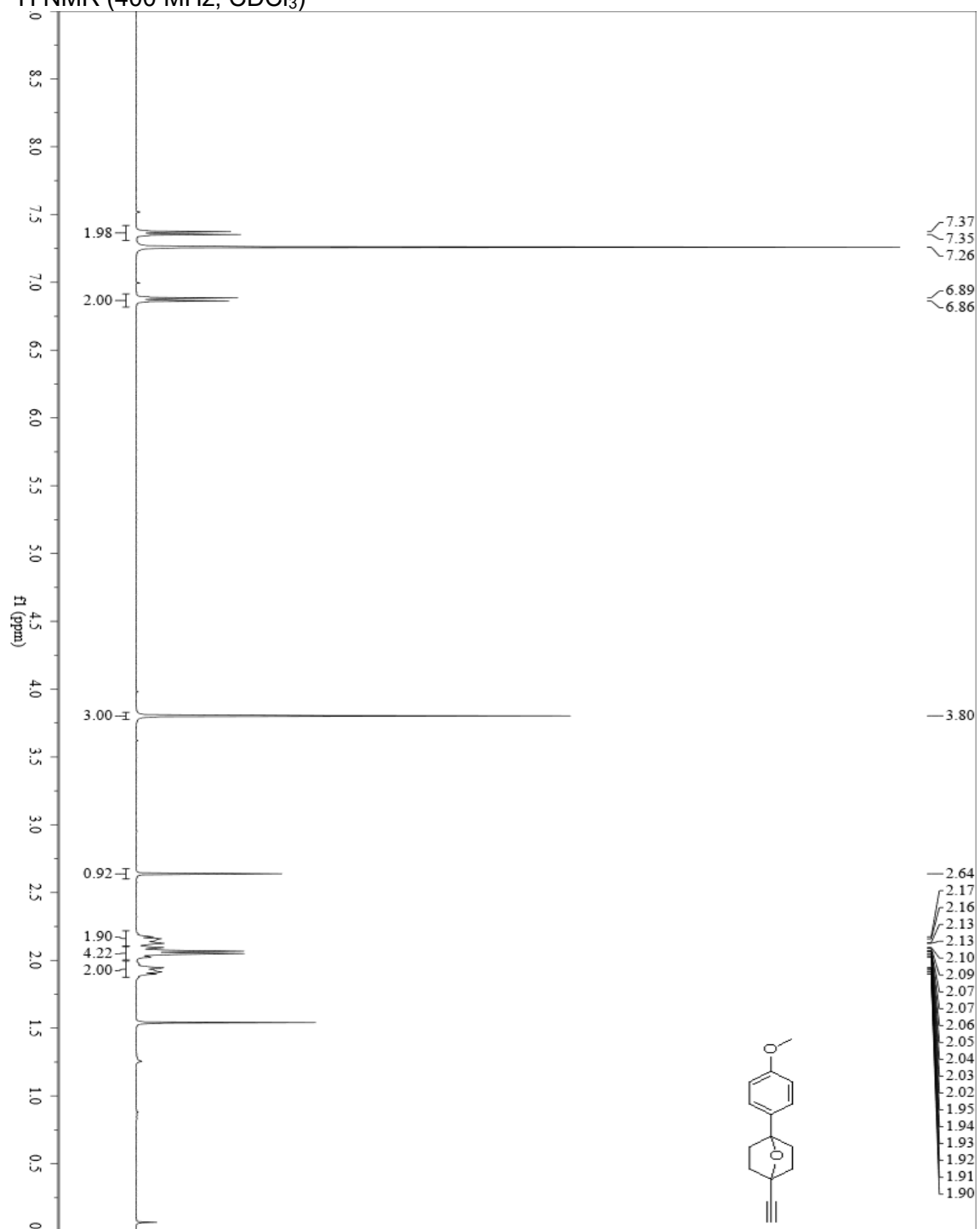
4.3.2e (1-(4-methoxyphenyl)-4-(p-tolyl)-7-oxabicyclo[2.2.1]heptane)  
<sup>1</sup>H NMR (400 MHz, CDCl<sub>3</sub>)



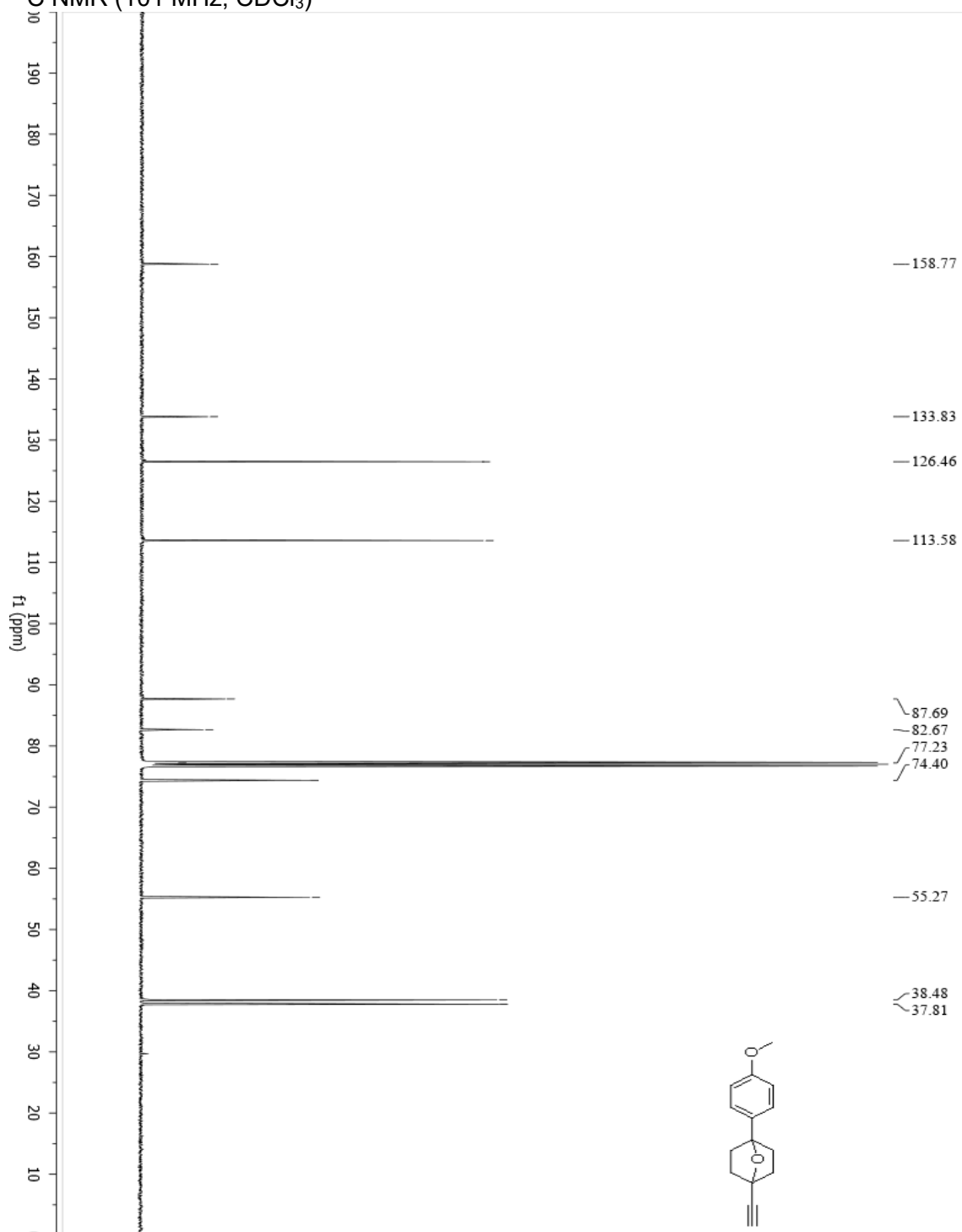
4.3.2f (1-(4-methoxyphenyl)-4-phenyl-7-oxabicyclo[2.2.1]heptane)  
<sup>13</sup>C NMR (101 MHz, CDCl<sub>3</sub>)



4.3.2f (1-(4-methoxyphenyl)-4-phenyl-7-oxabicyclo[2.2.1]heptane)  
<sup>1</sup>H NMR (400 MHz, CDCl<sub>3</sub>)

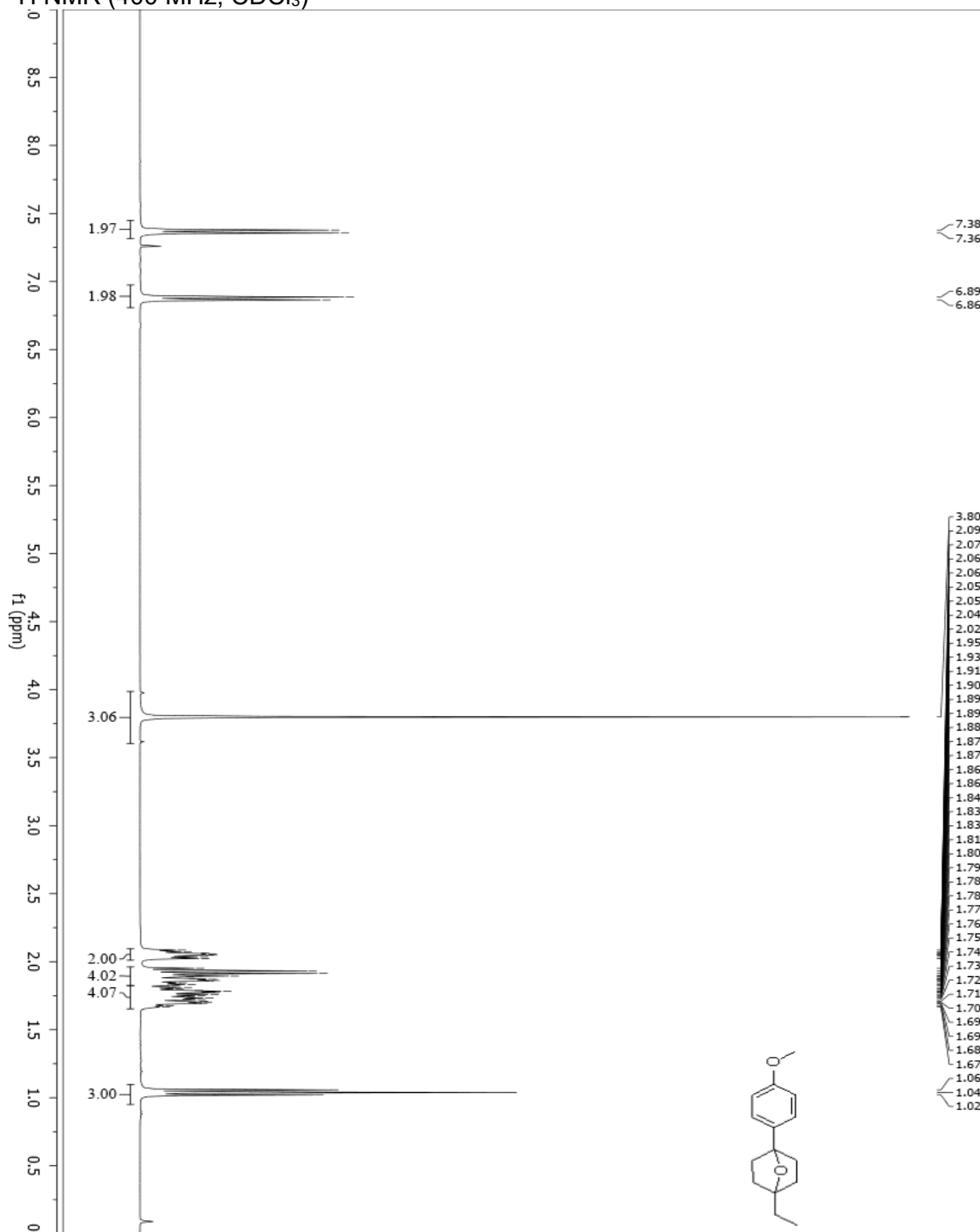


4.3.2g (1-ethynyl-4-(4-methoxyphenyl)-7-oxabicyclo[2.2.1]heptane)  
<sup>13</sup>C NMR (101 MHz, CDCl<sub>3</sub>)

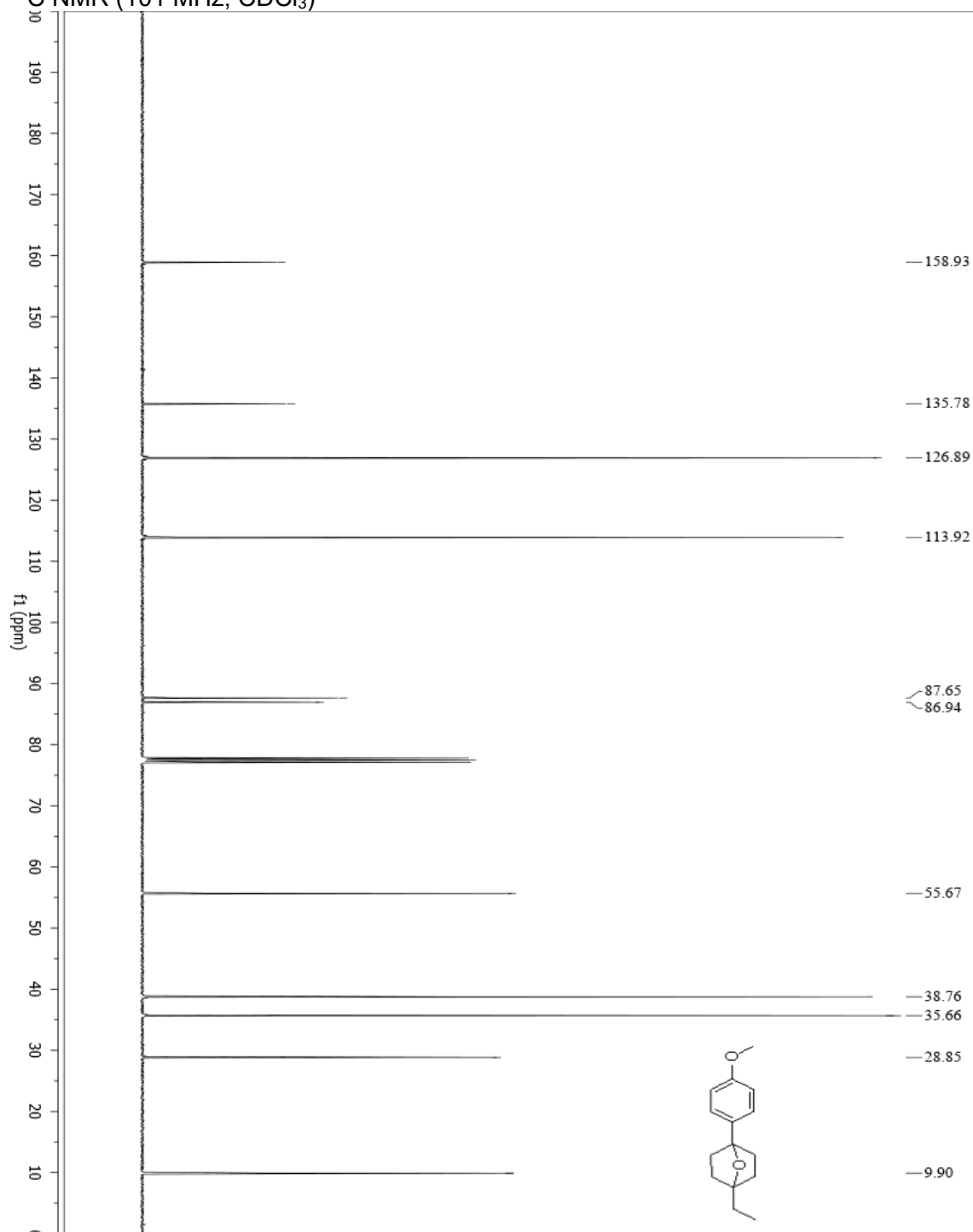




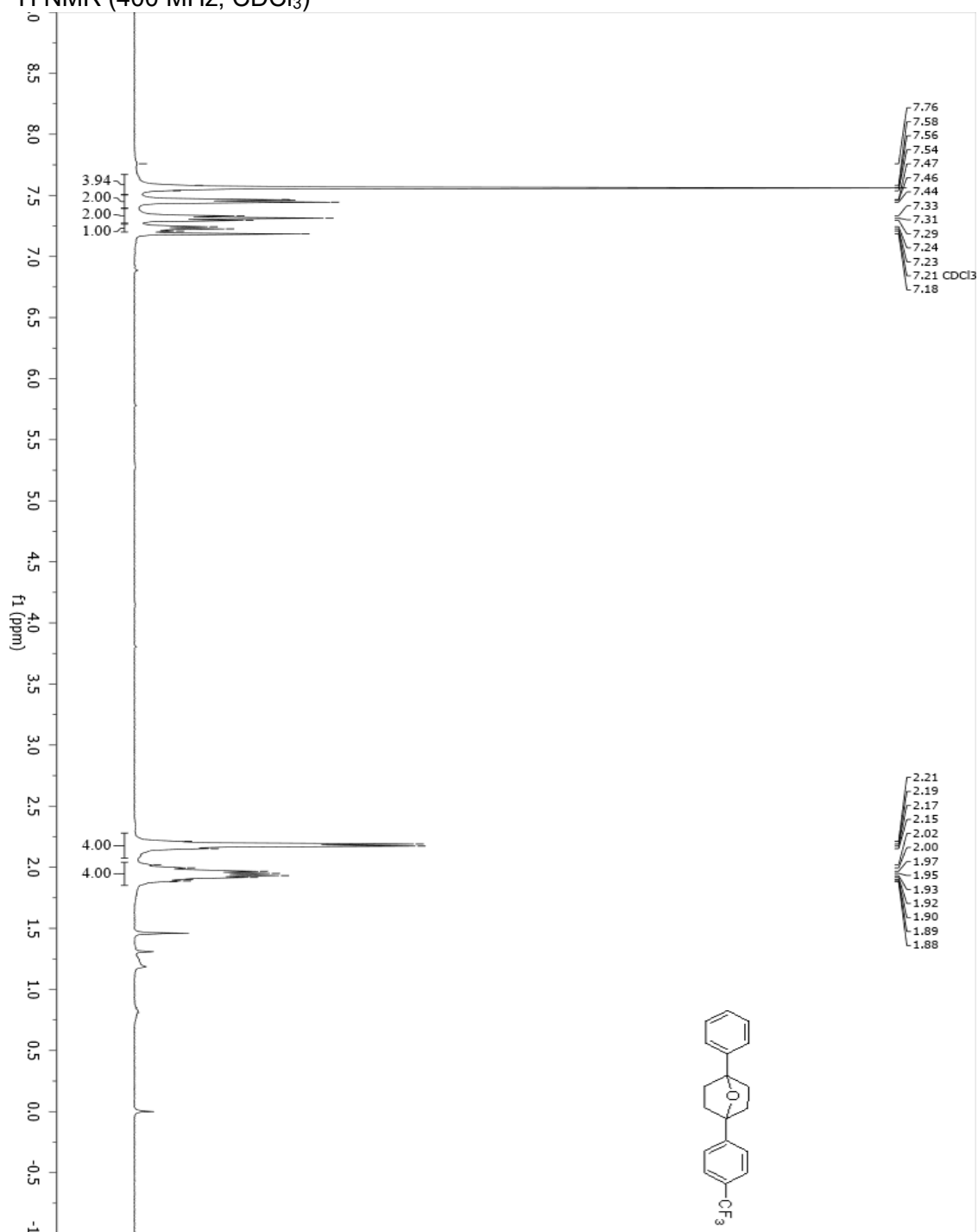
4.3.2g (1-ethynyl-4-(4-methoxyphenyl)-7-oxabicyclo[2.2.1]heptane)  
<sup>1</sup>H NMR (400 MHz, CDCl<sub>3</sub>)



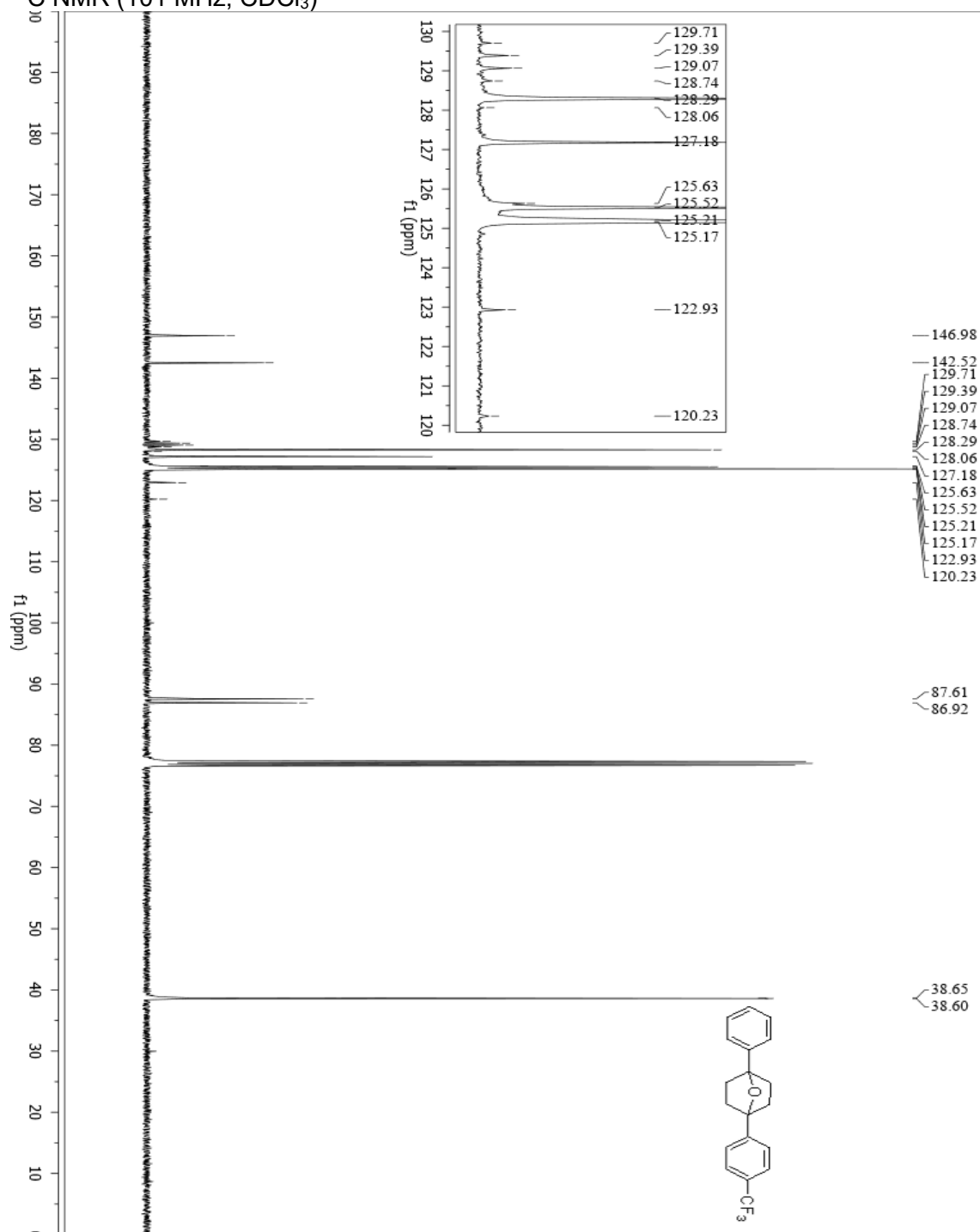
4.3.2h (1-ethyl-4-(4-methoxyphenyl)-7-oxabicyclo[2.2.1]heptane)  
<sup>13</sup>C NMR (101 MHz, CDCl<sub>3</sub>)



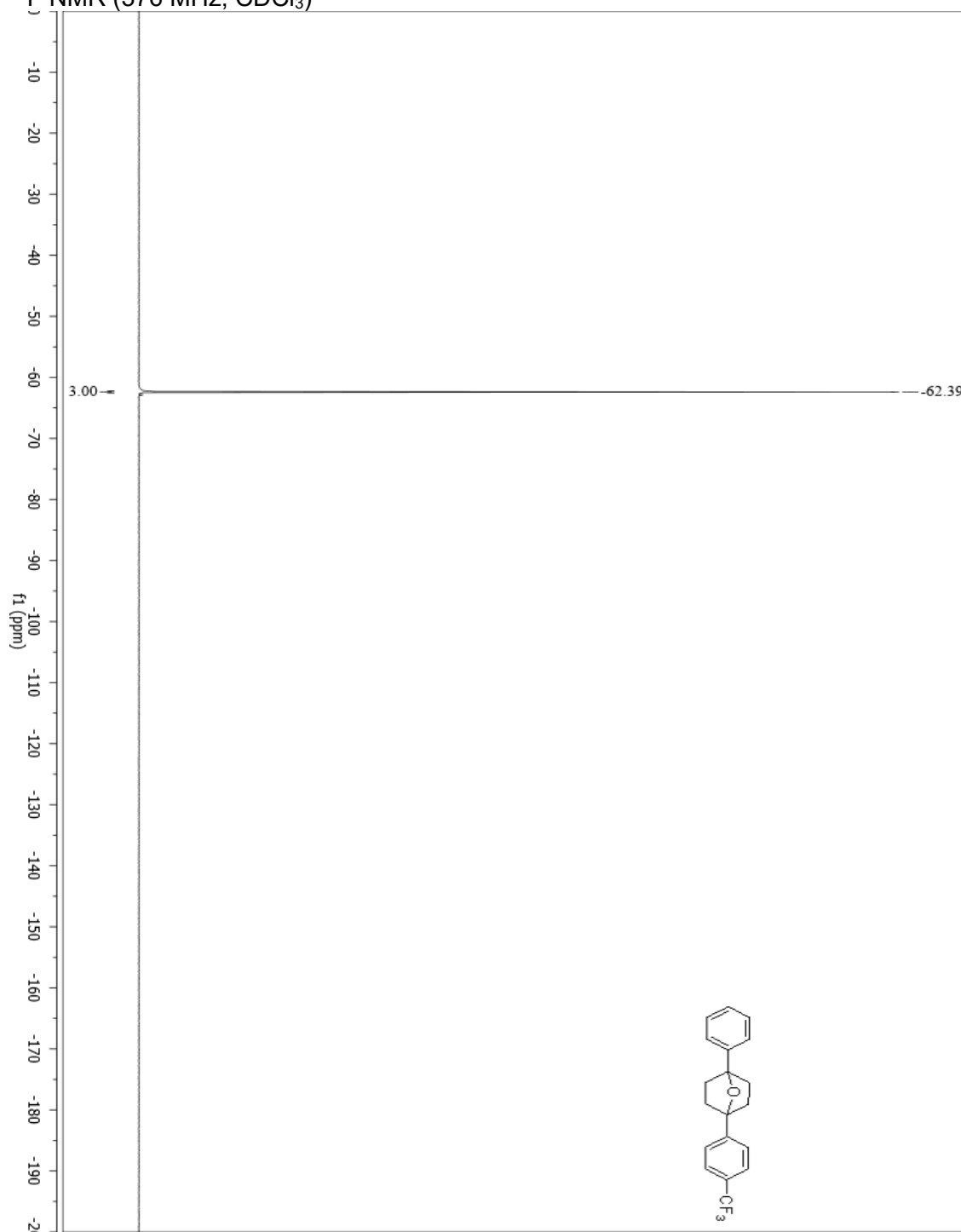
4.3.2h (1-ethyl-4-(4-methoxyphenyl)-7-oxabicyclo[2.2.1]heptane)  
<sup>1</sup>H NMR (400 MHz, CDCl<sub>3</sub>)



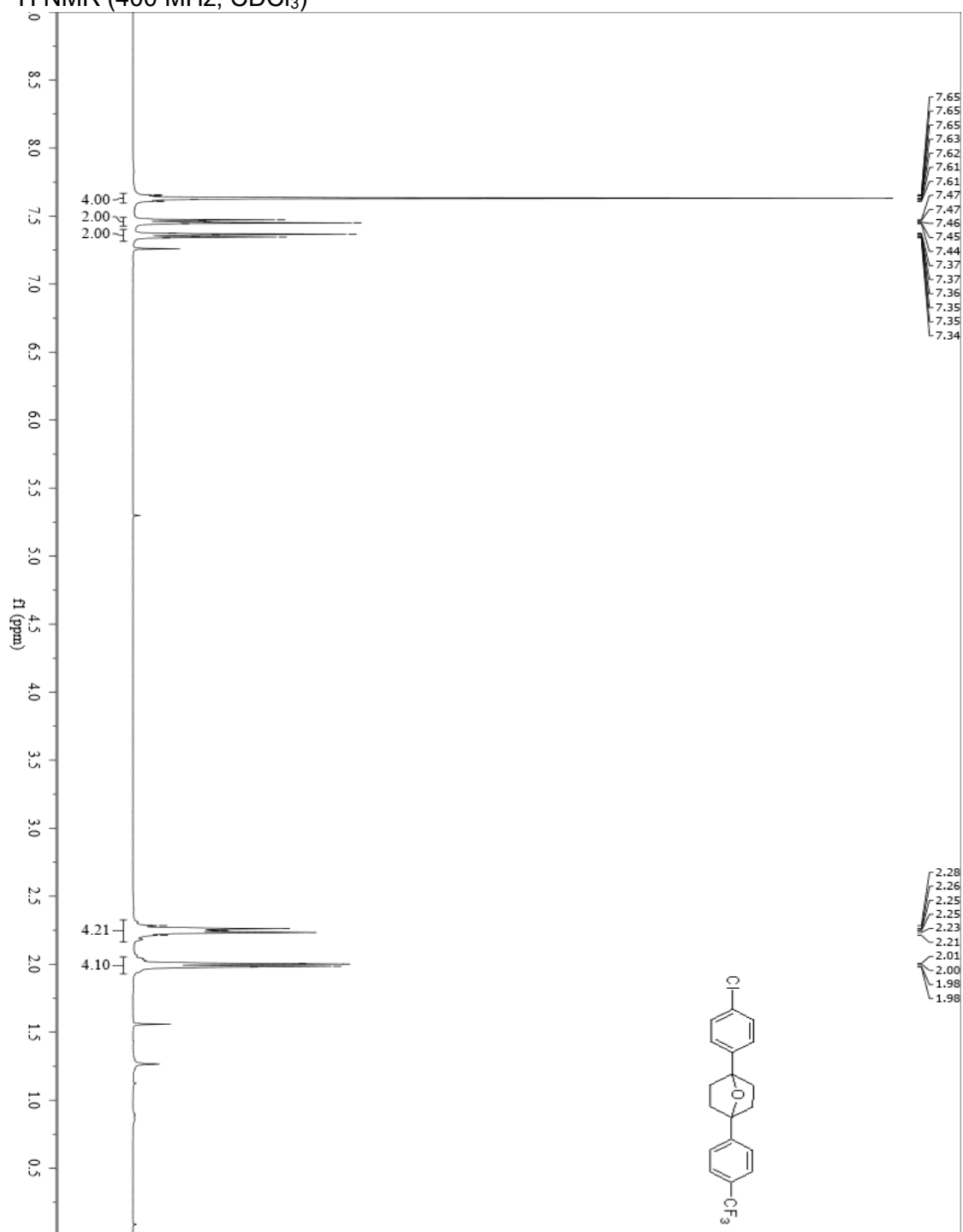
4.3.2i (1-phenyl-4-(4-(trifluoromethyl)phenyl)-7-oxabicyclo[2.2.1]heptane)  
<sup>13</sup>C NMR (101 MHz, CDCl<sub>3</sub>)



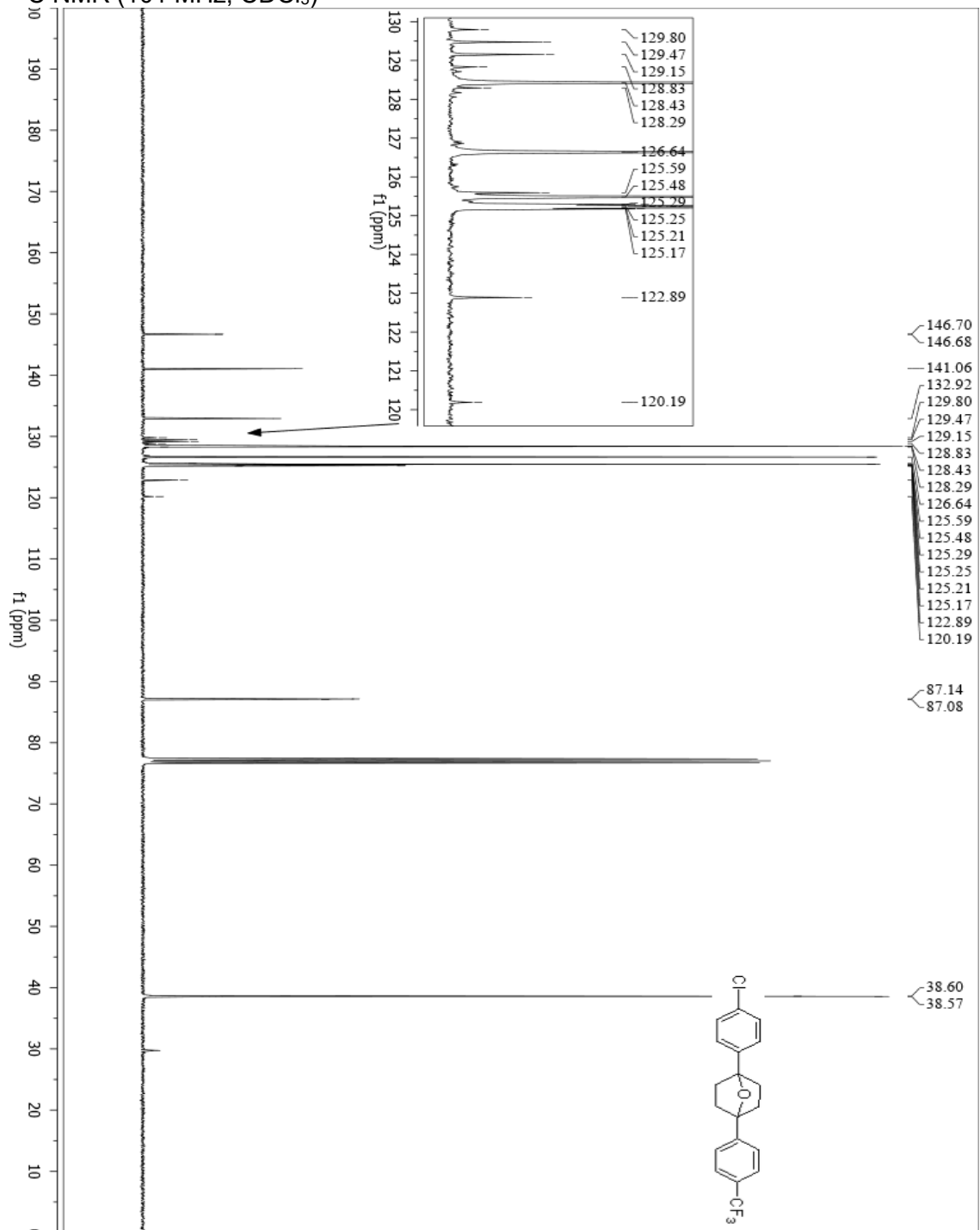
4.3.2i (1-phenyl-4-(4-(trifluoromethyl)phenyl)-7-oxabicyclo[2.2.1]heptane)  
<sup>19</sup>F NMR (376 MHz, CDCl<sub>3</sub>)



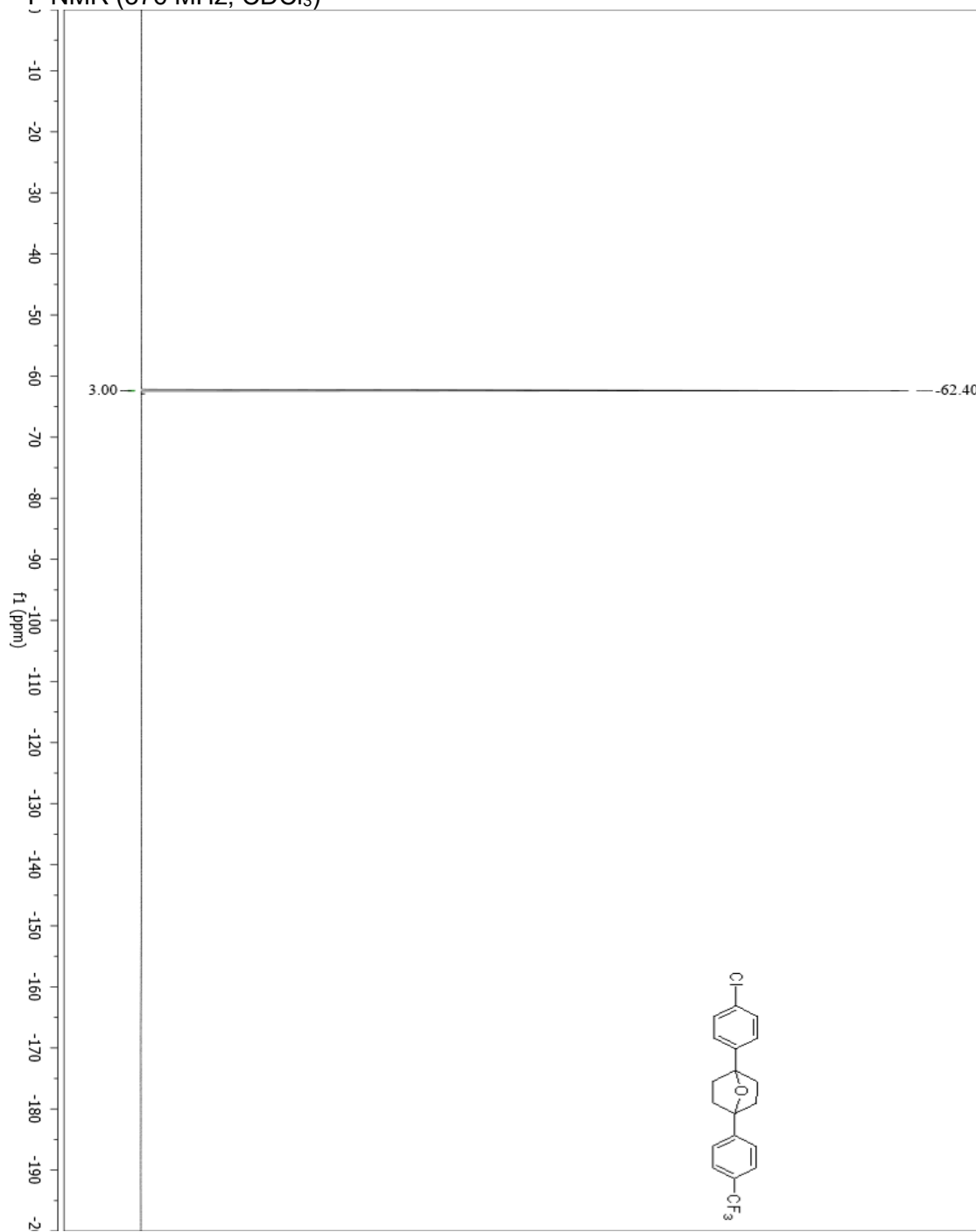
4.3.2i (1-phenyl-4-(4-(trifluoromethyl)phenyl)-7-oxabicyclo[2.2.1]heptane)  
<sup>1</sup>H NMR (400 MHz, CDCl<sub>3</sub>)



4.3.2k (1-(4-chlorophenyl)-4-(4-(trifluoromethyl)phenyl)-7-oxabicyclo[2.2.1]heptane)  
<sup>13</sup>C NMR (101 MHz, CDCl<sub>3</sub>)

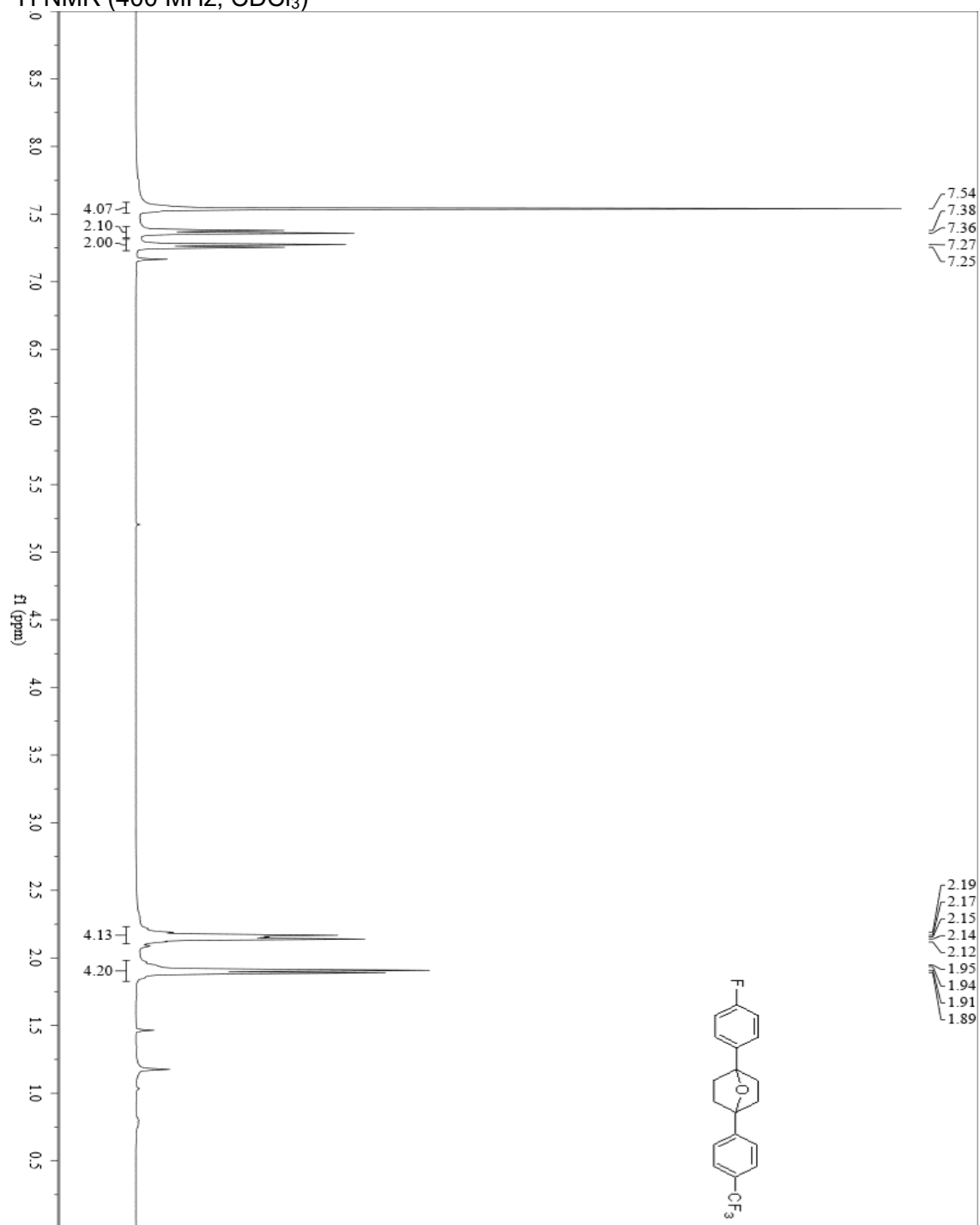


4.3.2k (1-(4-chlorophenyl)-4-(4-(trifluoromethyl)phenyl)-7-oxabicyclo[2.2.1]heptane)  
<sup>19</sup>F NMR (376 MHz, CDCl<sub>3</sub>)

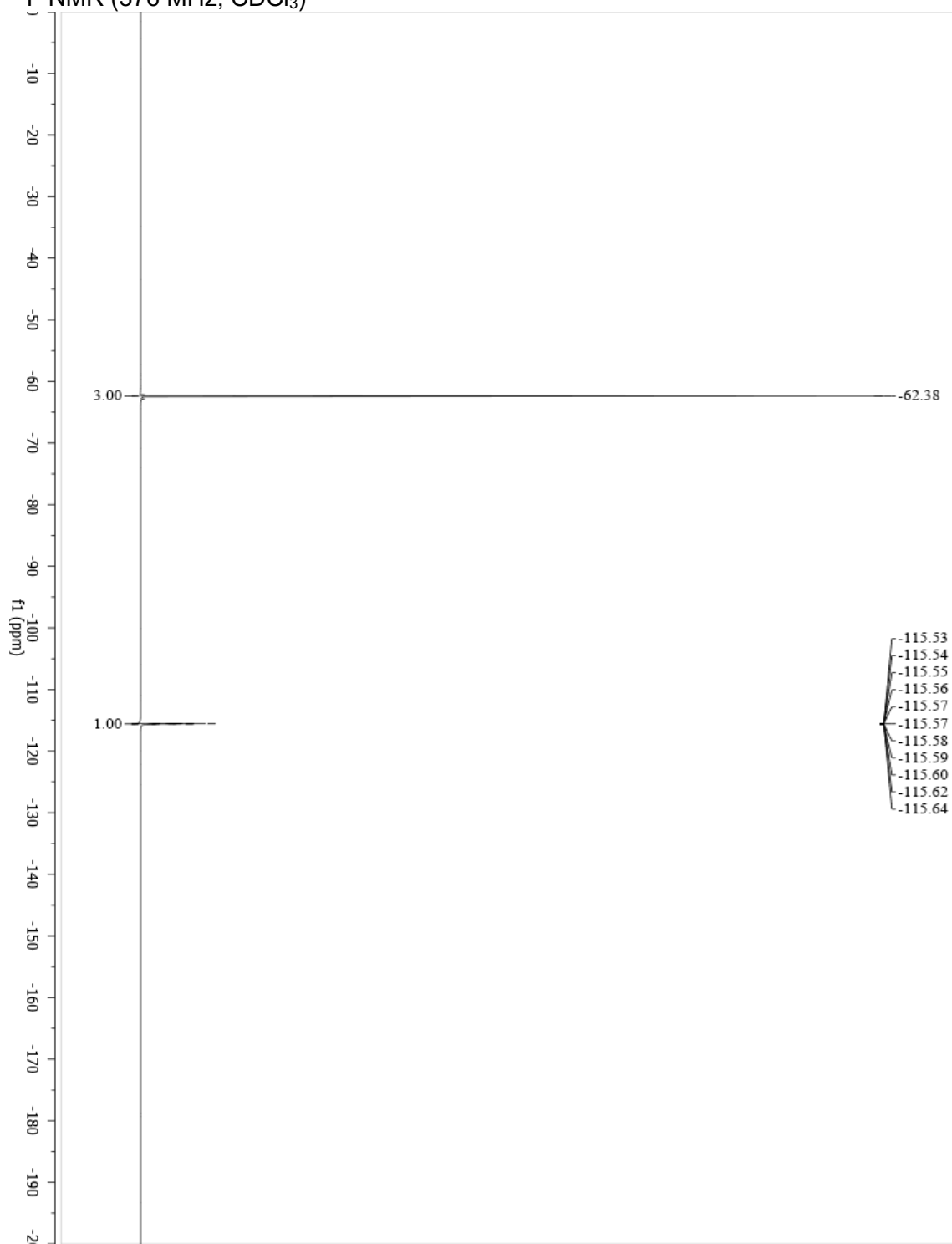




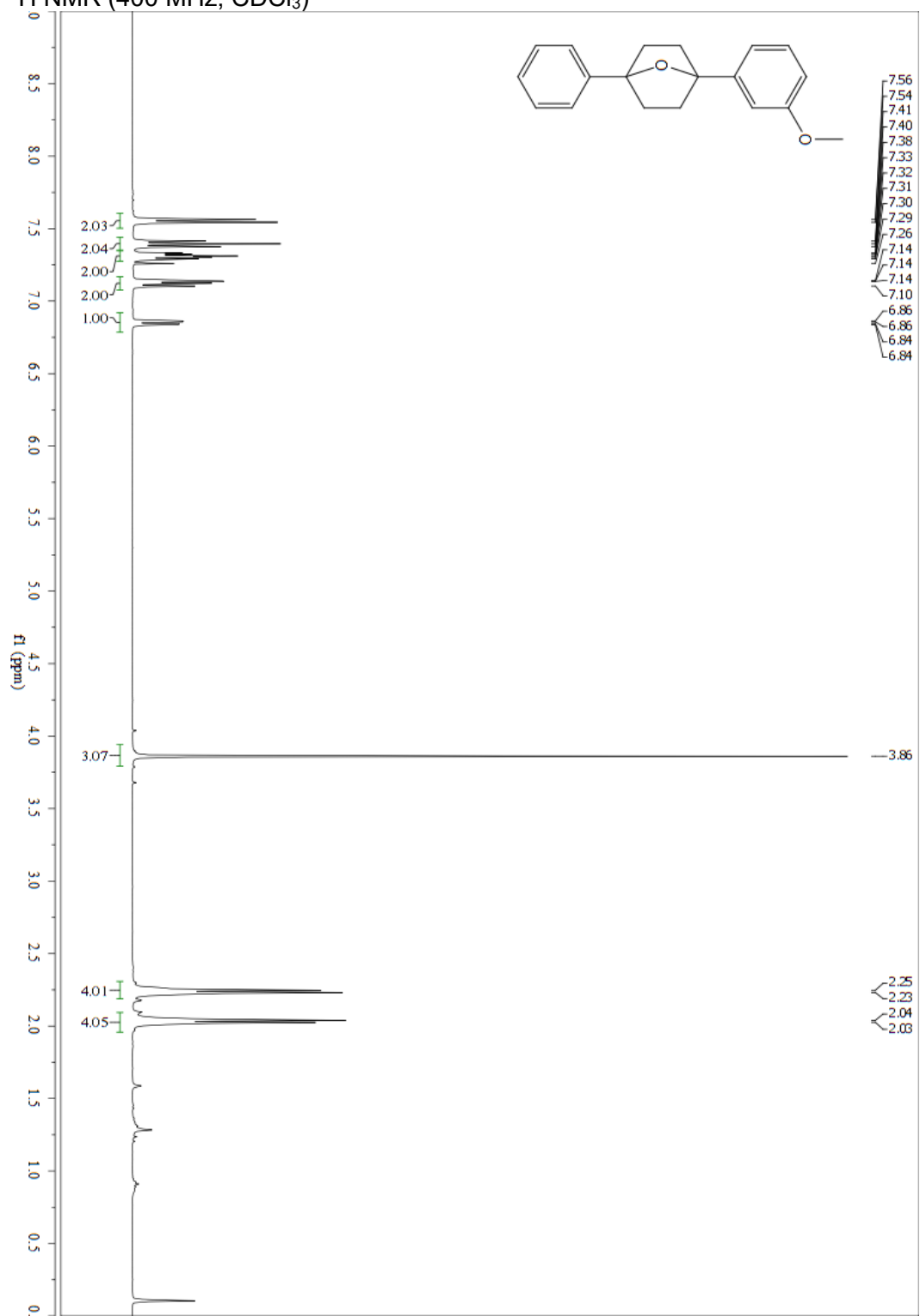
4.3.2k (1-(4-chlorophenyl)-4-(4-(trifluoromethyl)phenyl)-7-oxabicyclo[2.2.1]heptane)  
<sup>1</sup>H NMR (400 MHz, CDCl<sub>3</sub>)



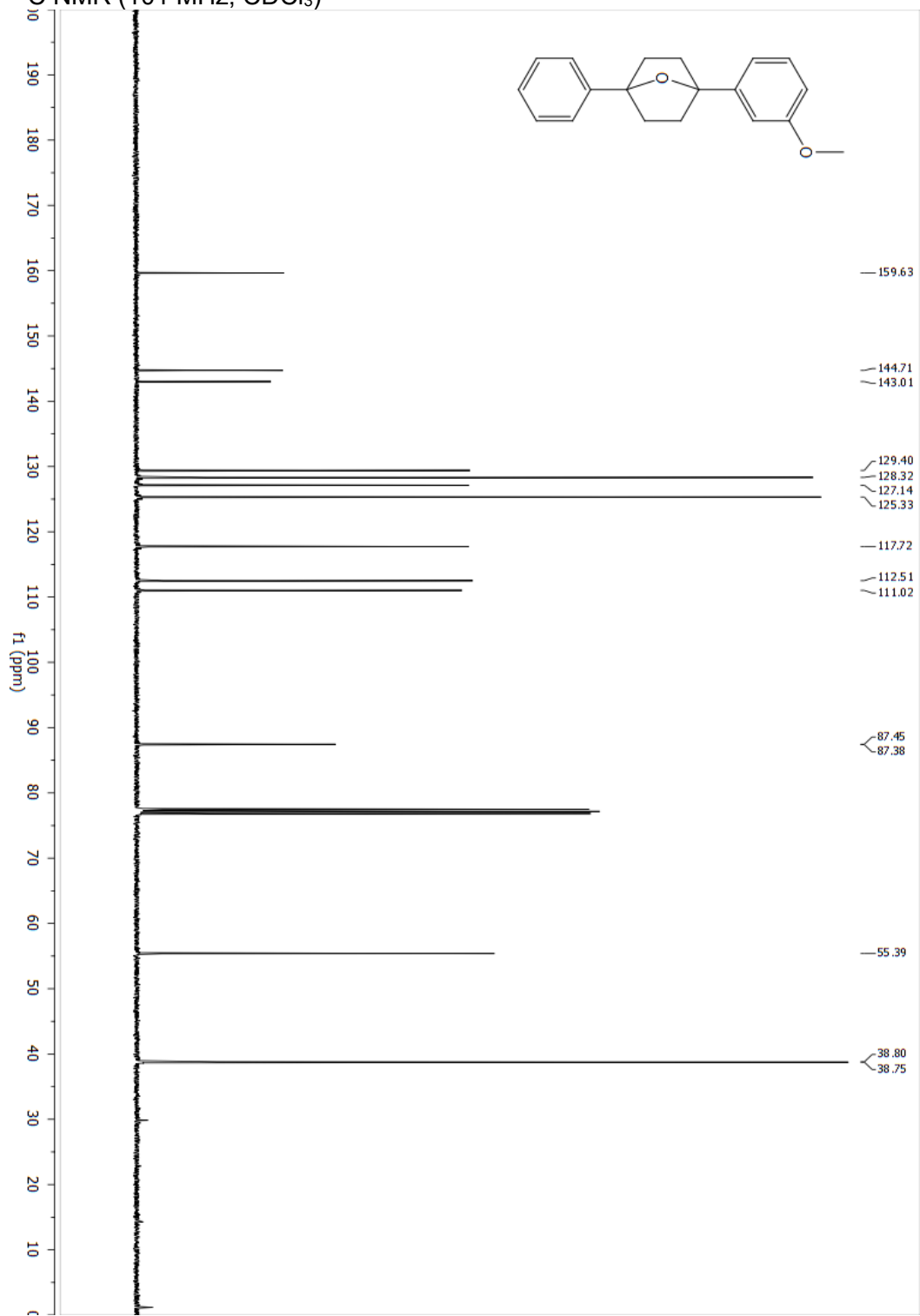
4.3.2j (1-(4-fluorophenyl)-4-(4-(trifluoromethyl)phenyl)-7-oxabicyclo[2.2.1]heptane)  
<sup>19</sup>F NMR (376 MHz, CDCl<sub>3</sub>)



4.3.2m (1-(3-methoxyphenyl)-4-phenyl-7-oxabicyclo[2.2.1]heptane)  
<sup>1</sup>H NMR (400 MHz, CDCl<sub>3</sub>)

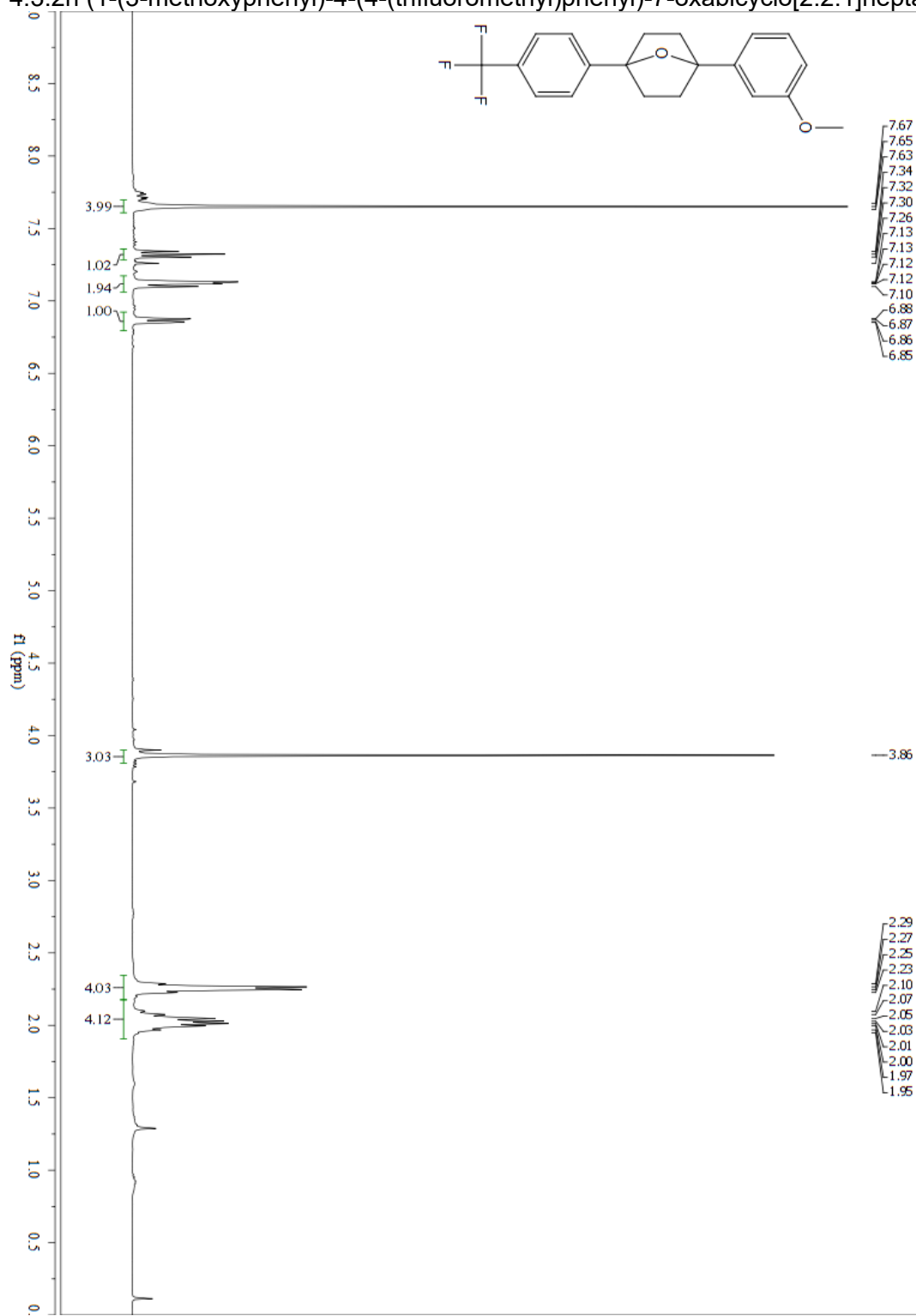


4.3.2m (1-(3-methoxyphenyl)-4-phenyl-7-oxabicyclo[2.2.1]heptane)  
<sup>13</sup>C NMR (101 MHz, CDCl<sub>3</sub>)

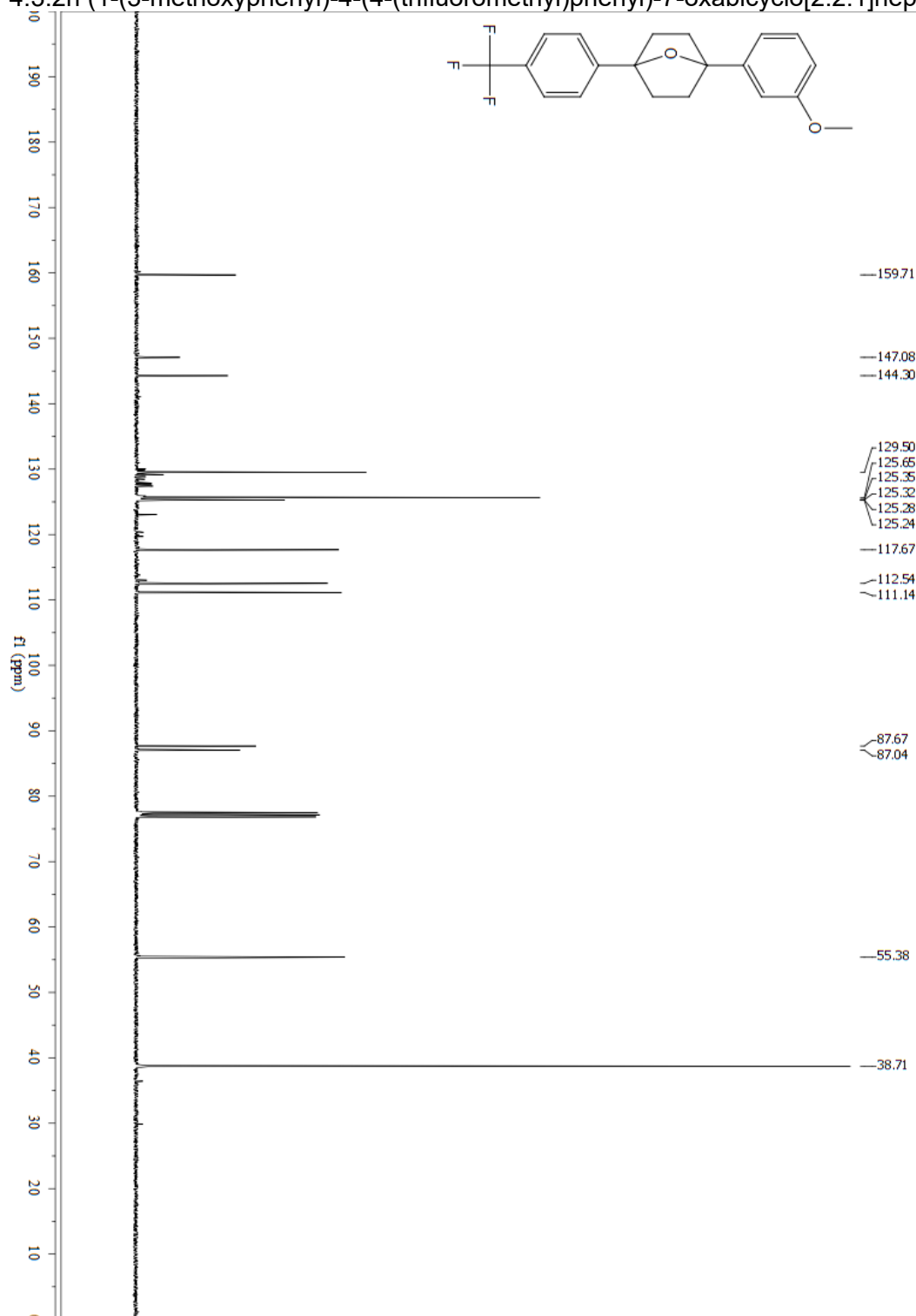


<sup>1</sup>H NMR (400 MHz, CDCl<sub>3</sub>)

4.3.2n (1-(3-methoxyphenyl)-4-(4-(trifluoromethyl)phenyl)-7-oxabicyclo[2.2.1]heptane)

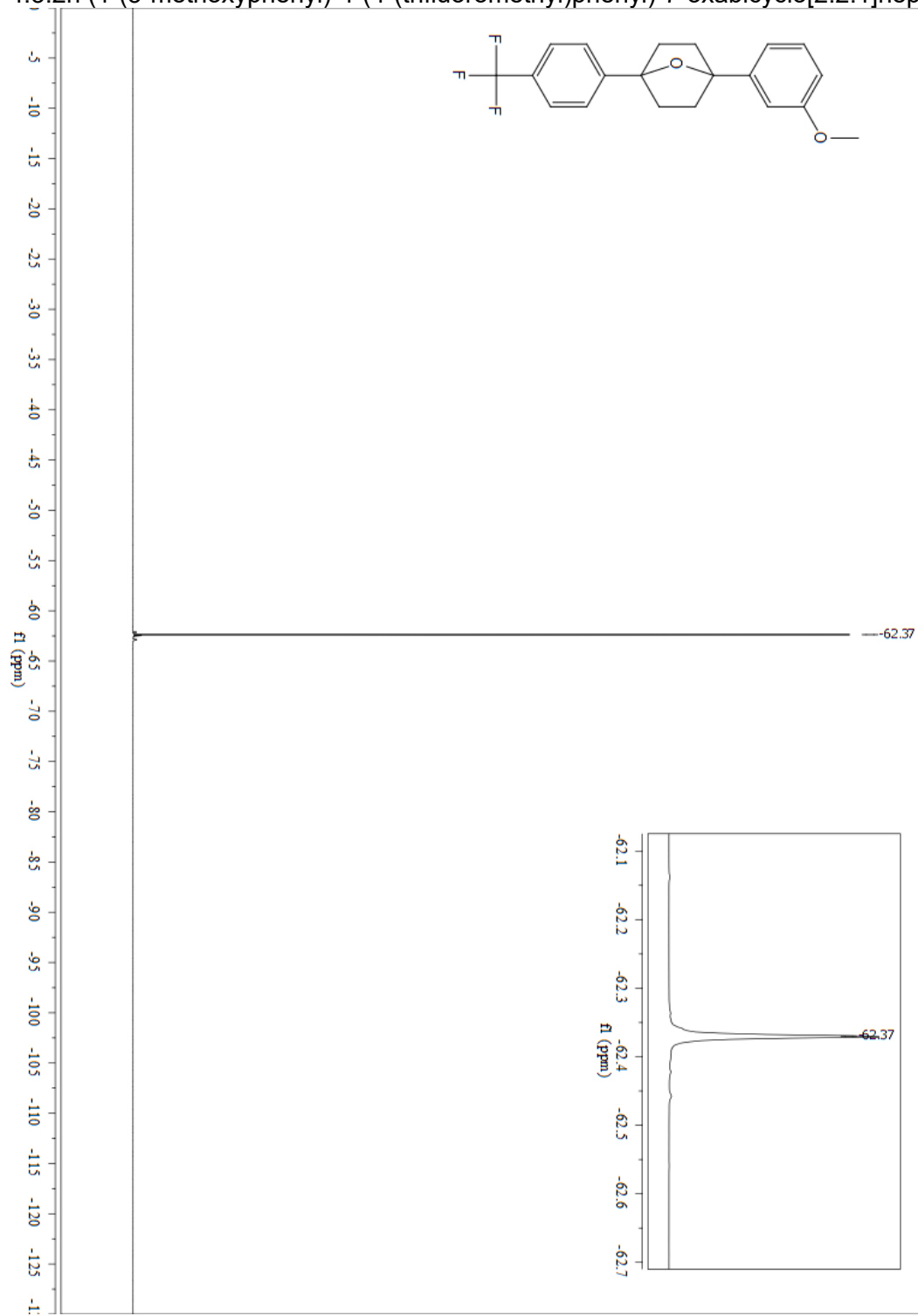


<sup>13</sup>C NMR (101 MHz, CDCl<sub>3</sub>)  
4.3.2n (1-(3-methoxyphenyl)-4-(4-(trifluoromethyl)phenyl)-7-oxabicyclo[2.2.1]heptane)



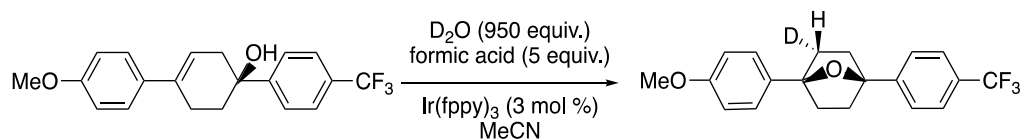
<sup>19</sup>F NMR (376 MHz, CDCl<sub>3</sub>)

4.3.2n (1-(3-methoxyphenyl)-4-(4-(trifluoromethyl)phenyl)-7-oxabicyclo[2.2.1]heptane)



## 4.12 Kinetics and Mechanistic Studies:

### 4.12.1 Deuterium Incorporation



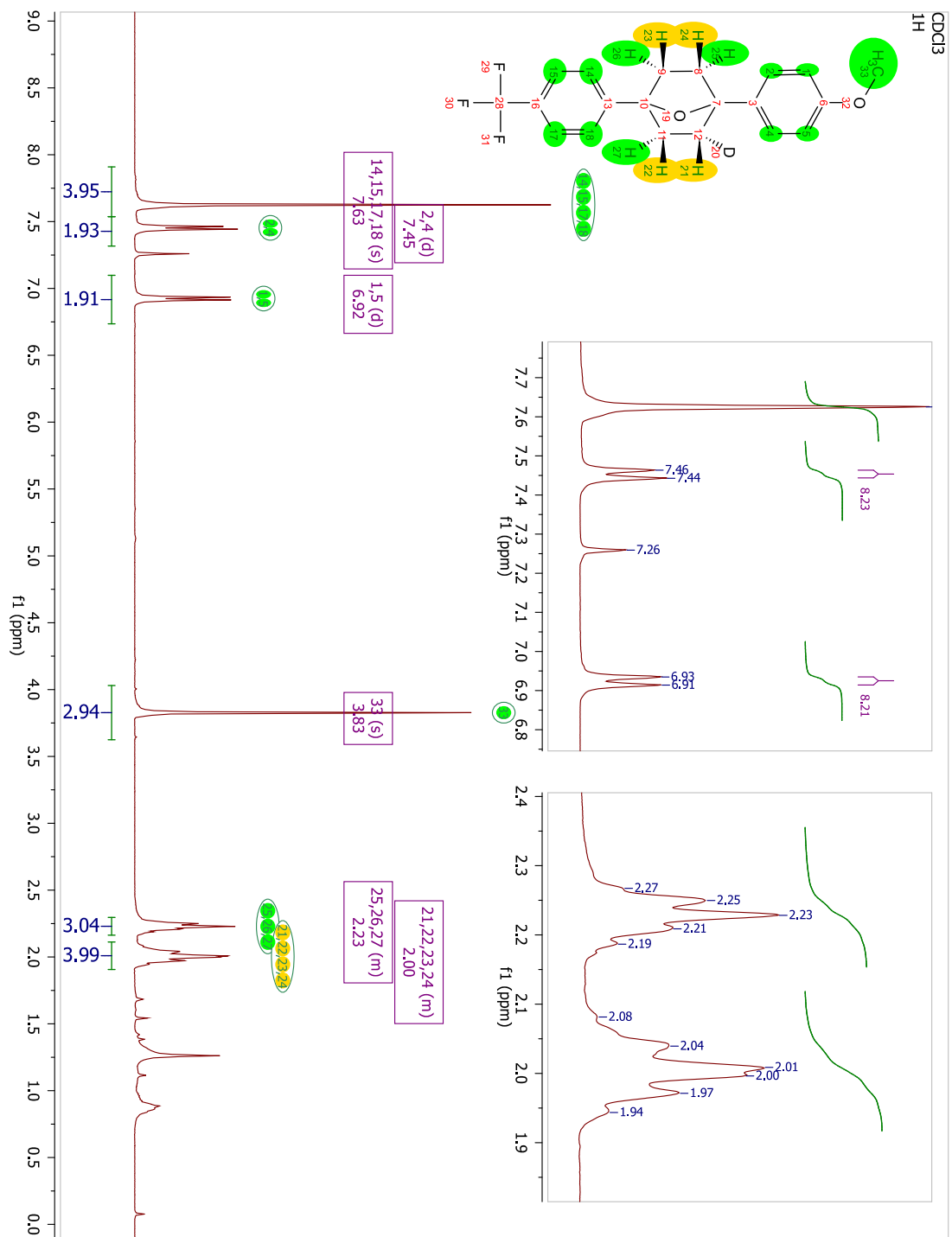
The general procedure A was carried out as in the synthesis of 4.3.2A, with the exception that 950 equivalents of D<sub>2</sub>O were added to the solution prior to degassing the solution. The spectrum was then simulated in Gaussian 09 according to the method of Bally and Rablen.<sup>289</sup> Averaged sets of degenerate signals are as follows: Set 1: 34 35 36; Set 2: 31 32; Set 3: 30 33; Set 4: 28 27 26 29; Set 5: 40 42 43 38; Set 6: 39 37 41 44. Mutual couplings were set to zero within degenerate averaged signals.

Minimized geometry of the product 4.3.2A at B3LYP/6-31G(d) is:

C,0.0882140903,-3.9421840255,1.9041454512  
C,0.0485318998,-2.6603123286,1.3589710991  
C,-1.0520209895,-1.8245527001,1.5833864337  
C,-2.1130592026,-2.3001919013,2.3669444944  
C,-2.0765143493,-3.5789073972,2.915961568  
C,-0.9731013071,-4.4050449092,2.6847748211  
C,-1.0919788126,-0.4281553663,1.0205259843  
C,0.6299679727,1.6737410538,-1.3155311574  
C,1.2075045064,0.7970780235,-2.2486869821  
C,2.0548659351,1.2665896012,-3.2427127992  
C,2.3424756005,2.6363173385,-3.338724768  
C,1.7708546238,3.5241807971,-2.4218134515  
C,0.9255281127,3.0343281366,-1.4213735648  
C,-0.9068327116,-5.7640752651,3.3234718755  
F,-2.1327590042,-6.3216335355,3.452939026  
F,-0.144415895,-6.6230845387,2.6101713931  
F,-0.3729192086,-5.7096789058,4.5679660325  
O,3.1859713897,2.9969001158,-4.3508843298  
C,3.5188824837,4.3682431329,-4.4887408578  
C,-1.8153125414,1.0739511264,-0.7139189533  
C,-2.3625336674,-0.0499657837,0.2061019224  
C,-0.8035140898,0.7056237457,2.0494769028  
C,-0.2641637906,1.8345401307,1.1297110726  
C,-0.3239345795,1.160531023,-0.2688569347  
O,-0.0424131881,-0.2221787161,0.0563955954  
H,0.940927416,-4.5865582248,1.7163483823  
H,0.8686794567,-2.2995378749,0.7489929612  
H,-2.9790675819,-1.6690826558,2.5476784335  
H,-2.9070873934,-3.9396572222,3.5141250533  
H,0.9947894206,-0.2644772957,-2.1775980499  
H,2.5109197352,0.5901361627,-3.9590971511  
H,1.9760939026,4.5875547853,-2.4692353921  
H,0.4943966272,3.7399487571,-0.7158636316  
H,4.1953554013,4.4283084265,-5.3433792927  
H,2.6302912223,4.9826934652,-4.68666037  
H,4.0292667132,4.7523130082,-3.5952699437  
H,-1.8694628031,0.7879748847,-1.7677566799  
H,-2.335088304,2.0302717329,-0.5983312197  
H,-2.7060530555,-0.9107676958,-0.3743701784  
H,-3.1875170091,0.2765539734,0.8469854636  
H,-0.0428781375,0.3753940679,2.7621366694  
H,-1.6962263374,0.9885700959,2.6158399921  
H,-0.8611976116,2.750519032,1.179173062  
H,0.769535061,2.0897837255,1.378582018

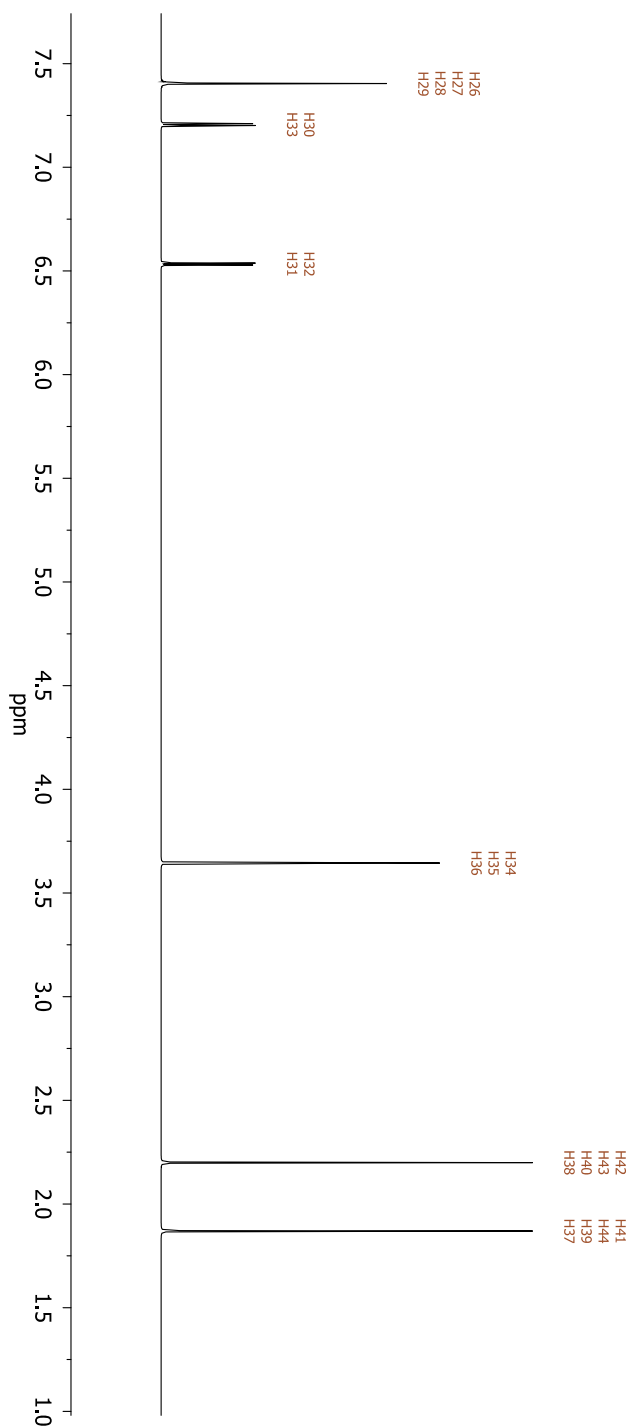
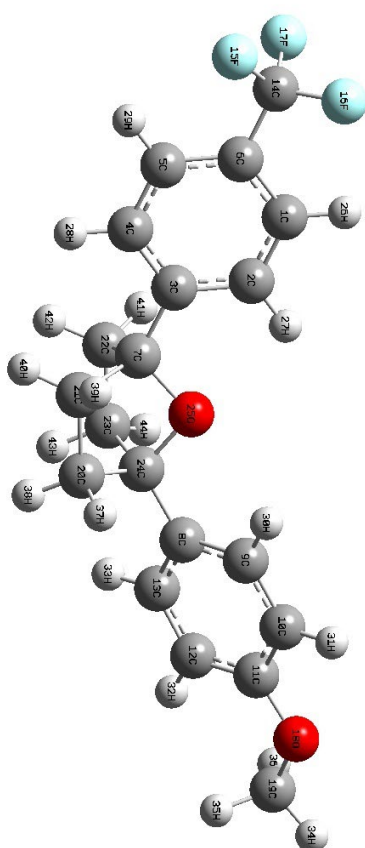
Experimental spectrum for the deuterated form of 4.3.2A, 4.3.d-2A



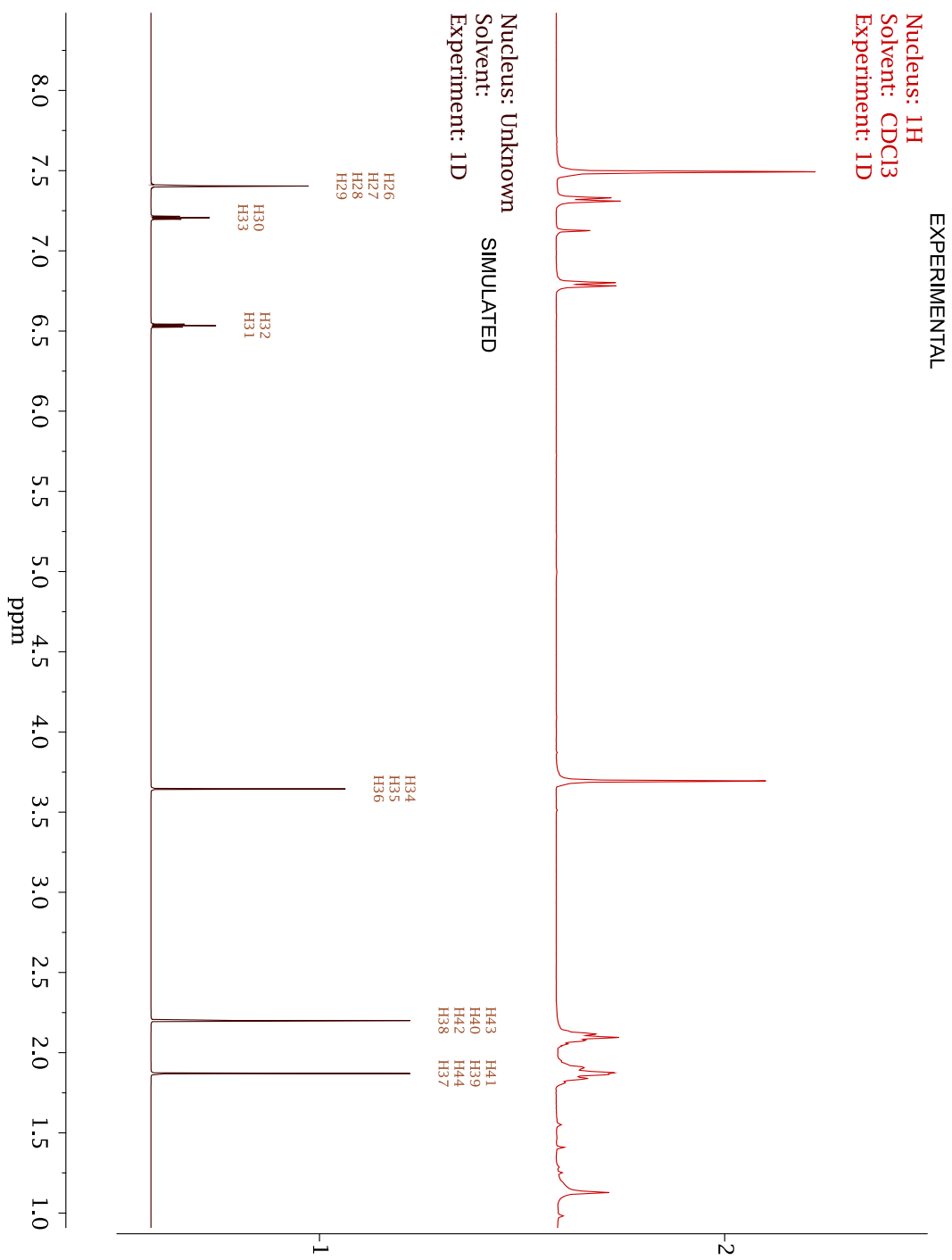


Simulated Unknown NMR Spectrum

Nucleus: Unknown  
Solvent:  
Experiment: 1D

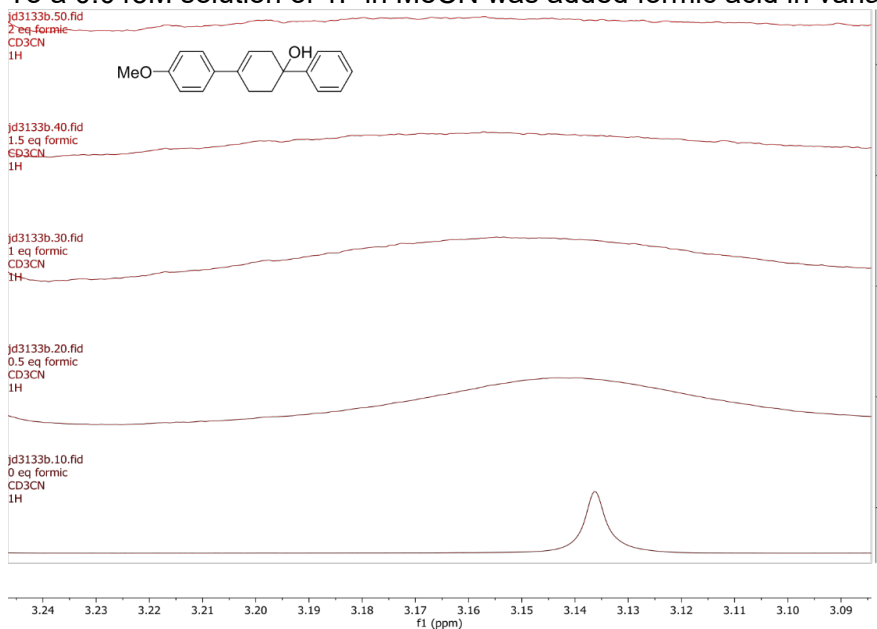


# Stacked Simulated and Experimental Spectra for 4.3.2A

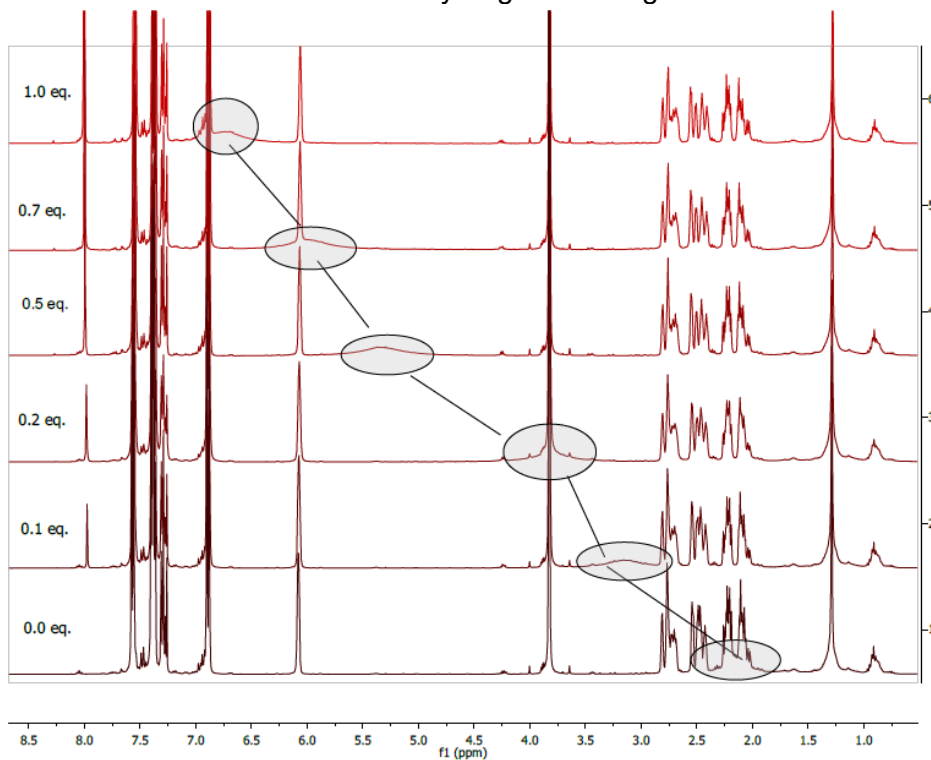


#### 4.12.2 Evidence for Hydrogen Bonding

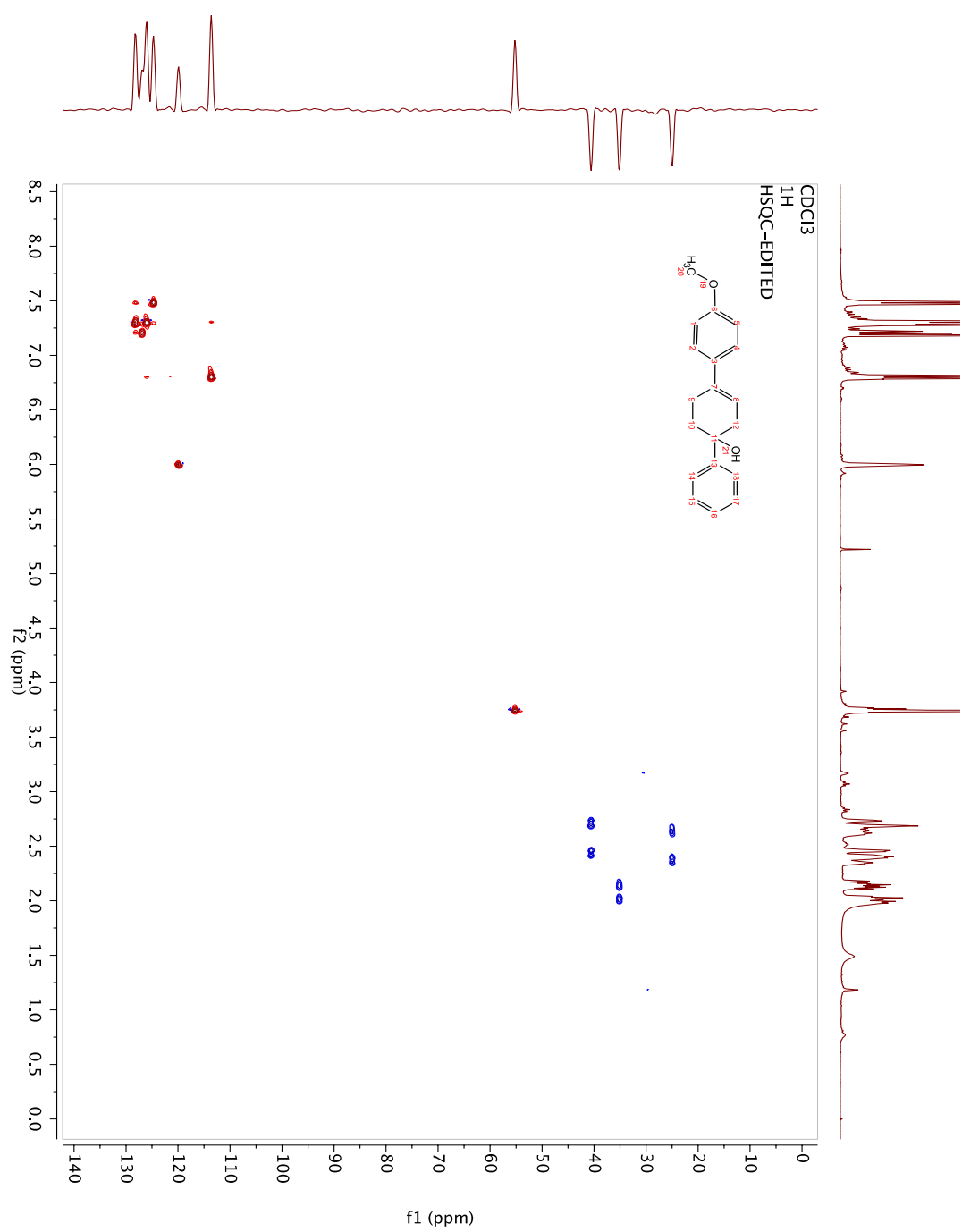
To a 0.045M solution of 1F in MeCN was added formic acid in variable amounts



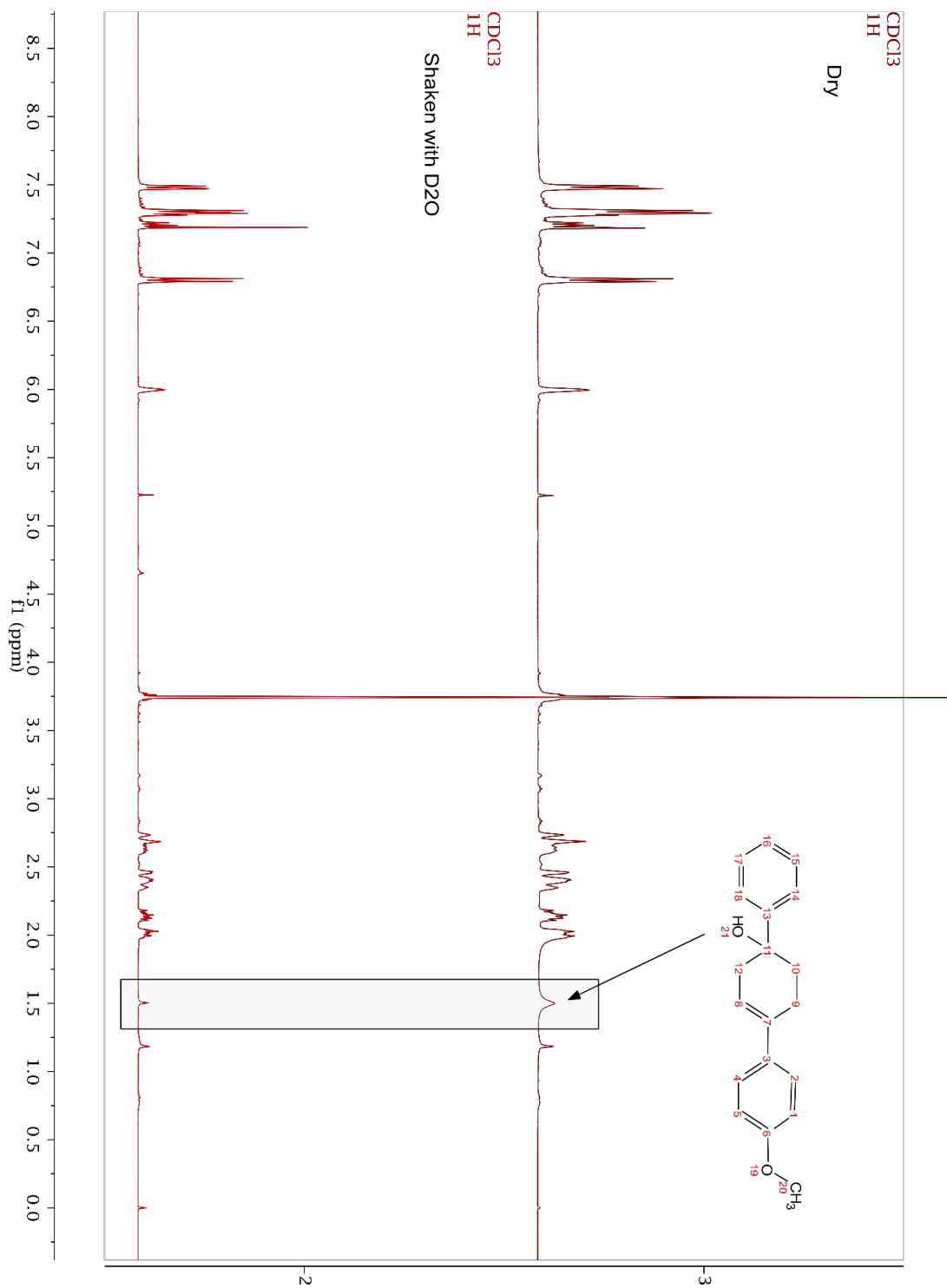
To a 0.045M solution of 1F in CDCl<sub>3</sub> was added formic acid in variable amounts. This change of solvent was used to emphasize hydrogen bonding, if present, and verify if the above titration result was due to hydrogen bonding.



HSQC of 1f to demonstrate the identity of the hydroxyl proton

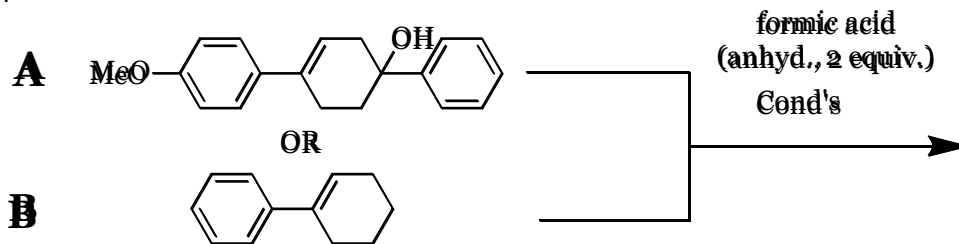


Deuterium exchange experiment with 4.3.1f to demonstrate the identity of the hydroxyl proton



### 4.12.3 Competition between 1-Ph-Cyclohexene and 4.3.1f

General procedure A was followed, except using 2 equivalents anhydrous formic acid (2 equiv., 2.5  $\mu$ L). The reactions were run either in the presence or absence of D<sub>2</sub>O (20 equiv. 40.5  $\mu$ L). Conversion was monitored by observing the disappearance of the vinylic proton via <sup>1</sup>H NMR.

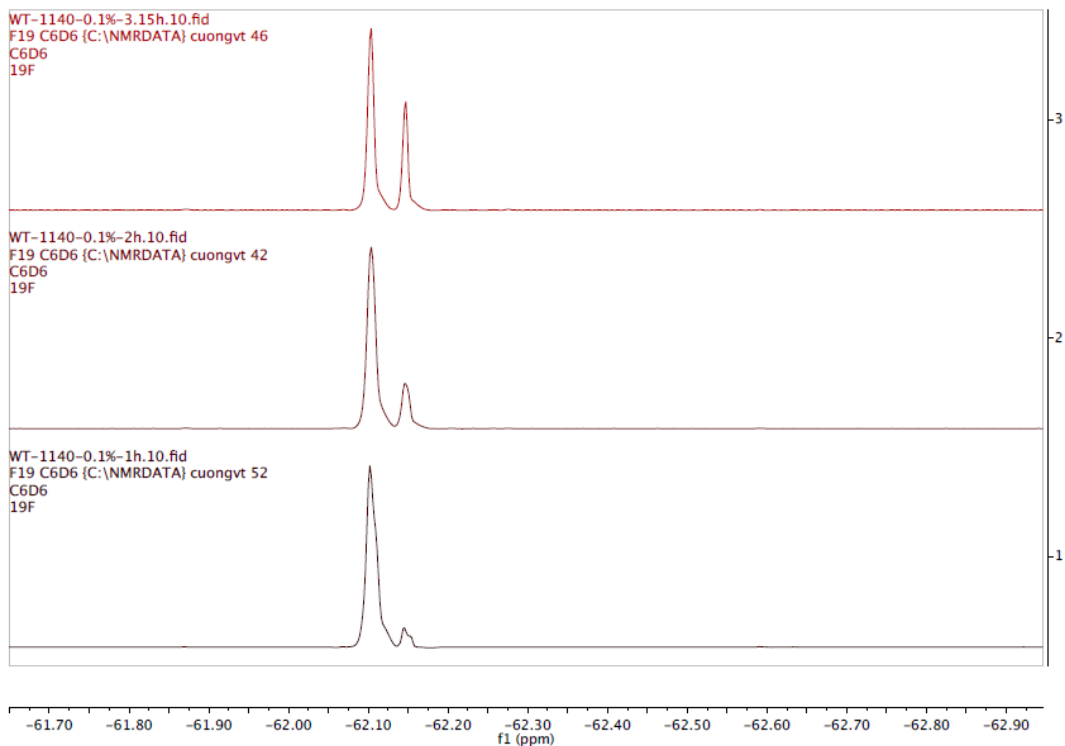


Substrate	A	A	B	B
anhydrous or D <sub>2</sub> O	a	D <sub>2</sub> O	D <sub>2</sub> O	a
time (minutes)	conversion (%)			
0	0	0	0	0
30	4	7	0	4
65	13	18	2	11
95	22	20	5	13
125	25	22	5	16
slope (error)	0.21 (0.010)	0.20 (0.017)	0.041 (0.0052)	0.14 (0.0070)

#### 4.12.4 Order of reactants:

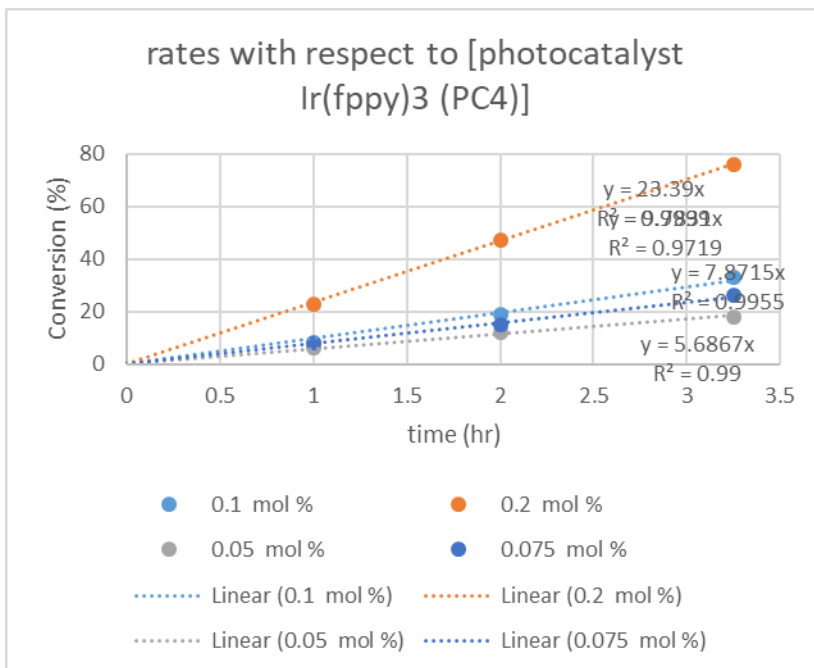
Order with respect to Photocatalyst:

General procedure F was followed with substrate 4.3.1A, except that the mol% photocatalyst was varied as shown. The conversion was measured by relative integration of  $^{19}\text{F}$  CF<sub>3</sub> signals.



time (hr)	Photocatalyst Loading (PC4)			
	0.2 mol %	0.1 mol %	0.075 mol %	0.05 mol %
	conv	conv	conv	conv
1	23	7	8	6
2	47	19	15	12
3.25	76	33	26	18
slope	23.39	9.78	7.87	5.69
slope error	0.08	0.55	0.15	0.15
order		1.26	1.11	1.02
		=LN(\$B10/C10)/LN(0.2/0.1))		
average order		1.13		
stddev		0.10		

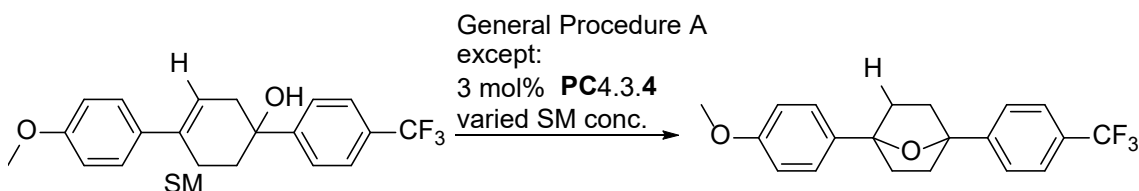




Order with respect to Substrate:

General Procedure A was followed, except as shown. Conversion monitored by watching the disappearance of the olefin proton via:  $^1\text{H}$  NMR

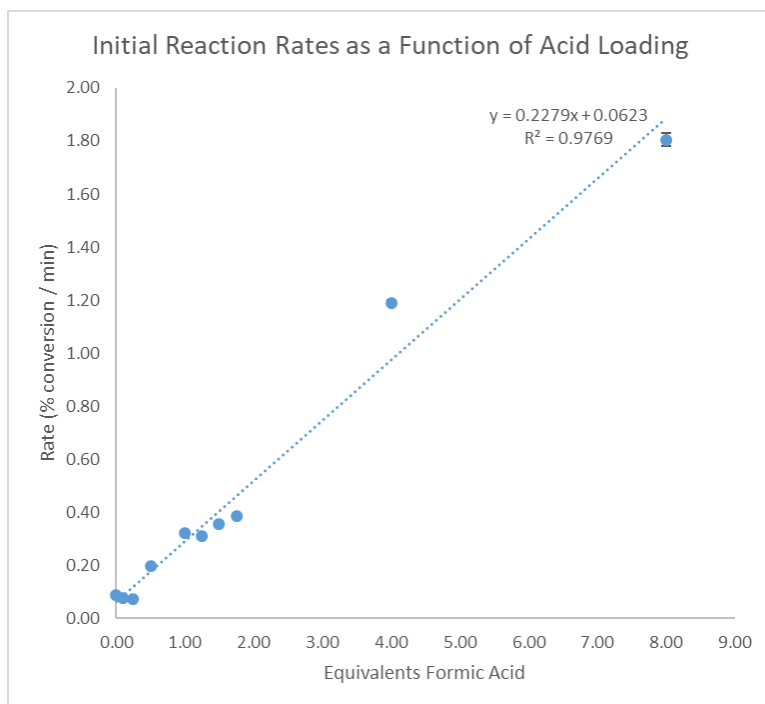
Using the logarithmic method, indicates that doubling the concentration of the substrate has little to no effect on the overall rate of the reaction. Hence, its order is, or is very near zero order.



time (min)	0.0072 mmol SM % conversion	-d[SM]/dt	0.0144 mmol SM % conversion	-d[SM]/dt
0	0	--	0	--
20	45	0.00972 mmol/h	19	0.00821 mmol/h
40	71	0.00767 mmol/h	35	0.00756 mmol/h

Rate Response to Acid Loading:

		eq formic											
		0.00	0.10	0.25	0.50	1.00	1.25	1.50	1.75	4.00	8.00		
time (m)	0	0	0	0	0	0	0	0	0	0	0	0	Time (min)
	10	2	1	0	0	2	4	5	5	18	29	15	
	20	1	2	0	2	4	6	8	8	35	55	30	
	30	1	1	0	5	7	10	13	13	54	80	45	
	40	3	3	3	7	12	12	16	15				
	50	4	2	4	9	15	15	18	19				
	60	9	3	4	13	22	17	23	25				
	70	7	3	4	15	21	22	27	27				
	80	10	8	5	17	31	23	28	29				
	90	9	8	8	20	33	24	35	35				
	100	6	7	7	21	33	32	36	39				
	110	10	12	9	22	35	36	40	42				
	120	9	7	9	25	39	44	43	47				
	130	12	10	9	25	40	37	47	50				
	150	15	11	11	28	47	45	50	59				
	170	13	16	14	33	53	54	59	64				
	slope		8.764E-02	7.754E-02	7.232E-02	1.972E-01	3.213E-01	3.109E-01	3.567E-01	3.863E-01	1.190E+00	1.805E+00	
slope error		0.47%	0.48%	0.27%	0.32%	0.65%	0.65%	0.45%	0.28%	0.87%	2.50%		



#### Kinetic evaluation

The observed rate expression is  $\text{Rate} = k^*[\text{Formic}][\text{Cat}]$ .

#### 4.12.5 Proton Inventory

General Procedure A was followed, except for the presence of either H<sub>2</sub>O or D<sub>2</sub>O, in triplicate (concurrently). To a clean, oven dried NMR tube, the cyclohexene starting material (0.0050 g, 0.0178 mmol, 1 equiv.), formic acid (0.036 mmol, 2 equiv.), Ir(Fppy)<sub>3</sub> stock solution (0.25 mM in anhydrous acetonitrile, 0.178 mL), and anhydrous acetonitrile (0.33 mL), and a deuterated benzene capillary were added. Solutions were degassed 10 minutes in the dark, at rt with argon bubbling. Conversions were measured via Bruker A400 1H NMR.

	Mol Fraction D2O			Mol Fraction D2O			Mol Fraction D2O			Mol Fraction D2O		
	0.0			0.1			0.2			0.5		
	A	B	C	A	B	C	A	B	C	A	B	C
0	0%	0%	0%	0%	0%	0%	0%	0%	0%	0%	0%	0%
20	3%	3%	6%	6%	2%	1%	1%	0%	2%	0%	10%	4%
40	6%	5%	3%	7%	3%	2%	3%	4%	2%	3%	9%	2%
60	13%	5%	6%	4%	7%	7%	4%	1%	1%	4%	18%	4%
80	16%	5%	6%	7%	7%	5%	5%	5%	13%	3%	10%	1%
100	17%	5%	7%	7%	13%	3%	11%	6%	14%	5%	20%	6%
160	22%	13%	10%	16%	16%	9%	15%	11%	8%	9%	13%	13%
220	24%	18%	13%	17%	21%	14%	17%	10%	9%	10%	16%	20%
280	34%	23%	18%	27%	30%	20%	27%	14%	48%	19%	23%	27%
slope	0.001283	0.000799	0.000646789	0.000904	0.00103	0.000650229	0.000893349	0.000522	0.001107798	0.000577	0.000945	0.000866972
slope error	8.6E-05	3.47E-05	4.59217E-05	5.92E-05	3.3E-05	4.45092E-05	4.07453E-05	3.8E-05	0.000221211	3.85E-05	0.00017	6.5653E-05
mole fraction D2O	0			0.1			0.2			0.5		
average slope/average slope0	1			0.94789916			0.924369748			0.875210084		
avgdev	0.024898063			0.014143731			0.021279307			0.014627931		
stddev	0.027132542			0.015907194			0.024208628			0.015838517		
max slope error	0.008595086			0.005915142			0.022121141			0.016968409		
total error	0.035727628			0.035727628			0.046329769			0.035727628		

	Mol Fraction D2O			Mol Fraction D2O		
	.8			1.0		
	A	B	C	A	B	C
	0%	I broke this tube	0%	0%	0%	0%
	1%		2%	2%	6%	3%
	2%		2%	-1%	9%	0%
	2%		5%	0%	5%	3%
	5%		7%	0%	8%	12%
	4%		5%	3%	10%	13%
	11%		10%	3%	13%	18%
	15%		16%	7%	4%	19%
	23%		21%	11%	13%	26%
slope	0.000718			0.000715596	0.00031	0.000517
slope error	4.33E-05		2.79967E-05	4.3E-05	0.000118	6.87452E-05
mole fraction D2O			0.8			1
average slope/average slope0			0.787815126			0.656722689
avgdev			0.000114679			0.024541284
stddev			0.000114679			0.027374568
max slope error			0.004333588			0.011776175
total error			0.035727628			0.039150743

#### 4.12.6 Calculations

Using Gaussian 09, dual dihedral coordinate scans were carried out at MP2/STO3G initially using the global minimum from a B3LYP/6-31+G optimization as a starting point. Finer detail of this cross section was generated at MP2/STO3G with the C<sup>1</sup> phenyl ring at 90 degrees, while varying the dihedral angle of the C<sup>4</sup> methoxyphenyl ring from -90 to 90 degrees in 2 degree increments. Geometries from the energy landscape were extracted for points of interest along the curve and optimizations were carried out in at MP2/cc-PVTZ theory level/basis set while holding the angle of the methoxyphenyl ring constant for these points. Vertical excitations were carried out as triplet state single point calculations of the optimized geometries generated in this way.

Gaussian 09, Revision C.01,

M. J. Frisch, G. W. Trucks, H. B. Schlegel, G. E. Scuseria,  
M. A. Robb, J. R. Cheeseman, G. Scalmani, V. Barone, B. Mennucci,  
G. A. Petersson, H. Nakatsuji, M. Caricato, X. Li, H. P. Hratchian,  
A. F. Izmaylov, J. Bloino, G. Zheng, J. L. Sonnenberg, M. Hada,  
M. Ehara, K. Toyota, R. Fukuda, J. Hasegawa, M. Ishida, T. Nakajima,  
Y. Honda, O. Kitao, H. Nakai, T. Vreven, J. A. Montgomery, Jr.,  
J. E. Peralta, F. Ogliaro, M. Bearpark, J. J. Heyd, E. Brothers,  
K. N. Kudin, V. N. Staroverov, T. Keith, R. Kobayashi, J. Normand,  
K. Raghavachari, A. Rendell, J. C. Burant, S. S. Iyengar, J. Tomasi,  
M. Cossi, N. Rega, J. M. Millam, M. Klene, J. E. Knox, J. B. Cross,  
V. Bakken, C. Adamo, J. Jaramillo, R. Gomperts, R. E. Stratmann,  
O. Yazyev, A. J. Austin, R. Cammi, C. Pomelli, J. W. Ochterski,  
R. L. Martin, K. Morokuma, V. G. Zakrzewski, G. A. Voth,  
P. Salvador, J. J. Dannenberg, S. Dapprich, A. D. Daniels,  
O. Farkas, J. B. Foresman, J. V. Ortiz, J. Cioslowski,  
and D. J. Fox, Gaussian, Inc., Wallingford CT, 2010.

## Cartesian Coordinates:

-90 deg mp2 ccptvz

C 4.26463 -0.98467 -0.05602  
C 4.96849 0.21922 0.01169  
C 4.26649 1.42824 0.04413  
C 2.87976 1.43197 0.01116  
C 2.15644 0.23410 -0.06605  
C 2.86898 -0.96469 -0.09056  
H 4.82961 2.34993 0.09311  
H 2.34625 2.37388 0.03415  
H 4.77926 -1.93268 -0.08422  
H 2.32989 -1.90233 -0.14675  
C -0.00178 0.21751 1.27253  
C -1.50040 0.48887 1.18821  
C -2.12409 -0.26964 0.01138  
C -1.51724 0.25061 -1.29371  
H 0.48280 0.95176 1.92039  
H 0.18437 -0.75405 1.74102  
H -1.67386 1.55774 1.05096  
H -1.99866 0.18632 2.10967  
H -1.90473 1.24888 -1.51232  
H -1.85125 -0.39827 -2.10656  
C 0.67580 0.24355 -0.07312  
C -0.01655 0.27486 -1.22537  
H 0.53588 0.30415 -2.15822  
O 6.32589 0.32114 0.04929  
C 7.04751 -0.89776 0.01718  
H 8.09653 -0.62483 0.05508  
H 6.80453 -1.52519 0.87634  
H 6.84967 -1.45164 -0.90201  
O -1.83227 -1.66319 0.14291  
H -0.90621 -1.76356 -0.11173  
C -3.62508 -0.11677 0.00154  
C -4.46688 -1.22971 0.05323  
C -5.85178 -1.06938 0.04536  
C -6.41454 0.20265 -0.01485  
C -5.58143 1.31885 -0.06727  
C -4.19882 1.15866 -0.05838  
H -4.02848 -2.21473 0.09917  
H -6.49016 -1.94175 0.08606  
H -7.48895 0.32473 -0.02126  
H -6.00622 2.31248 -0.11492  
H -3.56720 2.03706 -0.09909

-34 deg mp2 ccptvz

C 4.26772 -0.98708 -0.27067  
C 4.98075 0.17443 0.03399  
C 4.28169 1.35374 0.30624  
C 2.89606 1.37304 0.26970  
C 2.15724 0.22213 -0.04966  
C 2.87489 -0.95130 -0.30580  
H 4.84659 2.24515 0.54133  
H 2.38739 2.30556 0.47028  
H 4.77459 -1.91984 -0.46464  
H 2.33410 -1.86614 -0.51035  
C -0.06230 1.10364 0.86245  
C -1.55536 1.20287 0.56583  
C -2.12990 -0.16699 0.19353  
C -1.46684 -0.63463 -1.10240  
H 0.36803 2.10567 0.87405  
H 0.09780 0.70487 1.86844  
H -1.72220 1.89217 -0.26392  
H -2.08993 1.59051 1.43349  
H -1.84987 -0.05404 -1.94586  
H -1.75966 -1.67215 -1.28152  
C 0.68367 0.24259 -0.12539  
C 0.02724 -0.52163 -1.02327  
H 0.60905 -1.09118 -1.73941  
O 6.33730 0.25697 0.10054  
C 7.05306 -0.93360 -0.18027  
H 8.10342 -0.67832 -0.09165  
H 6.80953 -1.72066 0.53520  
H 6.84954 -1.28873 -1.19179  
O -1.84097 -1.10040 1.23670  
H -0.90148 -1.30839 1.15414  
C -3.62936 -0.10615 0.03849  
C -4.46975 -0.91985 0.80118  
C -5.85346 -0.84911 0.64618  
C -6.41653 0.03346 -0.27165  
C -5.58487 0.84897 -1.03716  
C -4.20345 0.77892 -0.88167  
H -4.03115 -1.60352 1.51167  
H -6.49067 -1.48620 1.24477  
H -7.49001 0.08649 -0.39053  
H -6.00984 1.53859 -1.75400  
H -3.57313 1.42053 -1.48432

-8 deg mp2 ccptvz

C 4.32866 -1.02044 -0.17272  
C 4.99074 0.18997 0.04930  
C 4.23734 1.35552 0.19467  
C 2.85349 1.31370 0.10782  
C 2.16193 0.11265 -0.12740  
C 2.93955 -1.04621 -0.25318  
H 4.75540 2.28724 0.37475  
H 2.31058 2.23942 0.22649  
H 4.87500 -1.94555 -0.27452  
H 2.46346 -2.00547 -0.39918  
C -0.05441 1.35520 0.13803  
C -1.54956 1.30094 -0.16207  
C -2.14303 -0.05000 0.23957  
C -1.48938 -1.12800 -0.62343  
H 0.37853 2.19336 -0.40996  
H 0.10847 1.57461 1.19721  
H -1.71713 1.45473 -1.22955  
H -2.06985 2.09583 0.37302  
H -1.86350 -1.05895 -1.64861  
H -1.79755 -2.10601 -0.24571  
C 0.68572 0.09087 -0.22608  
C 0.00651 -1.01524 -0.59926  
H 0.55744 -1.89949 -0.89387  
O 6.34036 0.33023 0.14702  
C 7.10721 -0.85261 -0.00045  
H 8.14405 -0.55031 0.09895  
H 6.86590 -1.58088 0.77546  
H 6.95338 -1.30475 -0.98154  
O -1.85685 -0.30440 1.61624  
H -0.91996 -0.53645 1.65444  
C -3.64245 -0.06276 0.07458  
C -4.48611 -0.35335 1.14883  
C -5.86988 -0.35986 0.97927  
C -6.42985 -0.07740 -0.26375  
C -5.59500 0.21322 -1.34134  
C -4.21345 0.22065 -1.17172  
H -4.04982 -0.57237 2.11124  
H -6.50958 -0.58669 1.82161  
H -7.50340 -0.08328 -0.39317  
H -6.01753 0.43400 -2.31229  
H -3.58083 0.44943 -2.01999

0 deg mp2 ccptvz

C 4.34861 -1.03543 -0.06629  
C 4.99214 0.20225 0.01786  
C 4.22100 1.36496 0.03110  
C 2.83772 1.29171 -0.04432  
C 2.16422 0.06115 -0.13697  
C 2.96000 -1.09210 -0.13704  
H 4.72443 2.31912 0.10241  
H 2.27963 2.21588 -0.02439  
H 4.90978 -1.95722 -0.07467  
H 2.50262 -2.06936 -0.19737  
C -0.05065 1.33005 -0.18900  
C -1.54020 1.20108 -0.49049  
C -2.14986 0.01511 0.25850  
C -1.49333 -1.26159 -0.26356  
H 0.40175 1.99626 -0.92542  
H 0.09009 1.81570 0.78107  
H -1.68830 1.05476 -1.56191  
H -2.06312 2.11422 -0.20467  
H -1.85764 -1.47933 -1.27140  
H -1.81042 -2.09516 0.36786  
C 0.68644 0.01234 -0.19864  
C 0.00312 -1.15088 -0.25934  
H 0.54863 -2.08561 -0.28251  
O 6.33975 0.37317 0.09246  
C 7.12436 -0.80713 0.08121  
H 8.15640 -0.47995 0.14567  
H 6.89227 -1.44558 0.93512  
H 6.97937 -1.37064 -0.84188  
O -1.88403 0.14858 1.65623  
H -0.95144 -0.07457 1.77238  
C -3.64702 -0.03696 0.08103  
C -4.50715 -0.02198 1.18106  
C -5.88853 -0.06993 0.99896  
C -6.42958 -0.13431 -0.28226  
C -5.57816 -0.15026 -1.38569  
C -4.19905 -0.10132 -1.20381  
H -4.08548 0.02754 2.17318  
H -6.54118 -0.05718 1.86157  
H -7.50130 -0.17177 -0.42127  
H -5.98594 -0.20048 -2.38630  
H -3.55329 -0.11377 -2.07271

This structure was found to have a twist in the cyclohexene dihedral angle, and was forced into planarity and reoptimized with modredundant freezes on dihedral angles for the cyclohexene ring and the C4-methoxyphenyl rotation angle to give the following structure, which is referenced in the energies as "unpuckered"



0 deg mp2/ccpvtz "unpuckered"  
C 4.35101223 -1.03699886 -0.05398961  
C 4.99350190 0.20318073 -0.10098595  
C 4.22025039 1.36194381 -0.17904529  
C 2.83577633 1.28179992 -0.21546103  
C 2.16310951 0.04791384 -0.17689751  
C 2.96127443 -1.10019087 -0.08719037  
H 4.72303237 2.31862925 -0.20903973  
H 2.27621449 2.20372015 -0.26940611  
H 4.91391696 -1.95545748 0.01115318  
H 2.50484583 -2.07884617 -0.04515215  
C -0.05522528 1.30612742 -0.29669550  
C -1.54464000 1.14237900 -0.60882600  
C -2.15059100 0.04134600 0.26281800  
C -1.49361133 -1.28428021 -0.15233235  
H 0.37871203 1.90042117 -1.10249864  
H 0.10656754 1.88057570 0.62010736  
H -1.69552800 0.88373600 -1.65840200  
H -2.06799300 2.08001300 -0.41936100  
H -1.84040352 -1.61937508 -1.13382023  
H -1.82137911 -2.03886732 0.56686436  
C 0.68441900 -0.00661400 -0.19975300  
C 0.00251600 -1.17046500 -0.13546900  
H 0.54855899 -2.10025513 -0.03963172  
O 6.34208230 0.38047787 -0.07371823  
C 7.12888195 -0.79560198 0.00765642  
H 8.16139563 -0.46371805 0.01744043  
H 6.91781976 -1.35122409 0.92274409  
H 6.96409428 -1.44316185 -0.85498915  
O -1.88104700 0.32174200 1.63790300  
H -0.94783500 0.11306100 1.77421100  
C -3.64817500 -0.03072200 0.09618700  
C -4.50524700 0.09925800 1.19101100  
C -5.88706700 0.03091100 1.01901100  
C -6.43159700 -0.16878200 -0.24669600  
C -5.58324000 -0.30009000 -1.34477100  
C -4.20369200 -0.23078700 -1.17308800  
H -4.08088500 0.25355700 2.17114900  
H -6.53732600 0.13385700 1.87737000  
H -7.50365000 -0.22181700 -0.37785300  
H -5.99374000 -0.45596700 -2.33331300  
H -3.56034800 -0.33410900 -2.03771100

60\_28 deg mp2 ccptvz

C 4.33710 -1.04912 0.16806  
C 4.98250 0.17003 -0.05264  
C 4.21764 1.31167 -0.30618  
C 2.83347 1.23675 -0.33062  
C 2.16169 0.02638 -0.09170  
C 2.94524 -1.10811 0.14410  
H 4.72991 2.24763 -0.48097  
H 2.26829 2.13840 -0.52252  
H 4.89795 -1.95444 0.34258  
H 2.46439 -2.06741 0.28229  
C -0.05015 0.97645 -0.93363  
C -1.52168 0.62758 -1.12340  
C -2.15395 0.21067 0.20810  
C -1.47358 -1.07079 0.69018  
H 0.44438 1.05961 -1.90327  
H 0.02738 1.96494 -0.47168  
H -1.61790 -0.19461 -1.83481  
H -2.06720 1.48199 -1.52522  
H -1.80323 -1.91606 0.07972  
H -1.81011 -1.27414 1.70951  
C 0.68810 -0.03230 -0.08836  
C 0.02167 -0.94769 0.64599  
H 0.59161 -1.62758 1.26883  
O 6.33226 0.34386 -0.05389  
C 7.11401 -0.80917 0.20629  
H 8.14761 -0.48184 0.17701  
H 6.89221 -1.22425 1.19079  
H 6.95491 -1.57598 -0.55359  
O -1.94735 1.24506 1.17294  
H -1.02605 1.16857 1.45258  
C -3.64235 0.00824 0.06659  
C -4.54822 0.71730 0.85813  
C -5.92044 0.51791 0.71318  
C -6.40637 -0.39178 -0.22208  
C -5.50892 -1.10428 -1.01564  
C -4.13903 -0.90422 -0.87168  
H -4.16913 1.42138 1.58279  
H -6.60913 1.07542 1.33373  
H -7.47105 -0.54522 -0.33259  
H -5.87376 -1.81431 -1.74555  
H -3.45670 -1.46591 -1.49708

90 deg mp2 ccptvz

C 4.34659 -1.05527 0.00544  
C 4.96358 0.19745 0.00907  
C 4.17781 1.35352 0.04004  
C 2.79411 1.25656 0.06653  
C 2.15740 0.00835 0.06947  
C 2.95319 -1.13672 0.03125  
H 4.67381 2.31419 0.04585  
H 2.19707 2.15961 0.09476  
H 4.92751 -1.96443 -0.01479  
H 2.47996 -2.11071 0.03114  
C 0.00277 -0.08196 -1.27269  
C -1.47911 -0.43504 -1.19457  
C -2.14394 0.27050 -0.00743  
C -1.51018 -0.23508 1.29066  
H 0.52639 -0.77909 -1.93102  
H 0.13628 0.90529 -1.72616  
H -1.59460 -1.51371 -1.07389  
H -1.99235 -0.14586 -2.11209  
H -1.84214 -1.25640 1.49358  
H -1.88007 0.38207 2.11260  
C 0.68009 -0.09246 0.07329  
C -0.01039 -0.17458 1.22417  
H 0.54215 -0.18272 2.15739  
O 6.31046 0.39693 -0.01457  
C 7.11674 -0.76770 -0.04534  
H 8.14379 -0.41947 -0.06174  
H 6.95682 -1.38435 0.84067  
H 6.92086 -1.36216 -0.93928  
O -1.92912 1.67964 -0.11802  
H -1.01061 1.82771 0.14073  
C -3.63431 0.03524 -0.00179  
C -4.53590 1.10096 -0.03766  
C -5.90992 0.86477 -0.03387  
C -6.40205 -0.43698 0.00648  
C -5.50895 -1.50646 0.04306  
C -4.13722 -1.27051 0.03823  
H -4.15220 2.10913 -0.06820  
H -6.59520 1.70131 -0.06216  
H -7.46814 -0.61792 0.00977  
H -5.87860 -2.52251 0.07522  
H -3.45834 -2.11344 0.06646

## synBoat MP2/cc-vptz

C	-2.20524	0.65437	1.29319
C	-1.72259	1.12518	0.05307
C	-2.43648	0.75249	-1.09972
C	-3.30889	-0.18189	1.3616
H	-1.69672	0.91909	2.21043
C	-3.98033	-0.57081	0.19823
H	-3.66908	-0.55192	2.31163
C	-3.53767	-0.09313	-1.04062
H	-4.0529	-0.3508	-1.95338
C	-0.56438	1.98864	-0.08621
C	0.29452	1.88625	-1.16679
H	-2.11972	1.16069	-2.05177
C	0.26496	2.42259	1.08712
C	1.52049	1.44731	1.06103
H	-0.26885	2.39202	2.03586
H	0.63449	3.44041	0.95213
C	1.45238	0.21105	0.10997
H	1.72406	1.03588	2.05076
H	2.38941	2.04077	0.77515
C	0.88174	0.53437	-1.3718
H	0.17896	-0.26753	-1.58546
H	1.67932	0.51866	-2.11204
H	1.06464	2.66055	-1.16946
O	0.6079	-0.77529	0.69597
O	-5.05059	-1.3892	0.37493
C	-5.72299	-1.81033	-0.80065
H	-5.05261	-2.35911	-1.46376
H	-6.52029	-2.46615	-0.4686
H	-6.15078	-0.9623	-1.33745
H	-0.28957	-0.41592	0.70643
C	2.83446	-0.38906	0.00362
C	3.85959	0.33	-0.62217
C	3.11787	-1.65624	0.51612
C	5.14046	-0.20208	-0.73113
H	3.65782	1.31298	-1.03118
C	4.40111	-2.19076	0.4056
H	2.32835	-2.21488	0.99509
C	5.41609	-1.468	-0.21548
H	5.91983	0.36821	-1.21833
H	4.60563	-3.17453	0.8064
H	6.41021	-1.885	-0.29972

final ether MP2/cc-pvtz

C 4.0247830362 -0.9593165114 -0.4513456739  
C 4.347175938 0.3446062122 -0.0637199133  
C 3.3303293687 1.2163787046 0.3309090711  
C 2.0058132461 0.7765331312 0.3394243926  
C 1.6747387532 -0.5193427007 -0.0503584981  
C 2.7035700764 -1.3819190084 -0.4468585979  
H 0.3444468452 -1.1996429913 2.15065667  
H 3.5491428591 2.2299375985 0.6297901249  
H 4.8243492453 -1.6194137751 -0.7576928962  
H 2.4723502269 -2.3930444299 -0.7569627253  
O -0.6600287581 0.1059613438 -0.0296324051  
C -0.2092875852 -1.8633818641 -1.183742278  
C -1.7313147292 -1.6002736517 -1.1692058269  
C -1.8736300402 -0.6643430588 0.0481548252  
C -1.6643323604 -1.4921895434 1.3314115623  
H 0.0467941493 -2.9133590765 -1.0507036342  
H 0.2477657089 -1.5093506184 -2.1056859878  
H -2.0501376851 -1.073224299 -2.0665100152  
H -2.3352681398 -2.5002712756 -1.0629341967  
H 1.2176599515 1.4513390444 0.6428285434  
H -1.9777248088 -0.9152905163 2.199356739  
H -2.2283486086 -2.4234618905 1.3125476893  
C 0.2642084452 -0.9989339449 0.0012398638  
C -0.1345124467 -1.7040304046 1.3136319565  
H 0.1673794547 -2.7503741861 1.3209214194  
O 5.6705079997 0.6665290916 -0.1087603357  
C 6.0070807689 1.986788472 0.2788116453  
H 5.7219282517 2.1815012531 1.3140571107  
H 7.0848381019 2.0612651437 0.1815210163  
H 5.5323574995 2.7242339674 -0.3705980397  
C -3.0750102357 0.2191991032 0.0175105283  
C -4.3102387492 -0.2624020631 0.4606238539  
C -5.4474308892 0.5386561195 0.3917772299  
C -5.3594463719 1.8334652134 -0.1161734794  
C -4.1298967462 2.3195937138 -0.5566164513  
C -2.9934905702 1.5162003499 -0.4950655054  
H -4.3839310706 -1.2649945222 0.8625490493  
H -6.3974934637 0.1549797954 0.7383193041  
H -6.2406149723 2.4583070609 -0.1652710907  
H -4.0548664704 3.3252472121 -0.9479554013  
H -2.0359752252 1.8860478013 -0.8334896433

antiChair\_coordinated to Fomic\_acid HF\_321G\_TS

O 1  
C -2.51794400 -0.87473100 1.46371700  
C -1.94468100 0.24025300 0.82411700  
C -2.62744800 0.79114600 -0.26514900  
C -3.68801300 -1.41790500 1.01585900  
H -2.02960700 -1.32106800 2.30443300  
C -4.34767700 -0.86011800 -0.08300600  
H -4.12941500 -2.27091600 1.48477000  
C -3.81009400 0.25079500 -0.71721000  
H -4.30815300 0.70196500 -1.54798900  
C -0.71385800 0.84181200 1.25129000  
C 0.05833900 1.69362600 0.41010000  
H -2.21840400 1.66046000 -0.73598100  
C 0.05985300 0.36121900 2.43841300  
C 1.13168100 -0.61409200 1.78658000  
H -0.50736800 -0.16181700 3.19392300  
H 0.60066900 1.18341200 2.88206700  
C 1.89030500 0.01259600 0.59358400  
H 0.63366200 -1.51791200 1.46231200  
H 1.85558900 -0.86688700 2.54893800  
C 0.90005400 0.64353300 -0.42068900  
H 0.27097000 -0.10875700 -0.87061300  
H 1.45563500 1.15647400 -1.18953000  
H 0.79029200 2.19781200 1.01978600  
C 2.76240400 -1.05577200 -0.06406700  
C 4.14025300 -0.96842500 0.04161300  
C 2.20798100 -2.12609300 -0.75485700  
C 4.95166800 -1.92913200 -0.53727400  
H 4.55706700 -0.14650300 0.58090900  
C 3.01783000 -3.08678500 -1.33241000  
H 1.14328300 -2.21645300 -0.84942400  
C 4.39505800 -2.99064400 -1.22629400  
H 6.01708900 -1.84634100 -0.44876900  
H 2.57566900 -3.90591200 -1.86482700  
O 2.71441200 1.05494400 1.14531100  
H 2.76516600 1.82104100 0.53833600  
O -5.50059000 -1.46160200 -0.44754700  
C -6.28344500 -0.99368200 -1.56728100  
H -5.71346800 -1.04476300 -2.48516700  
H -7.12636000 -1.66094500 -1.62078700  
H -6.62495000 0.01939400 -1.40299000  
H 5.02332300 -3.73404900 -1.67561100  
O 2.32018700 3.34301900 -0.65229100  
C 1.41413700 3.98284500 -1.18516400  
H 1.64232400 4.89168700 -1.72870500  
O 0.15114300 3.68895200 -1.18564800  
H -0.13266000 2.76488500 -0.50491700

Singlet Energies							
C4 angle	MP2/STO3G energy (Hartrees)	MP2/STO3G energy (kcal/mol - relative)	Boltzmann factor at 0 °C	Boltzmann factor at 25 °C	Boltzmann factor at 45 °C	% change 45 C to 25 C	% change 45 C to 0 C
-90	-871.172163	2.402920214	0.0120	0.0173	0.0224	22.5%	87.0%
-88	-871.172185	2.389491521	0.0123	0.0177	0.0228	22.4%	86.4%
-86	-871.172227	2.362759638	0.0129	0.0185	0.0238	22.2%	85.1%
-84	-871.17229	2.323352073	0.0138	0.0198	0.0254	21.8%	83.2%
-82	-871.172372	2.271959085	0.0152	0.0216	0.0275	21.4%	80.8%
-80	-871.172472	2.209333687	0.0171	0.0240	0.0304	20.9%	77.8%
-78	-871.172588	2.136668145	0.0195	0.0272	0.0341	20.3%	74.5%
-76	-871.172718	2.054903722	0.0227	0.0312	0.0388	19.6%	70.8%
-74	-871.172861	1.965232686	0.0268	0.0363	0.0447	18.8%	66.9%
-72	-871.173014	1.868847304	0.0320	0.0427	0.0520	18.0%	62.7%
-70	-871.173177	1.767002593	0.0386	0.0507	0.0611	17.1%	58.5%
-68	-871.173346	1.660953572	0.0469	0.0606	0.0723	16.2%	54.2%
-66	-871.173519	1.551955259	0.0573	0.0728	0.0859	15.2%	49.8%
-64	-871.173696	1.441262671	0.0703	0.0878	0.1023	14.2%	45.6%
-62	-871.173873	1.330193578	0.0862	0.1059	0.1220	13.2%	41.4%
-60	-871.174048	1.220002998	0.1057	0.1276	0.1452	12.1%	37.4%
-58	-871.174221	1.111883197	0.1289	0.1531	0.1723	11.1%	33.6%
-56	-871.174387	1.007277447	0.1563	0.1827	0.2033	10.1%	30.0%
-54	-871.174547	0.907378014	0.1879	0.2162	0.2381	9.2%	26.7%
-52	-871.174696	0.813377166	0.2235	0.2534	0.2762	8.3%	23.6%
-50	-871.174835	0.72652992	0.2622	0.2934	0.3169	7.4%	20.8%
-48	-871.17496	0.647840292	0.3032	0.3351	0.3589	6.6%	18.4%
-46	-871.175071	0.578437796	0.3445	0.3767	0.4005	6.0%	16.3%
-44	-871.175165	0.519138196	0.3843	0.4164	0.4399	5.4%	14.5%
-42	-871.175243	0.47063175	0.4202	0.4519	0.4750	4.9%	13.0%
-40	-871.175302	0.433420466	0.4500	0.4812	0.5038	4.5%	12.0%
-38	-871.175343	0.407755348	0.4718	0.5025	0.5247	4.2%	11.2%
-36	-871.175365	0.393573645	0.4843	0.5146	0.5366	4.1%	10.8%
-34	-871.17537	0.3904361	0.4871	0.5174	0.5393	4.1%	10.7%
-32	-871.175359	0.397840706	0.4805	0.5110	0.5330	4.1%	10.9%
-30	-871.175332	0.414657947	0.4658	0.4967	0.5190	4.3%	11.4%
-28	-871.175292	0.439570054	0.4449	0.4762	0.4989	4.6%	12.1%
-26	-871.175242	0.471008255	0.4199	0.4516	0.4747	4.9%	13.1%
-24	-871.175184	0.507152774	0.3929	0.4249	0.4484	5.2%	14.1%
-22	-871.175123	0.545807328	0.3659	0.3980	0.4218	5.6%	15.3%
-20	-871.175061	0.584838388	0.3405	0.3727	0.3965	6.0%	16.5%
-18	-871.175001	0.622112423	0.3179	0.3499	0.3738	6.4%	17.6%
-16	-871.174949	0.655056645	0.2992	0.3310	0.3548	6.7%	18.6%
-14	-871.174906	0.681976781	0.2847	0.3163	0.3400	7.0%	19.4%
-12	-871.174875	0.700990304	0.2749	0.3063	0.3300	7.2%	20.0%
-10	-871.17486	0.710842195	0.2699	0.3013	0.3249	7.3%	20.3%
-8	-871.17486	0.710591192	0.2701	0.3014	0.3250	7.3%	20.3%
-6	-871.174877	0.699923539	0.2754	0.3069	0.3305	7.2%	20.0%
-4	-871.174911	0.678901987	0.2863	0.3180	0.3417	6.9%	19.4%
-2	-871.174959	0.648279548	0.3029	0.3348	0.3587	6.6%	18.4%

Singlet Energies								
C4 angle	MP2/STO3G energy (Hartrees)	MP2/STO3G energy (kcal/mol - relative)	Boltzmann factor at 0 °C	Boltzmann factor at 25 °C	Boltzmann factor at 45 °C	% change 45 C to 25 C	% change 45 C to 0 C	
0	-871.175022	0.608871983	0.3257	0.3578	0.3817	6.3%	17.2%	
2	-871.175097	0.562122562	0.3550	0.3872	0.4110	5.8%	15.8%	
4	-871.175181	0.509537308	0.3911	0.4232	0.4467	5.3%	14.2%	
6	-871.175271	0.452810494	0.4342	0.4657	0.4886	4.7%	12.5%	
8	-871.175365	0.393573645	0.4843	0.5146	0.5366	4.1%	10.8%	
10	-871.175461	0.333709286	0.5408	0.5694	0.5899	3.5%	9.1%	
12	-871.175555	0.274660689	0.6029	0.6290	0.6476	2.9%	7.4%	
14	-871.175645	0.218184879	0.6690	0.6919	0.7081	2.3%	5.9%	
16	-871.175728	0.165725127	0.7369	0.7560	0.7694	1.7%	4.4%	
18	-871.175804	0.118599201	0.8037	0.8186	0.8290	1.3%	3.1%	
20	-871.175868	0.077999369	0.8662	0.8766	0.8839	0.8%	2.1%	
22	-871.175921	0.044992395	0.9205	0.9269	0.9313	0.5%	1.2%	
24	-871.17596	0.020519544	0.9629	0.9660	0.9681	0.2%	0.5%	
26	-871.175984	0.005271076	0.9903	0.9911	0.9917	0.1%	0.1%	
28	-871.175993	0	1.0000	1.0000	1.0000	0.0%	0.0%	
30	-871.175984	0.005208325	0.9905	0.9912	0.9918	0.1%	0.1%	
32	-871.175959	0.021147053	0.9618	0.9649	0.9671	0.2%	0.6%	
34	-871.175916	0.04812994	0.9151	0.9220	0.9267	0.5%	1.3%	
36	-871.175855	0.086156986	0.8532	0.8647	0.8726	0.9%	2.3%	
38	-871.175777	0.135165439	0.7796	0.7960	0.8075	1.4%	3.6%	
40	-871.175682	0.194778794	0.6985	0.7198	0.7349	2.0%	5.2%	
42	-871.175571	0.264620545	0.6142	0.6398	0.6580	2.8%	7.1%	
44	-871.175444	0.344125936	0.5305	0.5594	0.5802	3.6%	9.4%	
46	-871.175303	0.432416452	0.4508	0.4820	0.5046	4.5%	11.9%	
48	-871.17515	0.528676332	0.3776	0.4097	0.4333	5.5%	14.8%	
50	-871.174986	0.631838812	0.3122	0.3442	0.3681	6.5%	17.9%	
52	-871.174812	0.740837125	0.2554	0.2864	0.3098	7.6%	21.3%	
54	-871.174631	0.854353504	0.2072	0.2365	0.2589	8.7%	24.9%	
56	-871.174445	0.971383932	0.1670	0.1941	0.2151	9.8%	28.8%	
58	-871.174255	1.090610642	0.1341	0.1587	0.1782	10.9%	32.9%	
60	-871.174063	1.210904117	0.1074	0.1295	0.1473	12.1%	37.1%	
62	-871.173871	1.33100934	0.0861	0.1058	0.1218	13.2%	41.5%	
64	-871.173682	1.449796794	0.0692	0.0866	0.1009	14.3%	45.9%	
66	-871.173497	1.566199713	0.0558	0.0711	0.0840	15.3%	50.4%	
68	-871.173317	1.679088582	0.0453	0.0588	0.0702	16.3%	54.9%	
70	-871.173144	1.787459387	0.0371	0.0490	0.0592	17.3%	59.3%	
72	-871.17298	1.890308112	0.0307	0.0412	0.0503	18.2%	63.7%	
74	-871.172827	1.986567992	0.0257	0.0350	0.0432	19.0%	67.8%	
76	-871.172685	2.075297765	0.0219	0.0301	0.0375	19.8%	71.7%	
78	-871.172557	2.155556166	0.0189	0.0263	0.0331	20.4%	75.4%	
80	-871.172445	2.226339181	0.0165	0.0233	0.0296	21.0%	78.6%	
82	-871.172348	2.286768298	0.0148	0.0211	0.0269	21.5%	81.5%	
84	-871.17227	2.336027754	0.0135	0.0194	0.0248	22.0%	83.8%	
86	-871.172211	2.373239038	0.0126	0.0182	0.0234	22.3%	85.6%	
88	-871.172171	2.39777464	0.0121	0.0175	0.0225	22.5%	86.8%	
90	-871.172153	2.409069802	0.0118	0.0171	0.0221	22.6%	87.3%	
max	-871.172153		=EXP(-D94/(0.0019872041*273.15))=(G93-F93)/((G93))					
min	-871.175993							



Triplet Energies										
	c4 angle	MP2/cc-pvtz (Hartrees)	MP2/cc-pvtz (kcal/mol - relative)	MP2/cc-pvtz (kcal/mol - relative)	MP2/cc-pvtz (kcal/mol - relative to pdt)	Boltzmann factor at 0 °C	Boltzmann factor at 25 °C	Boltzmann factor at 45 °C	MP2/cc-pvtz (kcal/mol - forced distance relative to other triplets)	MP2/cc-pvtz (kcal/mol - triplet/ singlet gap)
	-90	-884.473037	30.3206435	126.1633827	88.9296435	124.103082				
	-34	-884.485216	22.68679723	118.5205365	81.28679723	118.283464				
	-8	-884.501476	12.48838523	108.3175915	71.0838523	107.299019				
	0	-884.502958	11.55363296	107.3873722	70.15363296	106.375401				
	28	-884.488677	20.51527724	116.3490165	79.11527724	116.349016				
	90	-884.472976	30.36748229	126.2012215	88.96748229	124.105906				
unpuckered	0	-884.52137	0	95.83373924	58.6	94.7861757				
max				-884.472976						
min				-884.52137						

Singlet Energies										
	c4 angle	MP2/cc-pvtz (Hartrees)	MP2/cc-pvtz (kcal/mol - relative)	MP2/cc-pvtz (kcal/mol - relative)	MP2/cc-pvtz (kcal/mol - relative to pdt)	Boltzmann factor at 0 °C	Boltzmann factor at 25 °C	Boltzmann factor at 45 °C	% change 45 C to 25 C	% change 45 C to 0 C
	-90	-883.809895	1.754891669	2.0603003	7.049436106	0.02246816	0.03088796	0.038434949	19.6%	71.1%
	-34	-883.812447	0.153455951	0.2370729	5.226208707	0.64612949	0.67023074	0.687303377	2.5%	6.4%
	-8	-883.810619	1.300386901	1.018672609	6.007708415	0.15312528	0.17921776	0.199671493	10.2%	30.4%
	0	-883.810505	1.309360279	1.011971214	6.00110702	0.1549989	0.18122574	0.201767278	10.2%	30.2%
	28	-883.812691	0	0	4.989135806	1	1	1	0.0%	0.0%
	90	-883.809849	1.783694333	2.095315302	7.084451108	0.02106455	0.02911542	0.036364163	19.9%	72.6%
unpuckered	0	-883.809849		-884.67242	6.036699331	0.1451615	0.17065953	0.19072229	10.5%	31.4%
max				-884.67075						
min				-884.67409						
			5.643000184							
	antiChair	-883.737949	52.54415236	51.6612472	51.6612472					
	synBoat	-883.728737	58.32470252	57.18953874	57.18953874					
	final product	-883.821684	0	0	0					
	max	-883.728737		-884.5909						
	min	-883.821684		-884.68204						

#### 4.12.7 References

1. Li, X.; Danishefsky, S. J., Cyclobutenone as a highly reactive dienophile: expanding upon Diels-Alder paradigms. *J. Am. Chem. Soc.* **2010**, *132* (32), 11004-11005.
2. Paton, R. S.; Kim, S.; Ross, A. G.; Danishefsky, S. J.; Houk, K. N., Experimental Diels-Alder Reactivities of Cycloalkenones and Cyclic Dienes Explained through Transition-State Distortion Energies. *Angew. Chem. Int. Ed.* **2011**, *123* (44), 10550-10552.
3. Ross, A. G.; Li, X.; Danishefsky, S. J., Intramolecular Diels-Alder reactions of cycloalkenones: translation of high endo selectivity to trans junctions. *J. Am. Chem. Soc.* **2012**, *134* (38), 16080-16084.
4. Medina, J. M.; McMahon, T. C.; Jimenez-Oses, G.; Houk, K. N.; Garg, N. K., Cycloadditions of cyclohexynes and cyclopentyne. *J. Am. Chem. Soc.* **2014**, *136* (42), 14706-9.
5. Shah, T. K.; Medina, J. M.; Garg, N. K., Expanding the Strained Alkyne Toolbox: Generation and Utility of Oxygen-Containing Strained Alkynes. *J. Am. Chem. Soc.* **2016**, *138* (14), 4948-4954.
6. Medina, J. M.; Ko, J. H.; Maynard, H. D.; Garg, N. K., Expanding the ROMP Toolbox: Synthesis of Air-Stable Benzonorbornadiene Polymers by Aryne Chemistry. *Macromolecules* **2017**, *50* (2), 580-586.
7. Blackman, M. L.; Royzen, M.; Fox, J. M., Tetrazine ligation: fast bioconjugation based on inverse-electron-demand Diels-Alder reactivity. *J. Am. Chem. Soc.* **2008**, *130* (41), 13518-13519.
8. Tasdelen, M. A.; Yagci, Y., Light-induced click reactions. *Angew. Chem. Int. Ed.* **2013**, *52* (23), 5930-8.
9. Arumugam, S.; Popik, V. V., Light-induced hetero-Diels-Alder cycloaddition: a facile and selective photoclick reaction. *J. Am. Chem. Soc.* **2011**, *133* (14), 5573-9.
10. Wang, Y.; Song, W.; Hu, W. J.; Lin, Q., Fast alkene functionalization in vivo by Photoclick chemistry: HOMO lifting of nitrile imine dipoles. *Angew. Chem. Int. Ed.* **2009**, *48* (29), 5330-5333.
11. Hoyle, C. E.; Lowe, A. B.; Bowman, C. N., Thiol-click chemistry: a multifaceted toolbox for small molecule and polymer synthesis. *Chem. Soc. Rev.* **2010**, *39* (4), 1355-1387.
12. Poloukhine, A. A.; Mbua, N. E.; Wolfert, M. A.; Boons, G. J.; Popik, V. V., Selective labeling of living cells by a photo-triggered click reaction. *J. Am. Chem. Soc.* **2009**, *131* (43), 15769-76.
13. Corey, E. J.; Tada, M.; LaMahieu, R.; Libit, L., trans-2-Cycloheptenone. *J. Am. Chem. Soc.* **1965**, *87* (9), 2051-2052.
14. Singh, A.; Fennell, C. J.; Weaver, J. D., Photocatalyst size controls electron and energy transfer: selectable E/Z isomer synthesis via C-F alkenylation. *Chem. Sci.* **2016**, *7* (11), 6796-6802.
15. Singh, K.; Staig, S. J.; Weaver, J. D., Facile synthesis of Z-alkenes via uphill catalysis. *J. Am. Chem. Soc.* **2014**, *136* (14), 5275-8.
16. Singh, K.; Fennell, C. J.; Coutsias, E. A.; Latifi, R.; Hartson, S.; Weaver, J. D., Light Harvesting for Rapid and Selective Reactions: Click Chemistry with Strain-Loadable Alkenes. *Chem-US* **2018**, *4* (1), 124-137.
17. Wei, X.-J.; Boon, W.; Hessel, V.; Noël, T., Visible-Light Photocatalytic Decarboxylation of  $\alpha,\beta$ -Unsaturated Carboxylic Acids: Facile Access to Stereoselective Difluoromethylated Styrenes in Batch and Flow. *ACS Catalysis* **2017**, *7* (10), 7136-7140.

18. Straathof, N. J. W.; Cramer, S. E.; Hessel, V.; Noël, T., Practical Photocatalytic Trifluoromethylation and Hydrotrifluoromethylation of Styrenes in Batch and Flow. *Angew. Chem. Int. Ed.* **2016**, *55* (50), 15549-15553.
19. Lin, Q.-Y.; Xu, X.-H.; Qing, F.-L., Chemo-, Regio-, and Stereoselective Trifluoromethylation of Styrenes via Visible Light-Driven Single-Electron Transfer (SET) and Triplet–Triplet Energy Transfer (TTET) Processes. *J Org Chem* **2014**, *79* (21), 10434-10446.
20. Metternich, J. B.; Gilmour, R., A Bio-Inspired, Catalytic E → Z Isomerization of Activated Olefins. *J. Am. Chem. Soc.* **2015**, *137* (35), 11254-11257.
21. Metternich, J. B.; Gilmour, R., One Photocatalyst, n Activation Modes Strategy for Cascade Catalysis: Emulating Coumarin Biosynthesis with (–)-Riboflavin. *J. Am. Chem. Soc.* **2016**, *138* (3), 1040-1045.
22. Metternich, J. B.; Gilmour, R., Photocatalytic E → Z Isomerization of Alkenes. *Synlett* **2016**, *27* (18), 2541-2552.
23. Fabry, D. C.; Ronge, M. A.; Rueping, M., Immobilization and Continuous Recycling of Photoredox Catalysts in Ionic Liquids for Applications in Batch Reactions and Flow Systems: Catalytic Alkene Isomerization by Using Visible Light. *Chem-Eur J* **2015**, *21* (14), 5350-5354.
24. Rackl, D.; Kreitmeier, P.; Reiser, O., Synthesis of a polyisobutylene-tagged fac-Ir(ppy)<sub>3</sub> complex and its application as recyclable visible-light photocatalyst in a continuous flow process. *Green Chem* **2016**, *18* (1), 214-219.
25. Stoll, M.; Hulstkamp, J.; Rouvé, A., Synthèses de produits macrocycliques à odeur musquée. 8e communication Synthèse de la civettone naturelle. *Helv. Chim. Acta* **1948**, *31* (2), 543-553.
26. Marshall, J., Trans-cycloalkenes and [a.b]betweenanenes, molecular jump ropes and double bond sandwiches. *Accounts Chem Res* **1980**, *13* (7), 213-218.
27. Cope, A. C.; Pike, R. A.; Spencer, C. F., Cyclic Polyolefins. XXVII. cis- and trans-Cycloöctene from N,N-Dimethylcycloöctylamine. *J. Am. Chem. Soc.* **1953**, *75* (13), 3212-3215.
28. Wallraff, G. M.; Michl, J., Low-temperature reactions of copper(I) triflate complexes of cis- and trans-cyclooctene cis- and trans-cycloheptene with trimethyl phosphite. Spectroscopic evidence for free trans-cycloheptene. *J Org Chem* **1986**, *51* (10), 1794-1800.
29. Inoue, Y.; Ueoka, T.; Kuroda, T.; Hakushi, T., Singlet photosensitization of simple alkenes. Part 4. cis-trans Photoisomerization of cycloheptene sensitized by aromatic esters. Some aspects of the chemistry of trans-cycloheptene. *J. Chem. Soc., Perkin Trans. 2* **1983**, *0* (7), 983-988.
30. Bonneau, R.; Jousot-Dubien, J.; Salem, L.; Yarwood, A. J., A trans cyclohexene. *J. Am. Chem. Soc.* **1976**, *98* (14), 4329-4330.
31. Dauben, W. G.; Van Riel, H. C. H. A.; Hauw, C.; Leroy, F.; Jousot-Dubien, J.; Bonneau, R., Photochemical formation of trans-1-phenylcyclohexene. Chemical proof of structure. *J. Am. Chem. Soc.* **1979**, *101* (7), 1901-1903.
32. Kropp, P. J., Photochemistry of cycloalkenes. V. Effects of ring size and substitution. *J. Am. Chem. Soc.* **1969**, *91* (21), 5783-5791.
33. Rosenberg, H. M.; Serve, M. P., Photolysis of 1-phenylcyclohexene in methanol. *J Org Chem* **1972**, *37* (1), 141-142.
34. Schuster, D. I.; Brown, R. H.; Resnick, B. M., Photochemistry of ketones in solution. 53. Stereospecific triplet-state photorearrangements of chiral 2-cyclohexenones: type A lumiketone rearrangement and phenyl migrations. *J. Am. Chem. Soc.* **1978**, *100* (14), 4504-4512.
35. Cozens, F. L.; McClelland, R. A.; Steenken, S., Observation of cationic intermediates in the photolysis of 1-phenylcyclohexene. *J. Am. Chem. Soc.* **1993**, *115* (12), 5050-5055.

36. Nikolai, J.; Loe, Ø.; Dominiak, P. M.; Gerlitz, O. O.; Autschbach, J.; Davies, H. M. L., Mechanistic Studies of UV Assisted [4 + 2] Cycloadditions in Synthetic Efforts toward Vibsanin E. *J. Am. Chem. Soc.* **2007**, *129* (35), 10763-10772.
37. Dorr, H.; Rawal, V. H., The Intramolecular Diels–Alder Reactions of Photochemically Generated trans-Cycloalkenones. *J. Am. Chem. Soc.* **1999**, *121* (43), 10229-10230.
38. Jin, S.; Nguyen, V. T.; Dang, H. T.; Nguyen, D. P.; Arman, H. D.; Larionov, O. V., Photoinduced Carboborative Ring Contraction Enables Regio- and Stereoselective Synthesis of Multiply Substituted Five-Membered Carbocycles and Heterocycles. *J. Am. Chem. Soc.* **2017**, *139* (33), 11365-11368.
39. Rono, L. J.; Yayla, H. G.; Wang, D. Y.; Armstrong, M. F.; Knowles, R. R., Enantioselective Photoredox Catalysis Enabled by Proton-Coupled Electron Transfer: Development of an Asymmetric Aza-Pinacol Cyclization. *J. Am. Chem. Soc.* **2013**, *135* (47), 17735-17738.
40. Lian, J.-J.; Chen, P.-C.; Lin, Y.-P.; Ting, H.-C.; Liu, R.-S., Gold-Catalyzed Intramolecular [3 + 2]-Cycloaddition of Arenyne-Yne Functionalities. *J. Am. Chem. Soc.* **2006**, *128* (35), 11372-11373.
41. Monkman, A. P.; Burrows, H. D.; Hamblett, I.; Navarathnam, S.; Svensson, M.; Andersson, M. R., The effect of conjugation length on triplet energies, electron delocalization and electron–electron correlation in soluble polythiophenes. *J. Chem. Phys.* **2001**, *115* (19), 9046-9049.
42. Flamigni, L.; Barbieri, A.; Sabatini, C.; Ventura, B.; Barigelletti, F., Photochemistry and Photophysics of Coordination Compounds: Iridium. In *Photochemistry and Photophysics of Coordination Compounds II*, Balzani, V.; Campagna, S., Eds. Springer Berlin Heidelberg: Berlin, Heidelberg, 2007; pp 143-203.
43. Dexter, D. L., A Theory of Sensitized Luminescence in Solids. *J. Chem. Phys.* **1953**, *21* (5), 836-850.
44. Head-Gordon, M.; Pople, J. A.; Frisch, M. J., MP2 energy evaluation by direct methods. *Chem. Phys. Lett.* **1988**, *153* (6), 503-506.
45. Cramer, C., Essentials of Computational Chemistry: Theories and Models. II ed.; John Wiley & Sons: 2004; p 216.
46. Dunning, T. H., Gaussian basis sets for use in correlated molecular calculations. I. The atoms boron through neon and hydrogen. *J. Chem. Phys.* **1989**, *90* (2), 1007-1023.
47. Banister, S. D.; Arnold, J. C.; Connor, M.; Glass, M.; McGregor, I. S., Dark Classics in Chemical Neuroscience:  $\Delta^9$ -Tetrahydrocannabinol. *ACS Chemical Neuroscience* **2019**, *10* (5), 2160-2175.
48. Teegardin, K.; Day, J. I.; Chan, J.; Weaver, J., Advances in Photocatalysis: A Microreview of Visible Light Mediated Ruthenium and Iridium Catalyzed Organic Transformations. *Org. Process Res. Dev.* **2016**, *20* (7), 1156-1163.
49. Johnson, R. P.; DiRico, K. J., Ab Initio Conformational Analysis of trans-Cyclohexene. *J. Org. Chem.* **1995**, *60* (4), 1074-1076.
50. Bally, T.; Rablen, P. R., Quantum-Chemical Simulation of <sup>1</sup>H NMR Spectra. 2. Comparison of DFT-Based Procedures for Computing Proton–Proton Coupling Constants in Organic Molecules. *J. Org. Chem.* **2011**, *76* (12), 4818-4830.
51. Anslyn, E.; Dougherty, D., Isotope Effects. In *Modern Physical Organic Chemistry*, University Science Books: 2006; pp 429-430.
52. Chandrasekhar, S.; Chandrashekar, G.; Reddy, M. S.; Srihari, P., A facile and chemoselective conjugate reduction using polymethylhydrosiloxane (PMHS) and catalytic B(C<sub>6</sub>F<sub>5</sub>)<sub>3</sub>. *Organic & Biomolecular Chemistry* **2006**, *4* (9), 1650-1652.

53. Günther, H., Chemical Shifts Through Hydrogen Bonding. In *NMR Spectroscopy*, John Wiley & Sons: 1995; pp 97-99.
54. See SI for details.
55. Gopalakrishnan, G.; Hogg, J. L., Differentiation of nucleophilic and general base catalysis in hydrolysis of N-acetylbenzotriazole using the proton inventory technique. *J Org Chem* **1981**, *46* (24), 4959-4964.
56. Corona-Martinez, D. O.; Taran, O.; Yatsimirsky, A. K., Mechanism of general acid-base catalysis in transesterification of an RNA model phosphodiester studied with strongly basic catalysts. *Org. Biomol. Chem.* **2010**, *8* (4), 873-880.
57. Plata, R. E.; Singleton, D. A., A Case Study of the Mechanism of Alcohol-Mediated Morita Baylis–Hillman Reactions. The Importance of Experimental Observations. *J. Am. Chem. Soc.* **2015**, *137* (11), 3811-3826.
58. Winter, A., Making a bad calculation. *Nature Chem.* **2015**, *7*, 473.
59. Pettersen, E. F.; Goddard, T. D.; Huang, C. C.; Couch, G. S.; Greenblatt, D. M.; Meng, E. C.; Ferrin, T. E., UCSF Chimera--a visualization system for exploratory research and analysis. *J. Comput. Chem.* **2004**, *25* (13), 1605-12.
60. Singh, A.; Teegardin, K.; Kelly, M.; Prasad, K. S.; Krishnan, S.; Weaver, J. D., Facile synthesis and complete characterization of homoleptic and heteroleptic cyclometalated Iridium(III) complexes for photocatalysis. *Journal of Organometallic Chemistry* **2015**, *776*, 51-59.
61. Bally, T.; Rablen, P. R., Quantum-Chemical Simulation of <sup>1</sup>H NMR Spectra. 2. Comparison of DFT-Based Procedures for Computing Proton–Proton Coupling Constants in Organic Molecules. *The Journal of Organic Chemistry* **2011**, *76* (12), 4818-4830.

## CHAPTER V

### SOLUBILITY OF IRIIDIUM AND RUTHENIUM ORGANOMETALLIC PHOTOREDOX CATALYSTS

#### 5.1 Overview



This chapter is adapted from *Org. Process Res. Dev.* **2019**, 23, 5, 1087. While I played a role in this investigation, the extent of my involvement was predominantly a supervisory role. I made recommendations and oversaw progress, but all accolades that can be afforded from this publication go to the primary authors, undergraduate researchers Daniel Jespersen and Brockton Keen, with lesser contributions from Duncan Mullins and Justin Briles. Anuradha Singh also contributed experimentally.

#### 5.2 Introduction

Recently, the footprint of photocatalysis has grown exponentially. Given the generally mild reaction conditions, many photocatalytic reactions are remarkable tolerant of functional groups, and as such have been used as a means of synthesis of complex organic molecules,<sup>75, 158, 283-288</sup> such as the synthetic core building block for the hepatitis-C drug elbasvir developed by the groups of DiRocco and Knowles,<sup>289</sup> or the perfluoroalkylated (hetero)aryl building blocks developed by the Stephenson group.<sup>290</sup> To date, however, no published industrial process has implemented any of the recently developed photocatalytic methods. As more photocatalysts are developed and give rise to a multitude of new reactions, the need for physical data regarding these catalysts increa

increases.<sup>75</sup> Unfortunately, these physical data are frequently absent from the literature, or reported in isolation, preventing logical comparisons between potential catalysts. In fact, we have often observed in the literature the excessive use photocatalysts beyond their solubility limits. Given the low natural abundance<sup>13, 291</sup> in the earth's crust and thus the exotic nature of iridium and ruthenium, any iridium or ruthenium-based photocatalyst used in a commercial process would need to be highly efficient. As such, awareness of the maximum photocatalyst concentration provides a clear starting point from which to initiate a reaction process. To help address this dearth of information, we provide herein solubility data for a wide

range of iridium-, and ruthenium-based photocatalysts in relevant solvents, and demonstrate how knowledge of this information can lead to improvements in catalyst efficiency within reactions from the literature.

The solubility of photocatalysts in various solvents is an important aspect of reactions. Too little catalyst will result in a suboptimal rate, as the low concentration cannot fully utilize the amount of light given it. On the other hand, at a high enough photocatalyst concentration, the penetration of light into the reaction vessel will become negligible, wherein almost all of the photons are absorbed by the photocatalysts very near the interface between the vessel and the reaction mixture, again retarding rates of reaction. To a large extent, this situation can be circumvented by use of a photo-flow setup, in which the path length of the light is kept very small by flowing the light absorbing reaction mixture through a small tube. At even higher concentrations, the photocatalysts precipitate. The precipitated photocatalysts almost certainly play no significant role in the reactions.<sup>40, 292</sup> In addition to significant monetary waste, in reference to the high cost of iridium or ruthenium catalysts discussed in this study, misinterpretation of the data can occur that can affect the development of the reaction. For instance, the catalyst loading is often used to make inferences about its effect on the reaction rate. However, this interpretation is highly suspect if the solubility limit of the photocatalyst is exceeded, because while the loading went up, the concentration remained constant. Finally, understanding of the solubility of the photocatalysts can heavily influence the choice of solvent used for purification or recovery of the photocatalysts, which becomes more important with scale.

### 5.3 Experimental

We limited the purview of this study to only commercially available, commonly implemented photocatalysts that are analogs to *fac*-Ir(ppy)<sub>3</sub> and Ru(bpy)<sub>3</sub>PF<sub>6</sub>. The solvents used in this study were those determined to be generally useful or commonly used in the laboratory setting.<sup>293</sup>

#### General Procedure A

For each solvent which could support a concentration greater than 1 ppt (part per thousand) of photocatalyst, ~1.5±0.1 mg of each catalyst was weighed into an 8 mL test tube. Solvent was incrementally added and after each subsequent addition, the mixture

was sonicated and centrifuged. An average time of sonication was 4 minutes. The necessary centrifugation time varied widely, depending on the solvent used, ranging from 2-4 minutes.<sup>26</sup> After centrifugation, the tube was inspected visually for particulate photocatalyst. If particulates were observed, additional solvent was added and the process repeated. Once a homogenous mixture was reached by visual examination, the mixture was centrifuged for a period of 60 minutes to ensure homogeneity. Due to the propensity for rapid evaporation of the more volatile solvents, it was necessary to measure the final volume of the solution in order to ensure an accurate result of the concentration at the end of the experiment.

### **General Procedure B**

For measuring in relatively nonsolvating solvents, general procedure A would be followed to the point that additional solvent could not be safely transferred into the test tube. The solution would then be capped with a septum and centrifuged for between 30 and 60 minutes. A majority of the supernatant would be removed, leaving enough to prevent disturbance of the precipitant photocatalyst. This would be repeated until there was no visual evidence of photocatalyst suspended in solution after centrifugation.

### **General Procedure C**

Into a clean 8 mL test tube was weighed  $\sim 1.0 \pm 0.1$  mg of photocatalyst. A solvent experimentally determined to readily solvate the photocatalyst was used to create a serial dilution. The solvent was then removed from the diluted solutions by evaporation and high vacuum in order to obtain an accurately weighed, small amount of photocatalyst. General Procedure A or B was then implemented.

### **General Procedure D**

For solvents in which less than 1 ppt photocatalyst was soluble, a different method was employed in order to avoid the use of copious amounts of solvent. To begin, each photocatalyst was dissolved in a clear, colorless, previously determined solvent in which it was highly soluble, and then serially diluted to 1000, 100, 10, and 1 ppm (part per million). To a new tube, an amount of solid photocatalyst ( $\sim 1$  mg) was added to each of the solvents. The heterogeneous mixture was then sonicated and centrifuged. Afterwards, the intensity of the color of the supernatant was then compared to the intensity of the solutions of known concentration, i.e. 1000, 100, 10, and 1 ppm (part per million). The solubility of each photocatalyst was then determined by comparison to the standard solutions, operating under the assumption that the color vibrancy, or intensity of emission, of each photocatalyst is constant across all solvents which appears reasonable based on our experience.

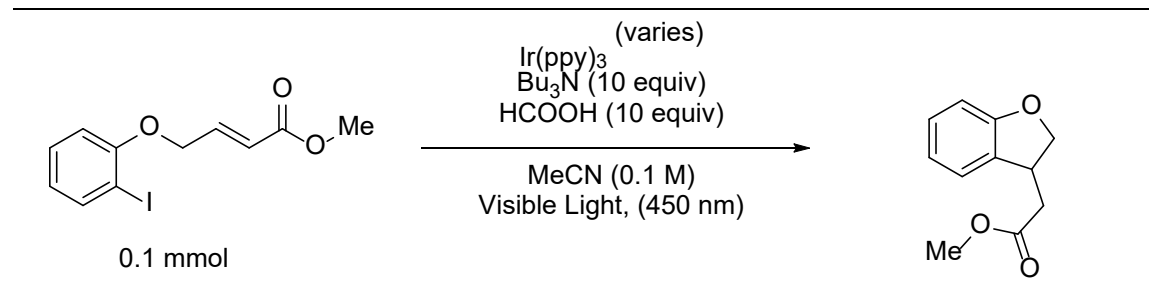
### **Photocatalytic Reaction Procedure**

All reagents were either obtained from commercial suppliers or synthesized according to literature methods. The majority of the photocatalysts used in the study were obtained through commercial sources, while some were synthesized using literature



methods.<sup>294</sup> Photocatalytic reactions were conducted in a light bath of blue LEDs (450 nm).

**Scheme 37:** Testing rates for the supersaturated literature reaction against variable concentrations of photocatalyst



A dry NMR tube was charged with reagents as indicated above (Scheme 37), varying the loading of photocatalyst. The reaction mixtures were sonicated to ensure homogeneity prior to introduction into the light bath. The reaction mixtures were monitored at the indicated timepoints by NMR spectroscopy and GCMS analysis of aliquots of the reaction mixture.<sup>42</sup>

#### 5.4 Discussion

While the primary purpose of this study is to provide important physical data on these photocatalysts, it would be fruitful to reassess reactions found in the literature making use of these catalysts. For example, the Stephenson group's 2012 paper concerning the harnessing of iodides for radical cyclization was found to be supersaturated with respect to photocatalyst, according to the data recorded in this study.<sup>295</sup> One of these reactions was recreated on a reduced scale and in tandem, implementing a range of catalyst loadings bounded by the concentration given in the procedure and concentrations less than the maximum presented in this study. Indeed, neither the initial rate, nor overall conversion of each reaction was observed to have any significant dependence on the concentration of the photocatalyst in the range between 0.25 mol% and 2.5 mol% reported in the original work. This finding demonstrates that judicious application of the solubility data for the photocatalysts presented here could represent a significant economic advantage, in addition to the obvious prudence toward ecological and earth abundance concerns.

In order to render the data more applicable in an industrial setting, an additional study was conducted in order to determine the solubility of certain representative photocatalysts in binary solutions of acetonitrile and water of varying mole fraction. The resulting data is presented below and in the respective tables pertaining to each photocatalyst. For charged species, the response to the use of a binary solvent system appears to correlate linearly with regard to the combination of the solubilities of those solvents (Figure 9). For the neutral *fac*-Ir(ppy)<sub>3</sub>, however, while the method of determination of solubility precludes the inclusion of explicit values, and requires reporting

as a range, the intensity of the coloration qualitatively diminishes with increasing mole fraction of water.

Solubility of Specific Photocatalysts in Binary Solutions of Acetonitrile and Water (Molar)	1:1 Acetonitrile:Water (v:v)	2:1 Acetonitrile:Water (v:v)	4:1 Acetonitrile:Water (v:v)	Acetonitrile
Mole Fraction of Acetonitrile	0.257	0.409	0.580	1.00
$\text{Ir}[\text{dF}(\text{CF}_3)\text{ppy}]_2(\text{dtbby})\text{PF}_6$	$3.6 \times 10^{-3}$	$8.5 \times 10^{-3}$	$6.1 \times 10^{-2}$	$1.3 \times 10^{-1}$
$\text{Ru}(\text{bpy})_3(\text{PF}_6)_2$	$1.3 \times 10^{-2}$	$1.7 \times 10^{-2}$	$4.4 \times 10^{-2}$	$1.4 \times 10^{-1}$

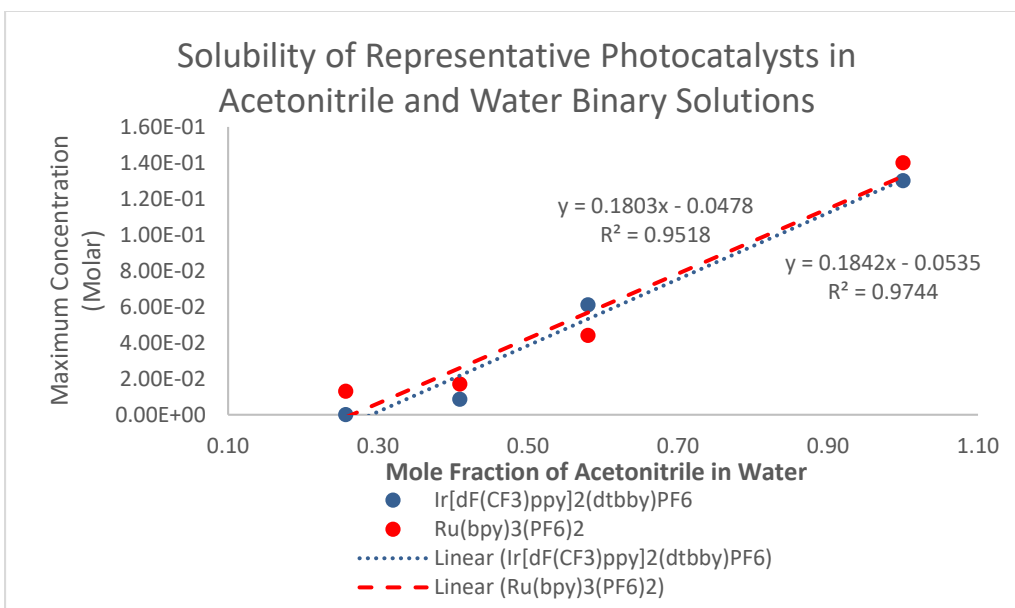
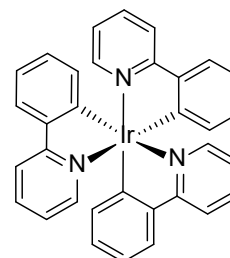


Figure 9. The solubility of photocatalysts in aqueous acetonitrile

<b><i>fac</i>-Ir(ppy)<sub>3</sub></b>		
CAS # 94928-86-6		
<b>Solvents</b>	<b>Molar Concentration</b>	<b>ppm</b>
Acetone <sup>23</sup>	6.0x10 <sup>-4</sup>	5.0x10 <sup>2</sup>
Acetonitrile <sup>23</sup>	4.1x10 <sup>-4</sup>	3.5x10 <sup>2</sup>
Dichloromethane <sup>23</sup>	7.3x10 <sup>-3</sup>	3.6x10 <sup>3</sup>
N,N-Dimethylformamide <sup>23</sup>	1.5x10 <sup>-3</sup>	1.0x10 <sup>3</sup>
Dimethylsulfoxide <sup>23</sup>	3.7x10 <sup>-3</sup>	2.2x10 <sup>3</sup>
Ethyl Acetate <sup>25</sup>	3.4x10 <sup>-4</sup>	2.5x10 <sup>2</sup>
Methanol <sup>25</sup>	1.1x10 <sup>-5</sup>	9.4x10 <sup>0</sup>
Methyl-t-butyl ether <sup>25</sup>	6.2x10 <sup>-5</sup>	5.5x10 <sup>1</sup>
N-Methyl 2-pyrrolidinone <sup>23</sup>	5.2x10 <sup>-2</sup>	3.3x10 <sup>4</sup>
Tetrahydrofuran <sup>23</sup>	2.1x10 <sup>-3</sup>	1.6x10 <sup>4</sup>
Toluene <sup>25</sup>	5.9x10 <sup>-4</sup>	4.4x10 <sup>2</sup>
Water <sup>23</sup>	-	<1
4:1 Acetonitrile:Water <sup>29</sup>	-	10-100
1:1 Acetonitrile:Water <sup>29</sup>	-	10-100



**Table 13**

<b><i>fac</i>-Ir(4'-Fppy)<sub>3</sub></b>		
CAS # 370878-69-6		
<b>Solvents</b>	<b>Molar Concentration</b>	<b>ppm</b>
Acetone <sup>23</sup>	8.0x10 <sup>-3</sup>	7.2x10 <sup>3</sup>
Acetonitrile <sup>23</sup>	9.2x10 <sup>-4</sup>	8.3x10 <sup>2</sup>
Dichloromethane <sup>23</sup>	4.2x10 <sup>-3</sup>	2.3x10 <sup>3</sup>
N,N-Dimethylformamide <sup>23</sup>	5.6x10 <sup>-2</sup>	4.2x10 <sup>4</sup>
Dimethylsulfoxide <sup>23</sup>	1.4x10 <sup>-2</sup>	8.9x10 <sup>3</sup>
Ethyl Acetate <sup>23</sup>	1.1x10 <sup>-3</sup>	8.7x10 <sup>2</sup>
Methanol <sup>25</sup>	5.6x10 <sup>-5</sup>	5.0x10 <sup>1</sup>
Methyl-t-butyl ether <sup>25</sup>	7.3x10 <sup>-5</sup>	7.0x10 <sup>1</sup>
N-Methyl 2-pyrrolidinone <sup>23</sup>	2.0x10 <sup>-1</sup>	1.4x10 <sup>5</sup>
Tetrahydrofuran <sup>23</sup>	1.8x10 <sup>-2</sup>	1.4x10 <sup>4</sup>
Toluene <sup>23</sup>	2.8x10 <sup>-4</sup>	2.3x10 <sup>2</sup>
Water <sup>23</sup>	-	<1

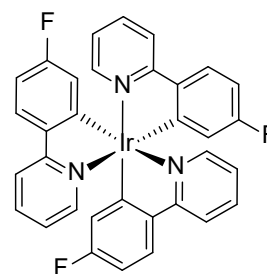


**Table 14**

<b>Ir(4'-CF<sub>3</sub>ppy)<sub>3</sub></b>		
CAS # 500295-52-3		
<b>Solvents</b>	<b>Molar Concentration</b>	<b>ppm</b>
Acetone <sup>23</sup>	1.4x10 <sup>-2</sup>	1.5x10 <sup>4</sup>
Acetonitrile <sup>23</sup>	1.5x10 <sup>-3</sup>	1.6x10 <sup>3</sup>
Dichloromethane <sup>23</sup>	1.0x10 <sup>-3</sup>	6.4x10 <sup>2</sup>
N,N-Dimethylformamide <sup>23</sup>	3.0x10 <sup>-2</sup>	2.7x10 <sup>4</sup>
Dimethylsulfoxide <sup>23</sup>	4.6x10 <sup>-3</sup>	3.6x10 <sup>3</sup>
Ethyl Acetate <sup>23</sup>	2.3x10 <sup>-3</sup>	2.2x10 <sup>3</sup>
Methanol <sup>25</sup>	5.6x10 <sup>-5</sup>	6.1x10 <sup>1</sup>
Methyl-t-butyl ether <sup>25</sup>	7.3x10 <sup>-5</sup>	8.4x10 <sup>1</sup>
N-Methyl 2-pyrrolidinone <sup>23</sup>	5.4x10 <sup>-2</sup>	4.4x10 <sup>4</sup>
Tetrahydrofuran <sup>23</sup>	1.4x10 <sup>-2</sup>	1.4x10 <sup>4</sup>
Toluene <sup>25</sup>	1.4x10 <sup>-4</sup>	1.4x10 <sup>2</sup>
Water <sup>23</sup>	-	<1

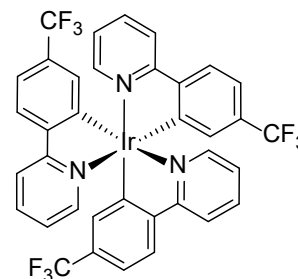


**Table 15**

<b>Ir(ppy)<sub>2</sub>(dtbbpy)PF<sub>6</sub></b>		
CAS # 676525-77-2		
<b>Solvents</b>	<b>Molar Concentration</b>	<b>ppm</b>
Acetone <sup>23</sup>	1.7x10 <sup>-1</sup>	2.0x10 <sup>5</sup>
Acetonitrile <sup>23</sup>	2.7x10 <sup>-1</sup>	3.2x10 <sup>5</sup>
Dichloromethane <sup>23</sup>	1.9x10 <sup>-1</sup>	1.3x10 <sup>5</sup>
N,N-Dimethylformamide <sup>23</sup>	1.4x10 <sup>-1</sup>	1.4x10 <sup>5</sup>
Dimethylsulfoxide <sup>23</sup>	1.5x10 <sup>-1</sup>	1.2x10 <sup>5</sup>
Ethyl Acetate <sup>23</sup>	8.1x10 <sup>-4</sup>	8.3x10 <sup>2</sup>
Methanol <sup>23</sup>	5.8x10 <sup>-3</sup>	6.7x10 <sup>3</sup>
Methyl-t-butyl ether <sup>29</sup>	-	10-100
N-Methyl 2-pyrrolidinone <sup>23</sup>	2.2x10 <sup>-1</sup>	1.9x10 <sup>5</sup>
Tetrahydrofuran <sup>25</sup>	3.6x10 <sup>-3</sup>	3.8x10 <sup>3</sup>
Toluene <sup>29</sup>	-	100-1000
Water <sup>29</sup>	-	1-10

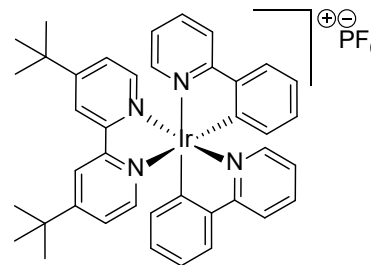


**Table 16**

<b>Ru(dmb)<sub>3</sub>(PF<sub>6</sub>)<sub>2</sub></b>		
CAS # 83605-44-1		
<b>Solvents</b>	<b>Molar Concentration</b>	<b>ppm</b>
Acetone <sup>23</sup>	2.2x10 <sup>-2</sup>	2.7x10 <sup>4</sup>
Acetonitrile <sup>23</sup>	6.4x10 <sup>-2</sup>	7.6x10 <sup>4</sup>
Dichloromethane <sup>23</sup>	9.9x10 <sup>-3</sup>	7.0x10 <sup>3</sup>
N,N-Dimethylformamide <sup>23</sup>	9.9x10 <sup>-2</sup>	9.9x10 <sup>4</sup>
Dimethylsulfoxide <sup>23</sup>	7.1x10 <sup>-2</sup>	6.1x10 <sup>4</sup>
Ethyl Acetate <sup>23</sup>	1.8x10 <sup>-3</sup>	1.9x10 <sup>3</sup>
Methanol <sup>23</sup>	3.9x10 <sup>-3</sup>	4.7x10 <sup>3</sup>
Methyl-t-butyl ether <sup>29</sup>	-	1-10
N-Methyl 2-pyrrolidinone <sup>23</sup>	1.2x10 <sup>-1</sup>	1.1x10 <sup>5</sup>
Tetrahydrofuran <sup>25</sup>	4.6x10 <sup>-5</sup>	4.9x10 <sup>1</sup>
Toluene <sup>29</sup>	-	1-10
Water <sup>25</sup>	4.0x10 <sup>-5</sup>	3.8x10 <sup>1</sup>

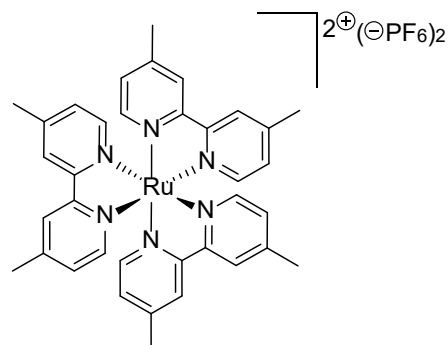


**Table 17**

<b>Ru(phen)<sub>3</sub>(PF<sub>6</sub>)<sub>2</sub></b>		
CAS # 60804-75-3		
<b>Solvents</b>	<b>Molar Concentration</b>	<b>ppm</b>
Acetone <sup>23</sup>	2.6x10 <sup>-2</sup>	3.6x10 <sup>4</sup>
Acetonitrile <sup>23</sup>	1.7x10 <sup>-1</sup>	2.3x10 <sup>5</sup>
Dichloromethane <sup>23</sup>	2.5x10 <sup>-3</sup>	2.0x10 <sup>3</sup>
N,N-Dimethylformamide <sup>23</sup>	2.5x10 <sup>-1</sup>	2.8x10 <sup>5</sup>
Dimethylsulfoxide <sup>23</sup>	2.8x10 <sup>-1</sup>	2.7x10 <sup>5</sup>
Ethyl Acetate <sup>29</sup>	-	1-10
Methanol <sup>23</sup>	5.5x10 <sup>-4</sup>	7.5x10 <sup>2</sup>
Methyl-t-butyl ether <sup>29</sup>	-	1-10
N-Methyl 2-pyrrolidinone <sup>23</sup>	1.9x10 <sup>-1</sup>	1.9x10 <sup>5</sup>
Tetrahydrofuran <sup>29</sup>	-	10-100
Toluene <sup>24</sup>	1.3x10 <sup>-5</sup>	1.6x10 <sup>1</sup>
Water <sup>29</sup>	-	10-100

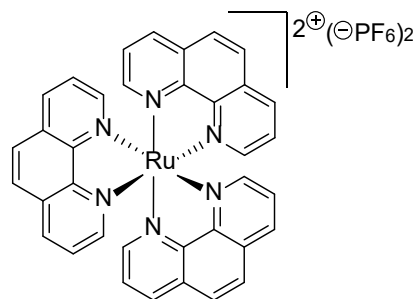


**Table 18**

<b>Ru(dtbbpy)<sub>3</sub>(PF<sub>6</sub>)<sub>2</sub></b>		
CAS # 75777-87-6		
<b>Solvents</b>	<b>Molar Concentration</b>	<b>ppm</b>
Acetone <sup>23</sup>	5.3x10 <sup>-2</sup>	8.0x10 <sup>4</sup>
Acetonitrile <sup>23</sup>	1.5x10 <sup>-1</sup>	2.3x10 <sup>5</sup>
Dichloromethane <sup>23</sup>	7.4x10 <sup>-2</sup>	6.6x10 <sup>4</sup>
N,N-Dimethylformamide <sup>23</sup>	1.5x10 <sup>-1</sup>	1.9x10 <sup>5</sup>
Dimethylsulfoxide <sup>23</sup>	6.1x10 <sup>-2</sup>	6.7x10 <sup>4</sup>
Ethyl Acetate <sup>29</sup>	-	100-1000
Methanol <sup>29</sup>	-	100-1000
Methyl-t-butyl ether <sup>29</sup>	-	10-100
N-Methyl 2-pyrrolidinone <sup>23</sup>	7.7x10	8.9x10 <sup>4</sup>
Tetrahydrofuran <sup>23</sup>	2.6x10 <sup>-3</sup>	3.5x10 <sup>3</sup>
Toluene <sup>29</sup>	-	1-10
Water <sup>29</sup>	-	1-10

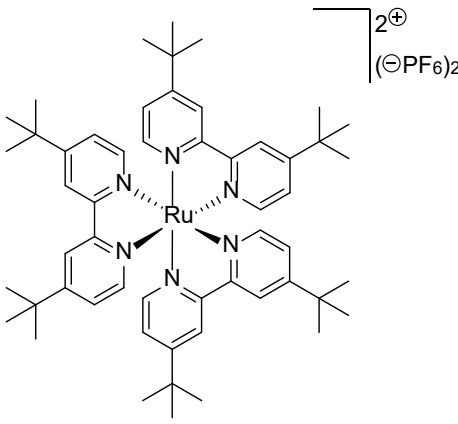


**Table 19**

<b>Ru(bpz)<sub>3</sub>(PF<sub>6</sub>)<sub>2</sub></b>		
CAS # 80907-56-8		
<b>Solvents</b>	<b>Molar Concentration</b>	<b>ppm</b>
Acetone <sup>29</sup>	-	100-1000
Acetonitrile <sup>29</sup>	-	100-1000
Dichloromethane <sup>29</sup>	-	10-100
N,N-Dimethylformamide <sup>23</sup>	4.4x10 <sup>-2</sup>	4.1x10 <sup>4</sup>
Dimethylsulfoxide <sup>23</sup>	3.7x10 <sup>-1</sup>	2.9x10 <sup>5</sup>
Ethyl Acetate <sup>29</sup>	-	10-100
Methanol <sup>29</sup>	-	100-1000
Methyl-t-butyl ether <sup>29</sup>	-	10-100
N-Methyl 2-pyrrolidinone <sup>23</sup>	1.8x10 <sup>-1</sup>	1.5x10 <sup>5</sup>
Tetrahydrofuran <sup>29</sup>	-	10-100
Toluene <sup>29</sup>	-	10-100
Water <sup>29</sup>	-	100-1000

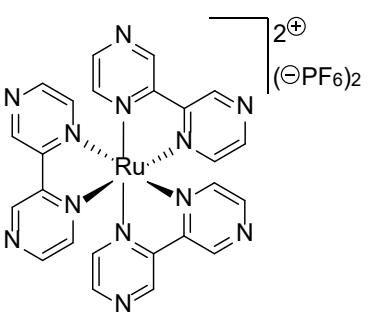


**Table 20**

<b>Ru(bpy)<sub>3</sub>(PF<sub>6</sub>)<sub>2</sub></b>		
CAS # 60804-74-2		
<b>Solvents</b>	<b>Molar Concentration</b>	<b>ppm</b>
Acetone <sup>23</sup>	3.3×10 <sup>-2</sup>	3.6×10 <sup>4</sup>
Acetonitrile <sup>23</sup>	1.4×10 <sup>-1</sup>	1.5×10 <sup>5</sup>
Dichloromethane <sup>29</sup>	-	100-1000
N,N-Dimethylformamide <sup>23</sup>	2.3×10 <sup>-1</sup>	2.1×10 <sup>5</sup>
Dimethylsulfoxide <sup>23</sup>	1.5×10 <sup>-1</sup>	1.2×10 <sup>5</sup>
Ethyl Acetate <sup>29</sup>	-	1-10
Methanol <sup>29</sup>	-	100-1000
Methyl-t-butyl ether <sup>29</sup>	-	1-10
N-Methyl 2-pyrrolidinone <sup>23</sup>	7.0×10 <sup>-2</sup>	5.8×10 <sup>4</sup>
Tetrahydrofuran <sup>29</sup>	-	10-100
Toluene <sup>29</sup>	-	1-10
Water <sup>29</sup>	-	100-1000
4:1 Acetonitrile:Water <sup>23</sup>	4.4×10 <sup>-2</sup>	-
2:1 Acetonitrile:Water <sup>23</sup>	1.7×10 <sup>-2</sup>	-
1:1 Acetonitrile:Water <sup>23</sup>	1.3×10 <sup>-2</sup>	-

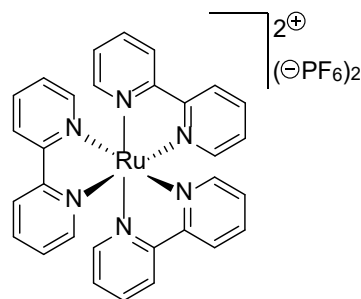


**Table 21**

<b><i>fac</i>-Ir(Fppy)<sub>3</sub></b>		
CAS # 387859-70-3		
<b>Solvents</b>	<b>Molar Concentration</b>	<b>ppm</b>
Acetone <sup>29</sup>	-	100-1000
Acetonitrile <sup>29</sup>	-	1000-100
Dichloromethane <sup>23</sup>	2.1×10 <sup>-3</sup>	1.2×10 <sup>3</sup>
N,N-Dimethylformamide <sup>23</sup>	2.0×10 <sup>-3</sup>	1.7×10 <sup>3</sup>
Dimethylsulfoxide <sup>29</sup>	-	100-1000
Ethyl Acetate <sup>29</sup>	-	100-1000
Methanol <sup>29</sup>	-	100-1000
Methyl-t-butyl ether <sup>29</sup>	-	100-1000
N-Methyl 2-pyrrolidinone <sup>23</sup>	1.7×10 <sup>-2</sup>	1.3×10 <sup>4</sup>
Tetrahydrofuran <sup>23</sup>	5.8×10 <sup>-3</sup>	5.0×10 <sup>3</sup>
Toluene <sup>29</sup>	-	100-1000
Water <sup>29</sup>	-	1-10

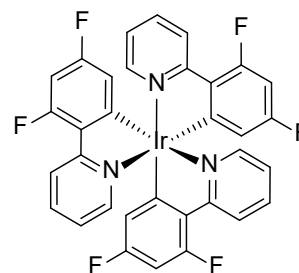


**Table 22**

<b>Ir(dtbppy)<sub>2</sub>(dtbbpy)PF<sub>6</sub></b>		
CAS # 808142-80-5		
<b>Solvents</b>	<b>Molar Concentration</b>	<b>ppm</b>
Acetone <sup>23</sup>	2.3x10 <sup>-2</sup>	3.3x10 <sup>4</sup>
Acetonitrile <sup>23</sup>	3.8x10 <sup>-2</sup>	5.5x10 <sup>4</sup>
Dichloromethane <sup>23</sup>	1.8x10 <sup>-1</sup>	1.5x10 <sup>5</sup>
N,N-Dimethylformamide <sup>23</sup>	1.5x10 <sup>-2</sup>	1.8x10 <sup>4</sup>
Dimethylsulfoxide <sup>23</sup>	5.3x10 <sup>-3</sup>	5.6x10 <sup>3</sup>
Ethyl Acetate <sup>23</sup>	8.6x10 <sup>-4</sup>	1.1x10 <sup>3</sup>
Methanol <sup>23</sup>	3.8x10 <sup>-3</sup>	5.5x10 <sup>3</sup>
Methyl-t-butyl ether <sup>29</sup>	-	100-1000
N-Methyl 2-pyrrolidinone <sup>23</sup>	4.8x10 <sup>-2</sup>	5.3x10 <sup>4</sup>
Tetrahydrofuran <sup>23</sup>	6.6x10 <sup>-3</sup>	8.5x10 <sup>3</sup>
Toluene <sup>23</sup>	2.0x10 <sup>-3</sup>	2.6x10 <sup>3</sup>
Water <sup>29</sup>	-	<1

**Table 23**

<b><i>fac</i>-Ir(tBuppy)<sub>3</sub></b>		
CAS # 359014-76-9		
<b>Solvents</b>	<b>Molar Concentration</b>	<b>ppm</b>
Acetone <sup>23</sup>	9.0x10 <sup>-3</sup>	9.5x10 <sup>3</sup>
Acetonitrile <sup>23</sup>	1.1x10 <sup>-3</sup>	1.1x10 <sup>3</sup>
Dichloromethane <sup>23</sup>	9.1x10 <sup>-3</sup>	5.7x10 <sup>3</sup>
N,N-Dimethylformamide <sup>23</sup>	7.4x10 <sup>-3</sup>	6.4x10 <sup>3</sup>
Dimethylsulfoxide <sup>23</sup>	8.4x10 <sup>-4</sup>	6.3x10 <sup>2</sup>
Ethyl Acetate <sup>23</sup>	1.7x10 <sup>-2</sup>	1.5x10 <sup>4</sup>
Methanol <sup>29</sup>	-	100-1000
Methyl-t-butyl ether <sup>29</sup>	-	100-1000
N-Methyl 2-pyrrolidinone <sup>23</sup>	1.4x10 <sup>-2</sup>	1.1x10 <sup>4</sup>
Tetrahydrofuran <sup>23</sup>	2.1x10 <sup>-2</sup>	1.9x10 <sup>4</sup>
Toluene <sup>23</sup>	3.5x10 <sup>-2</sup>	3.3x10 <sup>4</sup>
Water <sup>29</sup>	-	10-100

**Table 24**



<b>Ir[dF(CF<sub>3</sub>)ppy]<sub>2</sub>(dtbbpy)PF<sub>6</sub></b>		
CAS # 870987-63-6		
<b>Solvents</b>	<b>Molar Concentration</b>	<b>ppm</b>
Acetone <sup>23</sup>	9.9x10 <sup>-2</sup>	1.4x10 <sup>5</sup>
Acetonitrile <sup>23</sup>	1.3x10 <sup>-1</sup>	1.8x10 <sup>5</sup>
Dichloromethane <sup>23</sup>	5.6x10 <sup>-3</sup>	4.7x10 <sup>3</sup>
N,N-Dimethylformamide <sup>23</sup>	2.2x10 <sup>-1</sup>	2.6x10 <sup>5</sup>
Dimethylsulfoxide <sup>23</sup>	1.6x10 <sup>-1</sup>	1.7x10 <sup>5</sup>
Ethyl Acetate <sup>23</sup>	8.6x10 <sup>-3</sup>	1.1x10 <sup>4</sup>
Methanol <sup>23</sup>	2.4x10 <sup>-2</sup>	3.4x10 <sup>4</sup>
Methyl-t-butyl ether <sup>29</sup>	-	100-1000
N-Methyl 2-pyrrolidinone <sup>23</sup>	1.7x10 <sup>-2</sup>	1.8x10 <sup>-4</sup>
Tetrahydrofuran <sup>23</sup>	6.9x10 <sup>-3</sup>	8.8x10 <sup>3</sup>
Toluene <sup>29</sup>	-	100-1000
Water <sup>29</sup>	-	10-100
4:1 Acetonitrile:Water <sup>23</sup>	6.1x10 <sup>-2</sup>	-
2:1 Acetonitrile:Water <sup>23</sup>	8.5x10 <sup>-3</sup>	-
1:1 Acetonitrile:Water <sup>23</sup>	3.6x10 <sup>-3</sup>	-

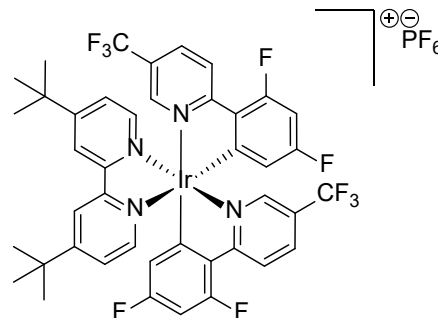


**Table 25**

<b>Ir(dmppy)<sub>2</sub>(dtbbpy)PF<sub>6</sub></b>		
CAS # 1607469-49-7		
<b>Solvents</b>	<b>Molar Concentration</b>	<b>ppm</b>
Acetone <sup>23</sup>	2.9x10 <sup>-1</sup>	3.6x10 <sup>5</sup>
Acetonitrile <sup>23</sup>	1.5x10 <sup>-1</sup>	1.8x10 <sup>5</sup>
Dichloromethane <sup>23</sup>	5.2x10 <sup>-1</sup>	3.8x10 <sup>5</sup>
N,N-Dimethylformamide <sup>23</sup>	5.8x10 <sup>-1</sup>	6.0x10 <sup>5</sup>
Dimethylsulfoxide <sup>23</sup>	1.0x10 <sup>-1</sup>	9.2x10 <sup>4</sup>
Ethyl Acetate <sup>23</sup>	9.5x10 <sup>-3</sup>	1.0x10 <sup>4</sup>
Methanol <sup>23</sup>	5.0x10 <sup>-3</sup>	6.2x10 <sup>3</sup>
Methyl-t-butyl ether <sup>29</sup>	-	10-100
N-Methyl 2-pyrrolidinone <sup>23</sup>	1.1x10 <sup>-1</sup>	1.0x10 <sup>5</sup>
Tetrahydrofuran <sup>23</sup>	1.1x10 <sup>-2</sup>	1.3x10 <sup>4</sup>
Toluene <sup>29</sup>	-	100-1000
Water <sup>29</sup>	-	1-10

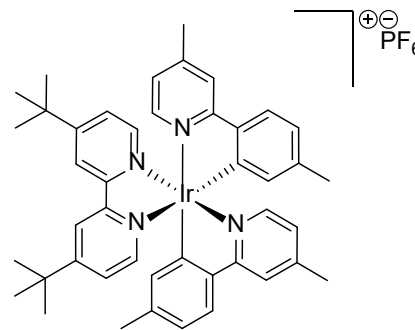


**Table 26**

**Table 13 – Table 26.** Maximum solubility of catalyst in various solvents, with some given as a range in ppm.<sup>25</sup>

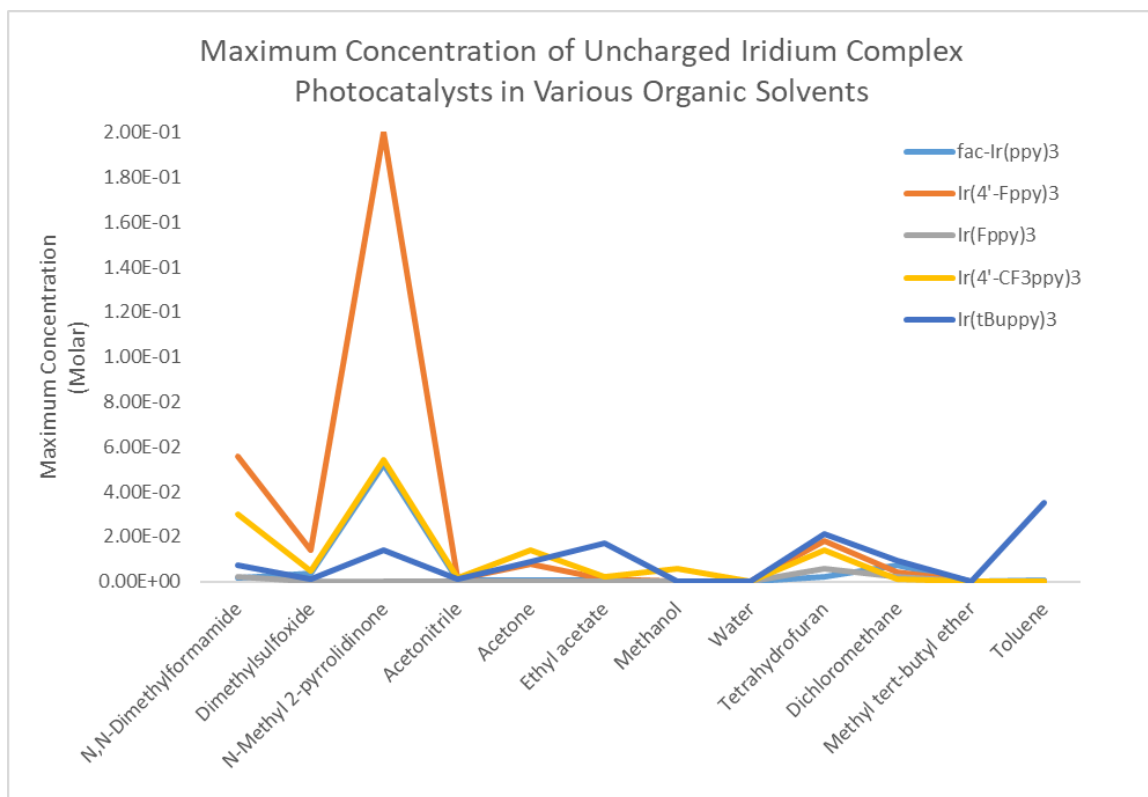


**Figure 10**

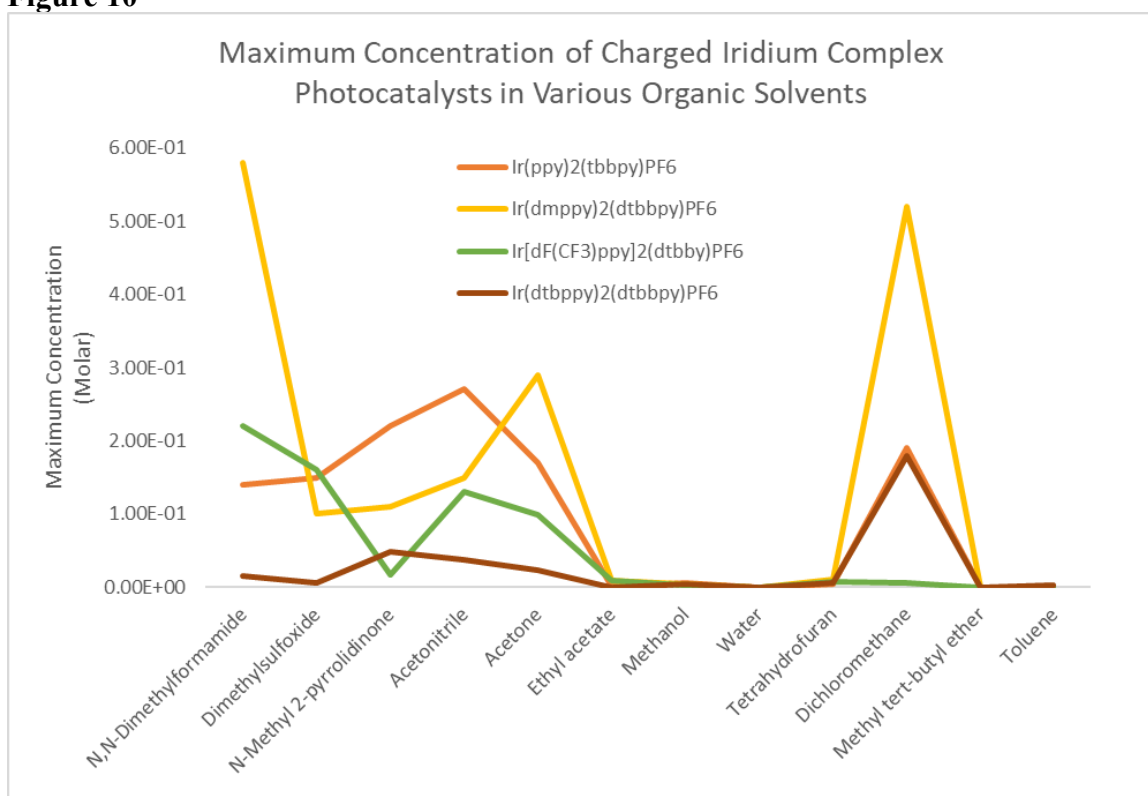


**Figure 11**

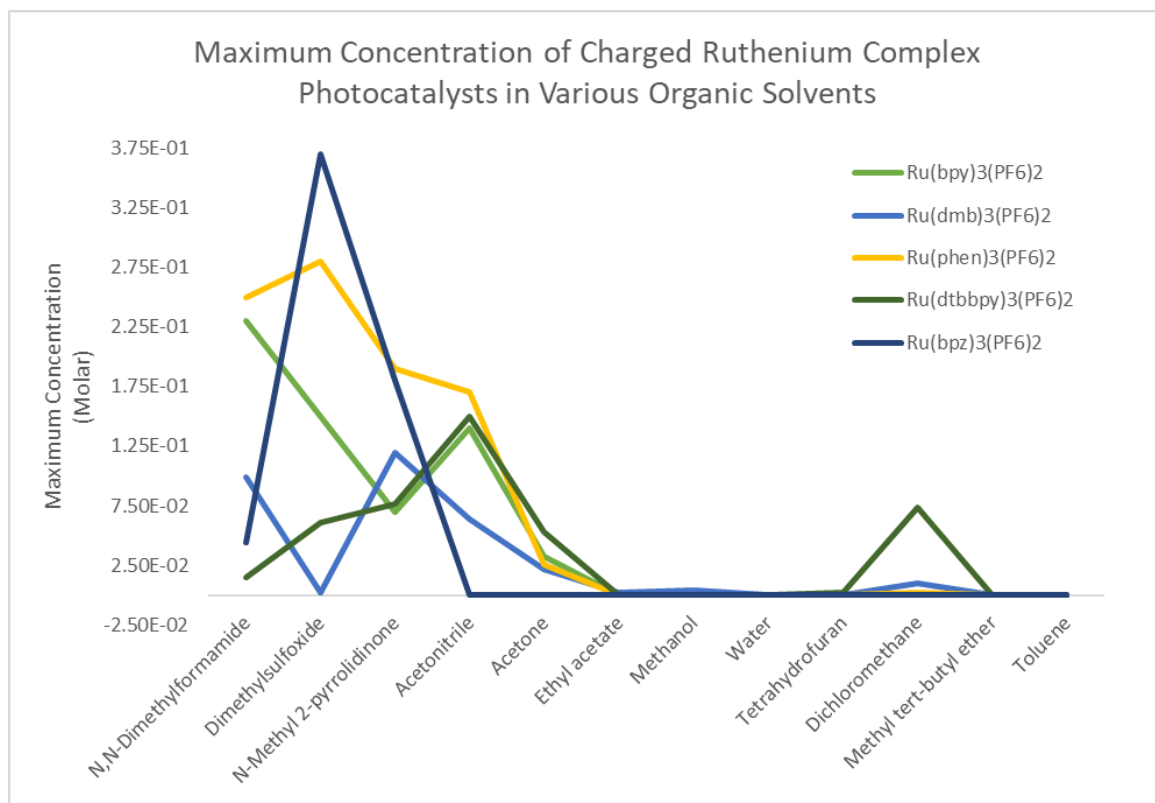


**Figure 12**

**Figure 10 – Figure 12.** Maximum concentration of iridium and ruthenium complex photocatalysts in common organic solvents<sup>293</sup>. Solvents are listed by decreasing Dipole Moment.<sup>296</sup>

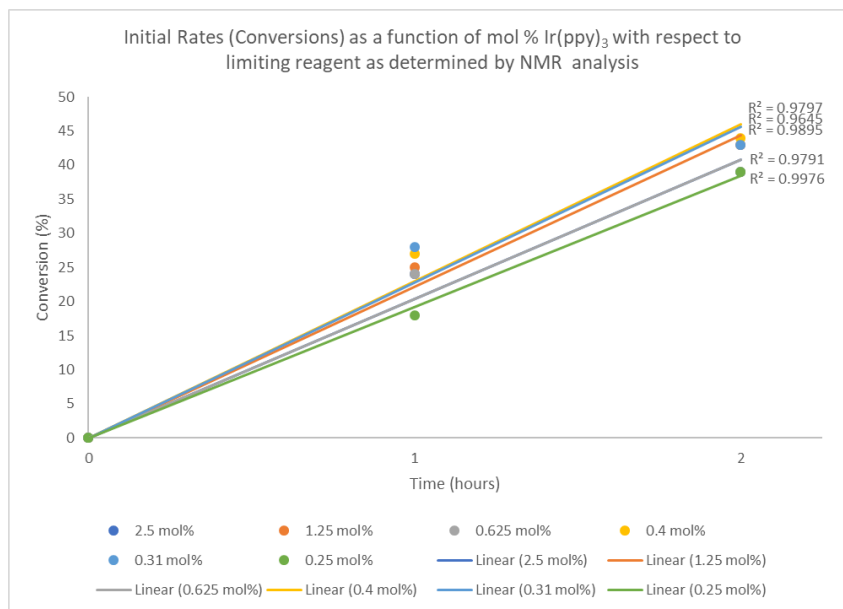
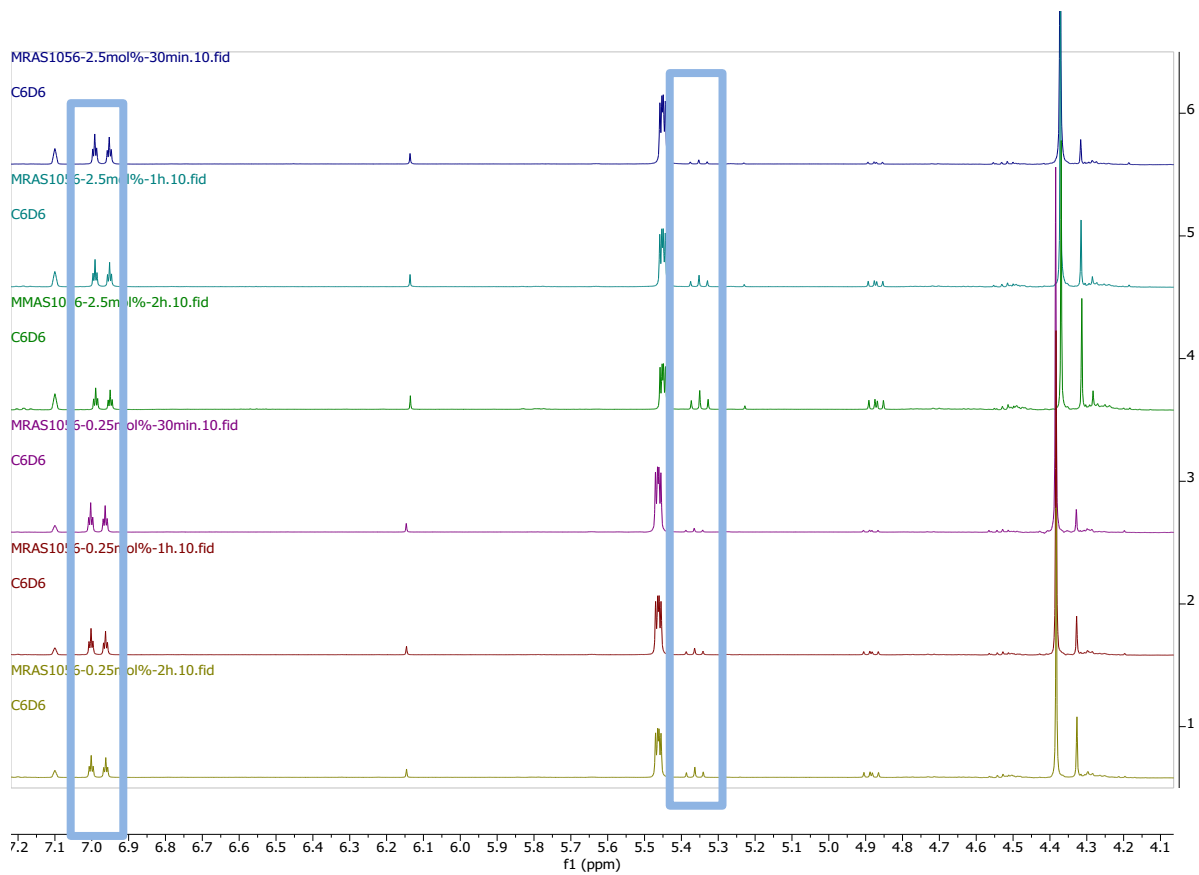
Concentration of Iridium and Ruthenium Complex Photocatalysts in Various Organic Solvents (Molar)	Acetone	Acetonitrile	Dichloromethane	N,N-Dimethylformamide	Dimethylsulfoxide	Ethyl acetate	Methanol	Methyl tert-butyl ether	N-Methyl 2-pyrrolidinone	Tetrahydrofuran	Toluene	Water
<b>Solvent Dipole Moment (D)</b>	2.78	3.51	1.53	3.91	3.86	1.84	1.77	1.36	3.75	1.75	0.36	1.76
<i>fac</i> -Ir(ppy) <sub>3</sub>	6.0x10 <sup>-4</sup>	4.2x10 <sup>-3</sup>	7.3x10 <sup>-3</sup>	1.5x10 <sup>-3</sup>	3.7x10 <sup>-3</sup>	3.3x10 <sup>-4</sup>	1.1x10 <sup>-5</sup>	6.2x10 <sup>-5</sup>	5.2x10 <sup>-2</sup>	2.1x10 <sup>-3</sup>	5.9x10 <sup>-4</sup>	<1.5x10 <sup>-6</sup>
<b>Ir(4'-Fppy)<sub>3</sub></b>	8.0x10 <sup>-3</sup>	9.2x10 <sup>-4</sup>	4.2x10 <sup>-3</sup>	5.6x10 <sup>-2</sup>	1.4x10 <sup>-2</sup>	1.1x10 <sup>-3</sup>	5.6x10 <sup>-5</sup>	7.4x10 <sup>-5</sup>	2.0x10 <sup>-1</sup>	1.8x10 <sup>-2</sup>	2.8x10 <sup>-4</sup>	<1.4x10 <sup>-6</sup>
<b>Ir(Fppy)<sub>3</sub></b>	1.0x10 <sup>-4</sup>	1.0x10 <sup>-3</sup>	2.1x10 <sup>-3</sup>	2.0x10 <sup>-3</sup>	1.0x10 <sup>-4</sup>	1.0x10 <sup>-4</sup>	1.0x10 <sup>-4</sup>	1.0x10 <sup>-4</sup>	1.7x10 <sup>-4</sup>	5.8x10 <sup>-3</sup>	1.0x10 <sup>-4</sup>	1.0x10 <sup>-6</sup>
<b>Ir(4'-CF<sub>3</sub>ppy)<sub>3</sub></b>	1.4x10 <sup>-2</sup>	1.5x10 <sup>-3</sup>	1.0x10 <sup>-3</sup>	3.0x10 <sup>-2</sup>	4.6x10 <sup>-3</sup>	2.3x10 <sup>-3</sup>	5.6x10 <sup>-3</sup>	7.3x10 <sup>-5</sup>	5.4x10 <sup>-2</sup>	1.4x10 <sup>-2</sup>	1.4x10 <sup>-4</sup>	<1.1x10 <sup>-6</sup>
<b>Ir(tBuppy)<sub>3</sub></b>	9.0x10 <sup>-3</sup>	1.1x10 <sup>-3</sup>	9.1x10 <sup>-3</sup>	7.4x10 <sup>-3</sup>	8.4x10 <sup>-4</sup>	1.7x10 <sup>-2</sup>	9.5x10 <sup>-5</sup>	9.5x10 <sup>-5</sup>	1.4x10 <sup>-2</sup>	2.1x10 <sup>-2</sup>	3.5x10 <sup>-2</sup>	9.5x10 <sup>-6</sup>
<b>Ir(ppy)<sub>2</sub>(tbbpy)PF<sub>6</sub></b>	1.7x10 <sup>-1</sup>	2.7x10 <sup>-1</sup>	1.9x10 <sup>-1</sup>	1.4x10 <sup>-1</sup>	1.5x10 <sup>-1</sup>	8.1x10 <sup>-4</sup>	5.8x10 <sup>-3</sup>	8.6x10 <sup>-6</sup>	2.2x10 <sup>-1</sup>	3.6x10 <sup>-3</sup>	8.6x10 <sup>-5</sup>	8.6x10 <sup>-7</sup>
<b>Ir(dmppy)<sub>2</sub>(dtbbpy)PF<sub>6</sub></b>	2.9x10 <sup>-1</sup>	1.5x10 <sup>-1</sup>	5.2x10 <sup>-1</sup>	5.8x10 <sup>-1</sup>	1.0x10 <sup>-1</sup>	9.5x10 <sup>-3</sup>	5.0x10 <sup>-3</sup>	8.1x10 <sup>-6</sup>	1.1x10 <sup>-1</sup>	1.1x10 <sup>-2</sup>	8.1x10 <sup>-5</sup>	8.1x10 <sup>-7</sup>
<b>Ir[d(CF<sub>3</sub>)ppy]<sub>2</sub>(dtbbpy)PF<sub>6</sub></b>	9.9x10 <sup>-2</sup>	1.3x10 <sup>-1</sup>	5.6x10 <sup>-3</sup>	2.2x10 <sup>-1</sup>	1.6x10 <sup>-1</sup>	8.6x10 <sup>-3</sup>	2.4x10 <sup>-3</sup>	7.0x10 <sup>-5</sup>	1.7x10 <sup>-2</sup>	6.9x10 <sup>-3</sup>	7.0x10 <sup>-5</sup>	7.0x10 <sup>-6</sup>
<b>Ir(dtbbpy)<sub>2</sub>(dtbbpy)PF<sub>6</sub></b>	2.3x10 <sup>-2</sup>	3.8x10 <sup>-2</sup>	1.8x10 <sup>-1</sup>	1.5x10 <sup>-2</sup>	5.3x10 <sup>-3</sup>	8.6x10 <sup>-5</sup>	3.8x10 <sup>-3</sup>	6.9x10 <sup>-5</sup>	4.8x10 <sup>-2</sup>	6.6x10 <sup>-3</sup>	2.0x10 <sup>-3</sup>	<6.9x10 <sup>-7</sup>
<b>Ru(bpy)<sub>3</sub>(PF<sub>6</sub>)<sub>2</sub></b>	3.3x10 <sup>-2</sup>	1.4x10 <sup>-1</sup>	9.1x10 <sup>-5</sup>	2.3x10 <sup>-1</sup>	1.5x10 <sup>-1</sup>	9.1x10 <sup>-7</sup>	9.1x10 <sup>-5</sup>	9.1x10 <sup>-7</sup>	7.0x10 <sup>-2</sup>	9.1x10 <sup>-6</sup>	9.1x10 <sup>-7</sup>	9.1x10 <sup>-5</sup>
<b>Ru(dmb)<sub>3</sub>(PF<sub>6</sub>)<sub>2</sub></b>	2.2x10 <sup>-2</sup>	6.4x10 <sup>-2</sup>	9.9x10 <sup>-3</sup>	9.9x10 <sup>-2</sup>	2.0x10 <sup>-3</sup>	1.8x10 <sup>-3</sup>	3.9x10 <sup>-3</sup>	8.3x10 <sup>-7</sup>	1.2x10 <sup>-1</sup>	4.6x10 <sup>-5</sup>	8.3x10 <sup>-7</sup>	4.0x10 <sup>-5</sup>
<b>Ru(phen)<sub>3</sub>(PF<sub>6</sub>)<sub>2</sub></b>	2.6x10 <sup>-2</sup>	1.7x10 <sup>-1</sup>	2.5x10 <sup>-3</sup>	2.5x10 <sup>-1</sup>	2.8x10 <sup>-1</sup>	7.3x10 <sup>-7</sup>	5.5x10 <sup>-4</sup>	7.3x10 <sup>-7</sup>	1.9x10 <sup>-1</sup>	7.3x10 <sup>-6</sup>	1.3x10 <sup>-5</sup>	7.3x10 <sup>-6</sup>
<b>Ru(dtbbpy)<sub>3</sub>(PF<sub>6</sub>)<sub>2</sub></b>	5.3x10 <sup>-2</sup>	1.5x10 <sup>-1</sup>	7.4x10 <sup>-2</sup>	1.5x10 <sup>-2</sup>	6.1x10 <sup>-2</sup>	6.6x10 <sup>-5</sup>	6.6x10 <sup>-5</sup>	6.6x10 <sup>-6</sup>	7.7x10 <sup>-2</sup>	2.6x10 <sup>-3</sup>	6.6x10 <sup>-7</sup>	6.6x10 <sup>-7</sup>
<b>Ru(bpz)<sub>3</sub>(PF<sub>6</sub>)<sub>2</sub></b>	9.1x10 <sup>-5</sup>	9.1x10 <sup>-5</sup>	9.1x10 <sup>-6</sup>	4.4x10 <sup>-2</sup>	3.7x10 <sup>-1</sup>	9.1x10 <sup>-6</sup>	9.1x10 <sup>-5</sup>	9.1x10 <sup>-6</sup>	1.8x10 <sup>-1</sup>	9.1x10 <sup>-6</sup>	9.1x10 <sup>-6</sup>	9.1x10 <sup>-5</sup>

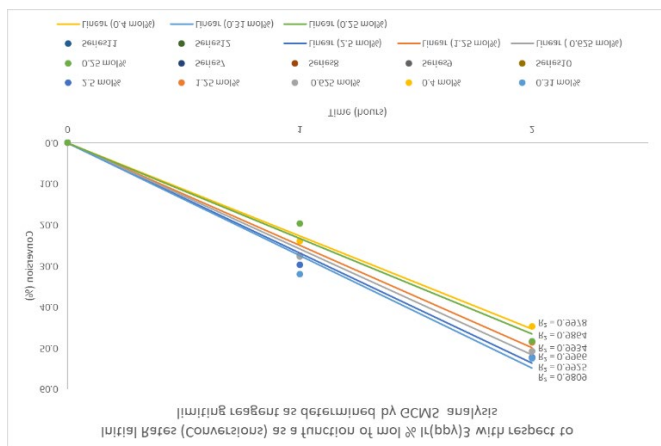
**Table 27**

Results of repeating literature reaction<sup>297</sup>

NMR conversions as a function of mol % Ir(ppy) <sub>3</sub> with respect to limiting reagent							std dev
time (h)	2.5 mol%	1.25 mol%	0.625 mol%	0.4 mol%	0.31 mol%	0.25 mol%	
0	0	0	0	0	0	0	
1	24	25	24	27	28	18	
2	39	43	39	44	43	39	
4	68	62	60	62	62	58	
6	83	79	74	77	69	68	
8	87	90	84	87	84	82	
20	100	100	100	100	100	100	
Slope of initial conversions (within the first halflife)							std dev
slope	19.5	21.5	19.5	22	21.5	19.5	1.096079
Note: integration at 4.7 and 4.2 ppm or 6.3 and 6.8 ppm							

GCMS conversions as a function of mol % Ir(ppy) <sub>3</sub> with respect to limiting reagent							std dev
time (h)	2.5 mol%	1.25 mol%	0.625 mol%	0.4 mol%	0.31 mol%	0.25 mol%	
0	0	0	0	0	0	0	
1	29.68	27.43	27.7	24	32.04	19.68	
2	52.17	48.59	50.7	44.7	52.51	48.32	
4	80.45	76	75.89	66	73.59	71.57	
6	93.7	89.8	87.2	83.27	87.76	82.91	
8	96.65	100	94.79	91.29	94.85	92.26	
20	100	100	100	100	100	100	
Slope of initial conversions (within the first halflife)							std dev
slope	26.085	24.295	25.35	22.35	26.255	24.16	1.3368103
Note: starting material's retention time 17.68 min and product's retention time 14.97 min							





## 5.5 Conclusion

We have determined and reported herein valuable physical data that was missing from the literature. The value of this data is evident when considering both the high cost of iridium and ruthenium and their relative terrestrial scarcity. It is our hope that disseminating these data will accelerate the adoption of photocatalysis not only as a routine laboratory procedure, but also in industry.

## 5.6 References

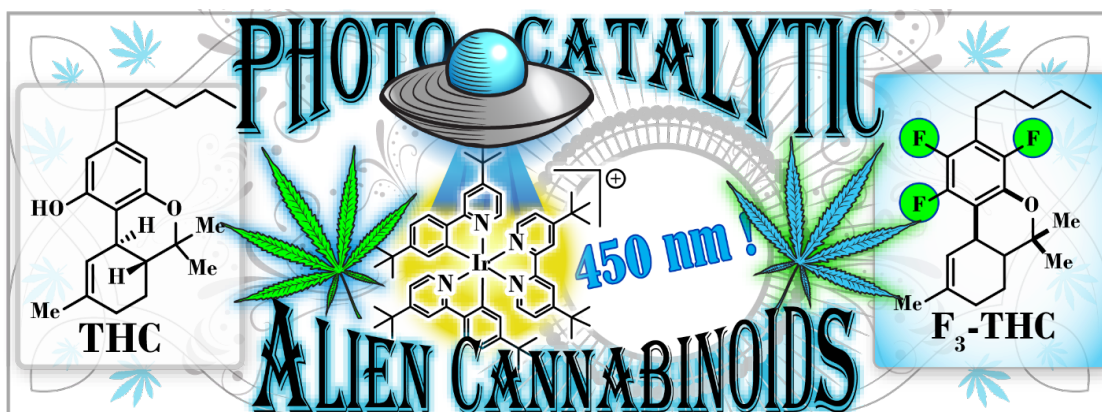
1. Prier, C. K.; Rankic, D. A.; MacMillan, D. W. C., Visible Light Photoredox Catalysis with Transition Metal Complexes: Applications in Organic Synthesis. *Chem. Rev.* **2013**, *113* (7), 5322-5363.
2. Teegardin, K.; Day, J. I.; Chan, J.; Weaver, J., Advances in Photocatalysis: A Microreview of Visible Light Mediated Ruthenium and Iridium Catalyzed Organic Transformations. *Org. Process Res. Dev.* **2016**, *20* (7), 1156-1163.
3. Marzo, L.; Pagire, S. K.; Reiser, O.; König, B., Visible-Light Photocatalysis: Does It Make a Difference in Organic Synthesis? *Angew. Chem. Int. Ed.* **2018**, *57* (32), 10034-10072.
4. Schultz, D. M.; Yoon, T. P., Solar Synthesis: Prospects in Visible Light Photocatalysis. *Science* **2014**, *343* (6174), 1239176.
5. Twilton, J.; Le, C.; Zhang, P.; Shaw, M. H.; Evans, R. W.; MacMillan, D. W. C., The merger of transition metal and photocatalysis. *Nat. Rev. Chem.* **2017**, *1*, 0052.
6. Michelin, C.; Hoffmann, N., Photocatalysis applied to organic synthesis – A green chemistry approach. *Curr. Opin. Green. Sustain. Chem.* **2018**, *10*, 40-45.
7. Douglas, J. J.; Sevrin, M. J.; Stephenson, C. R. J., Visible Light Photocatalysis: Applications and New Disconnections in the Synthesis of Pharmaceutical Agents. *Org. Process Res. Dev.* **2016**, *20* (7), 1134-1147.
8. Hoffmann, N., Proton-Coupled Electron Transfer in Photoredox Catalytic Reactions. *Eur. J. Org. Chem.* **2017**, *2017* (15), 1982-1992.
9. Yayla, H. G.; Peng, F.; Mangion, I. K.; McLaughlin, M.; Campeau, L.-C.; Davies, I. W.; DiRocco, D. A.; Knowles, R. R., Discovery and mechanistic study of a photocatalytic indoline dehydrogenation for the synthesis of elbasvir. *Chem. Sci.* **2016**, *7* (3), 2066-2073.

10. Beatty, Joel W.; Douglas, James J.; Miller, R.; McAtee, Rory C.; Cole, Kevin P.; Stephenson, Corey R. J., Photochemical Perfluoroalkylation with Pyridine  $\text{N-Oxides}$ : Mechanistic Insights and Performance on a Kilogram Scale. *Chem* **2016**, *1* (3), 456-472.
11. Wang, J.; Sanchez-Rosello, M.; Acena, J. L.; del Pozo, C.; Sorochinsky, A. E.; Fustero, S.; Soloshonok, V. A.; Liu, H., Fluorine in pharmaceutical industry: fluorine-containing drugs introduced to the market in the last decade (2001-2011). *Chem Rev* **2014**, *114* (4), 2432-506.
12. Hans Wedepohl, K., The composition of the continental crust. *Geochim. Cosmochim. Acta* **1995**, *59* (7), 1217-1232.
13. Banister, S. D.; Arnold, J. C.; Connor, M.; Glass, M.; McGregor, I. S., Dark Classics in Chemical Neuroscience:  $\Delta^9$ -Tetrahydrocannabinol. *ACS Chemical Neuroscience* **2019**, *10* (5), 2160-2175.
14. Devery Iii, J. J.; Douglas, J. J.; Nguyen, J. D.; Cole, K. P.; Flowers Ii, R. A.; Stephenson, C. R. J., Ligand functionalization as a deactivation pathway in a fac-Ir(ppy)<sub>3</sub>-mediated radical addition. *Chem. Sci.* **2015**, *6* (1), 537-541.
15. Prat, D.; Pardigon, O.; Flemming, H. W.; Letestu, S.; Ducandas, V.; Isnard, P.; Guntrum, E.; Senac, T.; Ruisseau, S.; Cruciani, P.; Hosek, P., Sanofi's Solvent Selection Guide: A Step Toward More Sustainable Processes. *Org. Process Res. Dev.* **2013**, *17* (12), 1517-1525.
16. Birch, A. J., 321. Reduction by dissolving metals. Part VII. The reactivity of mesomeric anions in relation to the reduction of benzene rings. *Journal of the Chemical Society (Resumed)* **1950**, (0), 1551-1556.
17. Singh, A.; Teegardin, K.; Kelly, M.; Prasad, K. S.; Krishnan, S.; Weaver, J. D., Facile synthesis and complete characterization of homoleptic and heteroleptic cyclometalated Iridium(III) complexes for photocatalysis. *J. Organomet. Chem* **2015**, *776*, 51-59.
18. Westphal, M. V.; Schafroth, M. A.; Sarott, R. C.; Imhof, M. A.; Bold, C. P.; Leippe, P.; Dhopeswarkar, A.; Grandner, J. M.; Katritch, V.; Mackie, K.; Trauner, D.; Carreira, E. M.; Frank, J. A., Synthesis of Photoswitchable  $\Delta^9$ -Tetrahydrocannabinol Derivatives Enables Optical Control of Cannabinoid Receptor 1 Signaling. *Journal of the American Chemical Society* **2017**, *139* (50), 18206-18212.
19. Nguyen, J. D.; D'Amato, E. M.; Narayanam, J. M. R.; Stephenson, C. R. J., Engaging unactivated alkyl, alkenyl and aryl iodides in visible-light-mediated free radical reactions. *Nat. Chem.* **2012**, *4*, 854.
20. Singh, A.; Fennell, C. J.; Weaver, J. D., Photocatalyst size controls electron and energy transfer: selectable E/Z isomer synthesis via C-F alkenylation. *Chemical Science* **2016**, *7* (11), 6796-6802.
21. Bally, T.; Rablen, P. R., Quantum-Chemical Simulation of <sup>1</sup>H NMR Spectra. 2. Comparison of DFT-Based Procedures for Computing Proton-Proton Coupling Constants in Organic Molecules. *The Journal of Organic Chemistry* **2011**, *76* (12), 4818-4830.
22. Rory, M.; Efrey, N.; Corey, S., *Arene Dearomatization via a Catalytic N-Centered Radical Cascade Reaction*. 2019.
23. Senaweera, S.; Weaver, J. D., Dual C-F, C-H Functionalization via Photocatalysis: Access to Multifluorinated Biaryls. *Journal of the American Chemical Society* **2016**, *138* (8), 2520-2523.
24. McClellan, A. L., *Tables of experimental dipole moments*. W.H. Freeman: San Francisco,, 1963; p 713 p.
25. Nguyen, J. D.; D'Amato, E. M.; Narayanam, J. M. R.; Stephenson, C. R. J., Engaging unactivated alkyl, alkenyl and aryl iodides in visible-light-mediated free radical reactions. *Nature Chemistry* **2012**, *4* (10), 854-859.

## CHAPTER VI

### POLYFLUORO-POLYCYCLIC DEAROMATIVE ARYLATION: A PHOTOCATALYTIC BIRCH-LIKE REDUCTION ENABLES C–C BOND FORMATION AND PROVIDES ACCESS TO UNNATURAL CANNABINOIDS

#### 6.1 Overview



This section is adapted from an unpublished work which was developed in collaboration with Sascha Grotjahn in the lab of Prof. Burkhard König at Institut für Organische Chemie, Universität Regensburg, Regensburg, Germany. Sascha and I are sharing primary authorship on this work. This work is complete except for some characterization data, which is currently unavailable due to the COVID-19 pandemic, which has shuttered labs around the world.

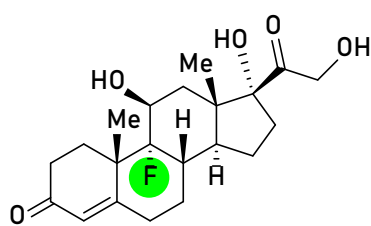
#### 6.2 Introduction

Fluorine has a greater ability than any other element to dramatically alter, often enhancing, the properties of functional molecules without dramatically altering the shape or function of the molecule. Perhaps due to the fact that there are few natural products that contain fluorine,<sup>2, 298-301</sup> which are usually toxic derivatives of fluoroacetate,<sup>302</sup> fluorination was historically overlooked as a legitimate direction for investigation. In 1953,<sup>303</sup> however, a fluorinated analog to hydrocortisone, fludrocortisone (6.2.1), was introduced to the literature. It was found to have a tenfold increase in glucocorticoid

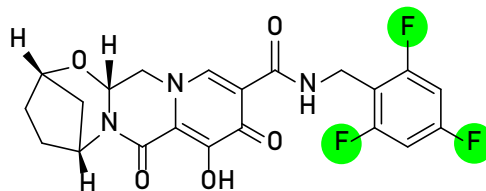
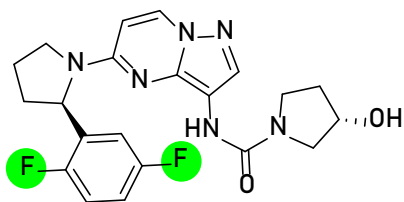
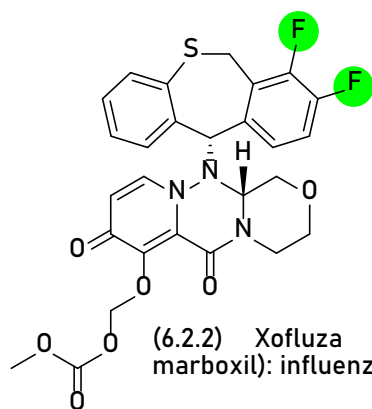


activity and up to 800 times the mineralocorticoid activity when compared to the non-fluorinated hormone, cortisol (table 28).<sup>304</sup> As time has passed, fluorination has assumed a lead role in discovery chemistry because of its ability to improve a host of properties in a multitude of applications.<sup>8, 24-25, 27, 305-306</sup> To further emphasize, an appreciation for the importance of fluorination in pharmaceuticals can be gained from by an examination of the drugs approved per annum by the U.S. FDA, of which typically 30%<sup>8, 307</sup> contain a C–F bond. In 2018, of U.S. FDA approved small molecule entities, 17 contained a C–F bond, 12 were fluoroarenes, and 3 were polyfluorinated arenes,<sup>308</sup> baloxavir marboxil (6.2.2), larotrectinib (6.2.3), and bictegrovir (6.2.4) indicating that *polyfluorination* specifically is becoming an increasingly important synthetic objective.

Table 28: Some Important Entries in the Fluoropharmacopeia



10X glucocorticoid activity  
800X mineralocorticoid activity  
vs. nonfluorinated counterpart



Despite the importance of fluorinated molecules in the pharmacopeia, linear syntheses to include fluorine are difficult. In contrast to more modern methods, methods for sequential fluorine installation such as the Balz-Schiemann and halox reactions exist,<sup>309</sup> but are difficult and are not typically functional group tolerant. Recent developments have increased the number of functional groups that can be transformed into fluorine,<sup>49, 309</sup> though while useful for monofluorination, these methods contribute little in the exploration of multifluorinated molecules, because they would require a library of multi-site prefunctionalized non-fluorinated starting materials in order to perform a comprehensive structure activity relationship study (SAR), and these starting materials are generally not available.

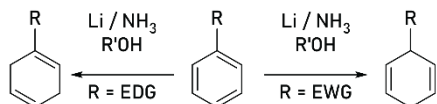
Some of us<sup>310-311</sup> have approached synthesis of organofluorines from the other way around. Rather than approaching fluorination through harsh, multi-step, or low yielding linear syntheses, the desired organofluorine can be realized by starting with all of the fluorines already in place, with poly- or perfluorinated core molecules, and replacing the unwanted fluorines through hydrodefluorination (HDF)<sup>139, 312-315</sup> or turning them into a desirable substituent through direct alkylation, alkenylation, arylation, and prenylation.<sup>141, 143, 311, 316-320</sup> Visible light photocatalysis with an iridium based photocatalyst has played a critical role in this area, and the interplay between photocatalytic C–F functionalizations and other methods has the potential to allow for sophisticated, but as of yet, largely unrealized SAR with respect to fluorine. Furthermore, the mild nature of these reactions may lend itself to the formation of unnatural products – fluorinated natural products,<sup>17</sup> which could create new opportunities to explore the effect of fluorination on the function of natural products—a mostly unexplored domain.

Previously, we showed it was possible to directly couple a perfluoroarene with an arene partner via C–F and C–H functionalization.<sup>18</sup> During this investigation,<sup>143</sup> careful assessment of some of the minor products in the crude reaction NMR spectra revealed vinylic <sup>1</sup>H signals, and GCMS analyses showed the [M+2] peak with respect to the expected product, a highly unexpected result. We expected that a cyclohexadienyl radical was a likely intermediate in the mechanism for the fluoroaryl arylation reaction, and that while the majority of the materials were proceeding through a mechanism in which they rearomatized – formally losing an H-atom in the process, under certain conditions the reduction of that intermediate had in fact gained an H-atom resulting in what amounts to a formal hydrogenation of the intended products.

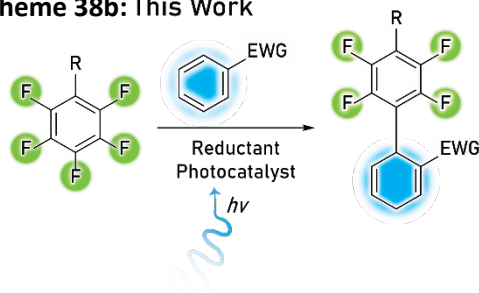
After careful isolation, we generated simulated NMR spectra of all possible perturbations of diene geometry for comparison to the experimental spectra, using the method of Bally and Rablen.<sup>282</sup> Of these, several contenders were similar to the experimental spectrum of 6.3.8, although the 1,4-diene in depicted in Scheme 1b appeared to most accurately match the experimental spectra (see section in supporting data labeled “Computational NMR spectra”).<sup>49</sup> Seeking more concrete data, we grew a crystal and submitted it for single crystal X-ray diffraction analysis, which confirmed the structure to that of (Table 30, 6.3.8). This product is structurally related to the product of a Birch<sup>19</sup> type dissolving metal reduction (Scheme 38a). However, in addition to the reduction, it simultaneously formed a new C–C bond. Another key difference is the regioselectivity of the diene, which differs from those formed under Birch conditions for substrates possessing an electron withdrawing group (Scheme 38a vs. 38b).<sup>321-322</sup> The conditions used for the Birch reaction (alkali metals in condensed liquid ammonia) are harsh and severely limit the scope of the reaction, while the reactions presented in here proceed in much milder conditions, and could be expected to be significantly more functional group tolerant. It is important to note that during the exploration of this methodology, a few photocatalytic dearomative methods have surfaced in the literature,<sup>323-325</sup> but the reaction discussed here is unique in that it does forms a C–C bond, yet does not require the pieces to be tethered together, it is not a spirocyclization, and it abstracts hydrogen (formally) from water.<sup>324</sup> We reasoned that because of the structural complexity, and functional richness

of these dienes it would be a valuable asset to the chemical community and set out to discover optimized conditions which would favor (Scheme 39) the formation of the reduced 1,4-diene.

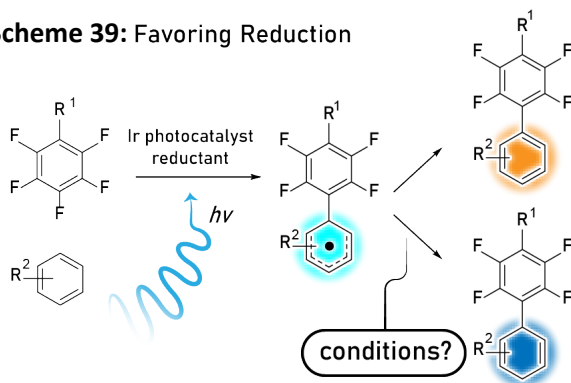
#### Scheme 38a: Birch Reduction



#### Scheme 38b: This Work



#### Scheme 39: Favoring Reduction



### 6.3 Optimization

Searching for optimal reaction conditions revealed the reaction to be somewhat odd, and one in which the mass balance apart from several major products consisted of many minor side products. Upon screening photocatalysts (table 29, entries 1-8), it was discovered that a somewhat oxidizing,<sup>74-75</sup> sterically bulky photocatalyst that has been thus far relatively underrepresented in the literature, the bis-4-(tert-butyl)-2-(4-(tert-butyl)phenyl)pyridine-4,4'-di-tert-butyl-2,2'-bipyridyl Iridium(III) hexafluorophosphate (Ir(dtbbpy)(dtbbpy)<sub>2</sub>PF<sub>6</sub>), with a triplet state emissive energy of 49.4 kcal/mol,<sup>72</sup> E<sub>0</sub>(Ir<sup>II</sup>/Ir<sup>III</sup>\*) = -1.04 V, and E<sub>0</sub>(Ir<sup>II</sup>/Ir<sup>III</sup>) = +1.13 V<sup>73</sup> was optimal. Recently, Chatterjee and Koenig<sup>326</sup> disclosed a dearomatization that is proposed to take place by triplet energy transfer followed by SET. However, because molecular radius of the photocatalyst has been shown to be critical for energy transfer to occur,<sup>316</sup> the large tert-butyl groups on this photocatalyst likely makes the probability of the necessary orbital overlap of the photocatalyst and the substrate unlikely. This is especially true given the difference in triplet state energies vs. the triplet emissive energy of competent energy transfer

photocatalysts *fac*-Ir(ppy)<sub>3</sub> at 55.2 kcal/mol<sup>316</sup> or *fac*-Ir(4-F-ppy)<sub>3</sub> at 58.6 kcal/mol.<sup>327</sup> It was discovered that the presence of water significantly enhances the reaction outcome (entries 9-12). Further, the addition of water causes the reaction to remain a pale yellow color, while in the absence of water, it darkens significantly. It could be that the presence of water further stabilizes a charged intermediate or transition state, or it could be serving to stabilize and solvate the fragmenting fluoride, a potentially very exothermic process (for more, see discussion of the mechanism below). It could also be serving a more abstruse role, like preventing the formation of light absorbing compounds that could photostarve the photocatalyst (Figure 12).<sup>328</sup> The screening for the identity of terminal reductants revealed tributylamine, and diisopropylethylamine (DIPEA, entry 13) to be very nearly identical, while all other reductants attempted gave poor or no results. We chose to utilize DIPEA due to its comparatively increased vapor pressure and water solubility, which we anticipated would facilitate product isolation. Precipitous decline in production of the intended diene was observed on either side of the optimized stoichiometry with respect to the amount of terminal reductant (entries 16-21). Hydrocarbon arene coupling partner (Ar-H) equivalents were found to be optimal at 3.0 (entries 22-24). Photocatalyst loading (entries 25-27) was found to be optimal for an NMR tube at 0.25 mol%, but product distribution was not affected at lower loadings. The reaction simply requires more time. Upon scaling the reaction up,

Table 29: Optimization of the Reaction Conditions

Reaction scheme: Ar-F + Ar-H + Photocatalyst + Reductant -> PDT + HDF

Entry	Equiv. Ar-H	R=	Equiv. DIPEA	Equiv. Water	0.25 Mol % PC	solvent	conc. (M)	Temp. (°C)	Time (Hrs)	PDT	HDF	conv.
<b>Photocatalyst Screen</b>												
1	2.6	Me	1.5	0	PC1	ACN	0.1	0	18	4	6	20
2	2.6	Me	1.5	0	PC2	ACN	0.1	0	18	1	2	7
3	2.6	Me	1.5	0	PC3	ACN	0.1	0	18	16	52	100
4	2.6	Me	1.5	0	PC4	ACN	0.1	0	18	15	32	73
5	2.6	Me	1.5	0	PC5	ACN	0.1	0	18	16	27	90
6	2.6	Me	1.5	0	PC6	ACN	0.1	0	18	9	20	51
7	2.6	Me	1.5	0	PC7	ACN	0.1	0	18	7	27	50
8	2.6	Me	1.5	0	PC8	ACN	0.1	0	18	3	7	25
<b>Chemical Structures of PC1-PC8</b>												
<b>Water Optimization</b>												
9	3.0	Me	1.1	0.0	0.25	ACN	0.1	0	18	8.6	24.8	48.7
10	3.0	Me	1.1	5	0.25	ACN	0.1	0	18	21.3	54.8	100
11	3.0	Me	1.1	15	0.25	ACN	0.1	0	18	22.0	48.5	100
12	3.0	Me	1.1	20	0.25	ACN	0.1	0	18	19.1	36.6	100
<b>Reductant Optimization</b>												
13	2.6	Me	DIPEA	15	0.25	ACN	0.1	rt	18	30.3	37.2	100
14	2.6	Me	TMP	15	0.25	ACN	0.1	rt	18	1.3	1.7	30.3
15	2.6	Me	TEA	15	0.25	ACN	0.1	rt	18	3.7	8.6	97.6
<b>DIPEA Optimization</b>												
16	2.6	Me	0.0	10	0.25	ACN	0.1	0	18	0.0	0.0	0.0
17	2.6	Me	0.5	10	0.25	ACN	0.1	0	18	13.8	28	57.0
18	2.6	Me	1.0	10	0.25	ACN	0.1	0	18	21.0	50.7	100
19	2.6	Me	1.2	10	0.25	ACN	0.1	0	18	18.8	48.3	100
20	2.6	Me	1.5	10	0.25	ACN	0.1	0	18	15.5	39.3	100
21	2.6	Me	3.0	10	0.25	ACN	0.1	0	18	8.5	29.5	100
<b>Ar-H Optimization</b>												
22	1.0	Me	1.2	10	0.25	ACN	0.1	0	18	10.5	46.5	100
23	3.0	Me	1.2	10	0.25	ACN	0.1	0	18	18.0	42.0	100
24	5.0	Me	1.2	10	0.25	ACN	0.1	0	18	18.3	36.3	100
<b>PC Loading</b>												
25	3.0	Me	1.1	10	0.50	ACN	0.1	0	18	14.5	26.5	100
26	3.0	Me	1.1	10	0.25	ACN	0.1	0	18	17.5	34.5	100
27	3.0	Me	1.1	10	0.10	ACN	0.1	0	18	9.5	20	75.6
<b>Temperature Screen</b>												
28	3.0	Me	1.1	15	0.25	ACN	0.1	-2	1.0	25.3	48.1	100
29	3.0	Me	1.1	15	0.25	ACN	0.1	rt	1.0	26.3	59.8	100
30	3.0	Me	1.1	15	0.25	ACN	0.1	50	1.0	28.7	66.1	100
31	3.0	Me	1.1	15	0.25	ACN	0.1	75	1.0	20.8	59.1	100

Conversions/yields determined against internal standard.  
Conducted in 1 mL solvent NMR tube.

however, the increased path length proved to slow the reaction rate. It was further found that the reaction depends heavily on reaction solvent, with poor or no reactivity in any solvent except acetonitrile. Curiously, the reaction was found to have very little sensitivity with respect to the temperature at which the reaction takes place (entries 28-31).

## 6.4 Scope

The reaction operates in a number of different fluoroarenes and coupling partners (Table 30). Reactions in which varying the Ar-H with benzoate esters (structures 6.3.5, 6.3.6, 6.3.9, 6.3.11, 6.3.13, 6.3.14, 6.3.15, 6.3.16, 6.3.17, 6.3.18, 6.3.19, and 6.3.20), ketones (6.3.8), benzonitriles (6.3.10), and amides (6.3.7, 6.3.12) progressed nicely, though in lower yields. In addition, separation of the material from the reaction mixture proved difficult, especially for those reactions in which the Ar-H was not appreciably volatile, such as the benzamides, and thus could not be separated *via* distillation. Variation of the fluoroarene revealed that a wide variety of fluoroarenes operated similarly, although variation of the Ar-H from 4-methyl to 4-tertbutyl benzoates resulted in somewhat better yields or easier separations. Interestingly, reaction with a bromopentafluorobenzene resulted in the typical 1,4 diene product connected at the position formerly occupied by the bromine (6.3.19). This is interesting because it serves as a mechanistic probe, suggesting the involvement of an aryl radical (see discussion below). The reaction with 3-chloro-2,4,5,6-tetrafluoropyridine also produces the dihydro product (6.3.20) and reveals an interesting property of the products. As should be expected,<sup>329</sup> the bicyclic motif is rotationally locked into conformation producing atropisomers which do not

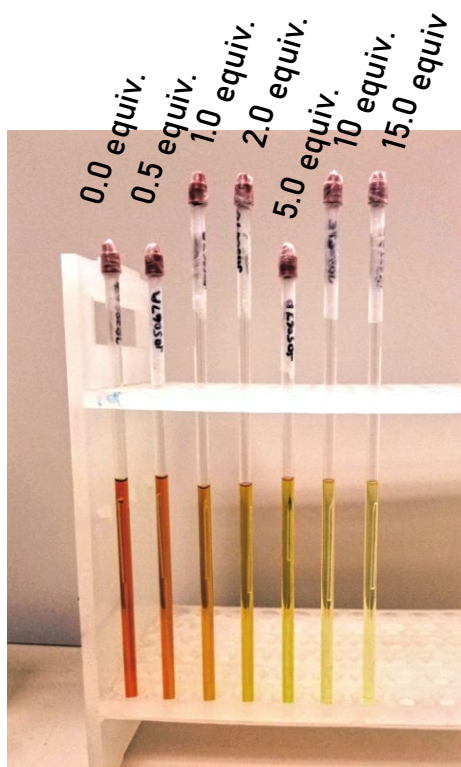


Figure 12: Darkening of Reaction as a Function of Equivalents Water Added

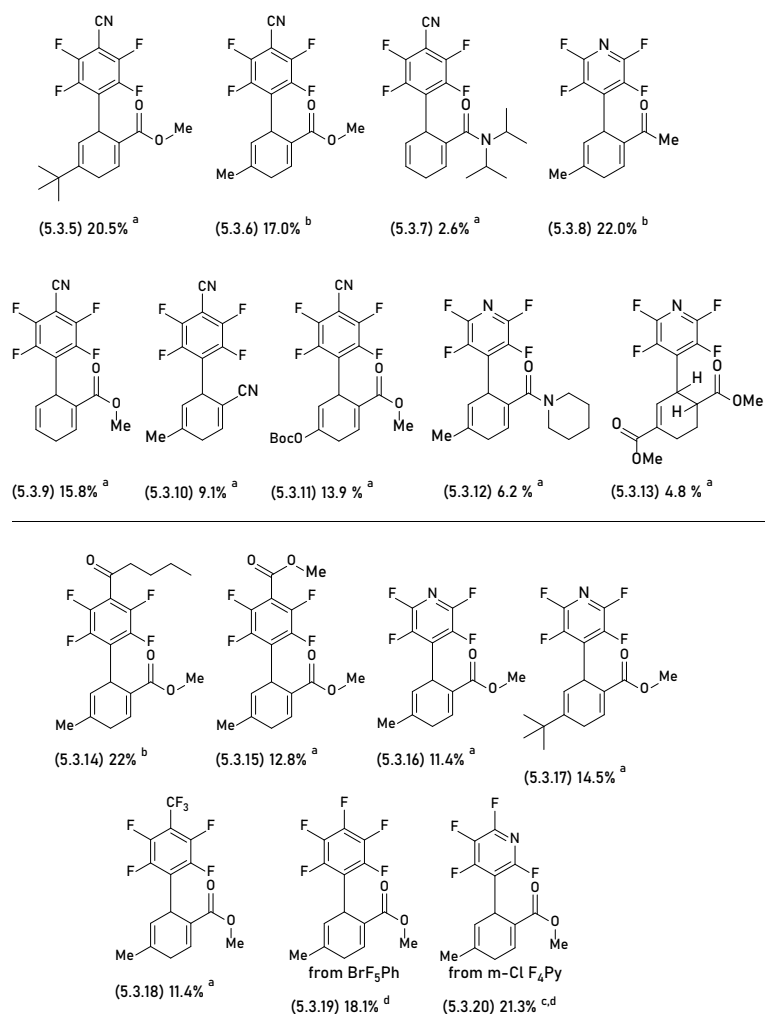
interconvert at room temperature, which are not evident with symmetrical fluoroarenes. In this case, the C-C bond formation gives rise to both axial and point chirality with a slight preference for one diastereomer (2.4:1). These diastereomers can be partially separated by recrystallization (1:1.9 – see characterization of 6.3.20 in supplementary data).<sup>49</sup> Under these conditions, although the reaction operates with all of the fluoroarenes shown here, reactions attempted with simple perfluorobenzene did not react at all, indicating that the fluoroaryl reduction potential (-2.11 V in DMF vs SCE)<sup>330</sup> is outside that reachable by the photocatalyst. While these yields are generally modest, this reaction provides a rapid increase in complexity from commercially available starting materials, and the reaction scales well. Compound 6.3.6 was run on a 10 mmol scale and produced 553 mg of fluorinated diene, and 947 mg diene 6.3.14 was produced from a 12.0 mmol scale batch reaction,

which was sufficient for downstream synthetic manipulations.<sup>49</sup>

While phenols are largely incompatible with these conditions due to their acidity, Boc-protected methyl paraben was investigated and found to be a competent coupling partner. Upon cleavage with TFA, this reaction provides a keto-cyclohex-enyl methyl carboxylate. The two-step process formally provides access to the product of Michael addition with the keto-tautomer of methyl paraben (Scheme 40, right).<sup>49</sup> With the five sites of reactive functional groups, it is both functional group dense, and a structure that would be extraordinarily difficult to reach given other methods. Such functionally dense structures should allow facile access to more complex classes of molecules.

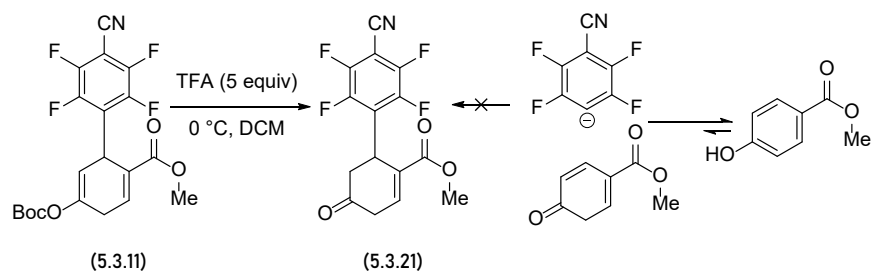
While phenols are largely incompatible with these conditions due to their acidity, Boc-protected methyl paraben was investigated and found to be a competent coupling partner. Upon cleavage with TFA, this reaction provides a keto-cyclohex-enyl methyl carboxylate. The two-step process formally provides access to the product of Michael addition with the keto-tautomer of methyl paraben (Scheme 40, right).<sup>49</sup> With the five sites of reactive functional groups, it is both functional group dense, and a structure that would be extraordinarily difficult to reach given other methods. Such functionally dense structures should allow facile access to more complex classes of molecules.

Table 30: Scope



Isolated yields. <sup>a</sup> Batch reaction conditions <sup>b</sup> Flow reaction conditions. <sup>c</sup> Produces atropisomers. <sup>d</sup> NMR yield

#### Scheme 40: Cleavage of the Boc Protecting Group



#### 6.5 Mechanism:

While the selectivity of the reaction involves C–F fragmentation selectivity, C–C bond formation regioselectivity, and C–H bond formation regioselectivity, and in certain cases—modest atropselectivity, it is remarkably predictable, forming only a single dearomatized isomer. The halogen selectivity follows trends we have previously observed in

photocatalytic C–F functionalization. The 4-position of any monosubstituted perfluoroarene preferentially fragments,<sup>135</sup> and when present, heavier halogens preferentially undergo fragmentation (structure 6.3.19 and 6.3.20, Table 30).<sup>139, 141, 143, 320</sup> Insofar as the regioselectivity of the C–C bond forming addition of the fluoroaryl fragment to the hydrocarbon aryl coupling partner, it appears to be dictated by the LUMO of the Ar–H partner. The reaction is selective for the carbon ortho to an electron withdrawing group. The reaction works best for substrates in which the predicted LUMO is larger at the ortho position and significantly smaller elsewhere.<sup>49</sup> Arenes lacking electron withdrawing groups fail to give any cyclohexadiene product, suggesting that the electron withdrawing functional group may play other critical roles. At this time, the driving forces that lead to the observed diene regioisomer are unclear.

As mentioned above, water played a critical role in the reaction. Darkening of the reaction mixture could be avoided by the addition of water. This accompanied much welcomed improvements in product distribution (Table 29 and Figure 12) and a reduction of the number of minor side products formed. This might be explained by the formation of cyanine dyes arising from oligomerization of the DIPEA, as those dyes are known to form under similar conditions and known to participate in photocatalytic reactions. The inclusion of water may prevent their formation, or hydrolyze them if they do form.<sup>331</sup>

We had presumed the amine indirectly (as the radical cation) served as the terminal reductant and source of H-atom in the formation of the diene. However, we found that when normal water was replaced with heavy water (15 equiv D<sub>2</sub>O, Scheme 41a), the reaction resulted in 69% deuterium incorporation into the diastereotopic methylene signal. Resubjecting the isolated product (6.4.22 or 6.4.23) to reaction conditions with the inclusion of D<sub>2</sub>O rather than H<sub>2</sub>O showed that post-reaction exchange was not operative (slow HDF was observed). Furthermore, the deuterium incorporation occurred with a *ca.* 3:1 (75%) selectivity on the side opposite the perfluoroaryl ring. These findings obviate the possibility of the reaction proceeding solely through a hydrogen atom transfer (HAT) process, because the bond dissociation energy of water at 117.9 kcal/mol<sup>332</sup> is far from the weakest bond (BDE for cyclohexadiene *ca.* 77 kcal/mol,<sup>325</sup> *ca.* 90 kcal/mol for neutral DIPEA, and *ca.* 42 kcal/mol as the DIPEA amine radical cation)<sup>137-138</sup> placing water well outside the realm of reasonable H-atom sources. It is more likely that the reaction proceeds through either an anionic reaction mechanism similar to the traditional Birch reaction, or through a proton coupled electron transfer (PCET) event in which the cyclohexadienyl radical is reduced to the carbanion and protonated. Because deuteration is incomplete, however, it is possible that the reaction is proceeding through both an anionic pathway and an HAT event.<sup>333</sup> It could be that the DIPEA is serving to provide a proton/deuteron source,<sup>334</sup> but it seems untenable to invoke a side reaction in which a catalytic cycle would incorporate deuterium into the amine when the reactions are complete in such a short time frame, and in the absence of a proton shuttle. Further, experiments aimed to identify more acidic or nonaqueous additives instead of water (isopropanol, ethanol, trifluoroethanol) that would favor the formation of the intended product proved fruitless, and in fact were deleterious to the



reaction. Curiously, the reaction is not appreciably sensitive to the rate of addition of the amine. In other words, decreasing the amount of amine in the reaction mixture vis-à-vis the amount of Ar–F should effect an increase in the relative amounts of intended product, because the cyclohexadienyl radical is expected to be able to abstract an H-atom from the amine radical cation, but not the amine, while in comparison the fluoroaryl radical could abstract an H-atom from either. These experiments did not affect the product distribution, suggesting that a different mechanism was operative, rather than proceeding through the H-atom abstraction by the cyclohexadienyl radical of the amine radical cation.

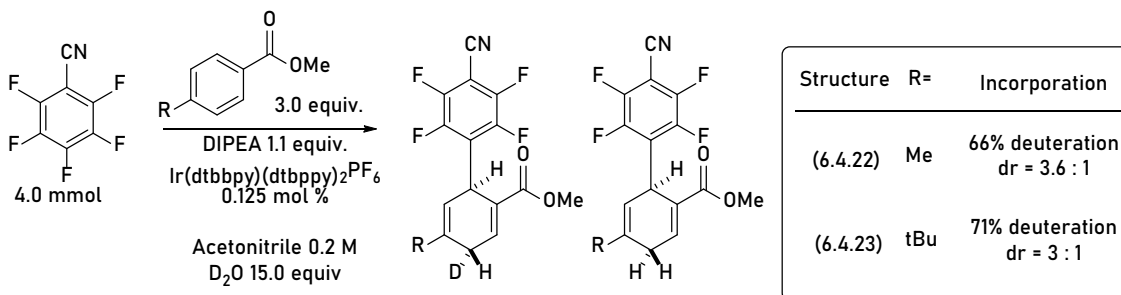
Upon further investigation, a kinetic isotope effect (KIE) was observed in parallel experiments where either H<sub>2</sub>O or D<sub>2</sub>O were included in the reaction mixture, with a  $k_H/k_D$  of 1.4, which is consistent with a secondary KIE, or a solvent KIE (Scheme 41b). This indicates that the rate determining step is not protonation of an anionic intermediate by water, nor is it a PCET event, steps for which a larger KIE could be expected.<sup>335</sup> It also indicates that if this observed KIE is a result of inclusion of the proton or deuteron, then the incorporation occurs prior to the rate determining step, as the reaction shouldn't demonstrate a KIE if the protonation or deuteration event occurs afterward. It could be that there is a pre-rate determining equilibrium, and that the protonation of the carbanionic intermediate is near the rate determining step. It could also be that fragmentation of a fluorine is the rate determining step, and that the observed KIE is a result of the solvation of the fragmenting fluoride,<sup>336</sup> for which a free energy of solvation of ca. 104.4 kcal/mol could be expected,<sup>337-338</sup> as compared with chloride and bromide, which are reported as 74.5 and -68.3 kcal/mol respectively.<sup>338</sup> Reactions with either bromopentafluorobenzene or 3-chloro-tetrafluoropyridine lead to a 1,4-diene product, replacing the bromine and the chlorine, respectively. Initial rates studies with these substrates indicate a KIE of 1.1, much less than analogous substrates in which a C–F bond is functionalized. This is of note because of the sizes of the halogens coupled with the lack of comparable KIE makes some potential intermediates unlikely (see below).

Because of the unknowns, we are presenting and considering several mechanistic possibilities (Scheme 42). The reaction is expected to proceed through a reductive quenching cycle, in which the triplet photocatalyst ( $E^0(\text{Ir}^{\text{II}}/\text{Ir}^{\text{III}*}) = -1.04 \text{ V}^{73}$ ) oxidizes an amine terminal reductant ( $E_{\text{ox}}$  ca. 0.5 V vs. SCE<sup>134</sup>). The reduced photocatalyst is then oxidized by a fluoroarene (A) to form the radical anion (B). This radical anion could fragment mesolytically to give the fluoroaryl radical (C) and a fluoride anion.<sup>139, 141, 143</sup> Based on BDEs, the fluoroaryl radical is expected to easily abstract an H-atom from DIPEA, or its corresponding radical cation, to give the major byproduct, the hydrodefluorinated product (D).

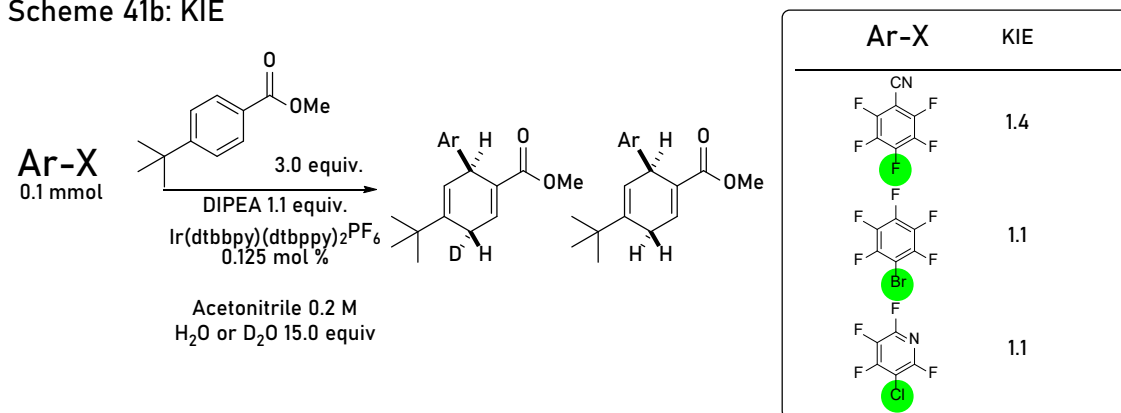
One might expect that the fluoroaryl radical anion (B) with its abundance of electron density could potentially act nucleophilically,<sup>339-340</sup> attacking the LUMO of the Ar–H to produce an intermediate distonic radical anion (F), or traverse a concerted addition/elimination pathway to produce a doubly allylic radical (G). It is possible too that the distonic radical anion (F) could fragment a fluoride in a stepwise manner to give the

delocalized radical (G). Further, it is possible that distonic radical anion (F) could proceed via reduction and subsequent protonation or PCET event (E) to give the 1,4-diene product (I) after fluoride extrusion, although this seems a somewhat untenable position because not only it would require the invocation of a double anion, if only transiently.

#### Scheme 41a: Deuteration



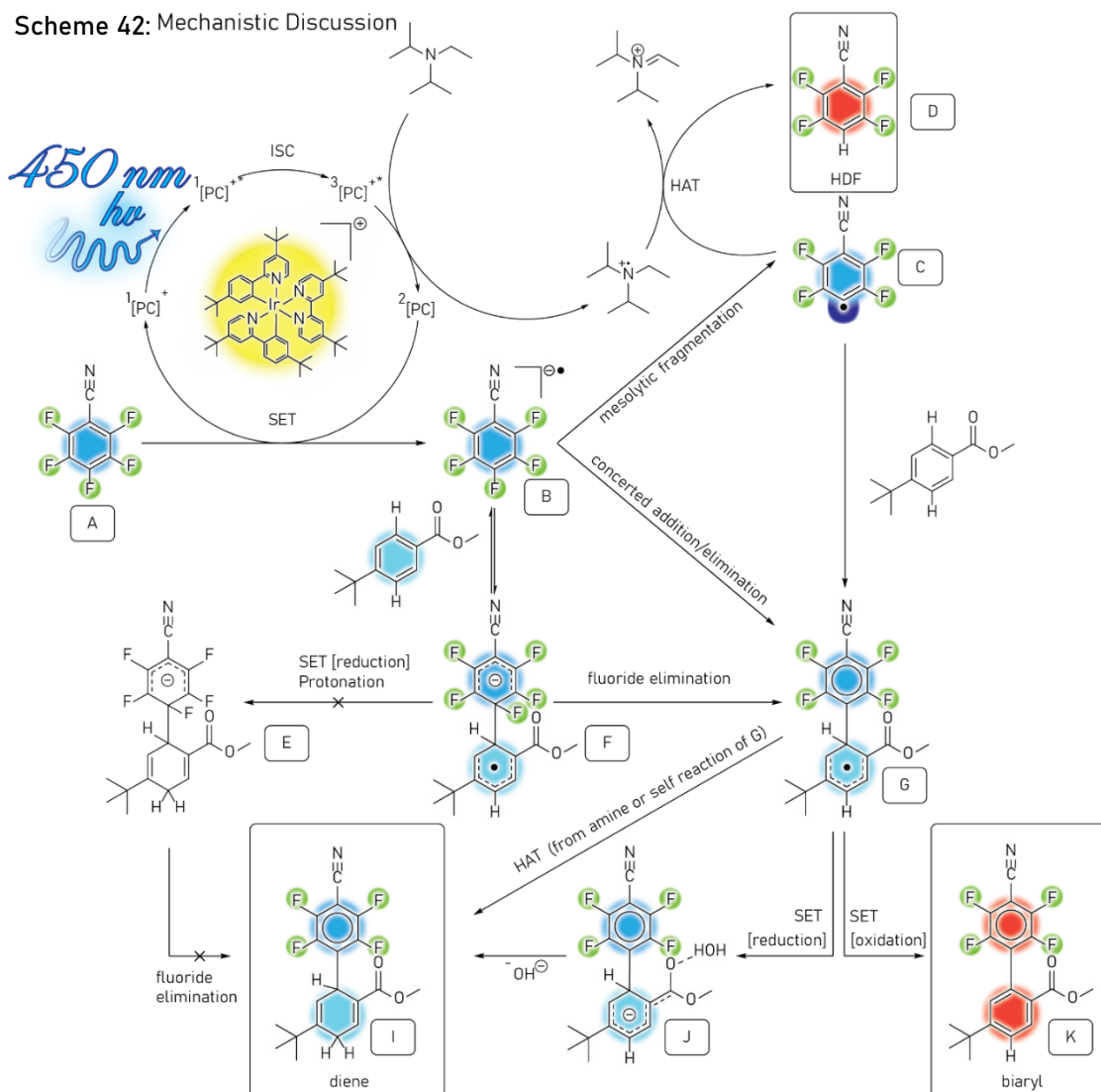
#### Scheme 41b: KIE



In contrast to previous reports of nucleophilic attack by related radical anions,<sup>340</sup> it is unconvincing that a well-defined distonic radical anion (F) intermediate is formed in this reaction. In light of the observation that both chlorinated and brominated fluoroarenes lead to the same 1,4-diene product, the rate enhancement observed upon increase of H<sub>2</sub>O, and that the observed KIE is significantly retarded in the presence of a fragmenting bromide or chloride, observations are consistent with fragmentation of the halogen being the slow step. In other words, the rate of halogen fragmentation increases as the size of the halogen increases and the corresponding radical anions are less reliant on solvation (compared to fluoride) to facilitate fragmentation. Consequently, the  $k_H/k_D$  diminishes as the rate of fragmentation increases, barring a mechanistic change between these substrates. This rate could be expected to be much more rapid upon forming an intermediate distonic radical anion (F), and that a solvent KIE, if observed at all, would be the same for all substrates, regardless of the fragmenting halogen. It is therefore more likely that, as with previous photocatalytic reactions we have reported, that we are proposing that the reaction occurs through the mesolytic fragmentation of the radical anion (B) to form the fluoroaryl radical (C) which then attacks the LUMO of the Ar-H, leading directly to (G).

It is again untenable to suppose that the reaction operates exclusively through a HAT event to give the observed 1,4-diene product (I), because it would be, as previously discussed, highly endergonic to abstract a hydrogen (or deuterium) from water, though the partial incorporation of protium may be best explained by a mechanistic bifurcation from intermediate G. Therefore, we propose that the delocalized, doubly allylic radical (G) is itself either reduced by the photocatalyst to give an anionic intermediate (J) which provides the observed 1,4-diene (I) upon protonation or oxidized to give the other observed major byproduct, the rearomatized biaryl product (K). It is possible too that the formation of the biaryl and the intended dienyl product originate from self-reaction of the radical G, in which the cyclohexadienyl radical abstracts an H-atom from another cyclohexadienyl radical G to form the observed reduced product (BDE *ca.* 77 kcal/mol for unsubstituted substrate),<sup>325</sup> although this pathway fails to account for the incorporation of the deuterium from water, but again the deuteration is incomplete. The amount of biaryl side product is always less than the amount of 1,4-diene, which supports a mechanistic bifurcation, although it is hardly conclusive.

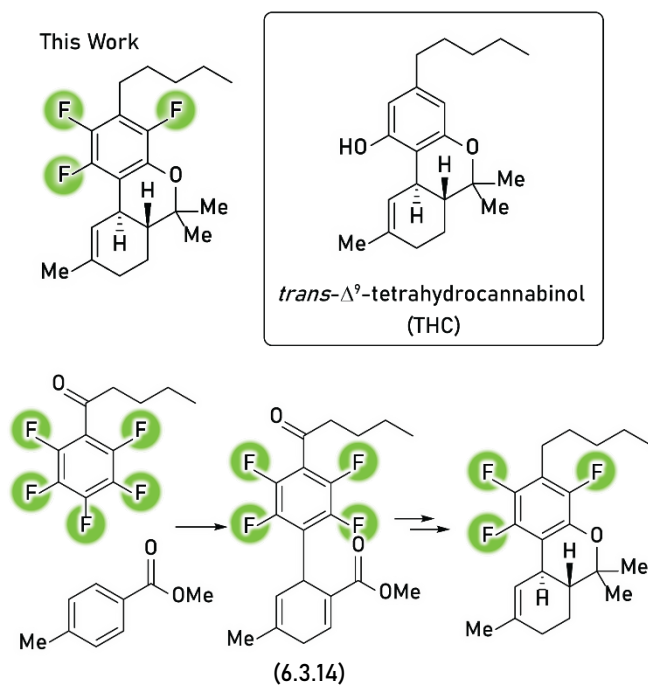
Scheme 42: Mechanistic Discussion



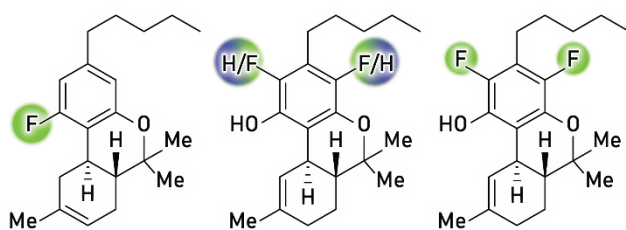
## 6.6 Application:

Returning to our original goal of enabling the synthesis of unnatural products, we were pleased to see that this motif maps very nicely onto the structural skeleton of classical cannabinoids (scheme 43a), the most prominent, and also most notorious of which is *trans*- $\Delta^9$ -tetrahydrocannabinol (THC),<sup>341</sup> the molecule not only responsible for most of the psychoactive effects of cannabis, but also many of its medicinal properties.

Scheme 43a: THC Fluoroanalog Target



Scheme 43b: Known Cannabinoid Fluoroanalogs

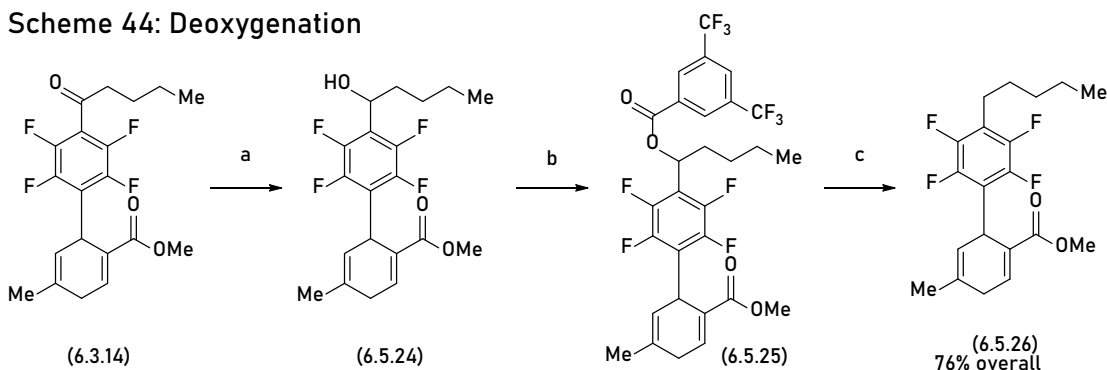


As no 3-perfluoroaryl substituted 1,4-cyclohexadienes have been reported previously we expected this structural motif could be a versatile synthetic building block of new unnatural products. Despite the extensive and ongoing research on classical cannabinoids,  $F_3$ -THC has, to the best of our knowledge, not been reported before. Related compounds with mono-<sup>342</sup> or di-fluorination<sup>343</sup> are known in the literature<sup>344-345</sup> and have been shown to have bioefficacy (Scheme 43b). This method allows access to a completely unknown series of trifluoro analogs with substitution at either the Ar-F or the Ar-H for diversification through a straightforward

series of reactions and importantly will allow us to investigate the role of the hydroxy group in the highly fluorinated scheme.

For the synthesis of F<sub>3</sub>-THC we chose diene (6.3.14) (Scheme 43a) as the most suitable starting material, because reactions toward a more direct route with the simple pentyl alkyl pentafluoroarene produced none of the intended intermediate materials, presumably because the reduction potential is too high with an electron donating group. Following the photo-Birch reaction we began investigation of methods for the deoxygenation of the aromatic ketone. Following a clean and unremarkable reduction of the ketone with NaCNBH<sub>3</sub>, we obtained (6.5.24) in high yield. We found the Barton-McCombie<sup>346</sup> approach attractive, and pursued the elegant photochemical approach developed by Reiser *et al.*,<sup>347</sup> which provided the intended deoxygenated product three straightforward steps<sup>347-348</sup> with a total yield of 76% (Scheme 44).

#### Scheme 44: Deoxygenation

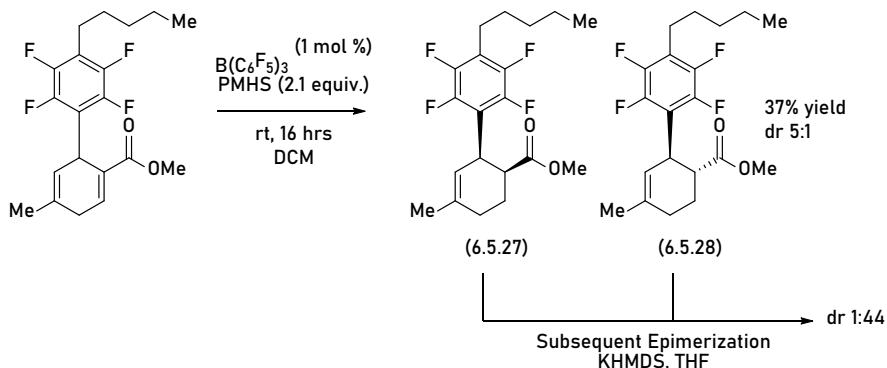


Reagents and conditions: (a) ZnI<sub>2</sub> (1.5 equiv.), NaBH<sub>3</sub>CN (7.5 equiv.), DCE, 80 °C, 97%; (b) bis(trifluoromethyl)benzoyl chloride (1.1 equiv.), 80 °C, 89%; (c) DIPEA (2.0 equiv.), [Ir(dtbbpy)(dtbppy)<sub>2</sub>]PF<sub>6</sub> (1.5 mol%), 45 °C, 455 nm irradiation, 86%.

Following the successful formation of the desired intermediate diene (26), reduction of the Michael system was addressed. This proved to be remarkably difficult. This was surprising given the expected electronic and steric differences between the alkenes, and yet, using a number of more common methods we observed unselective reaction, unintended side products, or poor conversion. The most reliable method was found to be a derivative of the method by Chandrasekhar *et al.*,<sup>349</sup> hydrogenation *via* polymethylhydrosiloxane (PHMS) with a strong Lewis acid, tris(pentafluorophenyl)borane (Scheme 45), which ultimately gave the hydrogenated product in modest yields and in a diastereomeric ratio of around 5:1 (varying between 4:1 and 6:1) in favor of the *cis* product (6.5.27) over the *trans* product (6.5.28). This reduction turned out to be sensitive towards the reaction conditions (further comments see SI). Epimerization to a 1:44 diastereomeric ratio in favor of the *trans* was achieved through the stoichiometric use of KHMDS in THF. Formation of the *trans* diastereomer (6.5.28) in excess is advantageous because the natural (*trans*) THC has a higher affinity for cannabinoid receptors than its *cis* counterpart. It could be reasonably expected that the fluorinated analogs would perform similarly. We expected the acidity of the ester's  $\alpha$ -hydrogen could be exploited through the use of a catalytic strong base to perform an epimerization to the *trans*. Curiously, however, it was found that

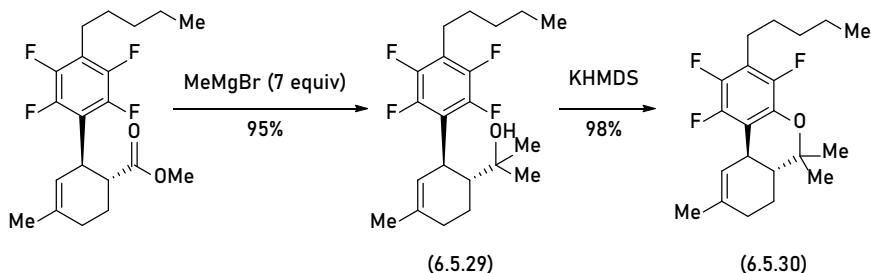
although catalytic amounts of KHMDS did improve the ratio in favor of the *trans* product, stoichiometric amounts were required in order to push the ratio to completeness, potentially with adventitious water serving as a proton source.<sup>49</sup>

#### Scheme 45: Reduction of the Michael System



Having determined a route to the *trans* intermediate cyclohexene (6.5.28), we then investigated the formation of the bridging ring (Scheme 46). We were hoping initially to be able to form the third ring through tandem nucleophilic addition of the methyls followed by subsequent  $S_NAr$  displacement of the fluoride. Unfortunately, this did not prove fruitful with either methyl Grignard or lithiate. Of note, while the *cis* and *trans* cyclohexenyl benzoates (6.5.27 & 6.5.28) were challenging to separate, upon substitution the corresponding *cis*- and *trans*- alcohols (6.5.29) showed different  $R_f$  values and could be more easily separated chromatographically. However, treating alcohol (6.5.29) with KHMDS afforded cyclization, similar to the work by Westphal, Trauner, Carreira, Frank and coworkers,<sup>343</sup> and provided the intended cannabinoid product (6.5.30) with a 93% yield over 2 steps (Scheme 46). Ultimately, the reaction starts with two commodity chemicals and takes place in 8 succinct steps with 6% overall yield. Furthermore, several points of diversification exist and could be used for further exploration of the motif. Several fluorinated cannabinoids are undergoing bioassay now. The results will be reported in due course.

#### Scheme 46: Intramolecular Cyclization



## 6.7 Conclusion:

We have demonstrated a new reaction that provides a new, direct route to 1,4-dienes. Further, we have shown that the reaction likely proceeds through an anionic intermediate, which opens the door for potential further diversification through a Birch-like alkylation. These dienes map readily onto the carbon framework of classical cannabinoids, which we have shown can be synthesized in short order which would otherwise have previously been prohibitively difficult to reach. In addition, the synthetic steps offer a wealth of synthetic possibilities for diversification. Further, we expect that the synthesis laid out herein can provide access to fluorinated analogs of existing CB1/CB2 agonists such as classical THC, related cannabinoids, or perrottetines. In addition, one of the major byproducts, the rearomatized biaryl species could lead (through a similar synthetic sequence shown below) to analogs of the natural cannabinoid cannabitol (CBN). Coupled with existing defluorination techniques and the possibilities present for downstream diversification, the possibilities for a complete SAR with respect to fluorination are accessible. Nonetheless, the reactivity is previously unknown and is orthogonal to any other dearomative mechanism known to the authors.

## 6.8 Acknowledgements:

The authors declare no conflict of interest.

## 6.9 References

1. Pauling, L., *J. Am. Chem. Soc.* **1932**, *54*, 3570.
2. Murphy, C. D.; Schaffrath, C.; O'Hagan, D., Fluorinated natural products: the biosynthesis of fluoroacetate and 4-fluorothreonine in *Streptomyces cattleya*. *Chemosphere* **2003**, *52* (2), 455-461.
3. Harper, D. B.; O'Hagan, D., *Nat. Prod. Rep* **1994**, *11*, 123.
4. Xu, X.-H.; Yao, G.-M.; Li, Y.-M.; Lu, J.-H.; Lin, C.-J.; Wang, X.; Kong, C.-H., 5-Fluorouracil derivatives from the sponge *Phakellia fusca*. *J. Nat. Prod.* **2003**, *66*, 285.
5. Tosaki, A.; Hearse, D. J., Fluoro-fatty acids and the impairment of cardiac function in the rat in vivo and in vitro. *Basic Res. Cardiol.* **1988**, (83), 158.
6. Welch, J. T., *Tetrahedron* **1987**, (43), 3123.
7. Gribble, G. W. In *Naturally occurring organofluorines*, Springer: 2002; pp 121-136.
8. Wang, J.; Sanchez-Rosello, M.; Acena, J. L.; del Pozo, C.; Sorochnikov, A. E.; Fustero, S.; Soloshonok, V. A.; Liu, H., Fluorine in pharmaceutical industry: fluorine-containing drugs introduced to the market in the last decade (2001-2011). *Chem Rev* **2014**, *114* (4), 2432-506.
9. Ismail, F. M. D., Important fluorinated drugs in experimental and clinical use. *J. Fluorine Chem.* **2002**, *118* (1), 27-33.
10. Böhm, H.-J.; Banner, D.; Bendels, S.; Kansy, M.; Kuhn, B.; Müller, K.; Obst-Sander, U.; Stahl, M., Fluorine in Medicinal Chemistry. **2004**, *5* (5), 637-643.
11. Isanbor, C.; O'Hagan, D., Fluorine in medicinal chemistry: A review of anti-cancer agents. *J. Fluorine Chem.* **2006**, *127* (3), 303-319.
12. Kirk, K. L., Fluorine in medicinal chemistry: Recent therapeutic applications of fluorinated small molecules. *J. Fluorine Chem.* **2006**, *127* (8), 1013-1029.

13. Morgenthaler, M.; Schweizer, E.; Hoffmann-Röder, A.; Benini, F.; Martin, R. E.; Jaeschke, G.; Wagner, B.; Fischer, H.; Bendels, S.; Zimmerli, D.; Schneider, J.; Diederich, F.; Kansy, M.; Müller, K., Predicting and Tuning Physicochemical Properties in Lead Optimization: Amine Basicities. **2007**, *2* (8), 1100-1115.
14. Müller, K.; Faeh, C.; Diederich, F., *Science* **2007**, *317*, 1881.
15. Kirk, K. L., Fluorination in Medicinal Chemistry: Methods, Strategies, and Recent Developments. *Organic Process Research & Development* **2008**, *12* (2), 305-321.
16. Hagmann, W. K., *J. Med. Chem.* **2008**, *51*, 4359.
17. Purser, S.; Moore, P. R.; Swallow, S.; Gouverneur, V., Fluorine in medicinal chemistry. *Chem. Soc. Rev.* **2008**, *37* (2), 320-330.
18. O'Hagan, D., Fluorine in health care: Organofluorine containing blockbuster drugs. *J. Fluorine Chem.* **2010**, *131* (11), 1071-1081.
19. Goekjian, P. G.; Wu, G.-Z.; Chen, S.; Zhou, L.; Jirousek, M. R.; Gillig, J. R.; Ballas, L. M.; Dixon, J. T., Synthesis of Fluorinated Macrocyclic Bis(indolyl)maleimides as Potential <sup>19</sup>F NMR Probes for Protein Kinase C. *J. Org. Chem.* **1999**, *64* (12), 4238-4246.
20. Moumné, R.; Pasco, M.; Prost, E.; Lecourt, T.; Micouin, L.; Tisné, C., Fluorinated Diaminocyclopentanes as Chiral Sensitive NMR Probes of RNA Structure. *J. Am. Chem. Soc.* **2010**, *132* (38), 13111-13113.
21. Cobb, S. L.; Murphy, C. D., <sup>19</sup>F NMR applications in chemical biology. *J. Fluorine Chem.* **2009**, *130* (2), 132-143.
22. Chen, H.; Viel, S.; Ziarelli, F.; Peng, L., <sup>19</sup>F NMR: a valuable tool for studying biological events. *Chem. Soc. Rev.* **2013**, *42* (20), 7971-7982.
23. Ametamey, S. M.; Honer, M.; Schubiger, P. A., Molecular Imaging with PET. *Chem. Rev.* **2008**, *108* (5), 1501-1516.
24. O'Hagan, D., Understanding organofluorine chemistry. An introduction to the C–F bond. *Chem. Soc. Rev.* **2008**, *37* (2), 308-319.
25. Böhm, H. J.; Banner, D.; Bendels, S.; Kansy, M.; Kuhn, B.; Müller, K.; Obst-Sander, U.; Stahl, M., Fluorine in Medicinal Chemistry. *ChemBioChem* **2004**, *5* (5), 637-643.
26. Hagmann, W. K., The Many Roles for Fluorine in Medicinal Chemistry. *J. Med. Chem.* **2008**, *51*, 4359.
27. Gillis, E. P.; Eastman, K. J.; Hill, M. D.; Donnelly, D. J.; Meanwell, N. A., Applications of Fluorine in Medicinal Chemistry. *J. Med. Chem.* **2015**, *58* (21), 8315-8359.
28. Purser, S.; Moore, P. R.; Swallow, S.; Gouverneur, V., Fluorine in medicinal chemistry. *Chemical Society Reviews* **2008**, *37* (2), 320-330.
29. Smart, B. E., Fluorine substituent effects (on bioactivity). *Journal of Fluorine Chemistry* **2001**, *109* (1), 3-11.
30. Shah, P.; Westwell, A. D., The role of fluorine in medicinal chemistry. *Journal of Enzyme Inhibition and Medicinal Chemistry* **2007**, *22* (5), 527-540.
31. Guengerich, F. P., Common and Uncommon Cytochrome P450 Reactions Related to Metabolism and Chemical Toxicity. *Chemical Research in Toxicology* **2001**, *14* (6), 611-650.
32. Bume, D. D.; Harry, S. A.; Lectka, T.; Pitts, C. R., Catalyzed and Promoted Aliphatic Fluorination. *The Journal of Organic Chemistry* **2018**, *83* (16), 8803-8814.
33. Szpera, R.; Moseley, D. F. J.; Smith, L. B.; Sterling, A. J.; Gouverneur, V., The Fluorination of C–H Bonds: Developments and Perspectives. *Angewandte Chemie International Edition* **2019**, *58* (42), 14824-14848.
34. Cheng, Q.; Ritter, T., New Directions in C–H Fluorination. *Trends in Chemistry* **2019**, *1* (5), 461-470.



35. Froese, R. D. J.; Whiteker, G. T.; Peterson, T. H.; Arriola, D. J.; Renga, J. M.; Shearer, J. W., Computational and Experimental Studies of Regioselective S<sub>N</sub>Ar Halide Exchange (HalEx) Reactions of Pentachloropyridine. *The Journal of Organic Chemistry* **2016**, *81* (22), 10672-10682.
36. Ye, Y.; Schimler, S. D.; Hanley, P. S.; Sanford, M. S., Cu(OTf)<sub>2</sub>-Mediated Fluorination of Aryltrifluoroborates with Potassium Fluoride. *J. Am. Chem. Soc.* **2013**, *135* (44), 16292-16295.
37. Ichiishi, N.; Canty, A. J.; Yates, B. F.; Sanford, M. S., Cu-Catalyzed Fluorination of Diaryliodonium Salts with KF. *Org. Lett.* **2013**, *15* (19), 5134-5137.
38. Lee, H. G.; Milner, P. J.; Buchwald, S. L., An Improved Catalyst System for the Pd-Catalyzed Fluorination of (Hetero)Aryl Triflates. *Org. Lett.* **2013**, *15* (21), 5602-5605.
39. Fier, P. S.; Luo, J.; Hartwig, J. F., Copper-Mediated Fluorination of Arylboronate Esters. Identification of a Copper(III) Fluoride Complex. *J. Am. Chem. Soc.* **2013**, *135* (7), 2552-2559.
40. Fier, P. S.; Hartwig, J. F., Copper-Mediated Fluorination of Aryl Iodides. *J. Am. Chem. Soc.* **2012**, *134* (26), 10795-10798.
41. Tang, P.; Furuya, T.; Ritter, T., Silver-Catalyzed Late-Stage Fluorination. *J. Am. Chem. Soc.* **2010**, *132* (34), 12150-12154.
42. Truong, T.; Klimovica, K.; Daugulis, O., Copper-Catalyzed, Directing Group-Assisted Fluorination of Arene and Heteroarene C-H Bonds. *J. Am. Chem. Soc.* **2013**, *135* (25), 9342-9345.
43. Lentz, D.; Braun, T.; Kuehnel, M. F., Synthesis of Fluorinated Building Blocks by Transition-Metal-Mediated Hydrodefluorination Reactions. *Angew. Chem. Int. Ed. Engl.* **2013**, *52* (12), 3328-3348.
44. Ahrens, T.; Kohlmann, J.; Ahrens, M.; Braun, T., Functionalization of Fluorinated Molecules by Transition-Metal-Mediated C-F Bond Activation To Access Fluorinated Building Blocks. *Chem. Rev.* **2015**, *115* (2), 931-972.
45. Weaver, J.; Senaweera, S., C-F activation and functionalization of perfluoro- and polyfluoroarenes. *Tetrahedron* **2014**, *70* (41), 7413-7428.
46. Kiplinger, J. L.; Richmond, T. G.; Osterberg, C. E., Activation of Carbon-Fluorine Bonds by Metal Complexes. *Chem. Rev.* **1994**, *94* (2), 373-431.
47. Amii, H.; Uneyama, K., C-F Bond Activation in Organic Synthesis. *Chem. Rev.* **2009**, *109* (5), 2119-2183.
48. Sandford, G., Pentafluoropyridine. In *Encyclopedia of Reagents for Organic Synthesis*, 2005.
49. Sun, A. D.; Love, J. A., Nickel-Catalyzed Selective Defluorination to Generate Partially Fluorinated Biaryls. *Organic Letters* **2011**, *13* (10), 2750-2753.
50. Wang, T.; Keyes, L.; Patrick, B. O.; Love, J. A., Exploration of the Mechanism of Platinum(II)-Catalyzed C-F Activation: Characterization and Reactivity of Platinum(IV) Fluoroaryl Complexes Relevant to Catalysis. *Organometallics* **2012**, *31* (4), 1397-1407.
51. Konovalov, V. V.; Laev, S. S.; Beregovaya, I. V.; Shchegoleva, L. N.; Shteingarts, V. D.; Tsvetkov, Y. D.; Bilkis, I., Fragmentation of Radical Anions of Polyfluorinated Benzoates. *The Journal of Physical Chemistry A* **2000**, *104* (2), 352-361.
52. Arndt, P.; Spannenberg, A.; Baumann, W.; Burlakov, V. V.; Rosenthal, U.; Becke, S.; Weiss, T., Reactions of Zirconocene 2-Vinylpyridine Complexes with Diisobutylaluminum Hydride and Fluoride. *Organometallics* **2004**, *23* (20), 4792-4795.
53. Schneider, H.; Hock, A.; Jaeger, A. D.; Lentz, D.; Radius, U., NHC-Alane Adducts as Hydride Sources in the Hydrodefluorination of Fluoroaromatics and Fluoroolefins. *European Journal of Inorganic Chemistry* **2018**, *2018* (36), 4031-4043.
54. Edelbach, B. L.; Fazlur Rahman, A. K.; Lachicotte, R. J.; Jones, W. D., Carbon-Fluorine Bond Cleavage by Zirconium Metal Hydride Complexes. *Organometallics* **1999**, *18* (16), 3170-3177.

55. Aizenberg, M.; Milstein, D., Homogeneous rhodium complex-catalyzed hydrogenolysis of C-F bonds. *Journal of the American Chemical Society* **1995**, *117* (33), 8674-8675.
56. Aizenberg, M.; Milstein, D., Catalytic Activation of Carbon-Fluorine Bonds by a Soluble Transition Metal Complex. *Science* **1994**, *265* (5170), 359-361.
57. Laev, S. S.; Shteingarts, V. D.; Bilkis, I. I., On the difference in the results of reductive defluorination of pentafluorobenzoic acid by sodium and zinc in liquid ammonia medium. *Tetrahedron Letters* **1995**, *36* (26), 4655-4658.
58. Ischay, M. A.; Anzovino, M. E.; Du, J.; Yoon, T. P., Efficient Visible Light Photocatalysis of [2+2] Enone Cycloadditions. *Journal of the American Chemical Society* **2008**, *130* (39), 12886-12887.
59. Nicewicz, D. A.; MacMillan, D. W. C., Merging Photoredox Catalysis with Organocatalysis: The Direct Asymmetric Alkylation of Aldehydes. *Science* **2008**, *322* (5898), 77-80.
60. Narayanam, J. M. R.; Tucker, J. W.; Stephenson, C. R. J., Electron-Transfer Photoredox Catalysis: Development of a Tin-Free Reductive Dehalogenation Reaction. *Journal of the American Chemical Society* **2009**, *131* (25), 8756-8757.
61. Ciamician, G., THE PHOTOCHEMISTRY OF THE FUTURE. *Science* **1912**, *36* (926), 385-394.
62. Srinivasan, R., Use of a  $\pi$ -Complex of an Olefin as a Photochemical Catalyst. *Journal of the American Chemical Society* **1963**, *85* (19), 3048-3049.
63. Baldwin, J. E.; Greeley, R. H., Cycloadditions. IV. Mechanism of the Photoisomerization of cis,cis-1,5-Cyclooctadiene to Tricyclo[3.3.0.0<sup>2,6</sup>]octane. *Journal of the American Chemical Society* **1965**, *87* (20), 4514-4516.
64. Salomon, R. G.; Kochi, J. K., Copper(I) catalysis in photocycloadditions. I. Norbornene. *Journal of the American Chemical Society* **1974**, *96* (4), 1137-1144.
65. Twilton, J.; Le, C.; Zhang, P.; Shaw, M. H.; Evans, R. W.; MacMillan, D. W. C., The merger of transition metal and photocatalysis. *Nature Reviews Chemistry* **2017**, *1* (7), 0052.
66. Shaw, M. H.; Twilton, J.; MacMillan, D. W. C., Photoredox Catalysis in Organic Chemistry. *The Journal of Organic Chemistry* **2016**, *81* (16), 6898-6926.
67. Romero, N. A.; Nicewicz, D. A., Organic Photoredox Catalysis. *Chemical Reviews* **2016**, *116* (17), 10075-10166.
68. Fagnoni, M.; Dondi, D.; Ravelli, D.; Albin, A., Photocatalysis for the Formation of the C-C Bond. *Chemical Reviews* **2007**, *107* (6), 2725-2756.
69. Xu, C.; Ravi Anusuyadevi, P.; Aymonier, C.; Luque, R.; Marre, S., Nanostructured materials for photocatalysis. *Chemical Society Reviews* **2019**, *48* (14), 3868-3902.
70. Flamigni, L.; Barbieri, A.; Sabatini, C.; Ventura, B.; Barigelletti, F., Photochemistry and Photophysics of Coordination Compounds: Iridium. In *Photochemistry and Photophysics of Coordination Compounds II*, Balzani, V.; Campagna, S., Eds. Springer Berlin Heidelberg: Berlin, Heidelberg, 2007; pp 143-203.
71. You, Y.; Nam, W., Photofunctional triplet excited states of cyclometalated Ir(III) complexes: beyond electroluminescence. *Chemical Society Reviews* **2012**, *41* (21), 7061-7084.
72. Daub, M. E.; Jung, H.; Lee, B. J.; Won, J.; Baik, M.-H.; Yoon, T. P., Enantioselective [2+2] Cycloadditions of Cinnamate Esters: Generalizing Lewis Acid Catalysis of Triplet Energy Transfer. *Journal of the American Chemical Society* **2019**, *141* (24), 9543-9547.
73. Amador, A. G.; Sherbrook, E. M.; Yoon, T. P., A Redox Auxiliary Strategy for Pyrrolidine Synthesis via Photocatalytic [3+2] Cycloaddition. *Asian Journal of Organic Chemistry* **2019**, *8* (7), 978-985.
74. Lowry, M. S.; Hudson, W. R.; Pascal, R. A.; Bernhard, S., Accelerated Luminophore Discovery through Combinatorial Synthesis. *J. Am. Chem. Soc.* **2004**, *126* (43), 14129-14135.

75. Teegardin, K.; Day, J. I.; Chan, J.; Weaver, J., Advances in Photocatalysis: A Microreview of Visible Light Mediated Ruthenium and Iridium Catalyzed Organic Transformations. *Organic Process Research & Development* **2016**, *20* (7), 1156-1163.
76. Holick, M. F.; Smith, E.; Pincus, S., Skin as the Site of Vitamin D Synthesis and Target Tissue for 1,25-Dihydroxyvitamin D<sub>3</sub>: Use of Calcitriol (1,25-Dihydroxyvitamin D<sub>3</sub>) for Treatment of Psoriasis. *Archives of Dermatology* **1987**, *123* (12), 1677-1683a.
77. Fuß, W., Previtamin D: Z-E photoisomerization via a Hula-twist conical intersection. *Physical Chemistry Chemical Physics* **2019**, *21* (13), 6776-6789.
78. Liu, R. S. H., Photoisomerization by Hula-Twist: A Fundamental Supramolecular Photochemical Reaction. *Accounts of Chemical Research* **2001**, *34* (7), 555-562.
79. Müller, A. M.; Lochbrunner, S.; Schmid, W. E.; Fuß, W., Low-Temperature Photochemistry of Previtamin D: A Hula-Twist Isomerization of a Triene. *Angewandte Chemie International Edition* **1998**, *37* (4), 505-507.
80. van der Horst, M. A.; Hellingwerf, K. J., Photoreceptor Proteins, "Star Actors of Modern Times": A Review of the Functional Dynamics in the Structure of Representative Members of Six Different Photoreceptor Families. *Accounts of Chemical Research* **2004**, *37* (1), 13-20.
81. Lewis, G. N.; Magel, T. T.; Lipkin, D., The Absorption and Re-emission of Light by cis- and trans-Stilbenes and the Efficiency of their Photochemical Isomerization. *Journal of the American Chemical Society* **1940**, *62* (11), 2973-2980.
82. Hammond, G. S.; Saltiel, J.; Lamola, A. A.; Turro, N. J.; Bradshaw, J. S.; Cowan, D. O.; Counsell, R. C.; Vogt, V.; Dalton, C., Mechanisms of Photochemical Reactions in Solution. XXII.1 Photochemical cis-trans Isomerization. *Journal of the American Chemical Society* **1964**, *86* (16), 3197-3217.
83. Lewis, F. D.; Bassani, D. M.; Caldwell, R. A.; Unett, D. J., Singlet State Cis,Trans Photoisomerization and Intersystem Crossing of 1-Arylpropenes. *Journal of the American Chemical Society* **1994**, *116* (23), 10477-10485.
84. Foote, C. S., Mechanisms of Photosensitized Oxidation. *Science* **1968**, *162* (3857), 963-970.
85. Albini, A., Photosensitization in Organic Synthesis. *Synthesis* **1981**, *1981* (04), 249-264.
86. Ohno, T.; Lichtin, N. N., Electron transfer in the quenching of triplet methylene blue by complexes of iron(II). *Journal of the American Chemical Society* **1980**, *102* (14), 4636-4643.
87. Srivastava, V.; Singh, P. P., Eosin Y catalysed photoredox synthesis: a review. *RSC Advances* **2017**, *7* (50), 31377-31392.
88. Dilling, W. L., Photochemical cycloaddition reactions of nonaromatic conjugated hydrocarbon dienes and polyenes. *Chemical Reviews* **1969**, *69* (6), 845-877.
89. Turro, N. J., Triplet-triplet excitation transfer in fluid solution: Applications to organic photochemistry. *Journal of Chemical Education* **1966**, *43* (1), 13.
90. Lindlar, H., Ein neuer Katalysator für selektive Hydrierungen. *Helvetica Chimica Acta* **1952**, *35* (2), 446-450.
91. Lindlar, H.; Dubuis, R.; Jones, F. N.; McKusick, B. C., Palladium Catalyst for Partial Reduction of Acetylenes. *Organic Syntheses* **1966**, *46*.
92. Overman, L. E.; Brown, M. J.; McCann, S. F.; Newbold, R. C.; Kende, A. S., (Z)-4-(Trimethylsilyl)-3-Buten-1-ol. *Organic Syntheses* **1990**, *68*.
93. Campos, K. R.; Cai, D.; Journet, M.; Kowal, J. J.; Larsen, R. D.; Reider, P. J., Controlled Semihydrogenation of Aminoalkynes Using Ethylenediamine as a Poison of Lindlar's Catalyst. *The Journal of Organic Chemistry* **2001**, *66* (10), 3634-3635.

94. Tucker, C. E.; Davidson, J.; Knochel, P., Mild and stereoselective hydroborations of functionalized alkynes and alkenes using pinacolborane. *The Journal of Organic Chemistry* **1992**, *57* (12), 3482-3485.
95. Brown, H. C.; Hamaoka, T.; Ravindran, N., Stereospecific conversion of alkenylboronic acids into alkenyl bromides with inversion of configuration. Striking differences in the stereochemistry of the replacement of the boronic acid substituent by bromine and iodine and its significance in terms of the reaction mechanism. *Journal of the American Chemical Society* **1973**, *95* (19), 6456-6457.
96. Brown, H. C.; Hamaoka, T.; Ravindran, N., Reaction of alkenylboronic acids with iodine under the influence of base. Simple procedure for the stereospecific conversion of terminal alkynes into trans-1-alkenyl iodides via hydroboration. *Journal of the American Chemical Society* **1973**, *95* (17), 5786-5788.
97. McGough, J. S.; Butler, S. M.; Cade, I. A.; Ingleson, M. J., Highly selective catalytic trans-hydroboration of alkynes mediated by borenium cations and B(C<sub>6</sub>F<sub>5</sub>)<sub>3</sub>. *Chemical Science* **2016**, *7* (5), 3384-3389.
98. Bergelson, L. D.; Barsukov, L. I.; Shemyakin, M. M., The stereochemistry of the Wittig reaction with non-stabilized and semistabilized ylids. *Tetrahedron* **1967**, *23* (6), 2709-2720.
99. Stork, G.; Zhao, K., A stereoselective synthesis of (Z)-1-iodo-1-alkenes. *Tetrahedron Letters* **1989**, *30* (17), 2173-2174.
100. The Nobel Prize in Chemistry 2005. <https://www.nobelprize.org/prizes/chemistry/2005/press-release/> (accessed 3/15/2020).
101. Gottumukkala, A. L.; Madduri, A. V. R.; Minnaard, A. J., Z-Selectivity: A Novel Facet of Metathesis. *ChemCatChem* **2012**, *4* (4), 462-467.
102. Werrel, S.; Walker, J. C. L.; Donohoe, T. J., Application of catalytic Z-selective olefin metathesis in natural product synthesis. *Tetrahedron Letters* **2015**, *56* (38), 5261-5268.
103. Singh, K.; Staig, S. J.; Weaver, J. D., Facile synthesis of Z-alkenes via uphill catalysis. *J. Am. Chem. Soc.* **2014**, *136* (14), 5275-8.
104. Lu, Z.; Yoon, T. P., Visible Light Photocatalysis of [2+2] Styrene Cycloadditions by Energy Transfer. *Angewandte Chemie International Edition* **2012**, *51* (41), 10329-10332.
105. Stoll, M.; Hulstkamp, J.; Rouvé, A., Synthèses de produits macrocycliques à odeur musquée. 8e communication Synthèse de la civettone naturelle. *Helv. Chim. Acta* **1948**, *31* (2), 543-553.
106. Marshall, J., Trans-cycloalkenes and [a.b]betweenanenes, molecular jump ropes and double bond sandwiches. *Accounts Chem Res* **1980**, *13* (7), 213-218.
107. Cope, A. C.; Pike, R. A.; Spencer, C. F., Cyclic Polyolefins. XXVII. cis- and trans-Cyclooctene from N,N-Dimethylcyclooctylamine. *J. Am. Chem. Soc.* **1953**, *75* (13), 3212-3215.
108. Wallraff, G. M.; Michl, J., Low-temperature reactions of copper(I) triflate complexes of cis- and trans-cyclooctene cis- and trans-cycloheptene with trimethyl phosphite. Spectroscopic evidence for free trans-cycloheptene. *J Org Chem* **1986**, *51* (10), 1794-1800.
109. Inoue, Y.; Ueoka, T.; Kuroda, T.; Hakushi, T., Singlet photosensitization of simple alkenes. Part 4. cis-trans Photoisomerization of cycloheptene sensitized by aromatic esters. Some aspects of the chemistry of trans-cycloheptene. *J. Chem. Soc., Perkin Trans. 2* **1983**, *0* (7), 983-988.
110. Verbeek, J.; Van Lenthe, J. H.; Timmermans, P. J. J. A.; Mackor, A.; Budzelaar, P. H. M., On the existence of trans-cyclohexene. *The Journal of Organic Chemistry* **1987**, *52* (13), 2955-2957.
111. Bonneau, R.; Jousot-Dubien, J.; Salem, L.; Yarwood, A. J., A trans cyclohexene. *J. Am. Chem. Soc.* **1976**, *98* (14), 4329-4330.

112. Dauben, W. G.; Van Riel, H. C. H. A.; Hauw, C.; Leroy, F.; Jousot-Dubien, J.; Bonneau, R., Photochemical formation of trans-1-phenylcyclohexene. Chemical proof of structure. *J. Am. Chem. Soc.* **1979**, *101* (7), 1901-1903.
113. Kropp, P. J., Photochemistry of cycloalkenes. V. Effects of ring size and substitution. *J. Am. Chem. Soc.* **1969**, *91* (21), 5783-5791.
114. Rosenberg, H. M.; Serve, M. P., Photolysis of 1-phenylcyclohexene in methanol. *J. Org. Chem.* **1972**, *37* (1), 141-142.
115. Schuster, D. I.; Brown, R. H.; Resnick, B. M., Photochemistry of ketones in solution. 53. Stereospecific triplet-state photorearrangements of chiral 2-cyclohexenones: type A lumiketone rearrangement and phenyl migrations. *J. Am. Chem. Soc.* **1978**, *100* (14), 4504-4512.
116. Cozens, F. L.; McClelland, R. A.; Steenken, S., Observation of cationic intermediates in the photolysis of 1-phenylcyclohexene. *J. Am. Chem. Soc.* **1993**, *115* (12), 5050-5055.
117. Li, X.; Danishefsky, S. J., Cyclobutenone as a highly reactive dienophile: expanding upon Diels-Alder paradigms. *J. Am. Chem. Soc.* **2010**, *132* (32), 11004-11005.
118. Paton, R. S.; Kim, S.; Ross, A. G.; Danishefsky, S. J.; Houk, K. N., Experimental Diels-Alder Reactivities of Cycloalkenones and Cyclic Dienes Explained through Transition-State Distortion Energies. *Angew. Chem. Int. Ed.* **2011**, *123* (44), 10550-10552.
119. Ross, A. G.; Li, X.; Danishefsky, S. J., Intramolecular Diels-Alder reactions of cycloalkenones: translation of high endo selectivity to trans junctions. *J. Am. Chem. Soc.* **2012**, *134* (38), 16080-16084.
120. Medina, J. M.; McMahon, T. C.; Jimenez-Oses, G.; Houk, K. N.; Garg, N. K., Cycloadditions of cyclohexynes and cyclopentyne. *J. Am. Chem. Soc.* **2014**, *136* (42), 14706-9.
121. Shah, T. K.; Medina, J. M.; Garg, N. K., Expanding the Strained Alkyne Toolbox: Generation and Utility of Oxygen-Containing Strained Alkynes. *J. Am. Chem. Soc.* **2016**, *138* (14), 4948-4954.
122. Medina, J. M.; Ko, J. H.; Maynard, H. D.; Garg, N. K., Expanding the ROMP Toolbox: Synthesis of Air-Stable Benzonorbornadiene Polymers by Aryne Chemistry. *Macromolecules* **2017**, *50* (2), 580-586.
123. Blackman, M. L.; Royzen, M.; Fox, J. M., Tetrazine ligation: fast bioconjugation based on inverse-electron-demand Diels-Alder reactivity. *J. Am. Chem. Soc.* **2008**, *130* (41), 13518-13519.
124. Tasdelen, M. A.; Yagci, Y., Light-induced click reactions. *Angew. Chem. Int. Ed.* **2013**, *52* (23), 5930-8.
125. Arumugam, S.; Popik, V. V., Light-induced hetero-Diels-Alder cycloaddition: a facile and selective photoclick reaction. *J. Am. Chem. Soc.* **2011**, *133* (14), 5573-9.
126. Wang, Y.; Song, W.; Hu, W. J.; Lin, Q., Fast alkene functionalization in vivo by Photoclick chemistry: HOMO lifting of nitrile imine dipoles. *Angew. Chem. Int. Ed.* **2009**, *48* (29), 5330-5333.
127. Hoyle, C. E.; Lowe, A. B.; Bowman, C. N., Thiol-click chemistry: a multifaceted toolbox for small molecule and polymer synthesis. *Chem. Soc. Rev.* **2010**, *39* (4), 1355-1387.
128. Poloukhine, A. A.; Mbua, N. E.; Wolfert, M. A.; Boons, G. J.; Popik, V. V., Selective labeling of living cells by a photo-triggered click reaction. *J. Am. Chem. Soc.* **2009**, *131* (43), 15769-76.
129. Nikolai, J.; Loe, Ø.; Dominiak, P. M.; Gerlitz, O. O.; Autschbach, J.; Davies, H. M. L., Mechanistic Studies of UV Assisted [4 + 2] Cycloadditions in Synthetic Efforts toward Vibsanin E. *J. Am. Chem. Soc.* **2007**, *129* (35), 10763-10772.
130. Dorr, H.; Rawal, V. H., The Intramolecular Diels-Alder Reactions of Photochemically Generated trans-Cycloalkenones. *J. Am. Chem. Soc.* **1999**, *121* (43), 10229-10230.
131. Jin, S.; Nguyen, V. T.; Dang, H. T.; Nguyen, D. P.; Arman, H. D.; Larionov, O. V., Photoinduced Carbaborative Ring Contraction Enables Regio- and Stereoselective Synthesis of

Multiply Substituted Five-Membered Carbocycles and Heterocycles. *J. Am. Chem. Soc.* **2017**, *139* (33), 11365-11368.

132. Ikezawa, H.; Kutal, C.; Yasufuku, K.; Yamazaki, H., Direct and sensitized valence photoisomerization of a substituted norbornadiene. Examination of the disparity between singlet- and triplet-state reactivities. *Journal of the American Chemical Society* **1986**, *108* (7), 1589-1594.
133. Islangulov, R. R.; Castellano, F. N., Photochemical Upconversion: Anthracene Dimerization Sensitized to Visible Light by a Rull Chromophore. *Angewandte Chemie International Edition* **2006**, *45* (36), 5957-5959.
134. McTiernan, C. D.; Morin, M.; McCallum, T.; Scaiano, J. C.; Barriault, L., Polynuclear gold(i) complexes in photoredox catalysis: understanding their reactivity through characterization and kinetic analysis. *Catalysis Science & Technology* **2016**, *6* (1), 201-207.
135. Shchegoleva, L. N.; Beregovaya, I. V.; Schastnev, P. V., Potential energy surface of C6F6<sup>-</sup> radical anion. *Chemical Physics Letters* **1999**, *312* (2), 325-332.
136. Clot, E.; Mégret, C.; Eisenstein, O.; Perutz, R. N., Exceptional Sensitivity of Metal–Aryl Bond Energies to ortho-Fluorine Substituents: Influence of the Metal, the Coordination Sphere, and the Spectator Ligands on M–C/H–C Bond Energy Correlations. *Journal of the American Chemical Society* **2009**, *131* (22), 7817-7827.
137. Beatty, J. W.; Stephenson, C. R. J., Amine Functionalization via Oxidative Photoredox Catalysis: Methodology Development and Complex Molecule Synthesis. *Accounts of Chemical Research* **2015**, *48* (5), 1474-1484.
138. Wayner, D. D. M.; Dannenberg, J. J.; Griller, D., Oxidation potentials of  $\alpha$ -aminoalkyl radicals: bond dissociation energies for related radical cations. *Chemical Physics Letters* **1986**, *131* (3), 189-191.
139. Senaweera, S. M.; Singh, A.; Weaver, J. D., Photocatalytic Hydrodefluorination: Facile Access to Partially Fluorinated Aromatics. *Journal of the American Chemical Society* **2014**, *136* (8), 3002-3005.
140. Kharasch, M. S.; Mayo, F. R., The Peroxide Effect in the Addition of Reagents to Unsaturated Compounds. I. The Addition of Hydrogen Bromide to Allyl Bromide. *Journal of the American Chemical Society* **1933**, *55* (6), 2468-2496.
141. Singh, A.; Kubik, J. J.; Weaver, J. D., Photocatalytic C–F alkylation; facile access to multifluorinated arenes. *Chemical Science* **2015**, *6* (12), 7206-7212.
142. Singh, A.; Fennell, C. J.; Weaver, J. D., Photocatalyst size controls electron and energy transfer: selectable E/Z isomer synthesis via C-F alkenylation. *Chem. Sci.* **2016**, *7* (11), 6796-6802.
143. Senaweera, S.; Weaver, J. D., Dual C–F, C–H Functionalization via Photocatalysis: Access to Multifluorinated Biaryls. *Journal of the American Chemical Society* **2016**, *138* (8), 2520-2523.
144. Priya, S.; Weaver, J. D., Prenyl Praxis: A Method for Direct Photocatalytic Defluoroprenylation. *Journal of the American Chemical Society* **2018**, *140* (47), 16020-16025.
145. Terrier, F., Rate and equilibrium studies in Jackson-Meisenheimer complexes. *Chemical Reviews* **1982**, *82* (2), 77-152.
146. Handel, H.; Pasquini, M. A.; Pierre, J. L., Effets de cryptands et activation de bases—VII11Partie précédente Réf. 1.: Réduction des halogénures de phényle par l'hydrure de potassium. *Tetrahedron* **1980**, *36* (22), 3205-3208.
147. Kwan, E. E.; Zeng, Y.; Besser, H. A.; Jacobsen, E. N., Concerted nucleophilic aromatic substitutions. *Nature Chemistry* **2018**, *10* (9), 917-923.
148. Neumann, C. N.; Hooker, J. M.; Ritter, T., Concerted nucleophilic aromatic substitution with (19)F(-) and (18)F(-). *Nature* **2016**, *534* (7607), 369-373.

149. Senger, N. A.; Bo, B.; Cheng, Q.; Keeffe, J. R.; Gronert, S.; Wu, W., The Element Effect Revisited: Factors Determining Leaving Group Ability in Activated Nucleophilic Aromatic Substitution Reactions. *The Journal of Organic Chemistry* **2012**, *77* (21), 9535-9540.
150. Bowler, J. T.; Wong, F. M.; Gronert, S.; Keeffe, J. R.; Wu, W., Reactivity in the nucleophilic aromatic substitution reactions of pyridinium ions. *Organic & Biomolecular Chemistry* **2014**, *12* (32), 6175-6180.
151. Bunnett, J. F.; Garbisch, E. W.; Pruitt, K. M., The "Element Effect" as a Criterion of Mechanism in Activated Aromatic Nucleophilic Substitution Reactions<sup>1,2</sup>. *Journal of the American Chemical Society* **1957**, *79* (2), 385-391.
152. Aksenov, V. V.; Vlasov, V. M.; Yakobson, G. G., Interaction of pentafluoropyridine with 4-nitrophenol and pentafluorophenol in the presence of potassium fluoride and 18-crown-6-ether. *Journal of Fluorine Chemistry* **1982**, *20* (4), 439-458.
153. Vlasov, V. M.; Aksenov, V. V.; Rodionov, P. P.; Beregovaya, I. V.; Shchegoleva, L. N., Unusual Lability of Pentafluorophenoxy Group in Reactions of Potassium Aroxides with Pentafluoropyridine. *Russian Journal of Organic Chemistry* **2002**, *38* (1), 115-125.
154. Rohrbach, S.; Smith, A. J.; Pang, J. H.; Poole, D. L.; Tuttle, T.; Chiba, S.; Murphy, J. A., Concerted Nucleophilic Aromatic Substitution Reactions. *Angewandte Chemie International Edition* **2019**, *58* (46), 16368-16388.
155. Singh, A.; Kubik, J. J.; Weaver, J. D., Photocatalytic C-F alkylation; facile access to multifluorinated arenes. *Chemical Science* **2015**.
156. Campagna, S.; Puntoriero, F.; Nastasi, F.; Bergamini, G.; Balzani, V., Photochemistry and Photophysics of Coordination Compounds: Ruthenium Photochemistry and Photophysics of Coordination Compounds I. *Top. Curr. Chem.* **2007**, *280*, 117-214.
157. Flamigni, L.; Barbieri, A.; Sabatini, C.; Ventura, B.; Barigelletti, F., Photochemistry and Photophysics of Coordination Compounds: Iridium Photochemistry and Photophysics of Coordination Compounds II. *Top. Curr. Chem.* **2007**, *281*, 143-203.
158. Prier, C. K.; Rankic, D. A.; MacMillan, D. W. C., Visible Light Photoredox Catalysis with Transition Metal Complexes: Applications in Organic Synthesis. *Chem. Rev.* **2013**, *113* (7), 5322-5363.
159. Kalyanasundaram, K.; Grätzel, M., Applications of functionalized transition metal complexes in photonic and optoelectronic devices. *Coord. Chem. Rev.* **1998**, *177* (1), 347-414.
160. Lowry, M. S.; Bernhard, S., Synthetically Tailored Excited States: Phosphorescent, Cyclometalated Iridium(III) Complexes and Their Applications. *Chem. Eur. J.* **2006**, *12* (31), 7970-7977.
161. Lalevee, J.; Peter, M.; Dumur, F.; Gigmès, D.; Blanchard, N.; Tehfe, M.-A.; Morlet-Savary, F.; Fouassier, J. P., Subtle Ligand Effects in Oxidative Photocatalysis with Iridium Complexes: Application to Photopolymerization. *Chem. Eur. J.* **2011**, *17* (52), 15027-15031.
162. Ischay, M. A.; Anzovino, M. E.; Du, J.; Yoon, T. P., Efficient Visible Light Photocatalysis of [2+2] Enone Cycloadditions. *J. Am. Chem. Soc.* **2008**, *130* (39), 12886-12887.
163. Pac, C.; Ihama, M.; Yasuda, M.; Miyauchi, Y.; Sakurai, H., Tris(2,2'-bipyridine)ruthenium(2+)-mediated photoreduction of olefins with 1-benzyl-1,4-dihydronicotinamide: a mechanistic probe for electron-transfer reactions of NAD(P)H-model compounds. *J. Am. Chem. Soc.* **1981**, *103* (21), 6495-6497.
164. Fukuzumi, S.; Mochizuki, S.; Tanaka, T., Photocatalytic reduction of phenacyl halides by 9,10-dihydro-10-methylacridine: control between the reductive and oxidative quenching pathways of tris(bipyridine)ruthenium complex utilizing an acid catalysis. *J. Phys. Chem.* **1990**, *94* (2), 722-726.

165. Narayanam, J. M. R.; Stephenson, C. R. J., Visible light photoredox catalysis: applications in organic synthesis. *Chem. Soc. Rev.* **2011**, *40* (1), 102-113.
166. Terrett, J. A.; Clift, M. D.; MacMillan, D. W. C., Direct  $\beta$ -Alkylation of Aldehydes via Photoredox Organocatalysis. *J. Am. Chem. Soc.* **2014**, *136* (19), 6858-6861.
167. Slinker, J. D.; Gorodetsky, A. A.; Lowry, M. S.; Wang, J.; Parker, S.; Rohl, R.; Bernhard, S.; Malliaras, G. G., Efficient yellow electroluminescence from a single layer of a cyclometalated iridium complex. *J. Am. Chem. Soc.* **2004**, *126* (9), 2763-7.
168. Juris, A.; Balzani, V.; Belser, P.; von Zelewsky, A., Characterization of the Excited State Properties of Some New Photosensitizers of the Ruthenium (Polypyridine) Family. *Helv. Chim. Acta* **1981**, *64* (7), 2175-2182.
169. Rillema, D. P.; Allen, G.; Meyer, T. J.; Conrad, D., Redox properties of ruthenium(II) tris chelate complexes containing the ligands 2,2'-bipyrazine, 2,2'-bipyridine, and 2,2'-bipyrimidine. *Inorg. Chem.* **1983**, *22* (11), 1617-1622.
170. Haga, M.; Dodsworth, E. S.; Eryavec, G.; Seymour, P.; Lever, A. B. P., Luminescence quenching of the tris(2,2'-bipyrazine)ruthenium(II) cation and its monoprotinated complex. *Inorg. Chem.* **1985**, *24* (12), 1901-1906.
171. Young, R. C.; Meyer, T. J.; Whitten, D. G., Electron transfer quenching of excited states of metal complexes. *J. Am. Chem. Soc.* **1976**, *98* (1), 286-287.
172. Prier, C. K.; Rankic, D. A.; MacMillan, D. W., Visible light photoredox catalysis with transition metal complexes: applications in organic synthesis. *Chem. Rev.* **2013**, *113* (7), 5322-63.
173. Farney, E. P.; Yoon, T. P., Visible-Light Sensitization of Vinyl Azides by Transition Metal Photocatalysis. *Angew. Chem., Int. Ed.* **2014**, *53* (3), 793-797.
174. Dedeian, K.; Djurovich, P. I.; Garces, F. O.; Carlson, G.; Watts, R. J., A new synthetic route to the preparation of a series of strong photoreducing agents: fac-tris-ortho-metalated complexes of iridium(III) with substituted 2-phenylpyridines. *Inorg. Chem.* **1991**, *30* (8), 1685-1687.
175. Grushin, V. V.; Herron, N.; LeCloux, D. D.; Marshall, W. J.; Petrov, V. A.; Wang, Y., New, efficient electroluminescent materials based on organometallic Ir complexes. *Chem. Commun.* **2001**, (16), 1494-1495.
176. Singh, A.; Teegardin, K.; Kelly, M.; Prasad, K. S.; Krishnan, S.; Weaver, J. D., Facile synthesis and complete characterization of homoleptic and heteroleptic cyclometalated Iridium(III) complexes for photocatalysis. *J. Organomet. Chem.* **2015**, *776*, 51-59.
177. Ladouceur, S.; Fortin, D.; Zysman-Colman, E., Enhanced Luminescent Iridium(III) Complexes Bearing Aryltriazole Cyclometallated Ligands. *Inorg. Chem.* **2011**, *50* (22), 11514-11526.
178. Swanick, K. N.; Ladouceur, S.; Zysman-Colman, E.; Ding, Z., Correlating electronic structures to electrochemiluminescence of cationic Ir complexes. *RSC Adv.* **2013**, *3* (43), 19961-19964.
179. Anderson, B. L.; Maher, A. G.; Nava, M.; Lopez, N.; Cummins, C. C.; Nocera, D. G., Ultrafast Photoinduced Electron Transfer from Peroxide Dianion. *J. Phys. Chem.* **2015**, *119* (24), 7422-7429.
180. Zou, Y.-Q.; Lu, L.-Q.; Fu, L.; Chang, N.-J.; Rong, J.; Chen, J.-R.; Xiao, W.-J., Visible-Light-Induced Oxidation/3+2 Cycloaddition/Oxidative Aromatization Sequence: A Photocatalytic Strategy To Construct Pyrrolo 2,1-a isoquinolines. *Angew. Chem., Int. Ed.* **2011**, *50* (31), 7171-7175.
181. Damrauer, N. H.; Boussie, T. R.; Devenney, M.; McCusker, J. K., Effects of Intraligand Electron Delocalization, Steric Tuning, and Excited-State Vibronic Coupling on the Photophysics of Aryl-Substituted Bipyridyl Complexes of Ru(II). *J. Am. Chem. Soc.* **1997**, *119* (35), 8253-8268.



182. Bernhard, S.; Barron, J. A.; Houston, P. L.; Abruña, H. D.; Ruglovksy, J. L.; Gao, X.; Malliaras, G. G., Electroluminescence in Ruthenium(II) Complexes. *J. Am. Chem. Soc.* **2002**, *124* (45), 13624-13628.
183. Lv, H.; Cai, Y.-B.; Zhang, J.-L., Copper-Catalyzed Hydrodefluorination of Fluoroarenes by Copper Hydride Intermediates. *Angew. Chem., Int. Ed.* **2013**, *52* (11), 3203-3207.
184. Kalyanasundaram, K., Photophysics, photochemistry and solar energy conversion with tris(bipyridyl)ruthenium(II) and its analogues. *Coord. Chem. Rev.* **1982**, *46*, 159-244.
185. Bryant, G. M.; Fergusson, J. E.; Powell, H. K. J., Charge-transfer and intraligand electronic spectra of bipyridyl complexes of iron, ruthenium, and osmium. I. Bivalent complexes. *Aust. J. Chem.* **1971**, *24* (2), 257-273.
186. Bueldt, L. A.; Prescimone, A.; Neuburger, M.; Wenger, O. S., Photoredox Properties of Homoleptic d6 Metal Complexes with the Electron-Rich 4,4',5,5'-Tetramethoxy-2,2'-bipyridine Ligand. *Eur. J. Inorg. Chem.* **2015**, *2015* (28), 4666-4677.
187. McNally, A.; Prier, C. K.; MacMillan, D. W. C., Discovery of an  $\alpha$ -Amino C-H Arylation Reaction Using the Strategy of Accelerated Serendipity. *Science* **2011**, *334* (6059), 1114-1117.
188. Singh, A.; Arora, A.; Weaver, J. D., Photoredox-Mediated C-H Functionalization and Coupling of Tertiary Aliphatic Amines with 2-Chloroazoles. *Organic letters* **2013**, *15*, 5390-5393.
189. Qin, Q.; Yu, S., Visible-Light-Promoted Redox Neutral C-H Amidation of Heteroarenes with Hydroxylamine Derivatives. *Org. Lett.* **2014**, *16* (13), 3504-3507.
190. Kim, H.; Kim, T.; Lee, D. G.; Roh, S. W.; Lee, C., Nitrogen-centered radical-mediated C-H imidation of arenes and heteroarenes via visible light induced photocatalysis. *Chem. Commun.* **2014**, *50* (66), 9273-9276.
191. Arora, A.; Teegardin, K. A.; Weaver, J. D., Reductive Alkylation of 2-Bromoazoles via Photoinduced Electron Transfer: A Versatile Strategy to Csp<sup>2</sup>-Csp<sup>3</sup> Coupled Products. *Org. Lett.* **2015**, *17* (15), 3722-3725.
192. Uraguchi, D.; Kinoshita, N.; Kizu, T.; Ooi, T., Synergistic Catalysis of Ionic Bronsted Acid and Photosensitizer for a Redox Neutral Asymmetric  $\alpha$ -Coupling of N-Arylaminomethanes with Aldimines. *J. Am. Chem. Soc.* **2015**, *137* (43), 13768-13771.
193. Senaweera, S.; Weaver, J. D., Dual C-F, C-H Functionalization via Photocatalysis: Access to Multifluorinated Biaryls. *J. Am. Chem. Soc.* **2016**, *138* (8), 2520-3.
194. Nguyen, J. D.; Matsuura, B. S.; Stephenson, C. R. J., A Photochemical Strategy for Lignin Degradation at Room Temperature. *J. Am. Chem. Soc.* **2014**, *136* (4), 1218-1221.
195. Wang, J.; Zheng, N., The cleavage of a C-C Bond in cyclobutylanilines by visible-light photoredox catalysis: Development of a [4+2] annulation method. *Angew. Chem., Int. Ed.* **2015**, *54* (39), 11424-11427.
196. Rono, L. J.; Yayla, H. G.; Wang, D. Y.; Armstrong, M. F.; Knowles, R. R., Enantioselective Photoredox Catalysis Enabled by Proton-Coupled Electron Transfer: Development of an Asymmetric Aza-Pinacol Cyclization. *J. Am. Chem. Soc.* **2013**.
197. Qin, Q.; Yu, S., Visible-Light-Promoted Remote C(sp<sup>3</sup>)-H Amidation and Chlorination. *Org. Lett.* **2015**, *17* (8), 1894-1897.
198. Tellis, J. C.; Primer, D. N.; Molander, G. A., Single-electron transmetalation in organoboron cross-coupling by photoredox/nickel dual catalysis. *Science* **2014**, *345* (6195), 433-436.
199. Labadie, J. W.; Stille, J. K., Mechanisms of the palladium-catalyzed couplings of acid chlorides with organotin reagents. *J. Am. Chem. Soc.* **1983**, *105* (19), 6129-6137.
200. Finch, A.; Gardner, P. J.; Pearn, E. J.; Watts, G. B., Thermochemistry of triphenylboron, tricyclohexylboron and some phenylboron halides. *T. Faraday Soc.* **1967**, *63*, 1880.

201. Noble, A.; MacMillan, D. W. C., Photoredox  $\alpha$ -Vinylolation of  $\alpha$ -Amino Acids and N-Aryl Amines. *J. Am. Chem. Soc.* **2014**, *136* (33), 11602-11605.
202. Beatty, J. W.; Stephenson, C. R. J., Synthesis of (-)-Pseudotabersonine, (-)-Pseudovincadifformine, and (+)-Coronaridine Enabled by Photoredox Catalysis in Flow. *J. Am. Chem. Soc.* **2014**, *136* (29), 10270-10273.
203. Di Rocco, D. A.; Dykstra, K.; Krska, S.; Vachal, P.; Conway, D. V.; Tudge, M., Late-stage functionalization of biologically active heterocycles through photoredox catalysis. *Angew. Chem., Int. Ed.* **2014**, *53* (19), 4802-4806.
204. Minisci, F.; Bernardi, R.; Bertini, F.; Galli, R.; Perchinnino, M., Nucleophilic character of alkyl radicals—VI. *Tetrahedron* **1971**, *27* (15), 3575-3579.
205. Molander, G. A.; Colombel, V.; Braz, V. A., Direct Alkylation of Heteroaryls Using Potassium Alkyl- and Alkoxyethyltrifluoroborates. *Org. Lett.* **2011**, *13* (7), 1852-1855.
206. Noble, A.; McCarver, S. J.; MacMillan, D. W. C., Merging Photoredox and Nickel Catalysis: Decarboxylative Cross-Coupling of Carboxylic Acids with Vinyl Halides. *J. Am. Chem. Soc.* **2015**, *137* (2), 624-627.
207. Chu, L.; Lipshultz, J. M.; MacMillan, D. W., Merging Photoredox and Nickel Catalysis: The Direct Synthesis of Ketones by the Decarboxylative Arylation of  $\alpha$ -Oxo Acids. *Angew. Chem., Int. Ed.* **2015**, *54* (27), 7929-33.
208. Lu, Z.; Yoon, T. P., Visible Light Photocatalysis of [2+2] Styrene Cycloadditions by Energy Transfer. *Angew. Chem., Int. Ed.* **2012**, *51* (41), 10329-10332.
209. Sahoo, B.; Hopkinson, M. N.; Glorius, F., Combining Gold and Photoredox Catalysis: Visible Light-Mediated Oxy- and Aminoarylation of Alkenes. *J. Am. Chem. Soc.* **2013**, *135* (15), 5505-5508.
210. Singh, K.; Staig, S. J.; Weaver, J. D., Facile Synthesis of Z-Alkenes via Uphill Catalysis. *J. Am. Chem. Soc.* **2014**, *136* (14), 5275-5278.
211. Osawa, M.; Hoshino, M.; Wakatsuki, Y., A Light-Harvesting tert-Phosphane Ligand Bearing a Ruthenium(II) Polypyridyl Complex as Substituent. *Angew. Chem., Int. Ed.* **2001**, *40* (18), 3472-3474.
212. Fabry, D. C.; Ronge, M. A.; Rueping, M., Immobilization and Continuous Recycling of Photoredox Catalysts in Ionic Liquids for Applications in Batch Reactions and Flow Systems: Catalytic Alkene Isomerization by Using Visible Light. *Chem. Eur. J.* **2015**, *21* (14), 5350-5354.
213. Maity, S.; Zhu, M.; Shinabery, R. S.; Zheng, N., Intermolecular [3+2] Cycloaddition of Cyclopropylamines with Olefins by Visible-Light Photocatalysis. *Angew. Chem., Int. Ed.* **2012**, *51* (1), 222-226.
214. Blum, T. R.; Zhu, Y.; Nordeen, S. A.; Yoon, T. P., Photocatalytic Synthesis of Dihydrobenzofurans by Oxidative [3+2] Cycloaddition of Phenols. *Angew. Chem., Int. Ed.* **2014**, *53* (41), 11056-11059.
215. Tyson, E. L.; Niemeyer, Z. L.; Yoon, T. P., Redox Mediators in Visible Light Photocatalysis: Photocatalytic Radical Thiol-Ene Additions. *J. Org. Chem.* **2014**, *79* (3), 1427-1436.
216. Oh, S. H.; Malpani, Y. R.; Ha, N.; Jung, Y.-S.; Han, S. B., Vicinal Difunctionalization of Alkenes: Chlorotrifluoromethylation with CF<sub>3</sub>SO<sub>2</sub>Cl by Photoredox Catalysis. *Org. Lett.* **2014**, *16* (5), 1310-1313.
217. Iqbal, N.; Jung, J.; Park, S.; Cho, E. J., Controlled Trifluoromethylation Reactions of Alkynes through Visible-Light Photoredox Catalysis. *Angew. Chem., Int. Ed.* **2014**, *53* (2), 539-542.
218. Tang, X.-J.; Thomason, C. S.; Dolbier, W. R., Jr., Photoredox-Catalyzed Tandem Radical Cyclization of N-Arylacrylamides: General Methods To Construct Fluorinated 3,3-Disubstituted 2-Oxindoles Using Fluoroalkylsulfonyle Chlorides. *Org. Lett.* **2014**, *16* (17), 4594-4597.

219. Andrews, R. S.; Becker, J. J.; Gagné, M. R., Investigating the Rate of Photoreductive Glucosyl Radical Generation. *Org. Lett.* **2011**, *13* (9), 2406-2409.
220. Penning, T. D.; Talley, J. J.; Bertenshaw, S. R.; Carter, J. S.; Collins, P. W.; Docter, S.; Graneto, M. J.; Lee, L. F.; Malecha, J. W.; Miyashiro, J. M.; Rogers, R. S.; Rogier, D. J.; Yu, S. S.; Anderson, G. D.; Burton, E. G.; Cogburn, J. N.; Gregory, S. A.; Koboldt, C. M.; Perkins, W. E.; Seibert, K.; Veenhuizen, A. W.; Zhang, Y. Y.; Isakson, P. C., Synthesis and Biological Evaluation of the 1,5-Diarylpyrazole Class of Cyclooxygenase-2 Inhibitors: Identification of 4-[5-(4-Methylphenyl)-3-(trifluoromethyl)-1H-pyrazol-1-yl]benzenesulfonamide (SC-58635, Celecoxib). *J. Med. Chem.* **1997**, *40* (9), 1347-1365.
221. Wang, J.; Sanchez-Rosello, M.; Acena, J. L.; del Pozo, C.; Sorochinsky, A. E.; Fustero, S.; Soloshonok, V. A.; Liu, H., Fluorine in pharmaceutical industry: fluorine-containing drugs introduced to the market in the last decade (2001-2011). *Chem. Rev.* **2014**, *114* (4), 2432-506.
222. Schimler, S. D.; Ryan, S. J.; Bland, D. C.; Anderson, J. E.; Sanford, M. S., Anhydrous Tetramethylammonium Fluoride for Room-Temperature S<sub>N</sub>Ar Fluorination. *J Org Chem* **2015**, *80* (24), 12137-12145.
223. Furuya, T.; Ritter, T., Fluorination of Boronic Acids Mediated by Silver(I) Triflate. *Org. Lett.* **2009**, *11* (13), 2860-2863.
224. Brooke, G. M., The preparation and properties of polyfluoro aromatic and heteroaromatic compounds. *J. Fluorine Chem.* **1997**, *86* (1), 1-76.
225. Campbell, M. G.; Ritter, T., Modern Carbon–Fluorine Bond Forming Reactions for Aryl Fluoride Synthesis. *Chem. Rev.* **2015**, *115* (2), 612-633.
226. Chambers, R. D.; Hutchinson, J.; Musgrave, W. K. R., Polyfluoro-heterocyclic compounds. Part I. The preparation of fluoro-, chlorofluoro-, and chlorofluorohydro-pyridines. *J. Chem. Soc.* **1964**, 3573.
227. Senaweera, S. M.; Weaver, J. D., Selective Perfluoro- and Polyfluoroarylation of Meldrum's Acid. *J Org Chem* **2014**, *79* (21), 10466-10476.
228. Senaweera, S. M.; Weaver, J. D., Dual C–F, C–H Functionalization via Photocatalysis; Access to Multi-Fluorinated Biaryls. *J. Am. Chem. Soc.* **2016**, *138*, 2520-2523.
229. Singh, A.; Kubik, J. J.; Weaver, J. D., Photocatalytic C-F alkylation; facile access to multifluorinated arenes. *Chem. Sci.* **2015**, *6* (12), 7206-7212.
230. Senaweera, S. M.; Singh, A.; Weaver, J. D., Photocatalytic Hydrodefluorination: Facile Access to Partially Fluorinated Aromatics. *J. Am. Chem. Soc.* **2014**, *136* (8), 3002–3005.
231. Singh, A.; Kubik, J. J.; Weaver, J. D., Photocatalytic C-F alkylation; facile access to multifluorinated arenes. *Chemical Science* **2015**, *6* (12), 7206-7212.
232. Senaweera, S.; Weaver, J. D., Photocatalytic C-F Reduction and Functionalization. *Aldrichimica Acta* **2016**, *49*, 45.
233. Senaweera, S. M.; Singh, A.; Weaver, J. D., Photocatalytic Hydrodefluorination: Facile Access to Partially Fluorinated Aromatics. *J. Am. Chem. Soc.* **2014**, *136* (8), 3002-3005.
234. Arora, A.; Weaver, J. D., Visible Light Photocatalysis for the Generation and Use of Reactive Azolyl and Polyfluoroaryl Intermediates. *Accounts Chem Res* **2016**, *49* (10), 2273-2283.
235. Weaver, J. D., Hydrodefluorination of Perfluoroarenes Meets Visible Light Photocatalysis. *Synlett* **2014**, *25* (14), 1946-1952.
236. LaBerge, N. A.; Love, J. A., Activation and Formation of Aromatic C–F Bonds. In *Organometallic Fluorine Chemistry*, Braun, T.; Hughes, R. P., Eds. Springer International Publishing: Cham, 2015; pp 55-111.
237. Hu, J.-Y.; Zhang, J.-L., Hydrodefluorination Reactions Catalyzed by Transition-Metal Complexes. In *Organometallic Fluorine Chemistry*, Braun, T.; Hughes, R. P., Eds. Springer International Publishing: Cham, 2015; pp 143-196.

238. Chambers, R. D.; Martin, P. A.; Sandford, G.; Williams, D. L. H., Mechanisms of reactions of halogenated compounds: Part 7. Effects of fluorine and other groups as substituents on nucleophilic aromatic substitution. *J. Fluorine Chem.* **2008**, *129* (10), 998-1002.
239. Sun, Y.; Sun, H.; Jia, J.; Du, A.; Li, X., Transition-Metal-Free Synthesis of Fluorinated Arenes from Perfluorinated Arenes Coupled with Grignard Reagents. *Organometallics* **2014**, *33* (4), 1079-1081.
240. Chambers, R. D.; Hassan, M. A.; Hoskin, P. R.; Kenwright, A.; Richmond, P.; Sandford, G., Polyhalogenated heterocyclic compounds: Part 45. Reactions of perfluoro-(4-isopropylpyridine) with oxygen, nitrogen and carbon nucleophiles [1]. *J. Fluorine Chem.* **2001**, *111* (2), 135-146.
241. Beyki, K.; Haydari, R.; Maghsoodlou, M. T., Synthesis of 2,3,5,6-tetrafluoro-pyridine derivatives from reaction of pentafluoropyridine with malononitrile, piperazine and tetrazole-5-thiol. *SpringerPlus* **2015**, *4* (1), 757.
242. Ono, N., *The Nitro Group in Organic Synthesis*. Wiley-VCH: 2001.
243. Colgin, N.; Tatum, N. J.; Pohl, E.; Cobb, S. L.; Sandford, G., Synthesis and molecular structure of a perfluorinated pyridyl carbanion. *J. Fluorine Chem.* **2012**, *133*, 33-37.
244. Vaidyanathaswamy, R.; Radha, K.; Dharani, M.; Raguraman, T. S.; Anand, R., Reaction of nitroalkanes with polyfluoroaromatic compounds. *J. Fluorine Chem.* **2012**, *144*, 33-37.
245. Prat, D.; Pardigon, O.; Flemming, H.-W.; Letestu, S.; Ducandas, V.; Isnard, P.; Guntrum, E.; Senac, T.; Ruisseau, S.; Cruciani, P.; Hosek, P., Sanofi's Solvent Selection Guide: A Step Toward More Sustainable Processes. *Organic Process Research & Development* **2013**, *17* (12), 1517-1525.
246. Bug, T.; Lemek, T.; Mayr, H., Nucleophilicities of Nitroalkyl Anions. *J Org Chem* **2004**, *69* (22), 7565-7576.
247. day, Prices of TMG and DBU.
248. Lee, L.; Kreutter, K. D.; Pan, W.; Crysler, C.; Spurlino, J.; Player, M. R.; Tomczuk, B.; Lu, T., 2-(2-Chloro-6-fluorophenyl)acetamides as potent thrombin inhibitors. *Bioorg. Med. Chem. Lett.* **2007**, *17* (22), 6266-6269.
249. Parikh, V. D.; Fray, A. H.; Kleinman, E. F., Synthesis of 8,9-difluoro-2-methyl-6-oxo-1,2-dihydropyrrolo[3,2,1-ij]quinoline-5-carboxylic acid. *J. Heterocyclic Chem.* **1988**, *25* (5), 1567-1569.
250. Pesti, J. A.; LaPorte, T.; Thornton, J. E.; Spangler, L.; Buono, F.; Crispino, G.; Gibson, F.; Lobben, P.; Papaioannou, C. G., Commercial Synthesis of a Pyrrolotriazine-Fluoroindole Intermediate to Brivanib Alaninate: Process Development Directed toward Impurity Control. *Org. Process Res. Dev.* **2014**, *18* (1), 89-102.
251. Brooke, G. M.; Burdon, J.; Tatlow, J. C., 172. Aromatic polyfluoro-compounds. Part VII. The reaction of pentafluoronitrobenzene with ammonia. *J. Chem. Soc.* **1961**, (0), 802-807.
252. Teegardin, K. A.; Weaver, J. D., Polyfluoroarylation of oxazolones: access to non-natural fluorinated amino acids. *Chemical Communications* **2017**.
253. Senaweera, S.; Weaver, J. D., *Currently unpublished work under review* **2017**.
254. Shipilov, A. I.; Zolotkova, E. E.; Igumnov, S. M., Chloro- and Bromo-defluorination of Hexafluorobenzene and Octafluorotoluene. *Russian Journal of Organic Chemistry* **2004**, *40* (8), 1117-1120.
255. Politzer, P.; Murray, J. S.; Clark, T.,  $\sigma$ -Hole Bonding: A Physical Interpretation. In *Halogen Bonding I*, Springer International Publishing Switzerland 2014: 2014; Vol. Volume 358 of the series Topics in Current Chemistry, pp 19-42.
256. Politzer, P.; Laurence, P. R.; Jayasuriya, K., Molecular electrostatic potentials: an effective tool for the elucidation of biochemical phenomena. *Environmental Health Perspectives* **1985**, *61*, 191-202.

257. Bürgi, H. B.; Dunitz, J. D.; Lehn, J. M.; Wipff, G., Stereochemistry of reaction paths at carbonyl centres. *Tetrahedron* **1974**, *30* (12), 1563-1572.
258. Billica, H. R. A., Homer, Catalyst, Raney Nickel, W-6. *Org. Synth.* **1949**, *29*, 24.
259. Subramanian, H.; Jasperse, C. P.; Sibi, M. P., Characterization of Bronsted acid-base complexes by 19F DOSY. *Org. Lett.* **2015**, *17* (6), 1429-32.
260. Gaussian 09, R. C.; Frisch, M. J.; Trucks, G. W.; Schlegel, H. B.; Scuseria, G. E.; Robb, M. A.; Cheeseman, J. R.; Scalmani, G.; Barone, V.; Mennucci, B.; Petersson, G. A.; Nakatsuji, H.; Caricato, M.; Li, X.; Hratchian, H. P.; Izmaylov, A. F.; Bloino, J.; Zheng, G.; Sonnenberg, J. L.; Hada, M.; Ehara, M.; Toyota, K.; Fukuda, R.; Hasegawa, J.; Ishida, M.; Nakajima, T.; Honda, Y.; Kitao, O.; Nakai, H.; Vreven, T.; J. A. Montgomery, J.; Peralta, J. E.; Ogliaro, F.; Bearpark, M.; Heyd, J. J.; Brothers, E.; Kudin, K. N.; Staroverov, V. N.; Keith, T.; Kobayashi, R.; Normand, J.; Raghavachari, K.; Rendell, A.; Burant, J. C.; Iyengar, S. S.; Tomasi, J.; Cossi, M.; Rega, N.; Millam, J. M.; Klene, M.; Knox, J. E.; Cross, J. B.; Bakken, V.; Adamo, C.; Jaramillo, J.; Gomperts, R.; Stratmann, R. E.; Yazyev, O.; Austin, A. J.; Cammi, R.; Pomelli, C.; Ochterski, J. W.; Martin, R. L.; Morokuma, K.; Zakrzewski, V. G.; Voth, G. A.; Salvador, P.; Dannenberg, J. J.; Dapprich, S.; Daniels, A. D.; Farkas, O.; Foresman, J. B.; Ortiz, J. V.; Cioslowski, J.; Fox, D. J., *Gaussian, Inc., Wallingford CT* **2010**.
261. Corey, E. J.; Tada, M.; LaMahieu, R.; Libit, L., trans-2-Cycloheptenone. *J. Am. Chem. Soc.* **1965**, *87* (9), 2051-2052.
262. Singh, K.; Fennell, C. J.; Coutias, E. A.; Latifi, R.; Hartson, S.; Weaver, J. D., Light Harvesting for Rapid and Selective Reactions: Click Chemistry with Strain-Loadable Alkenes. *Chem-Us* **2018**, *4* (1), 124-137.
263. Wei, X.-J.; Boon, W.; Hessel, V.; Noël, T., Visible-Light Photocatalytic Decarboxylation of  $\alpha,\beta$ -Unsaturated Carboxylic Acids: Facile Access to Stereoselective Difluoromethylated Styrenes in Batch and Flow. *ACS Catalysis* **2017**, *7* (10), 7136-7140.
264. Straathof, N. J. W.; Cramer, S. E.; Hessel, V.; Noël, T., Practical Photocatalytic Trifluoromethylation and Hydrotrifluoromethylation of Styrenes in Batch and Flow. *Angew. Chem. Int. Ed.* **2016**, *55* (50), 15549-15553.
265. Lin, Q.-Y.; Xu, X.-H.; Qing, F.-L., Chemo-, Regio-, and Stereoselective Trifluoromethylation of Styrenes via Visible Light-Driven Single-Electron Transfer (SET) and Triplet-Triplet Energy Transfer (TTET) Processes. *J. Org. Chem.* **2014**, *79* (21), 10434-10446.
266. Metternich, J. B.; Gilmour, R., A Bio-Inspired, Catalytic E  $\rightarrow$  Z Isomerization of Activated Olefins. *J. Am. Chem. Soc.* **2015**, *137* (35), 11254-11257.
267. Metternich, J. B.; Gilmour, R., One Photocatalyst, n Activation Modes Strategy for Cascade Catalysis: Emulating Coumarin Biosynthesis with (-)-Riboflavin. *J. Am. Chem. Soc.* **2016**, *138* (3), 1040-1045.
268. Metternich, J. B.; Gilmour, R., Photocatalytic E  $\rightarrow$  Z Isomerization of Alkenes. *Synlett* **2016**, *27* (18), 2541-2552.
269. Rackl, D.; Kreitmeier, P.; Reiser, O., Synthesis of a polyisobutylene-tagged fac-Ir(ppy)<sub>3</sub> complex and its application as recyclable visible-light photocatalyst in a continuous flow process. *Green Chem* **2016**, *18* (1), 214-219.
270. Rono, L. J.; Yayla, H. G.; Wang, D. Y.; Armstrong, M. F.; Knowles, R. R., Enantioselective Photoredox Catalysis Enabled by Proton-Coupled Electron Transfer: Development of an Asymmetric Aza-Pinacol Cyclization. *J. Am. Chem. Soc.* **2013**, *135* (47), 17735-8.
271. Lian, J.-J.; Chen, P.-C.; Lin, Y.-P.; Ting, H.-C.; Liu, R.-S., Gold-Catalyzed Intramolecular [3 + 2]-Cycloaddition of Arenyne-Yne Functionalities. *J. Am. Chem. Soc.* **2006**, *128* (35), 11372-11373.
272. Monkman, A. P.; Burrows, H. D.; Hamblett, I.; Navarathnam, S.; Svensson, M.; Andersson, M. R., The effect of conjugation length on triplet energies, electron delocalization

- and electron–electron correlation in soluble polythiophenes. *J. Chem. Phys.* **2001**, *115* (19), 9046-9049.
273. Dexter, D. L., A Theory of Sensitized Luminescence in Solids. *J. Chem. Phys.* **1953**, *21* (5), 836-850.
274. Head-Gordon, M.; Pople, J. A.; Frisch, M. J., MP2 energy evaluation by direct methods. *Chem. Phys. Lett.* **1988**, *153* (6), 503-506.
275. Cramer, C., Essentials of Computational Chemistry: Theories and Models. II ed.; John Wiley & Sons: 2004; p 216.
276. Dunning, T. H., Gaussian basis sets for use in correlated molecular calculations. I. The atoms boron through neon and hydrogen. *J. Chem. Phys.* **1989**, *90* (2), 1007-1023.
277. Teegardin, K.; Day, J. I.; Chan, J.; Weaver, J., Advances in Photocatalysis: A Microreview of Visible Light Mediated Ruthenium and Iridium Catalyzed Organic Transformations. *Org. Process Res. Dev.* **2016**, *20* (7), 1156-1163.
278. Johnson, R. P.; DiRico, K. J., Ab Initio Conformational Analysis of trans-Cyclohexene. *J Org Chem* **1995**, *60* (4), 1074-1076.
279. Bally, T.; Rablen, P. R., Quantum-Chemical Simulation of <sup>1</sup>H NMR Spectra. 2. Comparison of DFT-Based Procedures for Computing Proton–Proton Coupling Constants in Organic Molecules. *J Org Chem* **2011**, *76* (12), 4818-4830.
280. Anslyn, E.; Dougherty, D., Isotope Effects. In *Modern Physical Organic Chemistry*, University Science Books: 2006; pp 429-430.
281. Günther, H., Chemical Shifts Through Hydrogen Bonding. In *NMR Spectroscopy*, John Wiley & Sons: 1995; pp 97-99.
282. Sun, A. D.; Love, J. A., Nickel-Catalyzed Selective Defluorination to Generate Partially Fluorinated Biaryls. *Org. Lett.* **2011**, *13* (10), 2750-2753.
283. Gopalakrishnan, G.; Hogg, J. L., Differentiation of nucleophilic and general base catalysis in hydrolysis of N-acetylbenzotriazole using the proton inventory technique. *J Org Chem* **1981**, *46* (24), 4959-4964.
284. Corona-Martinez, D. O.; Taran, O.; Yatsimirsky, A. K., Mechanism of general acid-base catalysis in transesterification of an RNA model phosphodiester studied with strongly basic catalysts. *Org. Biomol. Chem.* **2010**, *8* (4), 873-880.
285. Plata, R. E.; Singleton, D. A., A Case Study of the Mechanism of Alcohol-Mediated Morita Baylis–Hillman Reactions. The Importance of Experimental Observations. *J. Am. Chem. Soc.* **2015**, *137* (11), 3811-3826.
286. Winter, A., Making a bad calculation. *Nature Chem.* **2015**, *7*, 473.
287. Pettersen, E. F.; Goddard, T. D.; Huang, C. C.; Couch, G. S.; Greenblatt, D. M.; Meng, E. C.; Ferrin, T. E., UCSF Chimera--a visualization system for exploratory research and analysis. *J. Comput. Chem.* **2004**, *25* (13), 1605-12.
288. Singh, A.; Teegardin, K.; Kelly, M.; Prasad, K. S.; Krishnan, S.; Weaver, J. D., Facile synthesis and complete characterization of homoleptic and heteroleptic cyclometalated Iridium(III) complexes for photocatalysis. *Journal of Organometallic Chemistry* **2015**, *776*, 51-59.
289. Bally, T.; Rablen, P. R., Quantum-Chemical Simulation of <sup>1</sup>H NMR Spectra. 2. Comparison of DFT-Based Procedures for Computing Proton–Proton Coupling Constants in Organic Molecules. *The Journal of Organic Chemistry* **2011**, *76* (12), 4818-4830.
290. Jaivel, N.; Uvarani, C.; Rajesh, R.; Velmurugan, D.; Marimuthu, P., Natural Occurrence of Organofluorine and Other Constituents from *Streptomyces* sp. TC1. *Journal of Natural Products* **2014**, *77* (1), 2-8.

291. Aldemir, H.; Kohlhepp, S. V.; Gulder, T.; Gulder, T. A. M., Structure of a Putative Fluorinated Natural Product from *Streptomyces* sp. TC1. *Journal of Natural Products* **2014**, *77* (11), 2331-2334.
292. Ayouf, M. S.; Cordes, D. B.; Slawin, A. M. Z.; O'Hagan, D., Total Synthesis of a Reported Fluorometabolite from *Streptomyces* sp. TC1 Indicates an Incorrect Assignment. The Isolated Compound Did Not Contain Fluorine. *Journal of Natural Products* **2014**, *77* (6), 1249-1251.
293. Jaivel, N.; Uvarani, C.; Rajesh, R.; Velmurugan, D.; Marimuthu, P., Correction to Natural Occurrence of Organofluorine and Other Constituents from *Streptomyces* sp. TC1. *Journal of Natural Products* **2015**, *78* (2), 343-343.
294. Walker, M. C.; Chang, M. C. Y., Natural and engineered biosynthesis of fluorinated natural products. *Chemical Society Reviews* **2014**, *43* (18), 6527-6536.
295. Fried, J.; Sabo, E. F., Halogenated Corticoids. I. 9 $\alpha$ -Halogen Derivatives of Cortisone and Hydrocortisone\*. *Journal of the American Chemical Society* **1957**, *79* (5), 1130-1141.
296. Ramsay, L.; Shelton, J.; Harrison, I.; Tidd, M.; Asbury, M., Spironolactone and potassium canrenoate in normal man. *Clinical Pharmacology & Therapeutics* **1976**, *20* (2), 167-177.
297. O'Hagan, D., Fluorine in health care: Organofluorine containing blockbuster drugs. *J. Fluorine Chem.* **2010**, *131* (11), 1071-1081.
298. Zhan, C.-G.; Landry, D. W., Theoretical Studies of Competing Reaction Pathways and Energy Barriers for Alkaline Ester Hydrolysis of Cocaine. *The Journal of Physical Chemistry A* **2001**, *105* (8), 1296-1301.
299. Zhou, Y.; Wang, J.; Gu, Z.; Wang, S.; Zhu, W.; Aceña, J. L.; Soloshonok, V. A.; Izawa, K.; Liu, H., Next Generation of Fluorine-Containing Pharmaceuticals, Compounds Currently in Phase II–III Clinical Trials of Major Pharmaceutical Companies: New Structural Trends and Therapeutic Areas. *Chemical Reviews* **2016**, *116* (2), 422-518.
300. Mei, H.; Han, J.; Fustero, S.; Medio-Simon, M.; Sedgwick, D. M.; Santi, C.; Ruzziconi, R.; Soloshonok, V. A., Fluorine-Containing Drugs Approved by the FDA in 2018. *Chemistry – A European Journal* **2019**, *25* (51), 11797-11819.
301. Furuya, T.; Klein, J. E. M. N.; Ritter, T., Carbon-Fluorine Bond Formation for the Synthesis of Aryl Fluorides. *Synthesis* **2010**, *2010* (11), 1804-1821.
302. Capdevila, L.; Meyer, T. H.; Roldán-Gómez, S.; Luis, J. M.; Ackermann, L.; Ribas, X., Chemodivergent Nickel(0)-Catalyzed Arene C–F Activation with Alkynes: Unprecedented C–F/C–H Double Insertion. *ACS Catalysis* **2019**, *9* (12), 11074-11081.
303. Luo, Z.-J.; Zhao, H.-Y.; Zhang, X., Highly Selective Pd-Catalyzed Direct C–F Bond Arylation of Polyfluoroarenes. *Organic Letters* **2018**, *20* (9), 2543-2546.
304. Chen, K.; Berg, N.; Gschwind, R.; König, B., Selective Single C(sp<sup>3</sup>)–F Bond Cleavage in Trifluoromethylarenes: Merging Visible-Light Catalysis with Lewis Acid Activation. *Journal of the American Chemical Society* **2017**, *139* (51), 18444-18447.
305. Vogt, D. B.; Seath, C. P.; Wang, H.; Jui, N. T., Selective C–F Functionalization of Unactivated Trifluoromethylarenes. *Journal of the American Chemical Society* **2019**, *141* (33), 13203-13211.
306. Matsunami, A.; Kayaki, Y.; Kuwata, S.; Ikariya, T., Nucleophilic Aromatic Substitution in Hydrodefluorination Exemplified by Hydrido-iridium(III) Complexes with Fluorinated Phenylsulfonyl-1,2-diphenylethylenediamine Ligands. *Organometallics* **2018**, *37* (12), 1958-1969.
307. Lu, J.; Khetrpal, N. S.; Johnson, J. A.; Zeng, X. C.; Zhang, J., “ $\pi$ -Hole- $\pi$ ” Interaction Promoted Photocatalytic Hydrodefluorination via Inner-Sphere Electron Transfer. *Journal of the American Chemical Society* **2016**, *138* (49), 15805-15808.

308. Singh, A.; Fennell, C. J.; Weaver, J. D., Photocatalyst size controls electron and energy transfer: selectable E/Z isomer synthesis via C–F alkenylation. *Chemical Science* **2016**, *7* (11), 6796-6802.
309. Nicholls, T. P.; Robertson, J. C.; Gardiner, M. G.; Bissember, A. C., Identifying the potential of pulsed LED irradiation in synthesis: copper-photocatalysed C–F functionalisation. *Chemical Communications* **2018**, *54* (36), 4589-4592.
310. Cao, D.; Pan, P.; Zeng, H.; Li, C.-J., Umpolung cross-coupling of polyfluoroarenes with hydrazones via activation of C–F bonds. *Chemical Communications* **2019**, *55* (63), 9323-9326.
311. Dai, P.; Ma, J.; Huang, W.; Chen, W.; Wu, N.; Wu, S.; Li, Y.; Cheng, X.; Tan, R., Photoredox C–F Quaternary Annulation Catalyzed by a Strongly Reducing Iridium Species. *ACS Catalysis* **2018**, *8* (2), 802-806.
312. Meyer, A. U.; Slanina, T.; Yao, C.-J.; König, B., Metal-Free Perfluoroarylation by Visible Light Photoredox Catalysis. *ACS Catalysis* **2016**, *6* (1), 369-375.
313. Senaweera, S.; Weaver, J. D., Dual C–F, C–H Functionalization via Photocatalysis: Access to Multifluorinated Biaryls. *J. Am. Chem. Soc.* **2016**, *138* (8), 2520-2523.
314. Birch, A. J., 321. Reduction by dissolving metals. Part VII. The reactivity of mesomeric anions in relation to the reduction of benzene rings. *Journal of the Chemical Society (Resumed)* **1950**, (0), 1551-1556.
315. Chapman, O. L.; Fitton, P., A General Synthesis of the Troponoid System Based on Solvolysis of 1,4-Dihydrobenzyl Tosylates. *Journal of the American Chemical Society* **1963**, *85* (1), 41-47.
316. Rory, M.; Efrey, N.; Corey, S., *Arene Dearomatization via a Catalytic N-Centered Radical Cascade Reaction*. 2019.
317. Dong, W.; Yuan, Y.; Xie, X.; Zhang, Z., Visible-Light-Driven Dearomatization Reaction toward the Formation of Spiro[4.5]deca-1,6,9-trien-8-ones. *Organic Letters* **2020**, *22* (2), 528-532.
318. Gao, Y.; DeYonker, N. J.; Garrett, E. C.; Wilson, A. K.; Cundari, T. R.; Marshall, P., Enthalpy of Formation of the Cyclohexadienyl Radical and the C–H Bond Enthalpy of 1,4-Cyclohexadiene: An Experimental and Computational Re-Evaluation. *The Journal of Physical Chemistry A* **2009**, *113* (25), 6955-6963.
319. Chatterjee, A.; König, B., Birch-Type Photoreduction of Arenes and Heteroarenes by Sensitized Electron Transfer. *Angewandte Chemie* **2019**, *131* (40), 14427-14432.
320. Day, J. I.; Singh, K.; Trinh, W.; Weaver, J. D., Visible Light Mediated Generation of trans-Arylcyclohexenes and Their Utilization in the Synthesis of Cyclic Bridged Ethers. *Journal of the American Chemical Society* **2018**, *140* (31), 9934-9941.
321. Rathnayake, M. D.; Weaver, J. D., A General Photocatalytic Route to Prenylation. *European Journal of Organic Chemistry* *n/a* (n/a).
322. Kumarasamy, E.; Raghunathan, R.; Sibi, M. P.; Sivaguru, J., Nonbiaryl and Heterobiaryl Atropisomers: Molecular Templates with Promise for Atropselective Chemical Transformations. *Chemical Reviews* **2015**, *115* (20), 11239-11300.
323. Loutfy, R. O.; Loutfy, R. O., The interrelation between polarographic half-wave potentials and the energies of electronic excited states. *Canadian Journal of Chemistry* **1976**, *54* (9), 1454-1463.
324. Rathnayake, M. D.; Weaver, J. D., Alkyl Halides via Visible Light Mediated Dehalogenation. *Organic Letters* **2019**, *21* (23), 9681-9687.
325. Boyarkin, O. V.; Koshelev, M. A.; Aseev, O.; Maksyutenko, P.; Rizzo, T. R.; Zobov, N. F.; Lodi, L.; Tennyson, J.; Polyansky, O. L., Accurate bond dissociation energy of water determined



- by triple-resonance vibrational spectroscopy and ab initio calculations. *Chemical Physics Letters* **2013**, 568-569, 14-20.
326. Costentin, C.; Savéant, J.-M., Concepts and tools for mechanism and selectivity analysis in synthetic organic electrochemistry. *Proceedings of the National Academy of Sciences* **2019**, 116 (23), 11147-11152.
327. Loh, Y. Y.; Nagao, K.; Hoover, A. J.; Hesk, D.; Rivera, N. R.; Colletti, S. L.; Davies, I. W.; MacMillan, D. W. C., Photoredox-catalyzed deuteration and tritiation of pharmaceutical compounds. *Science* **2017**, 358 (6367), 1182-1187.
328. Huynh, M. H. V.; Meyer, T. J., Proton-Coupled Electron Transfer. *Chemical Reviews* **2007**, 107 (11), 5004-5064.
329. Montanari, S.; Paradisi, C.; Scorrano, G., Thiol anions in nucleophilic aromatic substitution reactions with activated aryl halides. Attack on carbon vs attack on halogen. *The Journal of Organic Chemistry* **1993**, 58 (21), 5628-5631.
330. Bertran, J.; Gallardo, I.; Moreno, M.; Savéant, J.-M., Are Anion Radicals Nucleophiles and/or Outersphere Electron Donors? An Ab Initio Study of the Reaction of Ethylene and Formaldehyde Anion Radicals with Methyl Fluoride and Chloride. *Journal of the American Chemical Society* **1996**, 118 (24), 5737-5744.
331. Smothers, W. K.; Schanze, K. S.; Saltiel, J., Concerning the diene-induced photodechlorination of chloroaromatics. *Journal of the American Chemical Society* **1979**, 101 (7), 1895-1896.
332. Banister, S. D.; Arnold, J. C.; Connor, M.; Glass, M.; McGregor, I. S., Dark Classics in Chemical Neuroscience:  $\Delta^9$ -Tetrahydrocannabinol. *ACS Chemical Neuroscience* **2019**, 10 (5), 2160-2175.
333. Martin, B. R.; Jefferson, R. G.; Winckler, R.; Wiley, J. L.; Thomas, B. F.; Crocker, P. J.; Williams, W.; Razdan, R. K., Assessment of structural commonality between tetrahydrocannabinol and anandamide. *European Journal of Pharmacology* **2002**, 435 (1), 35-42.
334. Westphal, M. V.; Schafroth, M. A.; Sarott, R. C.; Imhof, M. A.; Bold, C. P.; Leippe, P.; Dhopeswarkar, A.; Grandner, J. M.; Katritch, V.; Mackie, K.; Trauner, D.; Carreira, E. M.; Frank, J. A., Synthesis of Photoswitchable  $\Delta^9$ -Tetrahydrocannabinol Derivatives Enables Optical Control of Cannabinoid Receptor 1 Signaling. *Journal of the American Chemical Society* **2017**, 139 (50), 18206-18212.
335. Breuer, A.; Haj, C. G.; Fogaça, M. V.; Gomes, F. V.; Silva, N. R.; Pedrazzi, J. F.; Del Bel, E. A.; Hallak, J. C.; Crippa, J. A.; Zuardi, A. W.; Mechoulam, R.; Guimarães, F. S., Fluorinated Cannabidiol Derivatives: Enhancement of Activity in Mice Models Predictive of Anxiolytic, Antidepressant and Antipsychotic Effects. *PLOS ONE* **2016**, 11 (7), e0158779.
336. Banister, S. D.; Stuart, J.; Kevin, R. C.; Edington, A.; Longworth, M.; Wilkinson, S. M.; Beinat, C.; Buchanan, A. S.; Hibbs, D. E.; Glass, M.; Connor, M.; McGregor, I. S.; Kassiou, M., Effects of Bioisosteric Fluorine in Synthetic Cannabinoid Designer Drugs JWH-018, AM-2201, UR-144, XLR-11, PB-22, 5F-PB-22, APICA, and STS-135. *ACS Chemical Neuroscience* **2015**, 6 (8), 1445-1458.
337. Barton, D. H. R.; McCombie, S. W., A new method for the deoxygenation of secondary alcohols. *Journal of the Chemical Society, Perkin Transactions 1* **1975**, (16), 1574-1585.
338. Rackl, D.; Kais, V.; Kreitmeier, P.; Reiser, O., Visible light photoredox-catalyzed deoxygenation of alcohols. *Beilstein Journal of Organic Chemistry* **2014**, 10, 2157-2165.
339. Lau, C. K.; Dufresne, C.; Belanger, P. C.; Pietre, S.; Scheiget, J., Reductive deoxygenation of aryl aldehydes and ketones and benzylic, allylic, and tertiary alcohols by zinc iodide-sodium cyanoborohydride. *The Journal of Organic Chemistry* **1986**, 51 (15), 3038-3043.

340. Chandrasekhar, S.; Chandrashekar, G.; Reddy, M. S.; Srihari, P., A facile and chemoselective conjugate reduction using polymethylhydrosiloxane (PMHS) and catalytic B(C<sub>6</sub>F<sub>5</sub>)<sub>3</sub>. *Organic & Biomolecular Chemistry* **2006**, 4 (9), 1650-1652.

341. Fulmer, G. R.; Miller, A. J. M.; Sherden, N. H.; Gottlieb, H. E.; Nudelman, A.; Stoltz, B. M.; Bercaw, J. E.; Goldberg, K. I., NMR Chemical Shifts of Trace Impurities: Common Laboratory Solvents, Organics, and Gases in Deuterated Solvents Relevant to the Organometallic Chemist. *Organometallics* **2010**, 29 (9), 2176-2179.

## 6.10 Experimental

### General Comments

All reactions were conducted in dried and deoxygenated solvents. Solvents for column chromatography were used without further purification. Commercially available starting materials were used as received.

### Melting Points

Melting points were determined on a Stuart SMP10 melting point apparatus and are reported uncorrected.

### NMR Analysis

NMR-spectra were recorded using a Bruker Advance 400 (400 MHz for <sup>1</sup>H, 101 MHz for <sup>13</sup>C, 376 MHz for <sup>19</sup>F) or a Bruker Neo 600 with BBO BBF-H-D-05 SmartProbe (599 MHz for <sup>1</sup>H, 564 MHz for <sup>19</sup>F, 151 MHz for <sup>13</sup>C), as noted. Chemical shifts are reported in ppm on the δ scale with residual solvent signal as internal standard<sup>341</sup>. As abbreviations for the multiplicity were used: s = singlet, d = doublet, t = triplet, q = quartet, m = multiplet, pt = pseudo triplet, app = apparent.

Analysis of reaction mixtures was performed in undeuterated solvents with either a DMSO-d<sub>6</sub> or C<sub>6</sub>D<sub>6</sub> capillary as reference. Spectra were analyzed using Topspin 4.0.6 or MestReNova 14.0.1-23559.

### Thin Layer Chromatography

Thin layer chromatography was done on with silica gel pre-coated aluminum sheets (Machery-Nagel, silica gel 60 G/UV254, 0.2 mm) and for visualization UV-light (254 nm) and potassium permanganate stain.

### X-Ray Analysis

X-Ray analysis was performed by the crystallography laboratory of the University of Regensburg. Structure solving was done by Florian Meurer.

### **Computational**

Calculations were conducted using Gaussian 09 RevE.01 on the HPC-cluster Athene at University of Regensburg or using Gaussian 09, Revision C.01 on Cowboy or Pete supercomputing clusters at the Oklahoma State University. Geometries at or near minima as determined by frequency calculation.

### **General Procedure A (batch) for formation of the 1,4-diene:**

In a darkened labspace, into a new 25 mL test tube fitted with a stirbar was charged the fluoroarene (2.0 mmol) and a stock solution consisting of the Ar-H (3.0 equiv.), DIPEA (1.1 equiv.), Ir(dtbubpy)(dtbuppy)<sub>2</sub>PF<sub>6</sub> (0.125 mol %), water (15 equiv.), a C<sub>6</sub>F<sub>6</sub> internal standard (1/6 equiv. – testing showed no difference between reactions in which the standard was included and those in which it was not), and acetonitrile (0.1 M). The test tube was fitted with a rubber septum. This solution was chilled to 0 °C and then sparged with argon for 10 minutes at 0 °C. The solution was attached to low, constant positive argon pressure and added to an irradiation bath at 460 nm and held at 0 °C until complete by NMR indication of complete consumption of SM. The reaction was then concentrated, extracted at least thrice with boiling hexanes, or until no remaining color was apparent in hexanes extracts. The pooled hexanes extracts were then concentrated and the resultant mixture heated in a 10 mL round bottomed flask at 90 °C under high vacuum for 1-2 hours. The resultant mixture was then dry loaded onto silica, and subjected to flash chromatography on a silica column with a hexanes and ethyl acetate mobile phase. The fractions containing the product were pooled and concentrated in a 20 mL scintillation vial. To the resultant oil was added a minimal amount of methanol, from which pure crystals formed upon repeated freezing of the solution in liquid nitrogen followed by vigorous shaking as the solution warmed.

### **General Procedure B (batch) for formation of the 1,4-diene:**

Perfluoroarene (12 mmol), aromatic trapping agent (31.2 mmol, 2.6 equiv.) and [Ir(dtbppy)(dtbppy)<sub>2</sub>]PF<sub>6</sub> (2 mg, 0.014 mol%) are dissolved in 120 mL of ACN inside a Tauchschaftreactor. DIPEA (14.4 mmol, 2.52 mL, 1.2 equiv.) is added within 60 h via syringe pump while irradiated at 455 nm. After three days the solvent is removed under reduced pressure. The residue is dissolved in 100 mL boiling hexane and filtered to remove insoluble components. The solvent is removed under reduced pressure and most of the Ar-H coupling partner distilled off with Kugelrohr distillation (for methyl toluate and methyl acetophenone: 95 °C, 1 mbar. 80-90% recovered). The residue is purified via

column chromatography and recrystallized from methanol. Crystallization usually is strongly inhibited if the product is not very pure. Addition of a seed crystal usually induces crystallization. If no crystal is available, repeatedly freezing the solution in liquid nitrogen and thawing can induced crystallization. After the first crystallization step photo-Birch dienes usually crystallize easily. A strongly yellow colored side product cannot be completely removed via column chromatography. After 1 – 3 crystallization steps the dienes are obtained as colorless solids.

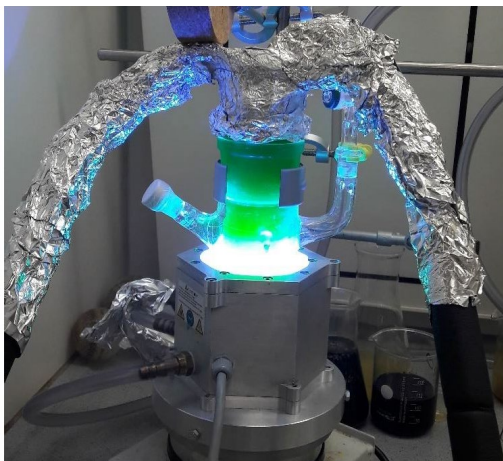
### **General Procedure C (flow) for formation of the 1,4-diene:**

In a darkened labspace, same as above except in 250 mL PFA round bottom flask test tube fitted with a stirbar was charged the fluoroarene and a stock solution consisting of the Ar-H (3.0 equiv.), DIPEA (1.1 equiv.), Ir(dtbubpy)(dtbuppy)<sub>2</sub>PF<sub>6</sub> (0.125 mol %), water (15 equiv.) and acetonitrile (0.1 M). The flask was fitted with a rubber septum. The solution was attached to low, constant positive argon pressure and circulated through PFA tubing via a peristaltic pump at 70 RPM, in which it was irradiated and held at room temp until complete by NMR indication of complete consumption of SM through analysis of aliquot.

### **General Procedure D (NMR scale)**

Same as general procedure A, except in a clean, dry NMR tube. A sealed melting point capillary containing a deuterated solvent was included in the NMR tube. The tube was then chilled to 0 deg. C. and degassed by sparging with argon through an 18-gauge stainless steel needle for 10 minutes. The NMR tube was fitted with a septum and sealed with parafilm.

### **Reaction Setup for Photo-Birch Arylation**



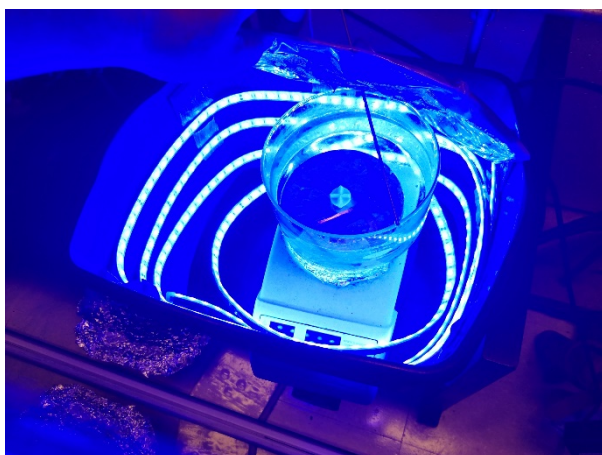
Large scale Tauchschaftreactor (below) reactions were conducted in a 120 mL vessel, irradiated by 24 OSRAM Osilon SSL 80 royal-blue LEDs ( $\lambda = 455$ )



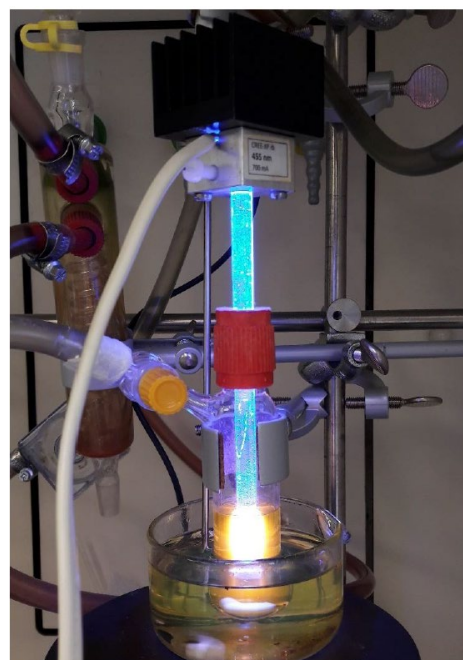
Reactions for substrate screening were conducted in sealed glass vials by irradiation with OSRAM Oslon SSL 80 royal-blue LEDs ( $\lambda = 455 \text{ nm} (\pm 15 \text{ nm})$ , 3.5 V, 700 mA), or in NMR tubes (as below)



Room temperature high intensity light bath (NMR scale) – lights are Solid Apollo Blue Waterproof 5050 72W LED Strip Light 465 nm SKU:

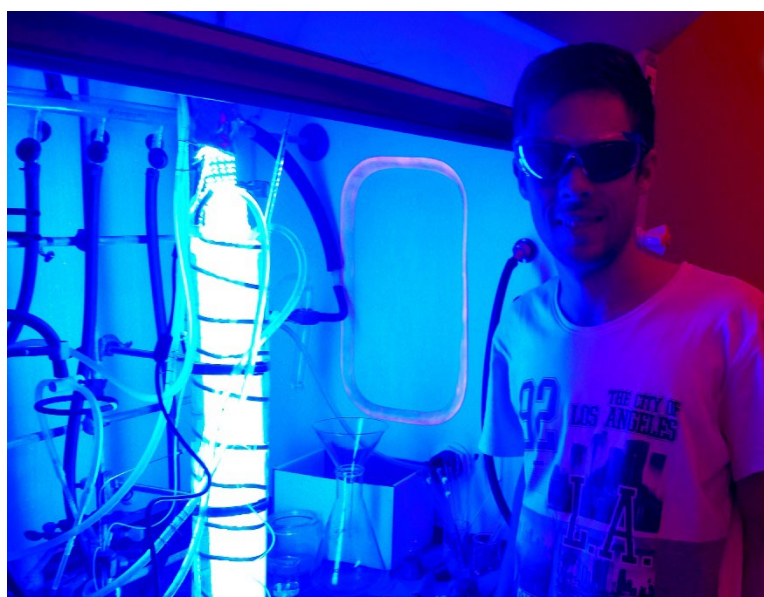
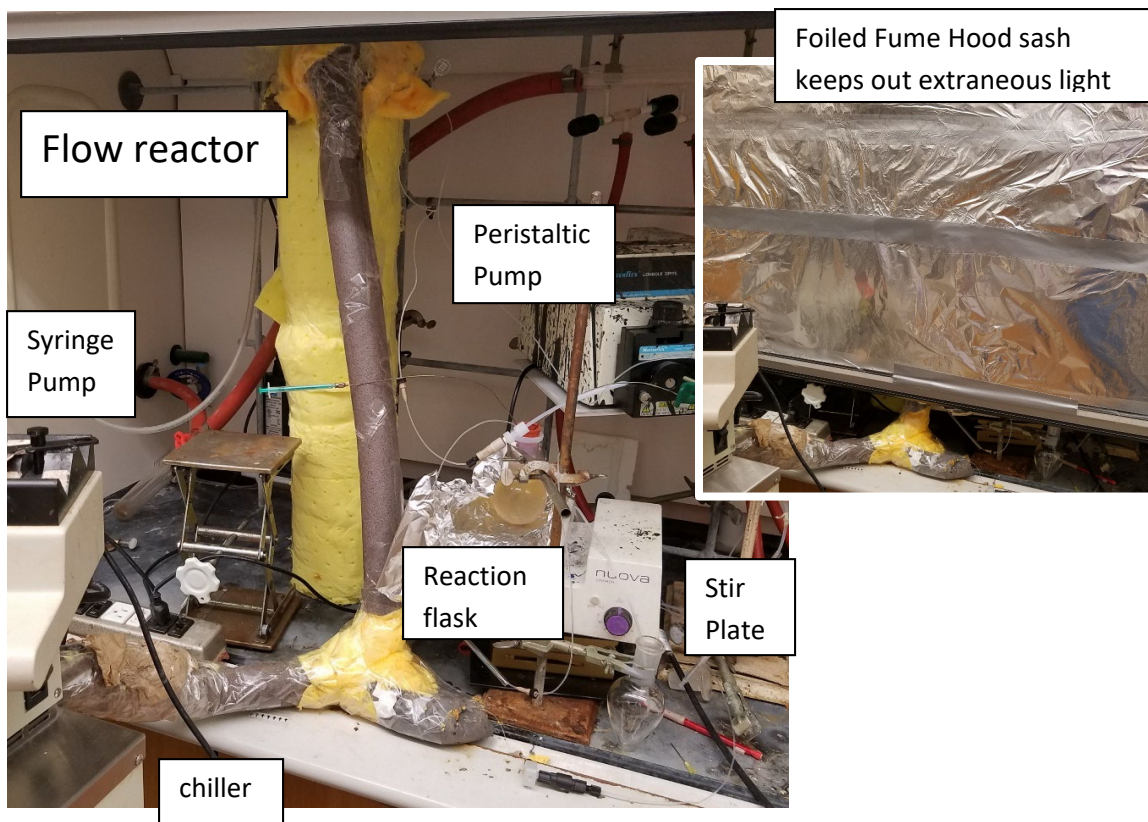


Variable temperature high intensity light bath (batch scale Gen Procedure A). Lights are Solid Apollo Blue Waterproof 5050 72W



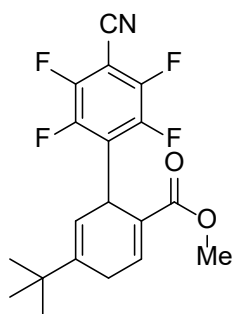
Deoxygenations were conducted in a 25 mL Schlenk tube. Irradiation was done via a single Cree-XP (rb455 nm 700 mA) through a glass rod.



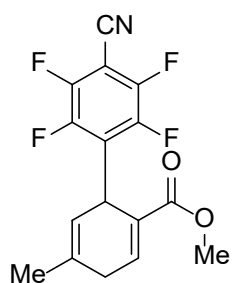


Sascha demonstrating LED intensity with insulation removed. Lights are Solid Apollo Blue Eco 3528 Double Row 96W LED Strip Light SKU: SA-LS-BL-3528-1200-24V

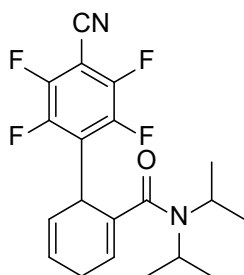
## 6.10.1 Compound Characterization



**(6.3.5) methyl 5-(tert-butyl)-4'-cyano-2',3',5',6'-tetrafluoro-1,4-dihydro-[1,1'-biphenyl]-2-carboxylate.** General Procedure A was followed. Colorless crystalline solid, **MP** 108-110 °C. **<sup>19</sup>F NMR** (376 MHz, Acetonitrile-*d*<sub>3</sub>) δ -136.63 (td, *J* = 16.0, 7.1 Hz, 2F), -143.09 (td, *J* = 16.0, 7.1 Hz, 2F). **<sup>1</sup>H NMR** (400 MHz, Acetonitrile-*d*<sub>3</sub>) δ 7.28 (t, *J* = 3.9 Hz, 1H), 5.60 – 5.36 (m, 1H), 4.89 (q, *J* = 6.1 Hz, 1H), 3.62 (s, 3H), 3.17 – 3.00 (m, 2H), 1.08 (s, 9H). **<sup>13</sup>C{<sup>1</sup>H} NMR** (151 MHz, Acetonitrile-*d*<sub>3</sub>) δ 165.59, 147.12 (ddt, *J* = 257.6, 17.2, 4.0 Hz), 145.25 (d, *J* = 248.2 Hz), 144.32, 140.64, 129.63 (t, *J* = 14.7 Hz), 125.79, 114.21, 107.93 (t, *J* = 3.8 Hz), 91.77 (tt, *J* = 17.6, 3.1 Hz), 51.30, 34.68, 33.14 (t, *J* = 2.1 Hz), 27.98, 26.44. **HRMS** (ESI/ion trap) *m/z*: [M - H<sup>+</sup>]<sup>-</sup> Calcd for C<sub>19</sub>H<sub>16</sub>F<sub>4</sub>NO<sub>2</sub><sup>-</sup> 366.1123; Found 366.1137. **NMR** yield: 32.9%. Isolated yield: 151.0 mg, 20.5 %



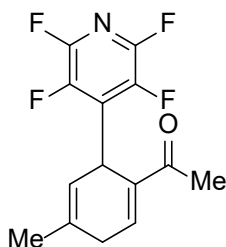
**(6.3.6) methyl 4'-cyano-2',3',5',6'-tetrafluoro-5-methyl-1,4-dihydro-[1,1'-biphenyl]-2-carboxylate.** General procedure B was followed. Colorless crystalline solid, **MP** 91-95°C. **<sup>19</sup>F NMR** (376 MHz, Chloroform-*d*) δ -133.47 (td, *J* = 16.6, 7.4 Hz, 2F), -141.19 (td, *J* = 15.9, 6.8 Hz, 2F). **<sup>1</sup>H NMR** (400 MHz, Chloroform-*d*) δ 7.25 (t, *J* = 3.8 Hz, 1H), 5.39 – 5.22 (m, 1H), 4.83 (q, *J* = 5.6 Hz, 1H), 3.67 (s, 3H), 2.98 (dd, *J* = 23.8, 7.9 Hz, 1H), 2.85 (dt, *J* = 23.9, 5.5 Hz, 1H), 1.76 (s, 3H). **<sup>13</sup>C{<sup>1</sup>H} NMR** (101 MHz, Chloroform-*d*) δ 166.01, 147.13 (ddt, *J* = 261.5, 16.6, 3.7 Hz), 145.21 (app-dm, *J* = 250.4 Hz), 140.25, 133.18, 129.54 (t, *J* = 14.3 Hz), 126.44, 117.45, 107.86 (t, *J* = 3.8 Hz), 92.26, 52.03, 33.18 (t, *J* = 2.1 Hz), 32.11, 22.65. **HRMS** (ESI/ion trap) *m/z*: [M - H<sup>+</sup>]<sup>-</sup> Calcd for C<sub>16</sub>H<sub>10</sub>F<sub>4</sub>NO<sub>2</sub><sup>-</sup> 324.0653; Found 324.0665. Isolated yield: 552.9 mg, 17.0 %



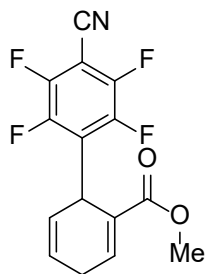
**(6.3.7) 4'-cyano-2',3',5',6'-tetrafluoro-N,N-diisopropyl-1,4-dihydro-[1,1'-biphenyl]-2-carboxamide.** General Procedure A was followed, except the Ar-H was not removed by heating under high vac, but rather separated by column chromatography, and the material was found to crystallize only from pentane. 40g silica column, material eluted with large amount of benzamide Ar-H. Second 24 g silica column was run on these combined fractions, which provided a peak which contained the intended product and the biaryl. Recrystallization from pentane. Colorless crystalline solid, **MP** 165-167 °C. **<sup>19</sup>F NMR** (376 MHz, Acetonitrile-*d*<sub>3</sub>) δ -135.27 – -135.57 (m, 2F), -142.00 – -142.19 (m, 2F). **<sup>1</sup>H NMR**

(400 MHz, Acetonitrile- $d_3$ )  $\delta$  6.03 – 5.91 (m, 2H), 5.67 (ddt,  $J$  = 10.0, 3.9, 2.1 Hz, 1H), 4.90 – 4.80 (m, 1H), 3.75 (s, 3H), 3.04 – 2.74 (m, 2H), 1.21 (d,  $J$  = 6.7 Hz, 6H), 1.01 (s, 6H).

**$^{13}\text{C}\{^1\text{H}\}$  NMR** (101 MHz, Acetonitrile- $d_3$ )  $\delta$  169.37, 147.63 (ddt,  $J$  = 258.7, 16.9, 4.0 Hz), 145.93 (app. dm,  $J$  = 248.4 Hz), 131.68, 130.68, 129.55, 128.71 (t,  $J$  = 15.0 Hz), 126.55, 125.11, 123.00, 108.31 (t,  $J$  = 3.8 Hz), 93.10 (tt,  $J$  = 17.6, 3.0 Hz), 33.60 (p,  $J$  = 1.5 Hz), 26.09, 20.49, 20.21. **HRMS** (ESI/ion trap)  $m/z$ :  $[\text{M} - \text{H}^+]^-$  Calcd for  $\text{C}_{20}\text{H}_{19}\text{F}_4\text{N}_2\text{O}^-$  379.1439; Found 379.1458. NMR yield: 25.0%. Isolated yield: 19.7 mg, 2.6 %



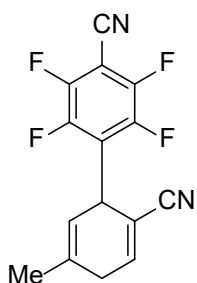
**(6.3.8) 1-(4-methyl-6-(perfluoropyridin-4-yl)cyclohexa-1,4-dien-1-yl)ethan-1-one** Synthesized according to general procedure 3 from pentafluoropyridine and p-methyl acetophenone. Purification via column chromatography (5% EA in PE) yielded mostly clean product, contaminated with rearomatized product as a viscous yellow liquid which solidified within three days. Recrystallization from n-hexane or MeOH yielded the clean product as a colorless crystalline solid (765 mg, 2.68 mmol, 22%). The structure of this compound could be definitely determined by single crystal X-ray diffractometry. TLC:  $R_f$  = 0.35 (hexanes/ethyl acetate 9:1).  **$^{19}\text{F}$ -NMR** (377 MHz,  $\text{CDCl}_3$ ):  $\delta$  = -92.86 – -93.10 (m, 2F), -146.26 – -146.51 (m, 2F).  **$^1\text{H}$ -NMR** (400 MHz,  $\text{CDCl}_3$ ):  $\delta$  [ppm] = 7.19 – 7.14 (m, 1H), 5.37 – 5.29 (m, 1H), 4.86 – 4.77 (m, 1H), 3.14 – 2.99 (m, 1H), 2.99 – 2.85 (m, 1H), 2.29 (s, 3H), 1.76 (s, 3H).  **$^{13}\text{C}$ -NMR** (101 MHz,  $\text{CDCl}_3$ ):  $\delta$  = 197.14, 144.76 – 144.35 (m), 142.34 – 141.92 (m), 141.92 – 141.50 (m), 141.06, 139.42 – 138.91 (m), 136.65 – 136.20 (m), 135.73, 132.55, 117.61, 32.34, 32.21, 25.02, 22.41. **HRMS** (+APCI): exact mass calc. for  $[\text{C}_{14}\text{H}_{11}\text{F}_4\text{O} + \text{NH}_4]^+$ :  $m/z$  = 303.1115, found: 303.1133.



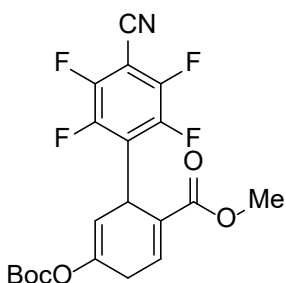
**(6.3.9) methyl 4'-cyano-2',3',5',6'-tetrafluoro-1,4-dihydro-[1,1'-biphenyl]-2-carboxylate.** General Procedure A was followed. 4g silica column. Colorless crystalline solid, **MP** 147-149 °C.  **$^{19}\text{F}$  NMR** (376 MHz, Acetonitrile- $d_3$ )  $\delta$  -136.45 (td,  $J$  = 16.0, 7.0 Hz), -143.01 (app. td,  $J$  = 16.1, 7.0 Hz).  **$^1\text{H}$  NMR** (400 MHz, Acetonitrile- $d_3$ )  $\delta$  7.25 (t,  $J$  = 4.0 Hz, 1H), 6.18 – 5.86 (m, 1H), 5.76 – 5.52 (m, 1H), 5.03 – 4.73 (m, 1H), 3.63 (s, 3H), 3.17 – 2.90 (m, 2H).  **$^{13}\text{C}\{^1\text{H}\}$  NMR** (101 MHz, Acetonitrile- $d_3$ )  $\delta$

166.63, 148.18 (ddt,  $J$  = 257.8, 17.1, 3.9 Hz), 146.24 (d,  $J$  = 247.6 Hz), 140.87 (t,  $J$  = 1.4 Hz), 130.08 (t,  $J$  = 14.7 Hz), 127.36, 126.24, 123.57, 108.88 (t,  $J$  = 3.8 Hz), 93.07 (tt,  $J$  = 17.5, 2.6 Hz), 52.35, 32.87 (p,  $J$  = 2.1 Hz), 27.83. **HRMS** (ESI/ion trap)  $m/z$ :  $[\text{M} - \text{H}^+]^-$  Calcd for  $\text{C}_{15}\text{H}_8\text{F}_4\text{NO}_2^-$  310.0497; Found 310.0509. NMR yield: 25.0%. Isolated yield: 98.5 mg, 15.8 %

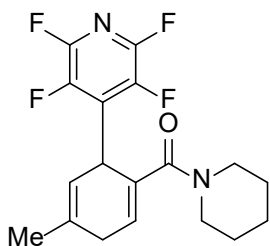




**(6.3.10) 2',3',5',6'-tetrafluoro-5-methyl-1,4-dihydro-[1,1'-biphenyl]-2,4'-dicarbonitrile.** General Procedure A was followed, except that the material was repeated recrystallized either from hexanes or methanol. Colorless crystalline solid, **MP** 117-120 °C. **<sup>19</sup>F** NMR (376 MHz, Chloroform-d)  $\delta$  -131.79 (td,  $J$  = 16.8, 7.3 Hz, 2F), -140.34 (td,  $J$  = 16.6, 6.5 Hz, 2F). **<sup>1</sup>H** NMR (400 MHz, Chloroform-d)  $\delta$  6.87 (td,  $J$  = 3.7, 1.6 Hz, 6H), 5.44 – 5.19 (m, 6H), 4.85 – 4.49 (m, 6H), 3.13 – 2.73 (m, 12H), 1.78 (s, 20H), 1.25 (s, 1H). **<sup>13</sup>C{<sup>1</sup>H}** NMR (151 MHz, Acetonitrile-d<sub>3</sub>)  $\delta$  147.41 (ddt,  $J$  = 259.1, 16.8, 3.9 Hz), 145.24 (ddt,  $J$  = 250.0, 11.7, 5.2 Hz), 144.98, 133.17, 131.75, 126.10 (t,  $J$  = 14.4 Hz), 115.44, 108.67, 107.69 (t,  $J$  = 3.9 Hz), 93.57 (tt,  $J$  = 17.4, 2.6 Hz), 34.20, 30.91, 21.73. **HRMS** (ESI/ion trap)  $m/z$ : [M - H<sup>+</sup>]<sup>-</sup> Calcd for C<sub>15</sub>H<sub>7</sub>F<sub>4</sub>N<sub>2</sub><sup>-</sup> 291.0551; Found 291.0552. NMR yield: 16.4%. Isolated yield: 30.0 mg, 9.1 %

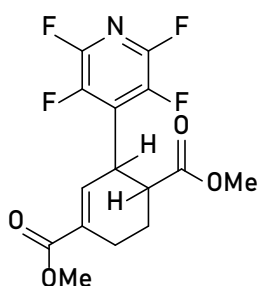


**(6.3.11) methyl 5-((tert-butoxycarbonyl)oxy)-4'-cyano-2',3',5',6'-tetrafluoro-1,4-dihydro-[1,1'-biphenyl]-2-carboxylate.** General Procedure A was followed, but with only 1 equivalent water, and the Ar-H was not removed by heating under high vac, but rather separated by column chromatography. 40 g silica column. Colorless crystalline solid, **MP** 104-105 °C. **<sup>19</sup>F** NMR (376 MHz, Chloroform-d)  $\delta$  -132.84 (td,  $J$  = 16.6, 7.3 Hz, 2F), -140.61 (td,  $J$  = 16.5, 15.8, 6.7 Hz, 2F). **<sup>1</sup>H** NMR (400 MHz, Chloroform-d)  $\delta$  7.13 (ddd,  $J$  = 4.4, 3.0, 1.0 Hz, 1H), 5.43 (dd,  $J$  = 4.3, 2.0 Hz, 1H), 4.98 (q,  $J$  = 6.1 Hz, 1H), 3.61 (s, 3H), 3.23 (ddt,  $J$  = 23.4, 7.5, 2.7 Hz, 1H), 3.06 (ddd,  $J$  = 23.4, 6.4, 4.6 Hz, 1H), 1.43 (s, 9H). **<sup>13</sup>C{<sup>1</sup>H}** NMR (101 MHz, Chloroform-d)  $\delta$  165.66, 151.00, 147.53, 147.49 (ddt,  $J$  = 262.2, 16.6, 3.1 Hz), 145.56 (d,  $J$  = 250.0 Hz), 138.95, 128.33 (t,  $J$  = 14.0 Hz), 126.64, 110.27, 107.99 (t,  $J$  = 3.6 Hz), 84.34, 52.57, 33.48, 31.39, 29.19, 28.08. **HRMS** (ESI/ion trap)  $m/z$ : [M - H<sup>+</sup>]<sup>-</sup> Calcd for C<sub>20</sub>H<sub>16</sub>F<sub>4</sub>NO<sub>5</sub><sup>-</sup> 426.0970; Found 426.0995. Isolated yield: 118.6 mg, 13.8 %



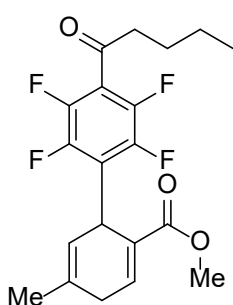
**(6.3.12) (4-methyl-6-(perfluoropyridin-4-yl)cyclohexa-1,4-dien-1-yl)(piperidin-1-yl)methanone.** General Procedure B was followed, at a 12 mmol scale, with 2.6 equiv. ArH, 10 equiv. water. The Ar-H was not removed by heating under high vac, but rather separated by column chromatography. Recrystallized from n-hexane. Colorless crystalline solid, **MP** °C. **<sup>19</sup>F** NMR (377 MHz, Chloroform-d)  $\delta$  -92.00 – -92.38 (m, 2F), -145.53 – -145.89 (m, 2F). **<sup>1</sup>H** NMR (400 MHz, Chloroform-d)  $\delta$  6.08 (ddd,  $J$  = 4.2, 2.9, 1.7 Hz, 1H), 5.32 (td,  $J$  = 3.1, 1.6 Hz, 1H), 4.93 (q,  $J$  = 6.4 Hz, 1H), 3.65 – 3.22 (m, 3H), 2.89 (dd,  $J$  = 23.3, 6.8 Hz, 1H), 2.75 (ddd,  $J$  = 22.9, 7.3, 4.0 Hz, 1H), 1.75 (s, 3H), 1.59 (p,  $J$  = 5.8 Hz, 2H), 1.53 – 1.18 (m, 5H). **<sup>13</sup>C{<sup>1</sup>H}** NMR (101 MHz, Chloroform-d)  $\delta$  168.58, 144.99 – 141.94 (m), 140.61 (dd,  $J$  = 260.6, 20.8 Hz), 135.44

(t,  $J = 13.3$  Hz), 133.46, 128.98, 128.32, 116.95, 34.37, 31.57, 30.93, 26.22, 24.54, 22.70, 14.10. Isolated yield: 220.0 mg, 6.2 % HRMS Need hrms, MP



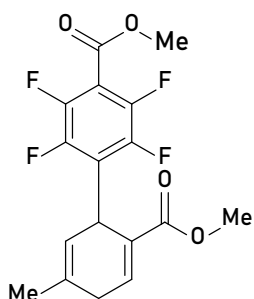
**(6.3.13) dimethyl 3-(perfluoropyridin-4-yl)cyclohex-1-ene-1,4-dicarboxylate**

$^{19}\text{F}$  NMR (376 MHz, Chloroform-*d*)  $\delta$  -90.76 – -91.23 (m, 2F), -142.62 – -143.66 (m, 2F).  $^1\text{H}$  NMR (400 MHz, Chloroform-*d*)  $\delta$  6.84 – 6.45 (m, 1H), 4.35 (d,  $J = 10.5$  Hz, 1H), 3.74 (s, 3H), 3.63 (s, 3H), 2.95 (ddd,  $J = 12.5, 10.4, 2.8$  Hz, 1H), 2.77 – 2.56 (m, 1H), 2.54 – 2.22 (m, 2H), 1.99 – 1.65 (m, 1H).  $^{13}\text{C}\{^1\text{H}\}$  NMR (101 MHz, Chloroform-*d*)  $\delta$  173.53, 166.59, 143.65 (dddd,  $J = 246.0, 16.5, 13.0, 3.1$  Hz), 140.70 (d,  $J = 259.5$ ), 134.78, 134.70 (tt,  $J = 14.3, 2.4$  Hz), 132.09, 52.37, 52.11, 43.24 (t,  $J = 2.2$  Hz), 35.77 (t,  $J = 2.0$  Hz), 26.03, 23.91. **HRMS** HRMS (ESI/ion trap)  $m/z$ :  $[\text{M} + \text{H}]^+$  Calcd for  $\text{C}_{15}\text{H}_{14}\text{F}_4\text{NO}_4^+$  348.0853; Found 348.0856. Isolated yield, 200 mg, 575.93  $\mu\text{mol}$ , 4.8%.



**(6.3.14) Methyl 2',3',5',6'-tetrafluoro-5-methyl-4'-pentanoyl-1,4-dihydro-[1,1'-biphenyl]-2-carboxylate**

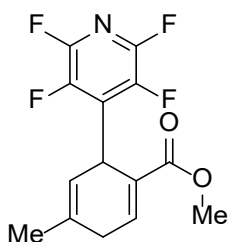
General procedure B was followed from 1-(perfluorophenyl)pentan-1-one and methyl *p*-toluate. Purification via column chromatography (5% EA in PE) yielded the product contaminated with variable amounts of rearomatized product as a yellow, viscous liquid. Recrystallization from MeOH yielded the product as colorless needles (947 mg, 2.46 mmol, 21%). **TLC**:  $R_f = 0.50$  (hexanes/ethyl acetate 9:1).  $^{19}\text{F}$ -NMR (377 MHz,  $\text{CDCl}_3$ ):  $\delta$  [ppm] = -143.85 – -14.17 (m, 4F)  $^1\text{H}$ -NMR (400 MHz, Chloroform-*d*)  $\delta$  7.24 – 7.17 (m, 1H), 5.42 – 5.21 (m, 1H), 4.78 (q,  $J = 6.2, 5.8$  Hz, 1H), 3.65 (s, 3H), 3.11 – 2.70 (m, 4H), 1.73 (t,  $J = 1.4$  Hz, 3H), 1.67 (p,  $J = 7.4$  Hz, 2H), 1.36 (h,  $J = 7.4$  Hz, 2H), 0.91 (t,  $J = 7.3$  Hz, 3H).  $^{13}\text{C}$ -NMR (101 MHz, Chloroform-*d*)  $\delta$  195.75, 166.14, 145.20 (ddt,  $J = 253.8, 16.3, 5.4$  Hz), 143.48 (dddd,  $J = 254.4, 17.6, 6.5, 5.0$  Hz), 139.69, 132.24, 126.97, 124.63 (t,  $J = 14.0$  Hz), 118.28, 118.08 (t,  $J = 17.8$  Hz), 51.83, 44.79, 32.64 (p,  $J = 1.9$  Hz), 32.04, 25.68, 22.55, 22.21, 13.83. **HRMS** (EI): exact mass calc. for  $\text{C}_{20}\text{H}_{20}\text{F}_4\text{O}_3$ :  $m/z = 384.1349$ , found: 384.1337  $[\text{M}]^+$ .



**(6.3.15) dimethyl 2',3',5',6'-tetrafluoro-5-methyl-1,4-dihydro-[1,1'-biphenyl]-2,4'-dicarboxylate**

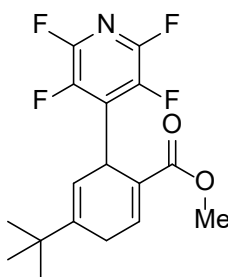
General Procedure A was followed. Product eluted at 5% EtOAc in Hexanes after 38 CV in 24 g column. Colorless crystalline solid, MP 91-95 °C.  $^{19}\text{F}$  NMR (564 MHz, Chloroform-*d*)  $\delta$  -139.20 (dd,  $J = 22.2, 12.6$  Hz, 2F (biaryl impurity)), -139.46 (dd,  $J = 22.6, 13.0$  Hz, 2F (biaryl impurity)), -140.33 – -140.90 (m, 2F), -142.99 – -143.96 (m, 2F).  $^1\text{H}$  NMR (599 MHz, Chloroform-*d*)  $\delta$  7.25 – 7.16 (m, 1H), 5.39 – 5.25 (m, 1H), 4.81

(q,  $J = 5.5, 5.0$  Hz, 1H), 3.95 (s, 3H), 3.66 (s, 2H), 2.97 (ddt,  $J = 24.8, 6.5, 2.4$  Hz, 1H), 2.83 (dt,  $J = 23.8, 5.5$  Hz, 1H), 1.74 (s, 3H).  **$^{13}\text{C}$  NMR** (151 MHz, Chloroform- $d$ )  $\delta$  166.15, 160.61, 145.29 (ddt,  $J = 249.6, 14.3, 4.7$  Hz), 144.74 (ddt,  $J = 256.7, 15.9, 4.4$  Hz), 139.79, 132.38, 126.94, 125.69 (t,  $J = 14.7$  Hz), 118.19, 110.51 (t,  $J = 15.8$  Hz), 53.27, 51.91, 32.74, 32.10, 22.63. **HRMS** (ESI/ion trap)  $m/z$ :  $[\text{M} + \text{Na}]^+$  Calcd for  $\text{C}_{17}\text{H}_{13}\text{F}_4\text{O}_4\text{Na}$  381.0726; Found 381.0707. Isolated yield: 99.6 mg, 13.8 %



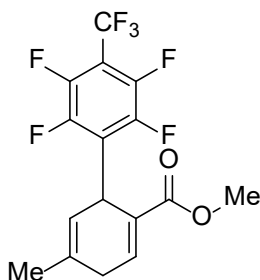
**(6.3.16) methyl 4-methyl-6-(perfluoropyridin-4-yl)cyclohexa-1,4-diene-1-carboxylate** General Procedure was followed.

Separation via 4 g chromatography column. Colorless crystalline solid, **MP** 93-96 °C.  **$^{19}\text{F}$  NMR** (564 MHz, Acetonitrile- $d_3$ )  $\delta$  -94.96 – -95.25 (m, 2F), -146.97 – -147.15 (m, 2F).  **$^1\text{H}$  NMR** (599 MHz, Acetonitrile- $d_3$ )  $\delta$  7.38 – 7.13 (m, 1H), 5.45 – 5.34 (m, 1H), 4.93 – 4.82 (m, 1H), 3.63 (s, 3H), 3.02 (app. dd,  $J = 24.3, 7.2$  Hz, 1H), 2.92 (dddt,  $J = 24.1, 6.5, 4.5, 0.9$  Hz, 1H), 1.79 – 1.76 (m, 3H).  **$^{13}\text{C}\{^1\text{H}\}$  NMR** (151 MHz, Acetonitrile- $d_3$ )  $\delta$  166.59, 144.30 (apparent d,  $J = 241.7$  Hz), 141.80 (apparent d,  $J = 256.9$  Hz), 137.49 (tt,  $J = 13.3, 2.2$  Hz), 134.31, 127.05, 117.70, 52.34, 34.12 (t,  $J = 1.9$  Hz), 32.42, 30.89, 22.57. **HRMS** (ESI/ion trap)  $m/z$ :  $[\text{M} - \text{H}]^-$  Calcd for  $\text{C}_{14}\text{H}_{10}\text{F}_4\text{NO}_2^-$  300.0653; Found 300.0658. NMR yield: 13.2%. Isolated yield: 69.1 mg, 11.4 %



**(6.3.17) methyl 4-(tert-butyl)-6-(perfluoropyridin-4-yl)cyclohexa-1,4-diene-1-carboxylate** General Procedure A was followed.

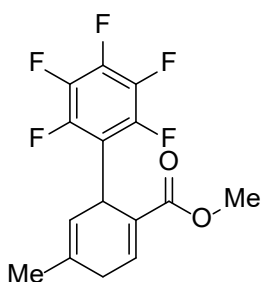
Colorless crystalline solid, **MP** 59-60 °C.  **$^{19}\text{F}$  NMR** (376 MHz, Chloroform- $d$ )  $\delta$  -91.85 – -92.17 (m, 2F), -145.34 – -145.88 (m, 2F).  **$^1\text{H}$  NMR** (400 MHz, Chloroform- $d$ )  $\delta$  7.30 (td,  $J = 3.9, 1.1$  Hz, 1H), 5.40 (dt,  $J = 4.3, 1.5$  Hz, 1H), 4.89 (q,  $J = 5.9$  Hz, 1H), 3.67 (s, 3H), 3.05 (ddd,  $J = 6.7, 4.0, 1.5$  Hz, 2H), 1.07 (s, 9H).  **$^{13}\text{C}\{^1\text{H}\}$  NMR** (101 MHz, Chloroform- $d$ )  $\delta$  165.93, 144.85, 143.56 (d,  $J = 248.4$  Hz), 141.09, 140.83 (d,  $J = 273.3$  Hz), 136.33 (t,  $J = 13.1$  Hz), 125.81, 114.11, 51.97, 35.24, 33.52 (t,  $J = 1.8$  Hz), 28.84, 26.89 (t,  $J = 1.6$  Hz). **HRMS** (ESI/ion trap)  $m/z$ :  $[\text{M} - \text{H}]^-$  Calcd for  $\text{C}_{17}\text{H}_{16}\text{F}_4\text{NO}_2^-$  342.1123; Found 342.1143. NMR yield: 16.7%. Isolated yield: 99.5 mg, 14.5 %



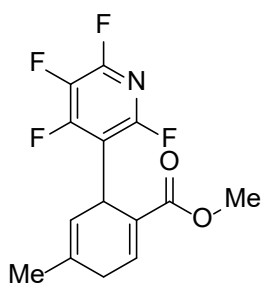
**(6.3.18) methyl 2',3',5',6'-tetrafluoro-5-(trifluoromethyl)-4'-methyl-1,1'-biphenyl-2-carboxylate** General Procedure A was followed, except the product was recrystallized from isopropanol.

Colorless crystalline solid, **MP** 104-105 °C.  **$^{19}\text{F}$  NMR** (564 MHz, Acetonitrile- $d_3$ )  $\delta$  -57.07 (t,  $J = 21.3$  Hz, 3F), -144.10 – -144.22 (m, 2F), -144.22 – -144.46 (m, 2F).  **$^1\text{H}$  NMR** (400 MHz, Acetonitrile- $d_3$ )  $\delta$  7.24 – 7.17 (m, 1H),

5.41 – 5.34 (m, 1H), 4.83 (q,  $J = 5.5$  Hz, 1H), 3.60 (s, 3H), 2.99 (ddt,  $J = 24.2, 6.6, 2.5$  Hz, 1H), 2.88 (ddd,  $J = 24.1, 6.5, 4.6$  Hz, 1H), 1.74 (s, 3H).  **$^{13}\text{C}\{^1\text{H}\}$  NMR** (151 MHz, Acetonitrile- $d_3$ )  $\delta$  166.63, 146.50 (d,  $J = 246.3$  Hz), 144.98 (d,  $J = 235.4$  Hz), 140.66, 133.82, 128.19 (t,  $J = 14.7$  Hz), 127.41, 122.18 (q,  $J = 273.3$  Hz), 108.51 – 107.35 (m), 52.23, 33.57 (t,  $J = 2.1$  Hz), 32.35, 22.49. **HRMS** (ESI/ion trap)  $m/z$ :  $[\text{M} - \text{H}^+]^-$  Calcd for  $\text{C}_{16}\text{H}_{10}\text{F}_7\text{O}_2^-$  367.0575; Found 367.0587. NMR yield: 29.3%. Isolated yield: 84.0 mg, 11.4 %



**(6.3.19) methyl 2',3',4',5',6'-pentafluoro-5-methyl-1,4-dihydro-[1,1'-biphenyl]-2-carboxylate** General Procedure A was followed from bromopentafluorobenzene. Colorless oily semisolid. Partial isolation was achieved via silica gel chromatography, 4 g hexanes/ethyl acetate.  **$^{19}\text{F}$  NMR** (376 MHz, Acetonitrile- $d_3$ )  $\delta$  -146.20 (dd,  $J = 21.2, 7.8$  Hz, 2F), -160.17 (td,  $J = 20.2, 1.1$  Hz, 1F), -165.56 – -165.83 (m, 2F).  **$^1\text{H}$  NMR** (400 MHz, Acetonitrile- $d_3$ )  $\delta$  7.22 – 7.12 (m, 1H), 5.41 – 5.34 (m, 1H), 4.74 (q,  $J = 6.1$  Hz, 1H), 3.03 – 2.90 (m, 1H), 2.92 – 2.79 (m, 1H), 1.73 (s, 3H).  **$^{13}\text{C}\{^1\text{H}\}$  NMR** (151 MHz, Acetonitrile- $d_3$ )  $\delta$  165.80, 145.43 (d,  $J = 245.3$  Hz), 139.77 (d,  $J = 247.4$  Hz), 139.30, 137.54 (d,  $J = 247.5$  Hz), 132.21, 129.19, 126.96, 118.18, 51.20, 31.87, 31.39, 21.53. **HRMS** (ESI/ion trap)  $m/z$ :  $[\text{M} - \text{H}^+]^-$  Calcd for  $\text{C}_{15}\text{H}_{10}\text{F}_5\text{O}_2^-$  317.0606; Found 317.0628. NMR yield, 18.1 %



**(6.3.20) methyl 4-methyl-6-(perfluoropyridin-3-yl)cyclohexa-1,4-diene-1-carboxylate** General Procedure A was followed with 3-chloro tetrafluoropyridine. Partial resolution of atropisomers was achieved through repeated recrystallizations. **HRMS** (ESI/ion trap)  $m/z$ :  $[\text{M} - \text{H}^+]^-$  Calcd for  $\text{C}_{14}\text{H}_{10}\text{F}_4\text{NO}_2^-$  300.0653; Found 300.0668. NMR yield: 21.3%. 2.4 : 1 dr.

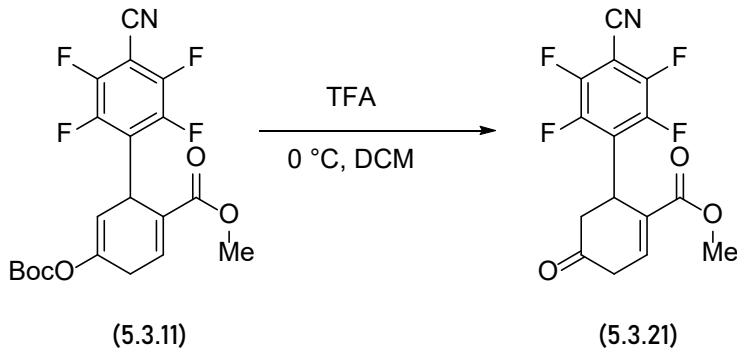
**Atropisomer 1 (Major):**

**$^{19}\text{F}$  NMR** (376 MHz, Acetonitrile- $d_3$ )  $\delta$  -73.99, -89.41 (ddd,  $J = 22.2, 18.8, 14.6$  Hz, 1F), -118.89 (q,  $J = 17.2$  Hz, 1F), -168.50 (ddd,  $J = 24.0, 21.8, 18.4$  Hz, 1F).  **$^1\text{H}$  NMR** (400 MHz, Acetonitrile- $d_3$ )  $\delta$  6.77 (m, 1H), 5.75 (m, 1H), 4.47 (q,  $J = 6.5$  Hz, 1H), 3.73 (s, 3H), 3.00 (ddp,  $J = 7.6, 3.9, 2.0$  Hz, 2H), 1.67 – 1.56 (m, 3H).  **$^{13}\text{C}\{^1\text{H}\}$  NMR** (151 MHz, Acetonitrile- $d_3$ )  $\delta$  167.56, 159.72 (d,  $J = 261.0$  Hz), 154.09 (d,  $J = 242.3$  Hz), 149.12 (d,  $J = 240.2$  Hz), 134.37 (d,  $J = 256.4$  Hz), 134.52, 130.39, 129.08, 122.37, 112.22, 52.32, 37.07, 26.80, 20.84.

**Atropisomer 2 (Minor):**

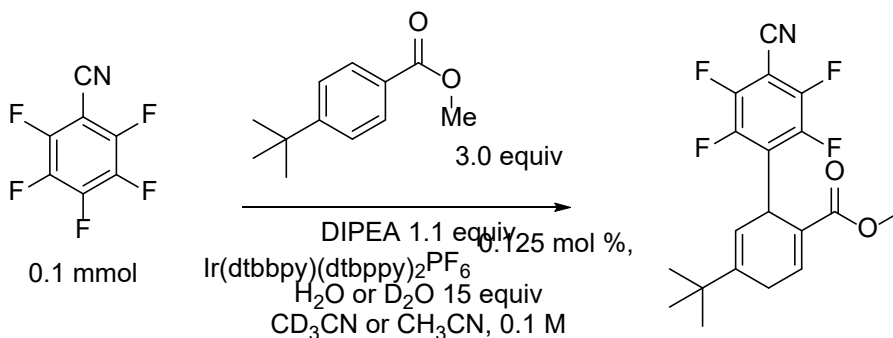
**$^{19}\text{F}$  NMR** (376 MHz, Acetonitrile- $d_3$ )  $\delta$  -74.63 (dt,  $J = 21.0, 14.3$  Hz), -90.73 (ddd,  $J = 21.9, 18.2, 14.8$  Hz, 1F), -119.82 (tdd,  $J = 18.2, 14.8, 1.2$  Hz, 1F), -169.33 (ddd,  $J = 23.9, 22.0, 18.4$  Hz, 1F).  **$^1\text{H}$  NMR** (400 MHz, Acetonitrile- $d_3$ )  $\delta$  7.22 (m, 1H), 5.40 (m, 1H), 4.74 – 4.60

(m, 1H), 3.62 (s, 3H), 3.07 – 2.94 (m, 1H), 2.94 – 2.79 (m, 1H), 1.77 (s, 3H). **<sup>13</sup>C{<sup>1</sup>H} NMR** (151 MHz, Acetonitrile-*d*<sub>3</sub>) δ 166.70, 159.33 (d, *J* = 262.2 Hz), 153.79 (d, *J* = 237.5 Hz), 148.40 (d, *J* = 244.8 Hz), 133.99 (d, *J* = 267.7 Hz), 133.50, 127.45, 112.00, 118.55, 52.18, 140.51, 32.56, 32.29, 22.46.



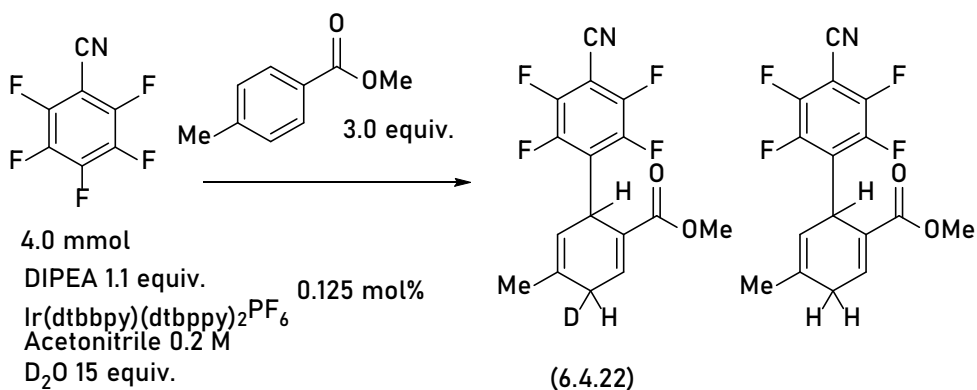
**(6.3.21) methyl 4'-cyano-2',3',5',6'-tetrafluoro-5-oxo-1,4,5,6-tetrahydro-[1,1'-biphenyl]-2-carboxylate**

methyl 5-((tert-butoxycarbonyl)oxy)-4'-cyano-2',3',5',6'-tetrafluoro-1,4-dihydro-[1,1'-biphenyl]-2-carboxylate (**6.3.11**) 5.0 mg (0.0117 mmol) was dissolved in DCM (0.02 M) in an NMR tube. Added 10 equivalents trifluoroacetic acid (TFA) and sonicated 2 hours. An additional 50 equivalents TFA was added and the mixture sonicated 2 hours. An additional 50 equivalents TFA was added and the mixture sonicated 2 hours, after which TLC indicated complete consumption of (11). **<sup>19</sup>F NMR** (376 MHz, Chloroform-*d*) δ -131.70 – -132.11 (m, 2F), -138.94 – -139.44 (m, 2F). **<sup>1</sup>H NMR** (400 MHz, Chloroform-*d*) δ 7.31 (dd, *J* = 4.4, 3.4 Hz, 1H), 4.88 (d, *J* = 8.5 Hz, 1H), 3.72 (s, 3H), 3.24 (s, 2H), 2.96 (dd, *J* = 15.7, 8.6 Hz, 1H), 2.63 (dd, *J* = 15.6, 3.1 Hz, 1H). **HRMS** (ESI/ion trap) *m/z*: [M - H<sup>+</sup>]<sup>-</sup> Calcd for C<sub>15</sub>H<sub>8</sub>F<sub>4</sub>NO<sub>3</sub><sup>-</sup> 326.0446; Found 326.0453. **NMR yield:** 94%

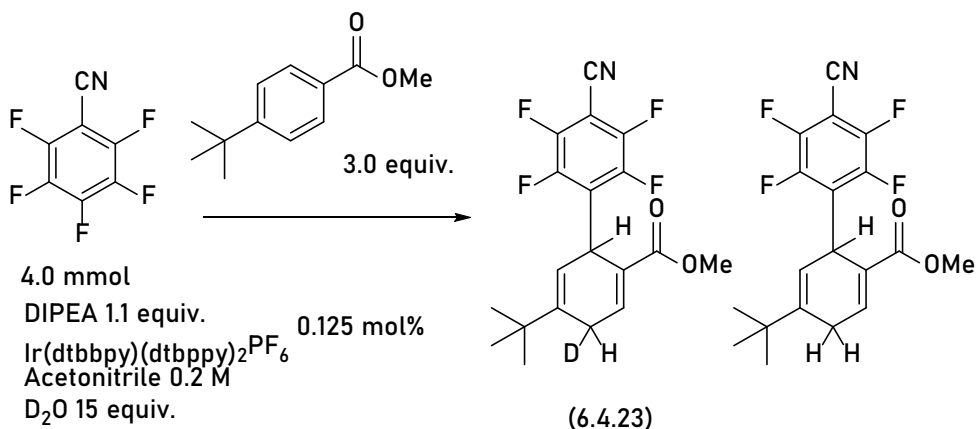


General procedure D was followed.

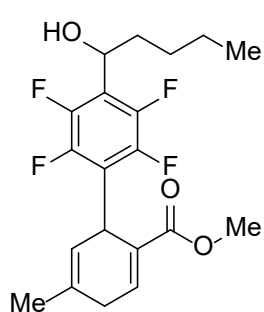
time	Temp.	Conc	solvent	Water	Comment
18 h	rt	0.1 M	$\text{CD}_3\text{CN}$	$\text{D}_2\text{O}$	D incorporated in product - m/z 368
			$\text{CH}_3\text{CN}$	$\text{D}_2\text{O}$	D incorporated in product - m/z 368
			$\text{CH}_3\text{CN}$	$\text{H}_2\text{O}$	no deuterium incorporation
			$\text{CD}_3\text{CN}$	$\text{H}_2\text{O}$	no deuterium incorporation



General Procedure A was followed, except with  $\text{D}_2\text{O}$  instead of  $\text{H}_2\text{O}$ . Colorless crystalline solid. Spectra agreed with nondeuterated spectra, except as shown. **HRMS** (ESI/ion trap) m/z:  $[\text{M} - \text{H}^+]^-$  Calcd for  $\text{C}_{16}\text{H}_9\text{DF}_4\text{NO}_2^-$  325.0716; Found 325.0730.

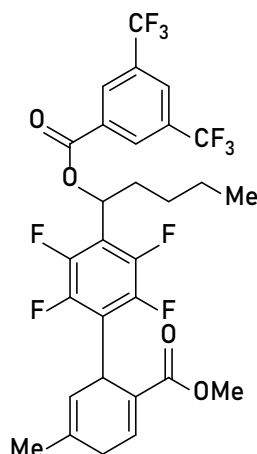


General Procedure A was followed, except with D<sub>2</sub>O instead of H<sub>2</sub>O. Colorless crystalline solid Spectra agreed with nondeuterated spectra, except as shown. **HRMS** (ESI/ion trap) *m/z*: [M - H<sup>+</sup>]<sup>-</sup> Calcd for C<sub>19</sub>H<sub>15</sub>DF<sub>4</sub>NO<sub>2</sub><sup>-</sup> 367.1185; Found 367.1195.



**(6.5.24) Methyl 2',3',5',6'-tetrafluoro-4'-(1-hydroxypentyl)-5-methyl-1,4-dihydro-[1,1'-biphenyl]-2-carboxylate**

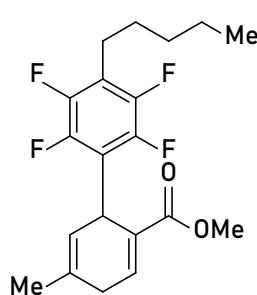
Reaction derived from literature procedure for deoxygenation of aromatic ketones.<sup>339</sup> Compound **(14)** (77 mg, 200 μmol) was dissolved in 1 mL DCE. Anhydrous ZnI<sub>2</sub> (96 mg, 300 μmol, 1.5 equiv.) and NaBH<sub>3</sub>CN (94 mg, 7.5 equiv.) were added and the dispersion heated to 80 °C for 6 h. After cooling to room temperature 2 mL 2M HCl was added dropwise until excess NaBH<sub>3</sub>CN was decomposed. The solution was extracted with DCM, the organic layer dried with Na<sub>2</sub>SO<sub>4</sub> and the solvent removed under reduced pressure. Purification via column chromatography (10% EA in PE) yielded the product as a slightly yellow viscous liquid (75 mg, 194 μmol, 97%). Solidifies from CHCl<sub>3</sub> as a white, waxy solid. **TLC**: *R<sub>f</sub>* = 0.30 (hexanes/ethyl acetate 9:1). **19F-NMR (377 MHz, CDCl<sub>3</sub>)**: δ [ppm] = -145.70 (dd, *J* = 21.51, 12.24 Hz, 2F), -146.51 (dd, *J* = 21.50, 12.24 Hz, 2F). **1H-NMR (400 MHz, CDCl<sub>3</sub>)**: δ [ppm] = 7.13 (d, *J* = 2.81 Hz, 1 H), 5.27 (s, 1 H), 5.00 – 4.89 (m, 1 H), 4.75 – 4.67 (m, 1 H), 3.58 (s, 3 H), 2.98 – 2.67 (m, 2 H), 2.20 – 2.07 (m, 1 H), 1.96 – 1.86 (m, 1 H), 1.80 – 1.70 (m, 1 H), 1.67 (s, 3 H), 1.44 – 1.11 (m, 5 H), 0.83 (t, 3 H). **<sup>13</sup>C{<sup>1</sup>H} NMR** (101 MHz, Chloroform-*d*) δ 166.33, 145.12 (d, *J* = 245.8 Hz), 144.37 (d, *J* = 245.0 Hz), 139.44, 131.63, 127.31, 120.87 (t, *J* = 14.7 Hz), 120.28 (t, *J* = 15.2 Hz), 118.81, 66.66, 51.70, 36.65, 32.28 (t, *J* = 2.2 Hz), 31.99, 31.64, 28.02, 22.69, 22.47, 22.37, 14.11, 13.91. **HRMS** (EI): exact mass calc. for C<sub>20</sub>H<sub>22</sub>F<sub>4</sub>O<sub>3</sub>: *m/z* = 386.1500, found: 386.1498 [M]<sup>+</sup>.



**(6.5.25) Methyl 4'-(1-((3,5-bis(trifluoromethyl)benzoyl)oxy)pentyl)-2',3',5,6'-tetrafluoro-5-methyl-1,4-dihydro-[1,1'-biphenyl]-2-carboxylate**

Compound **(24)** (900 mg, 2.33 mmol) was dissolved in 24 mL DCM and cooled in an ice bath. 3,5-bis(trifluoromethyl)benzoyl chloride (460  $\mu$ L, 1.1 equiv.) was added dropwise. The solution was warmed to room temperature and the solvent removed under reduced pressure. The residue was extracted with hot petroleum ether, most of the solvent was removed under reduced pressure and the product purified via column chromatography (0-10% EA in PE) to yield the product as a colorless viscous liquid as a mixture of diastereomers (1.30 g, 2.08 mmol, 89%). The diastereomers are not distinguishable in the  $^{19}\text{F}$  and  $^1\text{H}$  NMR, where they only lead to broadened or poorly resolved signals, but most of the  $^{13}\text{C}$  resonances appear as slightly split signals.

**TLC:**  $R_f$  = 0.70 (hexanes/ethyl acetate 9:1).  **$^{19}\text{F}$ -NMR (377 MHz, Chloroform- $d$ )**  $\delta$  - 63.62 (s, 6F), -144.34 – -144.57 (m, 2F), -145.02 (dd,  $J$  = 21.3, 12.2 Hz, 2F).  **$^1\text{H}$ -NMR (400 MHz,  $\text{CDCl}_3$ ):**  $\delta$  [ppm] = 8.49 (s, 2H), 8.07 (s, 1H), 7.22 – 7.18 (m, 1H), 6.31 (t,  $J$  = 7.43 Hz, 1H), 5.37 – 5.31 (m, 1H), 4.83 – 4.74 (m, 1H), 3.67 – 3.63 (2s, overlapping, 3H), 3.04 – 2.90 (m, 1H), 2.81 (dt,  $J$  = 23.74, 5.26 Hz, 1H), 2.33 – 2.20 (m, 1H), 2.11 – 2.00 (m, 1H), 1.77 – 1.70 (m, 3H), 1.51 – 1.25 (m, 4H + 2H impurities), 0.92 (t,  $J$  = 7.09 Hz, 3H).  **$^{13}\text{C}$ -NMR (101 MHz,  $\text{CDCl}_3$ ):**  $\delta$  166.28 (d,  $J$  = 4.8 Hz), 163.29 (d,  $J$  = 3.5 Hz), 145.32 (d,  $J$  = 246.5 Hz), 144.65 (d,  $J$  = 246.9 Hz), 139.59 (d,  $J$  = 8.2 Hz), 132.45 (q,  $J$  = 34.0 Hz), 132.16 (d,  $J$  = 2.2 Hz), 130.00 (d,  $J$  = 3.9 Hz), 127.24, 126.95 – 126.40 (m), 122.97 (q,  $J$  = 273.1 Hz), 122.41 (td,  $J$  = 14.7, 3.0 Hz), 118.70 (d,  $J$  = 2.2 Hz), 115.94 (t,  $J$  = 14.7 Hz), 69.40, 51.78 (d,  $J$  = 2.6 Hz), 33.44, 32.50, 32.09, 27.76, 22.69, 22.57, 22.33, 13.91.



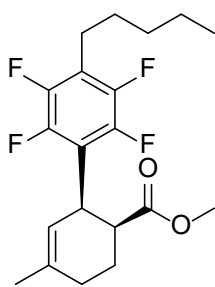
**(6.5.26) Methyl 2',3',5,6'-tetrafluoro-5-methyl-4'-pentyl-1,4-dihydro-[1,1'-biphenyl]-2-carboxylate**

According to a procedure derived from Reiser and coworkers. **(25)** (376 mg, 600  $\mu$ mol), 10 mg  $[\text{Ir}(\text{dtbbpy})(\text{dtbppy})_2]\text{PF}_6$  and DIPEA (210  $\mu$ L, 2 equiv.) were dissolved in a mixture of 15 mL acetonitrile and 1 mL of water. The solution was degassed and irradiated for 3 h at 455 nm while heating to 45  $^\circ\text{C}$ . After cooling to room temperature 20 mL petroleum ether was added, the solution washed with concentrated  $\text{K}_2\text{CO}_3$  solution and water, dried over  $\text{Na}_2\text{SO}_4$ , the solvent removed under reduced pressure and the residue purified via column chromatography (5% EA in PE) yielded the product contaminated with small amounts of rearomatized product as a slightly yellow viscous liquid. Recrystallization from MeOH yielded the product as colorless needles (193 mg, 521  $\mu$ mol, 86%). **TLC:**  $R_f$  = 0.70 (hexanes/ethyl acetate 9:1).

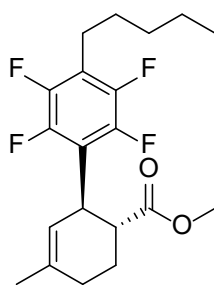
**$^{19}\text{F}$ -NMR (377 MHz,  $\text{CDCl}_3$ ):**  $\delta$  [ppm] = -146.66 – -147.14 (m, 4F).  **$^1\text{H}$ -NMR (400 MHz,  $\text{CDCl}_3$ ):**  $\delta$  [ppm] = 7.21 – 7.16 (m, 1H), 5.40 – 5.31 (m, 1H), 4.82 – 4.71 (m, 1H), 3.65 (s, 3H), 3.03 – 2.91 (m, 1H), 2.80 (dpt,  $J$  = 23.66, 5.42 Hz, 1H), 2.65 (t,  $J$  = 7.66, 2H), 1.74 (s, 3H), 1.62-1.52 (m, 2H), 1.26 – 1.28 (m, 4H), 0.89 (t,  $J$  = 6.94 Hz).  **$^{13}\text{C}$ -NMR (101 MHz,  $\text{CDCl}_3$ ):**  $\delta$  [ppm] = 166.2, 146.32 – 145.78 (m), 143.90 – 143.33 (m), 139.0, 131.2, 127.5,



119.1, 119.02 – 118.40 (m), 51.5, 32.1, 31.9, 31.3, 28.9, 22.6, 22.4, 22.3, 13.8. **HRMS** (EI): exact mass calc. for C<sub>20</sub>H<sub>22</sub>F<sub>4</sub>O<sub>2</sub>: m/z = 370.1556, found: 370.1545 [M]<sup>+</sup>.



(27)



(28)

**(6.5.27) & (6.5.28) Methyl 2',3',5',6'-tetrafluoro-5-methyl-4'-pentyl-1,2,3,4-tetrahydro-[1,1'-biphenyl]- 2-carboxylate**

Diene (26) (800 μmol) and PMHS (101 mg, 1.68 mmol, 2.1 equiv.) are put into a crimp vial under nitrogen. A solution of tris(pentafluorophenyl)borane (4 mg, 8 μmol, 1 mol%) in 4 mL DCM is added. The solution is stirred overnight at room temperature and stirred for another 24 h with saturated NH<sub>4</sub>F

solution or 2 h with TBAF•3H<sub>2</sub>O in DCM. Shorter times for quenching lead to incomplete cleavage of the silyl ethers formed and diminish the yield. The solution is extracted with DCM and column chromatography (5% EA in PE) yields the product. The products are obtained as mixtures of *cis* and *trans* isomer which are not separable by means of column chromatography. Column chromatography (5% EA in PE) yielded the product as a colorless, viscous liquid (26 mg, 70 μmol, 37%). Different reactions gave the product in varying *dr* (*cis/trans*) between 4 – 6 in favor of the *cis* diastereomer. The reaction seems to be notoriously sensitive towards reaction conditions and stoichiometry. A slight decrease in the amount of PMHS gave incomplete conversion while a slight increase led to a drastic decrease in yield. Due to the limited amount of material the reaction was not optimized further. An increase in yield should be possible with careful screening of different reaction conditions.

**(6.5.27) (*cis*) Methyl 2',3',5',6'-tetrafluoro-5-methyl-4'-pentyl-1,2,3,4-tetrahydro-[1,1'-biphenyl]- 2-carboxylate**

(NMR data derived from subtraction of the pure *trans* diastereomer)

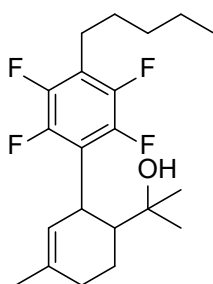
**TLC:** R<sub>f</sub> = 0.70 (hexanes/ethyl acetate 9:1)

**<sup>19</sup>F-NMR (377 MHz, CDCl<sub>3</sub>):** δ [ppm] = -142.16 (dd, J = 21.49, 12.18 Hz, 2F), -146.63 (dd, J = 21.85, 12.28 Hz, 2F). **<sup>1</sup>H-NMR (400 MHz, CDCl<sub>3</sub>):** δ [ppm] = 5.40 (d, J = 3.11 Hz, 1H), 4.18 (s, 1H), 3.52 (s, 3H), 3.00 – 2.92 (m, 1H), 2.67 (t, J = 7.62 Hz, 2H), 2.25 – 2.14 (m, 1H), 2.14 – 1.99 (m, 2H), 1.94 – 1.83 (m, 1H), 1.73 (s, 3H), 1.62 – 1.52 (m, 2H), 1.38 – 1.27 (m, 4H), 0.89 (t, J = 6.73 Hz, 3H). **<sup>13</sup>C{<sup>1</sup>H}-NMR (101 MHz, CDCl<sub>3</sub>):** δ [ppm] = 174.0, 146.60 – 154.75 (m), 144.19 – 143.46 (m), 136.2, 119.4 (t, J = 18.86), 117.0 (t, J = 14.82 Hz), 51.4, 43.7, 33.3, 31.3, 28.8, 28.7, 23.5, 22.7, 22.3, 21.4, 13.9. **HRMS** (EI): exact mass calc. for C<sub>20</sub>H<sub>24</sub>F<sub>4</sub>O<sub>2</sub>: m/z = 372.1707, found: 372.1706 [M]<sup>+</sup>.

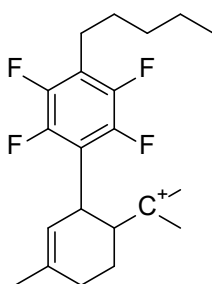
**(6.5.28) (*trans*) Methyl 2',3',5',6'-tetrafluoro-5-methyl-4'-pentyl-1,2,3,4-tetrahydro-[1,1'-biphenyl]- 2-carboxylate**

**TLC:** R<sub>f</sub> = 0.70 (hexanes/ethyl acetate 9:1)

**<sup>19</sup>F-NMR (377 MHz, CDCl<sub>3</sub>):** δ [ppm] = -144.61 (dd, J = 21.79, 12.49 Hz, 2F), -146.33 (dd, J = -22.05, 12.52 Hz, 2F). **<sup>1</sup>H-NMR (400 MHz, CDCl<sub>3</sub>):** δ [ppm] = 5.19 (s, 1H), 4.11 (d, J = 9.99 Hz, 1H), 3.58 (s, 3H), 2.94 – 2.86 (m, 1H), 2.67 (t, J = 7.62 Hz, 2H), 2.24 – 2.11 (m, 2H), 2.10 – 2.00 (m, 1H), 1.92 – 1.79 (m, 1H), 1.70 (s, 3H), 1.63 – 1.52 (m, 2H+2H impurities), 1.36 – 1.28 (m, 4H+2H impurities), 0.89 (t, J = 6.87 Hz, 3H+1H impurities). **<sup>13</sup>C{<sup>1</sup>H}-NMR (101 MHz, CDCl<sub>3</sub>):** δ [ppm] = 175.0, 146.34 – 145.80 (m), 143.84 – 143.40 (m), 134.6, 120.7, 51.7, 119.37 (t, J = 15.73 Hz), 119.02 (t, J = 18.98 Hz), 44.2, 34.9, 31.3, 29.3, 28.9, 26.7, 23.2, 22.7, 22.3, 13.9. **HRMS (EI):** exact mass calc. for C<sub>20</sub>H<sub>24</sub>F<sub>4</sub>O<sub>2</sub>: m/z = 372.1707, found: 372.1700 [M]<sup>+</sup>.



Exact Mass: 372.2076



Exact Mass: 355.2043

**(6.5.29) 2-(2',3',5',6'-Tetrafluoro-5-methyl-4'-pentyl-1,2,3,4-tetrahydro-[1,1'-biphenyl]-2-yl)propan-2-ol** A 3 M solution of MeMgBr in Et<sub>2</sub>O (7 equiv.) is added to a 2 M solution of ester (20 mg, 54 μmol) in dry THF at 0 °C. The solution is warmed to rt and stirred for 30 min. The reaction is quenched with saturated NH<sub>4</sub>Cl solution and extracted with ethyl acetate.

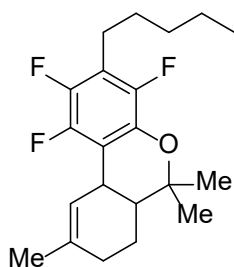
Column chromatography (20% EA in PE) yields the tertiary alcohol. The product was obtained as a colorless viscous liquid (19 mg, 51 μmol, 95%). *cis* and *trans* isomers are separable by column chromatography.

*cis*-**(6.5.29) TLC:** R<sub>f</sub> = 0.35 (hexanes/ethyl acetate 9:1). **<sup>19</sup>F-NMR (377 MHz, CDCl<sub>3</sub>):** δ [ppm] = -135.83 – -136.11 (m, 1F), 142.71 (dd, J = 22.37, 11.61 Hz, 1F), 146.10 (dd, J = 22.35, 12.15 Hz, 1 H), -146.40 (dd, J = 21.81, 11.68 Hz, 1F). **<sup>1</sup>H-NMR (400 MHz, CDCl<sub>3</sub>):** δ [ppm] = 5.30 – 5.24 (m, 1H), 4.08 – 4.00 (m, 1H), 2.68 (t, J = 7.63 Hz, 2H), 2.19 – 2.13 (m, 1H), 2.06 – 1.97 (m, 1H), 1.94 – 1.76 (m, 2H), 1.70 (s, 3H), 1.63 – 1.52 (m, 2H), 1.37 – 1.29 (4H), 1.07 (s, 3H), 1.00 (s, 3H), 0.89 (t, J = 6.85 Hz, 3H). **<sup>13</sup>C{<sup>1</sup>H}-NMR (101 MHz, CDCl<sub>3</sub>):** δ [ppm] = 135.71, 120.50, 119.33 – 118.69 (m), 72.68, 49.49, 32.02, 31.33, 30.81, 28.90, 28.34, 27.16, 23.42, 22.70, 22.31, 20.44, 20.33, 13.92. **HRMS (EI):** exact mass calc. for C<sub>21</sub>H<sub>28</sub>F<sub>4</sub>O: m/z = 372.2076, found: 354.1962 [M-H<sub>2</sub>O]<sup>+</sup>.

***trans*-(6.5.29)**

**TLC:** R<sub>f</sub> = 0.40 (hexanes/ethyl acetate 9:1)

**<sup>19</sup>F-NMR (377 MHz, CDCl<sub>3</sub>):** δ [ppm] = -144.51 – -144.94 (broad s, 2F), -146.84 (dd, J = 22.02, 12.18 Hz, 2F). **<sup>1</sup>H-NMR (400 MHz, CDCl<sub>3</sub>):** δ [ppm] = 5.05 (s, 1H), 3.82 (d, J = 9.25 Hz, 1H), 2.65 (t, J = 7.67 Hz, 2H), 2.25 – 2.10 (m, 2 H), 2.03 – 1.92 (m, 2H), 1.68 (s, 3H), 1.63 – 1.52 (m, 2H+1H impurities), 1.49 – 1.38 (m, 1H), 1.36 – 1.28 (m, 4 H), 1.20 (s, 3H), 1.12 (s, 3H), 0.93 (s, 1H), 0.89 (t, J = 6.95 Hz, 3H). **<sup>13</sup>C-NMR (101 MHz, CDCl<sub>3</sub>):** δ [ppm] = 146.33 – 145.46 (m), 143.86 – 143.05 (m), 135.2, 123.4 (t, J = 15.20 Hz), 117.8 (t, J = 18.90 Hz), 122.1, 73.7, 48.0, 34.1, 31.4, 30.2, 28.97, 28.94, 23.2, 22.6, 22.3.



**(6.5.30) 1,2,4-Trifluoro-6,6,9-trimethyl-3-pentyl-6a,7,8,10a-tetrahydro-6Hbenzo[**

**c]chromene (1-deoxy-1,2,4-trifluoro-THC) from tertiary alcohol (29) (14 mg,**

**cis:trans = 4:1) The product was obtained as a colorless liquid (13 mg, 37  $\mu$ mol, cis:trans**

**= 4:1, 98%). The tertiary alcohol is dissolved in dry THF. A 1 M**

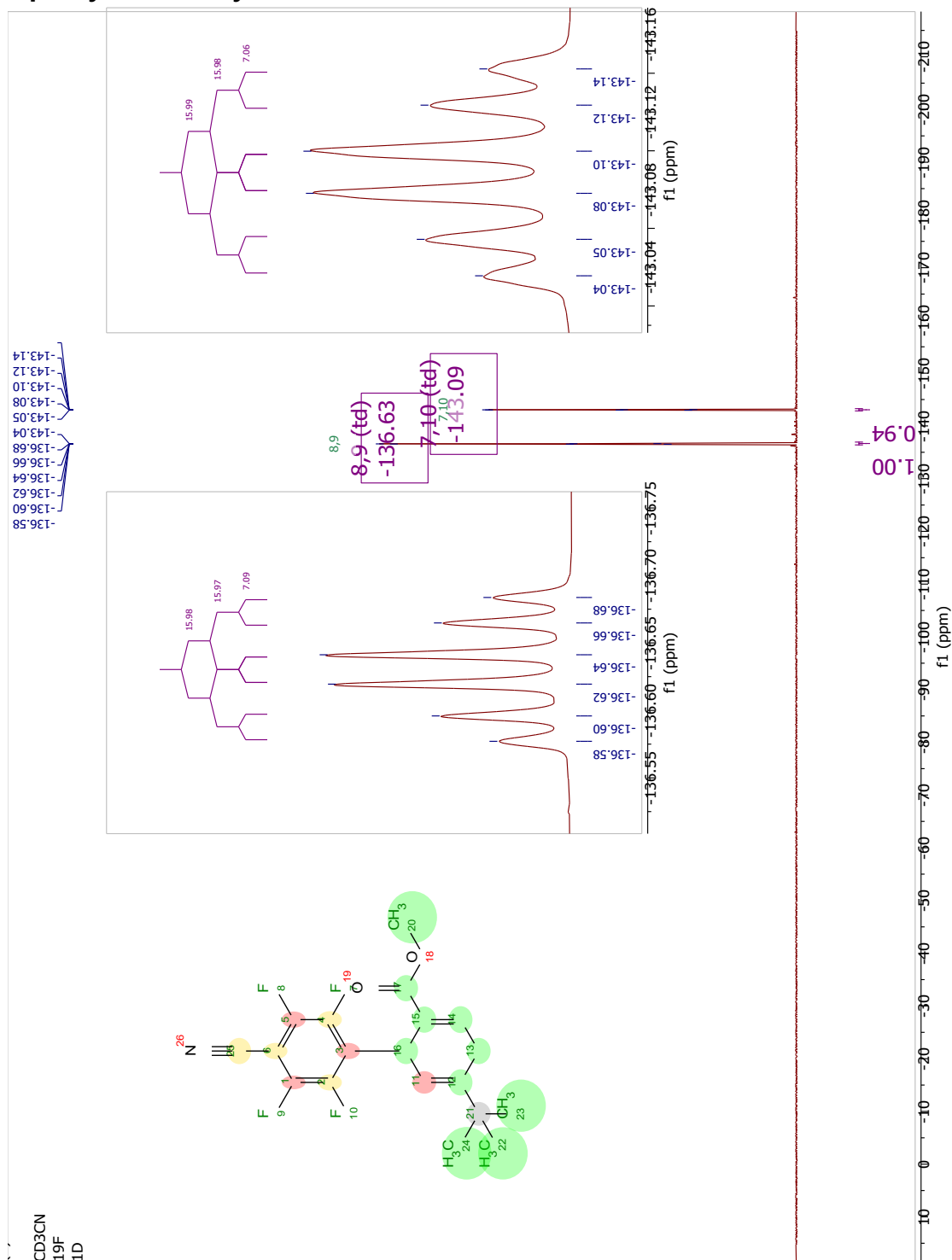
**solution of KHMDS in THF (1.5 equiv.) is added. The solution is heated to 40 °C for 15 minutes. The reaction is quenched with saturated  $\text{NH}_4\text{Cl}$  solution and extracted with ethyl acetate. Column chromatography (2% EA in PE) yields the target compound.**

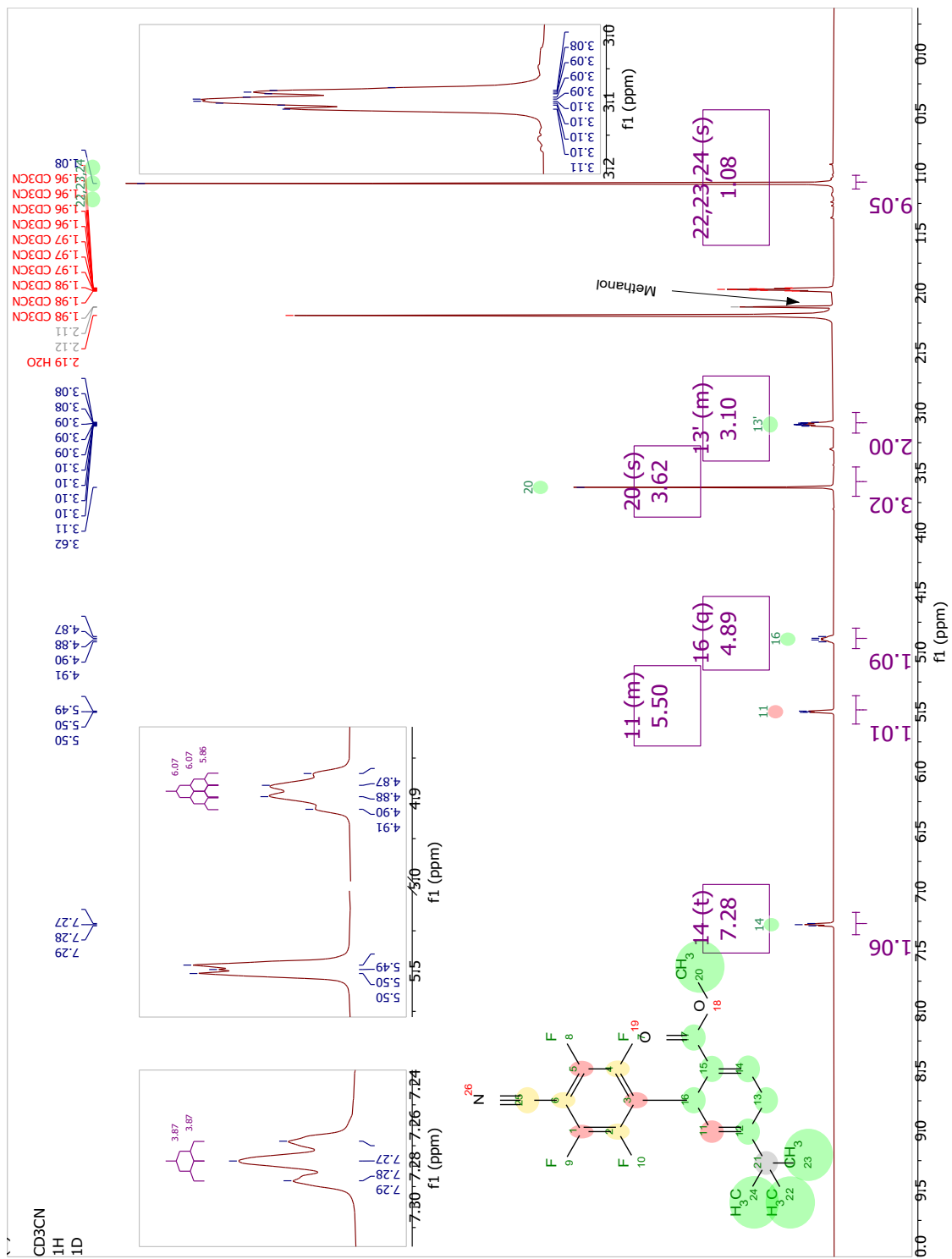
*cis*-**(6.5.30)**  **$^{19}\text{F}$ -NMR** (377 MHz,  $\text{CDCl}_3$ ):  $\delta$  [ppm] = -142.75 – -142.90 (m, 1F), -145.54 (d,  $J$  = 12 Hz, 1F), -153.50 (d,  $J$  = 22.41 Hz, 1F).  **$^1\text{H}$ -NMR** (400 MHz,  $\text{CDCl}_3$ ):  $\delta$  [ppm] = 6.39 – 6.31 (m, 1H), 4.03 – 3.96 (m, 1H), 2.97 (t,  $J$  = 7.53 Hz, 2H), alkyl region could not be analyzed due to overlaps from both diastereomers.

*trans*-**(6.5.30)**  **$^{19}\text{F}$ -NMR** (377 MHz,  $\text{CDCl}_3$ ):  $\delta$  [ppm] = -145.04 – -145.17 (m, 1F), -145.40 (d,  $J$  = 13.97 Hz, 1F), -154.26 (d,  $J$  = 22.81 Hz, 1F).  **$^1\text{H}$ -NMR** (400 MHz,  $\text{CDCl}_3$ ):  $\delta$  [ppm] = 6.41 (s, 1H), 3.69 (d,  $J$  = 11.35 Hz, 1H), alkyl region could not be analyzed due to overlaps from both diastereomers.

## 6.10.2 Spectra

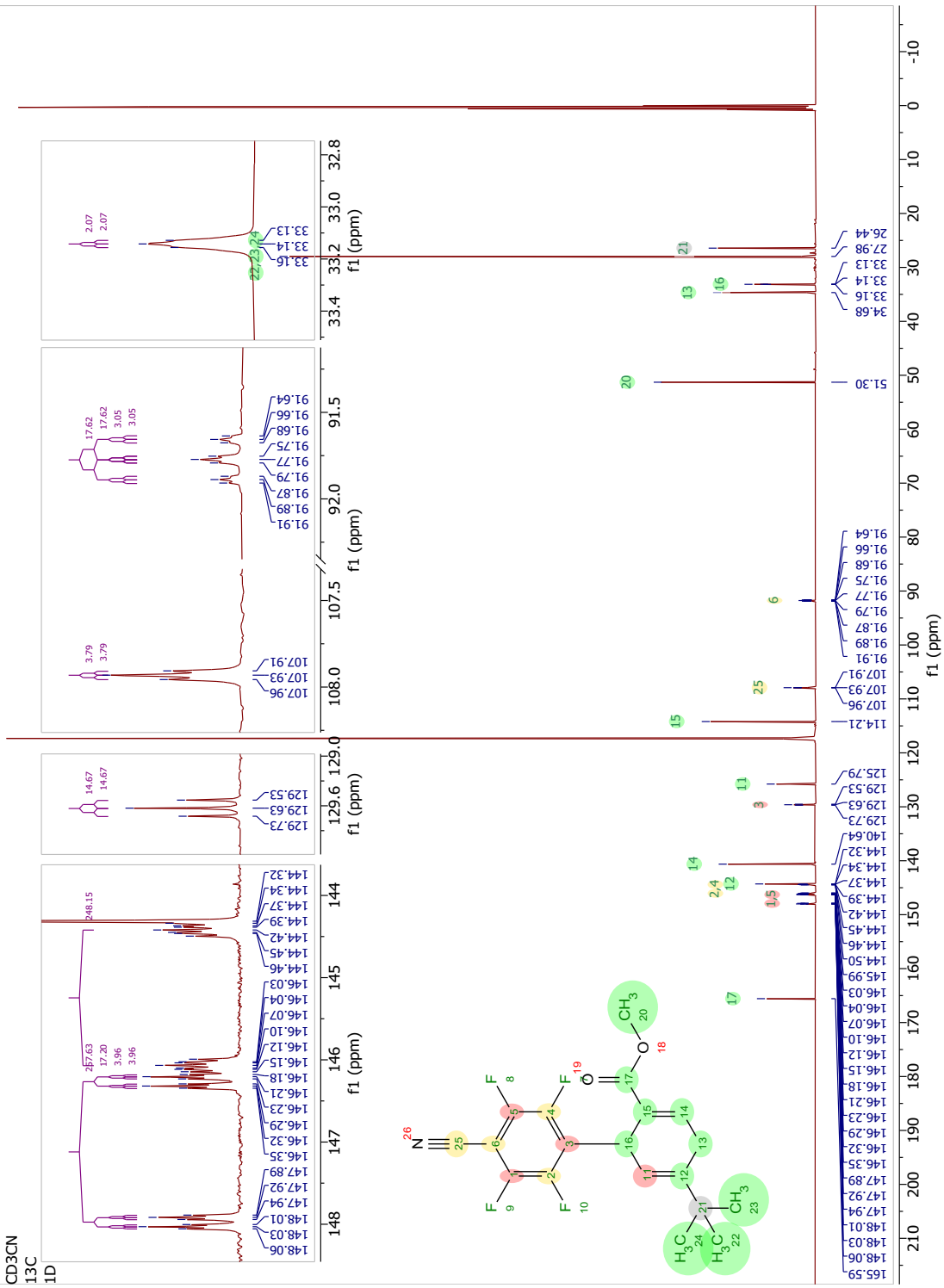
### (6.3.5) methyl 5-(tert-butyl)-4'-cyano-2',3',5',6'-tetrafluoro-1,4-dihydro-[1,1'-biphenyl]-2-carboxylate.



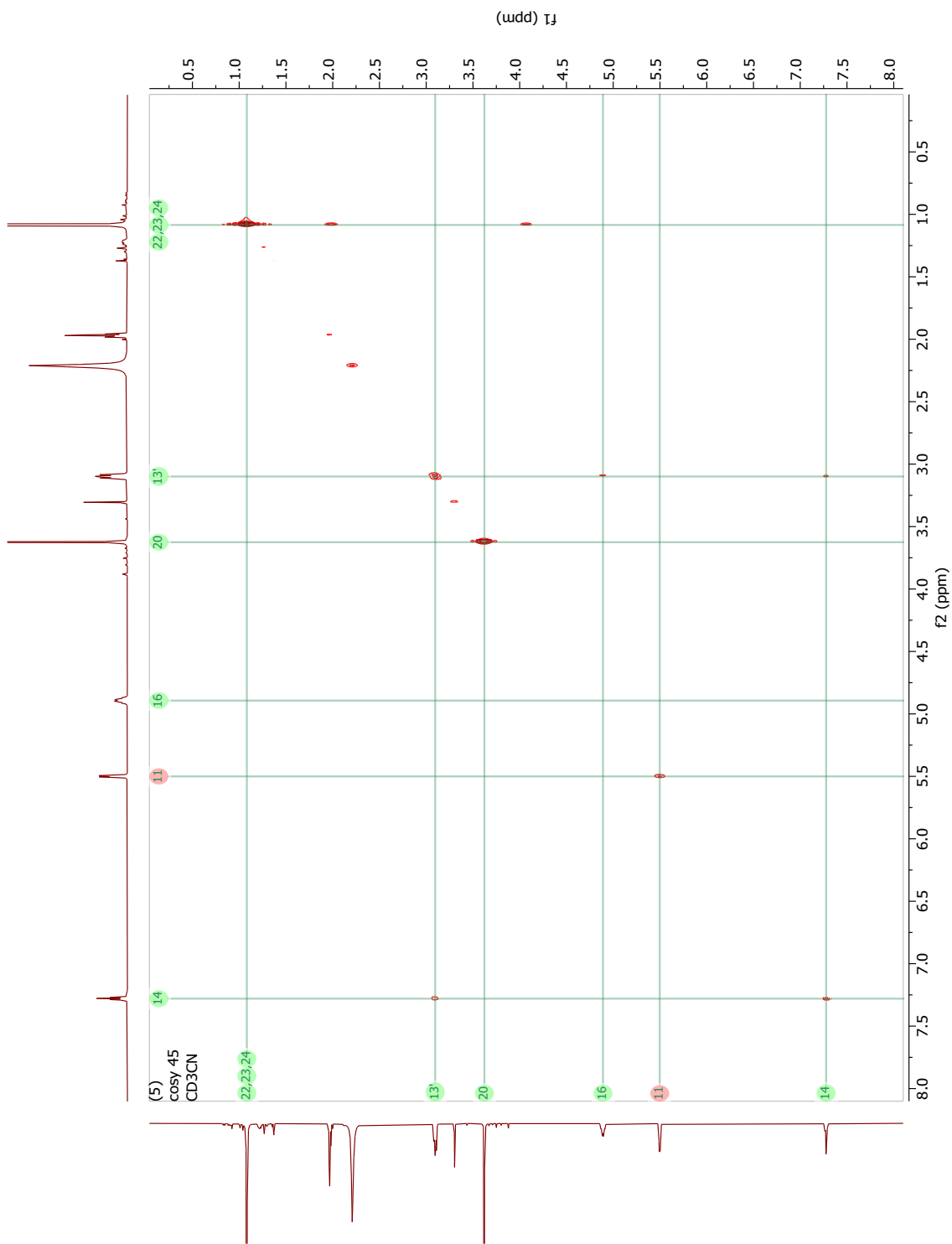


(5)

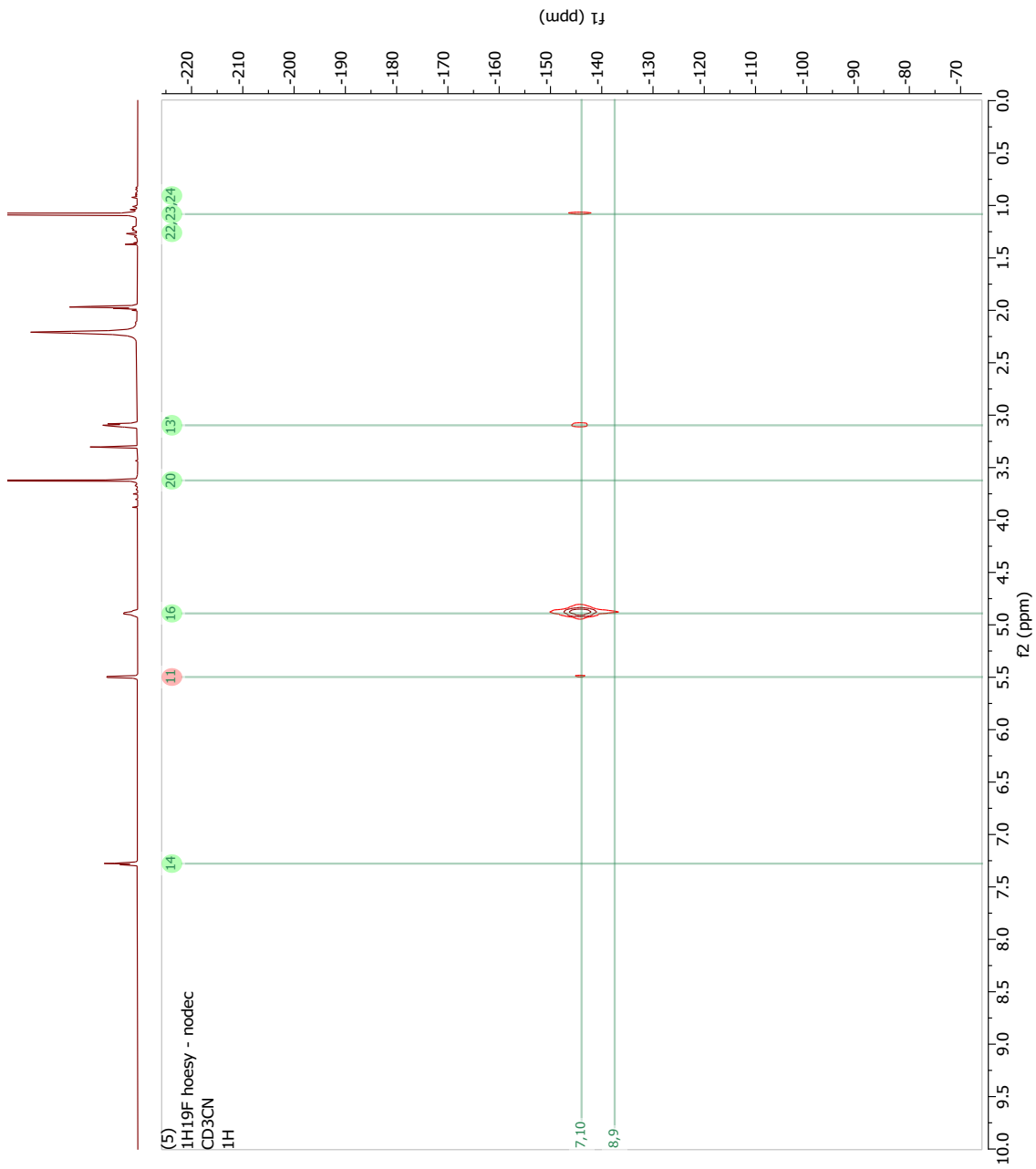
CD3CN  
13C  
1D

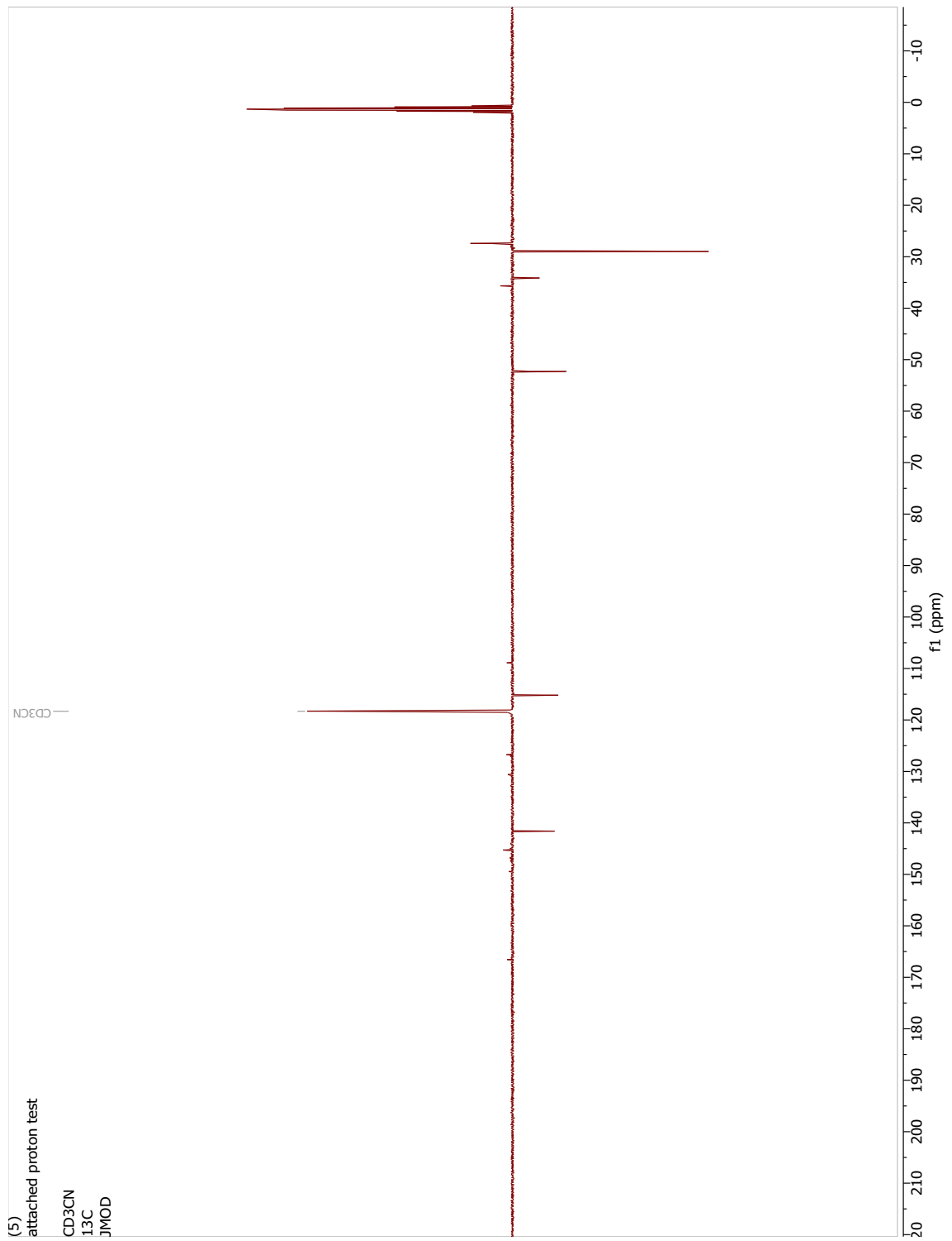


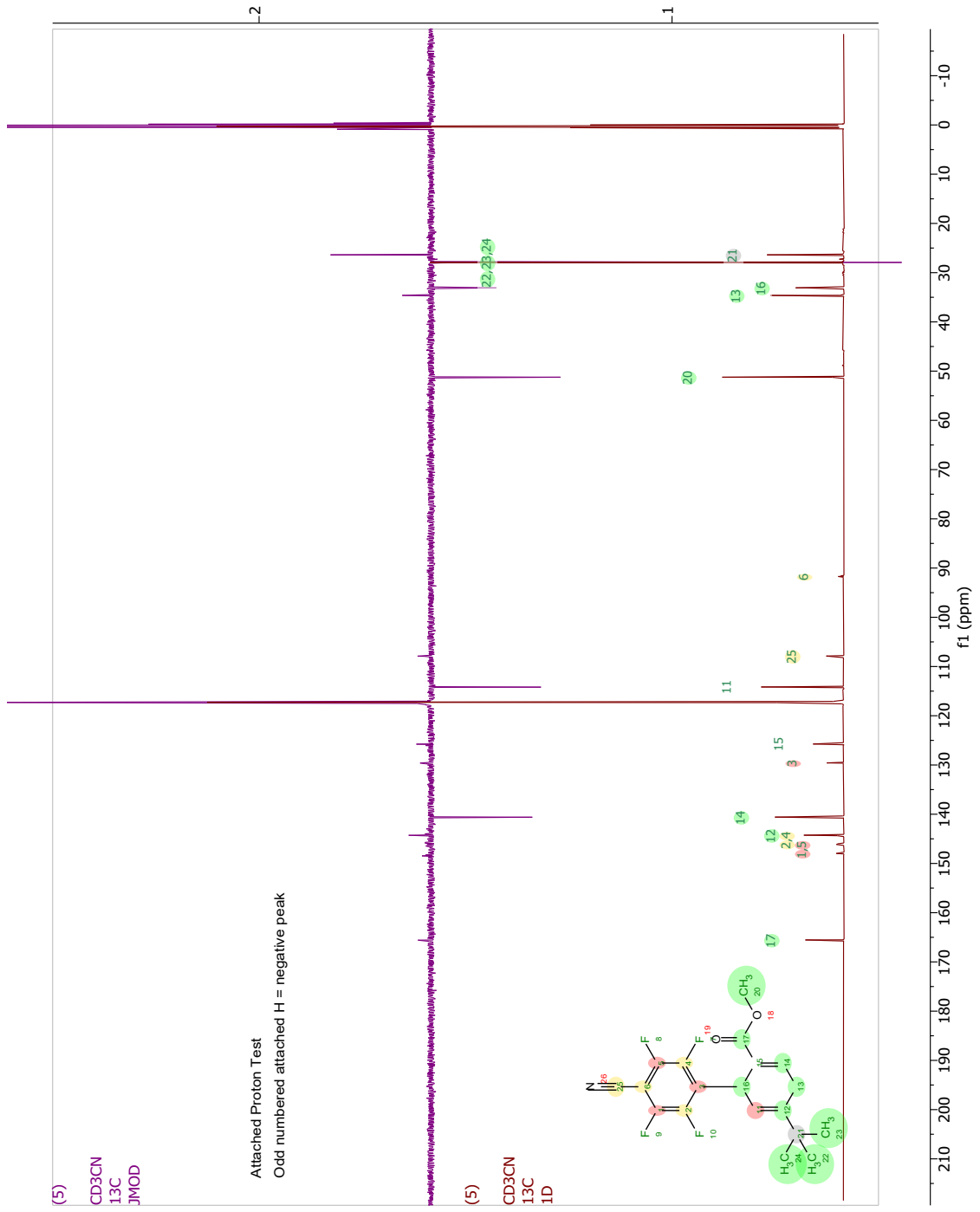




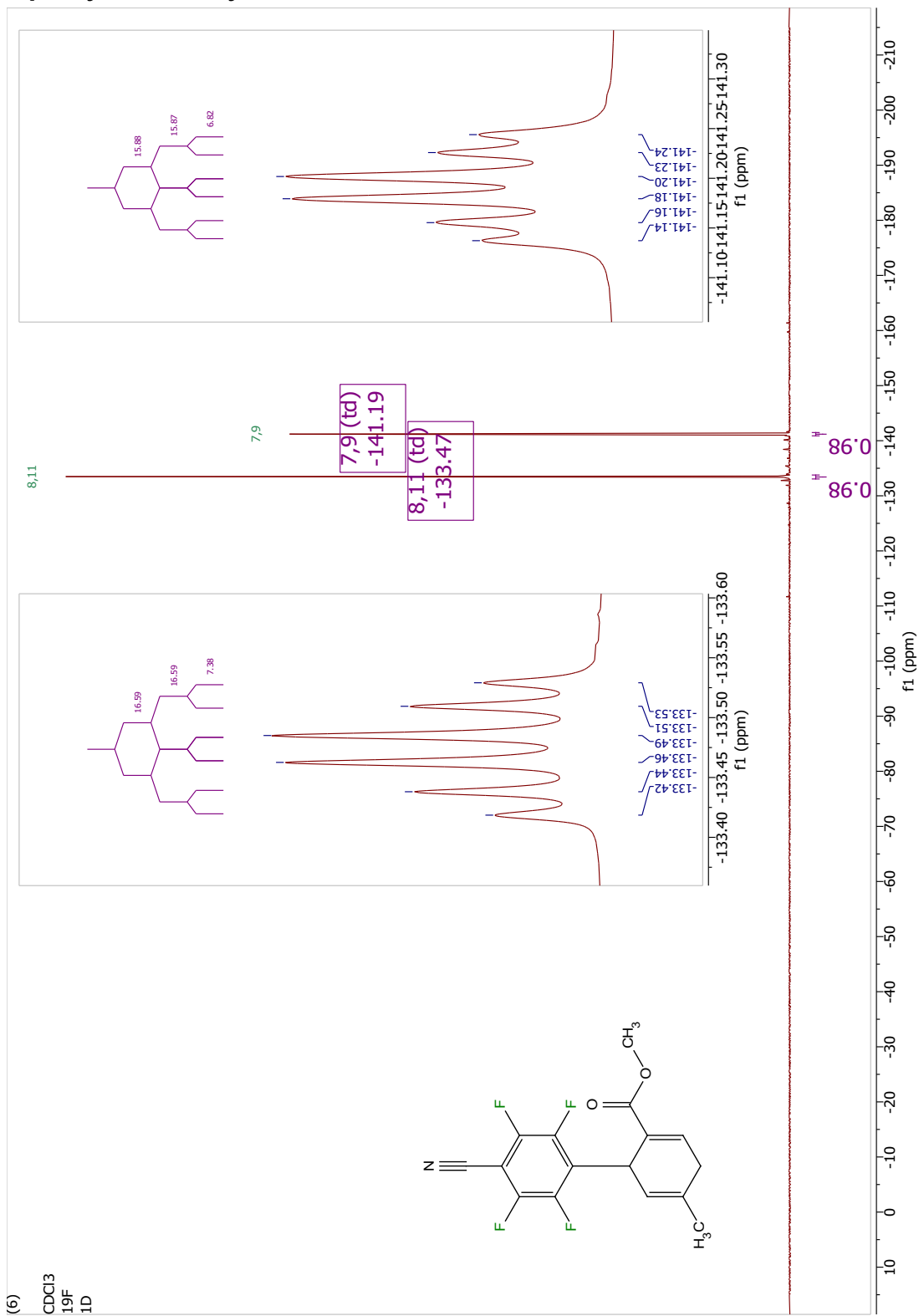








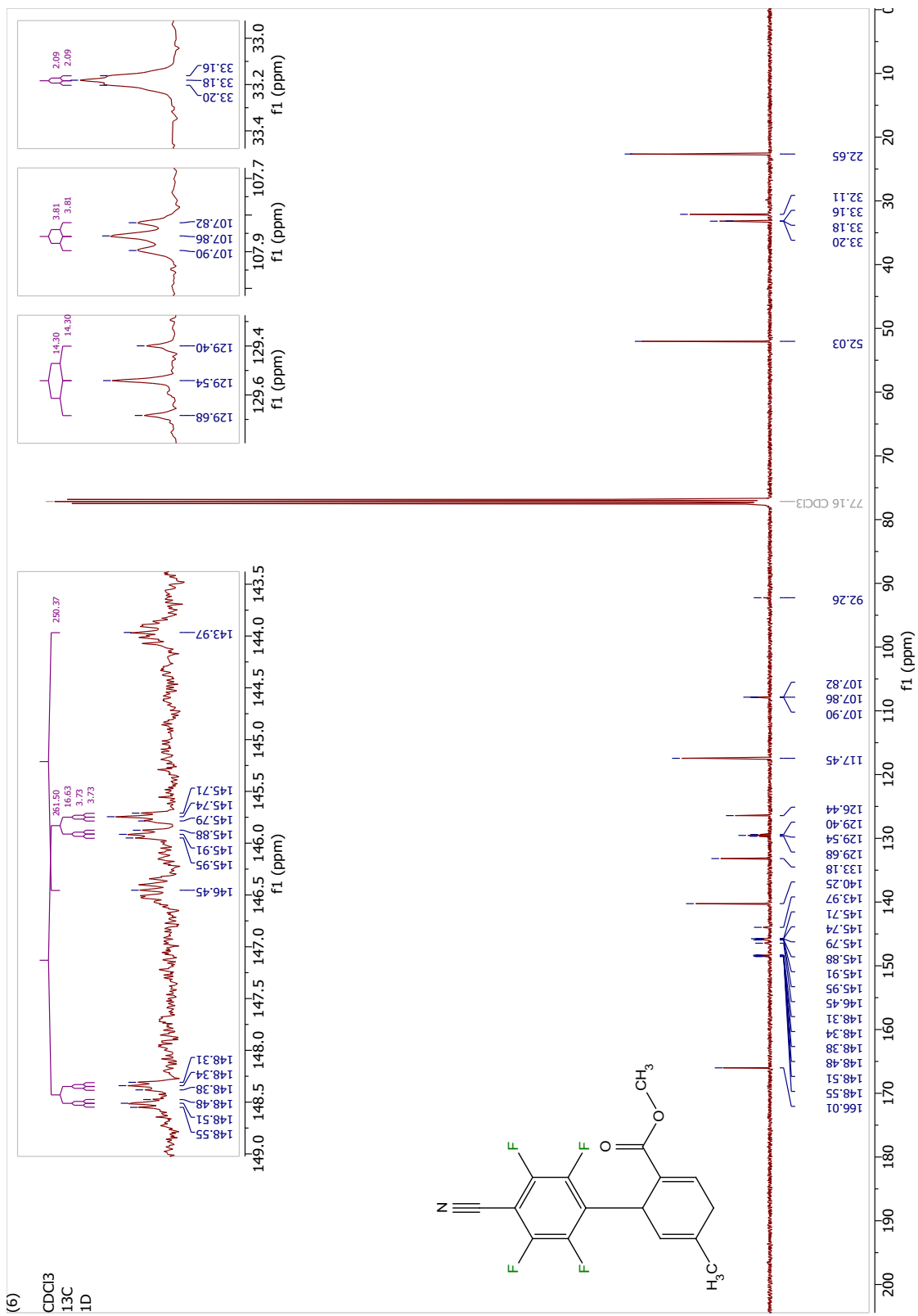
(6.3.6) methyl 4'-cyano-2',3',5',6'-tetrafluoro-5-methyl-1,4-dihydro-[1,1'-biphenyl]-2-carboxylate.



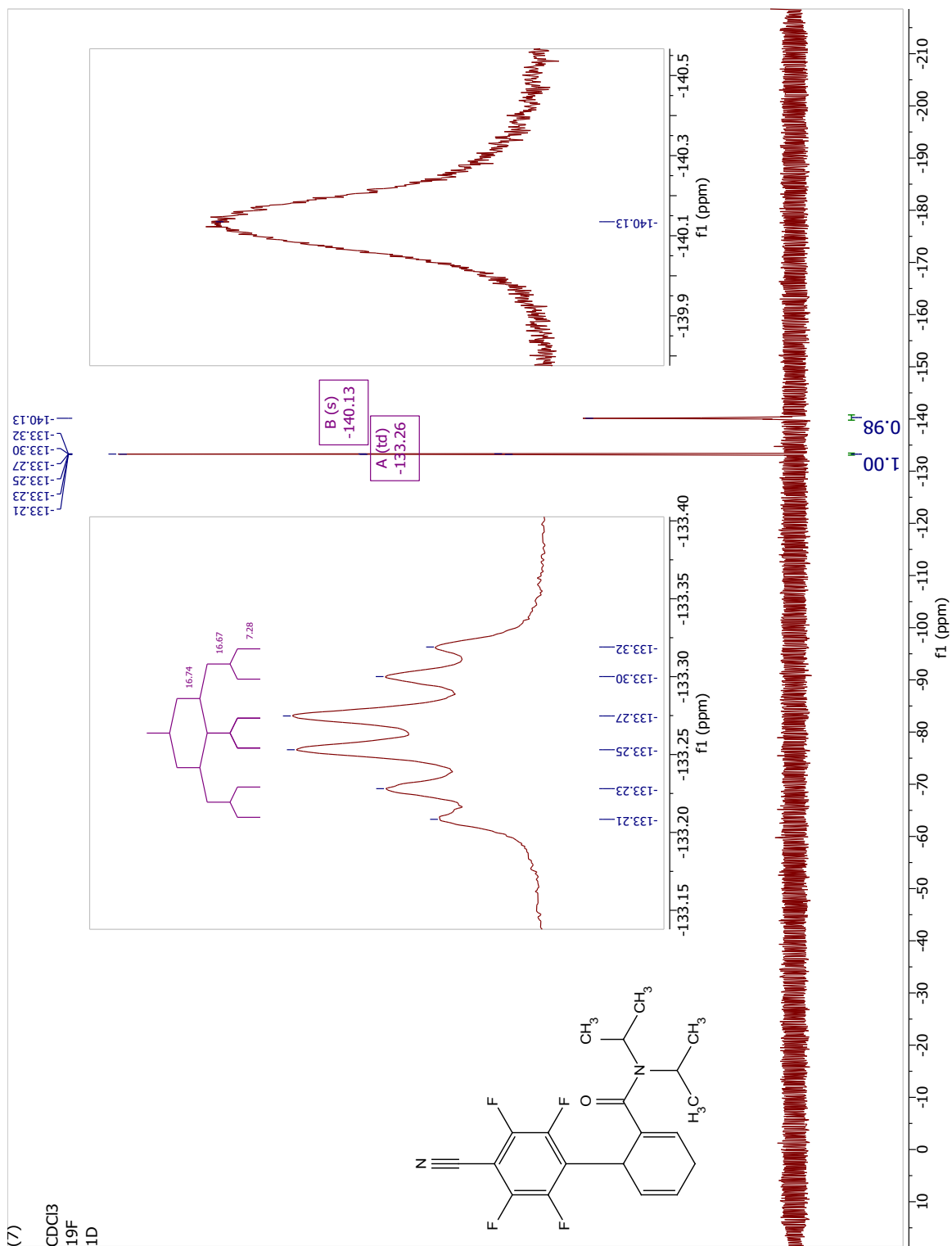


(6)

CDCl<sub>3</sub>  
13C  
1D

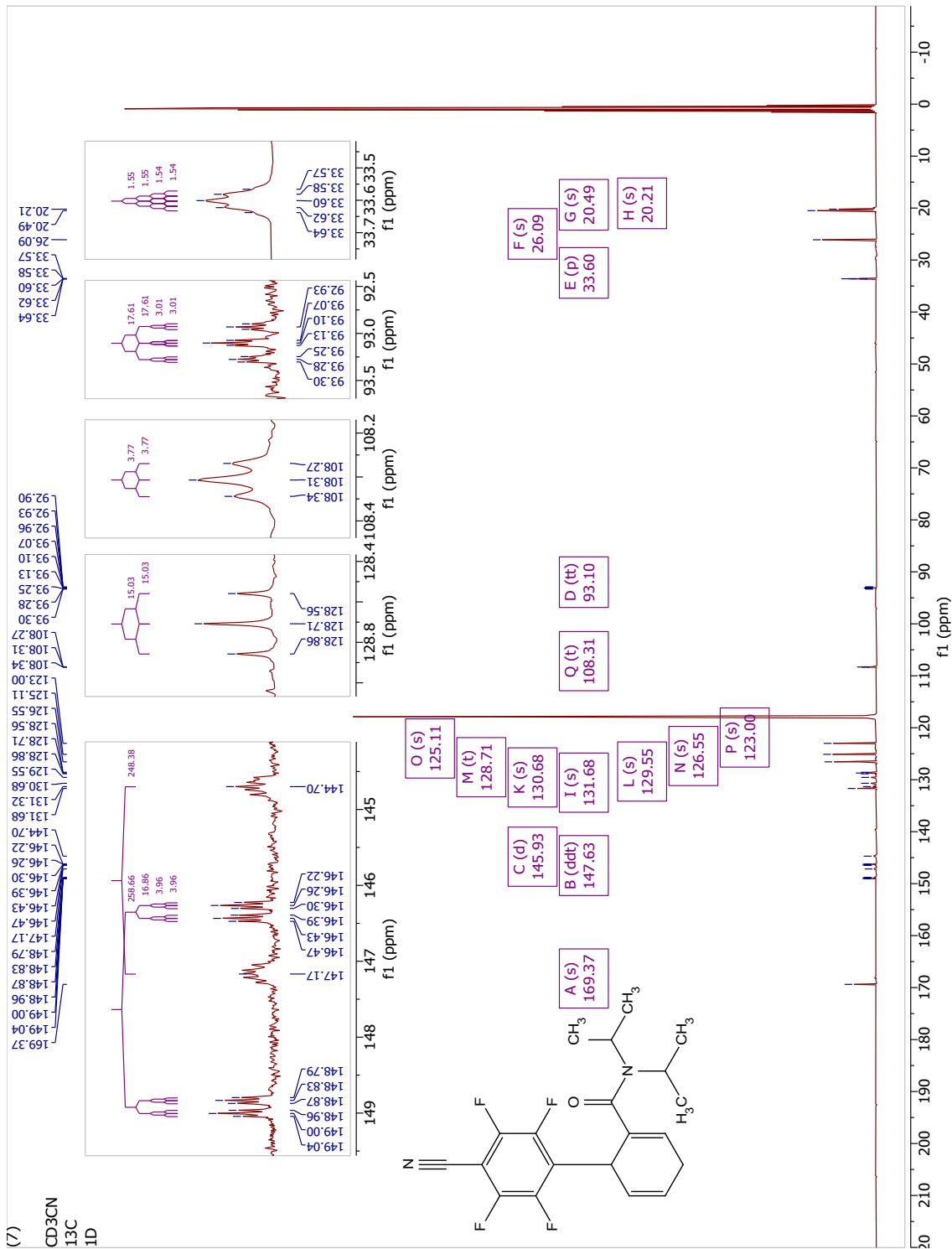


(6.3.7) 4'-cyano-2',3',5',6'-tetrafluoro-N,N-diisopropyl-1,4-dihydro-[1,1'-biphenyl]-2-carboxamide.

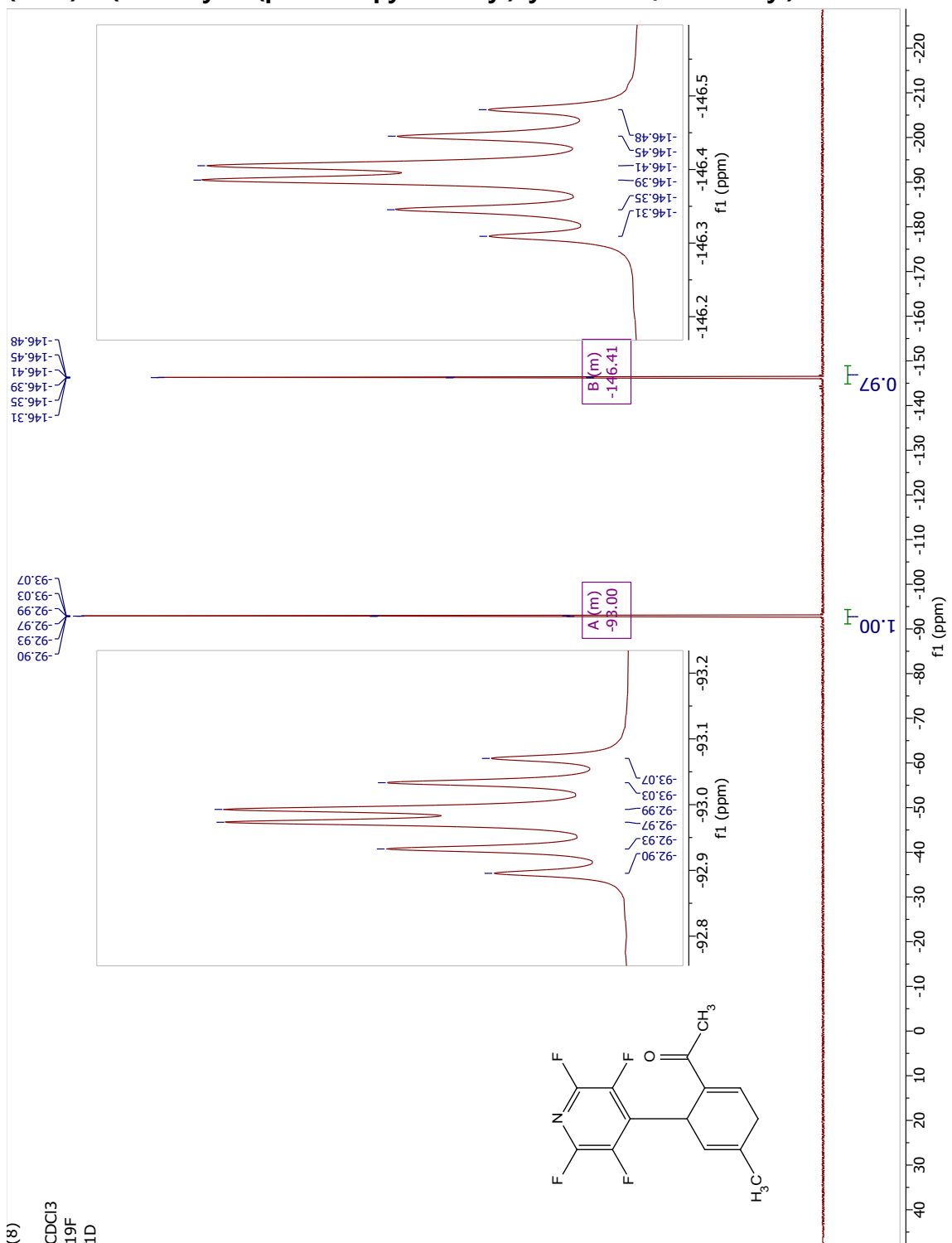








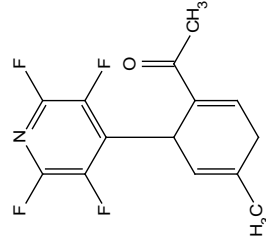
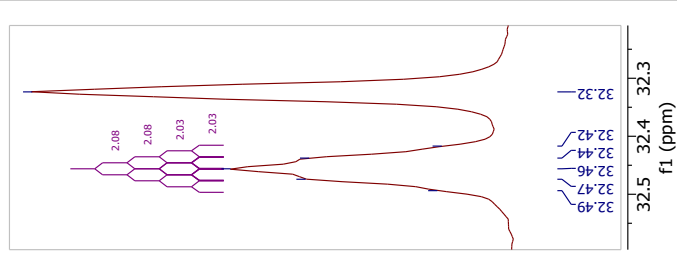
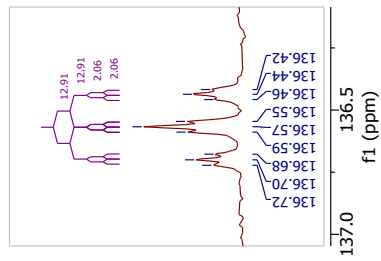
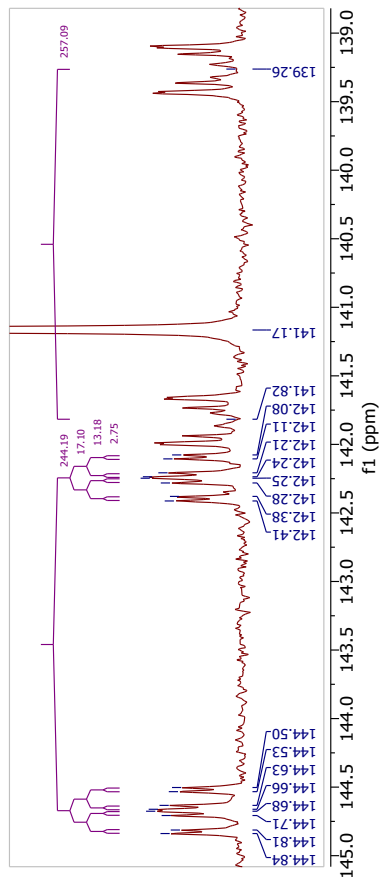
(6.3.8) 1-(4-methyl-6-(perfluoropyridin-4-yl)cyclohexa-1,4-dien-1-yl)ethan-1-one





(8)

CDCl<sub>3</sub>  
13C  
1D



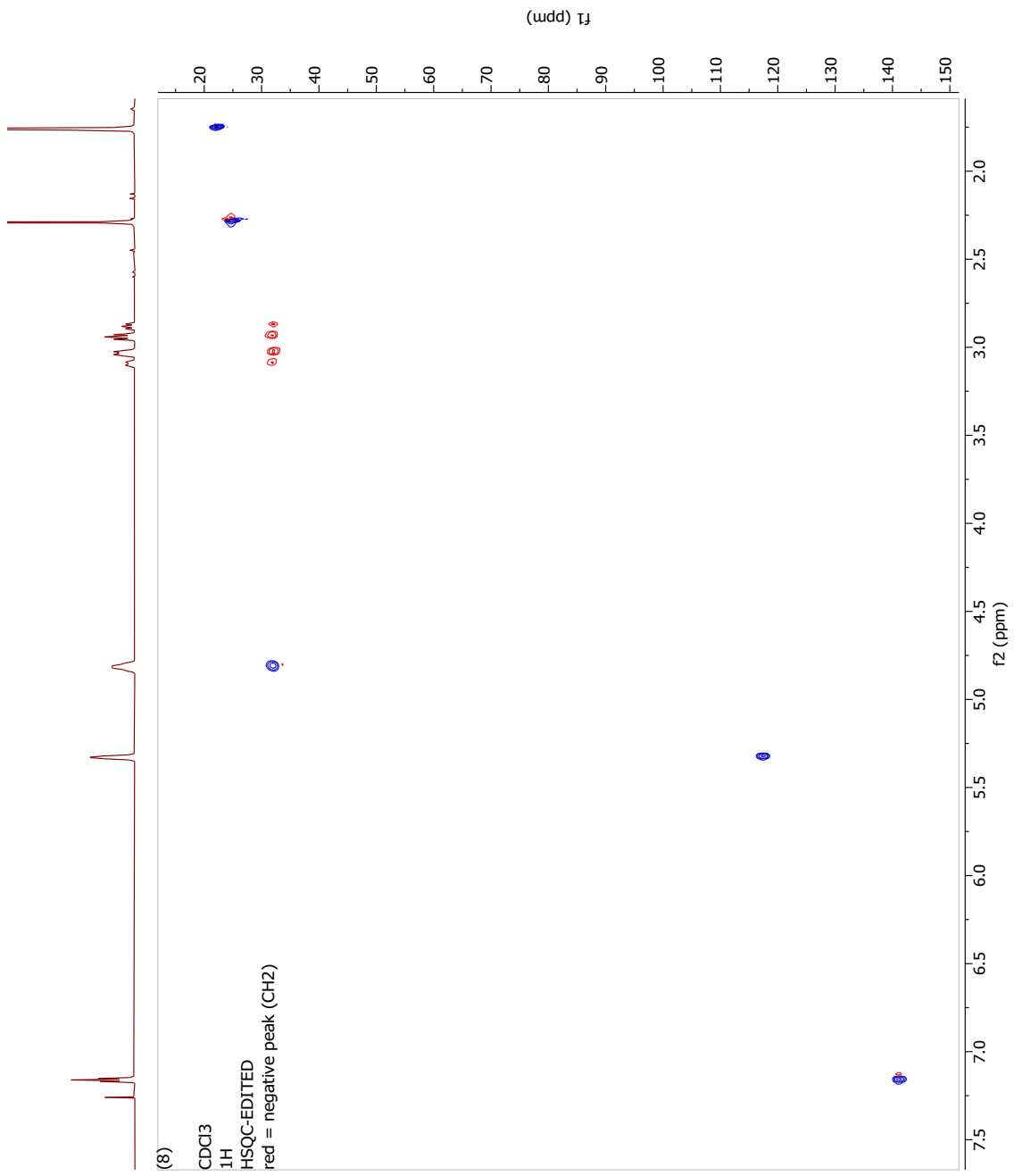
32.49  
32.47  
32.46  
32.44  
32.42  
32.32  
25.13  
22.53

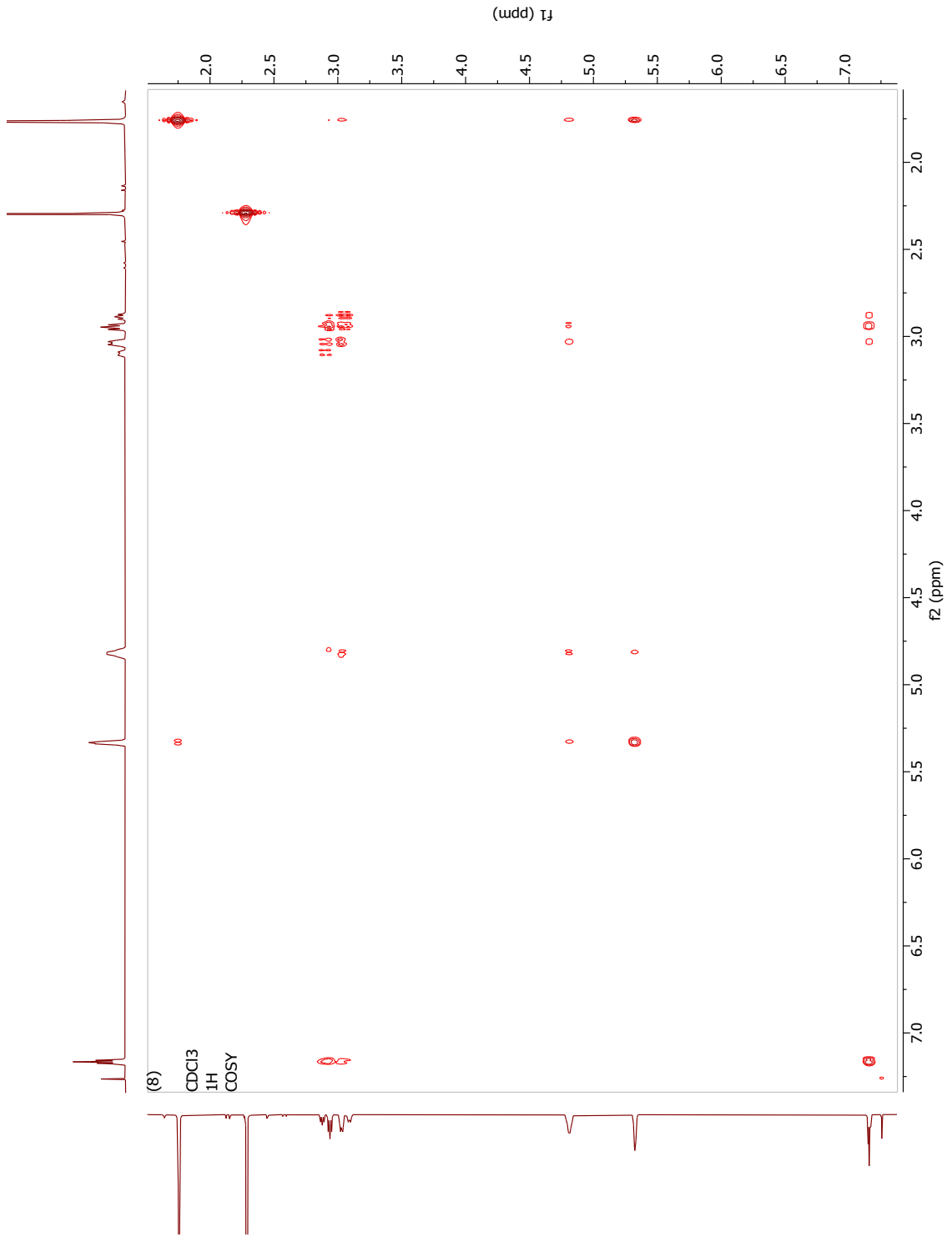
77.16 CDCl<sub>3</sub>

197.26  
144.84  
144.81  
144.71  
144.68  
144.66  
144.63  
144.53  
144.50  
142.41  
142.38  
142.28  
142.25  
142.24  
142.21  
142.11  
142.08  
141.82  
141.17  
139.26  
136.72  
136.70  
136.68  
136.59  
136.57  
136.55  
136.46  
136.44  
136.42  
135.85  
132.67  
117.73

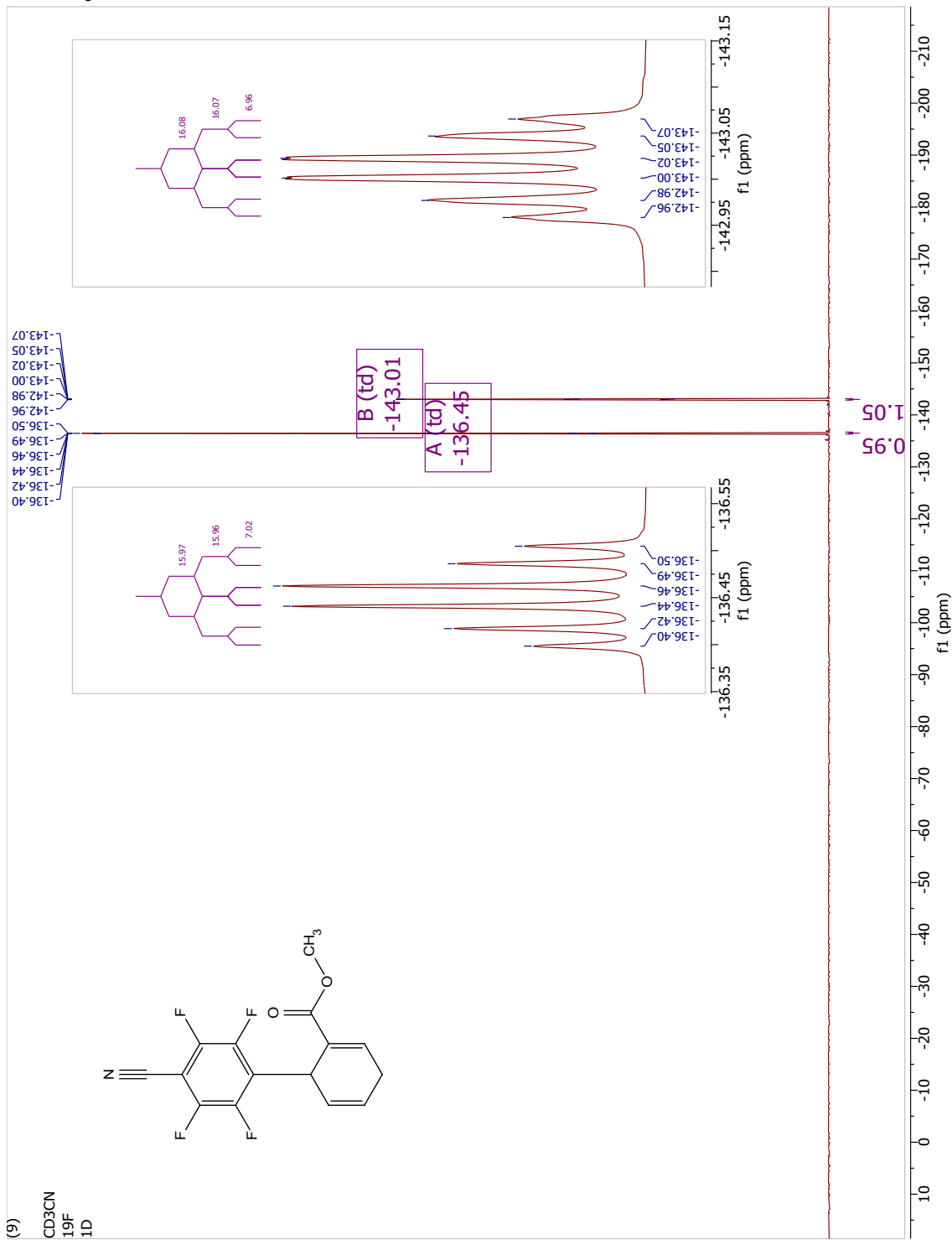
f1 (ppm)

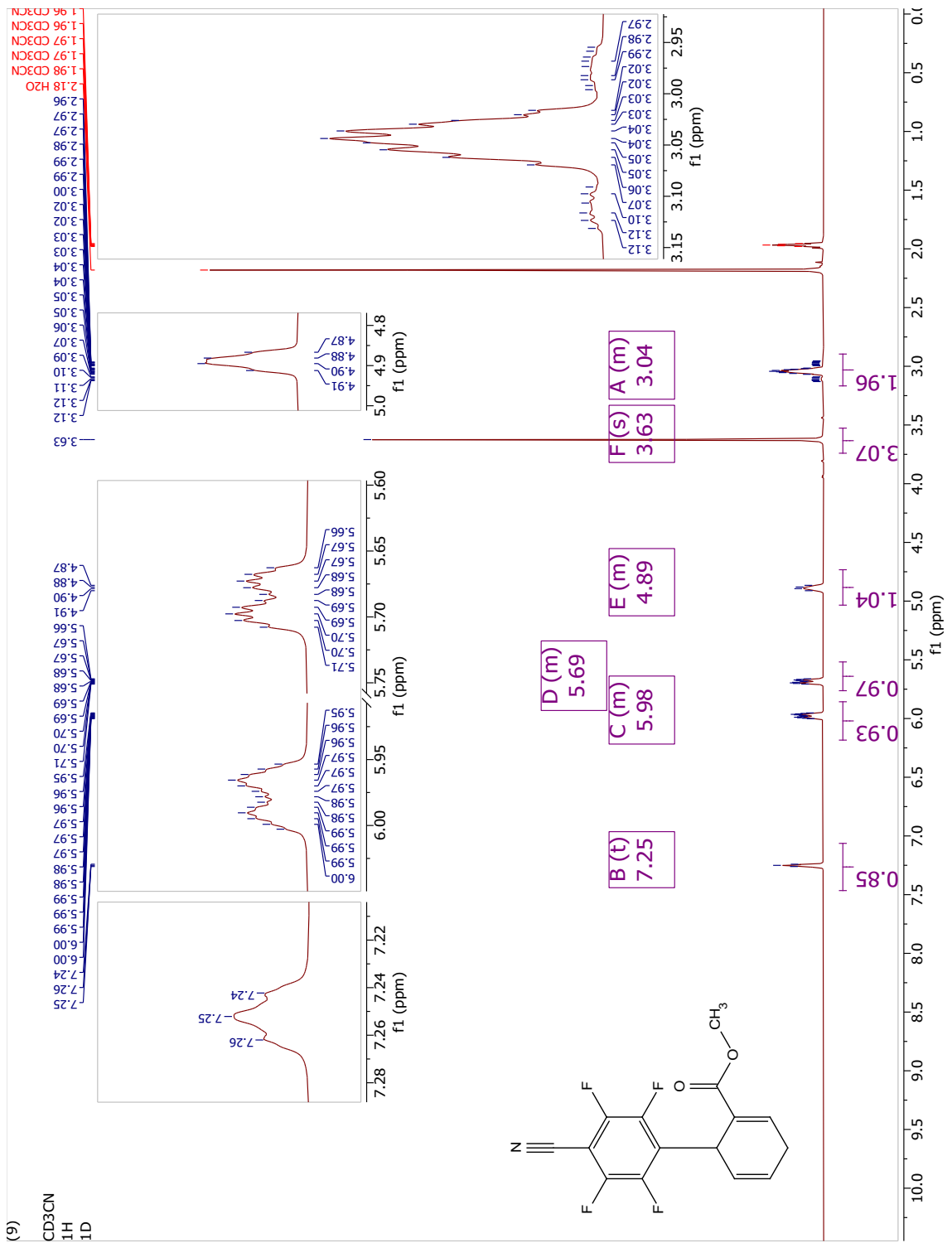
-3





(6.3.9) methyl 4'-cyano-2',3',5',6'-tetrafluoro-1,4-dihydro-[1,1'-biphenyl]-2-carboxylate.

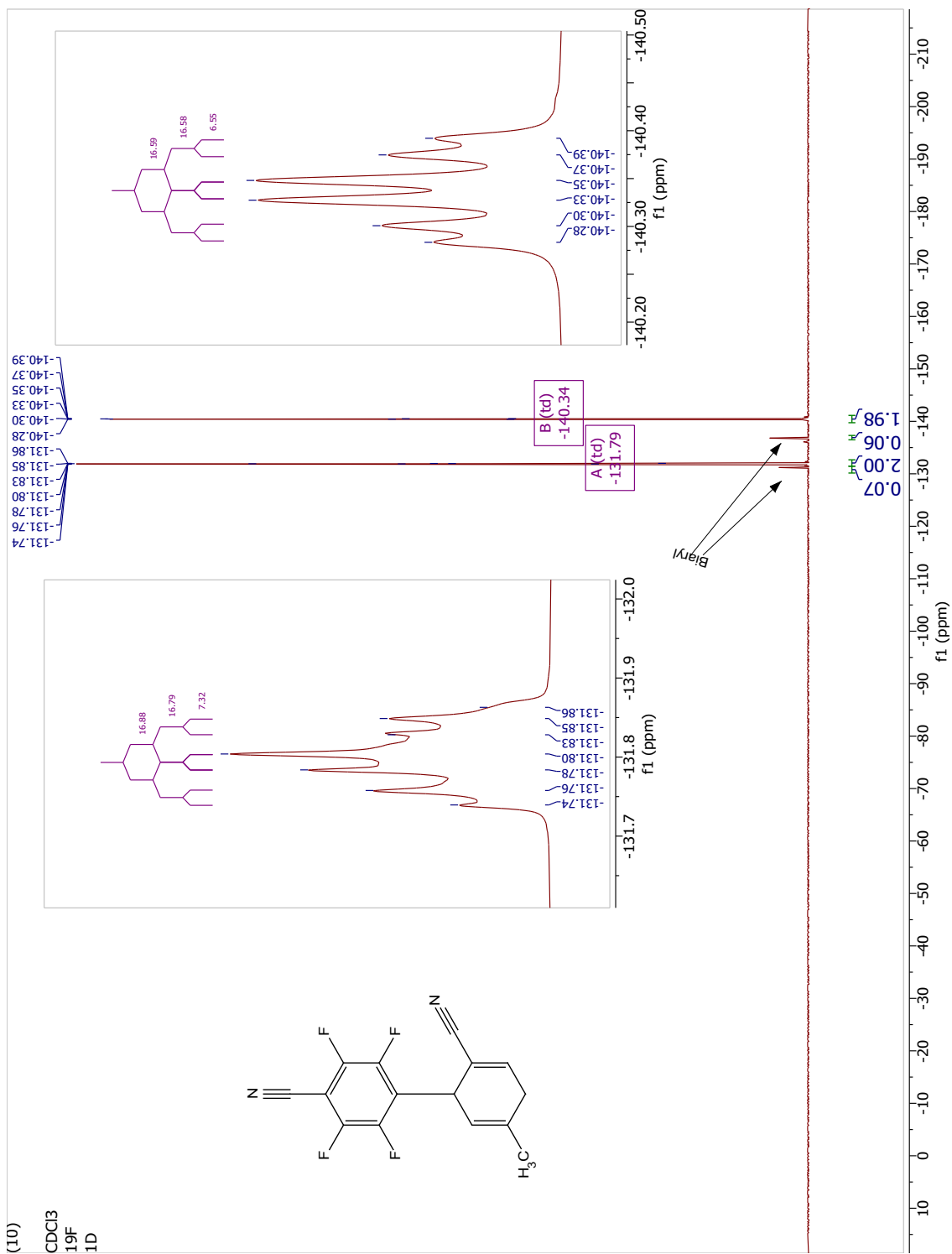


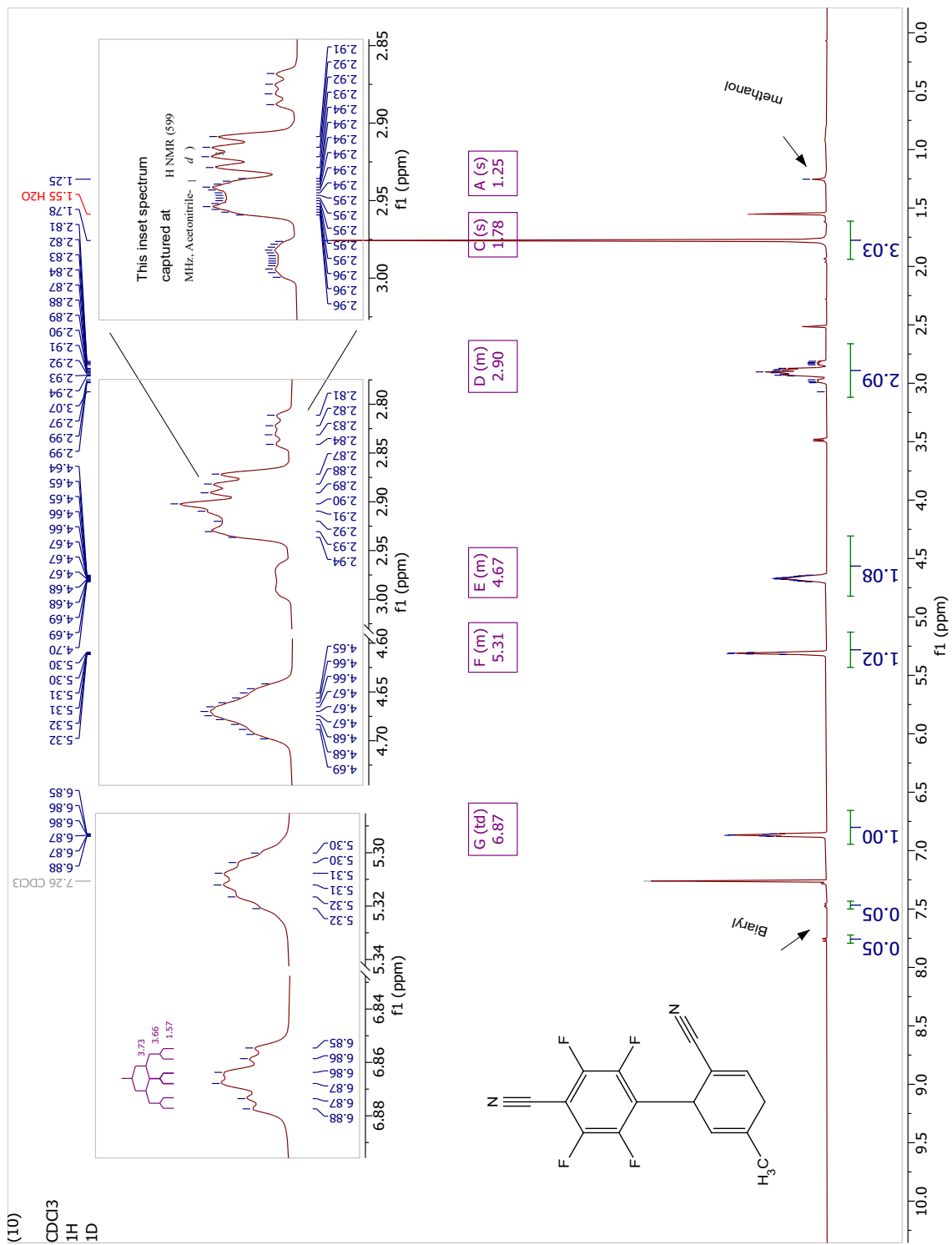






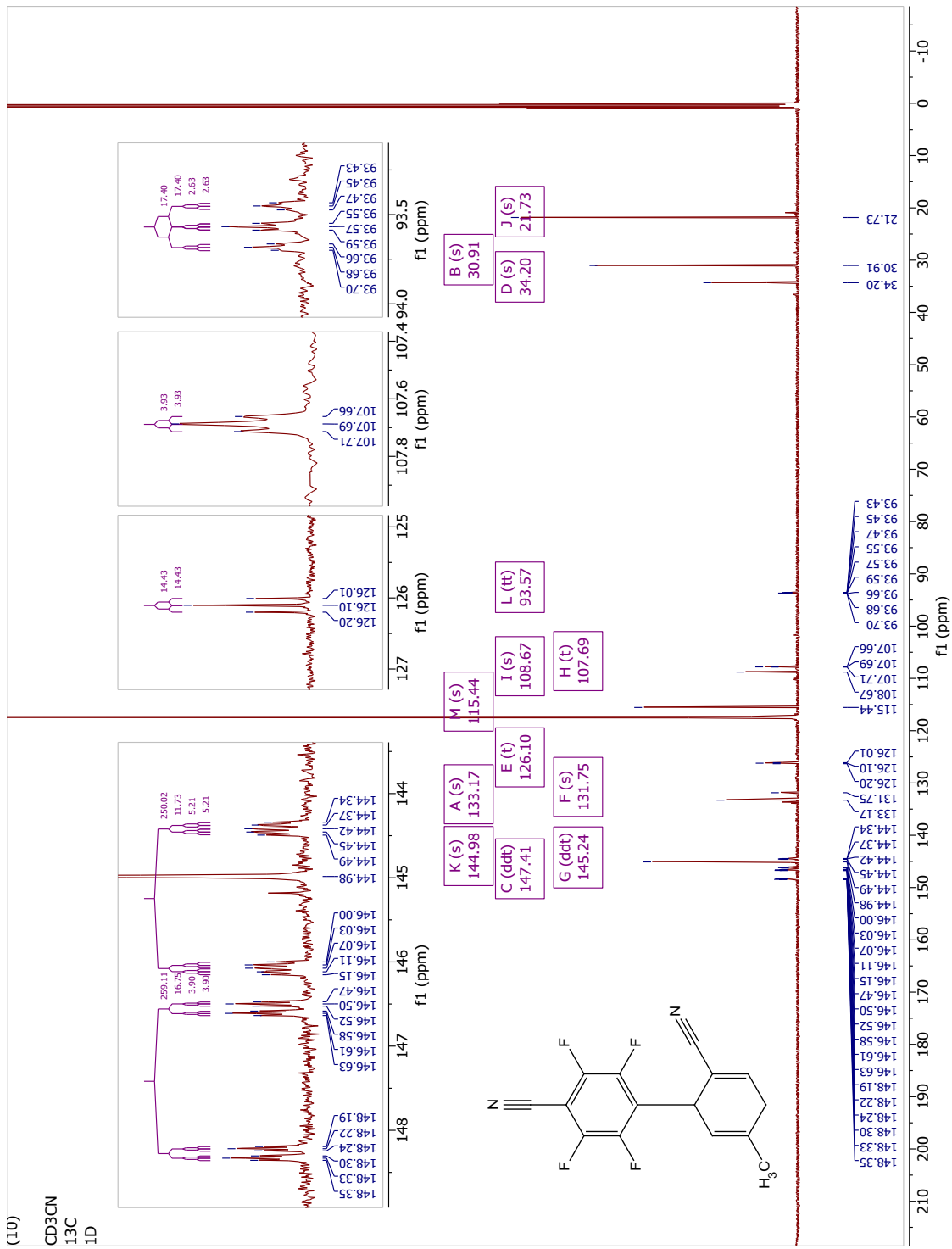
(6.3.10) 2',3',5',6'-tetrafluoro-5-methyl-1,4-dihydro-[1,1'-biphenyl]-2,4'-dicarbonitrile.



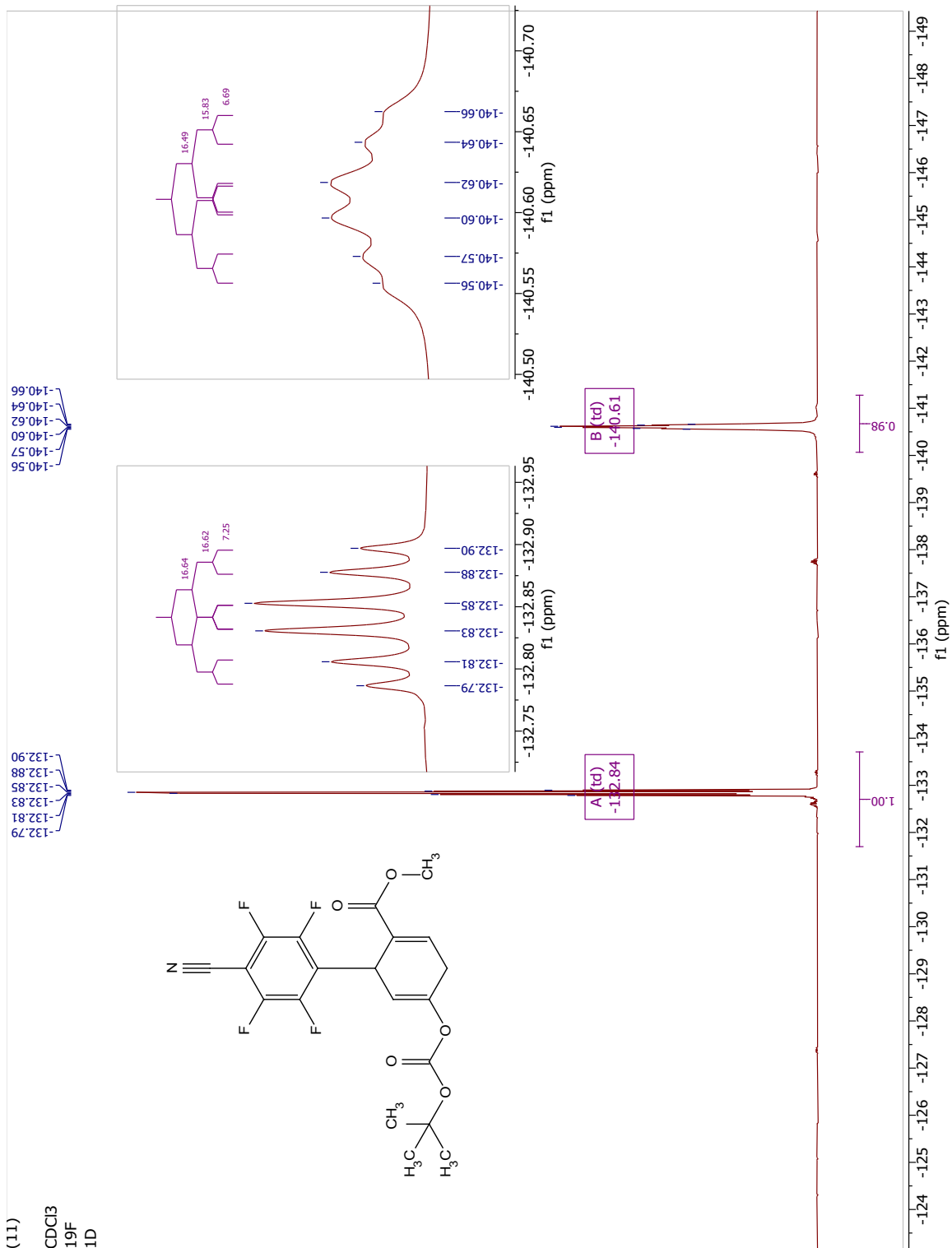


(10)

CD3CN  
13C  
1D

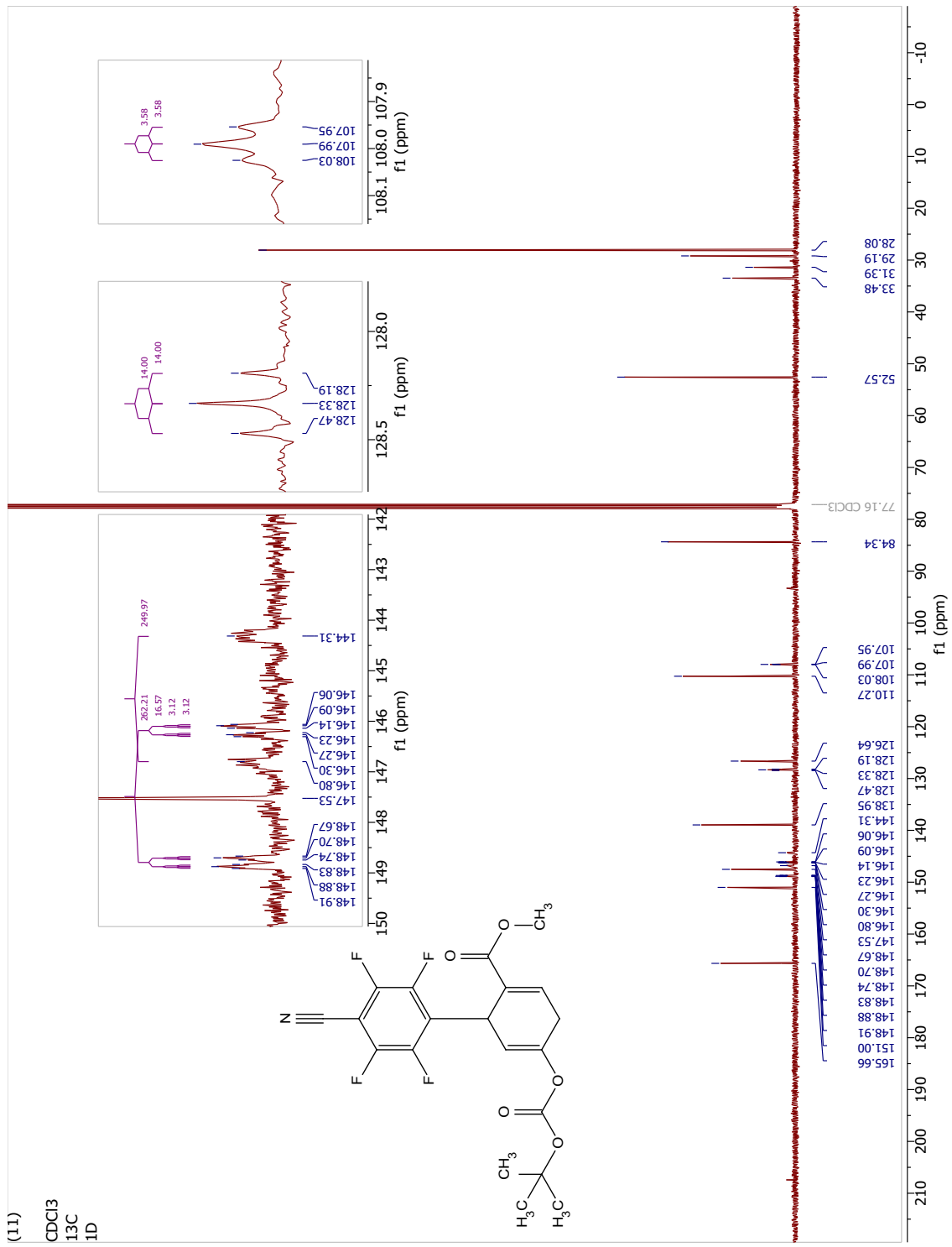


(6.3.11) methyl 5-((tert-butoxycarbonyl)oxy)-4'-cyano-2',3',5',6'-tetrafluoro-1,4-dihydro-[1,1'-biphenyl]-2-carboxylate.

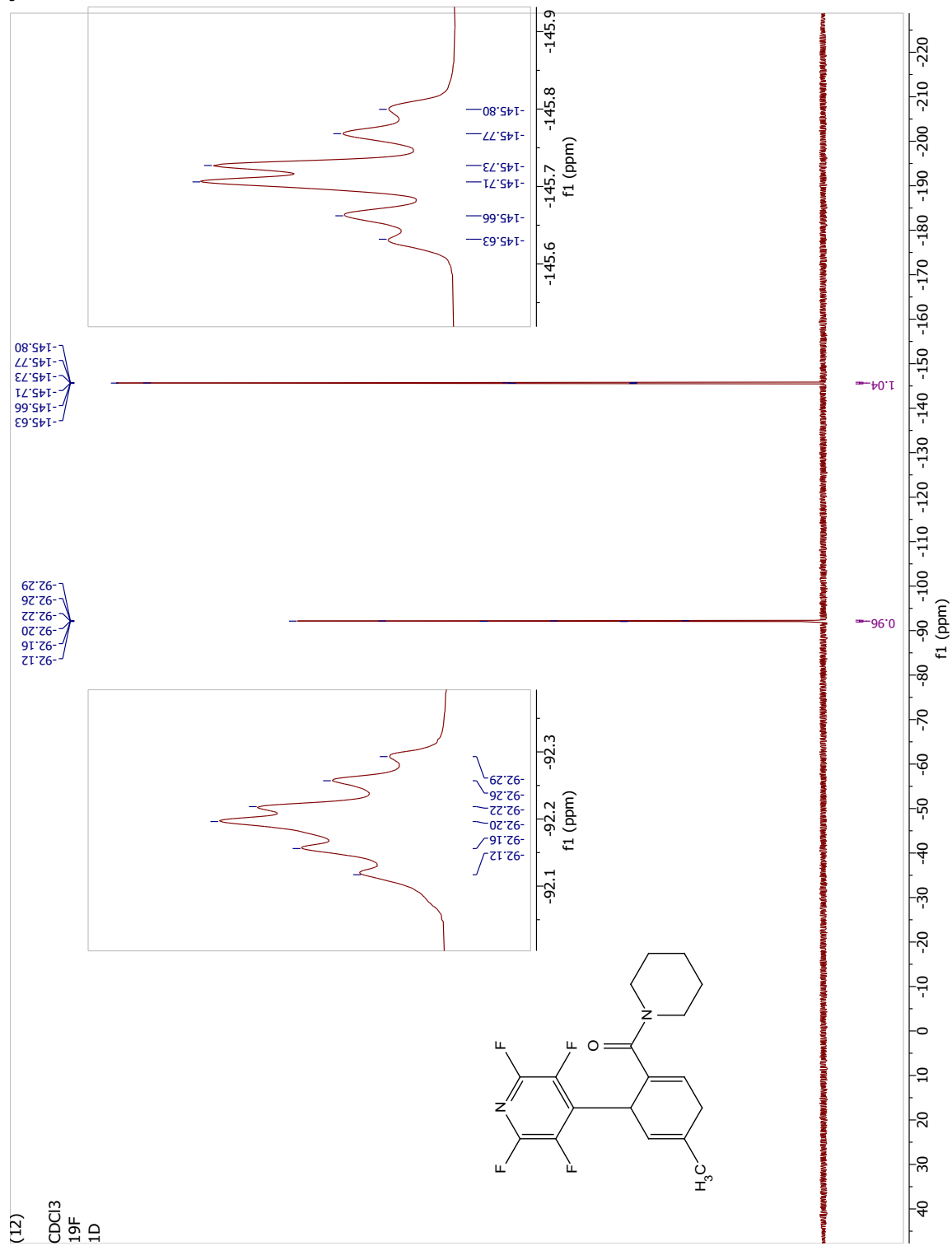




(11)  
CDCI3  
13C  
ID



(6.3.12) (4-methyl-6-(perfluoropyridin-4-yl)cyclohexa-1,4-dien-1-yl)(piperidin-1-yl)methanone

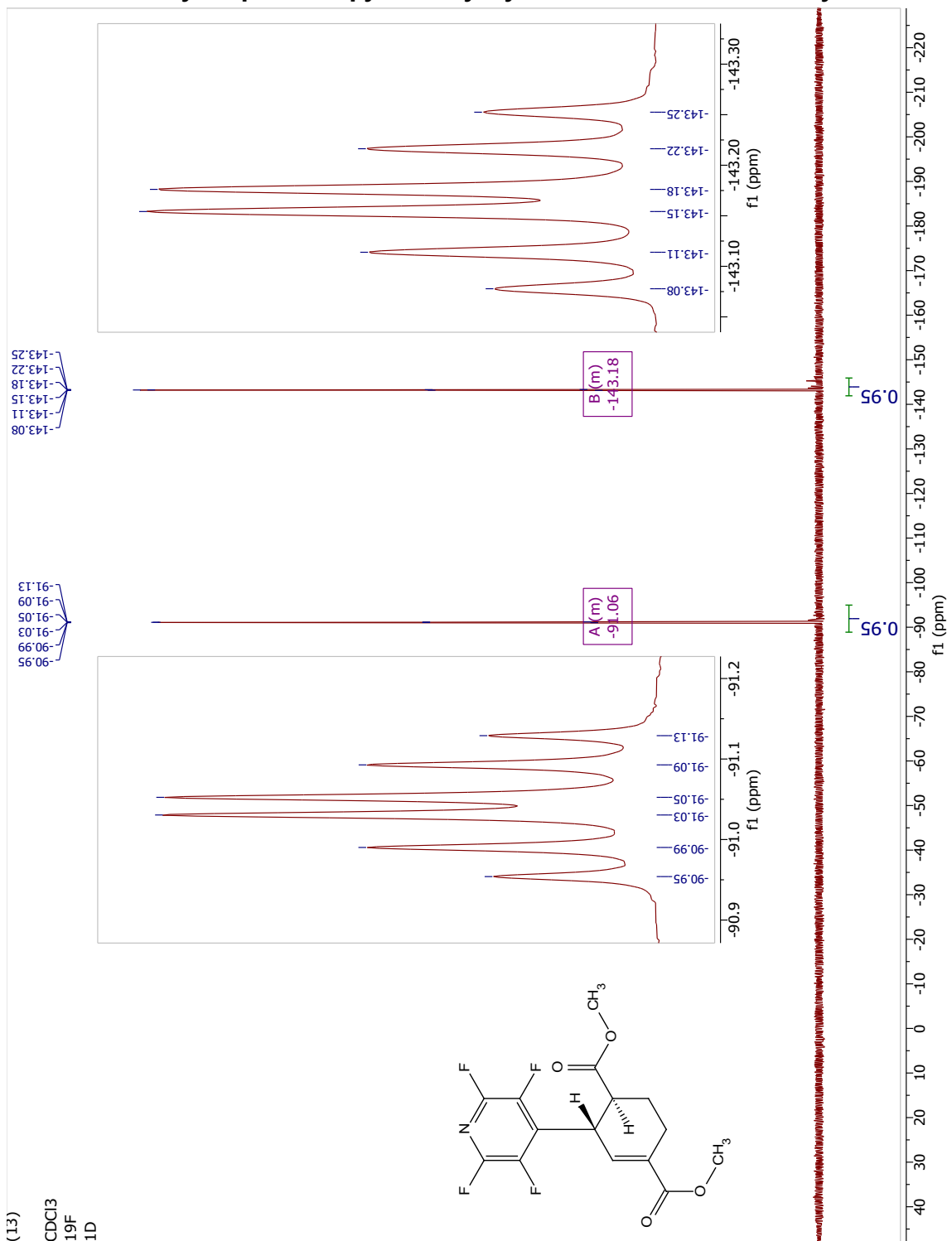






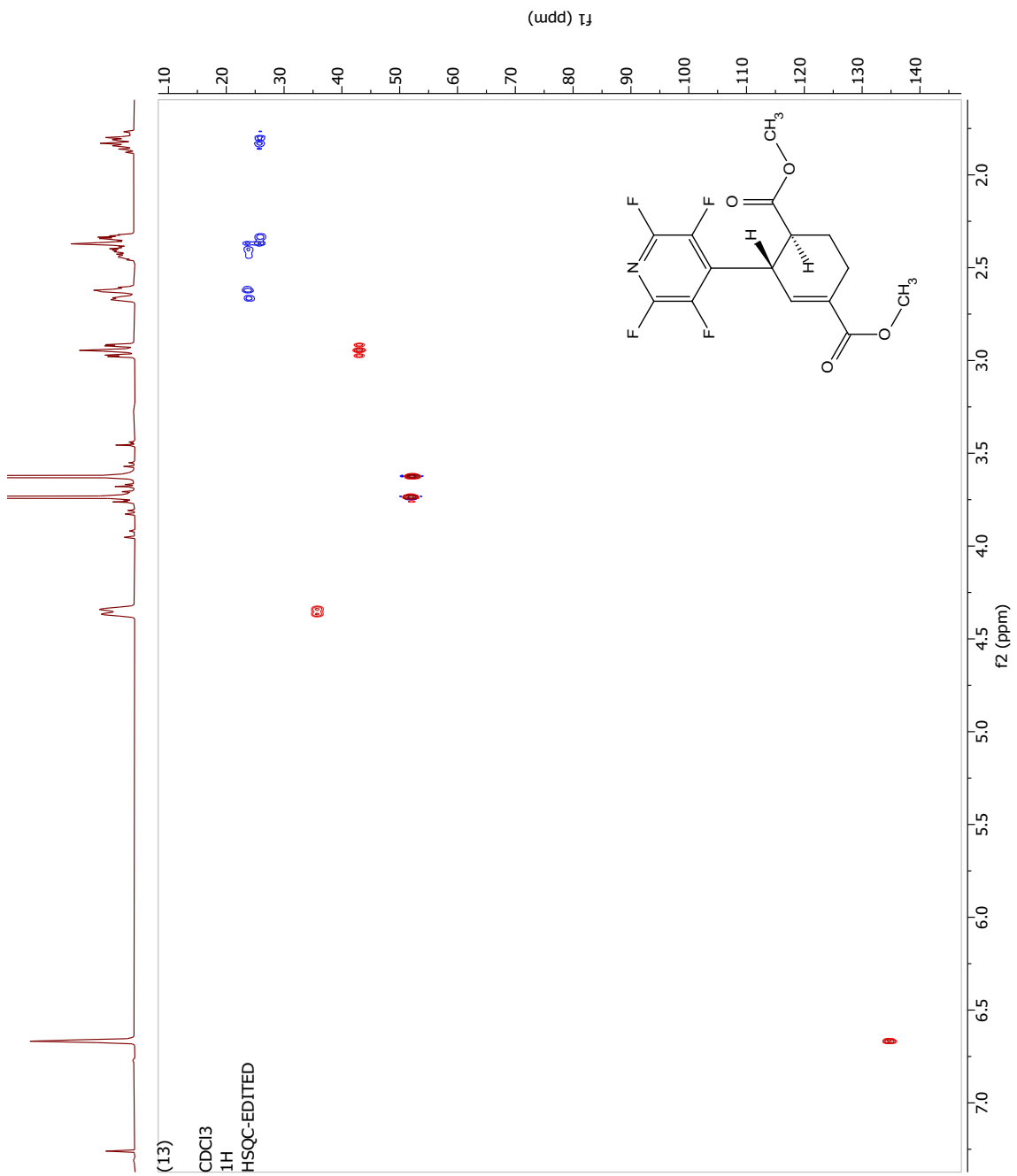


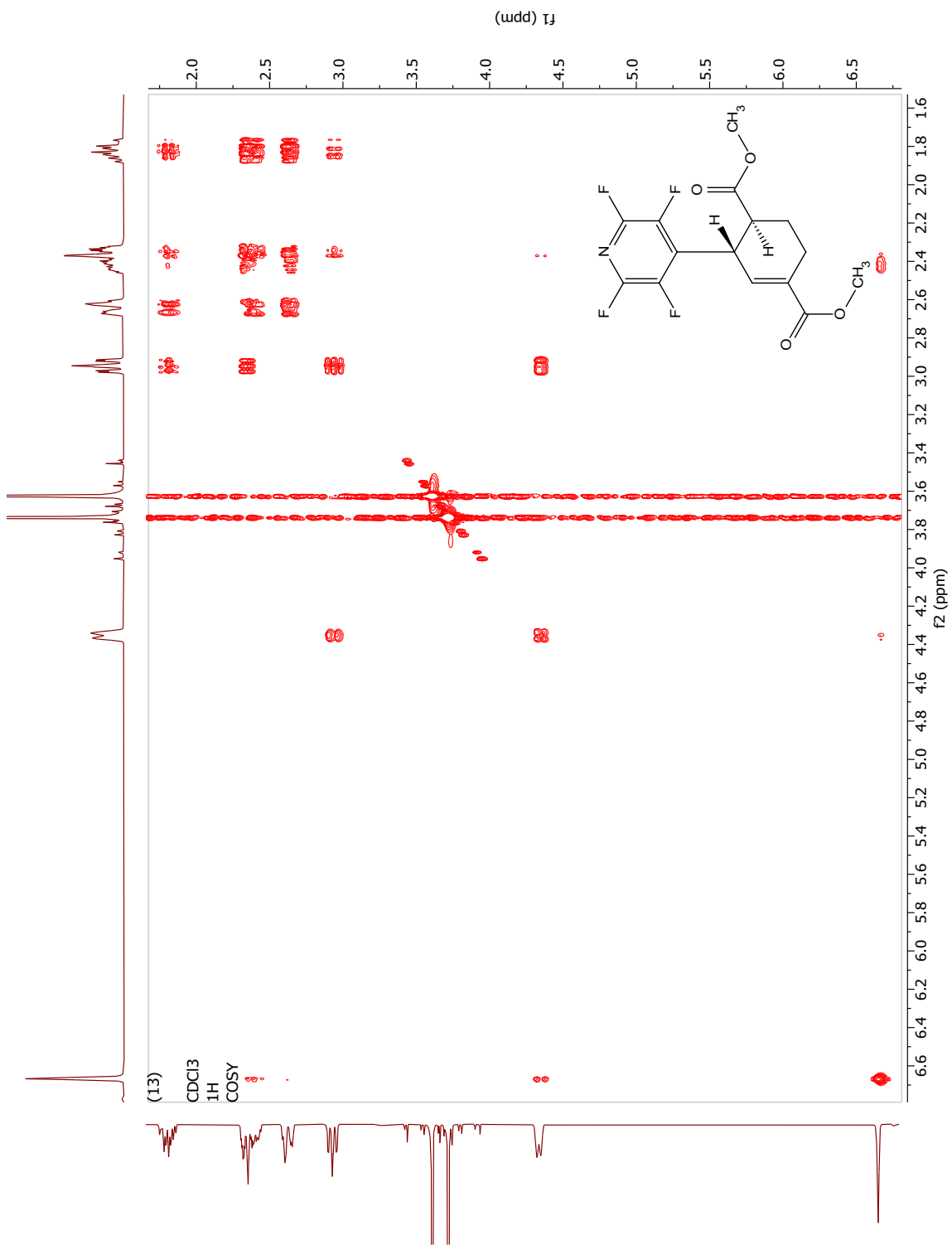
(6.3.13) dimethyl 3-(perfluoropyridin-4-yl)cyclohex-1-ene-1,4-dicarboxylate



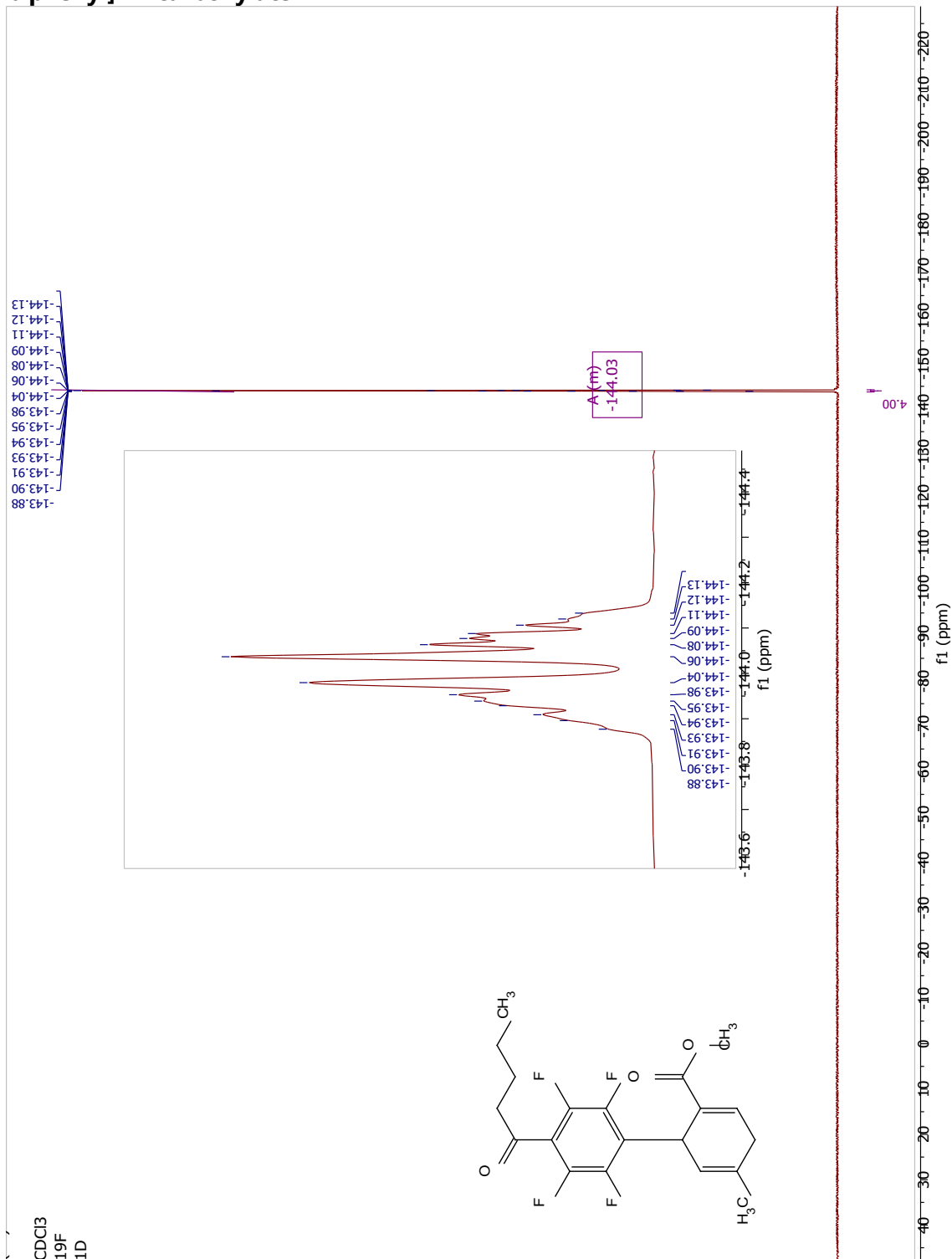






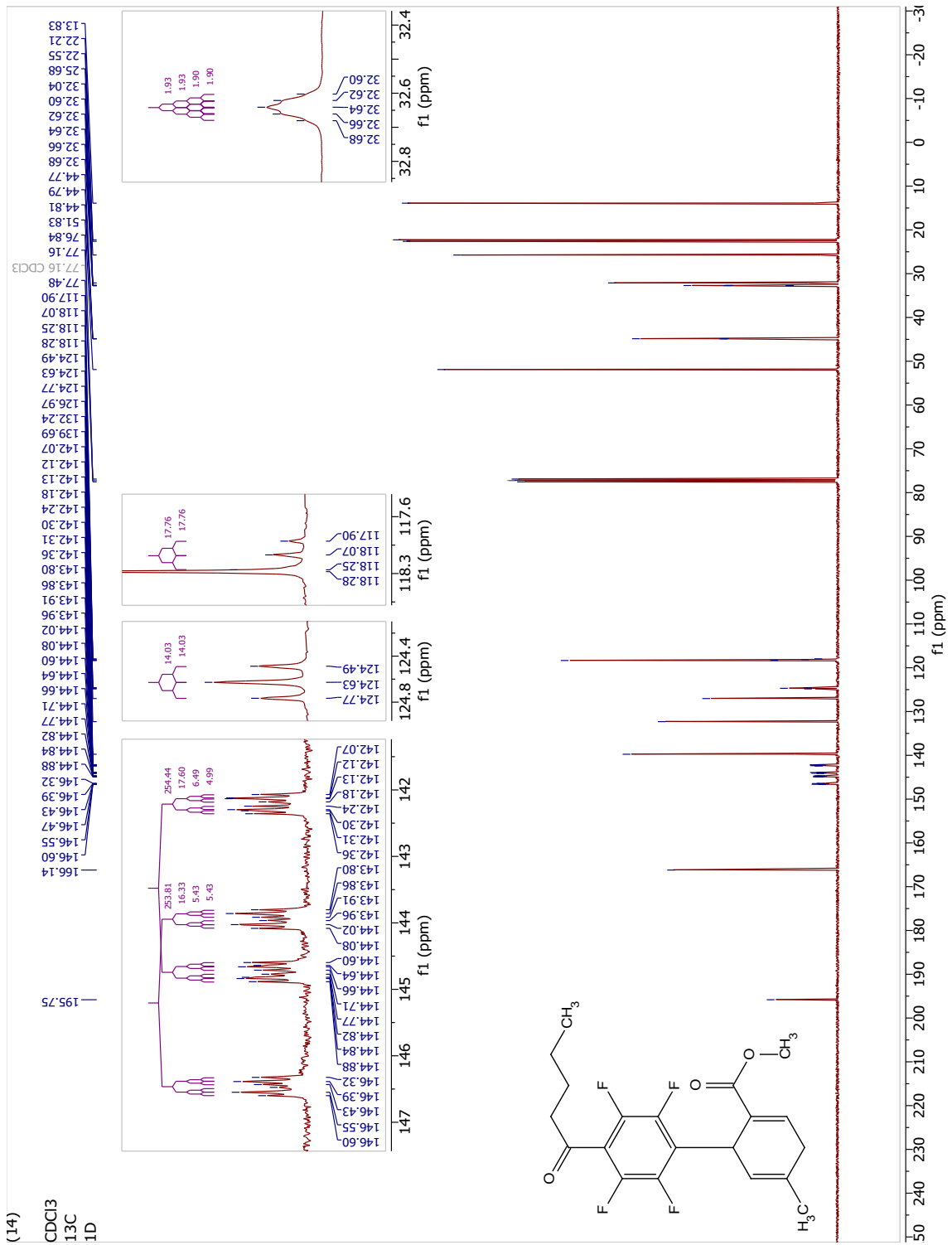


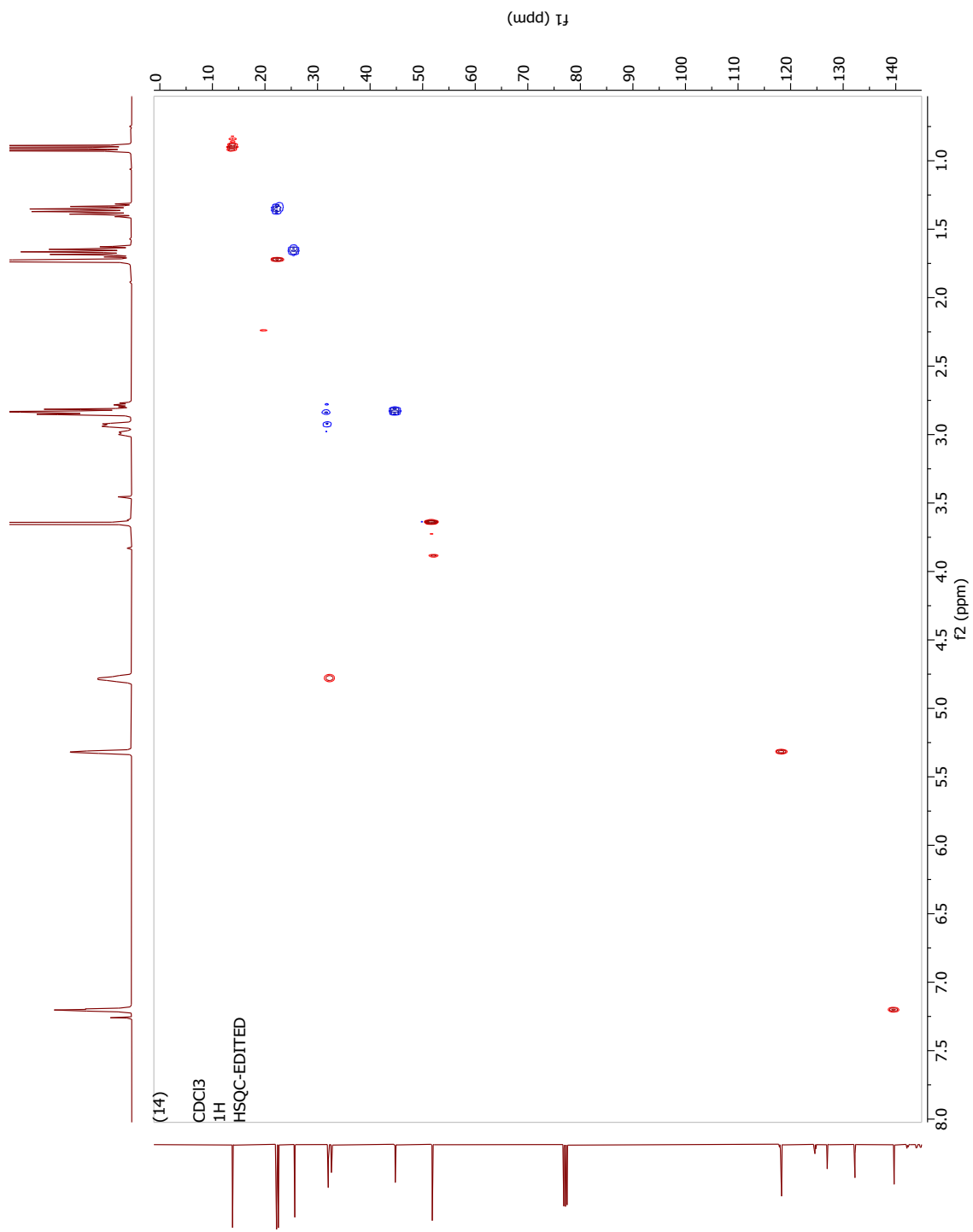
(6.3.14) Methyl 2',3',5',6'-tetrafluoro-5-methyl-4'-pentanoyl-1,4-dihydro-[1,1'-biphenyl]-2- carboxylate



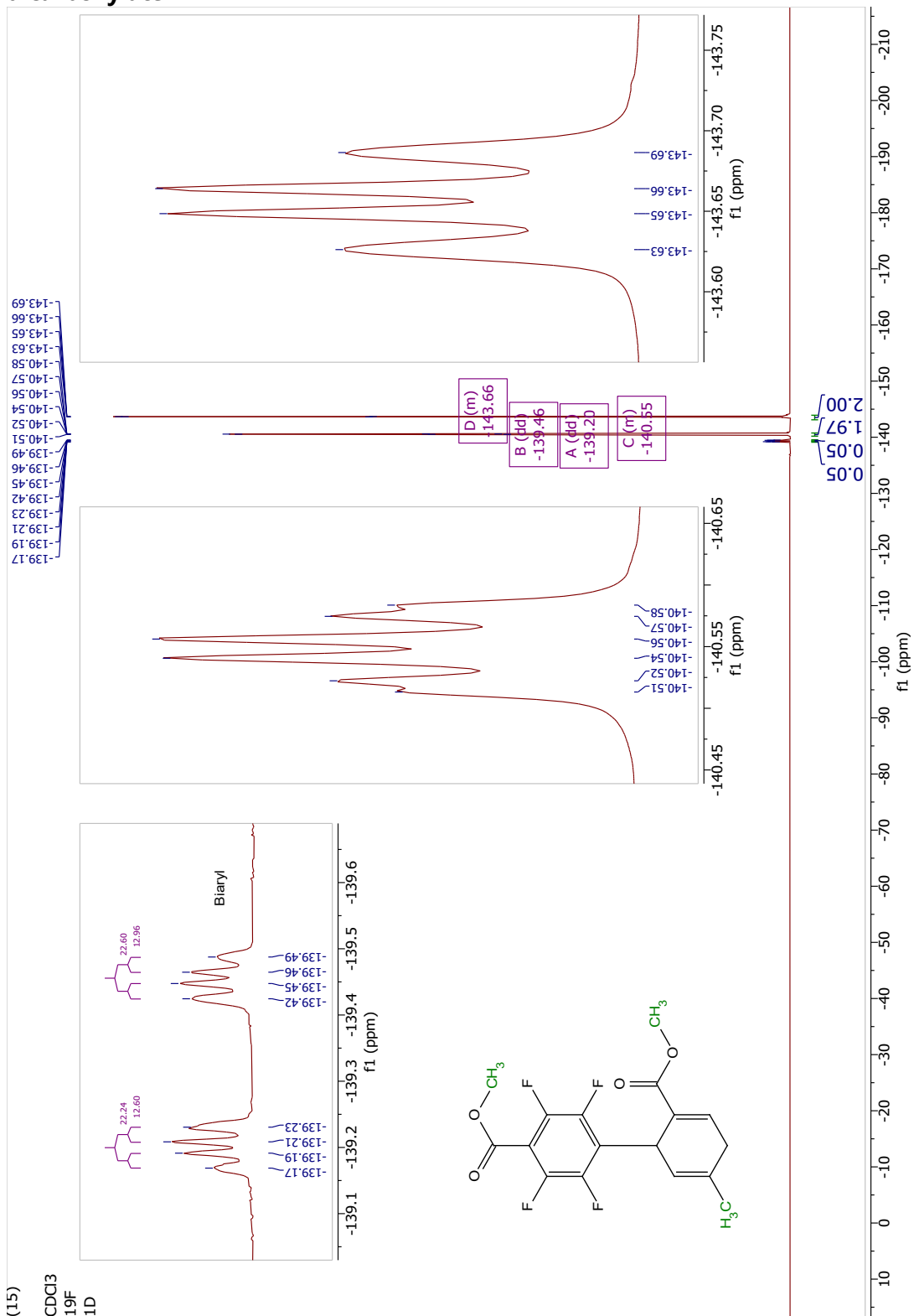








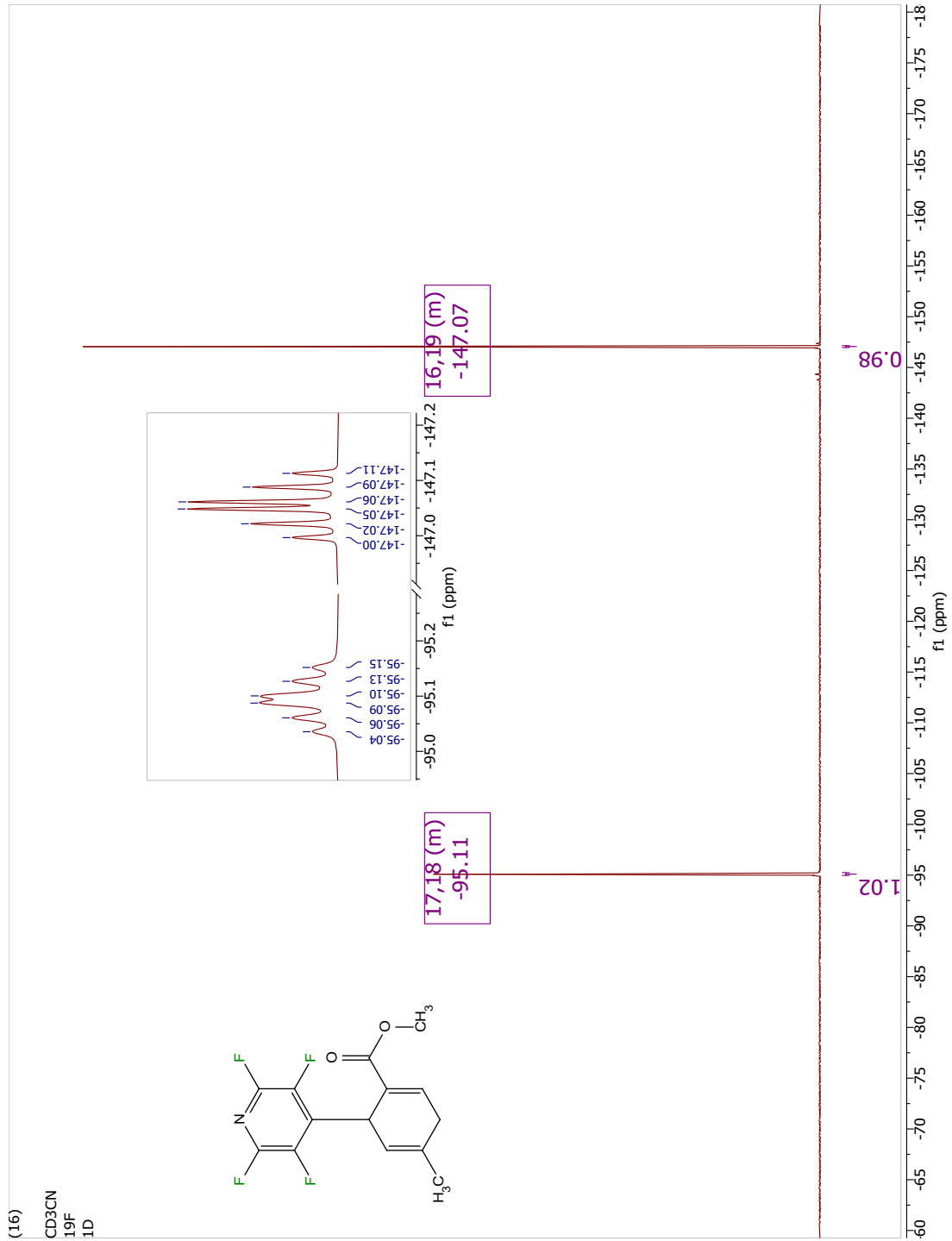
(6.3.15) dimethyl 2',3',5',6'-tetrafluoro-5-methyl-1,4-dihydro-[1,1'-biphenyl]-2,4'-dicarboxylate







(6.3.16) methyl 4-methyl-6-(perfluoropyridin-4-yl)cyclohexa-1,4-diene-1-carboxylate

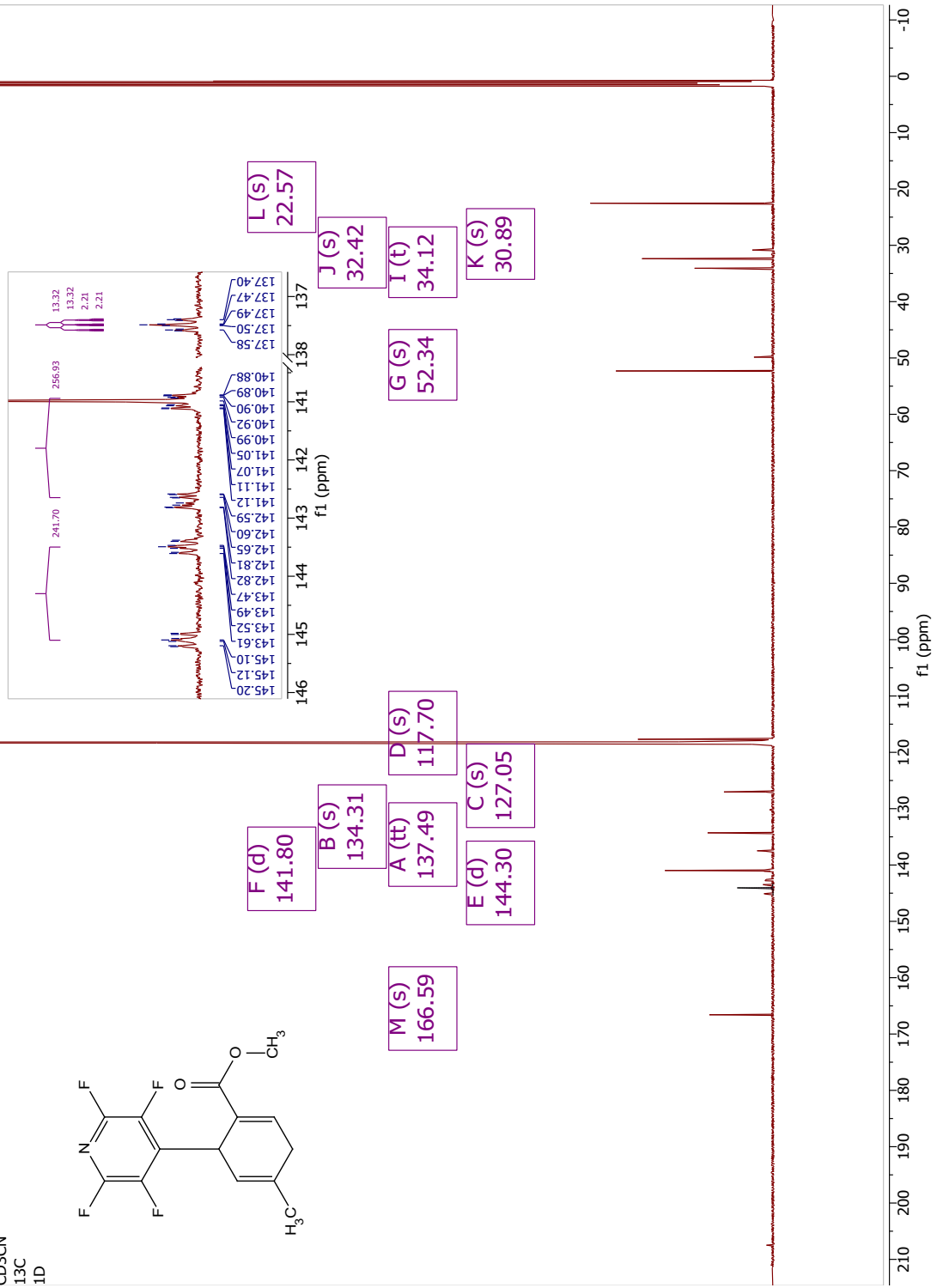
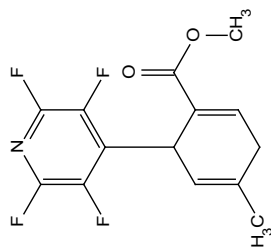


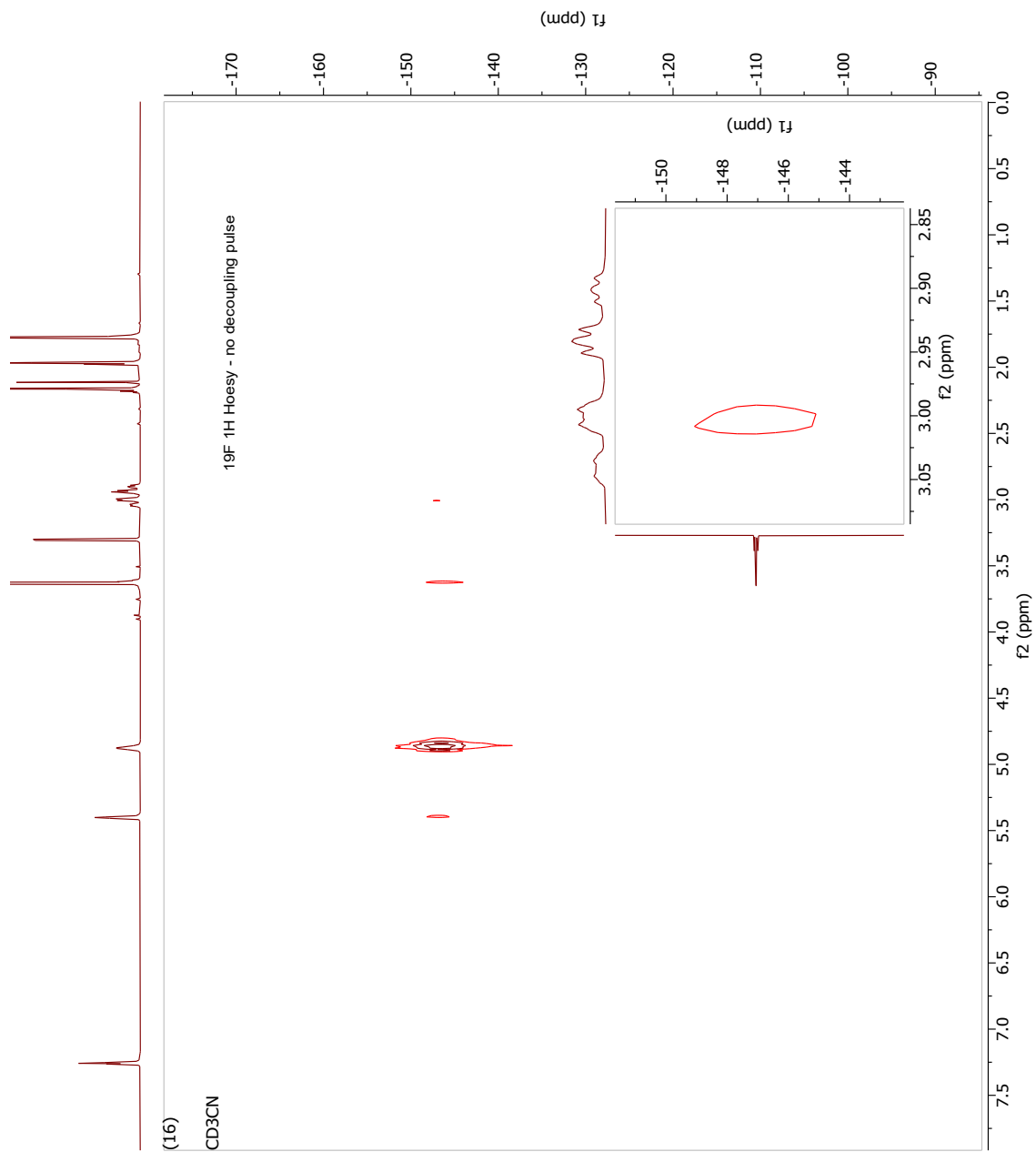




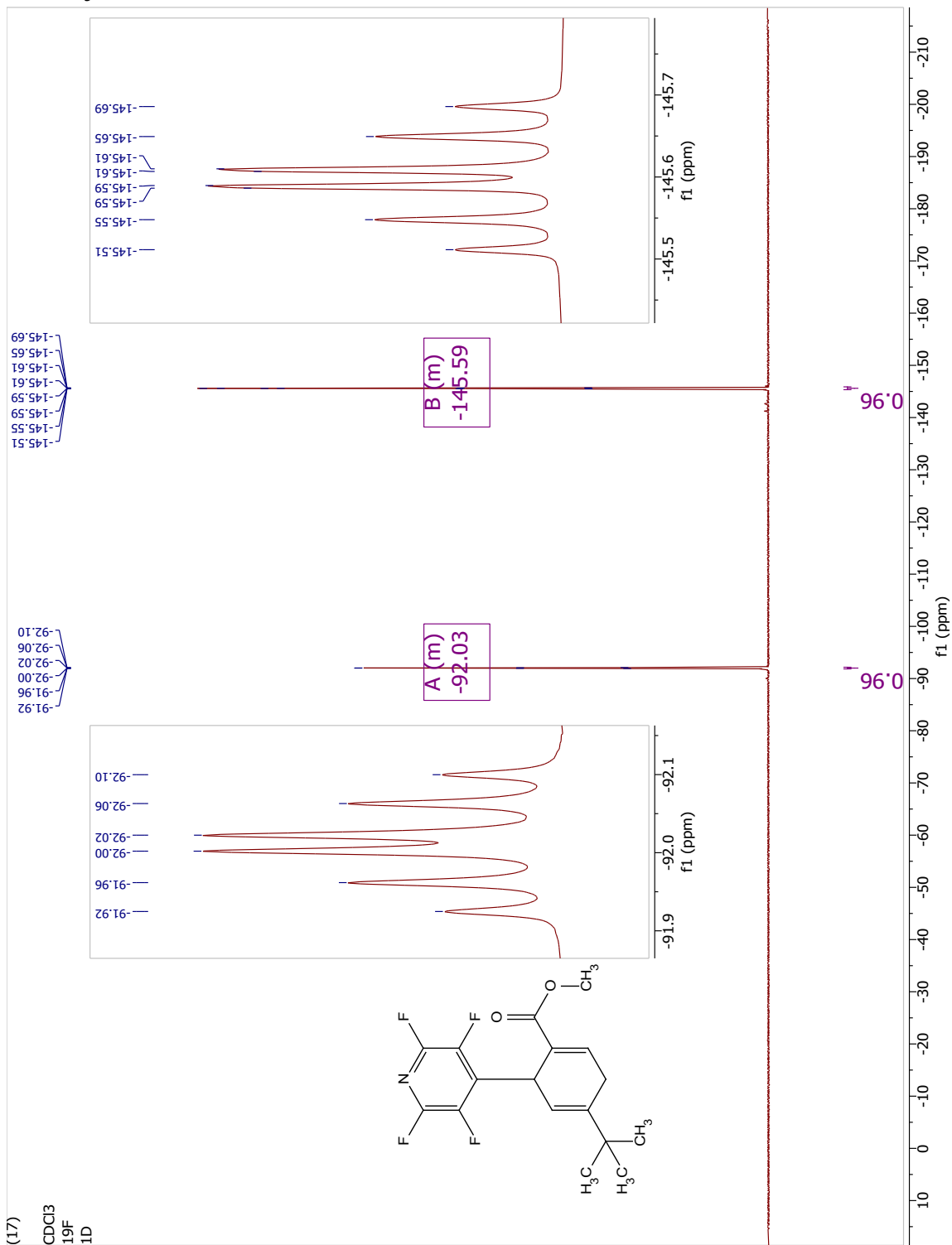
(16)

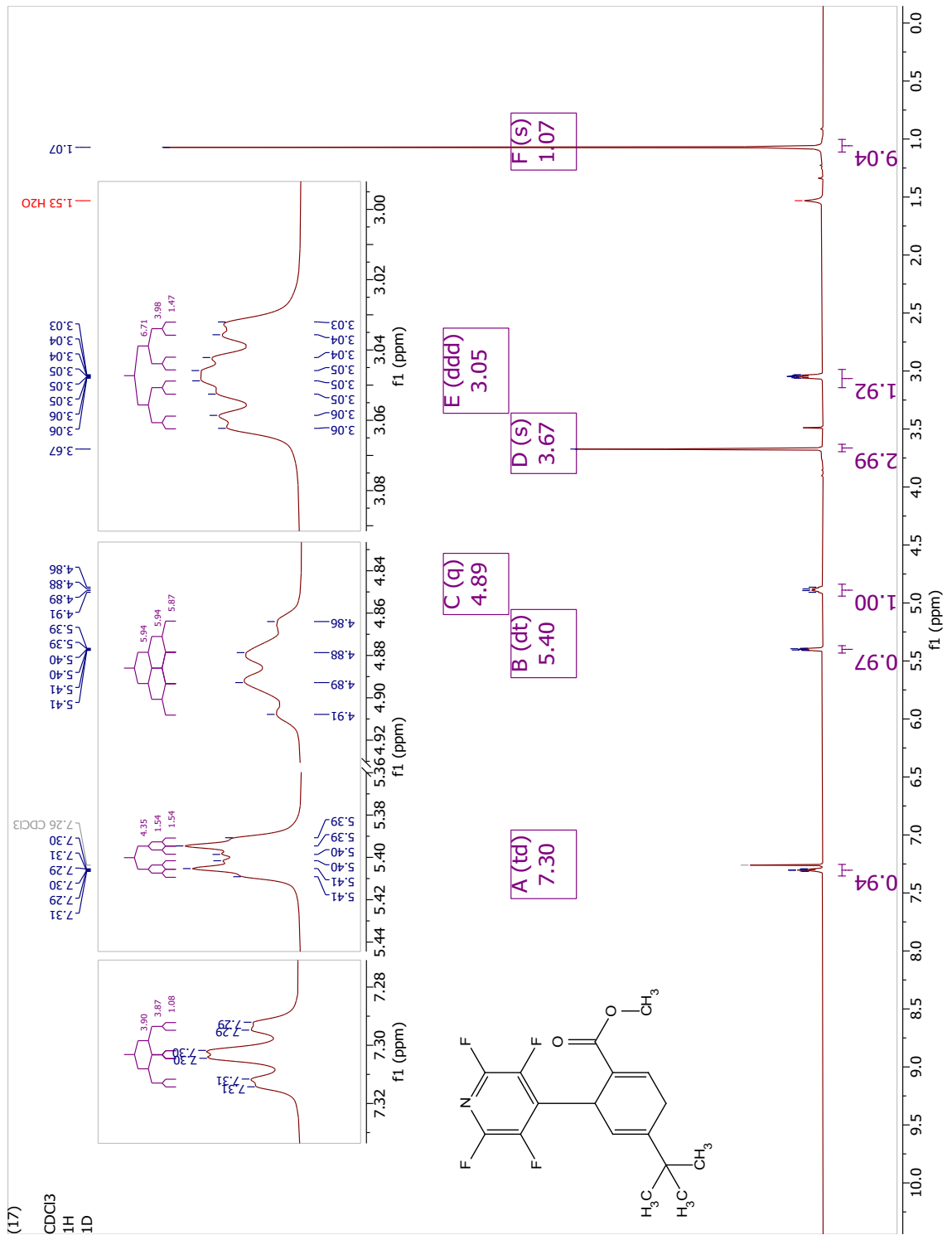
CD3CN  
13C  
1D

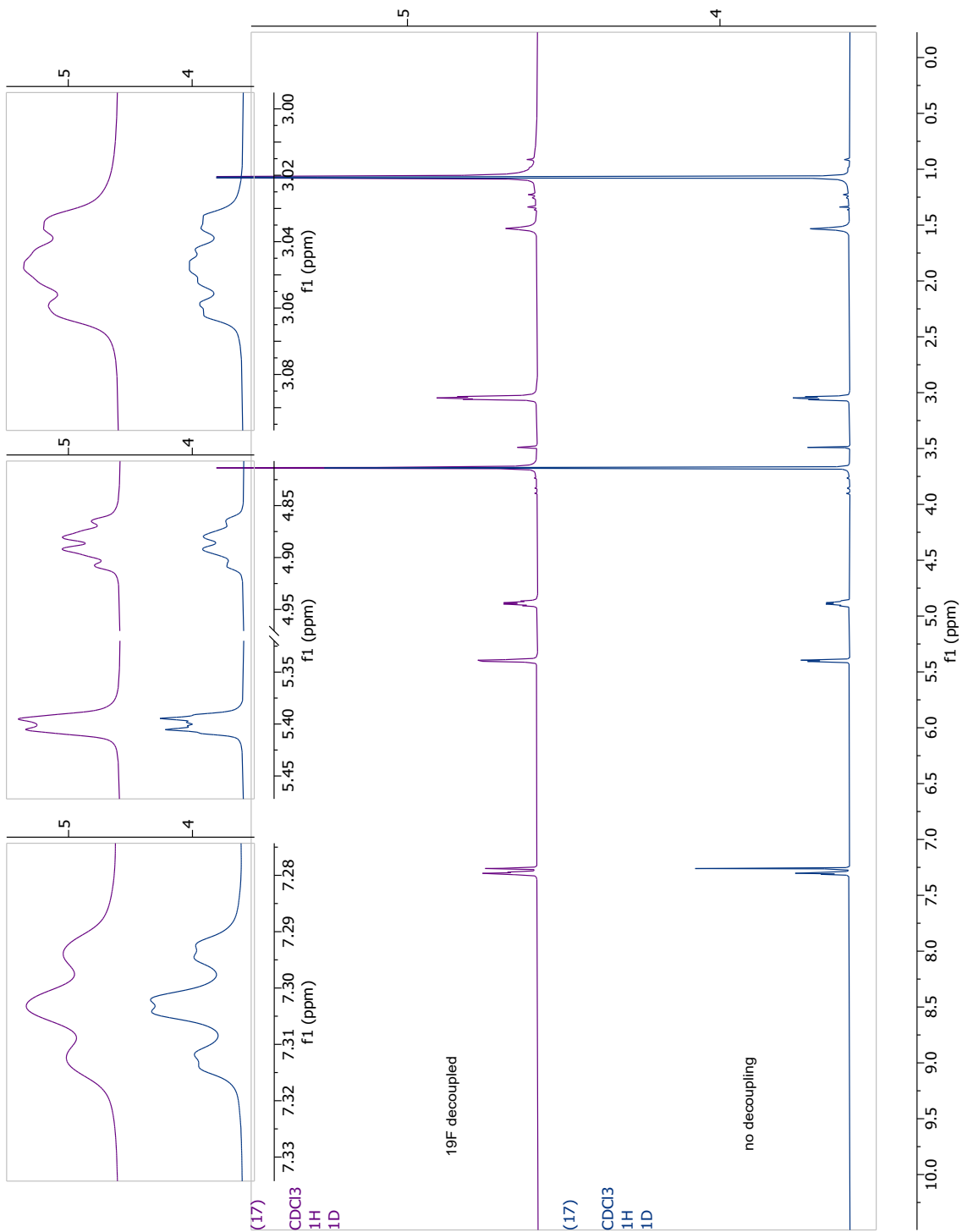




(6.3.17) methyl 4-(tert-butyl)-6-(perfluoropyridin-4-yl)cyclohexa-1,4-diene-1-carboxylate

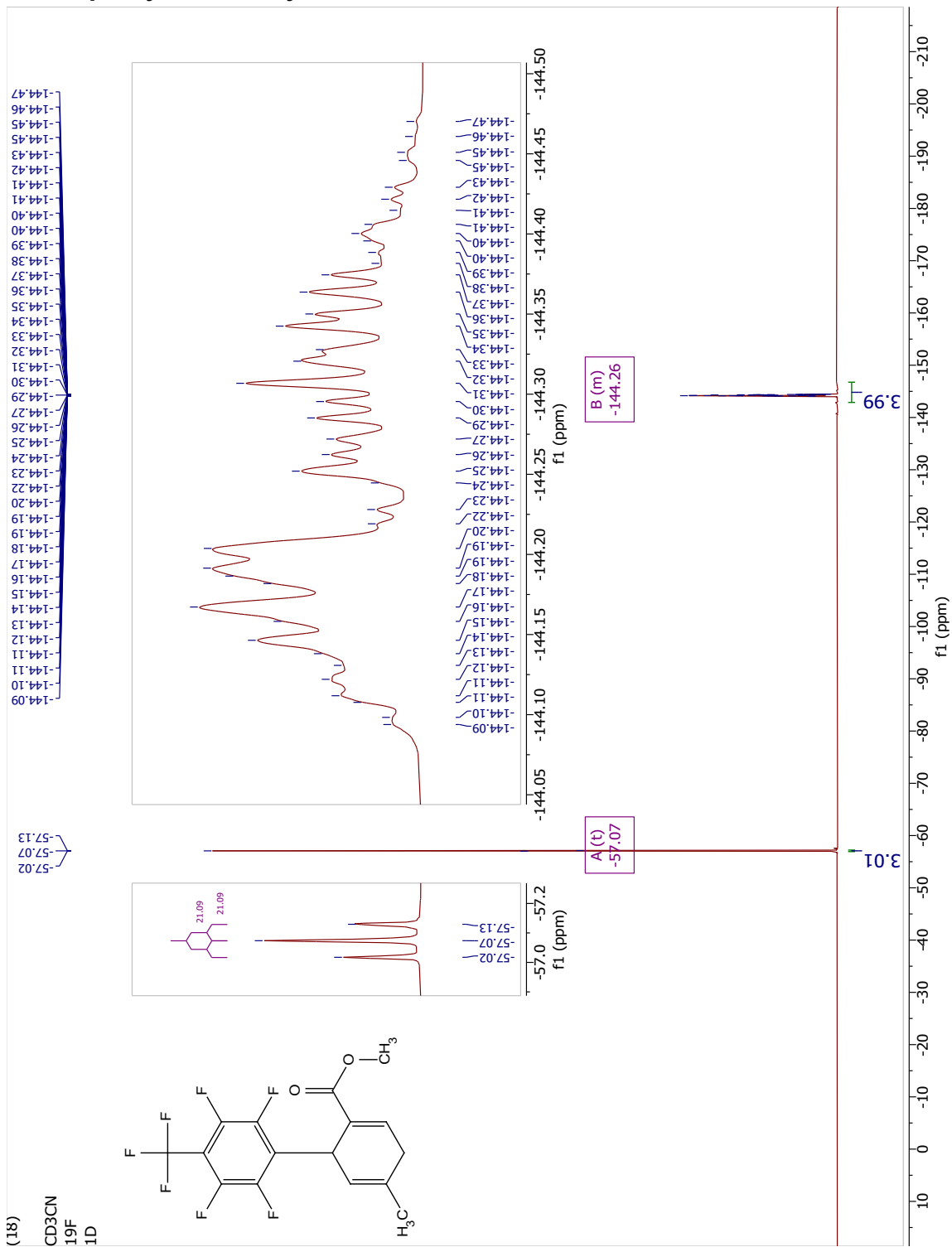








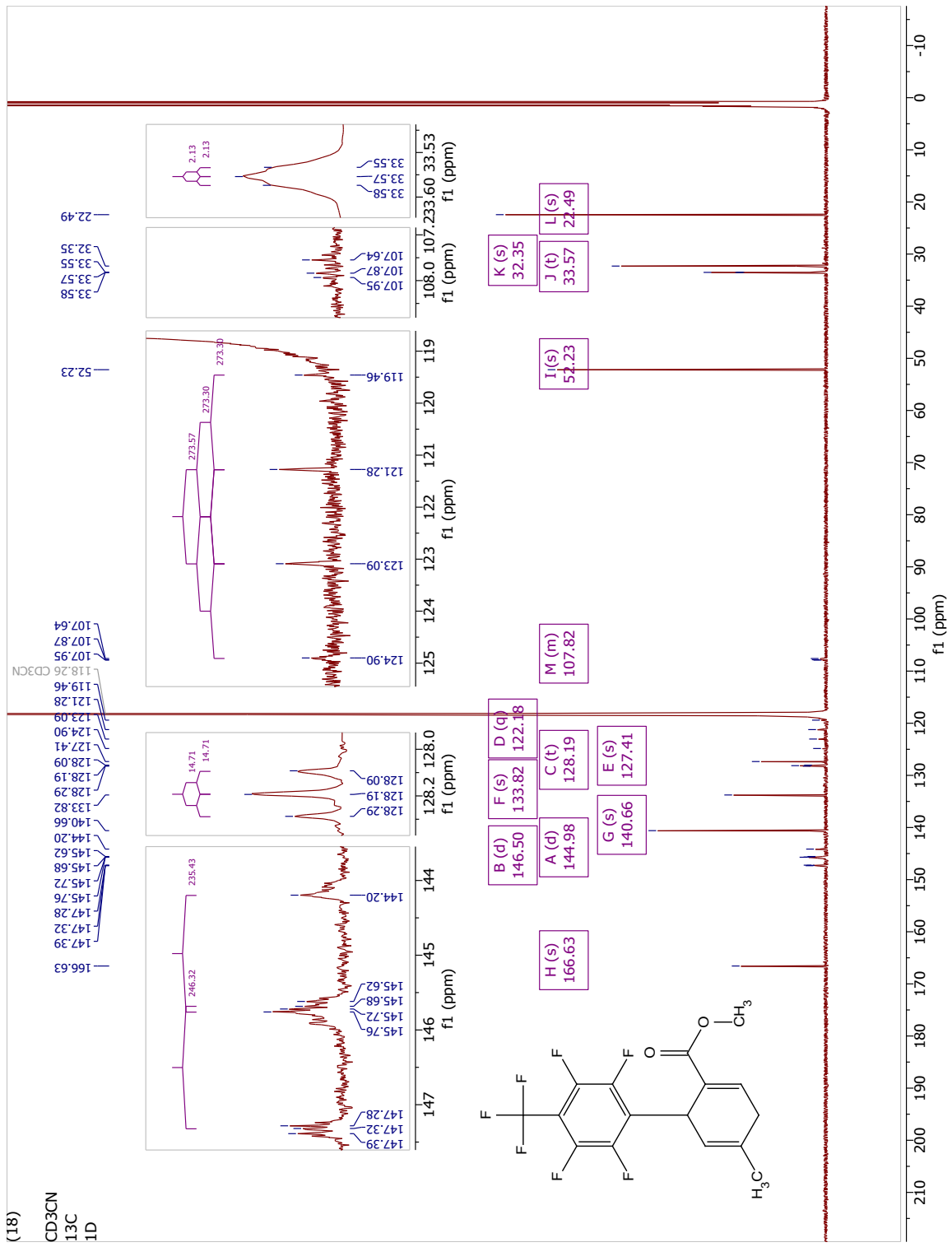
(6.3.18) methyl 2',3',5',6'-tetrafluoro-5-methyl-4'-(trifluoromethyl)-1,4-dihydro-[1,1'-biphenyl]-2-carboxylate



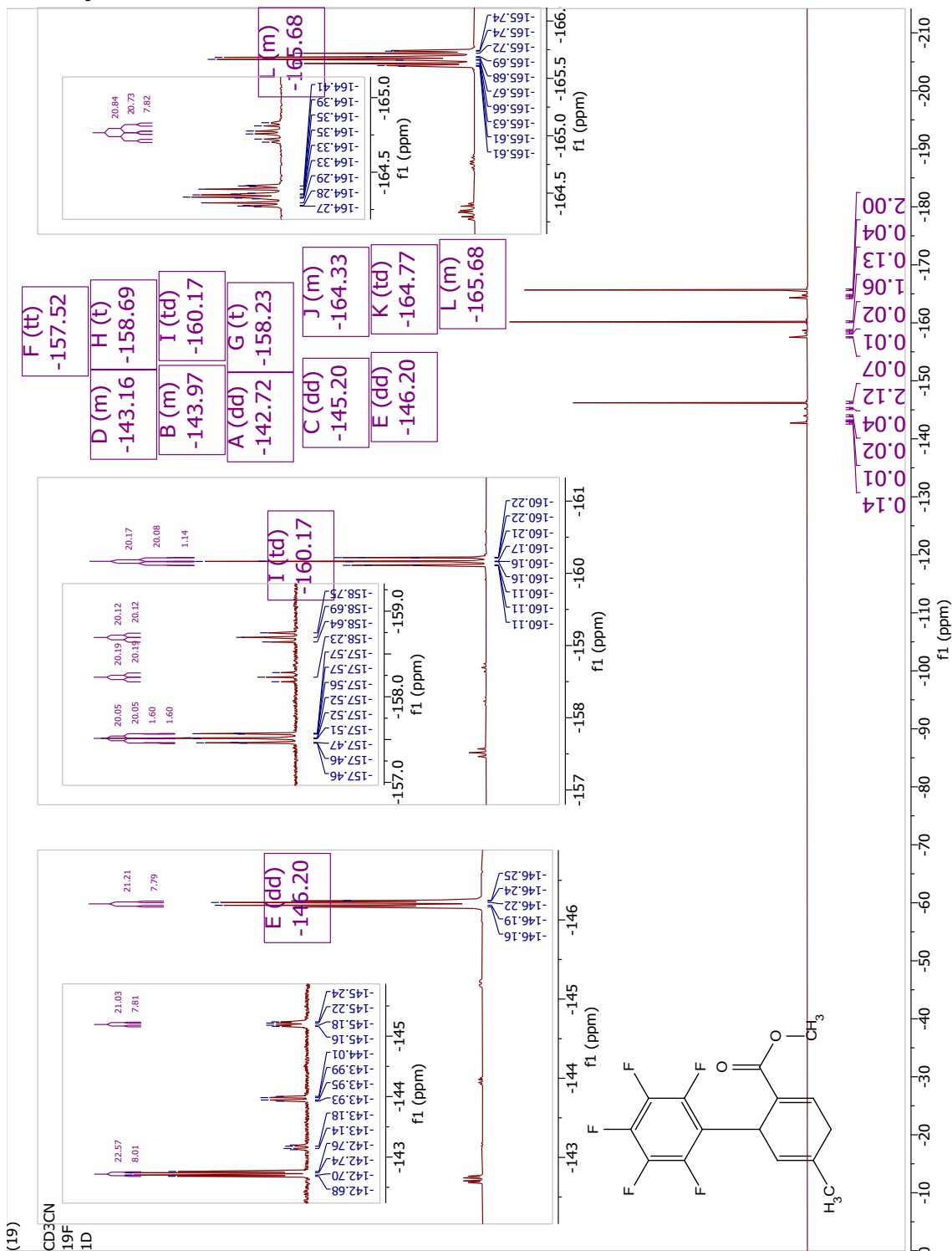


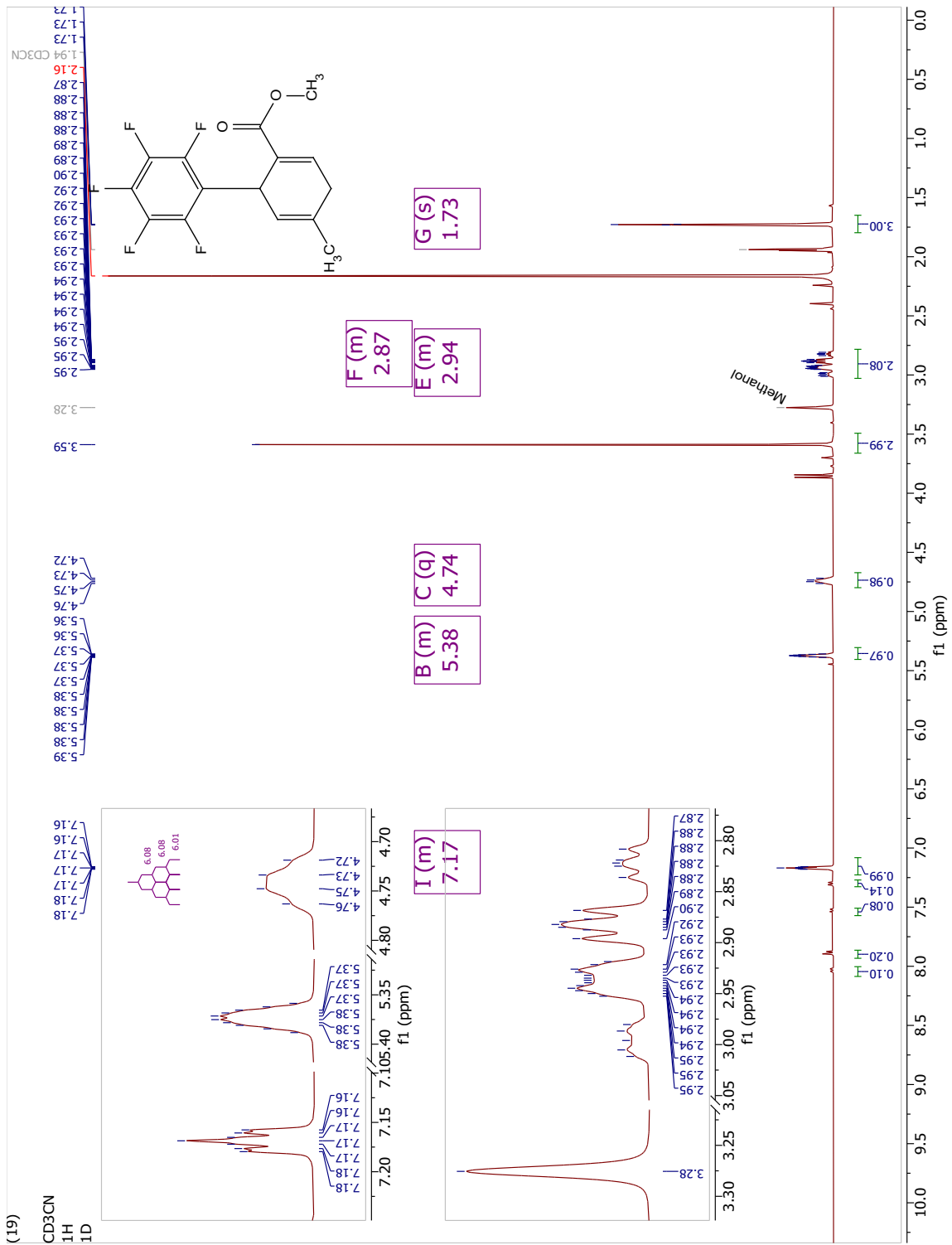


(18)  
CD3CN  
13C  
1D

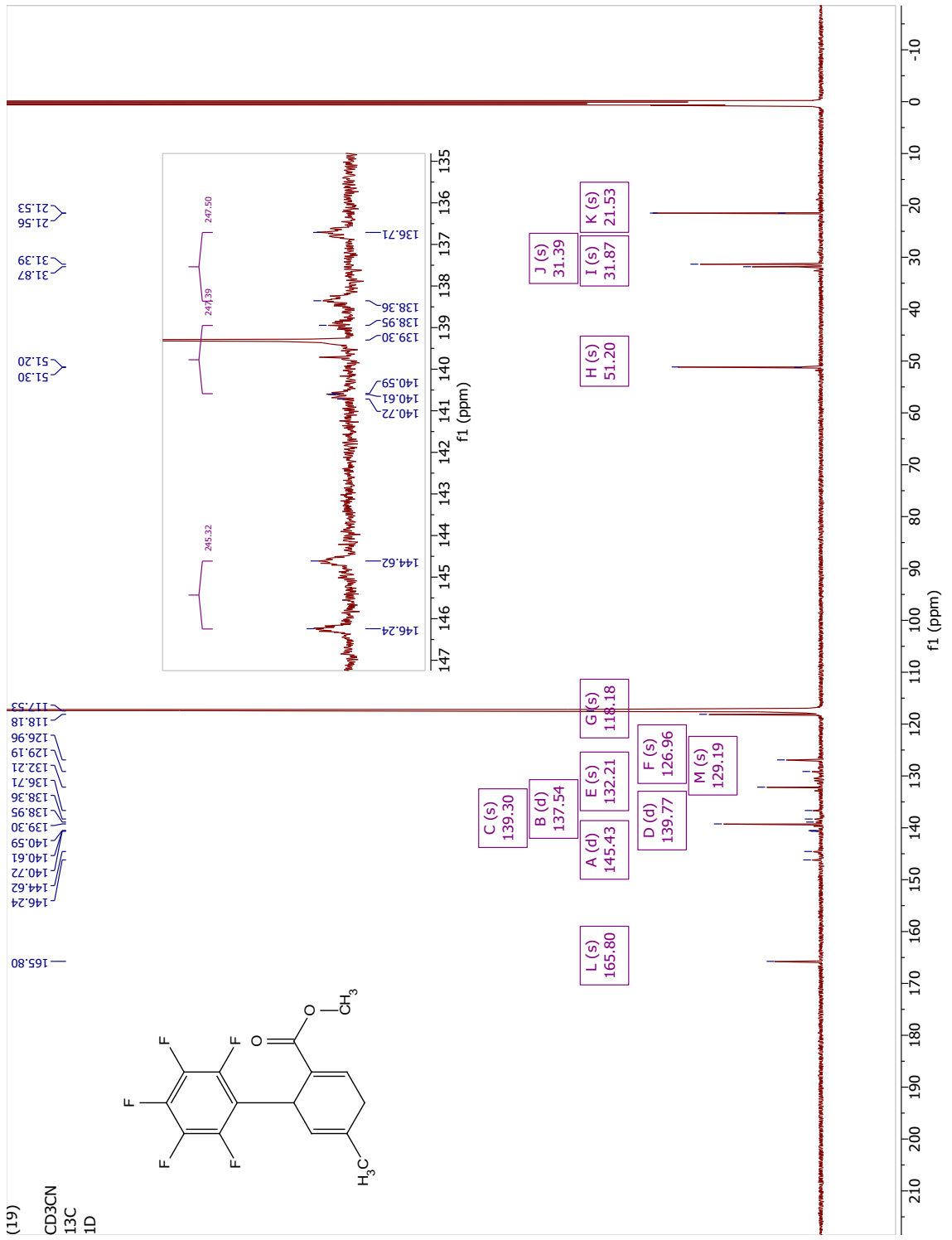
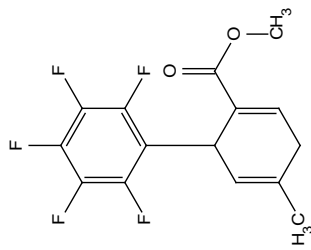


(6.3.19) methyl 2',3',4',5',6'-pentafluoro-5-methyl-1,4-dihydro-[1,1'-biphenyl]-2-carboxylate

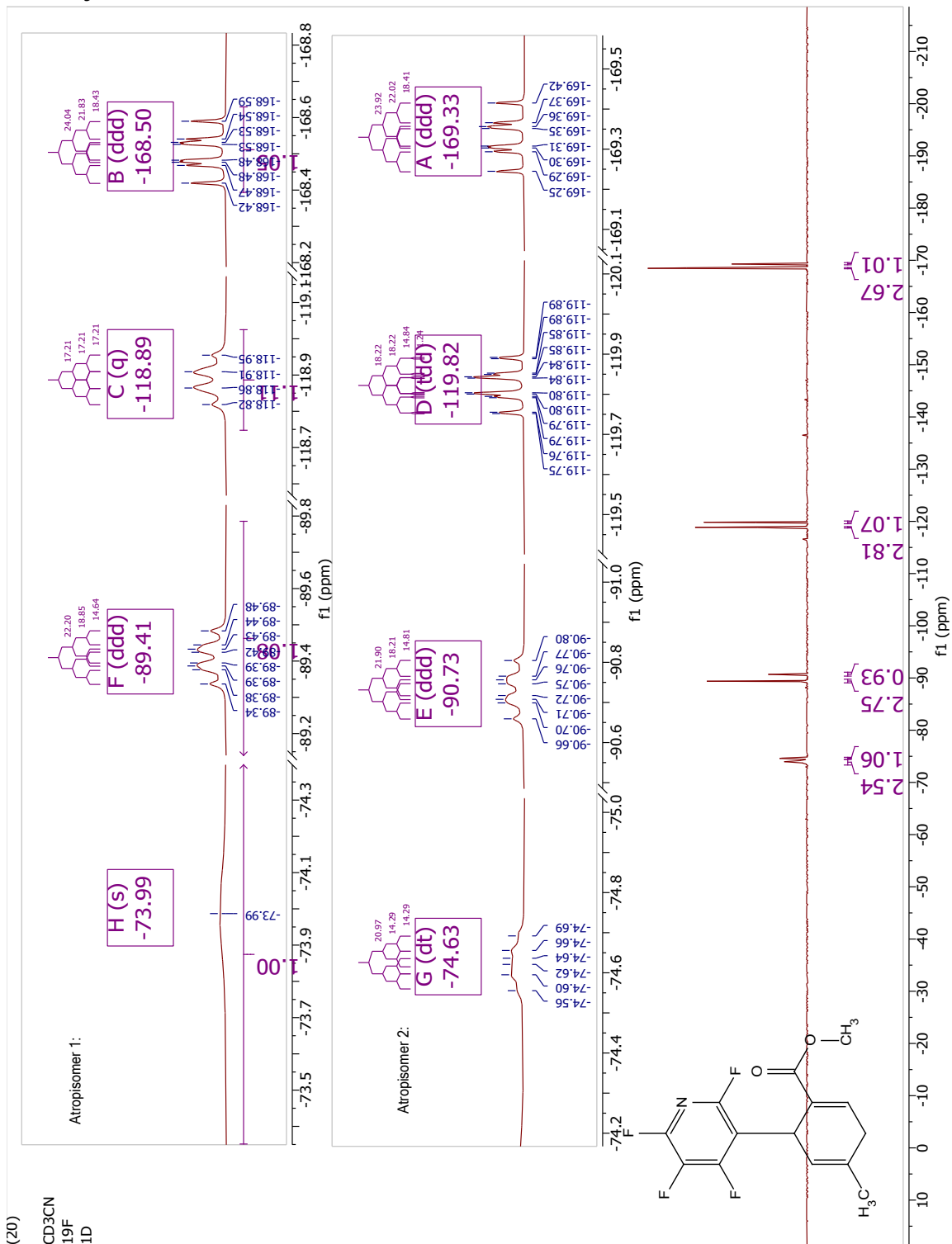


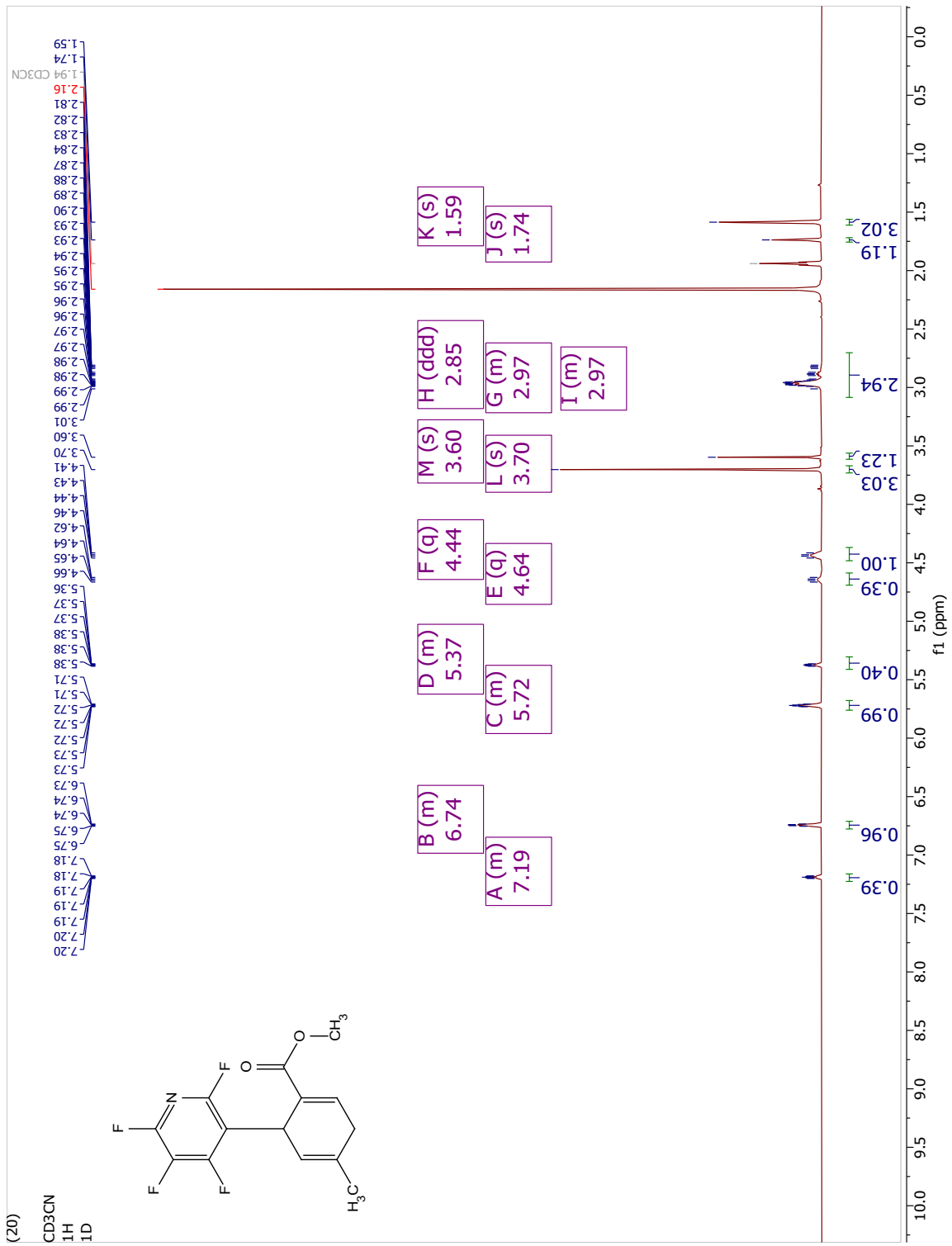


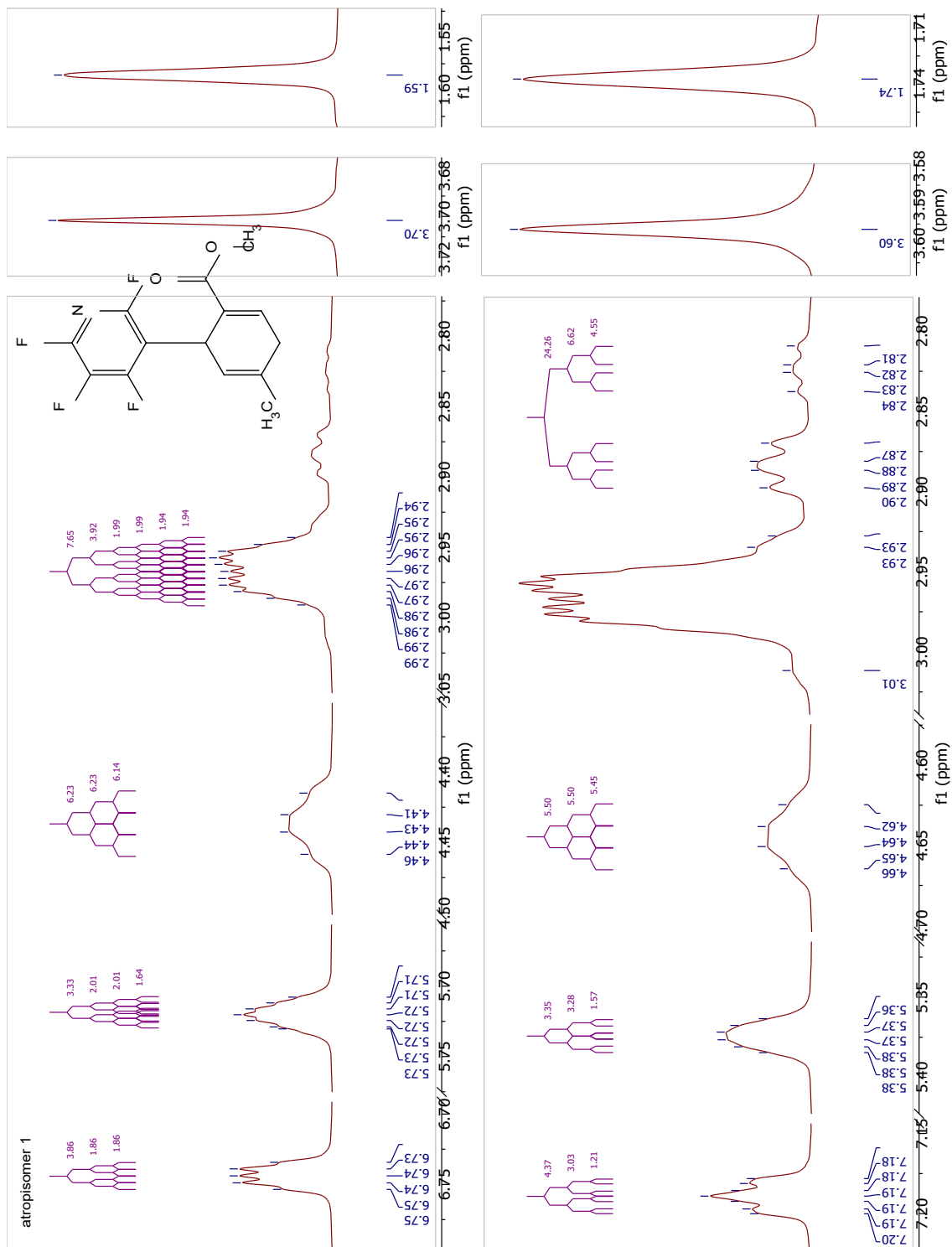
(19)  
CD3CN  
13C  
ID

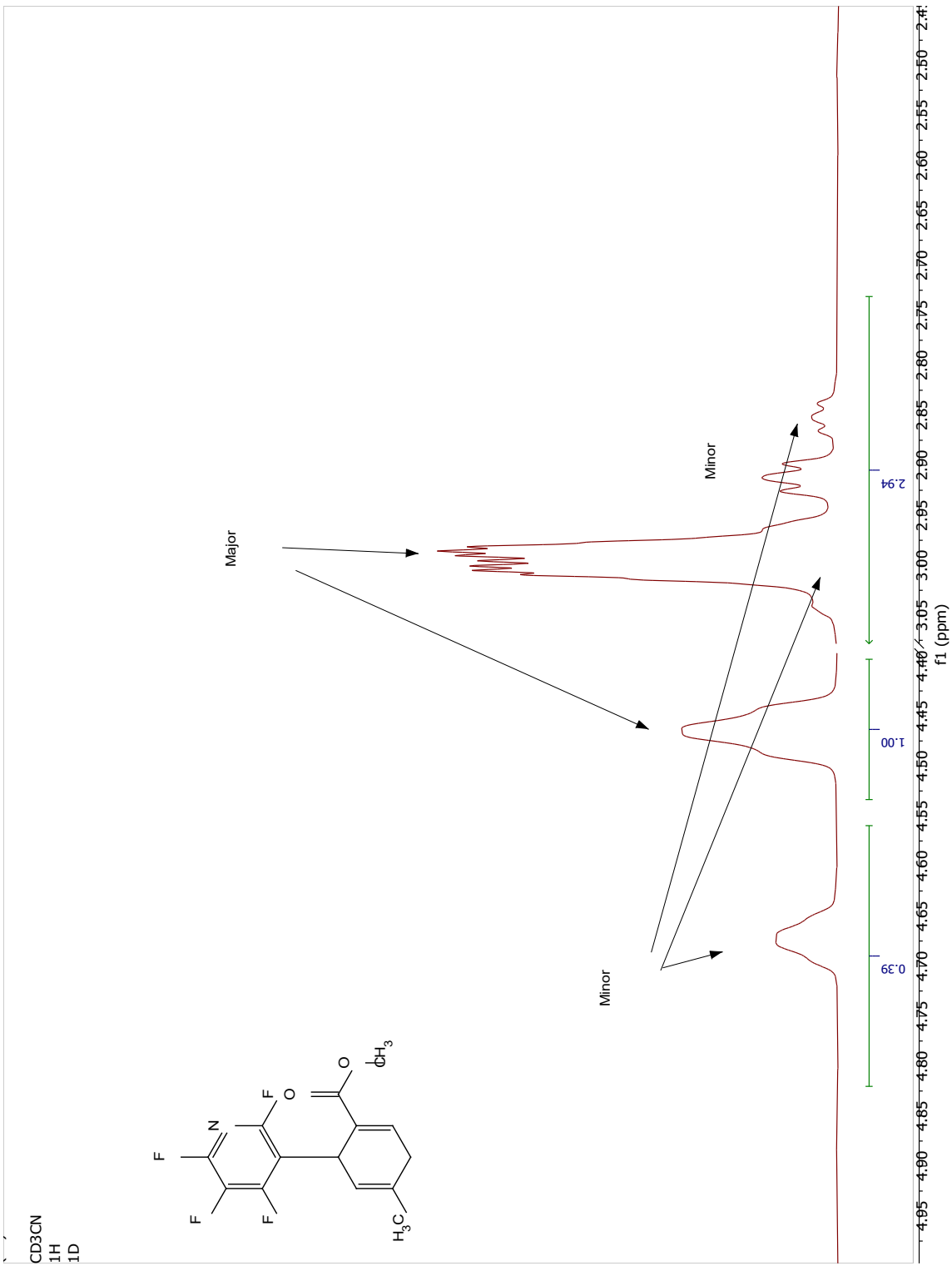


(6.3.20) methyl 4-methyl-6-(perfluoropyridin-3-yl)cyclohexa-1,4-diene-1-carboxylate

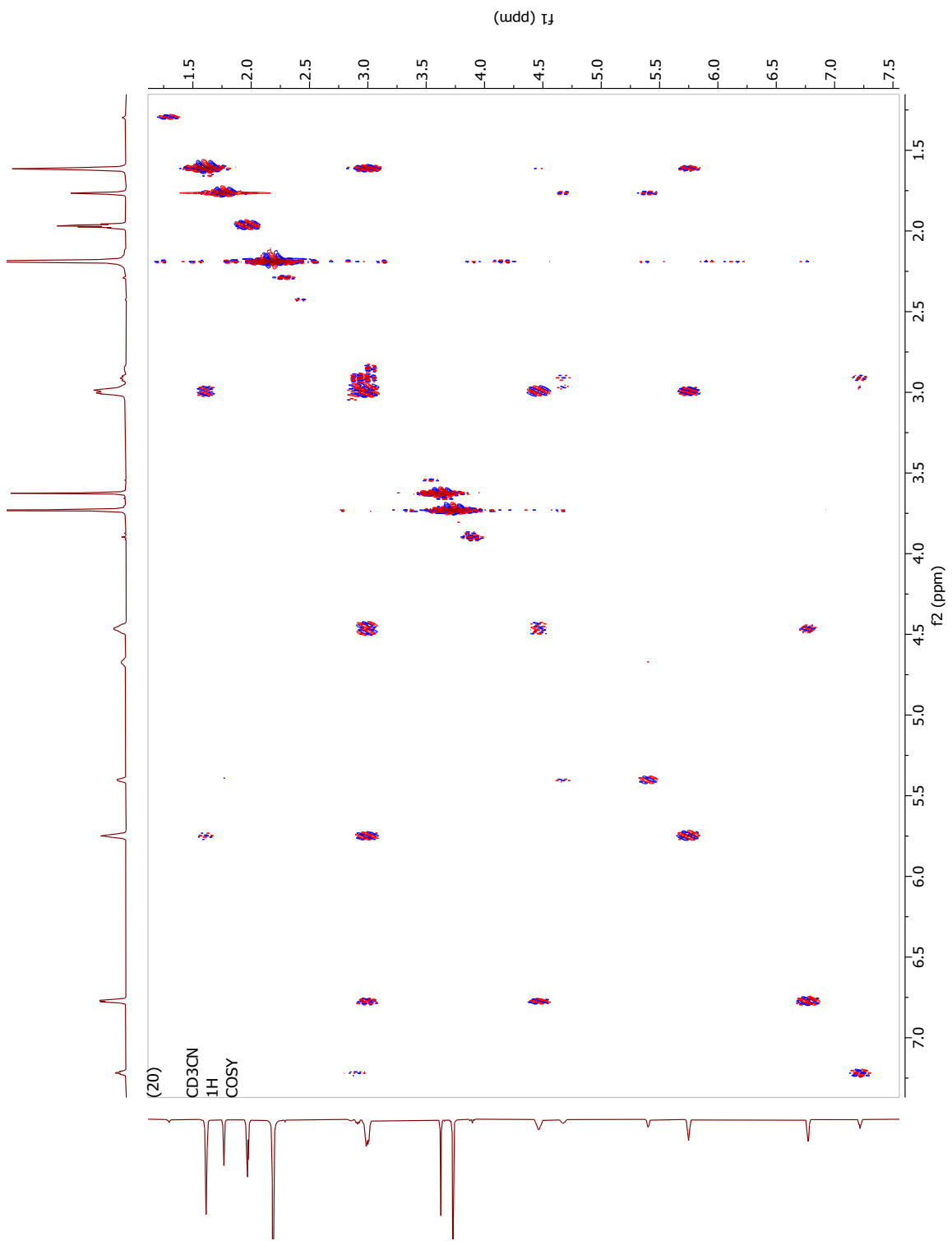


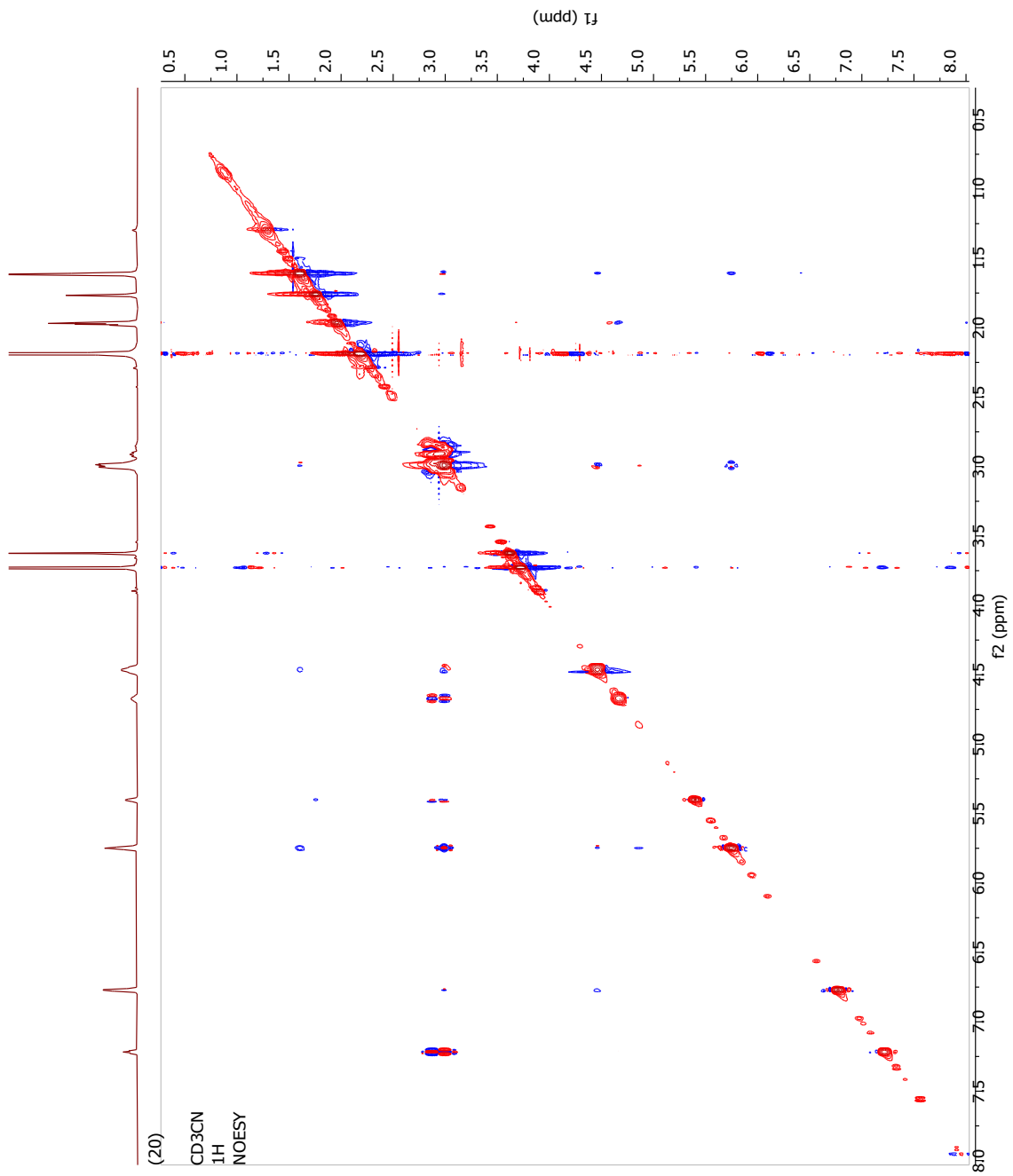


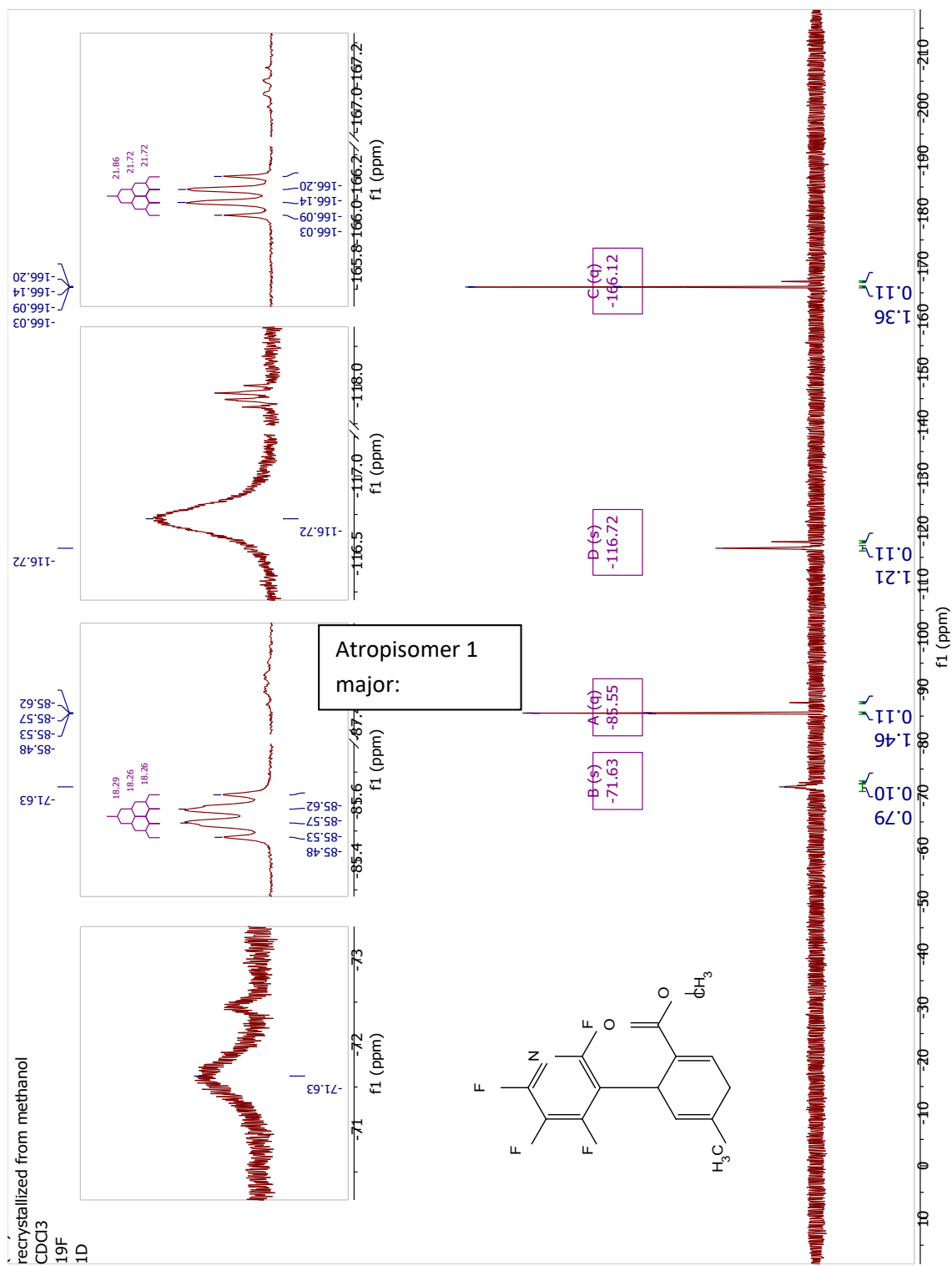


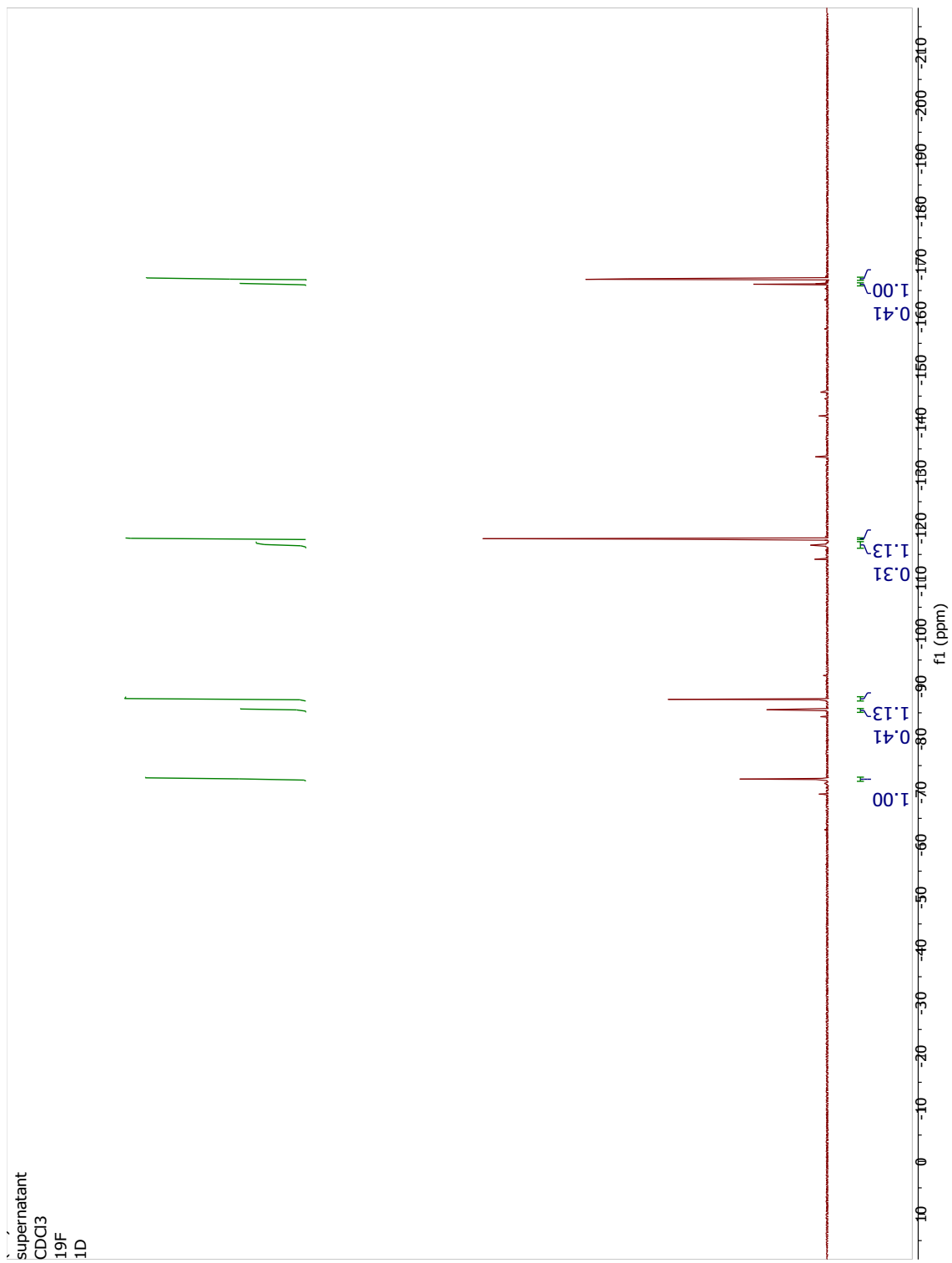




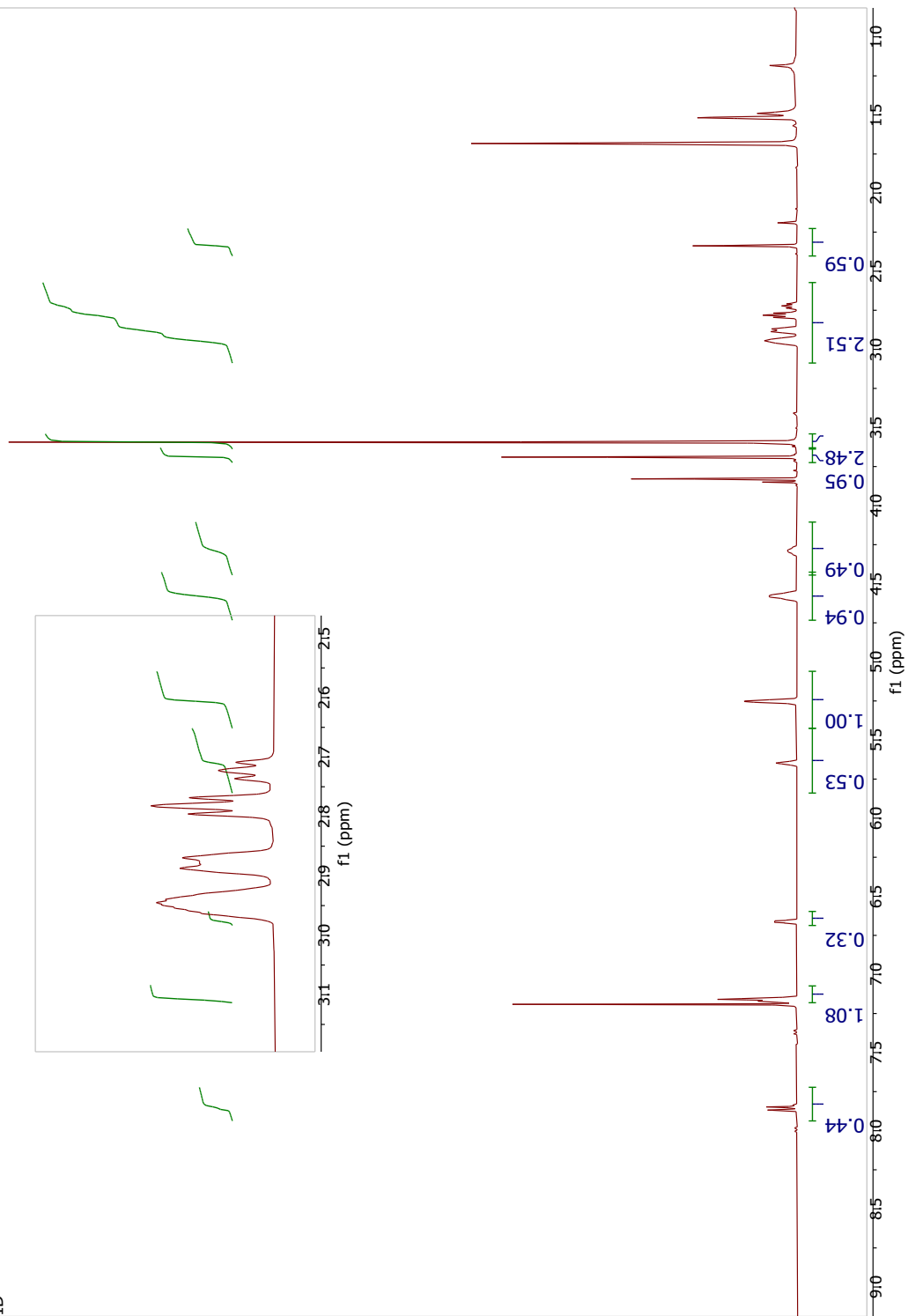


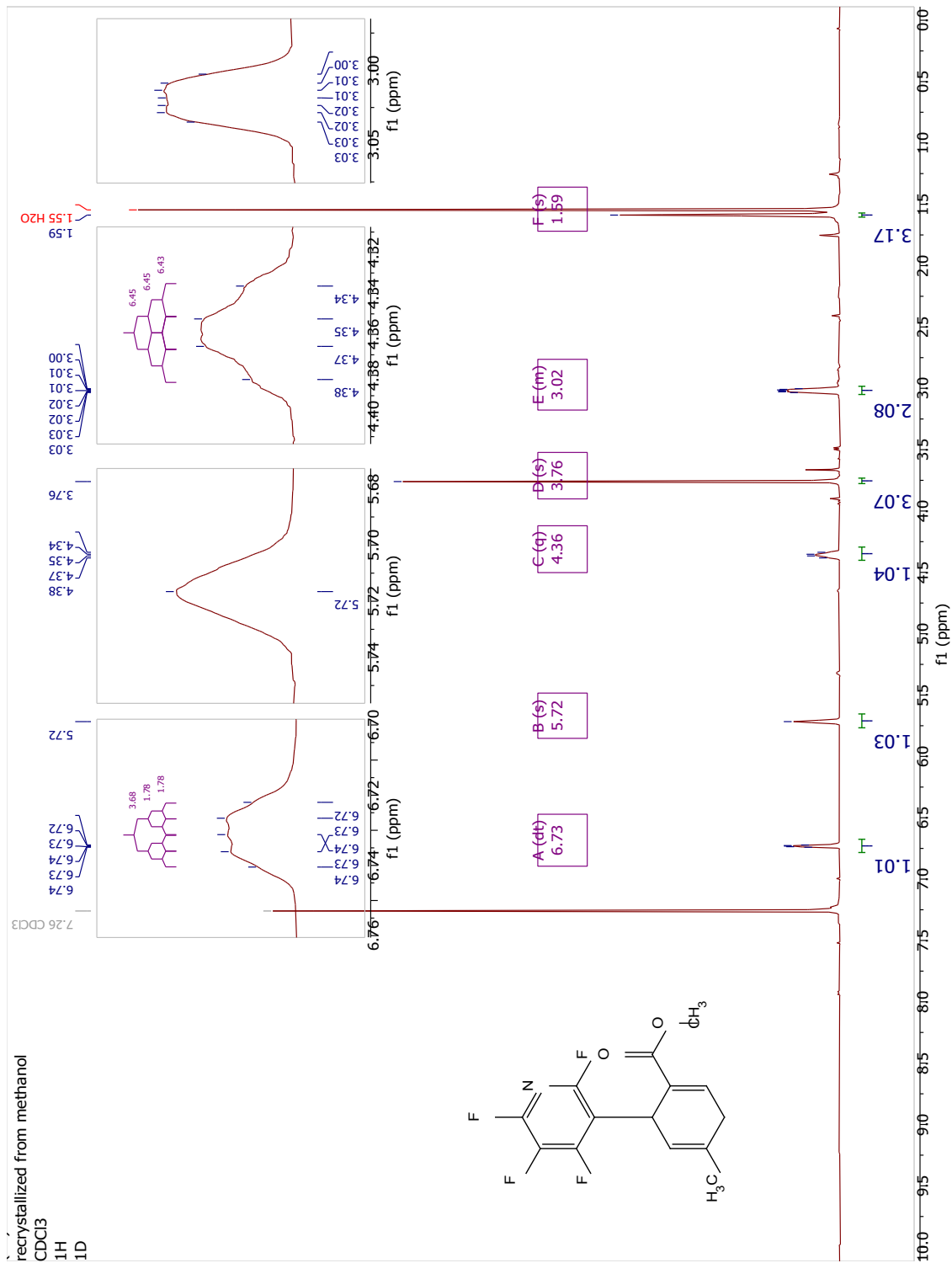






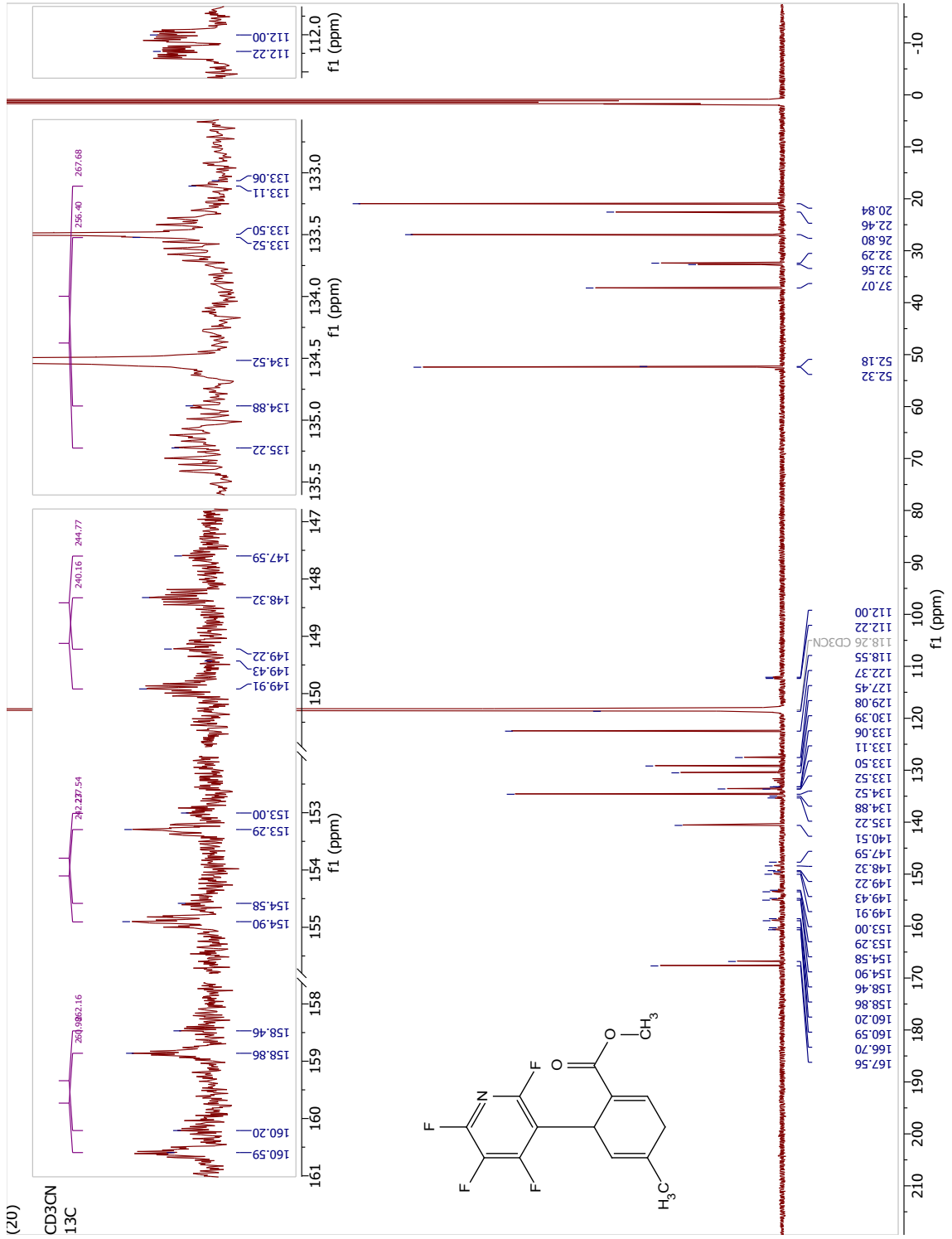
supernatant  
CDCl3  
1H  
1D

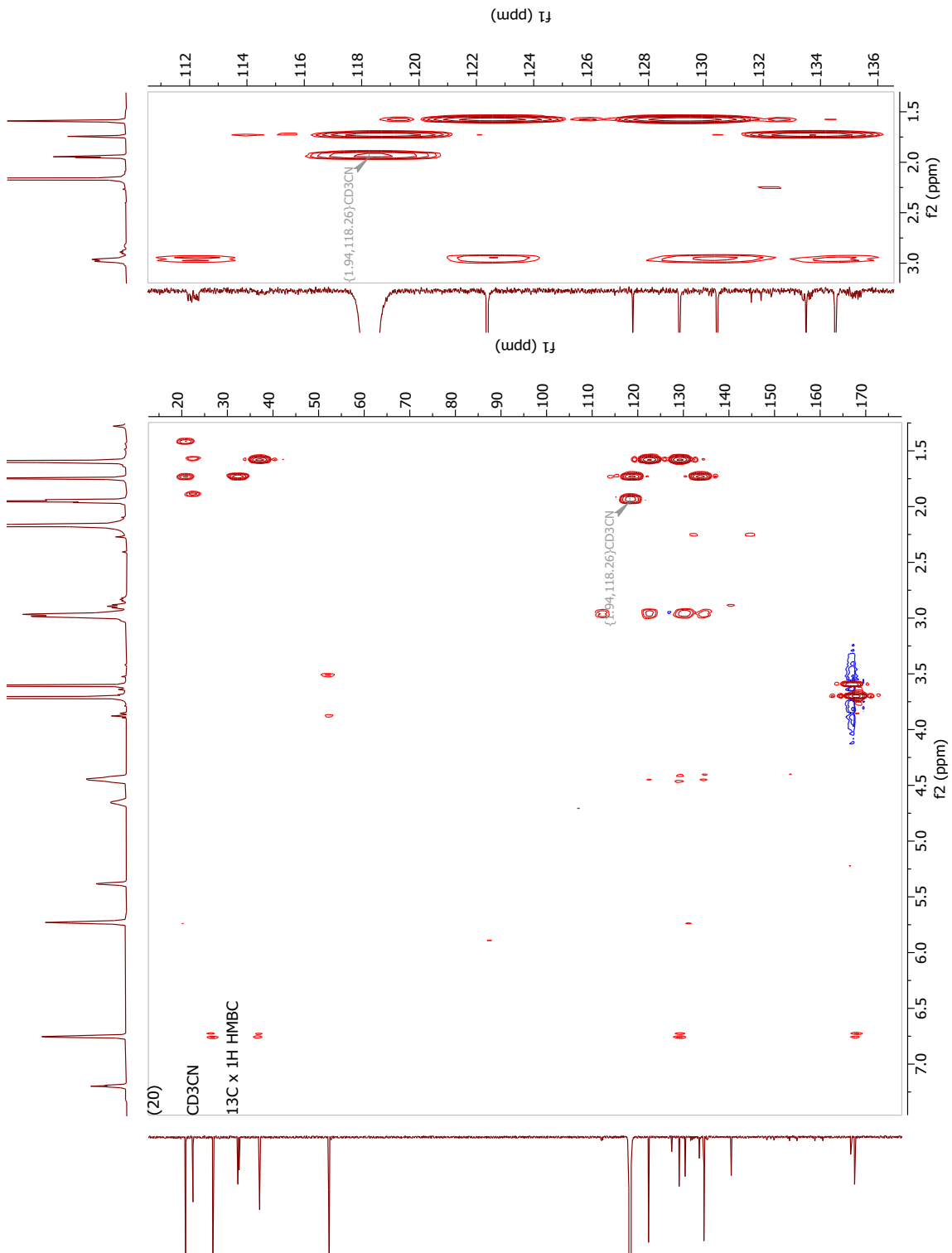




(20)

CD3CN  
13C





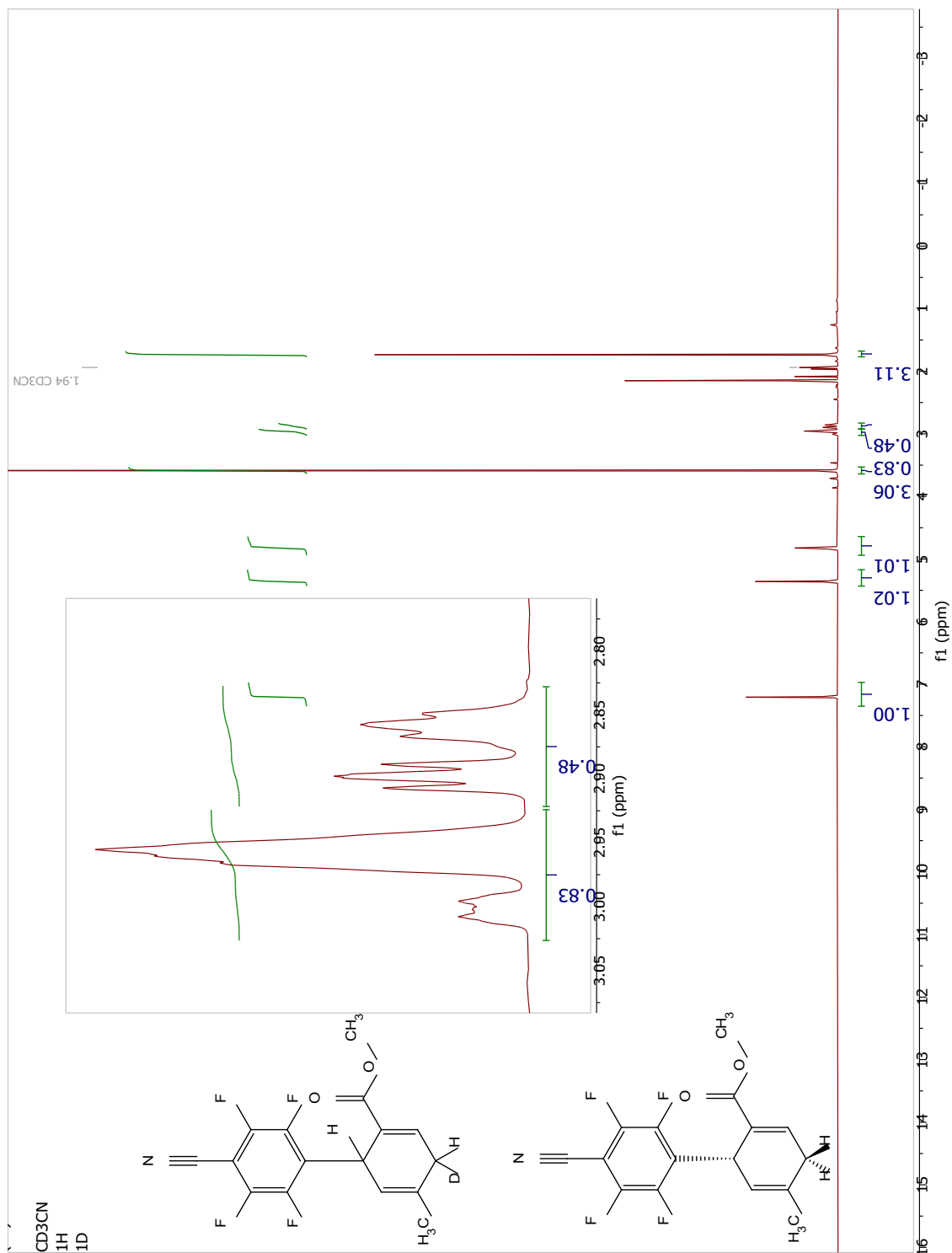




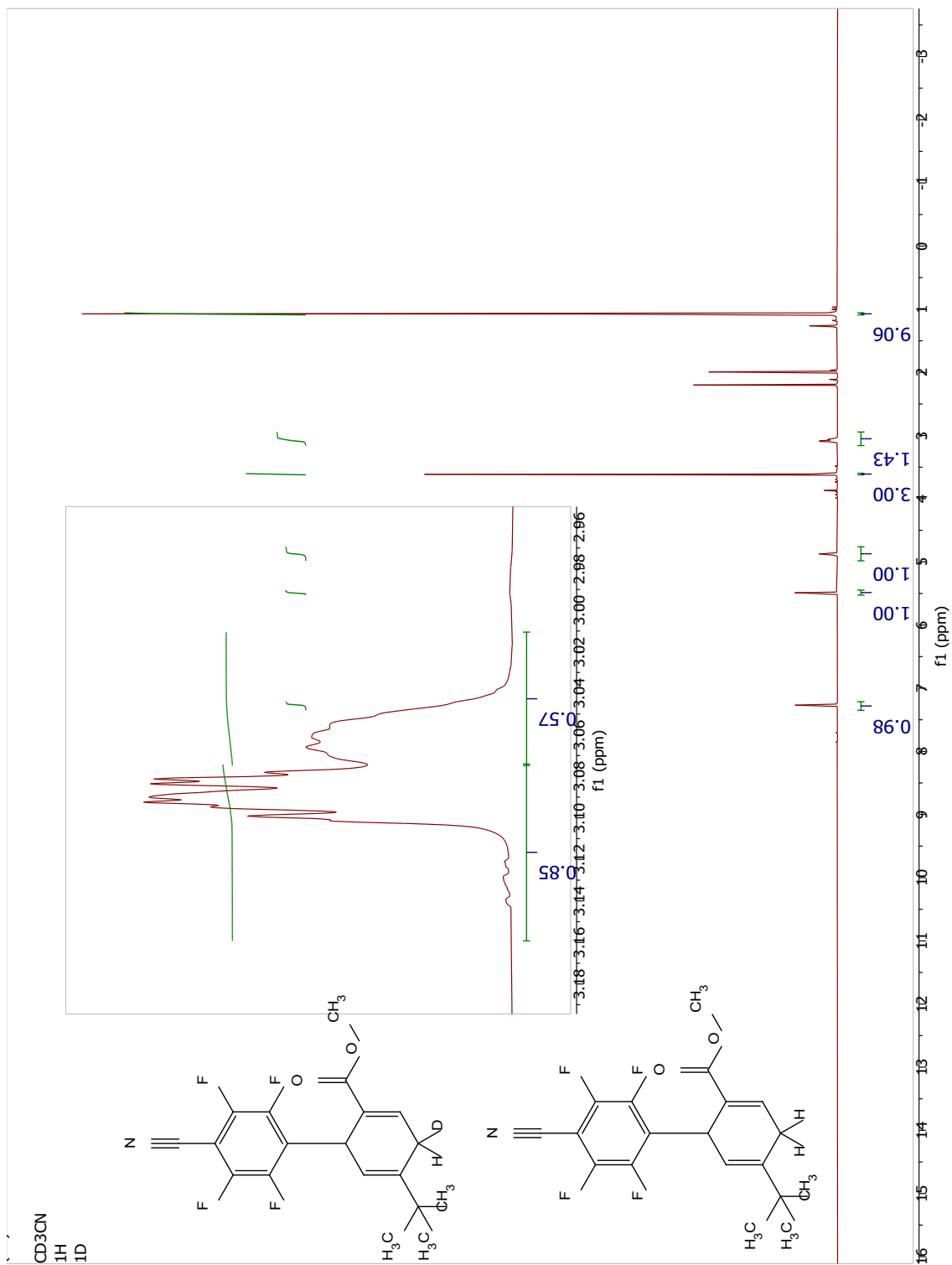




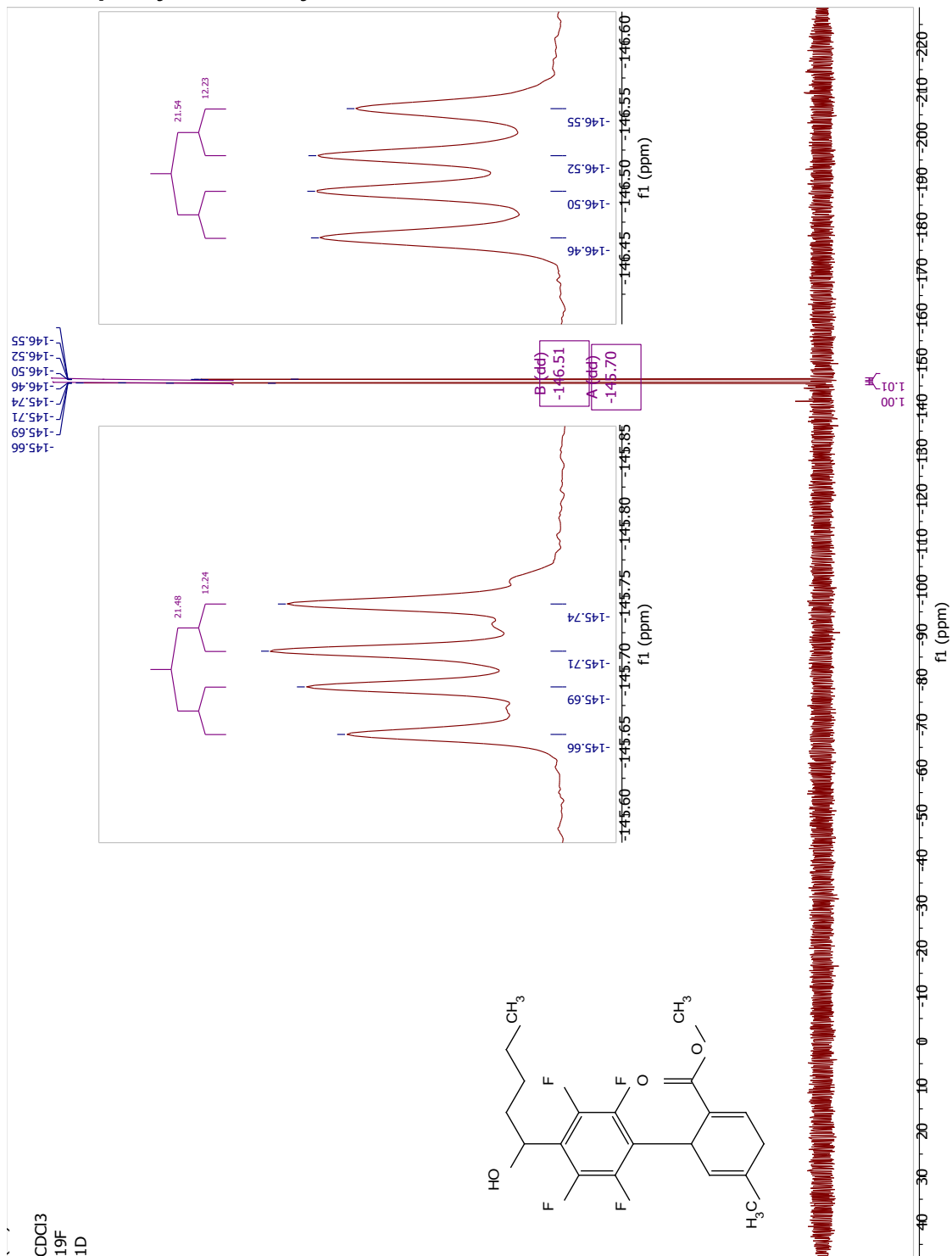
(6.4.22)



(6.4.23)



**(6.5.24) Methyl 2',3',5',6'-tetrafluoro-4'-(1-hydroxypentyl)-5-methyl-1,4-dihydro-[1,1'-biphenyl]-2-carboxylate**



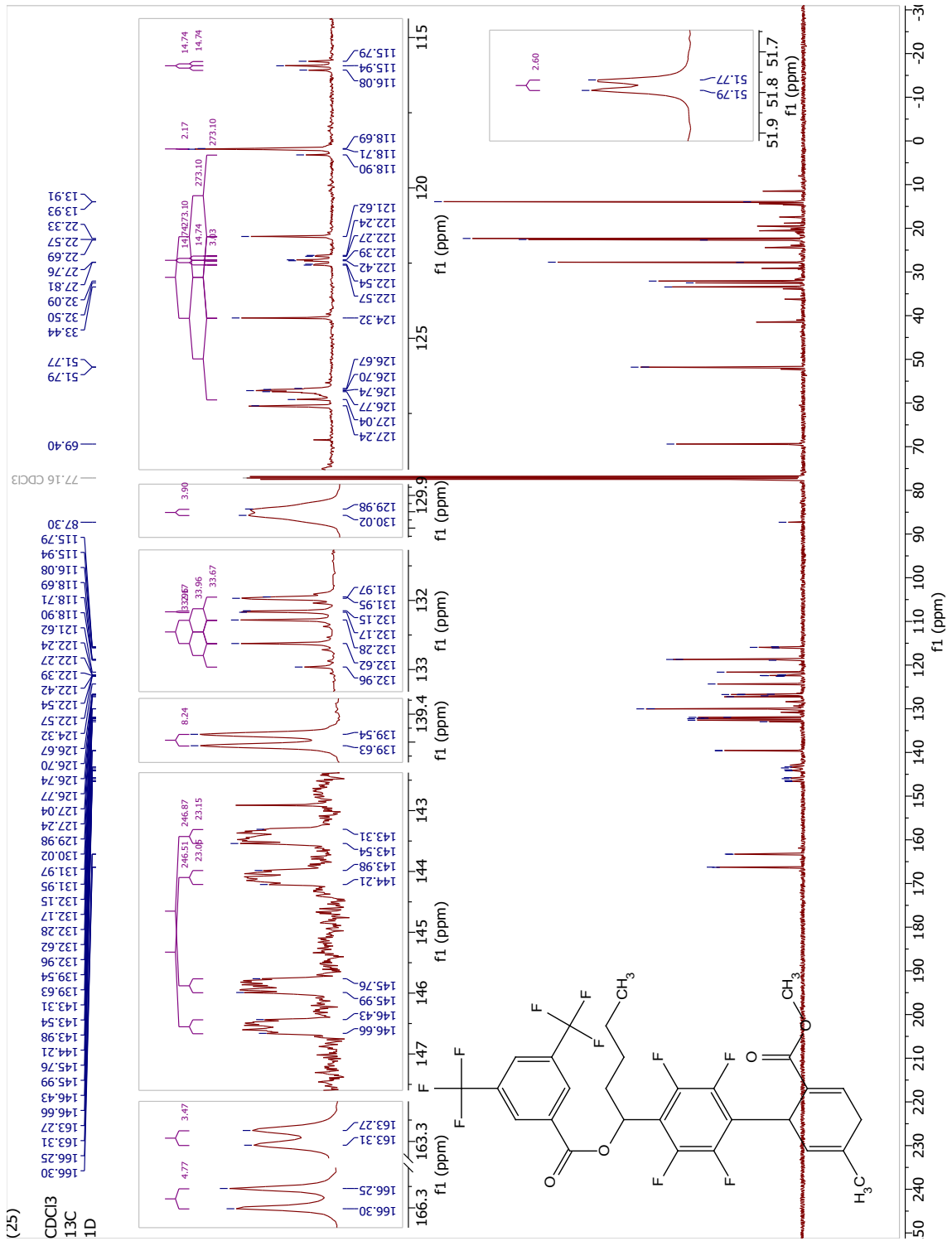




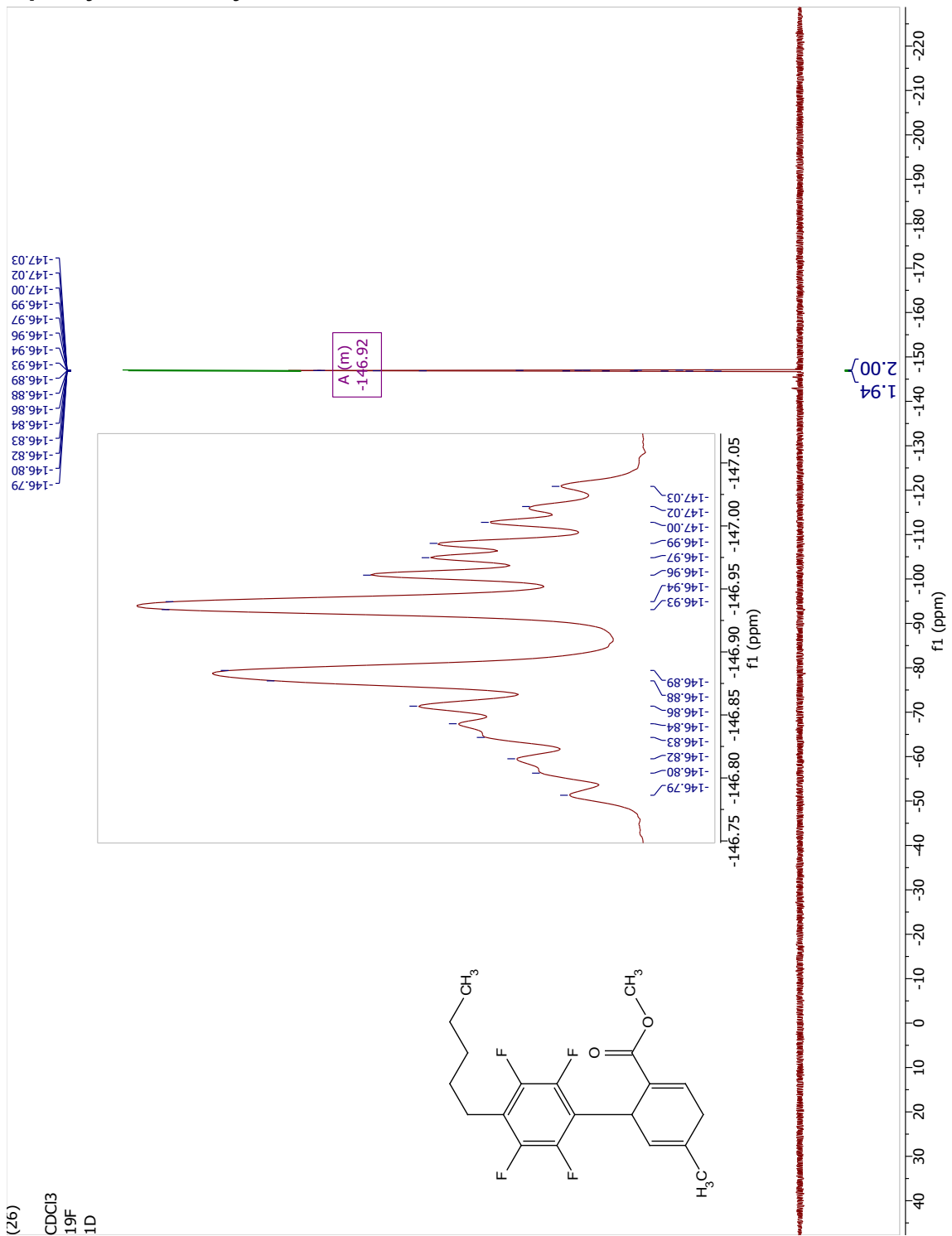


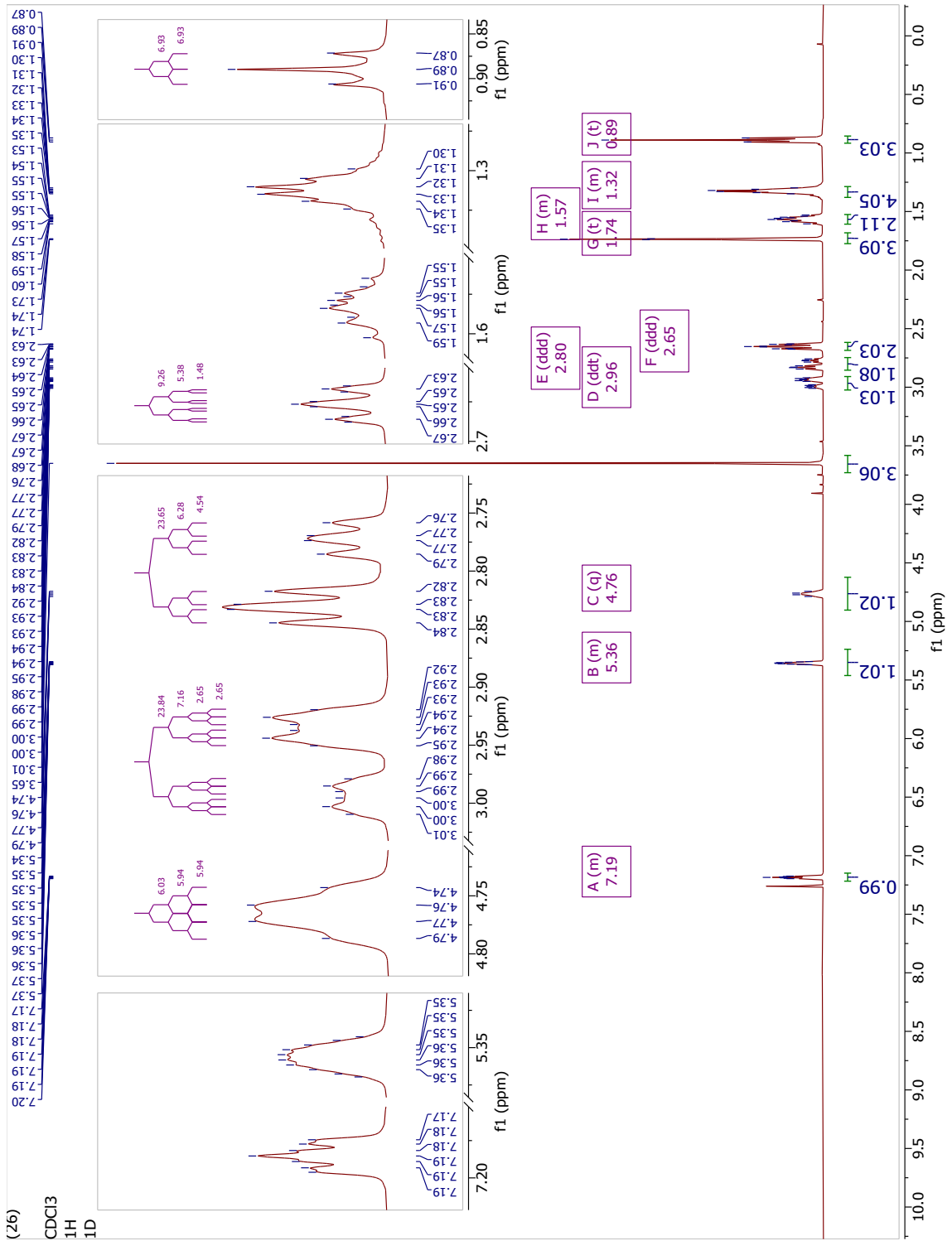




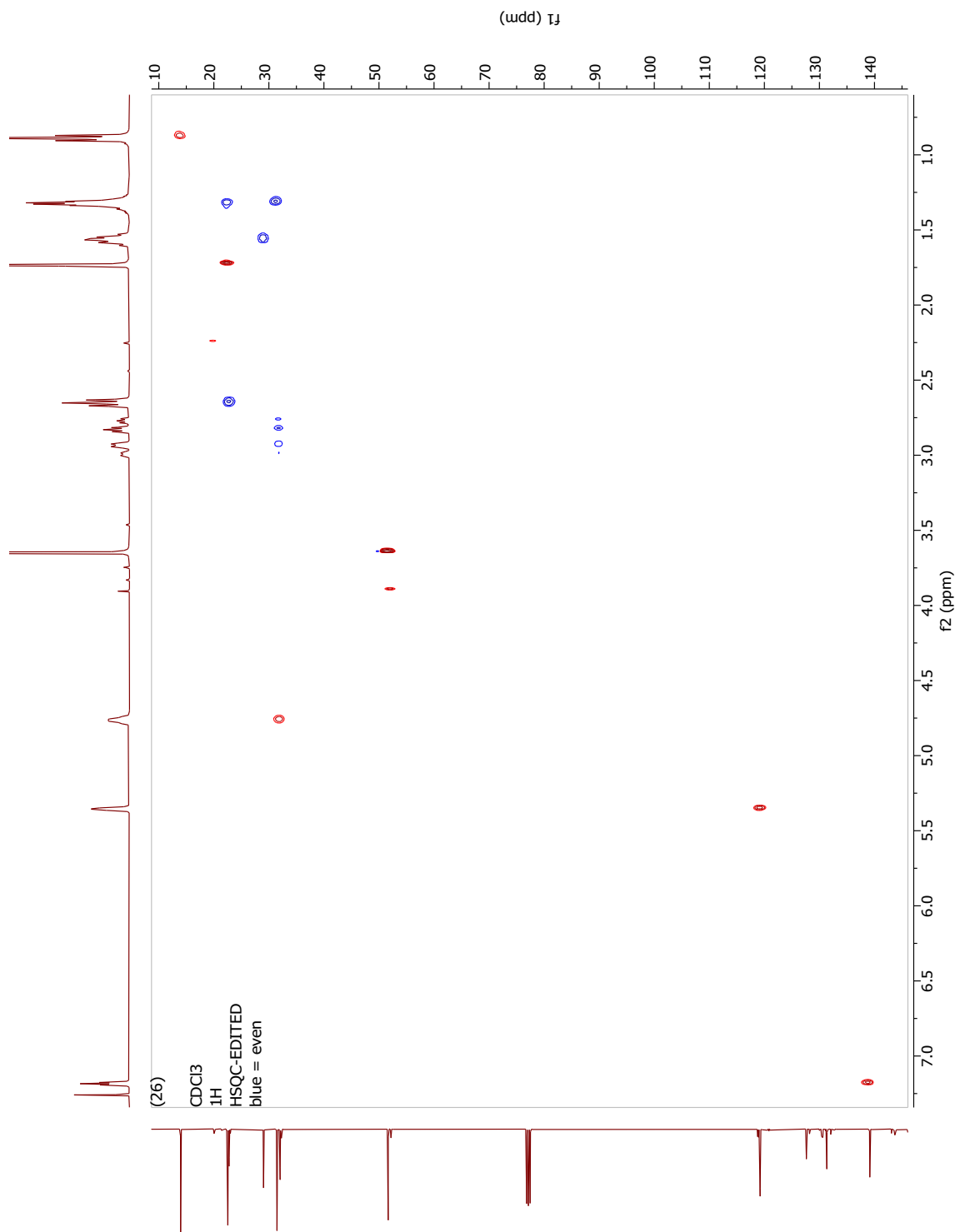


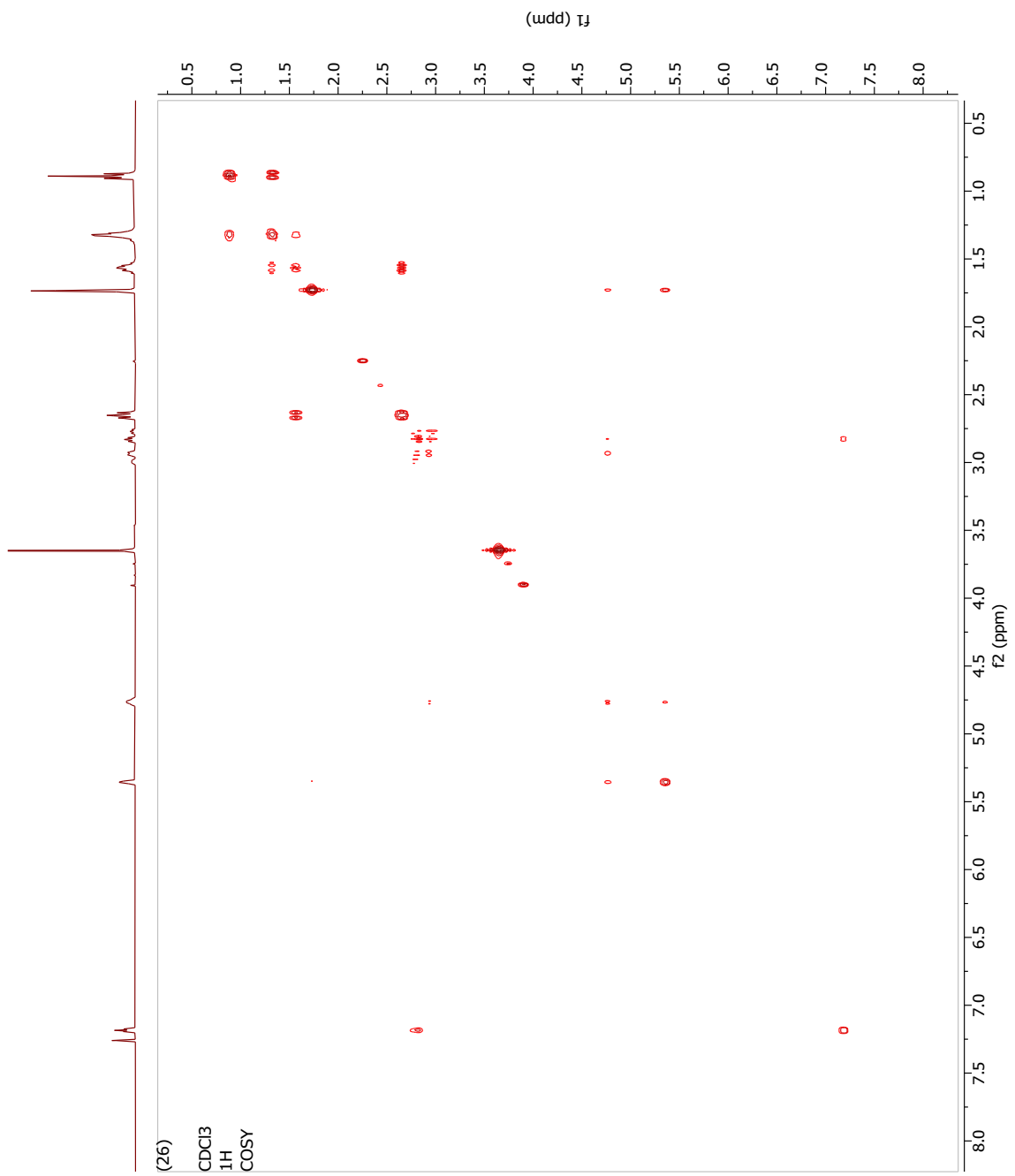
(6.5.26) Methyl 2',3',5',6'-tetrafluoro-5-methyl-4'-pentyl-1,4-dihydro-[1,1'-biphenyl]-2- carboxylate



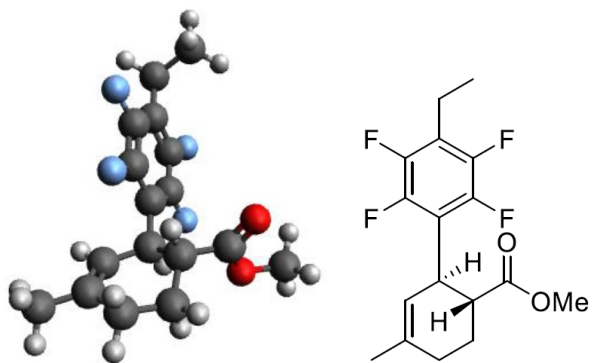












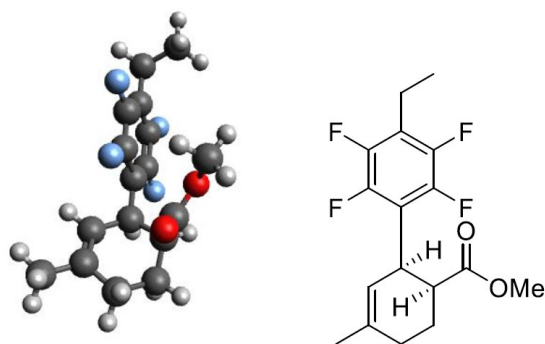
***trans*-Methyl-4'-ethyl-2',3',5',6'-tetrafluoro-5-methyl-1,2,3,4-tetrahydro-[1,1'-biphenyl]-2-carboxylate (6.5.28) model system**

Basis set: B3LYP/6-31G\* gas phase

Standard orientation (coordinates in Angstroms)

-----		
C	0	2.425000 0.371000 1.060000
C	0	1.045000 0.517000 1.183000
C	0	0.150000 -0.270000 0.456000
C	0	0.722000 -1.214000 -0.402000
C	0	2.100000 -1.357000 -0.523000
C	0	2.994000 -0.574000 0.208000
C	0	-1.356000 -0.096000 0.596000
C	0	-2.032000 -1.384000 1.032000
C	0	-3.216000 -1.820000 0.586000
C	0	-4.019000 -1.036000 -0.430000
C	0	-3.531000 0.409000 -0.591000
C	0	-1.994000 0.458000 -0.707000
C	0	-1.508000 1.861000 -1.030000
F	0	0.582000 1.454000 2.034000
C	0	-3.818000 -3.120000 1.054000
F	0	-0.070000 -2.009000 -1.148000
F	0	2.581000 -2.286000 -1.373000
F	0	3.222000 1.171000 1.797000
C	0	4.489000 -0.725000 0.052000
-----		
C	0	5.038000 0.012000 -1.183000
O	0	-0.982000 2.196000 -2.069000
O	0	-1.753000 2.719000 -0.011000
C	0	-1.323000 4.073000 -0.224000
H	0	-1.505000 0.656000 1.379000
H	0	-1.489000 -1.973000 1.770000
H	0	-3.981000 -1.558000 -1.399000
H	0	-5.079000 -1.035000 -0.139000
H	0	-3.988000 0.865000 -1.478000
H	0	-3.842000 1.008000 0.274000
H	0	-1.682000 -0.165000 -1.550000
H	0	-3.164000 -3.640000 1.761000
H	0	-4.789000 -2.956000 1.541000
H	0	-4.004000 -3.793000 0.205000
H	0	4.977000 -0.348000 0.956000
H	0	4.729000 -1.791000 -0.026000
H	0	6.122000 -0.124000 -1.258000
H	0	4.581000 -0.372000 -2.100000
H	0	4.832000 1.086000 -1.122000
H	0	-1.593000 4.612000 0.684000
H	0	-0.242000 4.110000 -0.386000
H	0	-1.827000 4.503000 -1.094000

Sum of electronic and thermal Free Energies = -1208.171102 E

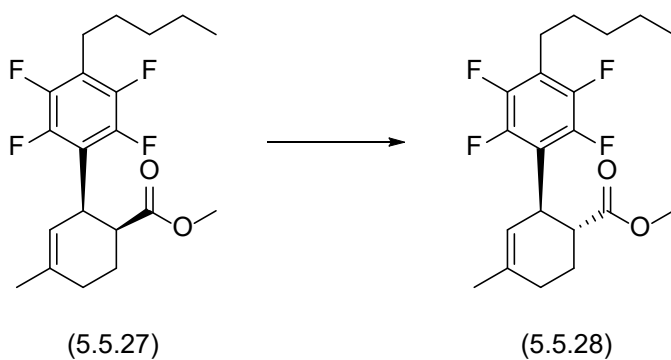


***cis*-Methyl-4'-ethyl-2',3',5',6'-tetrafluoro-5-methyl-1,2,3,4-tetrahydro-[1,1'-biphenyl]-2-carboxylate (6.5.27) model system**

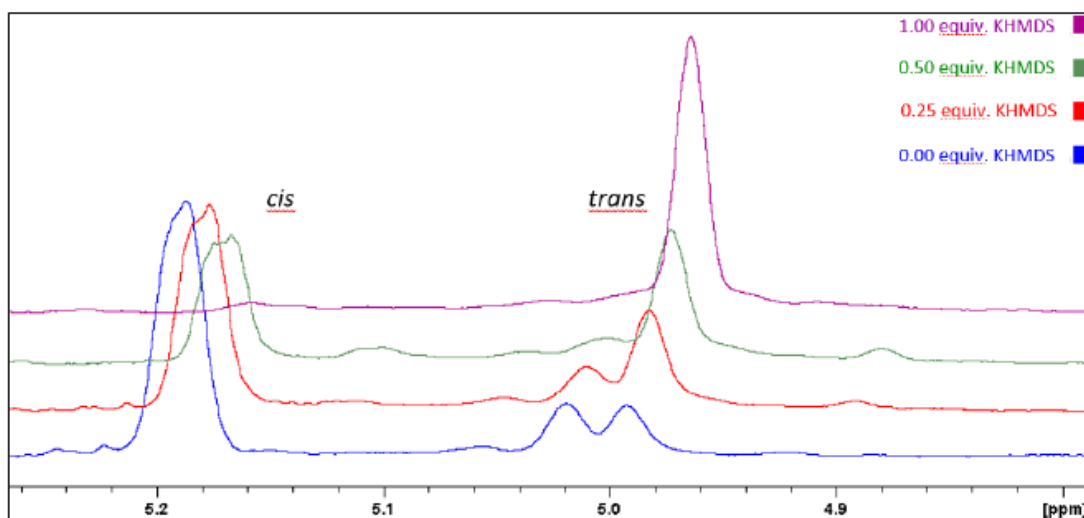
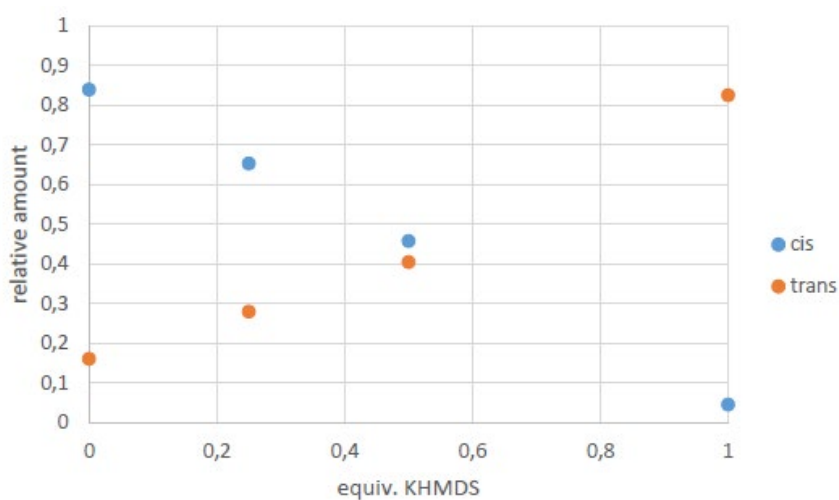
Basis set: B3LYP/6-31G\* gas phase  
Standard orientation (coordinates in  
Angstroms)

-----	
-----	
C O -2.545000 -1.338000 -0.354000	C O -4.466000 -0.049000 0.710000
C O -1.188000 -1.560000 -0.576000	C O -5.012000 1.104000 -0.151000
C O -0.198000 -0.769000 0.010000	O O 2.648000 2.072000 -0.561000
C O -0.655000 0.262000 0.834000	O O 0.608000 1.797000 -1.481000
C O -2.009000 0.484000 1.053000	C O 0.343000 3.185000 -1.216000
C O -2.997000 -0.313000 0.474000	H O 1.287000 -2.062000 -0.690000
C O 1.273000 -1.061000 -0.238000	H O 1.554000 -1.423000 1.938000
C O 2.090000 -1.122000 1.039000	H O 5.118000 -1.057000 -0.163000
C O 3.403000 -0.872000 1.108000	H O 4.534000 0.586000 0.047000
C O 4.204000 -0.449000 -0.102000	H O 3.454000 -1.603000 -1.777000
C O 3.433000 -0.562000 -1.428000	H O 3.928000 0.039000 -2.199000
C O 1.954000 -0.149000 -1.315000	H O 1.444000 -0.344000 -2.265000
C O 1.810000 1.346000 -1.052000	H O 4.637000 -0.005000 2.650000
F O -0.840000 -2.578000 -1.389000	H O 4.971000 -1.707000 2.340000
C O 4.163000 -0.966000 2.405000	H O 3.511000 -1.244000 3.240000
F O 0.228000 1.095000 1.419000	H O -4.616000 0.188000 1.769000
F O -2.374000 1.509000 1.852000	H O -5.026000 -0.965000 0.501000
F O -3.434000 -2.151000 -0.958000	H O -4.897000 0.886000 -1.218000
-----	
-----	

Sum of electronic and thermal Free Energies = -1208.165044 Eh

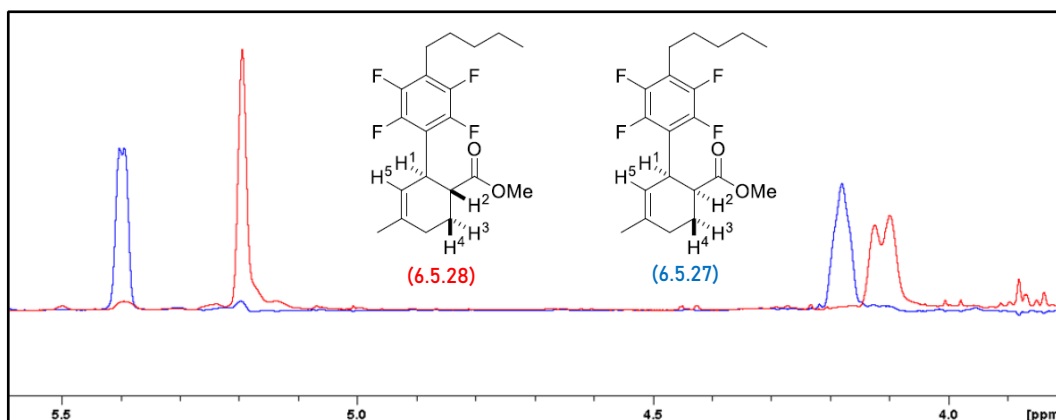


Addition of stoichiometric amounts of KHMDS in THF epimerizes the *cis* to the *trans* diastereomer.



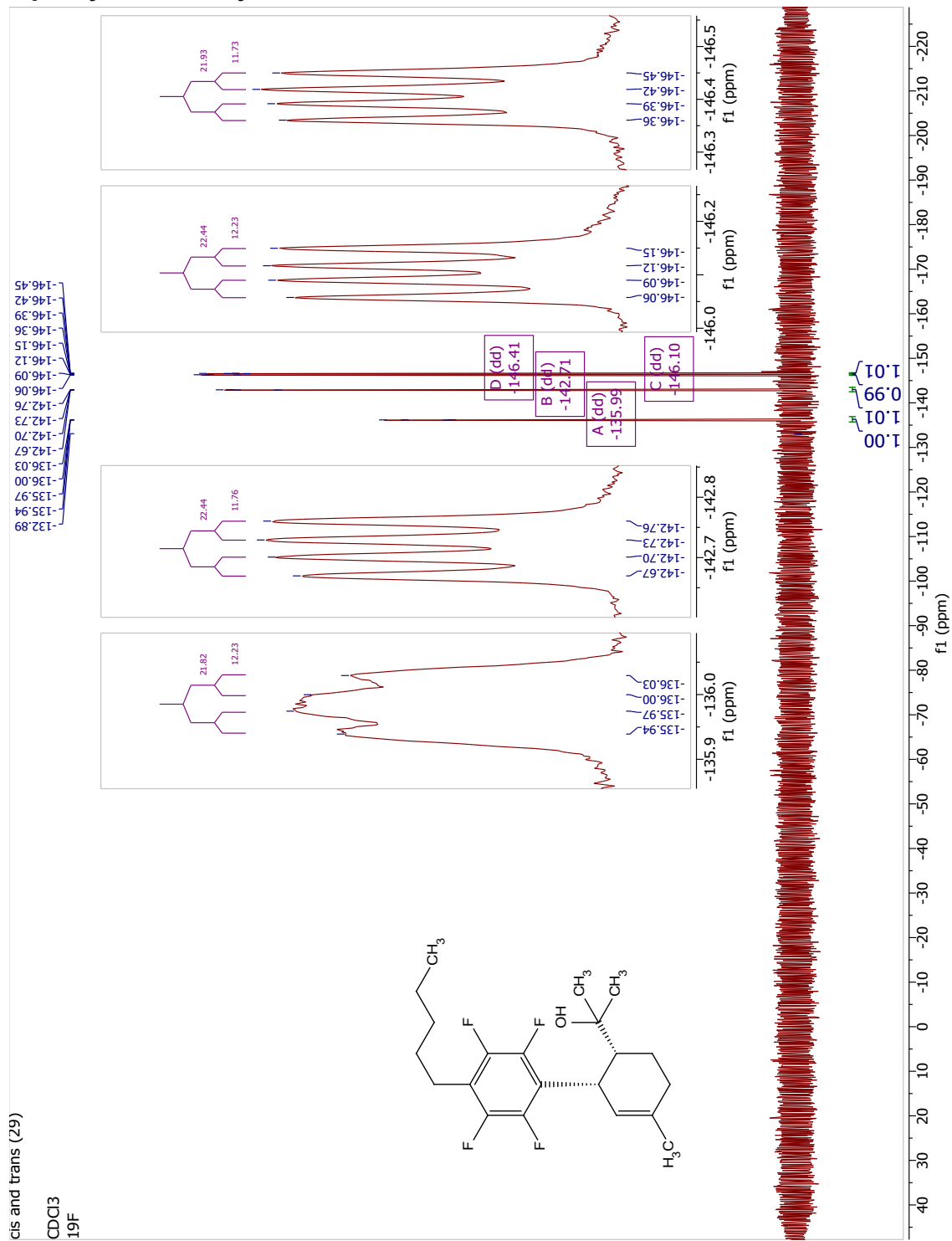
Epimerization of *cis*-(**6.5.27**) to *trans*-(**6.5.28**) (Top) Relative amounts determined via  $^1\text{H}$  NMR with THF (solvent) used as internal standard. (Bottom)  $^1\text{H}$  NMR showing the olefinic proton of *cis* and *trans*-**6.5.28**. Reaction conditions: SM ( $190\mu\text{M}$  in THF) inside

septum capped NMR tube. KHMDS (1M in THF) added stepwise. Values were corrected for dilution by additional THF from the KHMDS solution



Superposition of the <sup>1</sup>H NMR of (6.5.27) *cis*- and (6.5.28) *trans*-. Only the part showing the region of the olefinic (left) and benzylic (right) proton is depicted.

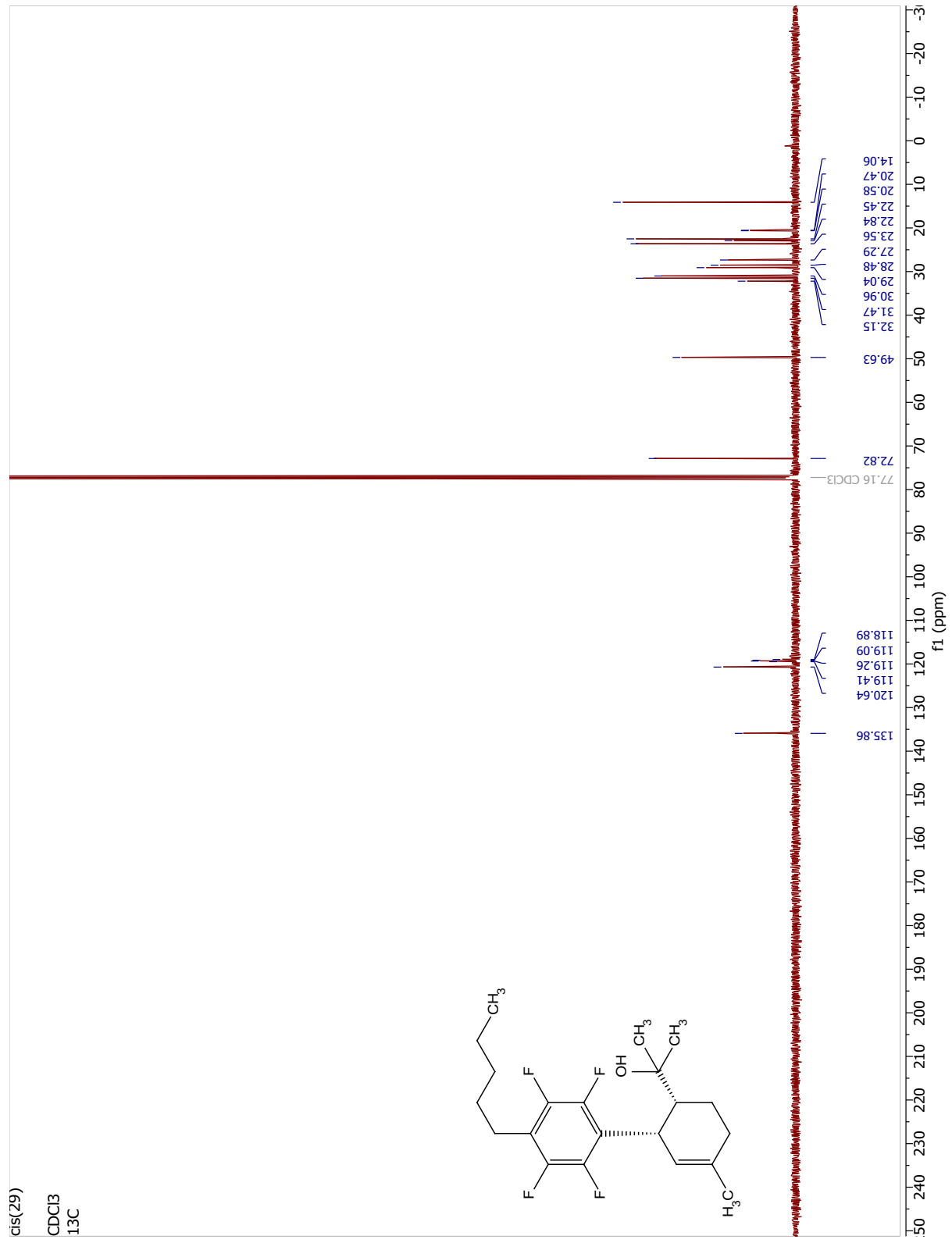
(6.5.29) Methyl 2',3',5',6'-tetrafluoro-5-methyl-4'-pentyl-1,2,3,4-tetrahydro-[1,1'-biphenyl]-2-carboxylate





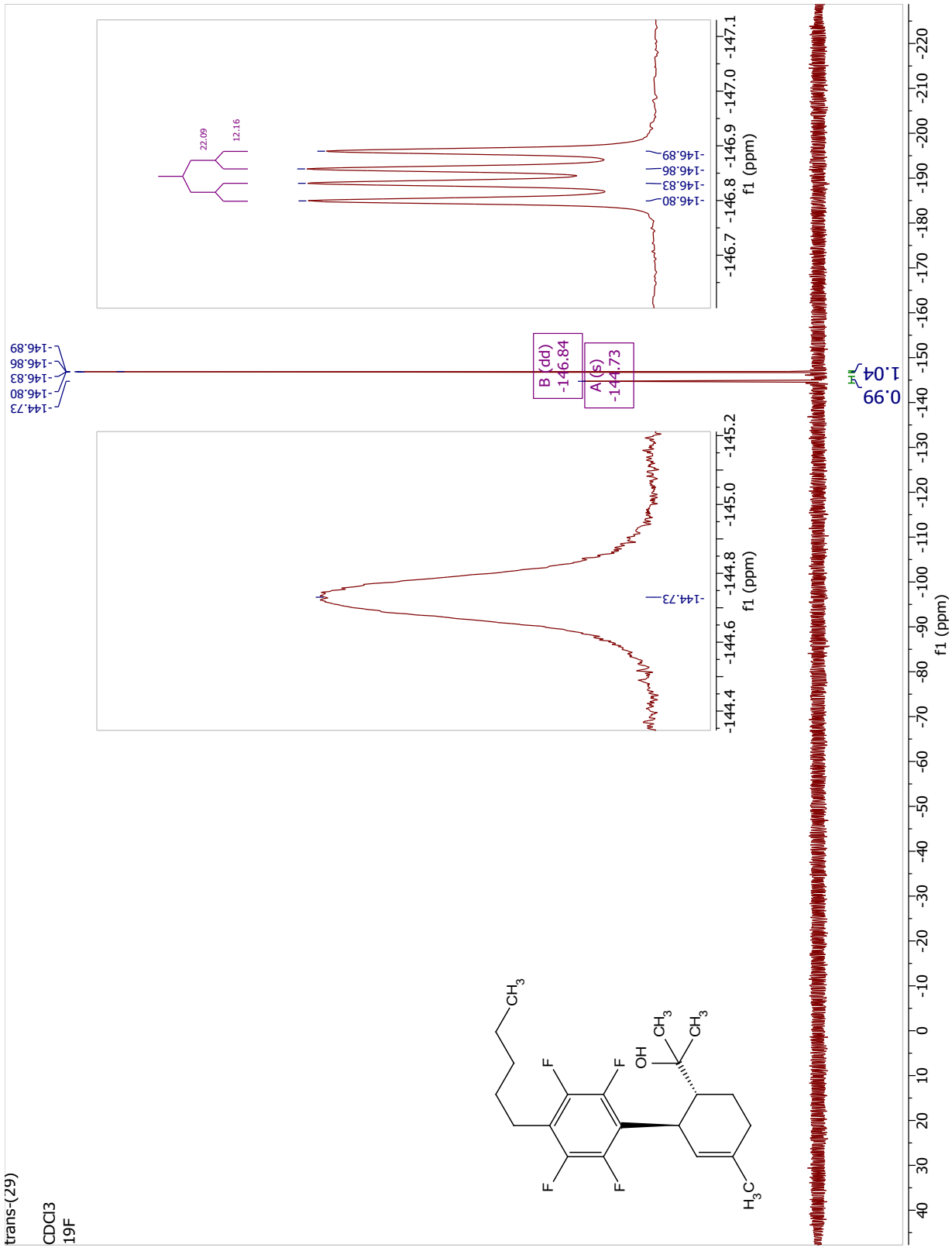
cis(29)

CDCl<sub>3</sub>  
13C



trans-(29)

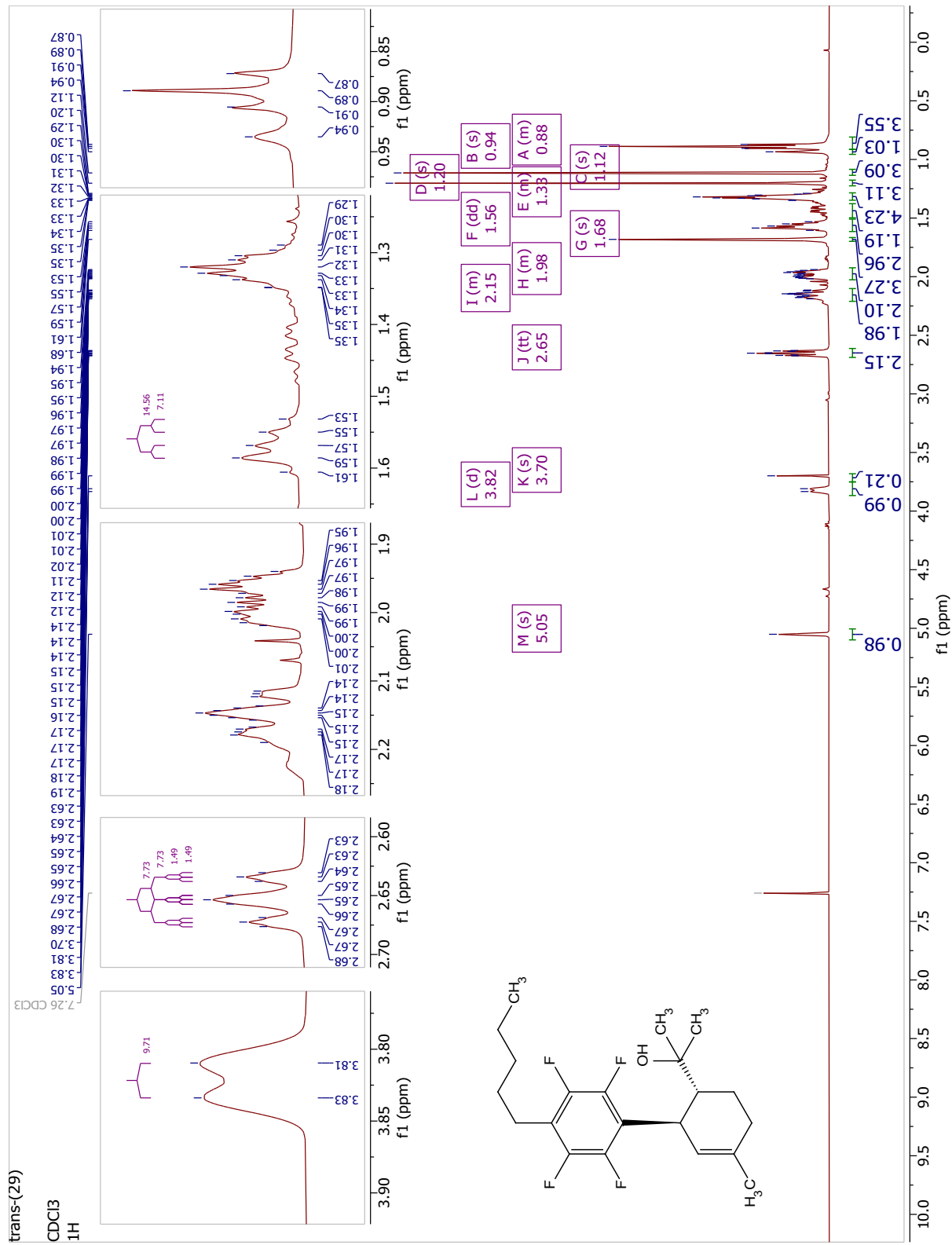
CDCl<sub>3</sub>  
19F





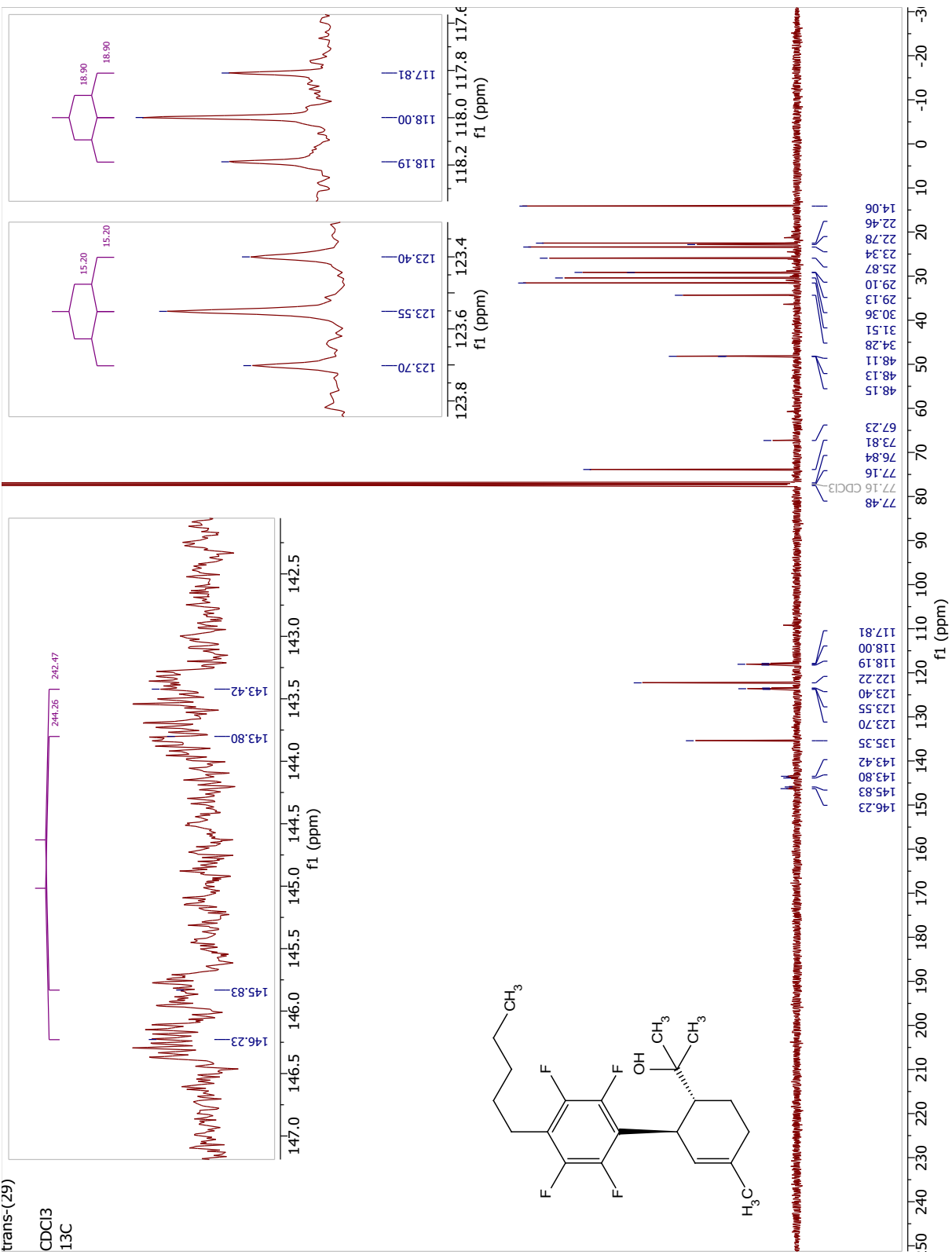
trans-(29)

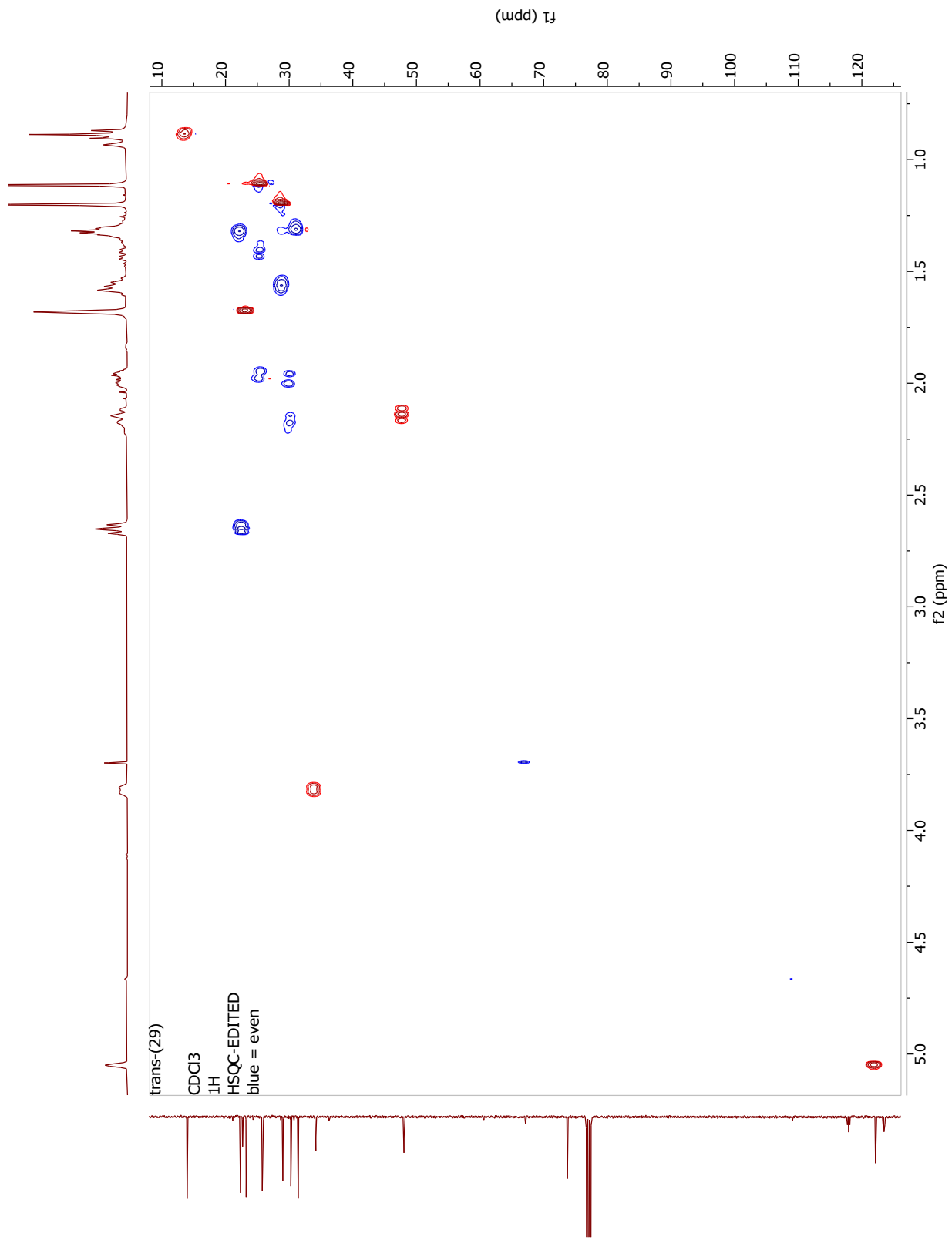
CDCl<sub>3</sub>  
1H

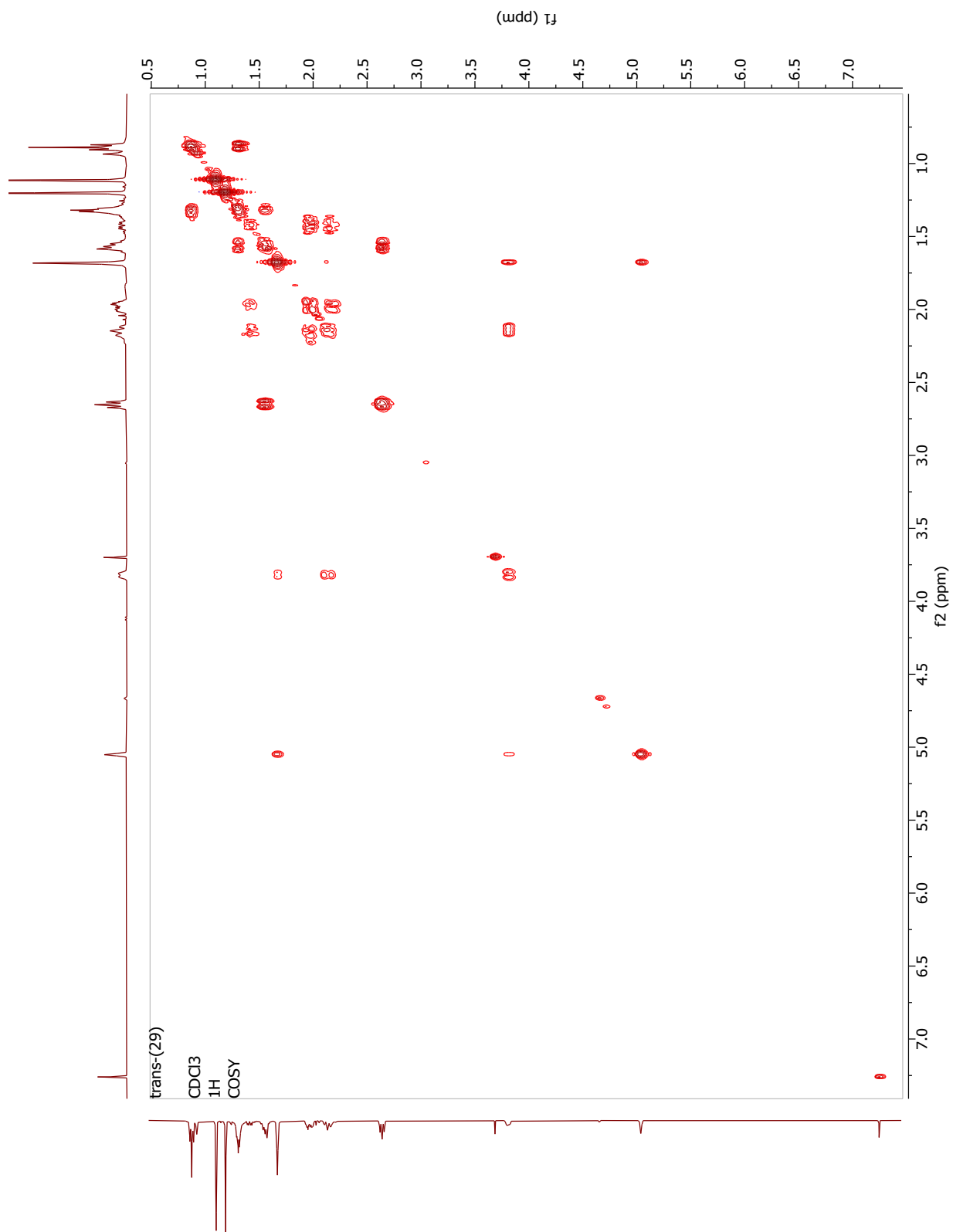


trans-(29)

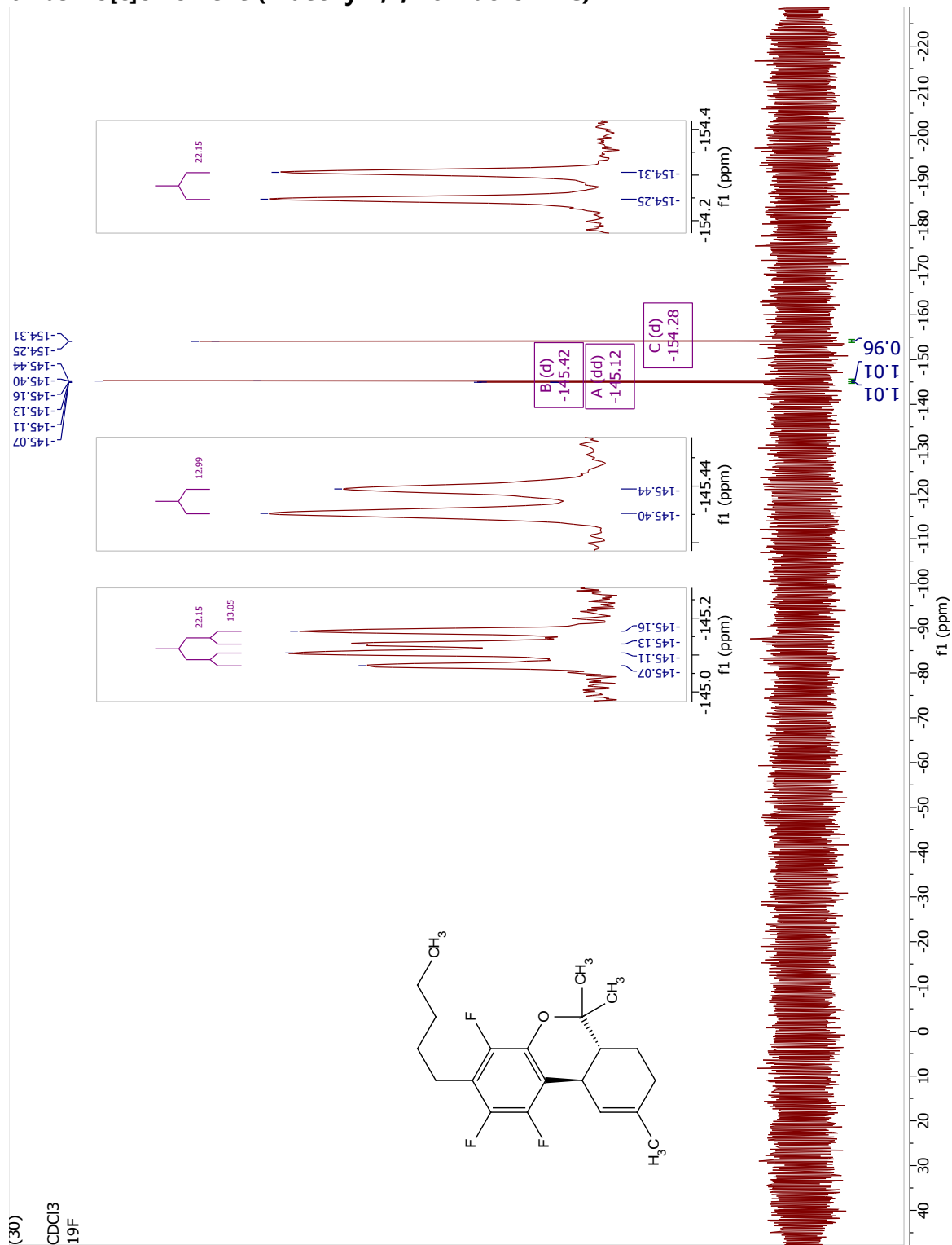
CDCl<sub>3</sub>  
13C

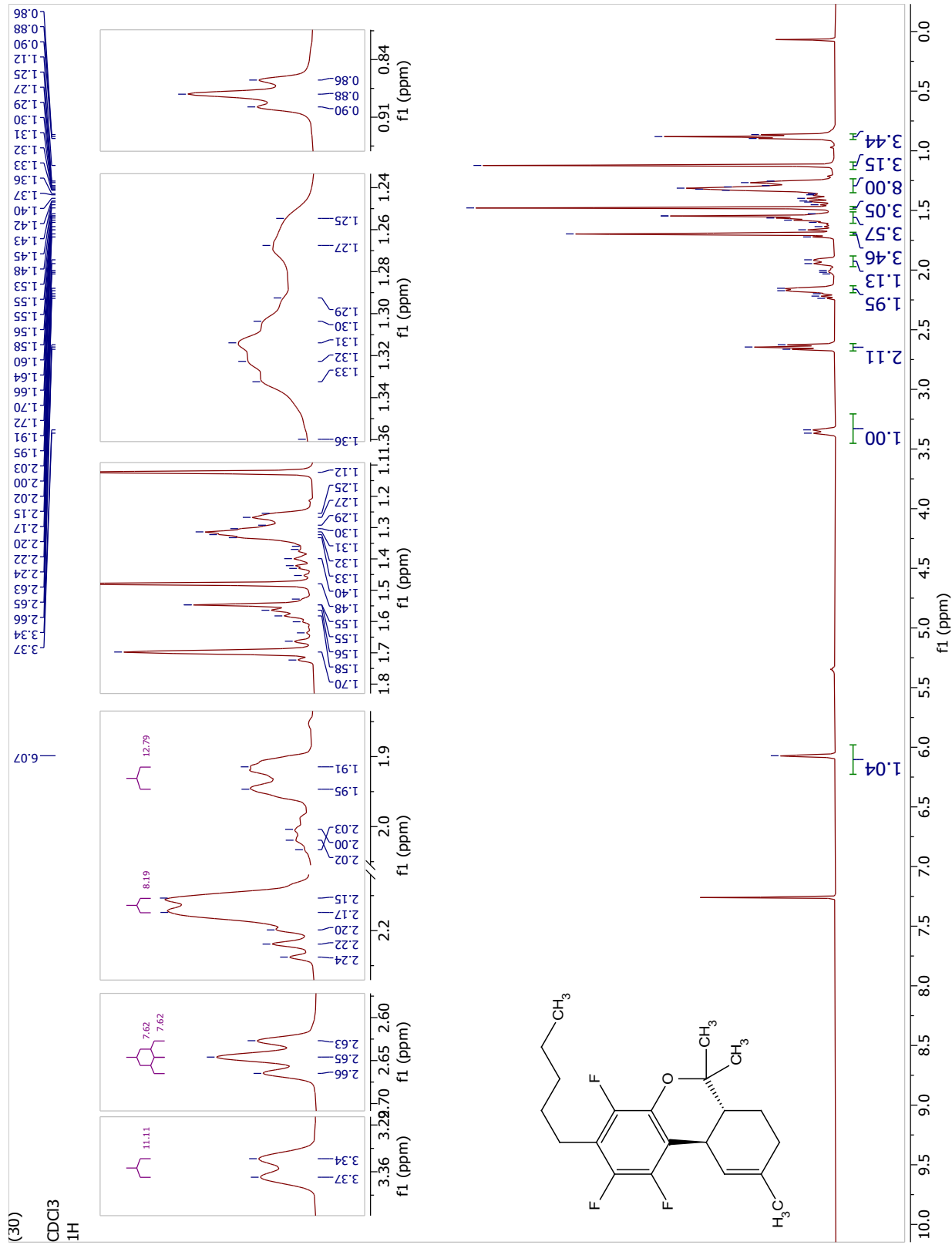






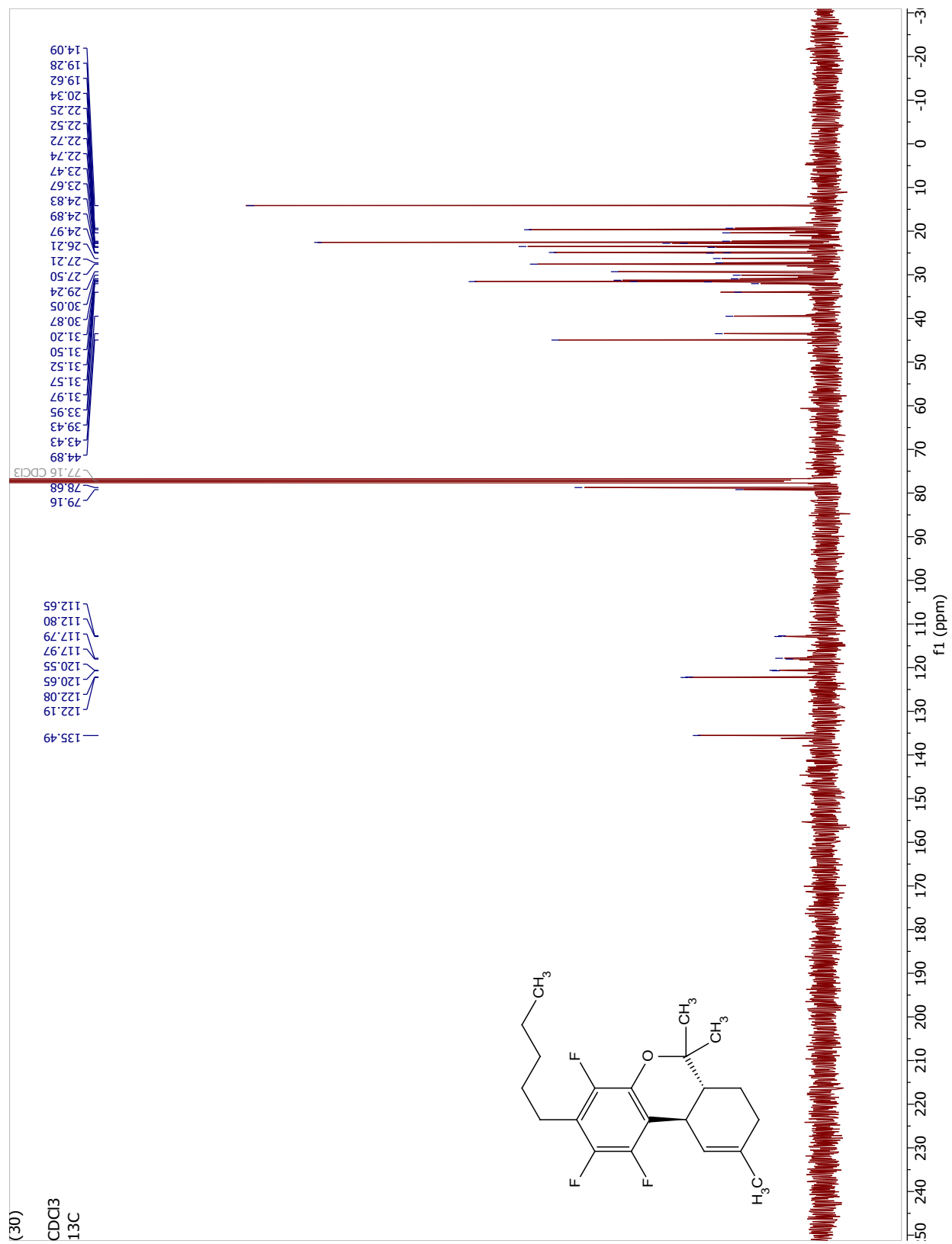
(6.5.30) 1,2,4-Trifluoro-6,6,9-trimethyl-3-pentyl-6a,7,8,10a-tetrahydro-6Hbenzo[c]chromene (1-deoxy-1,2,4-trifluoro-THC)

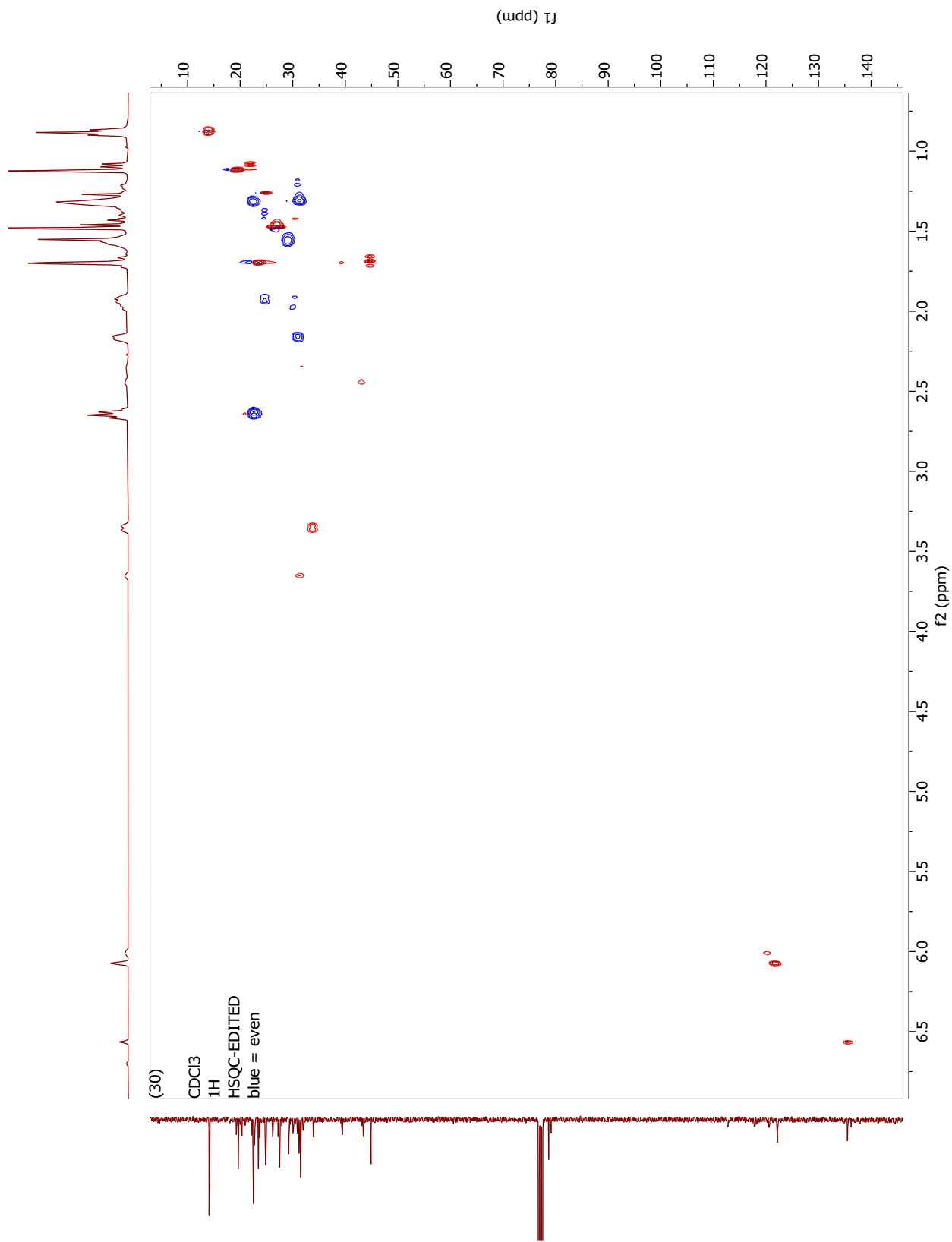




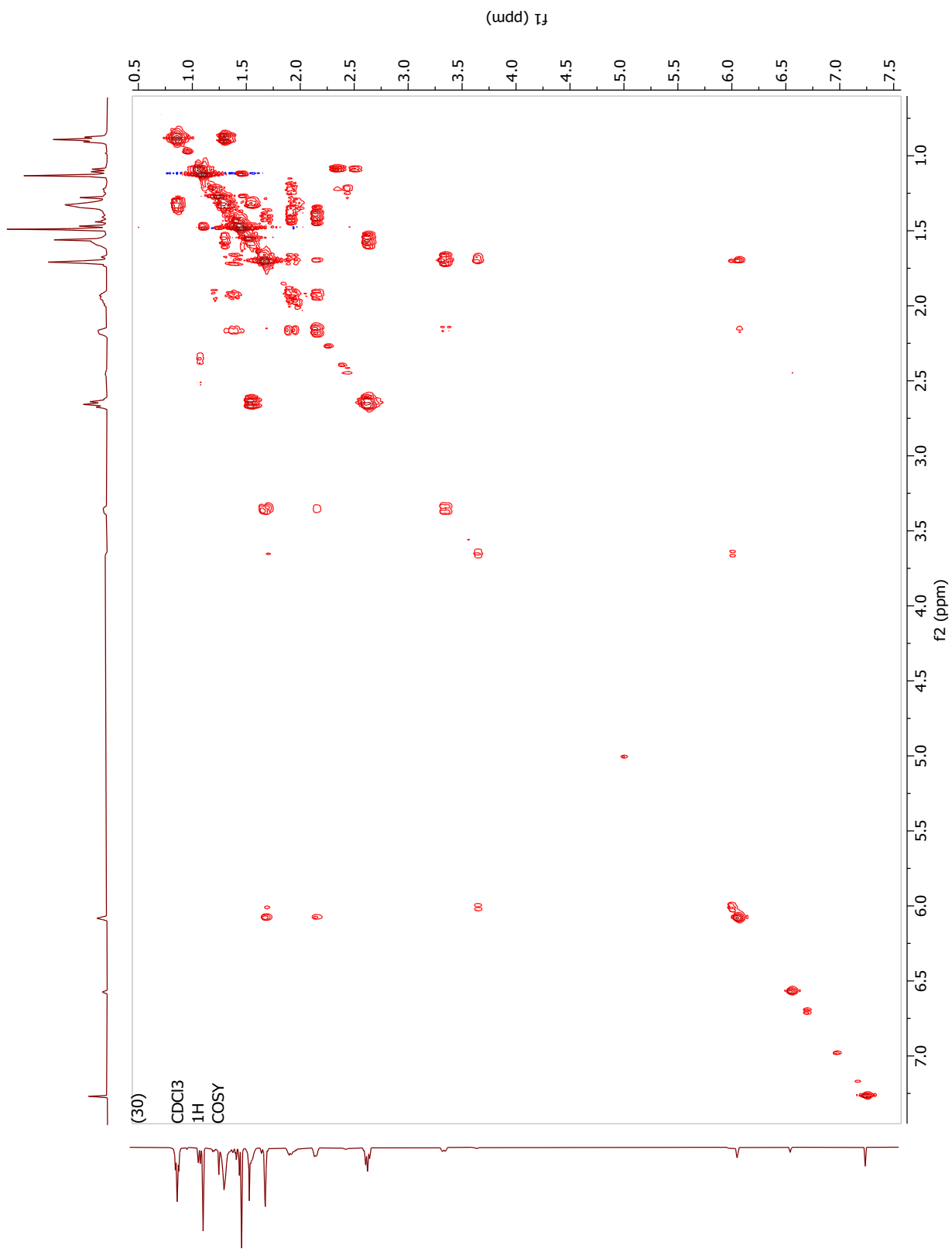
(30)

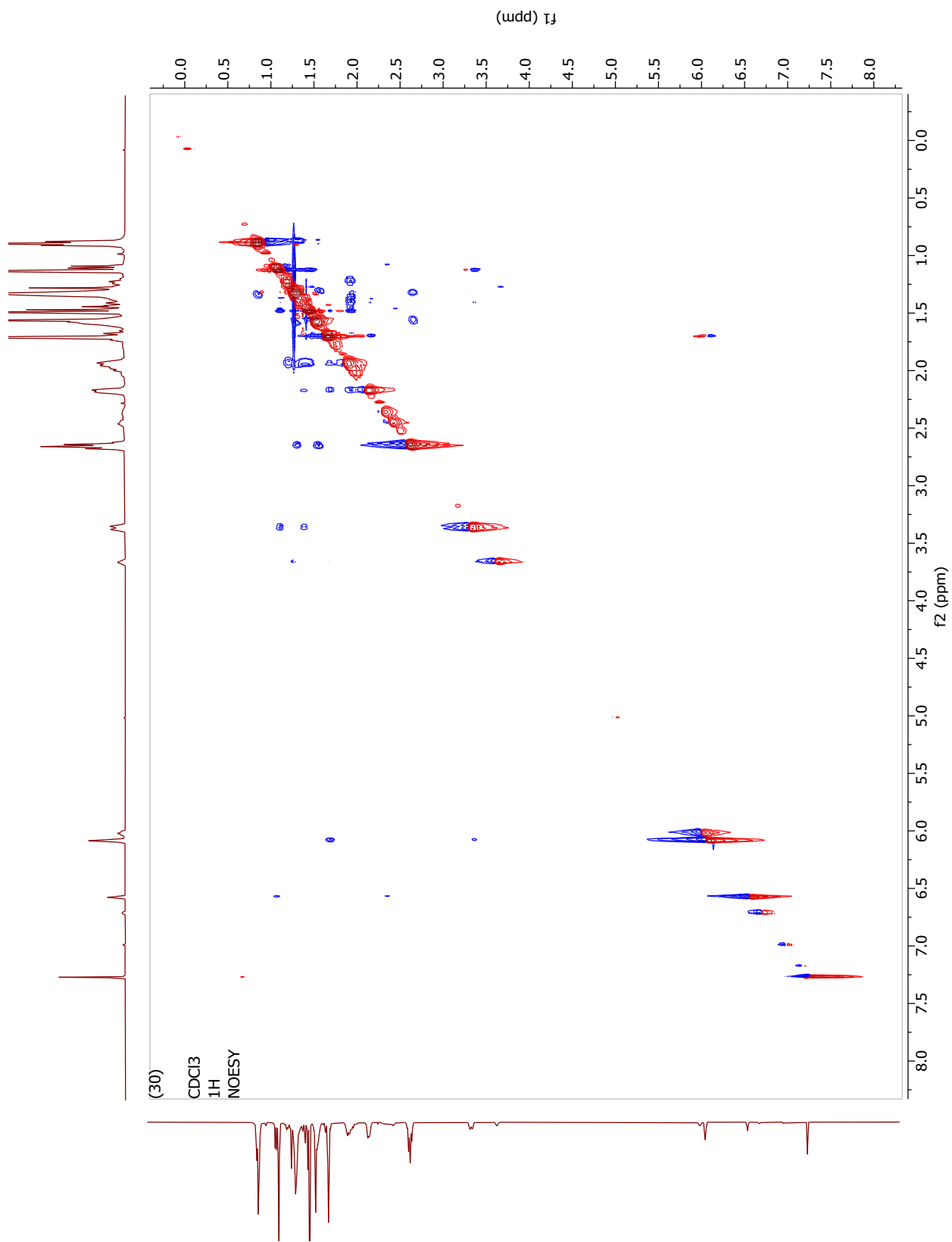
CDCl<sub>3</sub>  
13C

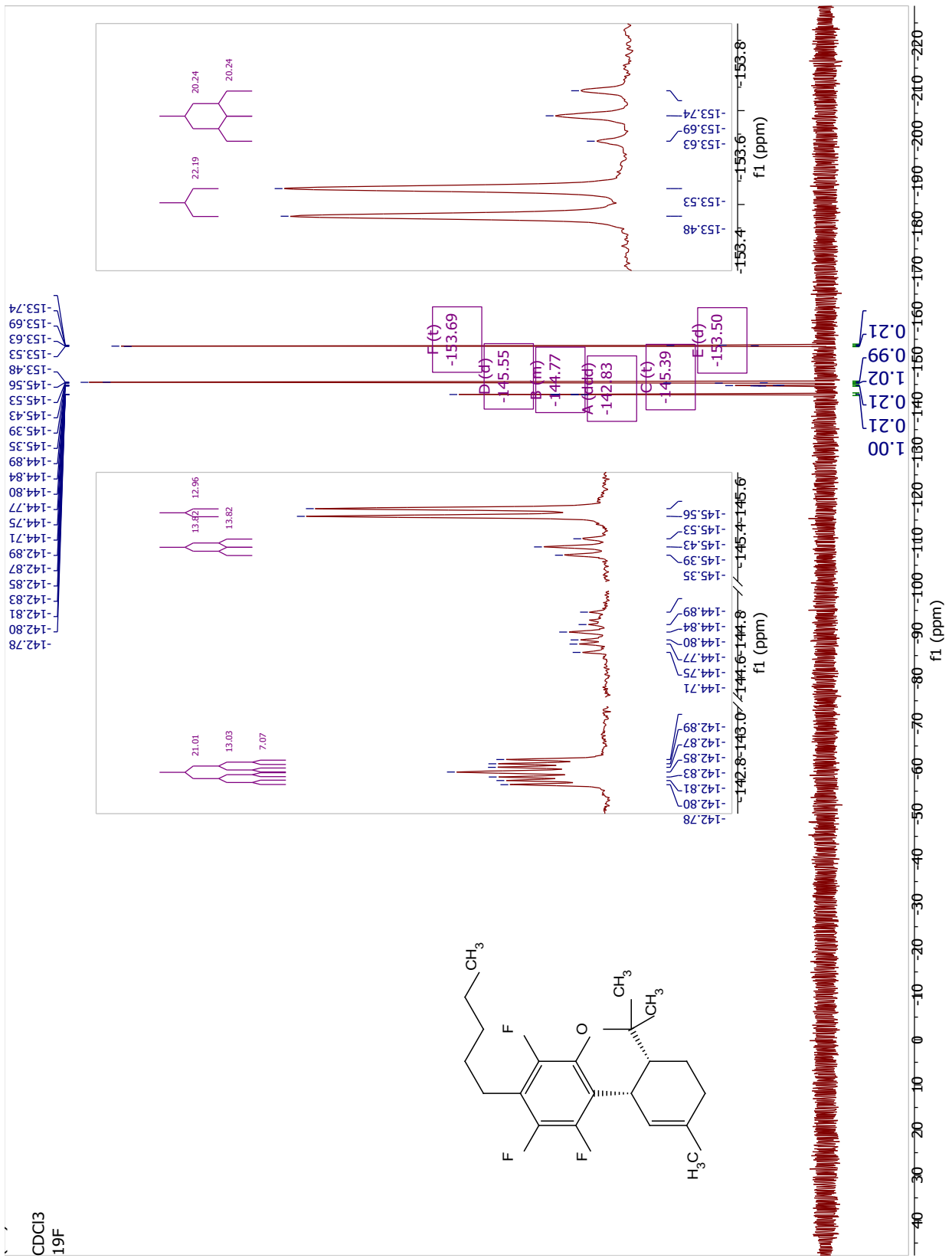






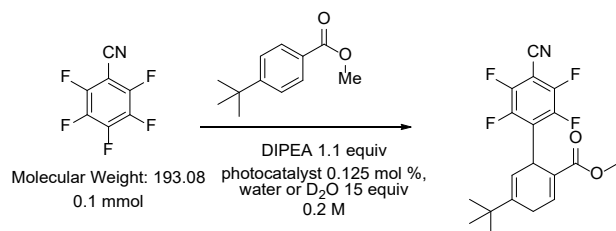




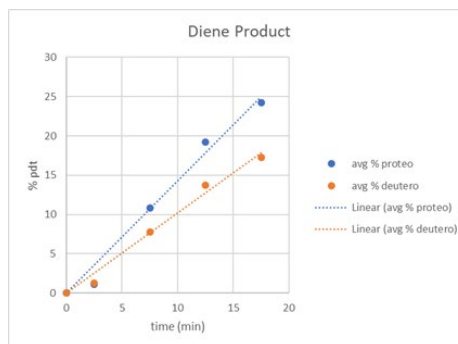




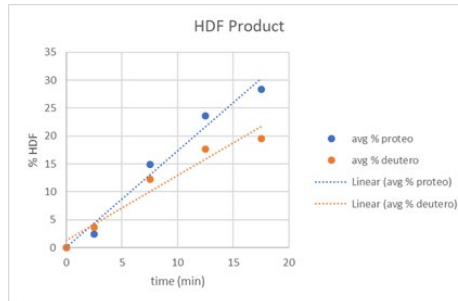
### 6.10.3 Kinetic Isotope Effect studies



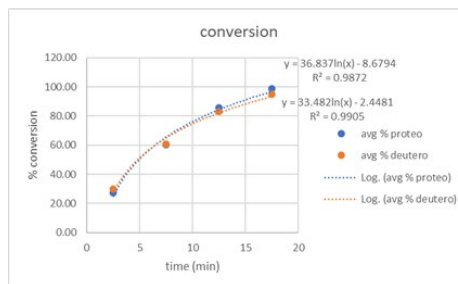
Diene product formation (%)						
time (min)	0	2.5	7.5	12.5	17.5	
H <sub>2</sub> O	JD5121A	0	0.17	2.08	3.78	4.9
	JD5121B	0	0.24	2.14	3.82	4.79
	JD5121C	0	0.28	2.26	3.92	4.86
D <sub>2</sub> O	JD5121D	0	0.25	1.48	2.68	3.37
	JD5121E	0	0.27	1.63	2.81	3.5
	JD5121F	0	0.26	1.54	2.76	3.48
avg % proteo	0	1.15	10.80	19.20	24.25	
stddev proteo	0	0.05	0.07	0.06	0.05	
avg % deuterio	0	1.30	7.75	13.75	17.25	
stddev deuterio	0	0.01	0.06	0.05	0.06	
		slope	intercept			
KH		1.48804878	0.00		KH/KD	
KD		1.04743902	0.00		1.42065433	

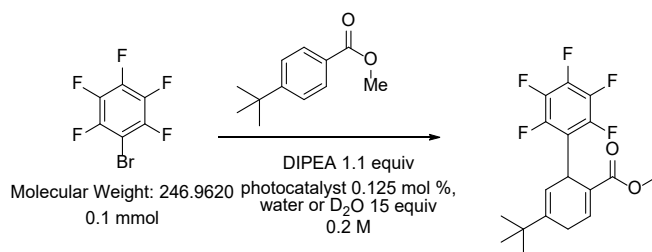


HDF product formation (%)					
time (min)	0	2.5	7.5	12.5	17.5
JD5121A	0	0.4	2.97	4.76	5.8
JD5121B	0	0.49	2.91	4.65	5.58
JD5121C	0	0.55	3.04	4.78	5.61
JD5121D	0	0.72	2.41	3.46	4.04
JD5121E	0	0.76	2.54	3.59	3.59
JD5121F	0	0.71	2.42	3.53	4.08
avg % proteo	0	2.40	14.87	23.65	28.32
stddev proteo	0	0.06	0.05	0.06	0.10
avg % deuterio	0	3.65	12.28	17.63	19.52
stddev deuterio	0	0.02	0.06	0.05	0.22
		slope	intercept		
KH		1.73073171	0.00		KH/KD
KD		1.16361789	0.00		1.48737118



Conversion (%)					
time (min)	0	2.5	7.5	12.5	17.5
JD5121A	0	15.26	8.82	3.4	0.64
JD5121B	0	14.4	7.8	2.77	0.05
JD5121C	0	14.03	7.24	2.51	0.04
JD5121D	0	14.23	7.89	3.56	1.21
JD5121E	0	13.96	7.6	3.22	0.92
JD5121F	0	13.89	8	3.33	0.94
avg % proteo	0	27.18	60.23	85.53	98.78
stddev proteo	0	0.52	0.65	0.37	0.28
avg % deuterio	0	29.87	60.85	83.15	94.88
stddev deuterio	0	0.15	0.17	0.14	0.13
		slope	intercept		
KH		5.57910569	0.00		KH/KD
KD		5.27256098	0.00		1.05813962





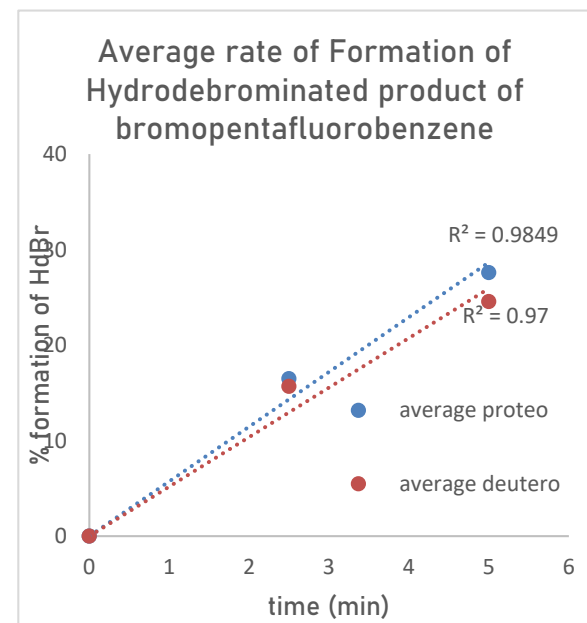
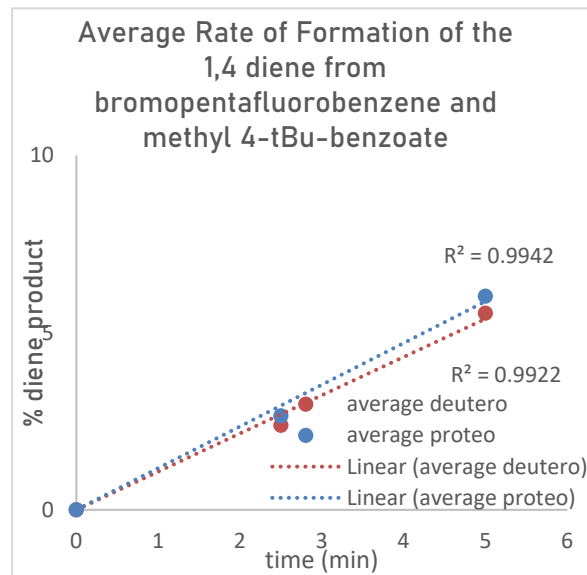
Formation of diene						
time (min)	integration			slope	average slope	stddev
	0	2.5	5			
H <sub>2</sub> O	0	0.4	0.89	0.178	0.176	0.00163
	0	0.38	0.87	0.174		
	0	0.38	0.88	0.176		
	as a %					
	0	2.74	6.1			
	0	2.62	6.01			
0	2.58	5.98				
average proteo			0	2.65	6.03	
D <sub>2</sub> O	0	0.36	0.79	0.158	0.165	0.00499
	0	0.32	0.85	0.17		
	0	0.36	0.83	0.166		
	as a %					
	0	2.41	5.41			
	0	2.25	5.46			
0	2.49	5.78				
average deuterio			0	2.38	5.55	

kH/kD  
1.069

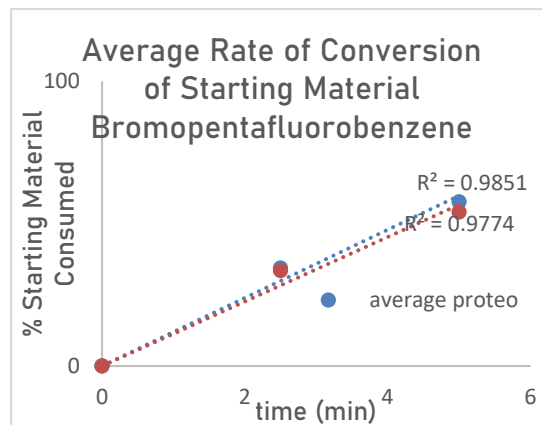
Formation of HDBr						
time (min)	integration			slope	average slope	stddev
	0	2.5	5			
H <sub>2</sub> O	0	2.55	4.14	0.828	0.805	0.01731
	0	2.33	4.01	0.802		
	0	2.34	3.93	0.786		
	as a %					
	0	17.5	28.4			
	0	16.1	27.7			
0	15.9	26.7				
average proteo			0	16.5	27.6	
D <sub>2</sub> O	0	2.29	3.54	0.708	0.731	0.01676
	0	2.21	3.68	0.736		
	0	2.34	3.74	0.748		
	as a %					
	0	15.4	24.2			
	0	15.5	24.4			
0	16.2	25				
average deuterio			0	15.7	24.6	

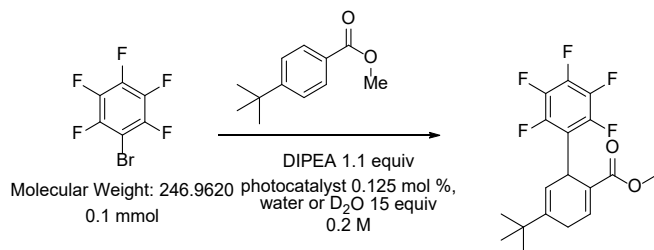
kH/kD  
1.102

Conversion of SM						
time (min)	integration			slope	average slope	stddev
	0	2.5	5			
H <sub>2</sub> O	15	9.34	6.14	-1.69	-1.68	0.01705
	14	9.73	6	-1.7		
	15	9.65	6.42	-1.66		
	as a %					
	0	36	57.9			
	0	32.8	58.6			
0	34.4	56.4				
average proteo			0	34.4	57.6	
D <sub>2</sub> O	15	10	7	-1.58	-1.57	0.02346



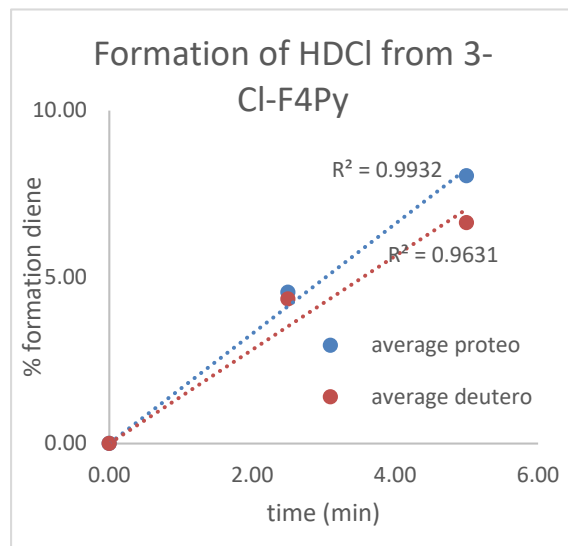
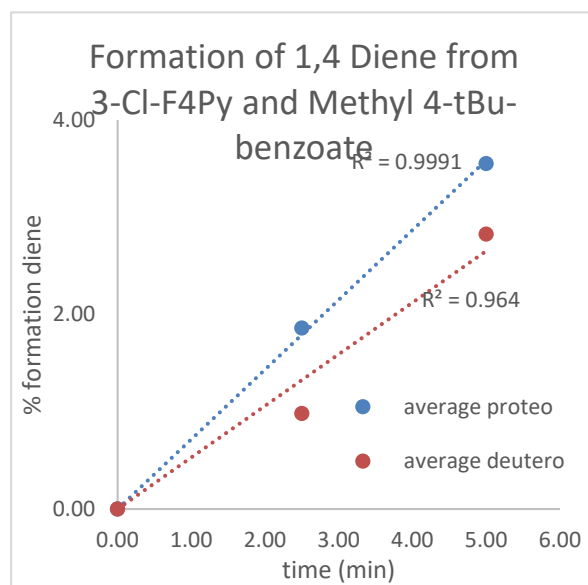
	14	9.58	6.55	-1.54
	14	9.38	6.48	-1.59
	as a %			
	0	32.8	53.1	
	0	32.7	54	
	0	35	55.1	
average proteo	0	33.5	54.1	
	kH/kD			
				1.071





Formation of diene						
time (min)	integration			slope	average slope	stddev
	0.00	2.50	5.00			
H <sub>2</sub> O	0.00	0.13	0.26	0.052	0.053	0.002
	0.00	0.16	0.28	0.056		
	0.00	0.16	0.26	0.052		
	as a %					
	0.00	1.58	3.65			
	0.00	2.01	3.76			
	0.00	2.00	3.24			
average proteo	0.00	1.86	3.55			
D <sub>2</sub> O	0.00	0.08	0.23	0.046	0.046	0.002
	0.00	0.08	0.22	0.044		
	0.00	0.08	0.24	0.048		
	as a %					
	0.00	1.00	2.88			
	0.00	0.97	2.65			
	0.00	0.98	2.94			
average deuterio	0.00	0.98	2.82			

kH/kD  
 1.1363



Formation of HDCl						
time (min)	integration			slope	average slope	stddev
	0	2.5	5			
H <sub>2</sub> O	0.00	0.34	0.61	0.122	0.121	0.002
	0.00	0.37	0.61	0.122		
	0.00	0.39	0.59	0.118		
	as a %					
	0.00	4.12	8.56			
	0.00	4.64	8.20			
	0.00	4.86	7.36			
average proteo	0.00	4.54	8.04			
D <sub>2</sub> O	0.00	0.34	0.53	0.106	0.108	0.003
	0.00	0.36	0.56	0.112		
	0.00	0.36	0.53	0.106		
	as a %					
	0.00	4.25	6.63			
	0.00	4.34	6.76			
	0.00	4.42	6.50			

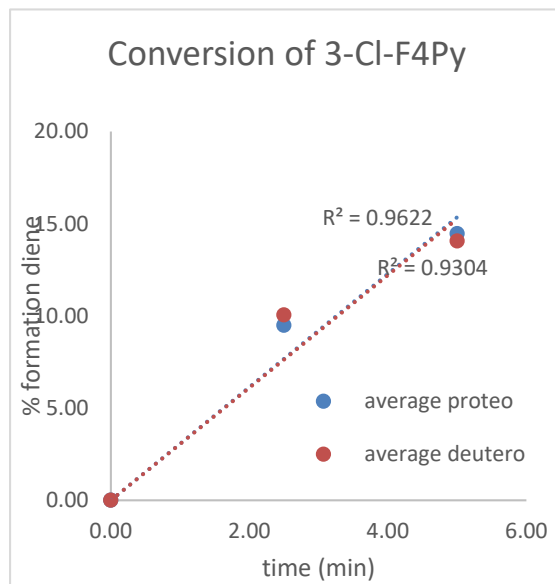


average deuterio	0.00	4.34	6.63
------------------	------	------	------

kH/kD  
1.095

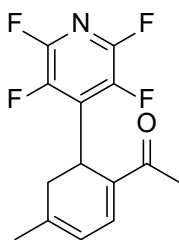
Consumption of SM							
	time (min)	integration			slope	average slope	stddev
		0	2.5	5			
H2O		8.25	7.13	6.90	0.270	-0.234	0.039
		7.97	7.44	7.07	0.180	-	-
		8.02	7.36	6.76	0.252	-	-
		as a %			-	-	-
		0.00	13.58	16.36	-	-	-
		0.00	6.65	11.29	-	-	-
		0.00	8.23	15.71	-	-	-
	average proteo	0.00	9.49	14.46	-	-	-
D2O		8.00	7.33	6.95	0.210	-0.229	0.035
		8.29	7.35	6.90	0.278	-	-
		8.15	7.30	7.15	0.200	-	-
		as a %			-	-	-
		0.00	8.38	13.13	-	-	-
		0.00	11.34	16.77	-	-	-
		0.00	10.43	12.27	-	-	-
	average deuterio	0.00	10.05	14.05	-	-	-

kH/kD  
1.0203



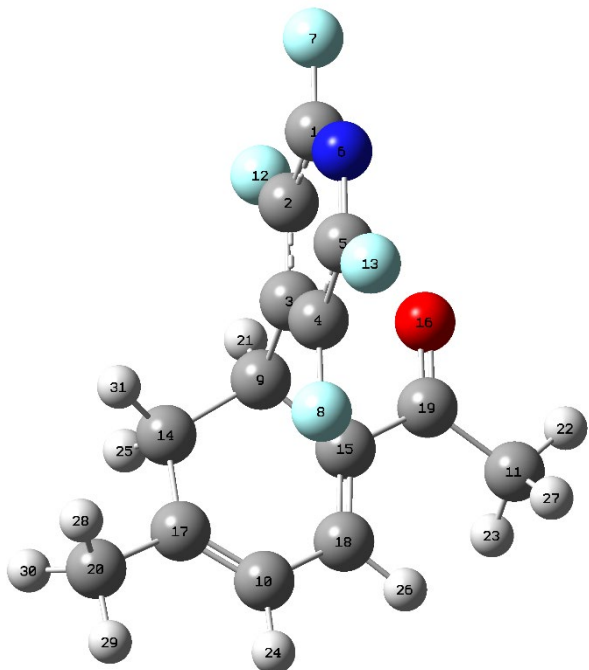
### 6.10.4 Computational NMR spectra

Computational NMR Spectra General Procedure: structures were built in Chem3d ver 17.1.0.105. Low energy conformational search was performed using stochastic conformational analysis was performed (MMF94), varying by 3 nm, generating 10 structures which were minimized in 500 steps. The low energy conformer was selected, exported as a PDB, and subjected to minimization in Gaussian. Methods same as described in Bally & Rablen.<sup>282</sup> Methyl signals were averaged following completion of calculation. Spectra were analyzed in MestreNova.

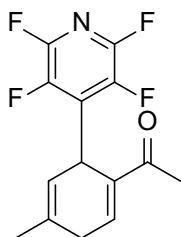


Diene Structure A

C	2.437508	3.506468	1.052895
C	2.12956	2.156784	0.89753
C	3.134767	1.244149	0.563841
C	4.412496	1.788777	0.417087
C	4.612408	3.155504	0.596863
N	3.650092	3.996418	0.906482
F	1.459861	4.357797	1.372831
F	5.464506	1.009242	0.113967
C	2.811558	-0.23701	0.390186
C	5.044653	-2.00826	-0.25495
C	2.380228	-0.64374	-3.53015
F	0.867334	1.749309	1.086835
F	5.846329	3.6491	0.451908
C	3.487286	-1.141	1.460206
C	3.094526	-0.71308	-1.03169
O	1.271948	0.558514	-1.78869
C	4.786576	-1.80011	1.051536
C	4.140228	-1.535	-1.28613
C	2.182532	-0.20868	-2.08474
C	5.691364	-2.2674	2.152091
H	1.732254	-0.30249	0.537386
H	1.599968	-0.18114	-4.13689
H	2.318611	-1.73324	-3.63271
H	5.941319	-2.54158	-0.56049
H	2.785889	-1.95024	1.718143
H	4.335194	-1.85604	-2.30613
H	3.360729	-0.33121	-3.90801
H	6.074526	-1.4134	2.72781
H	6.546521	-2.83005	1.765952
H	5.150945	-2.90561	2.865443
H	3.626284	-0.57378	2.388598

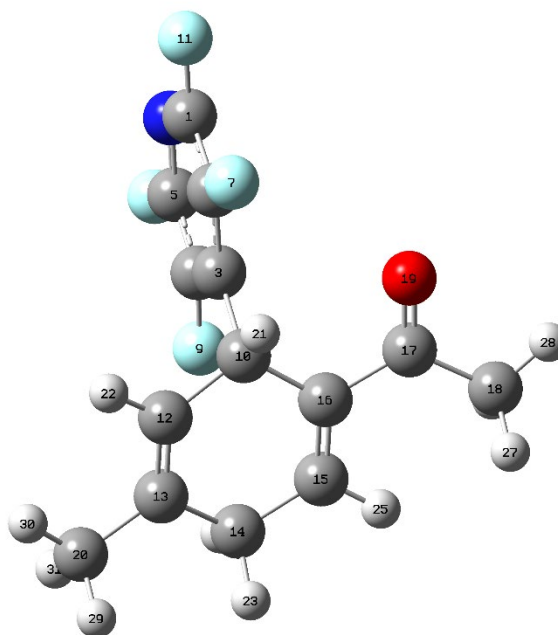




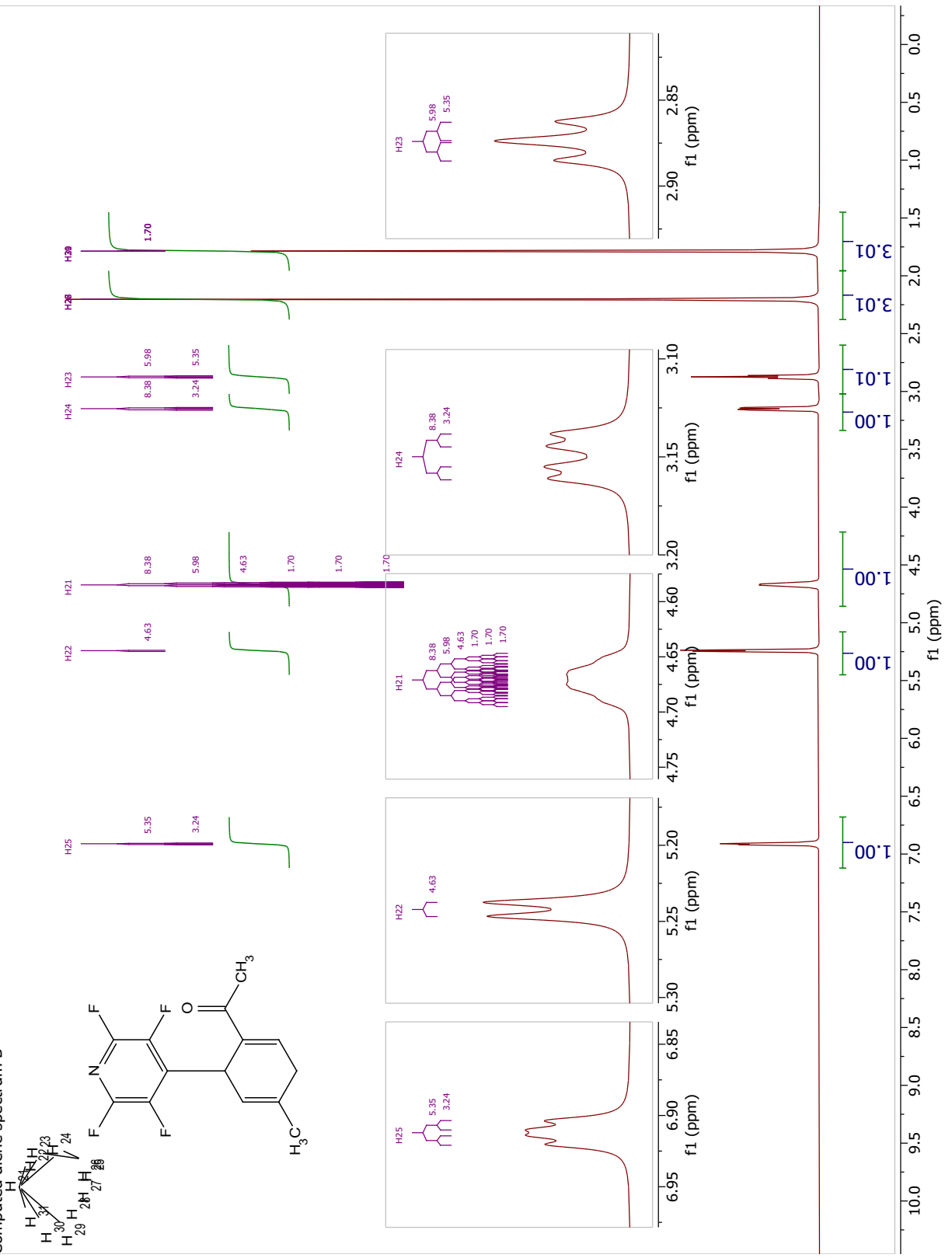


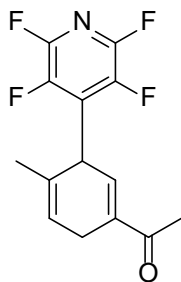
Diene Structure B

C	5.778514	3.517119	-0.67412
C	4.672493	2.811667	-0.20489
C	4.625901	1.423385	-0.3422
C	5.729266	0.839051	-0.96841
C	6.785255	1.637765	-1.39841
N	6.810622	2.94543	-1.25677
F	3.658906	3.477653	0.365667
F	7.832926	1.056553	-1.99159
F	5.788564	-0.49103	-1.16152
C	3.422108	0.612099	0.132987
F	5.803285	4.844896	-0.53386
C	2.702027	0.01108	-1.05509
C	2.627064	-1.2972	-1.31727
C	3.263163	-2.31347	-0.39875
C	3.735065	-1.74483	0.905326
C	3.818945	-0.43118	1.166235
C	4.275096	0.10206	2.483378
C	4.677056	-0.85752	3.592946
O	4.319923	1.311748	2.663839
C	1.920322	-1.84366	-2.52861
H	2.761634	1.332625	0.626897
H	2.242868	0.726347	-1.73571
H	2.558934	-3.13707	-0.20163
H	4.114764	-2.79432	-0.9103
H	4.020735	-2.46597	1.667851
H	5.512688	-1.49564	3.283111
H	3.84523	-1.51446	3.872002
H	4.977265	-0.27004	4.462176
H	1.099069	-2.51464	-2.24125
H	1.505519	-1.04375	-3.1492
H	2.605792	-2.4357	-3.15084



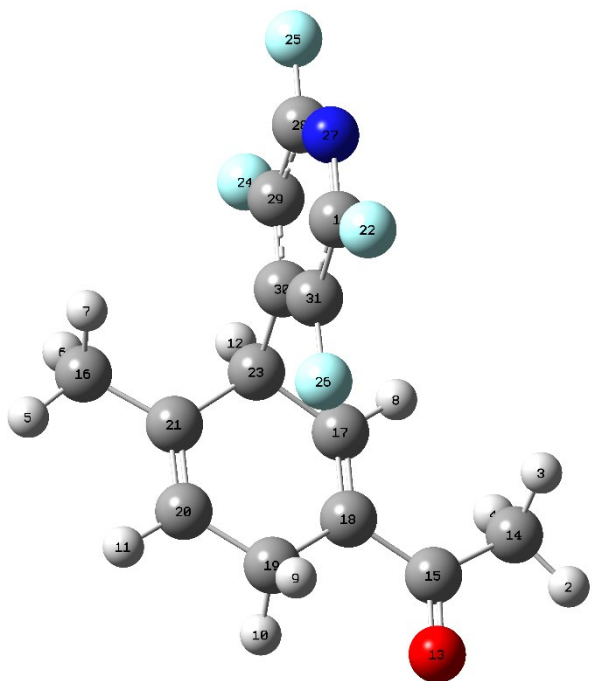
Computed diene spectrum B



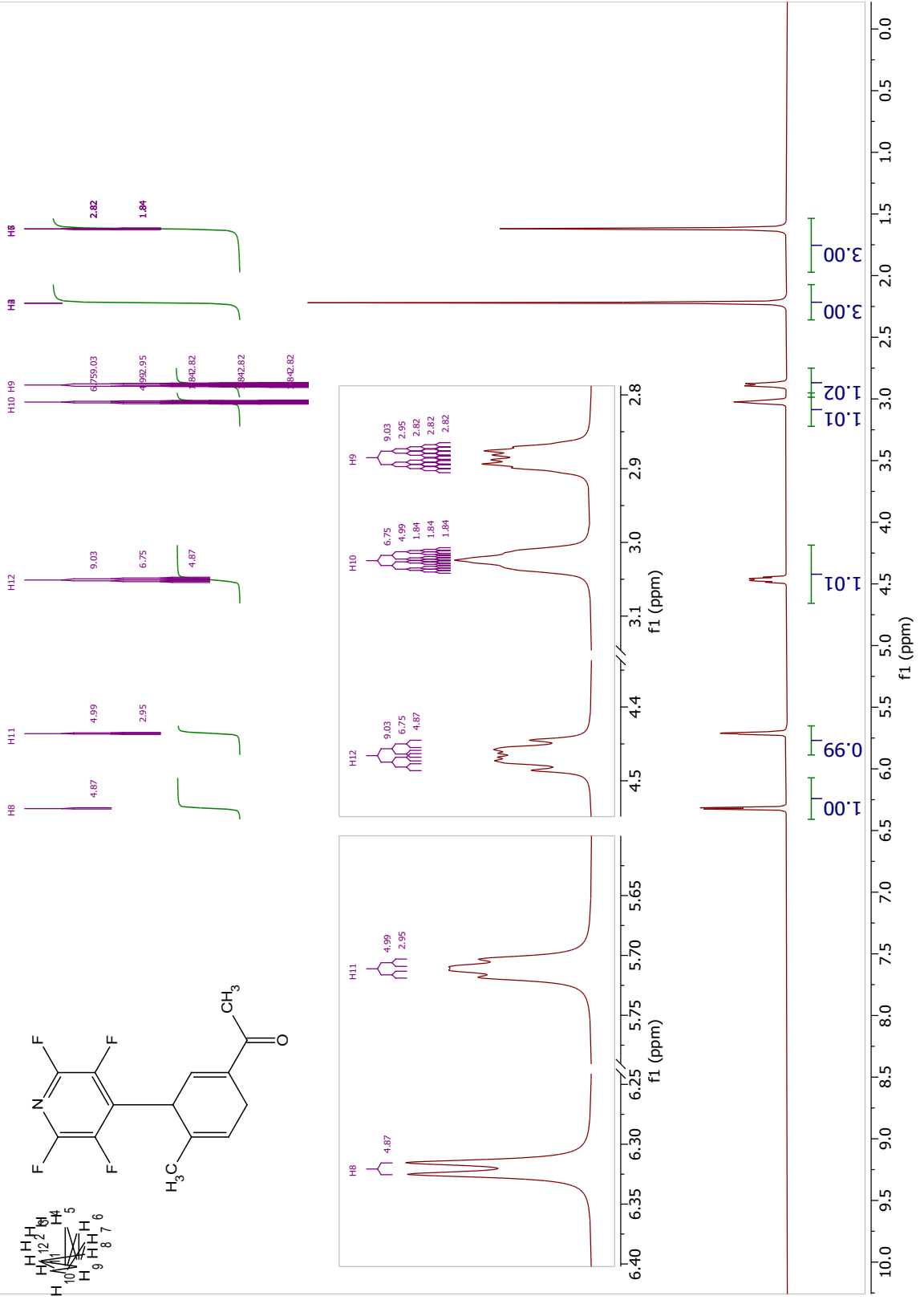
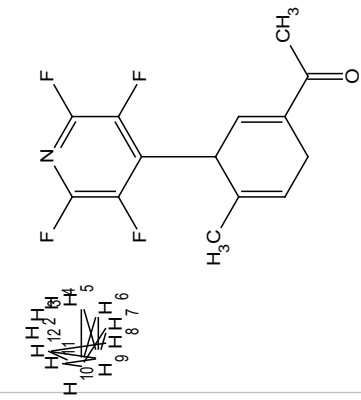


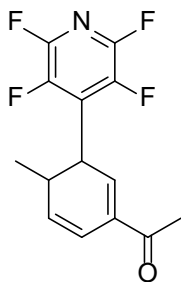
Diene Structure C

C	3.245211	3.363823	-0.58187
H	2.057594	-1.81474	4.457663
H	2.722236	-0.33298	3.722167
H	3.688029	-1.81398	3.736151
H	4.158207	-1.28067	-3.66239
H	5.664051	-1.11332	-2.73954
H	4.700723	0.313189	-3.11268
H	4.273673	-0.38182	1.887368
H	0.9804	-1.41767	-0.28853
H	1.714927	-2.98	-0.1193
H	2.370684	-2.14632	-2.37917
H	5.51141	-0.53024	-0.2486
O	1.010358	-2.51697	2.315185
C	2.667713	-1.42477	3.641216
C	2.034789	-1.84974	2.324768
C	4.632218	-0.74678	-2.83345
C	3.784337	-0.71261	0.97444
C	2.664178	-1.44819	1.027903
C	1.960584	-1.91486	-0.22059
C	2.750928	-1.67448	-1.47385
C	3.865355	-0.94075	-1.55117
F	2.0926	4.032682	-0.64854
C	4.445663	-0.27017	-0.31199
F	6.780871	1.42625	-0.3821
F	6.627914	4.116332	-0.5623
F	2.026889	1.344564	-0.47253
N	4.360052	4.063336	-0.60468
C	5.497647	3.407185	-0.53843
C	5.575358	2.018901	-0.44525
C	4.407033	1.254992	-0.41858
C	3.210369	1.973816	-0.49131



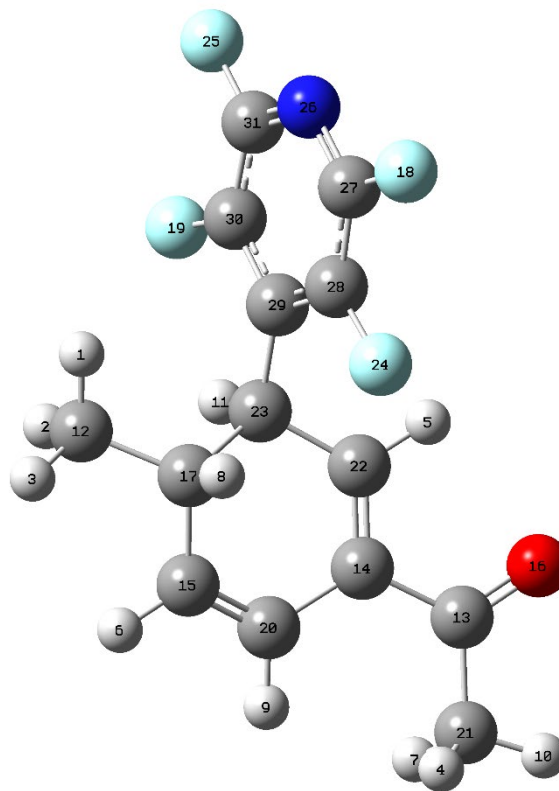
Computed diene spectrum C





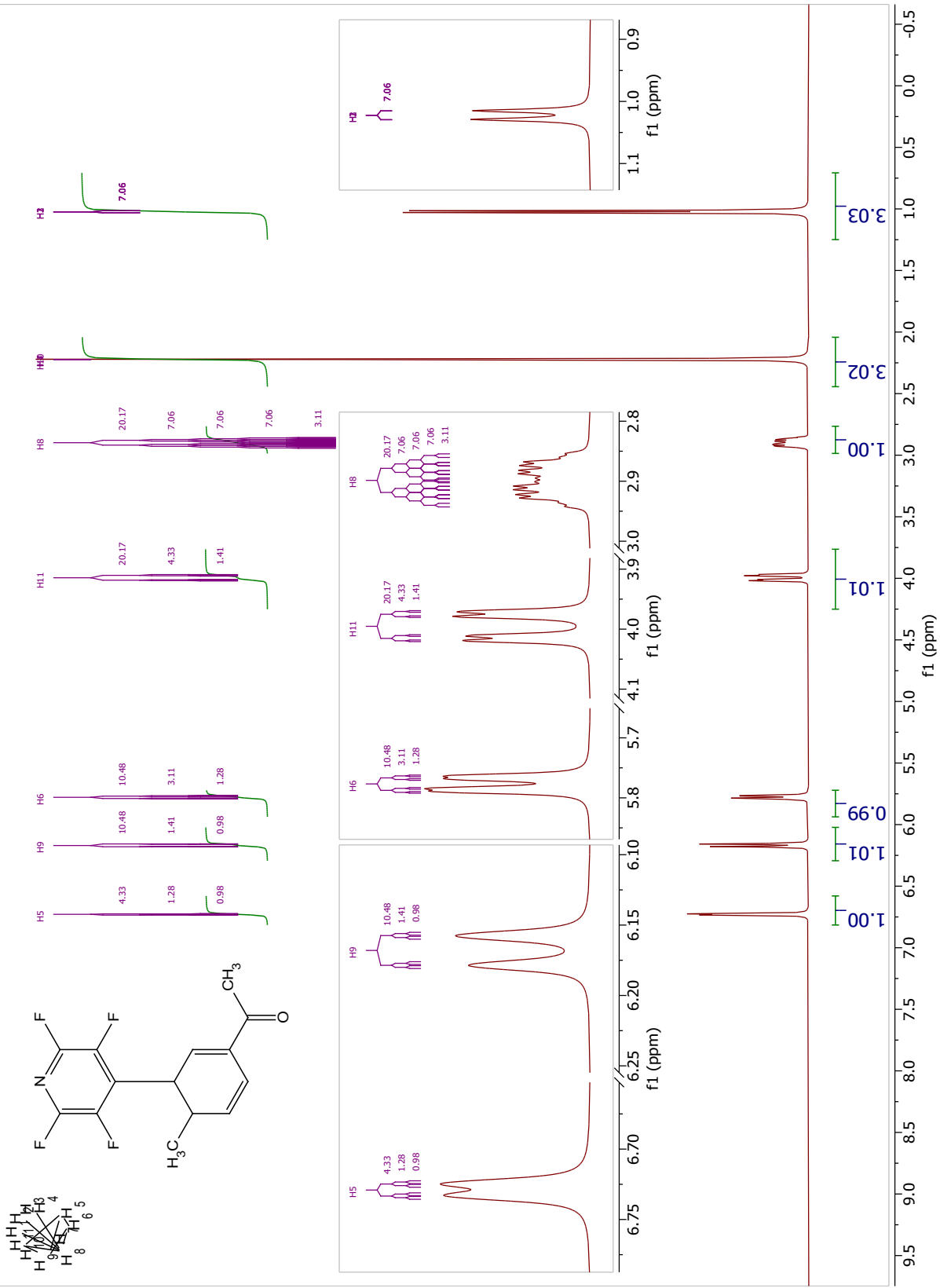
Diene Structure D

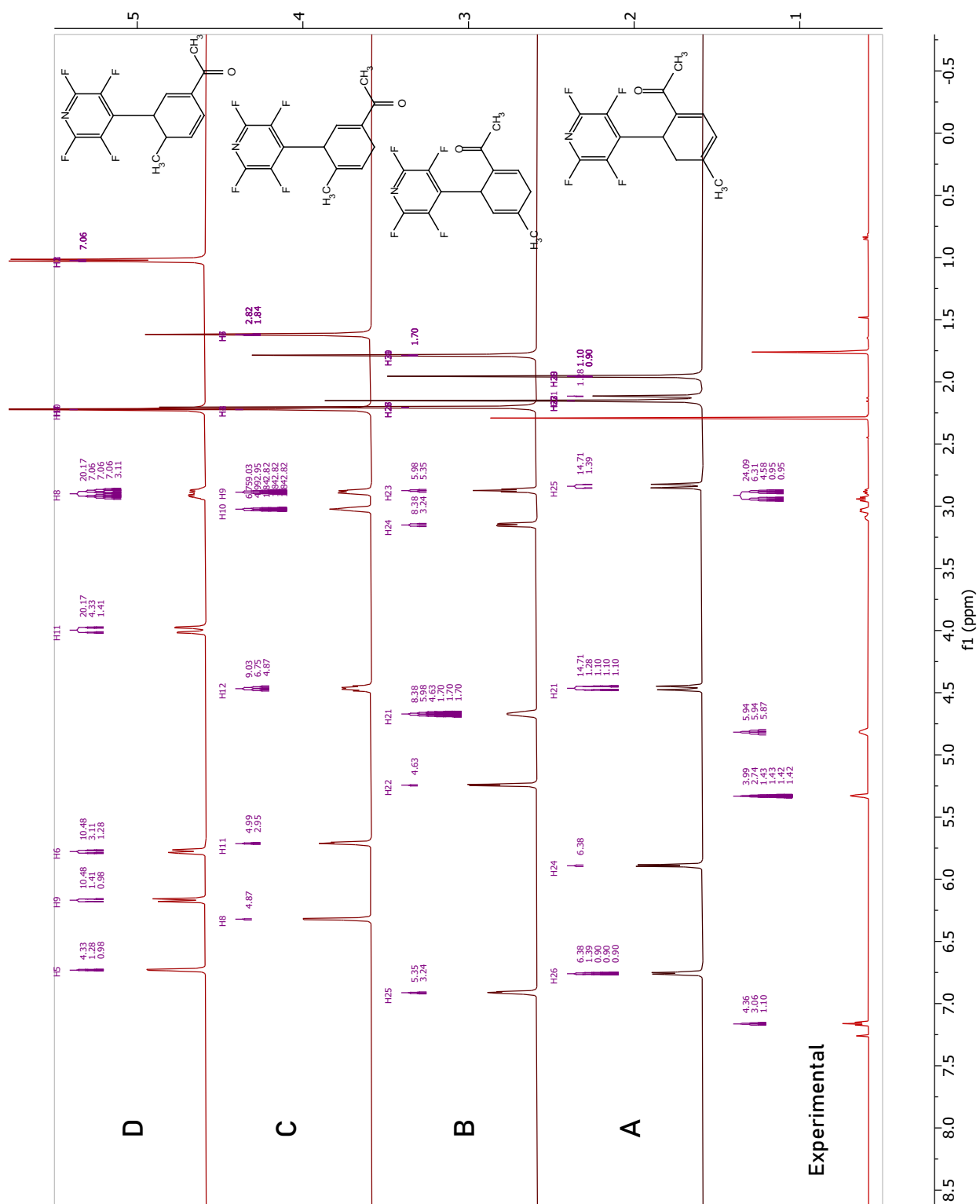
H	3.478092	0.704907	3.044957
H	2.474395	-0.74206	2.834845
H	4.110976	-0.88118	3.49941
H	5.774064	-3.49023	-2.52347
H	3.480614	0.438343	-1.95935
H	4.349214	-2.7202	1.817034
H	4.118192	-4.02681	-2.81673
H	5.075439	-0.11119	1.321001
H	4.342601	-3.50513	-0.48888
H	5.07806	-3.36263	-4.16562
H	2.166334	-0.1788	0.404693
C	3.496735	-0.3525	2.761997
C	4.357966	-1.87173	-2.81301
C	4.051014	-1.50223	-1.38735
C	4.200513	-2.01943	0.997938
O	4.205979	-1.06647	-3.71805
C	4.064966	-0.5513	1.349735
F	5.338939	4.571563	0.093153
F	0.933514	1.691376	1.166031
C	4.2055	-2.44991	-0.2725
C	4.865575	-3.27439	-3.09894
C	3.611299	-0.25359	-1.13232
C	3.204824	0.162525	0.265937
F	5.461933	1.892156	-0.25388
F	1.011948	4.377135	1.443719
N	3.175213	4.46323	0.766391
C	4.255753	3.836823	0.351001
C	4.319907	2.457089	0.172662
C	3.198039	1.667536	0.437304
C	2.065777	2.355245	0.877635
C	2.106627	3.740863	1.022647





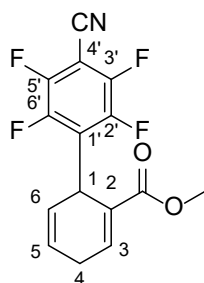
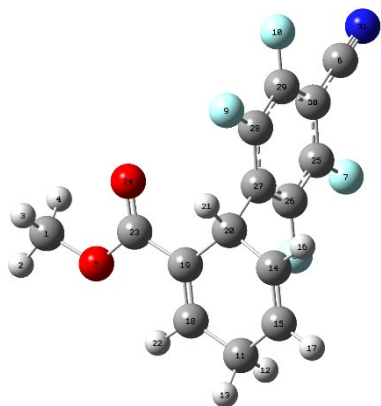
Computed diene spectrum D





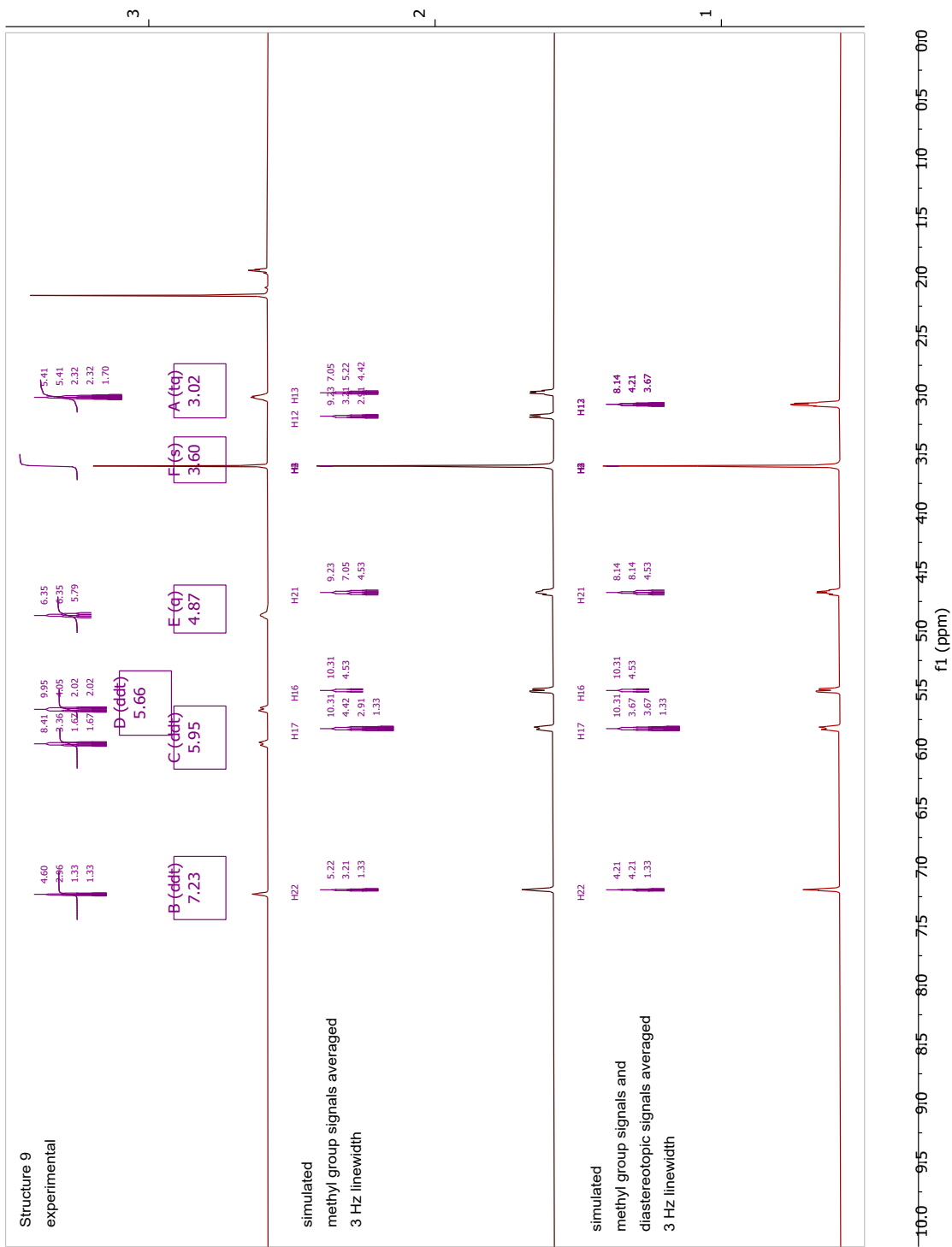
Experimental shift	Computational Shift: Structure A			$\Delta$	Computational Shift: Structure B		
	Integral		Integral		Integral		$\Delta$
7.16	1	6.76	1	0.40	6.91	1	0.25
5.33	1	5.89	1	-0.56	5.24	1	0.09
4.82	1	4.46	1	0.36	4.67	1	0.15
3.06	1	2.84	1	0.22	3.15	1	-0.09
2.91	1	2.11	1	0.80	2.87	1	0.04
2.29	3	2.15	3	0.14	2.20	3	0.09
1.76	3	1.96	3	-0.20	1.79	3	-0.03
std dev				0.41			0.10
mean				0.17			0.07

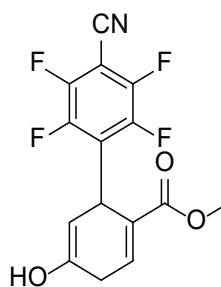
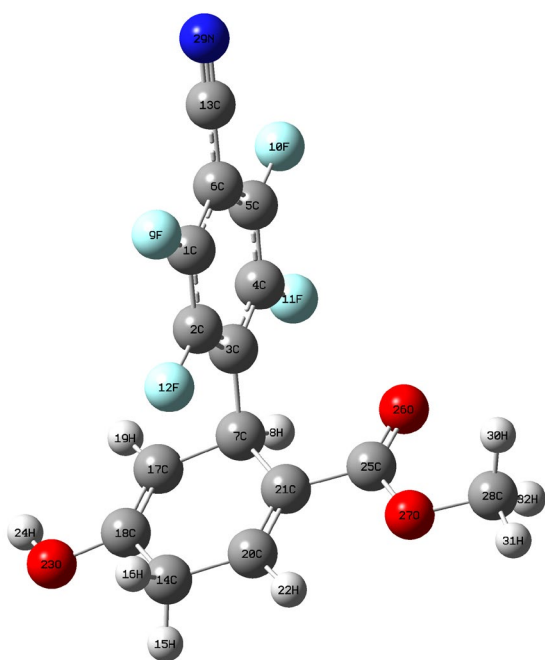
Computational Shift: Structure C			Computational Shift: Structure D		
Integral	$\Delta$		Integral	$\Delta$	
6.32	1	0.84	6.73	1	0.43
5.71	1	-0.38	6.17	1	-0.84
4.47	1	0.35	5.78	1	-0.96
3.02	1	0.04	3.99	1	-0.93
2.88	1	0.03	2.90	1	0.01
2.22	3	0.07	2.22	3	0.07
1.62	3	0.14	1.02	3	0.74
		0.35			0.65
		0.15			-0.21



methyl 4'-cyano-2',3',5',6'-tetrafluoro-1,4-dihydro-[1,1'-biphenyl]-2-carboxylate

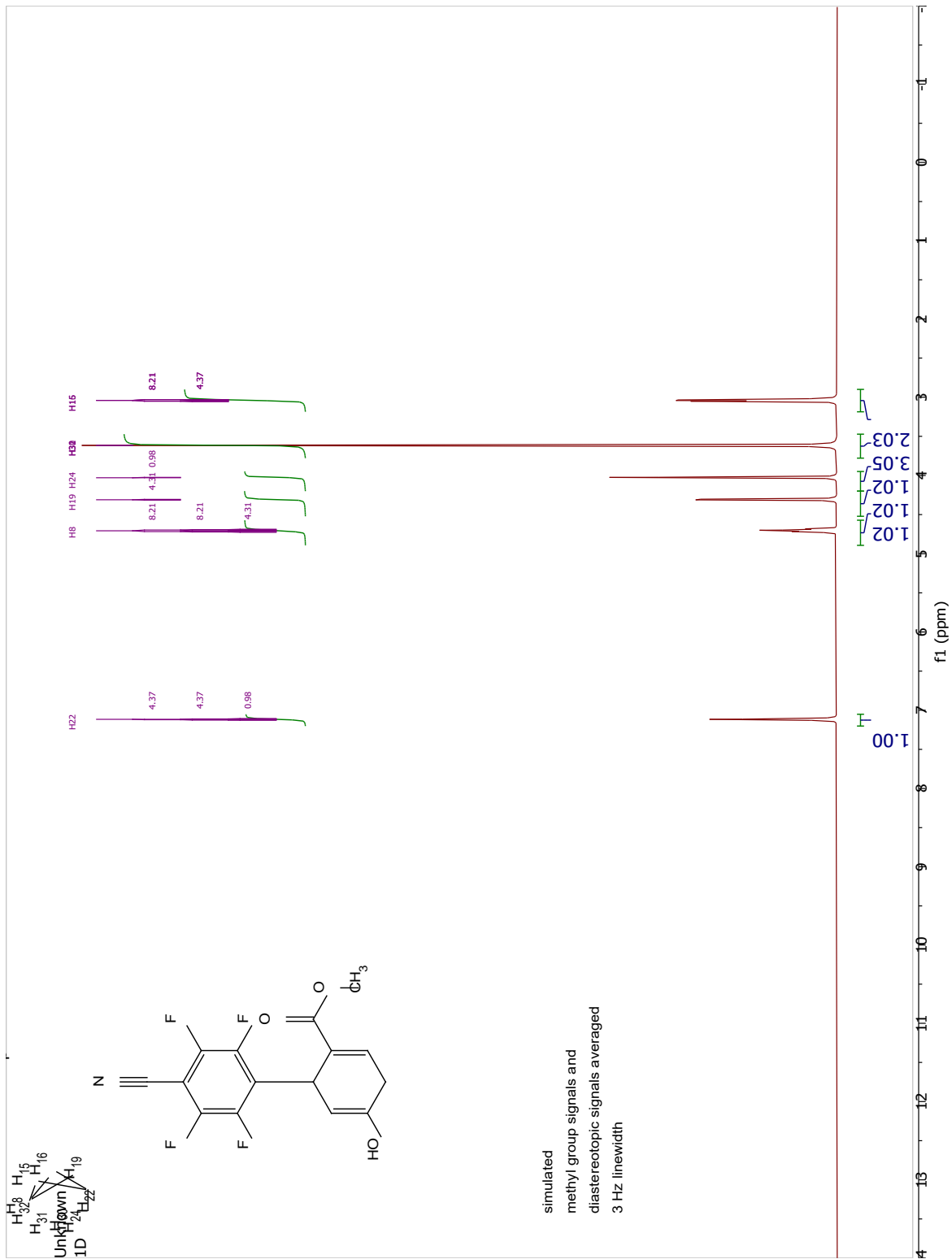
C	4.192810714943	-0.819316164610	4.137624952878	C	4.166442031493	-0.811495327757	1.782703198819
H	3.655127257694	-1.331856343321	4.935724697794	O	5.052172997302	0.024352461626	1.783916905947
H	5.262679481263	-1.036927887829	4.192217861469	C	2.193000828991	2.492964250246	-1.150169907753
H	4.046451432559	0.261739028424	4.207022499748	C	2.489200361368	1.144820004424	-0.989152856446
O	3.636201083005	-1.326261555225	2.913932792117	C	3.806144658448	0.679388399238	-0.923581330272
C	2.923569184108	4.826675737268	-1.431605591122	C	4.820518280424	1.633574857927	-1.040027588556
F	0.917234325705	2.884889470269	-1.202824555269	C	4.542952890827	2.985806023852	-1.204054324725
F	1.461793543937	0.285295108197	-0.890601332174	C	3.218783086482	3.441712166198	-1.262018944044
F	6.105932152525	1.257085469196	-1.002415025772	N	2.681949628197	5.955073386832	-1.570626394732
F	5.548688003209	3.856859546273	-1.309712507066				
C	2.004657199496	-2.906684136547	-0.669373379678	Experimental shift		Computational shift	$\Delta$ (EXP-COMP)
H	0.945074033085	-2.605514086352	-0.730976546496	(ppm)		(ppm)	
H	1.975789781640	-4.002161667699	-0.565818393282	7.25		7.19	0.06
C	3.678821887521	-1.588289453755	-1.967475294433	5.98		5.82	0.16
C	2.725786812786	-2.519307797476	-1.930565026565	5.69		5.5	0.19
H	4.170638350493	-1.340070665732	-2.905655421863	4.89		4.67	0.22
H	2.441037809609	-3.038836483290	-2.843227373178	3.63		3.6	0.03
C	2.613631083428	-2.308463291131	0.563131544489	3.04		3.08	-0.04
C	3.566315579346	-1.365484703016	0.539569169546				
C	4.136195466954	-0.804342129281	-0.754677789751				
H	5.228283051093	-0.854453632853	-0.689140334683				
H	2.257117002069	-2.671770584095	1.522856295056				

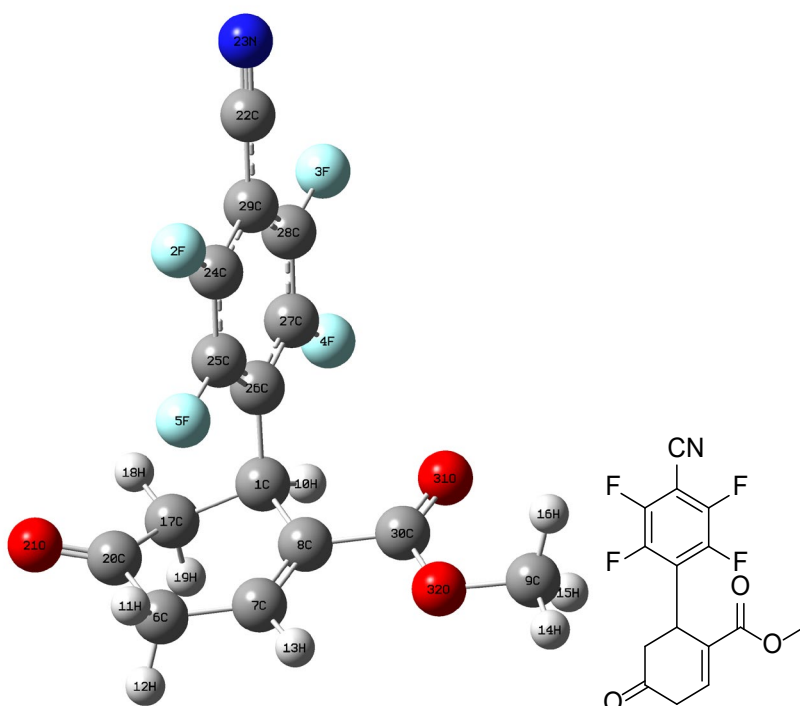




C,4.0474779807,2.8859128553,-0.7459591418  
 C,4.1543834056,1.5006991904,-0.7526648907  
 C,5.368688407,0.8445595536,-0.5232796308  
 C,6.4832370825,1.6617881122,-0.3095390911  
 C,6.3965440452,3.0487644824,-0.3024339851  
 C,5.1708837745,3.6944797325,-0.5199009798  
 C,5.5046910978,-0.6818346817,-0.5434243079  
 H,6.5288576892,-0.8829864716,-0.2125706992  
 F,2.8536731342,3.4542137542,-0.9648004322  
 F,7.4999817444,3.7768146018,-0.0886667644  
 F,7.6934258706,1.1092852347,-0.1073556603  
 F,3.0341857075,0.7895013458,-0.9879724493  
 C,5.0707129998,5.1181163488,-0.5175048786  
 C,3.3334427298,-2.5915183717,-1.3529285842  
 H,3.2890789533,-3.6850743889,-1.455728083  
 H,2.3322047916,-2.2360550766,-1.6425863493  
 C,5.3318054377,-1.2063063901,-1.9533886845  
 C,4.3530878397,-2.0481256554,-2.3075216803  
 H,6.0484476842,-0.8536343412,-2.6928947372  
 C,3.6124636151,-2.2208691397,0.0703648139  
 C,4.5699656386,-1.3598757651,0.4479232368  
 H,2.9921784955,-2.6835534145,0.8318873083  
 O,4.1570726211,-2.5318058316,-3.5725166466  
 H,4.8097502619,-2.1552026525,-4.179671725  
 C,4.8164245933,-1.0365984124,1.8798785771  
 O,5.7013483833,-0.2846942066,2.2535069524  
 O,3.9690752804,-1.6544390256,2.7304927305  
 C,4.1728470256,-1.3778759109,4.1303506045  
 N,4.9885659512,6.2779006661,-0.5171174682

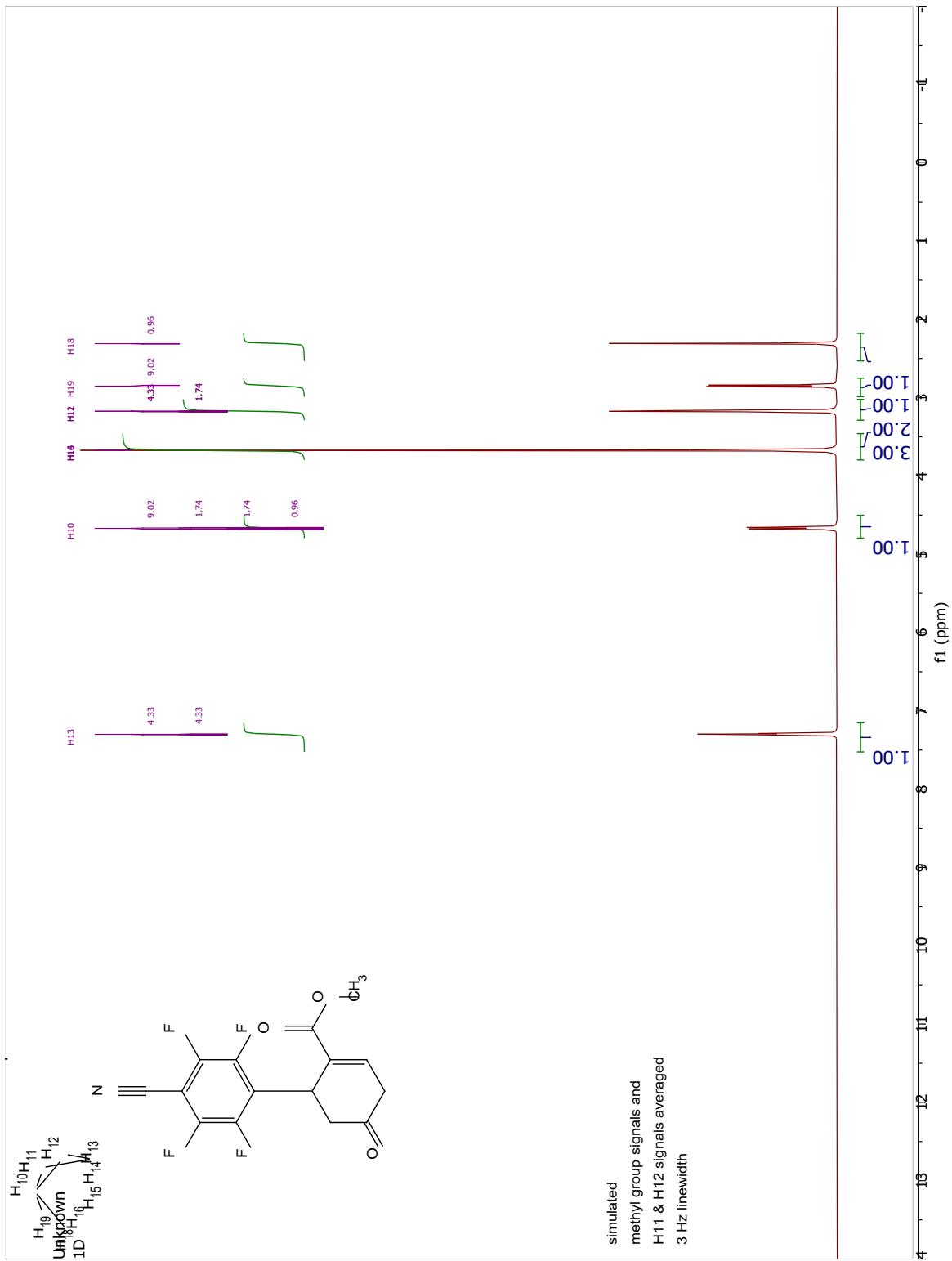
H,4.053747812,-0.3101957711,4.3283423712  
 H,3.4090621401,-1.9544375424,4.6510659633  
 H,5.1726878066,-1.691952828,4.4386143115





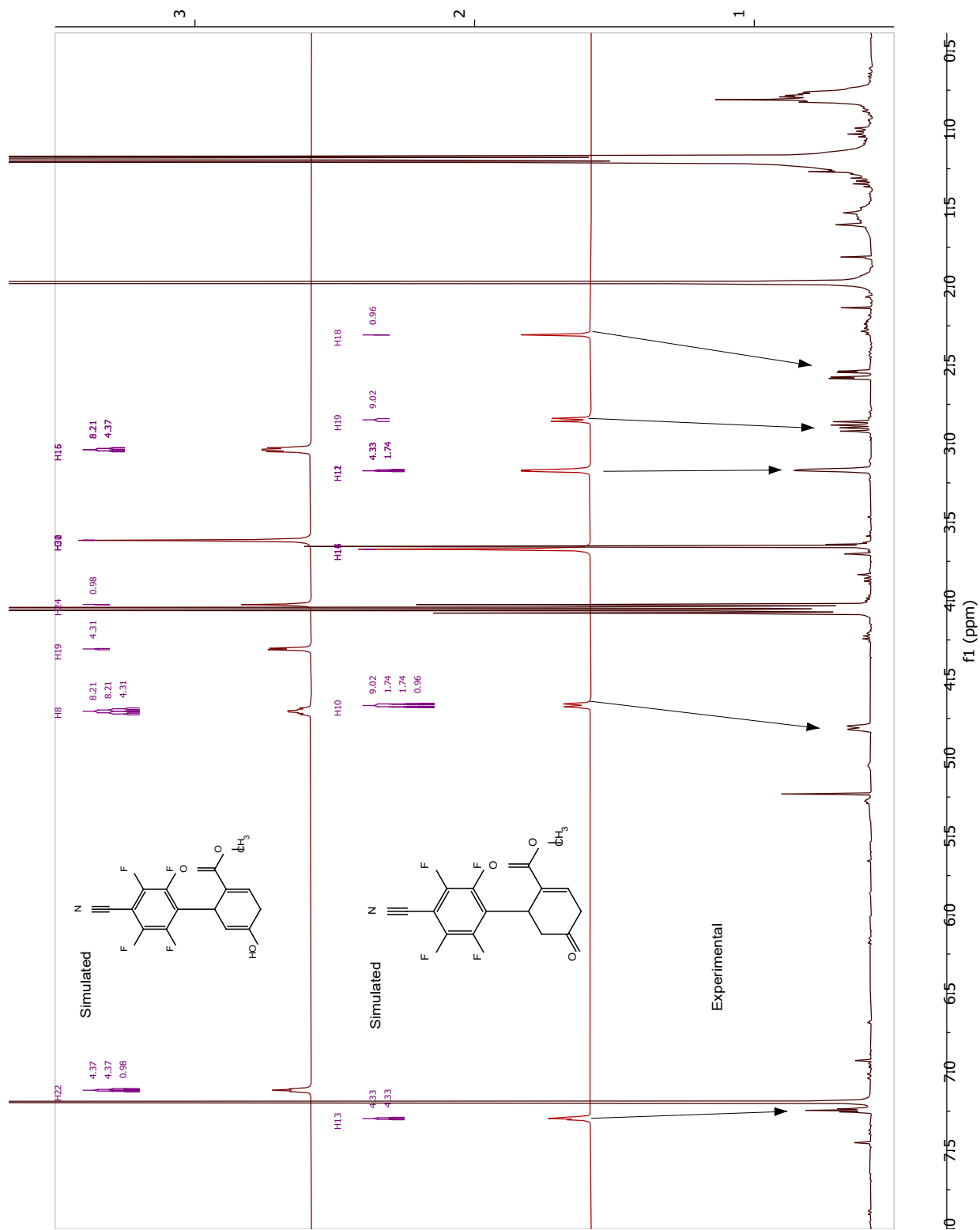
C,4.7380599398,0.5565131476,-1.0730995837  
 F,6.1249877932,-3.3885641316,1.549365348  
 F,2.8233983332,-3.8827657838,-1.8127540527  
 F,3.0240967819,-1.2830038702,-2.3984038766  
 F,6.3349370277,-0.7899701247,0.9725354083  
 C,6.9707803727,2.1473390784,0.1975105692  
 C,5.543710828,2.2036007557,0.6554403437  
 C,4.5471628786,1.4731572296,0.1278372754  
 C,1.6844934221,2.4547332939,2.2668242097  
 H,3.8883140391,0.7269282475,-1.7372314933  
 H,7.6248506827,1.8247220609,1.0173652784  
 H,7.3203687071,3.1572241549,-0.0674527393  
 H,5.3205494779,2.8640978039,1.4884888444  
 H,1.7619885559,3.1710714045,3.0838265705  
 H,0.9745742286,2.8019045598,1.5127322844  
 H,1.3681229787,1.477095168,2.6372128046  
 C,6.0217045026,0.9247928976,-1.8637248051  
 H,6.2916734634,0.1516831707,-2.5866881324  
 H,5.8029095743,1.8435699899,-2.4273841319  
 C,7.228129521,1.240715654,-0.9989693794  
 O,8.3467762447,0.8498583453,-1.2726686575  
 C,4.3576579808,-5.1028922426,0.197226556  
 N,4.2718769753,-6.2347985046,0.4479238429  
 C,5.3524547573,-2.8796629909,0.5821384461  
 C,5.4477116551,-1.527762895,0.2743162498  
 C,4.6669176189,-0.9271530147,-0.7179574588  
 C,3.791579784,-1.7736127549,-1.4089743409  
 C,3.6823325103,-3.1281208873,-1.1177651087  
 C,4.4621629099,-3.7127731021,-0.1095178879  
 C,3.1583854212,1.527125289,0.6658955667  
 O,2.2423303724,0.8632193662,0.2105058075  
 O,3.0110006616,2.3727286848,1.7064462426





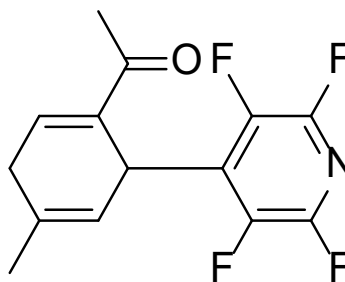
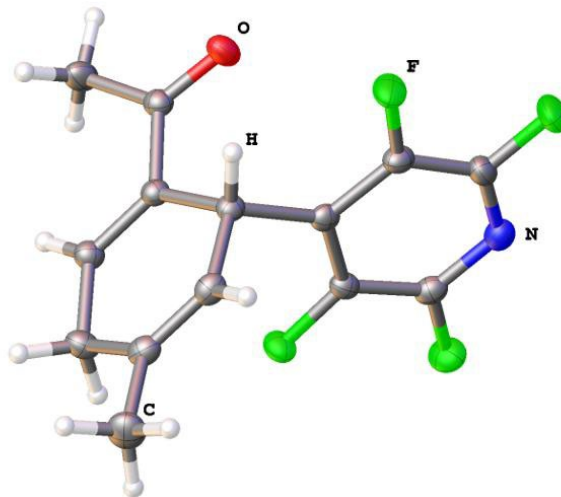
JD5143

Experimental shift	Integral	Computational Shift: ketone	Integral	$\Delta$	Computational Shift: hydroxyl	Integral	$\Delta$
7.31	1	7.30	1	0.01	7.12	1	0.19
4.88	1	4.67	1	0.21	4.70	1	0.18
3.72	3	3.67	3	0.05	3.62	3	0.10
3.24	2	3.17	2	0.07	3.04	2	0.20
2.96	1	2.85	1	0.11	4.03	1	-1.07
2.63	1	2.31	1	0.32	4.31	1	-1.68
std dev				0.11			0.75
mean				0.13			- 0.34



### 6.10.5 Single crystal X-ray diffraction analysis

Formula	C <sub>14</sub> H <sub>11</sub> F <sub>4</sub> NO
<i>D</i> <sub>calc.</sub> /g cm <sup>-3</sup>	1.522
$\mu$ /mm <sup>-1</sup>	1.201
Formula Weight	285.24
Colour	clear colourless
Shape	block
Size/mm <sup>3</sup>	0.12×0.11×0.08
<i>T</i> /K	123.00(10)
Crystal System	monoclinic
Space Group	<i>P</i> 2/ <i>a</i>
<i>a</i> /Å	13.6681(2)
<i>b</i> /Å	10.05445(18)
<i>c</i> /Å	18.1356(3)
$\alpha$ /°	90
$\beta$ /°	93.0274(15)
$\gamma$ /°	90
<i>V</i> /Å <sup>3</sup>	2488.81(7)
<i>Z</i>	8
<i>Z</i>	1
Wavelength/Å	1.54184
Radiation type	CuK $\alpha$
$\theta$ <sub>min</sub> /°	4.884
$\theta$ <sub>max</sub> /°	74.892
Measured Refl.	16570
Independent Refl.	2537
Reflections with <i>I</i> > 2( <i>I</i> )	2290
<i>R</i> <sub>int</sub>	0.0265
Parameters	183
Restraints	0
Largest Peak	0.257
Deepest Hole	-0.180
<i>Goof</i>	1.036
<i>wR</i> <sup>2</sup> (all data)	0.0857
<i>wR</i> <sup>2</sup>	0.0823
<i>R</i> <sup>1</sup> (all data)	0.0346
<i>R</i> <sup>1</sup>	0.0307



6.3.8

Fractional Atomic Coordinates ( $\times 10^4$ ) and Equivalent Isotropic Displacement Parameters ( $\text{\AA}^2 \times 10^3$ ) for **S046**.  
 $U_{eq}$  is defined as 1/3 of the trace of the orthogonalised  $U_{ij}$ .

Atom	x	y	z	$U_{eq}$
F4	4022.5(5)	5336.8(7)	4642.3(4)	25.04(18)
F3	4776.2(6)	7046.6(8)	5659.2(4)	29.33(19)
F1	2591.8(6)	9055.6(7)	3400.2(4)	31.4(2)
F2	3379.3(7)	10571.8(8)	4488.3(5)	38.0(2)
O1	4227.7(7)	7438.5(9)	2537.6(5)	26.7(2)
N1	4070.6(8)	8804.2(11)	5074.6(6)	24.4(2)
C10	3832.0(8)	6638.4(12)	4565.8(6)	18.9(2)
C9	3269.9(8)	7104.6(12)	3959.2(6)	18.4(2)
C11	4215.5(8)	7516.6(13)	5091.0(6)	21.3(2)
C3	3646.0(8)	5420.6(12)	2990.1(6)	17.8(2)
C7	2077.7(8)	5280.8(13)	3646.7(6)	21.4(3)
C4	3734.9(8)	4104.2(12)	3054.5(6)	20.2(2)
C2	4306.5(8)	6226.0(12)	2542.0(6)	19.7(2)
C8	2844.8(8)	6187.9(11)	3353.1(6)	18.3(2)
C13	3533.3(10)	9257.4(12)	4510.1(7)	24.4(3)
C6	2164.2(9)	3969.9(13)	3706.0(6)	22.2(3)
C12	3125.8(9)	8471.9(12)	3951.0(6)	22.3(3)
C5	3066.2(9)	3258.1(12)	3481.7(7)	23.5(3)
C1	5048.8(10)	5545.9(13)	2087.3(7)	26.9(3)
C14	1373.7(10)	3108.8(15)	3996.9(8)	32.5(3)

Anisotropic Displacement Parameters ( $\times 10^4$ ) **S046**. The anisotropic displacement factor exponent takes the form:  $-2\pi [h_2 a^* \times U_{11} + \dots + 2hka^* \times b^* \times U_{12}]$

Atom	$U_{11}$	$U_{22}$	$U_{33}$	$U_{23}$	$U_{13}$	$U_{12}$
F4	29.5(4)	19.3(4)	25.6(4)	3.0(3)	-5.0(3)	4.5(3)
F3	29.0(4)	33.2(4)	24.8(4)	2.3(3)	-8.6(3)	-1.1(3)
F1	45.0(5)	22.9(4)	25.5(4)	2.5(3)	-6.6(3)	11.2(3)
F2	61.4(6)	17.9(4)	34.4(4)	-2.8(3)	-0.8(4)	5.6(4)
O1	30.5(5)	18.3(5)	31.8(5)	2.4(3)	8.0(4)	-0.9(3)
N1	26.8(5)	25.1(6)	21.6(5)	-1.9(4)	4.1(4)	-3.6(4)
C10	17.5(5)	18.5(6)	20.9(5)	2.4(4)	3.5(4)	1.4(4)
C9	16.1(5)	21.1(6)	18.4(5)	0.9(4)	4.6(4)	1.0(4)
C11	18.2(5)	26.7(6)	19.0(5)	2.4(5)	1.7(4)	-1.3(5)
C3	17.4(5)	19.4(6)	16.5(5)	1.1(4)	0.6(4)	1.0(4)
C7	16.0(5)	27.6(6)	20.5(5)	-1.2(5)	1.4(4)	0.6(4)
C4	19.4(5)	20.0(6)	21.5(5)	1.7(4)	1.9(4)	1.6(4)
C2	20.7(5)	19.7(6)	18.6(5)	1.6(4)	0.0(4)	-0.5(4)
C8	18.6(5)	18.6(6)	17.8(5)	1.7(4)	-0.1(4)	2.8(4)
C13	32.2(6)	17.1(6)	24.6(6)	-0.3(5)	6.2(5)	0.8(5)
C6	19.2(6)	27.6(6)	19.6(6)	0.8(5)	0.2(4)	-3.1(5)
C12	25.4(6)	22.3(6)	19.2(5)	3.1(4)	2.1(4)	4.7(5)
C5	23.2(6)	19.7(6)	27.7(6)	4.6(5)	2.2(5)	-0.5(5)
C1	29.1(6)	23.5(6)	29.2(6)	3.2(5)	12.2(5)	0.5(5)
C14	27.5(7)	32.9(7)	37.6(7)	0.1(6)	7.9(6)	-8.4(6)

## Bond Lengths in Å.

Atom	Atom	Length/Å
F4	C10	1.3401(14)
F3	C11	1.3376(14)
F1	C12	1.3408(14)
F2	C13	1.3384(15)
O1	C2	1.2239(15)
N1	C11	1.3097(17)
N1	C13	1.3097(17)
C10	C9	1.3896(16)
C10	C11	1.3816(17)
C9	C8	1.5258(16)
C9	C12	1.3888(17)
C3	C4	1.3336(17)
C3	C2	1.4861(16)
C3	C8	1.5180(15)
C7	C8	1.5078(16)
C7	C6	1.3272(18)
C4	C5	1.4947(16)
C2	C1	1.5051(16)
C13	C12	1.3793(18)
C6	C5	1.5002(17)
C6	C14	1.5018(17)

F2	C13	C12	119.13(11)
N1	C13	F2	116.58(11)
N1	C13	C12	124.29(12)
C7	C6	C5	121.52(11)
C7	C6	C14	122.57(12)
C5	C6	C14	115.92(11)
F1	C12	C9	120.84(11)
F1	C12	C13	118.67(11)
C13	C12	C9	120.49(11)
C4	C5	C6	113.76(10)

## Bond Angles in Å.

Atom	Atom	Atom	Angle/°
C11	N1	C13	116.08(11)
F4	C10	C9	120.51(11)
F4	C10	C11	119.22(10)
C11	C10	C9	120.26(11)
C10	C9	C8	122.70(10)
C12	C9	C10	114.49(11)
C12	C9	C8	122.81(10)
F3	C11	C10	119.11(11)
N1	C11	F3	116.52(11)
N1	C11	C10	124.37(11)
C4	C3	C2	122.24(10)
C4	C3	C8	122.07(10)
C2	C3	C8	115.67(10)
C6	C7	C8	124.66(11)
C3	C4	C5	123.70(11)
O1	C2	C3	119.38(11)
O1	C2	C1	120.70(11)
C3	C2	C1	119.90(10)
C3	C8	C9	111.31(9)
C7	C8	C9	110.88(9)
C7	C8	C3	112.13(10)

Hydrogen Fractional Atomic Coordinates ( $\times 10^4$ ) and Equivalent Isotropic Displacement Parameters ( $\text{\AA}^2 \times 10^3$ ).  $U_{eq}$  is defined as 1/3 of the trace of the orthogonalised  $U_{ij}$ .

<b>Atom</b>	<b>x</b>	<b>y</b>	<b>z</b>	<b><math>U_{eq}</math></b>
H7	1503.07	5667.49	3797.01	26
H4	4241.62	3689.32	2820.42	24
H8	2519.41	6750.58	2973.05	22
H5A	3423.67	2934.21	3921.89	28
H5B	2869.87	2492.11	3184.22	28
H1A	4717.03	4990.19	1723.49	40
H1B	5474.97	5010.51	2403.05	40
H1C	5427.92	6203.12	1845.48	40
H14A	1627.89	2635.99	4425.23	49
H14B	1153.89	2484.33	3623.5	49
H14C	833.92	3655.67	4127.98	49

## VII

### ACKNOWLEDGEMENTS

This work was funded through the generous support of the NIH NIGMS award 5R01GM115697-02, HR-14-072, from the Oklahoma Center for the Advancement of Science and Technology, and Donors of the American Chemical Society Petroleum Research Fund award ACS-PRF 56159-DNI1. High-resolution mass spectrometry analyses were performed in the Genomics and Proteomics Center at Oklahoma State University, using resources supported by the NSF MRI and EPSCoR programs (award DBI/0722494). Molecular graphics and analyses were performed with the UCSF Chimera 1.11.2 package, Inkscape 0.92.0 r15299, FreeCAD 0.16, and GIMP 2.8.20. Chimera is developed by the Resource for Biocomputing, Visualization, and Informatics at the University of California, San Francisco (supported by NIGMS P41-GM103311). Inkscape and GIMP are available under GNU General Public License. FreeCad is available under the GNU Lesser General Public License. The computing for this project was performed at the OSU High Performance Computing Center at Oklahoma State University supported in part through the National Science Foundation grants OAC-1126330 and OAC-1531128. Some images were generated in part through Chimera,<sup>287</sup> which is developed by the Resource for Biocomputing, Visualization, and Informatics at the University of California, San Francisco (supported by NIGMS P41-GM103311).



VITA

JONATHAN ISAAC DAY

Candidate for the Degree of

Doctor of Philosophy

Thesis: FLUORINATION AND PHOTOCATALYSIS: NEW HORIZONS

Major Field: Chemistry

Biographical:

Education:

Completed the requirements for the Doctor of Philosophy in Chemistry at Oklahoma State University, Stillwater, Oklahoma in May, 2020.

Completed the requirements for the Bachelor of Science/Arts in Chemistry at Oklahoma State University, Stillwater, Oklahoma in December, 2015.

Professional Memberships:

American Chemical Society  
Phi Kappa Phi Honor Society